SEPSIS: BASIC, CLINICAL AND THERAPEUTIC APPROACHES

EDITED BY: Hong Zhou, Yan Kang, Lefu Lan and Daolin Tang
PUBLISHED IN: Frontiers in Pharmacology

frontiers Research Topics

ISSN 1664-8714
ISBN 978-2-88976-307-8
DOI 10.3389/978-2-88976-307-8

About Frontiers

Frontiers is more than just an open-access publisher of scholarly articles: it is a pioneering approach to the world of academia, radically improving the way scholarly research is managed. The grand vision of Frontiers is a world where all people have an equal opportunity to seek, share and generate knowledge. Frontiers provides immediate and permanent online open access to all its publications, but this alone is not enough to realize our grand goals.

Frontiers Journal Series

The Frontiers Journal Series is a multi-tier and interdisciplinary set of open-access, online journals, promising a paradigm shift from the current review, selection and dissemination processes in academic publishing. All Frontiers journals are driven by researchers for researchers; therefore, they constitute a service to the scholarly community. At the same time, the Frontiers Journal Series operates on a revolutionary invention, the tiered publishing system, initially addressing specific communities of scholars, and gradually climbing up to broader public understanding, thus serving the interests of the lay society, too.

Dedication to Quality

Each Frontiers article is a landmark of the highest quality, thanks to genuinely collaborative interactions between authors and review editors, who include some of the world's best academicians. Research must be certified by peers before entering a stream of knowledge that may eventually reach the public - and shape society; therefore, Frontiers only applies the most rigorous and unbiased reviews.
Frontiers revolutionizes research publishing by freely delivering the most outstanding research, evaluated with no bias from both the academic and social point of view. By applying the most advanced information technologies, Frontiers is catapulting scholarly publishing into a new generation.

What are Frontiers Research Topics?

Frontiers Research Topics are very popular trademarks of the Frontiers Journals Series: they are collections of at least ten articles, all centered on a particular subject. With their unique mix of varied contributions from Original Research to Review Articles, Frontiers Research Topics unify the most influential researchers, the latest key findings and historical advances in a hot research area! Find out more on how to host your own Frontiers Research Topic or contribute to one as an author by contacting the Frontiers Editorial Office: frontiersin.org/about/contact

SEPSIS: BASIC, CLINICAL AND THERAPEUTIC APPROACHES

Topic Editors:
Hong Zhou, Zunyi Medical University, China
Yan Kang, Sichuan University, China
Lefu Lan, Chinese Academy of Sciences (CAS), China
Daolin Tang, University of Texas Southwestern Medical Center, United States

Citation: Zhou, H., Kang, Y., Lan, L., Tang, D., eds. (2023). Sepsis: Basic, Clinical and Therapeutic Approaches. Lausanne: Frontiers Media SA.
doi: 10.3389/978-2-88976-307-8

Table of Contents

frontiers | Frontiers in Pharmacology

EDITORIAL
published: 11 May 2022
doi: 10.3389/fphar.2022.910332

Editorial: Sepsis: Basic, Clinical and Therapeutic Approaches

Yan Kang[1,2], *Daolin Tang*[3], *Lefu Lan*[4] *and Hong Zhou*[5]*

[1]Department of Critical Care Medicine, Institute of Critical Care Medicine, West China Hospital, Sichuan University, Chengdu, China, [2]West China Tianfu Hospital, Sichuan Universities, Chengdu, China, [3]Department of Surgery, UT Southwestern Medical Center, Dallas, TX, United States, [4]Shanghai Institute of Materia Medica, Chinese Academy of Sciences, Pudong Zhangjiang Hi-Tech Park, Shanghai, China, [5]Key Laboratory of Basic Pharmacology of Ministry of Education and Joint International Research Laboratory of Ethnomedicine of Ministry of Education, Zunyi Medical University, Zunyi, China

Keywords: sepsis, immune disorder, drugs, drug target, re-evaluation

Editorial on the Research Topic

Sepsis: Basic, Clinical and Therapeutic Approaches

Sepsis is a life-threatening organ dysfunction that affects millions of people globally; between one in six and one in three sepsis patients die each year (Evans et al., 2021). Its pathogenesis is complex and involves multiple systems and organs, and it requires comprehensive management. In particular, the immune system plays a core role through an early cytokine storm and late immunosuppression. However, no specific drug can effectively balance the uncontrolled immune reaction associated with sepsis (Evans et al., 2021). The Research Topic of this editorial focuses the development of new drugs and drug targets to combat sepsis. We believe that the research papers described below provide a new direction for investigations into drugs for the treatment of sepsis.

Autophagy is a conserved cellular biological process that plays an important role in maintaining the immune response, and is considered a new target for sepsis treatment (Ren et al., 2017). Liu et al. have described the role of transcription factor EB (TFEB) in the autophagy-lysosomal pathway. They found that some TFEB activators upregulated the mRNA expression of TFEB and, thereby, led to the activation of autophagy-lysosomal pathway (ALP) and promotion of the cellular clearance machinery.

Pathogen-associated molecular patterns, such as endotoxin/lipopolysaccharide (LPS), are important molecules associated with sepsis (van der Poll, et al., 2021). Qiao et al. demonstrated that capsaicin protects cardiomyocytes against LPS-induced damage via augmentation of 14-3-3γ-mediated autophagy. In the realm of herbal drugs, Wang et al. reported the effect of Xuebijing (XBJ), which is an add-on treatment that has been used for sepsis management for over 15 years in China. XBJ specifically targets sepsis-induced myocardial dysfunction, and it was found to significantly improve the survival of cecal ligation and puncture (CLP)-induced sepsis model mice by alleviating cardiac dysfunction. Its therapeutic effect was thought to be mediated by the combined action of its components paeoniflorin and hydroxysafflor yellow A.

Exosomes are vesicles derived from double invagination of the plasma membrane and are closely associated with immune responses. The cargos delivered by exosomes into recipient cells, especially immune cells, effectively alter their response and functions in sepsis (Murao et al., 2020). Qiu et al. investigated the effects and mechanisms of exosomes of multiple immune cells and the role of immune cell-derived exosomes in sepsis and provided an in-depth understanding of the mechanism of immune dysfunction in sepsis. Additionally, Murao et al. showed that exosomes transport cold-inducible RNA-binding protein (CIRP) from the intracellular to extracellular space in LPS- and CLP-induced sepsis mouse models. Thus, targeting exosome-mediated CIRP release may be a potential strategy for sepsis treatment.

Sepsis is often accompanied by metabolic disorders such as stress hyperglycemia, which damages host immune response and increases the risk of organ damage (Ali et al., 2008). Accordingly, the levels of endogenous glucagon-like peptide-1 (GLP-1) are tightly associated with the mortality of sepsis patients (Donnelly, 2012). In addition, Yang et al. reviewed the possible application of GLP-1 receptor agonists

OPEN ACCESS

Edited and reviewed by:
Salvatore Salomone,
University of Catania, Italy

***Correspondence:**
Hong Zhou
zhouh64@163.com

Specialty section:
This article was submitted to Experimental Pharmacology and Drug Discovery, a section of the journal Frontiers in Pharmacology

Received: *01 April 2022*
Accepted: *20 April 2022*
Published: *11 May 2022*

Citation:
Kang Y, Tang D, Lan L and Zhou H (2022) Editorial: Sepsis: Basic, Clinical and Therapeutic Approaches. Front. Pharmacol. 13:910332. doi: 10.3389/fphar.2022.910332

(GLP-1RAs), a new drug in diabetes treatment, for the treatment of sepsis. They suggested that GLP-1RAs not only regulated blood glucose homeostasis but also improved organ dysfunction, regulated immunity, and controlled inflammation and other functions (such as renal function) in sepsis. Their study provides a new perspective treatment for sepsis patients with stress hyperglycemia.

Epigenetic regulation plays an important role in the pathogenesis of sepsis (Falcão-Holanda et al., 2021). The epigenetic changes in sepsis include DNA methylation, histone modifications, and regulation of transcription via non-coding RNAs (Zhang et al., 2019). The bromodomain and extra-terminal (BET) protein family, an epigenetic regulator of gene transcription, has recently been recognized as a significant regulator of inflammation and immune response in sepsis. Wang et al. opined that BETs not only function as scaffolds to recruit different transcription factors and transcription elongation complexes, but also serve as switches to initiate gene transcription machinery in response to the interaction of BDs with acetylated chromatin either at gene promoters or in long-range cis regulatory elements. This mini-review summarizes the emerging roles and applications of BETs in sepsis.

Since 2019, the COVID-19 pandemic has been a threat to public health and killed millions of people worldwide (Alhazzani et al., 2021). In the early days of COVID-19, anti-pro-inflammatory cytokine antibodies were considered a promising treatment based on the observation that the over-release of pro-inflammatory cytokines was the cause of cytokine storms during COVID-19 (Schultze and Aschenbrenner, 2021). Accordingly, the systematic review by Wang et al. showed that the anti-cytokine antibodies tocilizumab, sarilumab, and anakinra could reduce mortality in patients with COVID-19; in particular, tocilizumab was not significantly associated with any serious adverse events or secondary infections. Further, Yuan et al. have also reviewed the potential of immune-related therapy in COVID-19 treatment and shed light on the current status of and advances in immune-related therapy for COVID-19 worldwide. In contrast to the promising effect of anti-cytokine therapy in COVID-19 treatment, in sepsis treatment, many clinical studies have found that antibodies have no therapeutic effect and may even increase mortality (Alhazzani et al., 2021). Thus, the use of anti-cytokine antibodies in the treatment of sepsis is controversial.

Treating sepsis with a combination of vitamins (such as vitamin C and vitamin D) and probiotics is currently an area of great interest. Kamel et al. demonstrated that both combinations of interventions, vitamin C plus vitamin B1 and vitamin D plus oral Lactobacillus probiotics, improved APACHE II scores and reduced sepsis incidence in trauma patients. Further, in their randomized, double-blinded, controlled clinical trial, severe trauma patients were stratified by leukocyte anti-sedimentation rate (LAR) into high-risk and low-risk groups for sepsis, and LAR combined with injury severity score was found to be a good predictor of sepsis.

In summary, the articles described here report on novel targets in immunotherapy and new therapeutic approaches in sepsis treatment. However, more research is required on new drug targets based on the pathophysiological mechanism of sepsis and re-evaluation of the data on existing drugs in clinical trials.

AUTHOR CONTRIBUTIONS

HZ, YK, DT, and LL drafted the manuscript. HZ, YK, DT, and LL revised, edited, and provided their final approval. All authors listed contributed to the work and approved it for publication.

ACKNOWLEDGMENTS

We thank the authors, editors, and reviewers who contributed to this Research Topic.

REFERENCES

Alhazzani, W., Evans, L., Alshamsi, F., Møller, M. H., Ostermann, M., Prescott, H. C., et al. (2021). Surviving Sepsis Campaign Guidelines on the Management of Adults with Coronavirus Disease 2019 (COVID-19) in the ICU: First Update. *Crit. Care Med.* 49 (3), e219–e234. doi:10.1097/CCM.0000000000004899

Ali, N. A., O'Brien, J. M., Jr, Dungan, K., Phillips, G., Marsh, C. B., Lemeshow, S., et al. (2008). Glucose Variability and Mortality in Patients with Sepsis. *Crit. Care Med.* 36, 2316–2321. doi:10.1097/ccm.0b013e3181810378

Donnelly, D. (2012). The Structure and Function of the Glucagon-like Peptide-1 Receptor and its Ligands. *Br. J. Pharmacol.* 166, 27–41. doi:10.1111/j.1476-5381.2011.01687.x

Evans, L., Rhodes, A., Alhazzani, W., Antonelli, M., Coopersmith, C. M., French, C., et al. (2021). Surviving Sepsis Campaign: International Guidelines for Management of Sepsis and Septic Shock 2021. *Crit. Care Med.* 49, e1063–e1143. doi:10.1097/CCM.0000000000005337

Falcão-Holanda, R. B., Brunialti, M. K. C., Jasiulionis, M. G., and Salomão, R. (2021). Epigenetic Regulation in Sepsis, Role in Pathophysiology and Therapeutic Perspective. *Front. Med. (Lausanne)* 8, 685333. doi:10.3389/fmed.2021.685333

Murao, A., Brenner, M., Aziz, M., and Wang, P. (2020). Exosomes in Sepsis. *Front. Immunol.* 11, 2140. doi:10.3389/fimmu.2020.02140

Ren, C., Zhang, H., Wu, T. T., and Yao, Y. M. (2017). Autophagy: A Potential Therapeutic Target for Reversing Sepsis-Induced Immunosuppression. *Front. Immunol.* 8, 1832. doi:10.3389/fimmu.2017.01832

Schultze, J. L., and Aschenbrenner, A. C. (2021). COVID-19 and the Human Innate Immune System. *Cell* 184, 1671–1692. doi:10.1016/j.cell.2021.02.029

van der Poll, T., Shankar-Hari, M., and Wiersinga, W. J. (2021). The Immunology of Sepsis. *Immunity* 54, 2450–2464. doi:10.1016/j.immuni.2021.10.012

Zhang, D., Tang, Z., Huang, H., Zhou, G., Cui, C., Weng, Y., et al. (2019). Metabolic Regulation of Gene Expression by Histone Lactylation. *Nature* 574, 575–580. doi:10.1038/s41586-019-1678-1

Conflict of Interest: The authors declare that the research was conducted in the absence of any commercial or financial relationships that could be construed as a potential conflict of interest.

frontiers in Pharmacology

REVIEW
published: 26 January 2021
doi: 10.3389/fphar.2020.609212

Potential of Immune-Related Therapy in COVID-19

Chunjue Yuan[1†], *Ruoyun Li*[1†], *Guohong Liu*[2*] *and Yunbao Pan*[1*]

[1]Department of Laboratory Medicine, Zhongnan Hospital of Wuhan University, Wuhan University, Wuhan, China, [2]Department of Radiology, Zhongnan Hospital of Wuhan University, Wuhan University, Wuhan, China

At the beginning of 2020, a sudden outbreak of new coronavirus, severe acute respiratory syndrome coronavirus 2 (SARS-CoV-2), infections led to anxiety, panic, and crisis among people worldwide. The outbreak first occurred in Wuhan, China, in late December 2019 and then spread rapidly across the globe, thus becoming a major public health emergency. Although the current epidemic situation in China tends to be stable, coronavirus disease 2019 (COVID-19) continues to spread globally. At present, no specific therapeutic drugs and vaccines are available against COVID-19. Also, the pathogenesis of the SARS-CoV-2 is not fully clear. Human immunity is important in SARS-CoV-2 infection. Studies have shown that excessive inflammation caused by SARS-CoV-2 infection and subsequent induced uncontrolled cytokine storm are the main causes of disease deterioration and death of severe patients. Therefore, immune-related research is of great significance for the prevention, control, and prognosis of COVID-19. This study aimed to review the latest research on immune-related treatment of COVID-19.

Keywords: SARS-CoV-2, COVID-19, vaccine, cytokine storm, convalescent plasma, mesenchymal stem cell

OPEN ACCESS

Edited by:
Yan Kang,
Sichuan University, China

Reviewed by:
Karthik Babu Mallilankaraman,
National University of Singapore, Singapore
Abdallah El-Sayed Allam,
Tanta University, Egypt

***Correspondence:**
Guohong Liu
liuguoh@outlook.com
Yunbao Pan
panyunbao@outlook.com

†These authors have contributed equally to this work and share first authorship

Specialty section:
This article was submitted to Translational Pharmacology, a section of the journal Frontiers in Pharmacology

Received: *22 September 2020*
Accepted: *17 December 2020*
Published: *26 January 2021*

Citation:
Yuan C, Li R, Liu G and Pan Y (2021) Potential of Immune-Related Therapy in COVID-19. Front. Pharmacol. 11:609212. doi: 10.3389/fphar.2020.609212

INTRODUCTION

In late December 2019, several patients with pneumonia of unknown etiology were detected in Wuhan, China. They were diagnosed with viral pneumonia, and the pathogen was subsequently isolated from patient samples. Electron microscopy showed that the pathogen presented a typical coronavirus morphology and was different from the coronavirus found in the past, which attracted great attention from the Chinese Center for Disease Control and Prevention, and an emergency response was urgently initiated. The viral genome sequence was first published on January 11, 2020, and confirmed as a completely new coronavirus named 2019 new coronavirus (nCoV) through sequence analysis and etiological studies (Zhu N et al., 2020). On February 11, 2020, the International Committee on Taxonomy of Viruses officially named the new coronavirus (2019-nCoV) severe acute respiratory syndrome coronavirus 2 (SARS-CoV-2) considering the phylogeny and taxonomy of the virus (Gorbalenya et al., 2020). On the same day, the World Health Organization announced that the disease caused by this virus was called coronavirus disease 2019 (COVID-19) (WHO, 2020a). Although most patients are mild to moderate and have a good prognosis, the mortality rate of critically ill patients is high. Therefore, cellular immunity and neutralizing antibodies are important in protection against infection with SARS-CoV-2. Anti-SARS-CoV-2 vaccines must induce strong cellular immunity and a high titer of neutralizing antibodies to fully protect vaccinated individuals. As for the lethal process of neocoronavirus infection, a hyperinflammatory syndrome known as secondary hemophagocytic lymphohistiocytosis (sHLH) appeared among part of COVID-19 patients because of cytokine storm, eventually leading to multiorgan failure (Mehta et al., 2020; Ruan et al., 2020); thus, finding solutions to prevent and reverse cytokine storm is also the key to the

rescue of severe COVID-19 patients (Huang et al., 2020). Since the outbreak of the epidemic, scientific researchers from all walks of life have devoted themselves to exploring a potential treatment for COVID-19. A management algorithm, which correlated the clinical features with laboratory and imaging findings, has been established for more appropriate diagnostic and therapeutic strategies (Galluccio et al., 2020). And current potential antiviral therapies are divided mainly into two aspects based on their action targets: 1) directly targeting the SARS-CoV-2 and 2) modulating immune cells or system. This study summarized mainly the research progress of potential treatment related to immunity.

TREATMENT AGAINST COVID-19

Up to August 10, 2020, more than 19.71 million people were diagnosed with COVID-19, leading to 720,000 deaths. As a safe and effective antiviral treatment against this epidemic is urgently needed, a series of studies are ongoing, including prevention and therapies.

Preventive Vaccines

Historic experience has proven that vaccines are the best way to prevent infectious diseases, but qualified vaccines need to undergo extensive trials to ensure their safety and effectiveness. A preclinical animal model test is required after the vaccine is developed, and a clinical trial can be declared only when the safety and effectiveness are ensured. Among these, the primary aim of phase I clinical evaluation is to explore the safety of the vaccine; the main purpose of phase II clinical evaluation is to report the efficacy and general safety information of the vaccine in the target population; and the purpose of phase III clinical evaluation is to comprehensively evaluate the protective effect and safety of the vaccine, which requires 1–4 years. Hundreds to thousands of volunteers were followed up for these assessments. Vaccine development against COVID-19 mainly focuses on viral vector, nucleic acid, and inactivated and recombinant proteins at present.

Viral Vector Vaccine

Adenovirus Recombinant New Corona Vaccine

After developing the Ebola vaccine with adenoviral vectors previously, the Academy of Military Medical Sciences and Tianjin CanSino Biological Inc. have rapidly developed a recombinant new coronavirus vaccine (Ad5-nCoV) with adenoviral vectors. Its safety and effectiveness have been verified in animal-related tests. On March 16, 2020, it became the first vaccine against the SARS-CoV-2 to enter the clinical trial in China (ChiCTR2000030906/NCT04313127). The vaccine carries spike (S) protein using modified human adenovirus type 5 (Ad5), leading to the neocoronavirus invasion (Chen Y et al., 2020). The immune system recognizes the virus antigen and develops an immune memory of S protein after the Ad5 vaccine injection. When attacked by the SARS-CoV-2, the memory immune system immediately recognizes and produces corresponding antibodies, thus achieving viral eradication. The 108 volunteers vaccinated in the phase I trial were mainly permanent residents of Wuhan and aged between 18 and 60 years. These volunteers were regularly followed up to determine whether adverse reactions occurred and whether anti-S protein-specific antibodies were produced *in vivo*. So far, 108 vaccinated volunteers have been in good health, and the overall progress of the phase I trial has been smooth. The phase II clinical trial of the Ad5-nCoV, which aimed at evaluating the immunogenicity and safety of the vaccine, was carried out in Wuhan among 508 volunteers with a broader age range on April 12 (ChiCTR2000031781/NCT04341389). Further, 250 participants aged more than 18 years were supposed to be in the middle-dose vaccine group, and 125 were in the low-dose and placebo groups, respectively. Immunogenicity was tested on days 0, 14, and 28 and 6 months after vaccination without hospitalization. The results of another clinical trial consisting of 696 participants (NCT04398147), conducted by CanSino with the Canadian partner, will also be revealed in December 2021. The global phase III clinical trial of the Ad5-nCoV, manufactured by CanSino and Beijing Institute of Biotechnology, started recruiting 40,000 volunteers of healthy adults aged 18 years old and above (NCT04526990). However, some risks are involved. If the human body has been previously infected with adenovirus type 5, it will produce its relevant antibodies, which will attack the vector rather than express the S protein if vaccinated with the recombinant vaccine, thereby rendering the vaccine ineffective (Zhu F-C et al., 2020; Shi et al., 2020).

AZD1222

The adenovirus vector vaccine AZD1222 (formerly known as ChAdOx1 nCoV-19) developed by AstraZeneca United Kingdom and Oxford University under the "Warp Speed" program is currently undergoing phase I/II clinical trials (NCT04324606) in the United Kingdom and phase III clinical trials in Brazil and South Africa. In phase I/II clinical trials (n = 1077, with an average age of 35 years) between April 23 and May 21, 543 participants were injected with AZD1222 and the other 534 received the meningococcal conjugate vaccine. Transformed from attenuated adenovirus, this replicator-defective chimpanzee virus vector carries a transgene that encodes the S protein of novel coronavirus. Patients will produce the S proteins after vaccination, thus triggering the immune system to produce antibodies against the virus. The results of phase I/II support the ongoing phase III clinical trial on a larger scale, as they have certified safety and immunogenicity of AZD1222, indicating its potential role in obstructing the pandemic of COVID-19 (Folegatti et al., 2020).

Nucleic Acid Vaccine

mRNA Vaccine

BNT162. BNT162, BioNTech's novel coronavirus vaccine candidate, went into clinical trials in late April and then entered overseas clinical trials in cooperation with Pfizer and Fosun Pharma. BNT162 includes four vaccine candidates: BNT162a1, BNT162b1, BNT162b2, and BNT162c2. On July 1, Pfizer posted on medRxiv about the positive results of phase I and part of phase II clinical trials of BNT162b1, which is the first

published clinical trial based on an mRNA vaccine technology. BNT162b2, one of the promising candidates for COVID-19, is a full-length S protein mRNA granted fast-track status by the Food and Drug Administration recently. It has been proved in phase I/II trials to induce T cells for better recognition of S epitopes, thus contributing to immune responses in older adults (NCT04380701) (Mulligan et al., 2020). The phase III clinical trial, in approximately 150 sites in six countries including 39 US states, has proved the safety and efficacy of BNT162b2 up to 95%. Revealed data demonstrated its good tolerance across all populations with 43,611 enrolled participants, and less older vaccinated people were reported with milder adverse events, which is consistent with an earlier study (Polack et al., 2020). Companies are planning to submit to the FDA for emergency use authorization (EUA) and share data with other regulatory agencies worldwide.

mRNA-1273

The phase I clinical trial of mRNA vaccine mRNA-1273, developed by the National Institutes of Health and Moderna, was officially launched on March 16 (NCT04283461). A total of 120 healthy volunteers, aged between 18 and 55 years, were recruited within 6 weeks to assess the safety and immunogenicity of mRNA-1273 (Laura and Johnson, 2020). This dominant vaccine also targets the S protein of the SARS-CoV-2. The S protein, which encodes the SARS-CoV-2, is delivered by lipid nanoparticles (LNPs) and regulated by mRNA, activating an immune response and thus curtailing the invasion of new coronavirus. In the phase I study, participants injected with mRNA-1273 twice developed robust neutralizing antibodies, whose neutralizing activity against SARS-COV-2 was reserved after 42 days. ModernaTX, Inc. started phase II trials on May 29, 2020, among 600 volunteers with doses of 50 mcg (NCT04405076), while phase III trials are supposed to recruit 30,000 healthy adults from 89 clinical trial spots throughout the United States. Volunteers will be randomly assigned to either a test group or a control group with a 100 μg dose of mRNA-1273 vaccine or a placebo saline injection, followed by a second dose 28 days later (NCT04470427). Compared with traditional vaccines, this vaccine is superior in a short development cycle, with no viral activity and good safety, and is expected to be used for COVID-19 prevention (Anderson et al., 2020).

DNA VACCINE

New Coronavirus Candidate DNA Vaccine INO-4800

On April 6, 2020, INO-4800, developed by INOVIO Pharmaceuticals, became the first new coronavirus candidate DNA vaccine to enter clinical trials. DNA vaccines insert specific antigen genes into eukaryotic expression vectors, directly injected or encapsulated by liposomes into the body, and their corresponding antigen proteins are expressed in the cells, inducing specific humoral and cellular immune responses, thus activating the body's immune system to achieve COVID-19 prevention. In phase I clinical studies during April (NCT04336410), INO-4800 has shown a robust neutralizing antibody and T-cell immune response to the virus in 40 enrolled participants aged 18–50 years; its phase I/II clinical effectiveness studies will also be performed by the Korean group in the summer of 2020 (NCT04447781) (Trevor et al., 2020).

GX-19

Genexine led the research on GX-19 on March 13, 2020, which was the first COVID-19 DNA vaccine with Korean FDA approval for phase I/IIa clinical trials (NCT04445389). It entered clinical trials on June 17; 60 healthy volunteers were injected in a two-dose trial during phase I. The trial was supposed to finish in 3 months. Later in September, phase IIa clinical trials among 150 participants (including placebos) were started to assess the safety and efficacy of GX-19, and the estimated completion date will be March 17, 2021 (Ye et al., 2020).

Inactivated Vaccine

PiCoVacc Vaccine

PiCoVacc vaccine, a polyvalent vaccine prepared by inactivating and purifying the virus using β-propiolactone, induces SARS-COV-2-specific neutralizing antibodies in mice, rats, and nonhuman primates as proposed by Qin et al., broadening a possible neutralization capability for the virus circulating globally (Gao et al., 2020). A majority of antigens and epitopes of the virus aim at conserved epitopes, thus reducing virus escape. Sinovac Biotech Co. has enrolled 144 volunteers aged 18–59 years for phase I and 600 for phase II (NCT04352608).

Recombinant Protein Vaccines

Pathogen-specific protein genes are inserted into appropriate expression systems via genetic engineering after recognizing their immunogenicity (such as *E. coli* yeast microbes). Proteins are cultivated on a large scale *in vitro* and further purified to become vaccines. Recombinant protein vaccines account for the majority of resistance to COVID-19 to date (nearly up to 42%), targeting the S protein of this virus.

NVX-CoV2373

Based on the gene sequence of COVID-19 (GenBank accession number, MN908947; nucleotides 21563–25384), Novavax generated an S protein antigen of this novel virus via its recombinant nanoparticle technology. Coupled with a unique saponin-based Matrix-M adjuvant, NVX-CoV2373 stimulates antigen presentation in local lymph nodes, enhancing the immune response and high levels of neutralizing antibodies. In preclinical trials, NVX-CoV2373 blocks the combination between S proteins and virus-targeted receptors. Clinical trials in phase I of NVX-CoV2373 recruited 131 participants aged 18–59 years (NCT04368988) to confirm its safety and immunogenicity and people aged 60–84 years are in need of expanding participant range in phase II trials up to 40 sites across Australia and/or the United States. This phase I/II trial is supposed to be complete on November 18, 2021 (Keech et al., 2020).

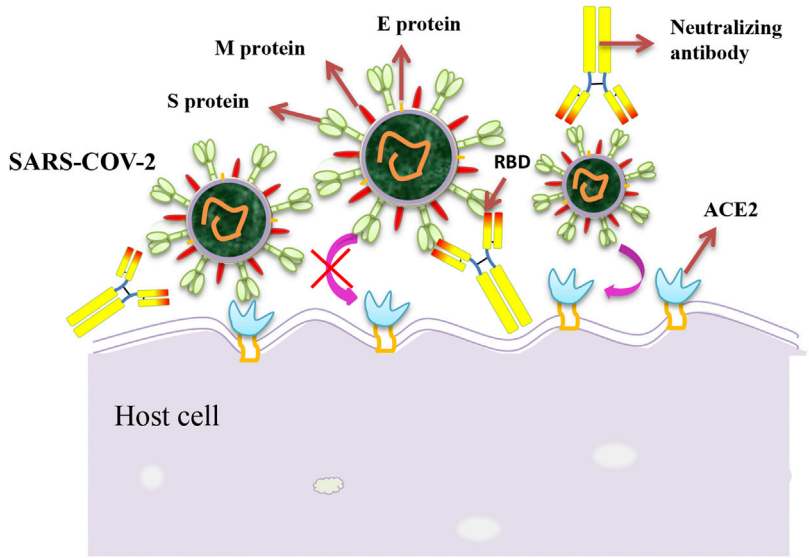

FIGURE 1 | Schematic diagram of the neutralization mechanism of the SARS-CoV-2. The interaction between spike proteins and cell receptors is necessary for membrane fusion and target cell entry. Monoclonal antibodies against the SARS-CoV-2 spike protein may inhibit the binding of the virus to its cellular receptor, thereby preventing the virus from entering the cell.

Therapeutic Options

Corticosteroids in COVID-19

Studies have shown that critically ill COVID-19 patients can develop a systemic inflammatory response, and uncontrolled cytokine storm caused by SARS-CoV-2 infection subsequently leads to lung injury, multisystem organ dysfunction, and eventually death. Corticosteroid, a potent anti-inflammatory, antifibrotic, and vasoconstrictive drug, has been previously applied in many other pulmonary infections to alleviate the condition of patients (Bozzette et al., 1990; Stockman et al., 2006; Rodrigo et al., 2013). Recently, a retrospective cohort study in China also revealed a potential mortality benefit of corticosteroids in COVID-19 (Chaomin et al., 2020), providing new clues on therapeutic approaches to novel coronavirus.

A number of studies on corticosteroids' role in SARS-CoV-2 infection have been carried out (Halpin et al., 2020; Peters et al., 2020). In the United Kingdom, a large open-label randomized trial recruited 6425 hospitalized patients with COVID-19. 2104 patients were treated with a 10-day course of dexamethasone (6 mg/d [oral or intravenous]) while the others received the standard of care, and mortality at 28 days showed the superiority in dexamethasone group (Horby et al., 2020). Meanwhile, Peter Horby et al. offered alternative options including prednisone 40 mg, methylprednisolone 32 mg, and hydrocortisone 160 mg (the total daily dose equivalencies to dexamethasone 6 mg). The World Health Organization (WHO) also performed a meta-analysis based on data from seven randomized clinical trials of corticosteroids in severe COVID-19 patients (PROSPERO CRD42020197242) (Sterne et al., 2020) and found that corticosteroids could reduce the risk of death in COVID-19 cases by 20%. WHO then issued living guidance for the use of corticosteroids in severe COVID-19 cases on September 2 (WHO, 2020b).

Though promising results were reported, putting corticosteroids into clinical use widely has been controversial (Bozzette et al., 1990; Stockman et al., 2006; Rodrigo et al., 2013, Prescott and Rice, 2020; Sanders et al., 2020). It is critical to weigh the potential benefits of corticosteroids against much potential harm associated with these drugs and clinicians should pay close attention to COVID-19 patients who are receiving corticosteroids for adverse effects and risk of reactivation of latent infections.

Convalescent Plasma Therapy

On the evening of February 13, Zhang Dingyu, president of Wuhan Jinyintan Hospital, publicly appealed for plasma donation from patients who recovered from new coronary pneumonia, as neutralizing antibodies in the plasma of recovered patients might help suffering patients (Wang Y et al., 2020). Thus, a clinical trial of convalescent plasma transfusion therapy was conducted on five severe patients by the team of Shenzhen Third People's Hospital (Shen et al., 2020); the patients included two women and three men aged 36–65 years. Applied plasma came from another five convalescent patients during their 10–22 days of hospitalization. The progression of COVID-19 enhanced rapidly after antiviral treatment because the viral load level was continuously high, thus leading to acute respiratory distress syndrome (ARDS). Specific antibody immunoglobulin G (IgG) in convalescent plasma bound to the SARS-CoV-2 with an antibody titer higher than 1:1000 and a neutralizing antibody titer greater than 40. The body temperature returned to normal within 3 days and the arterial partial pressure of oxygen/oxygen uptake concentration (PaO2/FiO2) increased within 12 days,

while the sequential organ failure assessment score decreased. The viral load also decreased to negative within 12 days with an increasing level of new coronavirus-specific antibody. The results suggested that the antibodies in the convalescent plasma might clear the virus and improve patient symptoms. The impact of the timing of plasma transfusion is not clear enough due to the small sample size and lack of a control group. Therefore, these observations remain to be evaluated in clinical trials.

Plasma therapy, also known as sclerotherapy, is the treatment of patients with corresponding diseases using the plasma, serum, or immunoglobulin from cured patients, which still has a large number of antibodies shortly after recovery. As a result, patients with the same disease can obtain passive immunity instantly through the input of exogenous antibodies. The safety, effectiveness, and applicability of this therapy have been controversial for a while. However, sclerotherapy is still new hope for the clinical treatment of the new coronavirus infection, considering previous research on SARS and the severe situation of the COVID-19 pandemic (Mair-Jenkins et al., 2015).

Monoclonal Antibody Therapy

The essence of plasma therapy is antibody therapy. The convalescent plasma of COVID-19 contains various antibodies that can be used to treat antibody-insufficient patients. China has pioneered in treating clinically critical patients using plasma therapy; preliminary clinical trials have shown improved symptoms in many patients. However, plasma therapy is still associated with many uncertainties, such as a limited source of therapeutic plasma and impurities in plasma that may cause safety risks. Relatively speaking, antibody drugs with single ingredients and precise doses are safer and more effective compared with plasma. Among these, monoclonal antibody drugs are the most commonly used. The mechanisms of monoclonal antibody therapy are mainly going to the following four pathways to block the virus from entering the cell: 1) the neutralizing antibody that binds to the S protein on the surface of the virus particle and blocks the binding between the S protein and ACE2; 2) neutralizing antibody that directly binds to ACE2 protein to block the combination of the virus and its receptor; 3) ACE2 analog that competitively binds to S protein on the surface of virus particles with ACE2; 4) antibody against cytokine storm. Apart from combining with the virus, the monoclonal antibody can prevent cytokine storm, which is one of the mortalities for a host of severe COVID-19 patients. Inhibiting interleukin-6 (IL-6), whose secretion leads to an overactive immune response, improves the treatment of severe COVID-19 patients by avoiding cytokine release syndrome (CRS) (Moore and June, 2020). Genentech started to recruit 330 severe COVID-19 patients from April in phase III clinical trial of Tocilizumab (NCT04320615), which is an inhibitor of IL-6. Regeneron Inc. also announced to enroll 400 patients in a clinical II/III trial with Sanofi, treating severe COVID-19 patients with another IL-6 inhibitor, Kevzara (NCT04359901).

CR3022

A previous study found that the receptor-binding domain (RBD) of the SARS-CoV-2 and SARS-CoV had a high similarity (73%) (Lu et al., 2020). Both of them could infect host cells by binding to the receptor angiotensin-converting enzyme II (ACE2). Another study on SARS-CoV revealed that the S protein on the surface of the viral envelope bound to the receptor ACE2 on host cells, thus mediating the adsorption and invasion of viruses (Gallagher and Buchmeier, 2001; Shanmugaraj et al., 2020). Monoclonal antibodies against SARS-CoV may also be involved in SARS-CoV-2 prevention, considering the similarity between the RBD structures of the SARS-CoV-2 and SARS-CoV (**Figure 1**). Ying Tianlei et al. expressed and purified several specific SARS-CoV antibodies with strong neutralizing activity, including m396 (Zhu et al., 2007), CR3014 (ter Meulen et al., 2004), CR3022 (ter Meulen et al., 2006), and specific human monoclonal antibody m336 for coronavirus of Middle East Respiratory Syndrome (MERS) (Ying et al., 2015). The RBD of SARS-CoV was determined by enzyme-linked immunosorbent assay (ELISA), showing that most SARS-CoV-specific antibodies did not bind to the SARS-CoV-2 RBD obviously except for CR3022, and its binding epitope on the SARS-CoV-2 RBD did not overlap with that of ACE2. This finding indicated that CR3022 had great potential for the prevention and treatment of SARS-CoV-2 infection. The study, which was published online on the preprint platform bioRxiv under the title "Potent binding of 2019 novel coronavirus spike protein by a SARS coronavirus-specific human monoclonal antibody," first reported that the SARS-CoV-specific human monoclonal antibody CR3022 could effectively bind to the SARS-CoV-2 RBD (Tian et al., 2020).

CD147

On March 14, 2020, a research paper titled "SARS-CoV-2 invades host cells via a novel route: CD147-spike protein" published on the preprint platform bioRxiv by a research team from the Fourth Military Medical University revealed a novel way for SARS-CoV-2 invasion: CD147-S protein (SP) (Wang K et al., 2020). CD147, also known as Basigin or EMMPRIN, is a transmembrane glycoprotein in the immunoglobulin superfamily (Cui et al., 2018). Previous studies showed that CD147 promoted the invasion of SARS-CoV into host cells while CD147 antagonistic peptide-9 inhibited SARS-CoV (Chen et al., 2017). Therefore, the research team investigated the possible role of CD147 in the invasion by novel coronaviruses based on the similarities between SARS-CoV and SARS-CoV-2, and the results confirmed their hypothesis. *In vitro* antiviral tests proved that mepolizumab, a humanized antibody against CD147, could significantly inhibit viral invasion (EC50 was 24.86 μg/ml; IC50 was 15.16 μg/ml) via immunoprecipitation and ELISA. Furthermore, the team used immunoelectron microscopy to observe the localization of CD147 and S proteins in SARS-CoV-2-infected Vero E6 cells (Wang K et al., 2020). All these findings suggested that CD147 might be a key target for specific anti-SARS-CoV-2 drugs.

A clinical trial was conducted by the team subsequently (NCT04275245) to investigate the efficacy and safety of mepolizumab against COVID-19. The enrolled volunteers were divided into two groups. The mepolizumab group was comprised of 17 patients with COVID-19 (4 normal, 6 severe, and 7 critical), while the control group was comprised of 11

TABLE 1 | General overview of potential immune-related therapies.

Related therapies			Outline	Research status
Preventive vaccine	Viral vector vaccine	Ad5-nCoV (Adenovirus Recombinant New Corona Vaccine)	Modified human adenovirus type 5 (Ad5) serves as a vector to carry S protein Chen Y et al. (2020), which mediates the invasion of target cells by the new coronavirus and enables the human body to produce immune memory of S protein	Phase I and phase II trials overall progress smoothly; the phase III clinical trial is being conducted
		AZD1222 (ChAdOx1 nCoV-19)	Transformed from attenuated adenovirus, this replicator-defective chimpanzee virus vector carries a transgene that encodes the S protein of novel coronavirus. Patients after vaccination produce antibodies against the virus	Phase I and phase II trials are completed; the phase III clinical trial is being conducted
	mRNA vaccine	BNT162	This is a full-length spike protein mRNA used to induce T cells for better recognition of spikes' epitopes	Positive results of phase I and part of phase II clinical trials of BNT162b1 are published; a global phase II/III clinical trial has been finished with an efficacy up to 95%
		mRNA-1273	Using lipid nanoparticles (LNPs) as carriers, prefusion of the spike protein stabilizing the SARS-CoV-2 was delivered into the human body to promote human immune response Anderson et al. (2020)	A phase I clinical trial (NCT04283461) was officially launched on March 16 to assess the safety and immunogenicity of mRNA-1273 Laura and Johnson (2020). The phase II and (NCT04405076) III clinical trials (NCT04470427) are being conducted
	DNA vaccine	INO-4800	Insertion of specific protein antigen genes into eukaryotic expression vectors, direct injection, or liposome encapsulation into the body induces specific humoral and cellular immune responses, thereby activating the body's immune system	INOVIO is the first new coronavirus DNA vaccine to enter clinical trials. Once the safety and immunogenicity data related to the phase I clinical study are available (NCT04336410), INOVIO will promote the phase I/II clinical effectiveness study as soon as possible (NCT04447781)
		GX-19		It entered clinical trials on June 19; phase IIa clinical trials among 150 participants (including placebos) will be started to assess the safety and efficacy of GX-19
	Inactivated vaccine	PiCoVacc	A majority of antigens and epitopes of the virus are aimed at conserved epitopes, thus reducing virus escape and broadening a possible neutralization capability for the virus circulating globally Gao et al. (2020)	It is the first published inactivated COVID-19 vaccine preclinically; phase I and phase II clinical trials are being conducted
	Recombinant protein vaccine	NVX-CoV2373	Coupled with the unique saponin-based Matrix-M adjuvant, NVX-CoV2373 stimulates antigen presentation in local lymph nodes, enhancing the immune response and high levels of neutralizing antibody. In preclinical trials, NVX-CoV2373 blocks the combination between spike proteins and virus-targeted receptors	Phase I trials are completed; phase I/II clinical trial is being conducted

(Continued on following page)

TABLE 1 | (*Continued*) General overview of potential immune-related therapies.

Related therapies			Outline	Research status
Therapeutic options	Corticosteroids		Corticosteroid, a potent anti-inflammatory, antifibrotic, and vasoconstrictive drug, has been previously applied in many other pulmonary infections to alleviate the condition of patients. It is also potential to be applied in approaches to COVID-19	A large open-label randomized trial recruited 6425 hospitalized patients with COVID-19 carried out in the United Kingdom, and mortality at 28 days showed the superiority in the dexamethasone group. The World Health Organization (WHO) also performed a meta-analysis (PROSPERO CRD42020197242) and then issued living guidance for the use of corticosteroids in severe COVID-19 cases on September 2 WHO (2020b)
	Convalescent plasma therapy		The plasma, serum, or immunoglobulin of convalescent patients with COVID-19 was extracted, and the passive immunity was obtained through the input of the external antibody, to kill the virus or pathogen *in vivo* and achieve the purpose of treating patients	The results showed that the antibodies in the plasma of the convalescent patients may help eliminate the virus and improve the symptoms of patients Shen et al. (2020). However, the sample size of this test is small, no control group is used, and the impact of the timing of plasma infusion is not clear. Therefore, these observations need to be evaluated in clinical trials
	Monoclonal antibody therapy	CR3022	Given the similarity between the RBD structures of the SARS-CoV-2 and SARS-CoV Lu et al. (2020), the research team purified several specific antibodies with strong neutralizing activity and targeting the SARS-CoV's RBD to study their binding to RBD of SARS-CoV ter Meulen et al. (2004), ter Meulen et al. (2006), Zhu et al. (2007), Ying et al. (2015)	CR3022 has a strong binding ability, indicating that it has great potential to be developed for the prevention and treatment of 2019-nCoV infection Tian et al. (2020)
		CD147	SP can bind to the receptor CD147 on host cells and thus mediate virus invasion Chen et al. (2017), Wang K et al. (2020). CD147 may be a key target for the development of specific anti-SARS-CoV-2 drugs	The results of the clinical trial (NCT 04275245) showed that the anti-CD147 humanized antibody mepolizumab could significantly inhibit the invasion of the virus into host cells Bian et al. (2020). Because the sample size of this study is small, and it is not a randomized controlled trial, the anti-COVID-19 ability of mepolizumab cannot be confirmed at present. A larger clinical trial is needed to verify the efficacy of mepolizumab further
		47D11	The immunofluorescence method detected the direct effect of 47D11 on the SARS virus and SARS-COV-2. Neutralizing antibodies can alter the course of infection in the host, thereby enhancing virus clearance or protecting an uninfected host exposed to the virus	Wang et al. tried 51 kinds of neutralizing antibodies against SARS hybridoma and picked out 47D11 antibody for its effectiveness against both viruses to determine whether an effective antibody existed against novel coronavirus, indicating its potential to prevent and treat COVID-19 and possibly also prevent other diseases in humans in the future Wang C et al. (2020)
		B38 and H4	Some neutralizing antibodies are potential virus-targeting monoclonal antibodies to avoid immune escape. The binding sites of B38 and ACE2 in receptor-binding domain (RBD) on the virus surface overlap, while H4 binds to other sites, indicating that this pair of antibodies can be used together clinically	On June 12, B38 and H4 isolated in a convalescent patient with coronavirus disease 2019 (COVID-19) were reported to block the combination between receptor-binding domain (RBD) and angiotensin-converting enzyme 2 (ACE2), meaning that they might be involved in virus prevention Wu et al. (2020)
		LY-CoV555	LY-CoV555, a lead anti-spike neutralizing monoclonal antibody affinitive to SARS-CoV-2, was obtained from a Covid-19 patient. It was developed by Eli Lilly after AbCellera's discovering	Phase I study of hospitalized COVID-19 patients (NCT04411628) has been completed and a long-term follow-up is ongoing. Phase II clinical trial (NCT04427501) showed that 2800 mg dose of LY-CoV555 tended to accelerate the viral decline by day 11. Phase III started in early August and stopped on October 13 considering its safety concern. On November 10, the FDA announced an EUA for LY-CoV555

(Continued on following page)

TABLE 1 | (*Continued*) General overview of potential immune-related therapies.

Related therapies		Outline	Research status
Therapeutic options	IVIG combined with low-molecular-weight heparin anticoagulation therapy	Clinical detection found that the number of peripheral blood lymphocytes in severe patients decreased significantly, while the level of inflammatory cytokines and D-dimer increased significantly Huang et al. (2020), Wang D. et al. (2020). The research team suggested that early IVIG combined with low-molecular-weight heparin anticoagulation therapy could effectively improve the immune function of patients and inhibit the occurrence of the cytokine storm Lin et al. (2020)	A randomized controlled clinical trial has been started (NCT 04261426)
	Mesenchymal stem cell therapy	It is expected that the prevention and reversal of the cytokine storm will become the key to rescuing severe patients with COVID-19 because of its strong anti-inflammatory and immune-regulatory effects, an improvement in the microenvironment, and promotion of the endogenous repair of the host Hashmi et al. (2016), Huang et al. (2020), Zhou et al. (2020)	It was found that mesenchymal stem cell therapy improved the prognosis of severe and critical patients rapidly and significantly, avoided cytokine storm effectively, and had no obvious side effects, thus providing new hope for the treatment of severe and critical patients with COVID-19 Leng et al. (2020)

hospitalized patients (4 normal, 4 severe, and 3 critical). The baseline characteristics of the two groups were basically balanced. The results were published later on March 24 (Bian et al., 2020). The overall improvement rate, defined as the proportion of patients discharged or with improved severity of illness, significantly improved in the mepolizumab group during the 7-, 14-, 21-, and 28-day follow-ups. The mepolizumab group also showed superiority in discharge and case severity of severe and critical patients compared with the control group. The negative rate and time of viral nucleic acid detection indicated virus clearance, which was significantly shorter (3 days) in the mepolizumab group compared with the control group (13 days). All these data suggested that mepolizumab treatment had a clear benefit in clearing the SARS-CoV-2. Also, the proportion of patients in the mepolizumab group whose lymphocyte counts and C-reactive protein concentrations returned to normal also increased significantly and rapidly. In terms of safety, patients treated with mepolizumab showed no adverse effects. CD147 is also a receptor for the ligand Cyclophilin A (CyPA), and their interaction is critical for inducing inflammation and chemotaxis (Dawar et al., 2017). Accordingly, it was speculated that mepolizumab could also block the interaction between CyPA and CD147, thereby inhibiting the inflammatory response caused by SARS-CoV-2 infection. The anti-COVID-19 ability of mepolizumab cannot be determined at present due to the limited sample size and the nonrandomized nature of the trial. Therefore, large-scale clinical trials are urgently needed to verify the efficacy of mepolizumab.

47D11

Both the SARS virus and SARS-COV-2 bind to their receptor ACE2 protein in the S1B domain, which is also the common target of antiviral drug investigations. Wang et al. tried 51 kinds of neutralizing antibodies against SARS hybridoma and examined the 47D11 antibody for its effectiveness against both viruses to determine whether an effective antibody existed against novel coronavirus. For further characterization, they recombined 47D11 into the human IgG1 homologous antibody. The immunofluorescence method detected the direct effect of 47D11 on the SARS virus and SARS-COV-2, while the MERS virus was used for negative comparisons. Neutralizing antibodies can alter the course of infection in the host, thereby enhancing virus clearance or protecting an uninfected host exposed to the virus. Thus, 47D11 has the potential to prevent and treat COVID-19 and possibly also prevent other diseases in the future (Wang C et al., 2020).

B38 and H4

Some neutralizing antibodies are potential virus-targeting monoclonal antibodies to avoid immune escape. On June 12, B38 and H4 isolated in a convalescent patient with COVID-19 were reported to block the combination between RBD and ACE2, indicating that they might be involved in virus prevention (Wu et al., 2020). Besides, the binding sites of B38

and ACE2 overlapped on RBD while H4 did not, indicating that this pair of antibodies could be used together clinically.

Narsoplimab

High concentrations of the SARS-CoV-2 prompt the local inflammatory environment and activate the lectin pathway of complement. Hence, patients tend to have endothelial injury and activation during the exudative phase of viral infection, thus leading to a life-threatening ARDS. Narsoplimab, a high-affinity fully human immunoglobulin gamma 4 (IgG4), has been reported to block the lectin pathway by binding to mannan-binding lectin-associated serine protease-2 (MASP-2), which binds to COVID-19 N protein in disease progression. The inhibition of MASP-2, which is located upstream in the lectin pathway, does not cause any difference in an adaptive immune response as the lytic arm of the classical pathway still exists. The results revealed by Alessandro Rambaldi et al. provided a novel sight into COVID-19 immunological therapy via complement inhibition (Rambaldi et al., 2020).

LY-CoV555

LY-CoV555 (also known as LY3819253), used to be an effective anti-spike neutralizing monoclonal antibody for SARS-CoV-2, was isolated from a blood sample of an early novel coronavirus patient in the United States. The antibody against novel coronavirus spike protein can prevent the attachment and entrance of the virus and is expected to prevent its infection, which also provides another treatment approach for COVID-19. Eli Lilly has completed a phase I study of hospitalized COVID-19 patients (NCT04411628) and a long-term follow-up is ongoing. In the interim analysis of phase II clinical trial (NCT04427501), the 2800 mg dose of LY-CoV555 showed efficacy in viral clearance by day 11 (Chen P et al., 2020). Phase III started in early August to evaluate the safety and efficacy of the developed neutralizing antibody (Lilly, 2020). After the 5-day treatment among 326 participants, the trial was suspended as the difference, which existed between the antibody-treated group and the placebo-treated group, exceeded a predetermined threshold for security. On November 10, the FDA announced a EUA for LY-CoV555 to treat patients aged 12 years and older weighing at least 40 kg who are at high risk of progressing to severe COVID-19 and it was administered as a one-time treatment with intravenous fluids, which provided a new way to prevent novel coronavirus from causing severe symptoms and even death in patients (Chen P et al., 2020).

Intravenous Human Immunoglobulin Combined With Low-Molecular-Weight Heparin Anticoagulation Therapy

The treatment mechanism of COVID-19, as a new infectious disease, is still unclear. Cao et al. proposed a reasonable hypothesis on the potential pathogenesis of COVID-19 based on theoretical research and clinical observation and divided the disease progression into three stages: viremia stage, acute stage (pneumonia stage), and convalescent stage (Lin et al., 2020). Viruses enter the lungs and peripheral blood through the mucosa and respiratory tract. If the patient has a good immune function and no other basic diseases, the body can kill the virus quickly and enter the recovery period. If the patient is immunocompromised or damaged and has basic diseases such as diabetes and hypertension, the human immune system cannot eliminate the virus and cause aggravation of the disease. The clinical tests revealed that the number of peripheral blood lymphocytes significantly reduced in severe patients, while the levels of inflammatory cytokines and D-dimer significantly increased. Close to 20% of patients with COVID-19 had abnormal coagulation function, and almost all severe and critically ill patients had coagulation disorders (Chen N et al., 2020; Huang et al., 2020; Wang D et al., 2020). Based on the aforementioned hypotheses and clinical observations on the underlying pathogenesis, the research team suggested that early intravenous human immunoglobulin (IVIG) combined with low-molecular-weight heparin anticoagulation therapy effectively improved the immune function of patients and inhibited the occurrence of the cytokine storm. That is, patients with COVID-19 were immediately treated with adequate doses of IVIG [0.3–0.5 g/(kg · d) for 5 days] and low-molecular-weight heparin anticoagulation when the number of peripheral blood lymphocytes significantly reduced, the levels of inflammatory cytokines (such as interleukin 6) significantly increased, and coagulation D-dimer levels were four times higher than the upper limit of normal. Also, the laboratory indicators were closely monitored for the side effects after anticoagulation treatment (Lin et al., 2020).

IVIG is a blood product extracted from the plasma of healthy people through a series of complex biotechnologies and administered via intravenous injection. Its main components are broad-spectrum antiviral and bacterial IgG antibodies. After intravenous infusion, the IgG antibodies in the blood of the recipients can be rapidly increased to effectively identify and neutralize pathogens, prevent excessive immunity, maintain immune homeostasis, and cause other effects. A randomized controlled clinical trial on the use of IVIG in treating severe SARS-CoV-2 infection has been initiated (NCT04261426). Despite the excellent efficacy of IVIG in treating influenza (Liu et al., 2016) and SARS (Ho et al., 2004), a large amount of clinical trial data from patients with COVID-19 remain the key to supporting this therapy.

Mesenchymal Stem Cell Therapy

Mesenchymal stem cells (MSCs) are characterized by strong anti-inflammatory and immune-regulatory activities, improving the microenvironment of the body and promoting the endogenous repair of the host. The safety and efficacy of MSC therapy have been demonstrated in many clinical trials, especially in immune-mediated inflammatory diseases, such as graft-versus-host disease (Hashmi et al., 2016) and systemic lupus erythematosus (Zhou et al., 2020). Given the strong immune-regulatory capacity of MSCs, the team recruited seven patients with COVID-19 for MSC transplantation to explore the potential of MSCs to treat patients with COVID-19 by observing the changes in immune and inflammatory system functions and the occurrence of side effects within 14 days after transplantation (Leng et al., 2020). MSC transplantation

therapy could rapidly and significantly improve the prognosis of severe and critical patients and effectively avoid the cytokine storm, without obvious side effects. This study provided new ideas and hope for treating severe and critical patients with COVID-19, besides hormone therapy and anti-inflammatory therapy.

CONCLUSION

In summary, this study was elaborated on the potential immune-related therapies from specific prevention to the prognosis of severe patients (**Table 1**). These therapies have initially achieved promising results. However, scientific, rigorous preclinical studies and clinical trials are needed to ensure the efficacy and safety of these therapies before they are widely used in treating COVID-19. Research on COVID-19 is still underway globally, and it is believed that the SARS-CoV-2 will be eradicated shortly.

AUTHOR CONTRIBUTIONS

YP and GL conceived the study, reviewed and helped to draft the manuscript. CY and RL drafted the manuscript.

REFERENCES

Anderson, E. J., Rouphael, N. G., Widge, A. T., Jackson, L. A., Roberts, P. C., Makhene, M., et al. (2020). Safety and immunogenicity of SARS-CoV-2 mRNA-1273 vaccine in older adults. *N. Engl. J. Med.*, 383 (25), 2427–2438. doi:10.1056/NEJMoa2028436

Bian, H. J., Zheng, Z.-H., Wei, D., Zhang, Z., Kang, W.-Z., Hao, C.-Q., et al. (2020). Meplazumab treats COVID-19 pneumonia: an open-labelled, concurrent controlled add-on clinical trial. medRxiv. doi:10.1101/2020.03.21.20040691

Bozzette, S., Sattler, F. R., Chiu, J., Wu, A. W., Gluckstein, D., Kemper, C., et al. (1990). A controlled trial of early adjunctive treatment with corticosteroids for Pneumocystis carini pneumonia in the acquired immunodeficiency syndrome. California Collaborative Treatment Group. *N. Engl. J. Med.* 323 (21), 1451–1457. doi:10.1056/NEJM199011223232104

Chaomin, W., Xiaoyan, C., Yanping, C., Jia'an, X., Xing, Z., Sha, X., et al. (2020). Risk factors associated with acute respiratory distress syndrome and death in patients with coronavirus disease 2019 pneumonia in Wuhan, China. *JAMA Intern. Med.* 180 (7), 934–943. doi:10.1001/jamainternmed.2020.0994

Chen, J., Xia, S., Yang, X., Chen, H., Li, F., Liu, F., et al. (2017). Human cytomegalovirus encoded miR-US25-1-5p attenuates CD147/EMMPRIN-mediated early antiviral response. *Viruses* 9 (12), 365. doi:10.3390/v9120365

Chen, N., Zhou, M., Dong, X., Qu, J., Gong, F., Han, Y., et al. (2020). Epidemiological and clinical characteristics of 99 cases of 2019 novel coronavirus pneumonia in Wuhan, China: a descriptive study. *Lancet* 395 (10223), 507–513. doi:10.1016/S0140-6736(20)30211-7

Chen, P., Nirula, A., Heller, B., Gottlieb, R. L., Boscia, J., Morris, J., et al. (2020). SARS-CoV-2 Neutralizing Antibody LY-CoV555 in Outpatients with Covid-19. *N. Engl. J. Med.* [Epub ahead of print]. doi:10.1056/NEJMoa2029849

Chen, Y., Liu, Q., and Guo, D. (2020). Emerging coronaviruses: genome structure, replication, and pathogenesis. *J. Med. Virol.* 92 (4), 418–423. doi:10.1002/jmv.25681

Cui, J., Huang, W., Wu, B., Jin, J., Jing, L., Shi, W. P., et al. (2018). N-glycosylation by N-acetylglucosaminyltransferase V enhances the interaction of CD147/basigin with integrin beta1 and promotes HCC metastasis. *J. Pathol.* 245 (1), 41–52. doi:10.1002/path.5054

Dawar, F. U., Wu, J., Zhao, L., Khattak, M. N., Mei, J., and Lin, L. (2017). Updates in understanding the role of cyclophilin A in leukocyte chemotaxis. *J. Leukoc. Biol.* 101 (4), 823–826. doi:10.1189/jlb.3RU1116-477R

Folegatti, P. M., Ewer, K. J., Aley, P. K., Angus, B., Becker, S., Belij-Rammerstorfer, S., et al. (2020). Safety and immunogenicity of the ChAdOx1 nCoV-19 vaccine against SARS-CoV-2: a preliminary report of a phase 1/2, single-blind, randomised controlled trial. *Lancet* 396 (10249), 467–478. doi:10.1016/S0140-6736(20)31604-4

Gallagher, T. M., and Buchmeier, M. J. (2001). Coronavirus spike proteins in viral entry and pathogenesis. *Virology* 279 (2), 371–374. doi:10.1006/viro.2000.0757

Galluccio, F., Ergonenc, T., Garcia Martos, A., Allam, A. E.-S., Pérez-Herrero, M., Aguilar, R., et al. (2020). Treatment algorithm for COVID-19: a multidisciplinary point of view. *Clin. Rheumatol.* 39 (7), 2077–2084. doi:10.1007/s10067-020-05179-0

Gao, Q., Bao, L., Mao, H., Wang, L., Xu, K., Yang, M., et al. (2020). Development of an inactivated vaccine candidate for SARS-CoV-2. *Science* 369 (6499), eabc1932. doi:10.1126/science.abc1932

Gorbalenya, A. E., Baker, S. C., Baric, R. S., de Groot, R. J., Drosten, C., Gulyaeva, A. A., et al. (2020). Severe acute respiratory syndrome-related coronavirus: the species and its viruses – a statement of the Coronavirus Study Group. bioRxiv. doi:10.1101/2020.02.07.937862

Halpin, D. M. G., Singh, D., and Hadfield, R. M. (2020). Inhaled corticosteroids and COVID-19: a systematic review and clinical perspective. *Eur. Respir. J.* 55 (5), 2001009. doi:10.1183/13993003.01009-2020

Hashmi, S., Ahmed, M., Murad, M. H., Litzow, M. R., Adams, R. H., Ball, L. M., et al. (2016). Survival after mesenchymal stromal cell therapy in steroid-refractory acute graft-versus-host disease: systematic review and meta-analysis. *Lancet Haematol.* 3 (1), e45–e52. doi:10.1016/S2352-3026(15)00224-0

Ho, J. C., Wu, A. Y., Lam, B., Ooi, G. C., Khong, P. L., Ho, P. L., et al. (2004). Pentaglobin in steroid-resistant severe acute respiratory syndrome. *Int. J. Tubercul. Lung Dis.* 8 (10), 1173–1179. doi:10.1080/01902140490489126

Horby, P., Lim, W. S., Emberson, J. R., Mafham, M., Bell, J. L., and Linsell, L. (2020). Dexamethasone in hospitalized patients with Covid-19 – preliminary report. *N. Engl. J. Med.* [Epub ahead of print]. doi:10.1056/NEJMoa2021436

Huang, C., Wang, Y., Li, X., Ren, L., Zhao, J., Hu, Y., et al. (2020). Clinical features of patients infected with 2019 novel coronavirus in Wuhan, China. *Lancet* 2020, 395(10223), 497–506. doi:10.1016/S0140-6736(20)30183-5

Keech, C., Albert, G., Cho, I., Robertson, A., Reed, P., Neal, S., et al. (2020). Phase 1–2 trial of a SARS-CoV-2 recombinant spike protein nanoparticle vaccine. *N. Engl. J. Med.* 383 (24), 2320–2332. doi:10.1056/NEJMoa2026920

Laura, N., and Johnson, C. K. (2020). *AP Exclusive: coronavirus vaccine test opens with 1st doses*. Durango, CO: The Gurango Herald.

Leng, Z., Zhu, R., Hou, W., Feng, Y., Yang, Y., Han, Q., et al. (2020). Transplantation of ACE2- mesenchymal stem cells improves the outcome of patients with COVID-19 pneumonia. *Aging Dis.* 11 (2), 216–228. doi:10.14336/AD.2020.0228

Lilly, E. (2020). *Lilly initiates phase 3 trial of LY-CoV555 for prevention of COVID-19 at long-term care facilities in partnership with the National Institute of Allergy and Infectious Diseases*. Indianapolis, IN: Eli Lilly and Company.

Lin, L., Lu, L., Cao, W., and Li, T. (2020). Hypothesis for potential pathogenesis of SARS-CoV-2 infection-a review of immune changes in patients with viral pneumonia. *Emerg. Microb. Infect.* 9 (1), 727–732. doi:10.1080/22221751.2020.1746199

Liu, Q., Zhou, Y. H., and Yang, Z. Q. (2016). The cytokine storm of severe influenza and development of immunomodulatory therapy. *Cell. Mol. Immunol.* 13 (1), 3–10. doi:10.1038/cmi.2015.74

Lu, R., Zhao, X., Li, J., Niu, P., Yang, B., Wu, H., et al. (2020). Genomic characterisation and epidemiology of 2019 novel coronavirus: implications for virus origins and receptor binding. *Lancet* 395 (10224), 565–574. doi:10.1016/S0140-6736(20)30251-8

Mair-Jenkins, J., Saavedra-Campos, M., Baillie, J. K., Cleary, P., Khaw, F. M., Lim, W. S., et al. (2015). The effectiveness of convalescent plasma and hyperimmune immunoglobulin for the treatment of severe acute respiratory infections of viral etiology: a systematic review and exploratory meta-analysis. *J. Infect. Dis.* 211 (1), 80–90. doi:10.1093/infdis/jiu396

Mehta, P., McAuley, D. F., Brown, M., Sanchez, E., Tattersall, R. S., Manson, J. J., et al. (2020). COVID-19: consider cytokine storm syndromes and immunosuppression. *Lancet* 395 (10229), 1033–1034. doi:10.1016/S0140-6736(20)30628-0

Moore, J. B., and June, C. H. (2020). Cytokine release syndrome in severe COVID-19. *Science* 368, 473–474. doi:10.1126/science.abb8925

Mulligan, M. J., Lyke, K. E., Kitchin, N., Absalon, J., Gurtman, A., Lockhart, S., et al. (2020). Phase I/II study of COVID-19 RNA vaccine BNT162b1 in adults. *Nature* 586 (7830), 589–593. doi:10.1038/s41586-020-2639-4

Peters, M. C., Sajuthi, S, Deford, P., Christenson, S., Rios, C. L., Montgomery, M. T., et al. (2020). COVID-19 related genes in sputum cells in asthma: relationship to demographic features and corticosteroids. *Am. J. Respir. Crit. Care Med.* 202 (1), 83–90. doi:10.1164/rccm.202003-0821OC

Polack, F. P., Thomas, S. J., Kitchin, N., Absalon, J., Gurtman, A., Lockhart, S., et al. (2020). Safety and efficacy of the BNT162b2 mRNA Covid-19 vaccine. *N. Engl. J. Med.* 383, 2603–2615. doi:10.1056/NEJMoa2034577

Prescott, H. C., and Rice, T. W. (2020). Corticosteroids in COVID-19 ARDS: evidence and hope during the pandemic. *JAMA* 324, 1292–1295. doi:10.1001/jama.2020.16747

Rambaldi, A., Gritti, G., Micò, M. C., Frigeni, M., Borleri, G., Salvi, A., et al. (2020). Endothelial injury and thrombotic microangiopathy in COVID-19: treatment with the lectin-pathway inhibitor narsoplimab. *Immunobiology* 225 (6), 152001. doi:10.1016/j.imbio.2020.152001

Rodrigo, C., Leonardi-Bee, J., Nguyen-Van-Tam, J., and Lim, W. S. (2013). *Corticosteroids as adjunctive therapy in the treatment of influenza*. New Jersey: John Wiley & Sons.

Ruan, Q., Yang, K., Wang, W., and Song, J., (2020). Clinical predictors of mortality due to COVID-19 based on an analysis of data of 150 patients from Wuhan, China. *Intensive Care Med.* 46, 846–848. doi:10.1007/s00134-020-05991-x

Sanders, J. M., Monogue, M. L., Jodlowski, T. Z., and Cutrell, J. B. (2020). Pharmacologic treatments for coronavirus disease 2019 (COVID-19) a review. *J. Am. Med. Assoc.* 323 (18), 1824–1836. doi:10.1001/jama.2020.6019

Shanmugaraj, B., Siriwattananon, K., Wangkanont, K., and Phoolcharoen, W. (2020). Perspectives on monoclonal antibody therapy as potential therapeutic intervention for Coronavirus disease-19 (COVID-19). *Asian Pac. J. Allergy Immunol.* 38 (1), 10–18. doi:10.12932/AP-200220-0773

Shen, C., Wang, Z., Zhao, F., Yang, Y., Li, J., Yuan, J., et al. (2020). Treatment of 5 critically Ill patients with COVID-19 with convalescent plasma. *J. Am. Med. Assoc.* 323 (16), 1582–1589. doi:10.1001/jama.2020.4783

Shi, Y., Wang, N., and Zou, Q. M. (2020). Progress and challenge of vaccine development against 2019 novel coronavirus (2019-nCoV). *Zhonghua Yu Fang Yi Xue Za Zhi* 54 (6), 614–619. doi:10.3760/cma.j.cn112150-20200317-00366

Sterne, J. A. C, Murthy, S., Diaz, J. V., Slutsky, A. S., Villar, J., Angus, D. C., et al. (2020). Association between administration of systemic corticosteroids and mortality among critically Ill patients with COVID-19: a meta-analysis. *J. Am. Med. Assoc.* 324 (13), 1330–1341. doi:10.1001/jama.2020.17023

Stockman, L. J., Bellamy, R., and Garner, P. (2006). SARS: systematic review of treatment effects. *PLoS Med.* 3 (9), e343. doi:10.1371/journal.pmed.0030343

ter Meulen, J., Bakker, A. B., van den Brink, E. N., Weverling, G. J., Martina, B. E., Haagmans, B. L., et al. (2004). Human monoclonal antibody as prophylaxis for SARS coronavirus infection in ferrets. *Lancet* 363 (9427), 2139–2141. doi:10.1016/S0140-6736(04)16506-9

ter Meulen, J., van den Brink, E. N., Poon, L. L., Marissen, W. E., Leung, C. S., Cox, F., et al. (2006). Human monoclonal antibody combination against SARS coronavirus: synergy and coverage of escape mutants. *PLoS Med.* 3 (7), e237. doi:10.1371/journal.pmed.0030237

Tian, X., Li, C., Huang, A., Xia, S., Lu, S., Shi, Z., et al. (2020). Potent binding of 2019 novel coronavirus spike protein by a SARS coronavirus-specific human monoclonal antibody. *Emerg. Microb. Infect.* 9 (1), 382–385. doi:10.1080/22221751.2020.1729069

Trevor, R. F. S., Patel, A., Ramos, S., Elwood, D., Zhu, X., Yan, J., et al. (2020). Immunogenicity of a DNA vaccine candidate for COVID-19. *Nat. Commun.* 11 (1), 2601. doi:10.1038/s41467-020-16505-0

Wang, C., Li, W., Drabek, D., Okba, N. M. A., and Bosch, B. J. (2020). A human monoclonal antibody blocking SARS-CoV-2 infection. *Nat. Commun.* 11 (1), 2251. doi:10.1038/s41467-020-16256-y

Wang, D., Hu, B., Hu, C., Zhu, F., Liu, X., Zhang, J., et al. (2020). Clinical characteristics of 138 hospitalized patients with 2019 novel coronavirus-infected Pneumonia in Wuhan, China. *J. Am. Med. Assoc.* 323 (11), 1061–1069. doi:10.1001/jama.2020.1585

Wang, K., Chen, W., Zhou, Y.-S., Lian, J.-Q., Zhang, Z., Du, P., et al. (2020). SARS-CoV-2 invades host cells via a novel route: CD147-spike protein. bioRxiv. doi:10.1101/2020.03.14.988345

Wang, Y., Huo, P., Dai, R., Lv, X., Yuan, S., Zhang, Y., et al. (2020). Convalescent plasma may be a possible treatment for COVID-19: a systematic review. *Int. Immunopharm.* 92, 1475–1483. doi:10.1002/jmv.25961

WHO (2020a). General's remarks at the media briefing on 2019-nCoV. Available at: https://www.who.int/director-general/speeches/detail/who-director-general-s-remarks-at-the-media-briefing-on-2019-ncov-on-11-february-2020 (Accessed February 11, 2020).

WHO (2020b). Corticosteroids for COVID-19. Available at: https://www.who.int/publications/i/item/WHO-2019-nCoV-Corticosteroids-2020.1 (Accessed September 2, 2020).

Wu, Y., Wang, F., Shen, C., Peng, W., Li, D., Zhao, C., et al. (2020). A noncompeting pair of human neutralizing antibodies block COVID-19 virus binding to its receptor ACE2. *Science* 368 (6496), 1274–1278. doi:10.1126/science.abc2241

Ye, T., Zhong, Z., García-Sastre, A., Schotsaert, M., and De Geest, B. G. (2020). Current status of COVID-19 (Pre)Clinical vaccine development. *Angew. Chem. Int. Ed.* 59 (43), 18885–18897. doi:10.1002/anie.202008319

Ying, T., Prabakaran, P., Du, L., Shi, W., Feng, Y., Wang, Y., et al. (2015). Junctional and allele-specific residues are critical for MERS-CoV neutralization by an exceptionally potent germline-like antibody. *Nat. Commun.* 6, 8223. doi:10.1038/ncomms9223

Zhou, T., Li, H. Y., Liao, C., Lin, W., and Lin, S. (2020). Clinical efficacy and safety of mesenchymal stem cells for systemic lupus erythematosus. *Stem Cell. Int.* 2020, 6518508. doi:10.1155/2020/6518508

Zhu, F.-C., Li, Y.-H., Guan, X.-H., Hou, L.-H., Wang, W.-J., Li, J.-X., et al. (2020). Safety, tolerability, and immunogenicity of a recombinant adenovirus type-5 vectored COVID-19 vaccine: a dose-escalation, open-label, non-randomised, first-in-human trial. *Lancet* 395 (10240), 1845–1854. doi:10.1016/S0140-6736(20)31208-3

Zhu, N., Zhang, D., Wang, W., Li, X., Yang, B., Song, J., et al. (2020). A novel coronavirus from patients with Pneumonia in China, 2019. *N. Engl. J. Med.* 382 (8), 727–733. doi:10.1056/NEJMoa2001017

Zhu, Z., Chakraborti, S., He, Y., Roberts, A., Sheahan, T., Xiao, X., et al. (2007). Potent cross-reactive neutralization of SARS coronavirus isolates by human monoclonal antibodies. *Proc. Natl. Acad. Sci. U.S.A.* 104 (29), 12123–12128. doi:10.1073/pnas.0701000104

Conflict of Interest: The authors declare that the research was conducted in the absence of any commercial or financial relationships that could be construed as a potential conflict of interest.

frontiers in Pharmacology

MINI REVIEW
published: 11 March 2021
doi: 10.3389/fphar.2021.642294

Pharmacological Modulation of BET Family in Sepsis

Nian Wang, Runliu Wu, Paul B. Comish, Rui Kang and Daolin Tang**

Department of Surgery, UT Southwestern Medical Center, Dallas, TX, United States

The Third International Consensus Definitions for Sepsis and Septic Shock (Sepsis 3.0) recommended defining sepsis as a life-threatening organ dysfunction caused by the host's uncontrolled response to infection. The bromodomain and extra-terminal (BET) protein family (such as BRD2, BRD3, and BRD4), an epigenetic regulator of gene transcription, has recently been recognized as a significant septic regulator of inflammation and immune response, including cytokine and chemokine production. Mechanistically, the two N-terminal conserved tandem bromodomains (namely the first bromodomain [BD1] and the second bromodomain [BD2]) favor the binding of BETs to acetylated histones or transcription factors, thereby initiating gene transcription machinery after CycT1 and CDK9 (also known as P-TEFb) are recruited to gene promoters to phosphorylate RNA pol II. Notably, BD1 and BD2 are not functionally redundant because they have different target genes in innate immune cells. Small-molecule BET inhibitors (BETis) for different BDs, such as I-BET, JQ1, I-BET151, apabetalone, RVX-297, and dBET1 have shown promising therapeutic effects in experimental sepsis models. This mini-review summarizes the emerging roles of BETs and the applications of BETis in sepsis, discusses the existing shortcomings of BETis, and introduces possible future research directions in this area.

Keywords: bromodomain and extra-terminal, inhibitor, innate immune, inflammation, sepsis

OPEN ACCESS

Edited by:
Abdur Rauf,
University of Swabi, Pakistan

Reviewed by:
Md. Sahab Uddin,
Southeast University, Bangladesh
Olesya Kharenko,
Zenith Epigenetics Ltd., Canada

****Correspondence:***
Rui Kang
rui.kang@utsouthwestern.edu
Daolin Tang
daolin.tang@utsouthwestern.edu

Specialty section:
This article was submitted to Experimental Pharmacology and Drug Discovery, a section of the journal Frontiers in Pharmacology

Received: *15 December 2020*
Accepted: *25 January 2021*
Published: *11 March 2021*

Citation:
Wang N, Wu R, Comish PB, Kang R and Tang D (2021) Pharmacological Modulation of BET Family in Sepsis. Front. Pharmacol. 12:642294. doi: 10.3389/fphar.2021.642294

INTRODUCTION

Sepsis is a medical condition driven by an unrestricted host response to infection and subsequent multiple organ dysfunction or failure (Singer et al., 2016). While bacterial infections are considered to be the most common causes of sepsis, other pathogen infections, such as fungus, virus, and parasite, also initiate sepsis (Dolin et al., 2019). Despite considerable medical advances in recent years, especially intensive care support and the application of antibiotics, the mortality rate of patients with sepsis remains high (>25%). Once patients develop septic shock with multiple organ dysfunction syndrome (MODS), the mortality rate can reach as high as 70% (Rudd et al., 2020). Thus, sepsis is still a big challenge in modern medicine.

The pathophysiology of sepsis is complex and involves multiple steps (Kang et al., 2018; Chen et al., 2019). Cytokine storm, a well-established mechanism for sepsis, results in uncontrolled inflammatory responses (Chousterman et al., 2017). However, antibody drugs targeting cytokines (e.g., tumor necrosis factor [TNF] and interleukin 6 [IL6]), inflammatory pathways (e.g., toll like receptor 4 [TLR4]), or endotoxin, as well as empiric antibiotic therapies have little or disappointing benefit for patients with sepsis (Chaudhry et al., 2013). Since the production of inflammation and immune response genes involved in sepsis is strictly controlled at the transcriptional, posttranscriptional, translational, and posttranslational levels, targeting these regulatory pathways may reasonably provide potential treatment strategies for sepsis (Carson et al., 2011; Vachharajani and McCall, 2019).

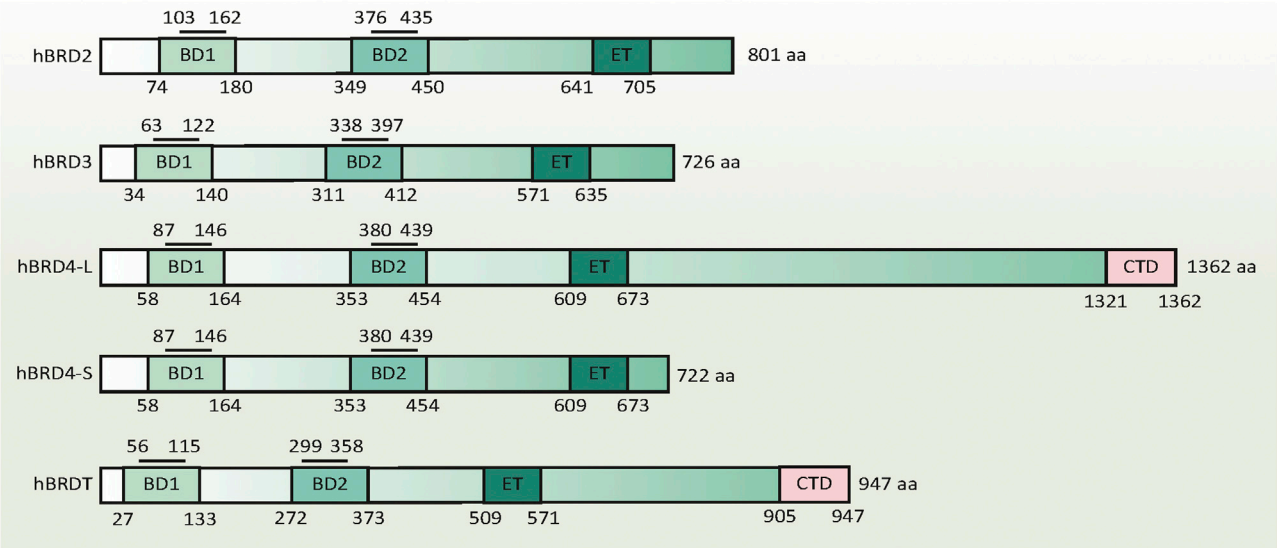

FIGURE 1 | Domain structure of human BET family proteins. The numbers below the columns indicate the amino acid boundaries of each domain in each BET. The numbers above the column indicate the amino acid boundaries of the acetyl-lysine binding sites in the BD1 and BD2 domains. The amino acid sequence alignment is based on published information, using the following accession numbers retrieved from the GenBank database: hBRD2, NM_005104; hBRD3, NM_007371.4; hBRD4-L, NM_058243; hBRD4-S, NM_014299; and hBRDT, NM_001242805. Abbreviations BD1, the first bromodomain; BD2, the second bromodomain; BRD, bromodomain protein (numbers 2-4); CTD, C-terminal domain; ET, extra-terminal domain

The epigenome describes all heritable chemical modifications added to DNA and histone proteins, which regulates the transcription of genes in the genome without affecting the DNA sequence (Zhang and Cao, 2019). The main epigenetic machinery includes DNA alterations (e.g., methylation and oxidation), histone modifications (e.g., acetylation, ubiquitination, phosphorylation, and methylation), and microRNA regulations (Topper et al., 2020). As a reversible chromatin modification, histone acetylation is affected by histone acetyltransferases (HATs, "epigenetic writer") and histone deacetylases (HDACs, "epigenetic eraser"). After acetylation, the acetylated lysine within the N-terminal tail protruding from the histone core of the nucleosome is recognized by the epigenetic reader and bound to their specific structural domains (e.g., bromodomain), leading to the activation of nuclear transcription factor and subsequent gene transcription (Peserico and Simone, 2011). Hence, epigenetic readers are molecular gatekeepers of gene expression and become promising drug targets of diseases.

Bromodomain is an evolutionarily conserved protein-protein interaction module, which comprises approximately 110 amino acids that recognize acetylated lysine residues within histones and other proteins. 61 bromodomain modules, including bromodomain and extra-terminal domain (BET) family (Filippakopoulos et al., 2012), have been identified in various species. The BET protein family, including BRD2, BRD3, BRD4, and BRDT, plays a complex role in coordinating innate immune responses through epigenetic regulation of gene transcription.

In this mini-review, we not only outline the structure and function of BET family in innate immunity (**Figure 1** and **Figure 2**), but also summarize the application of various BET inhibitors (BETis) in experimental models of sepsis (**Table 1**). These emerging knowledge may help to further develop novel anti-sepsis strategies.

CHARACTERISTICS OF BETS IN INNATE IMMUNITY

Expression of BETs

Normally, the expression of BRDT is restricted to the testis, while the expression of BRD2, BRD3, or BRD4 is commonly found in the nucleus of other cells (including immune cells). Under pathological conditions, the expression of BETs may be further changed (upregulation or downregulation) to meet the requirements for orchestrating a genetic regulatory response (Bachtel et al., 2019; Hong et al., 2020). In the case of sepsis, according to the type of pathogen infection, the expression of BRD2, BRD3 or BRD4 shows heterozygosity and diversity in immune cells. For example, BRD4 expression can be up-regulated, down-regulated or unchanged in activated macrophages or memory $CD4^+$ T cells during virus infection (Bachtel et al., 2019). The expression profile of the BETs may not be a good biomarker of sepsis, although they have functions in innate immunity (discussed later). While several miRNAs (e.g., miR-218-5p, miR-29a, and miRNA-302e) act as the posttranscriptional regulators of BRD4 expression (Lin et al., 2018; Li et al., 2019; Tang et al., 2019), the transcriptional regulatory mechanisms controlling the expression of BETs remain obscure.

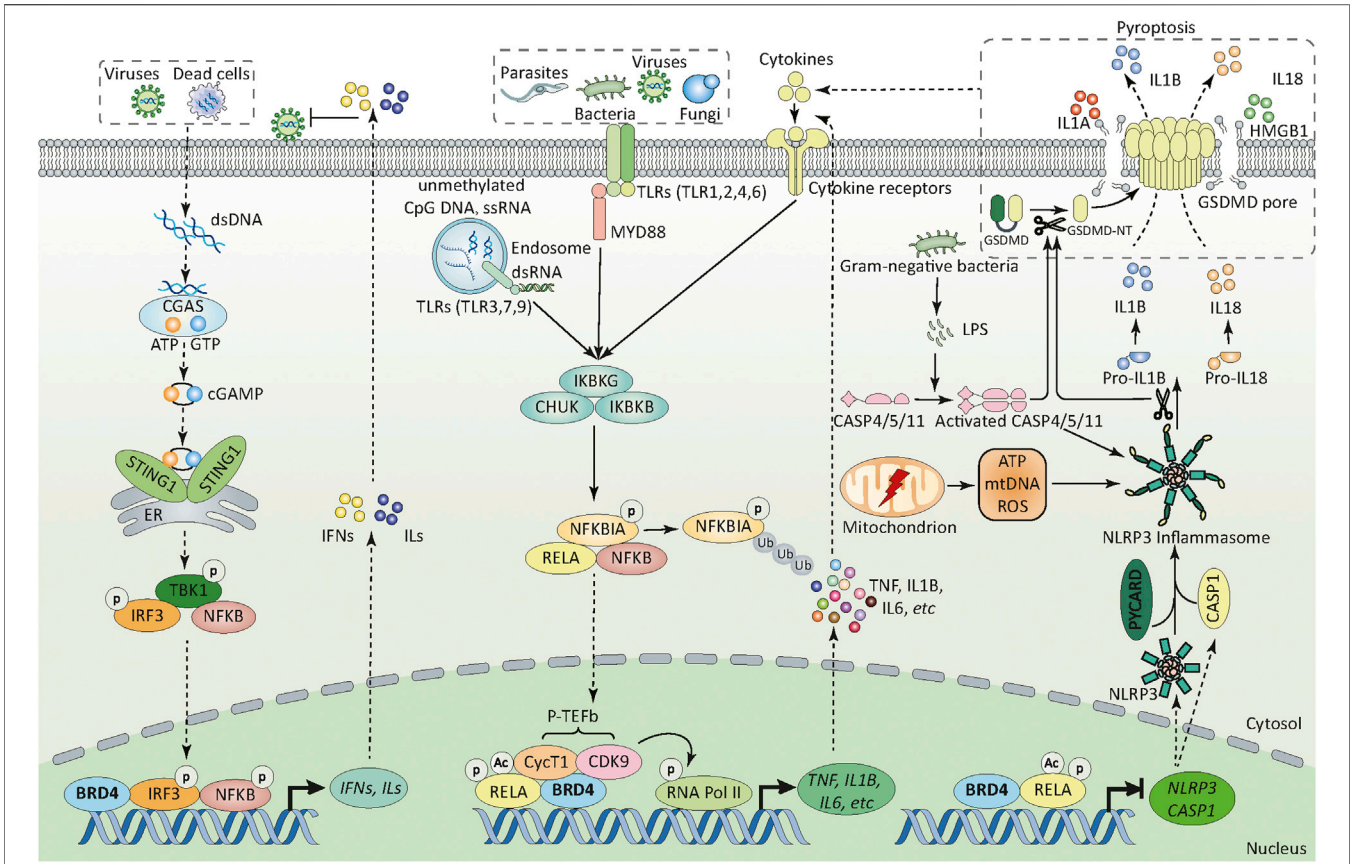

FIGURE 2 | BRD4 in innate immunity. BRD4 can sense and orchestrate different PRR-mediated innate immunity through transcriptional regulation. First, upon pathogen infection (e.g., bacteria, fungi, parasites, and viruses), BRD4 regulates the activation of different TLR-mediated NF-κB pathways through promoting the phosphorylation of RELA at Ser276 and its acetylation at Lys310. In addition, BRD4 recruits CycT1 and CDK9 (also known as P-TEFb) to the promoters of target genes which can phosphorylate RNA pol II at serine 2 and 5, thereby initiating gene transcriptional machinery. Second, BRD4 can promote or inhibit the activation of NLRP3 inflammasome pathway through transcriptional regulation of NRLP3 and CASP1 in a RELA-dependent manner. BRD4-mediated NLRP3 expression in innate immunity is context dependent. Third, cytoplasmic DNA derived from viruses and dead cells activates CGAS and produces endogenous cyclic dinucleotide cGAMP, which further binds to STING1 located in the endoplasmic reticulum, then induces the dimerization and translocation of STING1 from the ER to the perinuclear region. During trafficking, STING1 recruits and activates TBK1, stimulates the phosphorylation and nuclear translocation of IRF3, and to a lesser extent NFKB1, which leads to the production of type 1 IFN and other inflammatory cytokines (e.g., TNF and IL6).; Abbreviations: ATP, adenosine triphosphate; BRD4, bromodomain containing 4; CASP1, caspase 1; CASP4, caspase 4; CASP5, caspase 5; CASP11, caspase 11; CDK9, cyclin-dependent kinase 9; cGAMP, cyclic GMP-AMP; CGAS, cyclic GMP-AMP synthase; CHUK, component of inhibitor of nuclear factor kappa B kinase complex; CycT1, cyclin T1; dsDNA, double-stranded DNA; dsRNA, double-stranded RNA; ER, endoplasmic reticulum; HMGB1, high mobility group box 1, IFN, interferon; IKBKB, inhibitor of nuclear factor kappa B kinase regulatory subunit beta; IKBKG, inhibitor of nuclear factor kappa B kinase regulatory subunit gamma; ILs, interleukins; IL1A, interleukin 1 alpha; IL1B, interleukin 1 beta; IL18, interleukin 18; IL6, interleukin 6;IRF3, interferon regulatory factor 3; GSDMD, gasdermin D; GSDMD-NT, gasdermin D N-terminal domain; GTP, guanosine triphosphate; LPS, lipopolysaccharide; mtDNA, mitochondrial DNA; MYD88, myeloid differentiation primary response 88 (MYD88); NFKBIA, NFKB inhibitor alpha; NFKB1, nuclear factor kappa B subunit 1; NLRP3, NLR family pyrin domain containing 3; p-TEFb, positive transcription elongation factor b; PYCARD, PYD and CARD domain containing; RELA, RELA proto-oncogene; RNA pol II, RNA polymerase II; ROS, reactive oxygen species; ssRNA, single-stranded RNA; STING1, stimulator of interferon response cGAMP interactor 1; TBK1, TANK binding kinase 1; TLR, toll-like receptor (numbers 1-9); TNF, tumor necrosis factor.

Structure of BETs

Although the amino acid length of each BET is different, they have a similar protein secondary structure: two N-terminal conserved tandem bromodomains (namely the first bromodomain [BD1] and the second bromodomain [BD2]) and a unique C-terminal extraterminal (ET) domain. These BDs contain four alpha helices, which are separated by a variable loop region to form a central hydrophobic cavity. Acetylated lysine residues in histone tails and other proteins (e.g., RELA proto-oncogene [RELA] and tumor protein p53 [TP53]) are recognized through this central hydrophobic pocket by anchoring to a conserved asparagine residue (Filippakopoulos et al., 2012). Unlike other bromodomain proteins, BETs prefer to bind to diacetylated lysine residues with an optimal spacing of two amino acids (Kac-XX-Kac) closely located in the protein sequence. The acetyl-lysine binding sites in BD1 and BD2 containing 59 amino acids have unique binding selectivity and are not redundant in function (**Figure 1**). BD1 binds chromatin components, especially diacetylated residues on histone H4 (e.g., H4K5Ac, H4K8Ac, and H4K12Ac). BD2 accommodates a wide range of diacetylated residues and facilitates the recruitment of BETs to induce gene

TABLE 1 | BET inhibitors in sepsis.

Inhibitor	Target	IC50	Septic animal or cell model	Dose of BETi	Administration method	Target molecule and main action	Chemical structure	Ref
I-BET (GSK525762A)	BRD4 (BD1)	32.5–42.5 nM	Cecal ligation puncture (CLP)-treated mice	30 mg/kg	Intravenous injection (i.v.), twice daily for 2 days	Downregulation of IL6, IFNB1, IL1B, IL12A, CXCL9 and CCL12, *etc.*	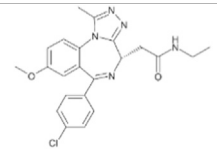	Nicodeme et al. (2010)
			Heat-killed Salmonella typhimurium (strain IR71, 5×10^9/kg, i.v.)-treated mice	30 mg/kg	i.v., twice daily for 2 days			
			LPS (5 mg/kg, intraperitoneal injection [i.p.])-treated mice	30 mg/kg	i.v., twice daily for 2 days			
			LPS (100 ng/ml)-induced mouse immortalized bone marrow-derived macrophages (iBMDMs)	5 μM	Pretreatment (at 30 min before LPS stimulation)			
(+)-JQ1	BRD2, BRD4 (BD1 and BD2)	77/33 nM (BD1 and BD2)	LPS (20 mg/kg, i.p.)-treated mice	50 mg/kg	i.p., at 2 h before and 24 h after LPS injection	Downregulation of IL6 and TNF	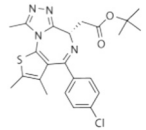	Belkina et al. (2013) Wienerroither et al. (2014)
			L. monocytogenes (strain LO28, multiplicity of infection [MOI] = 20)-infected mouse iBMDMs (4 h)	250 nM	Pretreatment (at 1 h before infection and left in the culture medium during infection	Downregulation of NOS2, IL6, IL1RN, TNF, SLAMF1, IRF8, MXD1, IL19, IFITM1, GBP2, IFNB, DUSP2, *etc.*		
			L. monocytogenes (strain LO28, MOI = 20)-infected mouse (24 h)	50 mg/kg	i.p.			
			LPS (100 ng/ml)-treated mouse primary astrocytes (24 h)	100 nM	Pretreatment (at 30 min before LPS stimulation)	Downregulation of SERPINE1		Choi et al. (2015))
I-BET151 (GSK1210151A)	BRD2, BRD3, and BRD4 (BD1 and BD2)	0.5 μM (BRD2), 0.25 μM (BRD3), and 0.79 μM (BRD4)	LPS (20 mg/kg, i.p.)-treated mice	10 mg/kg	i.v., at 60 min before or 90 min after LPS challenge	Downregulation of IL6	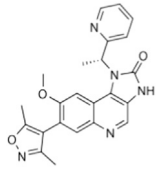	Seal et al. (2012)
Apabetalone (RVX-208 or RVX-000222)	BRD4 (BD2)	87 ± 10 μM (BD1); 0.51 ± 0.041 mM (BD2)	LPS (10 μg, i.p.)-induced endotoxemic mice	150 mg/kg	Gavage for 7 days	Downregulation of APCS, A2M, CD14, and CCR2	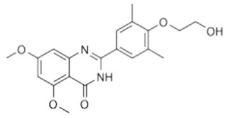	Wasiak et al. (2020)
RVX-297	BRD2 and BRD4 (BD2)	30 and 80 nM,	LPS (5 or 10 μg, i.p.)-induced endotoxemic mice	75 mg/kg	Gavage at 4 h before LPS stimulation and again when stimulated with LPS	Downregulation of IL6, IL17, CSF2, CCL2, IL2, TNF, and IFNG	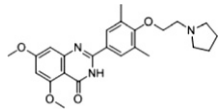	Jahagirdar et al. (2017)
			LPS (1 μg/ml)-induced mouse BMDMs (3 h)	10 μM	Combined treatment with LPS			
dBET1	BRD2 and BRD4	20 nM	LPS (10 ng/ml)-treated microglia (24 h)	1 μM	Pretreatment (at 1h before LPS stimulation)	Downregulation of NOS2, IL1B, TNF, CCL2, IL6, PTGS2, and MMP9	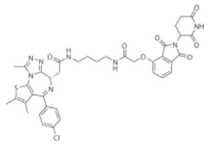	DeMars et al. (2018)

transcription, which is relatively more permissive (Moriniere et al., 2009; Gamsjaeger et al., 2011).

As for the C-terminal ET domain in each BET, they contain a helical architecture, including an acidic surface, shaped in a continuous ridge. Because the ET domain is responsible for the interaction between proteins, BETs act as scaffold proteins for the recruitment of transcription factors and coactivators. Other domains, such as motif B and Ser/Glu/Asp-rich region (SEED), are conserved in the C-terminal moiety of each BET, whereas the C-terminal domain (CTD) and motif A are not present in every BET (Florence and Faller, 2001). This may be the structural basis for distinguishing the functional differences of each BET. Intriguingly, since the regions in BETs are weakly reminiscent of kinase motifs, BETs exhibit intrinsic kinase activities, which may initiate gene transcription by directly phosphorylating RNA polymerase II (Pol II) at serine 2 and 5 (Denis et al., 2000; Devaiah et al., 2012). Notably, the kinase motifs of BETs lack homology with other known kinase domains. Given this, it is necessary to develop specific BETis targeting kinase activity in the future.

Function of BETs

BETs not only function as scaffolds to recruit different transcription factors (e.g., RELA, JUN, and MYC) and transcription elongation complexes (e.g., P-TEFb), but also serves as switches to initiate gene transcription machinery upon the interaction of BDs with acetylated chromatin either at gene promoters or in long range cis regulatory elements (namely "enhancers") (Filippakopoulos and Knapp, 2014). Consequently, BETs regulate the expression of various immune and inflammatory genes in innate immunity.

One of the key events of infection-related innate immunity is the recognition of evolutionary conserved structures on pathogens (namely pathogen-associated molecular patterns [PAMPs]) through different pattern recognition receptors (PRRs) expressed in immune and non-immune cells. Main PRRs include transmembrane (e.g., toll-like receptors [TLRs]) and intracellular (e.g., nucleotide-binding oligomerization domain (NOD)-like receptors [NLRs]) PRRs (Tang et al., 2012). Infection-mediated tissue damage can further amplify the systemic inflammatory response through the release of endogenous damage-associated molecular patterns (DAMPs) (e.g., high mobility group box 1 [HMGB1] and host DNA) by dead or dying cells (Kang, et al., 2014). In these processes, BET plays a role in coordinating gene transcription mediated by PAMPs or DAMPs, which decides the outcome of infection via interaction with TLR, inflammasome, and DNA sensor pathways (**Figure 2**).

TLRs are central PRRs responsible for recognizing PAMP to trigger the expression of immune mediators by activating transcription factors, such as nuclear factor kappa B (NFKB) and interferon regulatory factors (IRFs). 10 TLRs (TLR1-10) in humans and 13 TLRs (TLR1-13) in mice have been identified, which show different subcellular localizations and PAMP recognition preferences. TLR-1, -2, -4, -5, and -6 are located at the extracellular surface and bind to the components of microbial cell walls and membranes of pathogens (e.g., lipopolysaccharide [LPS], lipoteichoic acid, and lipoproteins). TLR-3, -7, -8, and -9 are mainly expressed in the endoplasmic reticulum and endosome, and detect microbial nucleic acids, such as double or single-stranded RNA from RNA viruses and DNA presented in bacteria and viruses. BET affects the signal pathway of TLRs through two potential mechanisms. On one hand, BETs directly mediate the transcription upregulation of TLR-2, -4, and -6 genes, thereby activating TLR pathway (Nicodeme et al., 2010; Meng et al., 2014; Zhao et al., 2019). On the other hand, BET may promote or inhibit TLR signaling-mediated gene expression through the modulation of activity of NFKB or IRFs in a context-dependent manner. Although the role of BETs in shaping TLR-1, -2, -3, -4, -6, -7, and -9 signaling has been largely demonstrated, their functions in control of TLR-5, -8, and -10, as well as other transmembrane PRRs, are still a mystery.

The inflammasome machinery is important in the innate immune system, which not only mediates the maturation and release of the interleukin-1 (IL1) family (e.g., IL1B and IL18), but also promotes the activation of caspase-1 (CASP1) or CASP4/5/11 to trigger gasdermin D (GSDMD)-dependent pyroptosis to release DAMPs (e.g., HMGB1). One of the largest subfamilies of inflammasomes is called NLR inflammasomes. According to the structure of N-terminal domain, NLRs are further divided into four subfamilies (namely NLRA, NLRB, NLRC, and NLRP) to recognize PAMPs or DAMPs. Among them, the NLR family pyrin domain containing 3 (NLRP3) inflammasome is best characterized and shows sustained activation in sepsis through canonical CASP1-dependent or non-canonical CASP4/5/11-mediated pathway. Interestingly, BETs confer opposite effects on NRLP3 activation depending on cell types. For example, the inhibition of BRD4 alleviates the inflammatory response by blocking TNF-related NRLP3 activation in rat nucleus pulposus cells (Hong et al., 2020). However, the inhibition of BRD4 prevents proliferation and epithelial mesenchymal transition in kidney cancer cells by increasing RELA-mediated NLRP3 expression and subsequent pyroptosis (Tan et al., 2020). Parallel to membrane TLR4, CASP11 acts as a cytoplasmic receptor for LPS in macrophages to trigger endotoxemia in mice. Defining the role of BETs in the regulation of cytoplasmic LPS signaling may further determine the pathological roles of BETs in bacterial infection.

Another multifunctional regulator of innate immunity is the DNA sensor. In addition to TLR9, a receptor essential for identifying unmethylated CpG DNA, cyclic GMP-AMP synthase (CGAS) plays a broad role in the recognition of various types of DNA and their metabolites produced by microorganisms and hosts. After the endogenous second messenger cyclic GMP-AMP (cGAMP) is synthesized by CGAS, cGAMP binds to stimulator of interferon response cGAMP interactor 1 (STING1, also known as STING or TMEM173), resulting in the transcriptional activation of NFKB1 and IRF3, thereby increasing the production of type I interferon and pro-inflammatory cytokines (Chen et al., 2016). The activation of the CGAS-STING1 pathway is related to BRD4 inhibition-mediated antiviral immunity (Wang et al., 2020), indicating that BRD4 is a repressor of the STING1 pathway. Unlike viral infection, excessive activation of STING1

mediates lethal inflammation and systemic coagulation, leading to bacterial septic shock in mice, partly through the activation of NFKB1 and the inflammasome pathway (Zhang et al., 2020; Zhou et al., 2020). This STING1-dependent inflammatory pathway in sepsis seems to depend on the plasma membrane receptor ALK receptor tyrosine kinase (ALK), not cytoplasmic CGAS (Zeng et al., 2017). On this basis, we urgently need to figure out how BRD4 controls the dual role of STING1 pathway in innate immunity.

Application of BETis in Sepsis and Septic Shock

According to the structure of BETs, some chemical compounds have been developed to disrupt or compete the binding of BD1 and BD2 to acetylated histones and transcription factors. The first-generation BETis are also considered pan-BETis because they have no selectivity for BD1 and BD2. Since the BDs between different BETs have a high degree of homology, these BETis cannot distinguish individual member of the BETs. While selective BD1-BETis and BD2-BETis show different inhibition activity of BET, BD1-BETis seems to be as effective as pan-BETis in some cases (Gilan et al., 2020). However, a recent study has shown that BD1 is primarily required for steady stage gene expression, whereas both BD1 and BD2 in all BETs are required for acute phase gene expression during inflammation (Gilan et al., 2020). Theoretically, BD2-BETis may be predominantly effective in the treatment of acute inflammation, including the hyperinflammatory state in the early stage of sepsis. Below, we summarize the potential applications of BETis in experimental sepsis (**Table 1**).

I-BET

I-BET (also known as I-BET762 or GSK525762A) was discovered in 2010 (Nicodeme et al., 2010). It binds to BD1 of BRD4 at the acetyl-lysine (AcK)-binding pocket, which enables two I-BET molecules to bind to the tandem BDs of BET with high affinity. I-BET can successfully compete with AcK within the recognition pocket of BET. I-BET is highly selective and effectively displaces the tetra-acetylated H4 peptide previously bound to the BET tandem BD. Pre-treatment of bone marrow derived macrophages (BMDMs) with I-BET results in the downregulation of 38 and 151 of the LPS-inducible immune genes (including cytokines and chemokines) at 1 and 4 h, respectively. Moreover, the administration of I-BET protects mice from experimental sepsis caused by endotoxemia, polymicrobial peritonitis, and cecal ligation and puncture (CLP). The myeloid lineage-specific *Brd4* conditional knockout mice (termed *Brd4* CKO) are used to further investigate the pathological effects of BRD4 in sepsis. Surprisingly, *Brd4* CKO mice are resistant to endotoxemia, but are more susceptible to intraperitoneal injection of group B *Streptococcus*-induced infection (Bao et al., 2017), which may result from the compromised innate immune response to clear bacteria *in vivo*. These findings not only demonstrate the importance of BRD4 in innate immunity against bacterial infection, but also highlight an unknown function of BRD4 in regulating the activity of bacterial LPS and non-LPS components.

JQ1

JQ1 (best known as (+)-JQ1), the most widely used BETi reported in 2010, is a thienotriazolodiazepine which competitively binds to both BD1 and BD2 of BETs with acetylated lysine. It exhibits prominent anti-inflammatory and immunoregulatory activity in endotoxemic mice by reducing the levels of IL6 and TNF, and rescues mice from LPS-induced death (Belkina et al., 2013). In BMDMs infected with heat-killed *L. monocytogenes*, JQ1 also inhibits the expression of cytokines, such as nitric oxide synthase 2 (NOS2), IL6, and interleukin 1 receptor antagonist (IL1RN) (Wienerroither et al., 2014). Moreover, JQ1 inhibits LPS-induced the upregulation of inflammatory cytokines and serpin family E member 1 (SERPINE1) in mouse primary astrocytes through the depletion of BRD2 recruitment and H3K4me3 enrichment at the promoter region of SERPINE1 (Choi et al., 2015). In addition to bacterial infection, JQ1 also inhibits the upregulation of immune genes (e.g., IL1B, IL6, interferon beta 1 [IFNB1], ISG15 ubiquitin like modifier [ISG15], and interferon gamma [IFNG]) during infection with viruses (e.g., *Pseudorabies virus*, *Herpes simplex virus*, and *Ectromelia virus*), fungi (e.g., *Candida albicans* and *Aspergillus fumigatus*), and parasites (e.g., *Schistosoma japonicum*) (Wang et al., 2021; Dominguez-Andres et al., 2019; Wang et al., 2020). Despite its strong anticancer activity, the toxicity and side effects of JQ1 for the treatment of sepsis may not be optimistic, and extensive research is needed.

I-BET151

I-BET151 (also known as GSK1210151A), which belongs to the quinoline isoxazole BET family bromodomain inhibitors, was developed in 2012 and has good oral bioavailability with a similar effect as I-BET (Seal et al., 2012). The administration of I-BET151 also protects mice from LPS-induced death (endotoxemia). Interestingly, I-BET151 cannot affect LPS-induced TNF production, but significantly inhibits LPS-mediated IL6 production. Since both TNF and IL6 are NFKB target genes, I-BET151 may regulate endotoxemia in an NFKB-independent manner. Another open question is whether I-BET151 can be used to inhibit the signal transducer and activator of transcription 3 (STAT3)-related immune pathway, because the inflammatory mediator IL6 is a well-known activator of the STAT3 pathway.

Apabetalone and RVX-297

Apabetalone (also known as RVX-208 or RVX-000222), an oral BETi selective for BD2 within BETs, is currently used in phase 3 clinical trials for the treatment of coronary artery disease, diabetes, and chronic kidney failure. In a mouse model of lethal endotoxemia, apabetalone prevents liver damage by inhibiting the expression of alpha-2-macroglobulin and serum amyloid P. In patients with cardiovascular disease, apabetalone provides benefit for limiting chronic cytokine signaling (Wasiak et al., 2020). Thus, this action of apabetalone might also serve as an effective therapy in treating patient with sepsis and MODS, especially sepsis-induced cardiomyopathy. BRD2 is a direct target of apabetalone (Gordon et al., 2020). Since apabetalone can inhibit the expression of angiotensin-converting enzyme 2 (ACE2), the receptor utilized by the SARS-CoV-2 particles to gain entry into human cells, it is becoming a promising drug for the treatment of COVID-19 and

concomitant sepsis (Gilham et al., 2020). RVX-297, a 4-quinazolinone derivative related to RVX-208, is two times more selective for BD2 than RVX-208. RVX-297 also decreases the production of multiple cytokines in endotoxemic mice (Jahagirdar et al., 2017), highlighting its potential anti-inflammatory activities in lethal infection.

dBET1

In recent years, the degradation of BETs using proteolytic targeting chimera (PROTAC) has shown excellent targeting ability and activity. The advantage of BETs degradation rather than inhibition is that it may lead to selective suppression of individual BET-dependent genes. Indeed, PROTAC-based BETis (e.g., dBET1, MZ-1, and ARV-825) exhibit promising immunoregulatory activities in various disease models (Suarez-Alvarez et al., 2017; DeMars et al., 2018; Tsujikawa et al., 2019). DBET1 is a conjugate of (+)-JQ1 and cereblon E3 ubiquitin ligase ligand (phthalimide), which can induce highly selective cereblon-dependent BET degradation *in vitro* and *in vivo*. dBET1 effectively inhibits LPS-induced the expression of proinflammatory factors (e.g., NOS2, prostaglandin-endoperoxide synthase 2 [PTGS2], IL1B, TNF, C-C motif chemokine ligand 2 [CCL2], IL6, and matrix metallopeptidase 9 [MMP9]) in the microglia by degrading BRD2 and BRD4 in a time- and dose-dependent manner (DeMars et al., 2018). These activities make DBET1 a promising drug candidate for the treatment of sepsis. However, since the complete loss of BRD2 and BRD4 is lethal, when DBET1 is administered systemically, uncontrolled degradation of BRDs in normal cells may bring toxicity. Therefore, the therapeutic window and adverse reactions of dBET1 needs to be carefully defined in future studies.

CONCLUSION AND OUTLOOK

Sepsis and septic shock cause more than 11 million deaths each year (Rudd et al., 2020), which is currently compounded by the COVID-19-related septic deaths (Tang et al., 2020). Because of their transcriptional control of immune and inflammatory genes, BETs have become druggable targets for the treatment of diseases, including sepsis (Wang et al., 2021). Although the existing preclinical data seems encouraging, there are still some problems to be solved considering its translational application. First, the unique functions of different BETs in different stages of sepsis are still poorly understood. Second, the dosage and administration time of BETis are undefined and need to be further explored. In the late stage of sepsis, the immune system of patients may be suppressed or even paralyzed, thus necessitating an optimal, individualized therapeutic regimen. Third, since most BETis have predominant anti-cancer activity, more attention should be paid to their long-term toxicity and side effects. Fourth, developing new kinds of BETis with high efficacy and low toxicity through new technology/concept (e.g., PROTACs, lysosome-targeting chimeras [LYTACs], or phase separation) are always important for future studies.

AUTHOR CONTRIBUTIONS

RK and DT conceived of the topic for this review. All authors listed have made a substantial, direct, and intellectual contribution to the work, and approved it for publication.

REFERENCES

Bachtel, N. D., Beckerle, G. A., Mota, T. M., Rougvie, M. M., Raposo, R. A. S., Jones, R. B., et al. (2019). Short communication: expression of host restriction factors by memory CD4+ T cells differs between healthy donors and HIV-1-Infected individuals with effective antiretroviral therapy. *AIDS Res. Hum. Retroviruses* 35, 108–111. doi:10.1089/AID.2018.0162

Bao, Y., Wu, X., Chen, J., Hu, X., Zeng, F., Cheng, J., et al. (2017). Brd4 modulates the innate immune response through Mnk2-eIF4E pathway-dependent translational control of IκBα. *Proc. Natl. Acad. Sci. USA* 114, E3993–E4001. doi:10.1073/pnas.1700109114

Belkina, A. C., Nikolajczyk, B. S., and Denis, G. V. (2013). BET protein function is required for inflammation: Brd2 genetic disruption and BET inhibitor JQ1 impair mouse macrophage inflammatory responses. *J. Immunol.* 190, 3670–3678. doi:10.4049/jimmunol.1202838

Carson, W. F., Cavassani, K. A., Dou, Y., and Kunkel, S. L. (2011). Epigenetic regulation of immune cell functions during post-septic immunosuppression. *Epigenetics* 6, 273–283. doi:10.4161/epi.6.3.14017

Chaudhry, H., Zhou, J., Zhong, Y., Ali, M. M., McGuire, F., Nagarkatti, P. S., et al. (2013). Role of cytokines as a double-edged sword in sepsis. *In Vivo*. 27, 669–684.

Chen, R., Zeng, L., Zhu, S., Liu, J., Zeh, H. J., Kroemer, G., et al. (2019). cAMP metabolism controls caspase-11 inflammasome activation and pyroptosis in sepsis. *Sci. Adv.* 5, eaav5562. doi:10.1126/sciadv.aav5562

Chen, Q., Sun, L., and Chen, Z. J. (2016). Regulation and function of the cGAS-STING pathway of cytosolic DNA sensing. *Nat. Immunol.* 17, 1142–1149. doi:10.1038/ni.3558

Choi, C. S., Hong, S. H., Sim, S., Cho, K. S., Kim, J. W., Yang, S. M., et al. (2015). The epigenetic reader BRD2 as a specific modulator of PAI-1 expression in lipopolysaccharide-stimulated mouse primary astrocytes. *Neurochem. Res.* 40, 2211–2219. doi:10.1007/s11064-015-1710-2

Chousterman, B. G., Swirski, F. K., and Weber, G. F. (2017). Cytokine storm and sepsis disease pathogenesis. *Semin. Immunopathol.* 39, 517–528. doi:10.1007/s00281-017-0639-8

DeMars, K. M., Yang, C., Castro-Rivera, C. I., and Candelario-Jalil, E. (2018). Selective degradation of BET proteins with dBET1, a proteolysis-targeting chimera, potently reduces pro-inflammatory responses in lipopolysaccharide-activated microglia. *Biochem. Biophys. Res. Commun.* 497, 410–415. doi:10.1016/j.bbrc.2018.02.096

Denis, G. V., Vaziri, C., Guo, N., and Faller, D. V. (2000). RING3 kinase transactivates promoters of cell cycle regulatory genes through E2F. *Cell Growth Differ.* 11, 417–424.

Devaiah, B. N., Lewis, B. A., Cherman, N., Hewitt, M. C., Albrecht, B. K., Robey, P. G., et al. (2012). BRD4 is an atypical kinase that phosphorylates serine2 of the RNA polymerase II carboxy-terminal domain. *Proc. Natl. Acad. Sci. USA*. 109, 6927–6932. doi:10.1073/pnas.1120422109

Dolin, H. H., Papadimos, T. J., Chen, X., and Pan, Z. K. (2019). Characterization of pathogenic sepsis etiologies and patient profiles: a novel approach to triage and treatment. *Microbiol. Insights*. 12, 1178636118825081. doi:10.1177/1178636118825081

Domínguez-Andrés, J., Ferreira, A. V., Jansen, T., Smithers, N., Prinjha, R. K., Furze, R. C., et al. (2019). Bromodomain inhibitor I-BET151 suppresses immune responses during fungal-immune interaction. *Eur. J. Immunol.* 49, 2044–2050. doi:10.1002/eji.201848081

Filippakopoulos, P., and Knapp, S. (2014). Targeting bromodomains: epigenetic readers of lysine acetylation. *Nat. Rev. Drug Discov.* 13, 337–356. doi:10.1038/nrd4286

Filippakopoulos, P., Picaud, S., Mangos, M., Keates, T., Lambert, J. P., and Barsyte-Lovejoy, D., et al. (2012). Histone recognition and large-scale structural analysis of the human bromodomain family. *Cell* 149, 214–231. doi:10.1016/j.cell.2012.02.013

Florence, B., and Faller, D. V. (2001). You bet-cha: a novel family of transcriptional regulators. *Front Biosci.* 6, D1008–D1018. doi:10.2741/florence

Gamsjaeger, R., Webb, S. R., Lamonica, J. M., Billin, A., Blobel, G. A., and Mackay, J. P. (2011). Structural basis and specificity of acetylated transcription factor GATA1 recognition by BET family bromodomain protein Brd3. *Mol. Cell Biol.* 31, 2632–2640. doi:10.1128/MCB.05413-11

Gilan, O., Rioja, I., Knezevic, K., Bell, M. J., Yeung, M. M., Harker, N. R., et al. (2020). Selective targeting of BD1 and BD2 of the BET proteins in cancer and immunoinflammation. *Science*. 368, 387–394. doi:10.1126/science.aaz8455

Gilham, D., Fu, L., Tsujikawa, L. M., Rakai, B., Wasiak, S., and Stotz, S., et al. (2020). Apabetalone (RVX-208) reduces ACE2 expression in human cell culture systems, which could attenuate SARS-CoV-2 viral entry. *Circulation*. 142, A14112. doi:10.1161/circ.142.suppl_3.14112

Gordon, D. E., Jang, G. M., Bouhaddou, M., Xu, J., Obernier, K., White, K. M., et al. (2020). A SARS-CoV-2 protein interaction map reveals targets for drug repurposing. *Nature* 583, 459–468. doi:10.1038/s41586-020-2286-9

Hong, J., Li, S., Markova, D. Z., Liang, A., Kepler, C. K., Huang, Y., et al. (2020). Bromodomain-containing protein 4 inhibition alleviates matrix degradation by enhancing autophagy and suppressing NLRP3 inflammasome activity in NP cells. *J. Cell Physiol.* 235, 5736–5749. doi:10.1002/jcp.29508

Jahagirdar, R., Attwell, S., Marusic, S., Bendele, A., Shenoy, N., and McLure, K. G., et al. (2017). RVX-297, a BET bromodomain inhibitor, has therapeutic effects in preclinical models of acute inflammation and autoimmune disease. *Mol. Pharmacol.* 92, 694–706. doi:10.1124/mol.117.110379

Kang, R., Zeng, L., Zhu, S., Xie, Y., Liu, J., Wen, Q., et al. (2018). Lipid peroxidation drives Gasdermin D-mediated pyroptosis in lethal polymicrobial sepsis. *Cell Host Microbe.* 24, 97–108.e4. doi:10.1016/j.chom.2018.05.009

Kang, R., Chen, R., Zhang, Q., Hou, W., Wu, S., Cao, L., et al. (2014). HMGB1 in health and disease. *Mol. Aspects Med.* 40, 1–116. doi:10.1016/j.mam.2014.05.001

Li, S., Cui, W., Song, Q., Zhou, Y., and Li, J. (2019). miRNA-302e attenuates inflammation in infantile pneumonia though the RelA/BRD4/NF-κB signaling pathway. *Int. J. Mol. Med.* 44, 47–56. doi:10.3892/ijmm.2019.4194

Lin, Y. C., Wang, F. S., Yang, Y. L., Chuang, Y. T., and Huang, Y. H. (2018). MicroRNA-29a mitigation of toll-like receptor 2 and 4 signaling and alleviation of obstructive jaundice-induced fibrosis in mice. *Biochem. Biophys. Res. Commun.* 496, 880–886. doi:10.1016/j.bbrc.2018.01.132

Meng, S., Zhang, L., Tang, Y., Tu, Q., Zheng, L., Yu, L., et al. (2014). BET inhibitor JQ1 blocks inflammation and bone destruction. *J. Dent Res.* 93, 657–662. doi:10.1177/0022034514534261

Morinière, J., Rousseaux, S., Steuerwald, U., Soler-López, M., Curtet, S., Vitte, A. L., et al. (2009). Cooperative binding of two acetylation marks on a histone tail by a single bromodomain. *Nature*. 461, 664–668. doi:10.1038/nature08397

Nicodeme, E., Jeffrey, K. L., Schaefer, U., Beinke, S., Dewell, S., Chung, C. W., et al. (2010). Suppression of inflammation by a synthetic histone mimic. *Nature* 468, 1119–1123. doi:10.1038/nature09589

Peserico, A., and Simone, C. (2011). Physical and functional HAT/HDAC interplay regulates protein acetylation balance. *J. Biomed. Biotechnol.* 2011, 371832. doi:10.1155/2011/371832

Rudd, K. E., Johnson, S. C., Agesa, K. M., Shackelford, K. A., Tsoi, D., Kievlan, D. R., et al. (2020). Global, regional, and national sepsis incidence and mortality, 1990-2017: analysis for the Global Burden of Disease Study. *Lancet* 395, 200–211. doi:10.1016/S0140-6736(19)32989-7

Seal, J., Lamotte, Y., Donche, F., Bouillot, A., Mirguet, O., Gellibert, F., et al. (2012). Identification of a novel series of BET family bromodomain inhibitors: binding mode and profile of I-BET151 (GSK1210151A). *Bioorg. Med. Chem. Lett.* 22, 2968–2972. doi:10.1016/j.bmcl.2012.02.041

Singer, M., Deutschman, C. S., Seymour, C. W., Shankar-Hari, M., Annane, D., Bauer, M., et al. (2016). The Third international Consensus Definitions for sepsis and septic shock (Sepsis-3). *JAMA*. 315, 801–810. doi:10.1001/jama.2016.0287

Suarez-Alvarez, B., Morgado-Pascual, J. L., Rayego-Mateos, S., Rodriguez, R. M., Rodrigues-Diez, R., Cannata-Ortiz, P., et al. (2017). Inhibition of bromodomain and extraterminal domain family proteins ameliorates experimental renal damage. *J. Am. Soc. Nephrol.* 28, 504–519. doi:10.1681/ASN.2015080910

Tan, Y. F., Wang, M., Chen, Z. Y., Wang, L., and Liu, X. H. (2020). Inhibition of BRD4 prevents proliferation and epithelial-mesenchymal transition in renal cell carcinoma via NLRP3 inflammasome-induced pyroptosis. *Cell Death Dis.* 11, 239. doi:10.1038/s41419-020-2431-2

Tang, D., Kang, R., Coyne, C. B., Zeh, H. J., and Lotze, M. T. (2012). PAMPs and DAMPs: signal 0s that spur autophagy and immunity. *Immunol Rev.* 249, 158–175. doi:10.1111/j.1600-065X.2012.01146.x

Tang, D., Comish, P., and Kang, R. (2020). The hallmarks of COVID-19 disease. *PLoS Pathog.* 16, e1008536. doi:10.1371/journal.ppat.1008536

Tang, K., Zhao, J., Xie, J., and Wang, J. (2019). Decreased miR-29b expression is associated with airway inflammation in chronic obstructive pulmonary disease. *Am. J. Physiol. Lung Cell Mol Physiol.* 316, L621–L629. doi:10.1152/ajplung.00436.2018

Topper, M. J., Vaz, M., Marrone, K. A., Brahmer, J. R., and Baylin, S. B. (2020). The emerging role of epigenetic therapeutics in immuno-oncology. *Nat. Rev. Clin. Oncol.* 17, 75–90. doi:10.1038/s41571-019-0266-5

Tsujikawa, L. M., Fu, L., Das, S., Halliday, C., Rakai, B. D., Stotz, S. C., et al. (2019). Apabetalone (RVX-208) reduces vascular inflammation *in vitro* and in CVD patients by a BET-dependent epigenetic mechanism. *Clin. Epigenetics* 11, 102. doi:10.1186/s13148-019-0696-z

Vachharajani, V., and McCall, C. E. (2019). Epigenetic and metabolic programming of innate immunity in sepsis. *Innate Immun.* 25, 267–279. doi:10.1177/1753425919842320

Wang, J., Li, G. L., Ming, S. L., Wang, C. F., Shi, L. J., Su, B. Q., et al. (2020). BRD4 inhibition exerts anti-viral activity through DNA damage-dependent innate immune responses. *PLoS Pathog.* 16, e1008429. doi:10.1371/journal.ppat.1008429

Wang, N., Wu, R., Tang, D., and Kang, R. (2021). The BET family in immunity and disease. *Signal Transduct Target Ther.* 6, 23. doi:10.1038/s41392-020-00384-4

Wasiak, S., Gilham, D., Daze, E., Tsujikawa, L. M., Halliday, C., Stotz, S. C., et al. (2020). Epigenetic modulation by apabetalone counters cytokine-driven acute phase response in vitro, in mice and in patients with cardiovascular disease. *Cardiovasc. Ther.* 2020, 9397109. doi:10.1155/2020/9397109

Wienerroither, S., Rauch, I., Rosebrock, F., Jamieson, A. M., Bradner, J., Muhar, M., et al. (2014). Regulation of NO synthesis, local inflammation, and innate immunity to pathogens by BET family proteins. *Mol. Cell Biol.* 34, 415–427. doi:10.1128/MCB.01353-13

Zeng, L., Kang, R., Zhu, S., Wang, X., Cao, L., Wang, H., et al. (2017). ALK is a therapeutic target for lethal sepsis. *Sci. Transl. Med.* 9, eaan5689. doi:10.1126/scitranslmed.aan5689

Zhang, H., Zeng, L., Xie, M., Liu, J., Zhou, B., Wu, R., et al. (2020). TMEM173 drives lethal coagulation in sepsis. *Cell Host Microbe*. 27, 556–570.e6. doi:10.1016/j.chom.2020.02.004

Zhang, Q., and Cao, X. (2019). Epigenetic regulation of the innate immune response to infection. *Nat. Rev. Immunol.* 19, 417–432. doi:10.1038/s41577-019-0151-6

Zhao, J., Meng, Z., Xie, C., Yang, C., Liu, Z., Wu, S., et al. (2019). B7-H3 is regulated by BRD4 and promotes TLR4 expression in pancreatic ductal adenocarcinoma. *Int. J. Biochem. Cell Biol.* 108, 84–91. doi:10.1016/j.biocel.2019.01.011

Zhou, B., Liu, J., Zeng, L., Zhu, S., Wang, H., Billiar, T. R., et al. (2020). Extracellular SQSTM1 mediates bacterial septic death in mice through insulin receptor signalling. *Nat. Microbiol.* 5, 1576–1587. doi:10.1038/s41564-020-00795-7

Conflict of Interest: The authors declare that the research was conducted in the absence of any commercial or financial relationships that could be construed as a potential conflict of interest.

frontiers in Pharmacology

ORIGINAL RESEARCH
published: 13 April 2021
doi: 10.3389/fphar.2020.614024

Paeoniflorin and Hydroxysafflor Yellow A in Xuebijing Injection Attenuate Sepsis-Induced Cardiac Dysfunction and Inhibit Proinflammatory Cytokine Production

Xin-Tong Wang[1,2], Zhen Peng[1,2], Ying-Ying An[1,2], Ting Shang[1,2], Guangxu Xiao[1,2], Shuang He[1,2], Xi Chen[1], Han Zhang[1], Yuefei Wang[1], Tao Wang[1], Jun-Hua Zhang[1], Xiumei Gao[1], Yan Zhu[1,2] and Yuxin Feng[1,2]**

[1]State Key Laboratory of Component-based Chinese Medicine, Tianjin University of Traditional Chinese Medicine, Tianjin, China, [2]Research and Development Center of TCM, Tianjin International Joint Academy of Biotechnology and Medicine, Tianjin, China

OPEN ACCESS

Edited by:
Hong Zhou,
Zunyi Medical University, China

Reviewed by:
Guo-Chang Fan,
University of Cincinnati, United States
Santosh Kumar Mishra,
Indian Veterinary Research Institute (IVRI), India

***Correspondence:**
Yan Zhu
yanzhu.harvard@icloud.com
Yuxin Feng
fengyn@live.com

Specialty section:
This article was submitted to Experimental Pharmacology and Drug Discovery, a section of the journal Frontiers in Pharmacology

Received: 05 October 2020
Accepted: 07 December 2020
Published: 13 April 2021

Citation:
Wang X-T, Peng Z, An Y-Y, Shang T, Xiao G, He S, Chen X, Zhang H, Wang Y, Wang T, Zhang J-H, Gao X, Zhu Y and Feng Y (2021) Paeoniflorin and Hydroxysafflor Yellow A in Xuebijing Injection Attenuate Sepsis-Induced Cardiac Dysfunction and Inhibit Proinflammatory Cytokine Production. Front. Pharmacol. 11:614024. doi: 10.3389/fphar.2020.614024

Sepsis-induced myocardial dysfunction is a major contributor to the poor outcomes of septic shock. As an add-on with conventional sepsis management for over 15 years, the effect of Xuebijing injection (XBJ) on the sepsis-induced myocardial dysfunction was not well understood. The material basis of Xuebijing injection (XBJ) in managing infections and infection-related complications remains to be defined. A murine cecal ligation and puncture (CLP) model and cardiomyocytes *in vitro* culture were adopted to study the influence of XBJ on infection-induced cardiac dysfunction. XBJ significantly improved the survival of septic-mice and rescued cardiac dysfunction *in vivo*. RNA-seq revealed XBJ attenuated the expression of proinflammatory cytokines and related signalings in the heart which was further confirmed on the mRNA and protein levels. Xuebijing also protected cardiomyocytes from LPS-induced mitochondrial calcium ion overload and reduced the LPS-induced ROS production in cardiomyocytes. The therapeutic effect of XBJ was mediated by the combination of paeoniflorin and hydroxysafflor yellow A (HSYA) (C0127-2). C0127-2 improved the survival of septic mice, protected their cardiac function and cardiomyocytes while balancing gene expression in cytokine-storm-related signalings, such as TNF-α and NF-κB. In summary, Paeoniflorin and HSYA are key active compounds in XBJ for managing sepsis, protecting cardiac function, and controlling inflammation in the cardiac tissue partially by limiting the production of IL-6, IL-1β, and CXCL2.

Keywords: Xuebijing injection, septic shock, sepsis-induced myocardial dysfunction, paeoniflorin (Pae), hydroxysafflor yellow A (HSYA), cytokine storm, CXCL2/MIP-2

HIGHLIGHTS

- Xuebijing injection protected cardiac function during systemic infection partially by down-regulating the expression of pro-inflammatory cytokines and related pathways in the cardiac tissue.
- Paeoniflorin and hydroxysafflor yellow A in XBJ rescued mice from septic shock.

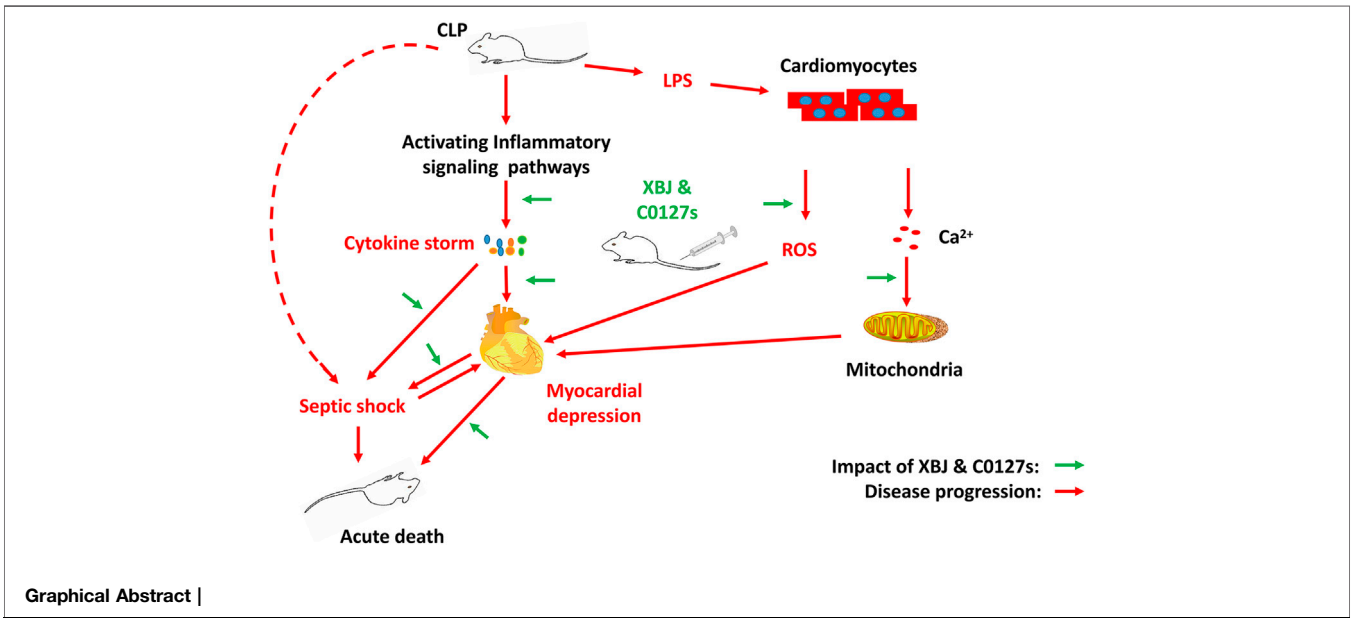

Graphical Abstract |

- Paeoniflorin and hydroxysafflor yellow A in XBJ protected cardiac function in septic mice partially by inhibiting the expression of pro-inflammatory cytokines/chemokines and related pathways in the cardiac tissue.

INTRODUCTION

The mortality rate in septic shock generally exceeds 40% (Beesley et al., 2018). Sepsis-induced cardiomyopathy (SIC), a frequent incident in sepsis, contributes to the poor outcomes of septic shock (Ehrman et al., 2018; Martin et al., 2019). Circulating proinflammatory cytokines act directly on cardiomyocytes and vasculatures to compromise myocardial performance (Ehrman et al., 2018). It is believed that TNF-α, IL-1β, and IL-6 are major contributors to SIC (Pathan et al., 2004; Liu et al., 2017; Martin et al., 2019).

Results of clinical trials suggested that beta-adrenergic agonists and levosimendan were not effective in improving outcomes in sepsis patients (Gordon et al., 2016; Walley, 2018). Medications improving cardiovascular function and targeting proinflammatory cytokines showed therapeutic potentials to manage sepsis and sepsis-induced myocardial dysfunction (Li et al., 2007; Walley, 2018). However, targeting TLR4 signaling with Eritoran did not improve survival in sepsis patients (Opal et al., 2013; Martin et al., 2019). Murine monoclonal anti-TNF-α improved ventricular function in patients with septic shock. But it did not improve patient survival (Vincent et al., 1992; Abraham et al., 1998).

Approved to treat sepsis and septic shock as an add-on in China since 2004, Xuebijing injection significantly improved the survival of severe pneumonia patients in a large-scale clinical trial (Cheng et al., 2016; Zhang et al., 2018; Song et al., 2019). Showing promising clinical effect in managing severe COVID-19 and saving thousands of lives in China, it was recently approved to treat moderate and severe CVOID-19 in China (Fan et al., 2020). Activating circulation and remove stasis, XBJ maintains the balance of the immune system and renders organ protections during systemic infection (Liu et al., 2014a; Chen et al., 2018; Shang et al., 2019). Paeoniflorin claims the highest concentration and hydroxysafflor yellow A claims the 2nd highest concentration among all detectable compounds in Xuebijing injection (Cheng et al., 2016; Shang et al., 2019; Li et al., 2020a). A series of studies indicated these two compounds are promising Xuebijing constituents of therapeutic importance (Cao et al., 2011; Zhai and Guo, 2016b; Cheng et al., 2016; Zou et al., 2018; Shang et al., 2019). Paeoniflorin improved survival and cardiac function in LPS-treated rodents (Cao et al., 2011; Zhai and Guo, 2016b; Liu et al., 2016). HSYA improved ischaemia-induced cardiac haemodynamics by stimulating nucleolin-mediated angiogenesis (Zou et al., 2018).

Though XBJ has been used to treat sepsis as an add-on for over one and a half decades, several key questions remain to be addressed: 1. What's the influence of XBJ on sepsis-induced cardiac dysfunction? 2. What are the mechanisms of XBJ in managing sepsis-induced cardiac dysfunction? 3. Which compounds in XBJ play major roles in managing septic shock? 4. Which compounds in XBJ play a major role in managing sepsis-induced cardiac dysfunction? In this study, we try to address these questions by evaluating the impact of XBJ and its key compounds (paeoniflorin and hydroxysafflor yellow A) on cardiac function in a clinical relevant shock model (Barth et al., 2006) and investigating the molecular mechanism.

MATERIALS AND METHODS

Chemicals and Reagents

Xuebijing injection (catalog number: z20040033, batch number: 1905061) was manufactured by Tianjin Chase Sun Pharmaceutical Co., Ltd (Tianjin, China). Paeoniflorin (CAS #:23180-57-6), Hydroxysafflor yellow A (CAS #: 78281-02-4), Ferulic acid (CAS # 537- 98-4), and protocatechuic aldehyde (CAS #: 139-85-5) were

purchased from Shanghai Yuanye Biotechnology Co., Ltd. (Shanghai, China). Mouse NT-proBNP ELISA (Cat#: ZC-37812-96T) kit, DCFH-DA (Cat#:CA1410-100T), RIPA tissue/cell lysate (Cat#: R0020), SDS-PAGE gel kit, and Rainbow 245 Spectrum Marker (Cat#:PR 1920), Mouse IL-6 ELISA kit (Cat#:ZC-37988-96T), Mouse IL-1β ELISA kit (Cat#:ZC-37974-96T), and EasySee Western Blot Kit (Lot#:O30807) were purchased from Solarbio (Beijing, China). The primary antibody of rabbit anti-CXCL2 (bs-1162R) was purchased from Bioss Inc., (Beijing, China) and GAPDH, 1:4,000 (14C10) was from Cell Signaling Technology (Beverly, MA, United States). The secondary antibody Goat anti-Rabbit IgG (1:4,000) (ZB-2301) was purchased from ZS bio (Beijing, China). 2, 2, 2-Tribromoalcohol (Cat#:T48402) and Bacterial lipopolysaccharide (Cat#: L2880-10 MG) were purchased from Sigma Aldrich (St. Louis, MO, United States). Rhod2-AM (Cat#: zy0129) and Anti-GRP78 (BiP) antibody (ab21685) were purchased from Abcam (Cambridge, MA, United States).

Animals

This study was carried out following the recommendations of the Guide for the Care and Use of Laboratory Animals (NIH Publication No. 85-23, revised 1996, United States) and the recommendations in the Guidance for the Care and Use of Laboratory Animals issued by the Ministry of Science and Technology of China. All experiments were approved by the Experimental Animal Ethics Committee of Tianjin University of Traditional Chinese Medicine (Tianjin, China) and performed in accordance with its guidelines (license number: TCM-LAE-20170017). Male ICR mice, 6-week-old, were purchased from Beijing Vital River Laboratory Animal Technology Co., Ltd. (Beijing, China, Certificate no.: SCXK Jing 2012-0001). They were kept under controlled temperature (22 ± 2°C) and relative humidity (40% ± 5%) conditions, fed commercial rat food and purified water, and had a 12-h light/dark cycle.

Cecal Ligation and Puncture

As described previously (Rittirsch et al., 2009; Chen et al., 2018), the abdomen of an anesthetized mouse was depilated, and an incision of less than 1 cm was cut with scissors to expose the cecum which was ligated with a 2–0 line 1/3 from the ileocecal valve. An 18G-needle was used to perforate the cecum (one hole), and then a small amount of feces a little feces was squeezed out. After the operation, the cecum was returned to the original position, the wound was sutured with a 4–0 suture, and the mouse was kept on an electric blanket after the operation.

Drug Administration

The animals were randomly divided into five groups, sham group, CLP group, CLP + Xuebijing group, CLP + C0127 group, and CLP + C0127-2 group. C0127 was defined as the combination of paeoniflorin (2 mg/ml, CAS #:23180-57-6), hydroxysafflor yellow A (0.5 mg/ml, CAS #: 78281-02-4), ferulic acid (0.02 mg/ml, CAS # 537-98-4), and protocatechuic aldehyde (0.01 mg/ml, CAS #: 139-85-5) at the indicated concentrations (Shang et al., 2019). C0127-2 was defined as the combination of paeoniflorin (2 mg/ml, CAS #:23180-57-6) and hydroxysafflor yellow A (0.5 mg/ml, CAS #: 78281-02-4) at the indicated concentration. Paeoniflorin (2 mg/ml, CAS #:23180-57-6), hydroxysafflor yellow A (0.5 mg/ml, CAS #: 78281-02-4), ferulic acid (0.02 mg/ml, CAS # 537-98-4), and protocatechuic aldehyde (0.01 mg/ml, CAS #: 139-85-5) were dissolved in PBS before the tail-vein injection. Drug treatment was started three days before the cecal ligation and puncture, Xuebijing (9 ml/kg), C0127 (9 ml/kg), C0127-2 (9 ml/kg) were administered twice/day by tail-vein injections to the corresponding groups. Two hrs after CLP, XBJ (9 ml/kg) and C0127s (9 ml/kg) were administered every 12 h by tail-vein injection. Saline was administered to sham and CLP group by every 12 h by tail-vein injection. Mice were feed and supplied with water daily.

RNA Samples Collection

Twenty-four hours after CLP surgery, the hearts of mice (including normal mice, CLP group, XBJ treatment group, C0127 treatment group, C0127-2 treatment group) were collected. The intracavity blood was washed with normal saline, and the hearts were immediately placed into liquid nitrogen. The hearts were later used for high-throughput sequencing on an Illumina sequencing platform (4 in each group). RNA was extracted from cardiac tissue using standard extraction method as described (Lyu et al., 2018a) and was reverse transcribed using NEB Next®Ultra™RNA library preparation kit for Illumina®.

RNA-Seq

RNA Quantification and Quality Testing

RNA degradation and contamination was monitored on 1% agarose gels. RNA purity was checked using the NanoPhotometer® spectrophotometer (IMPLEN, CA, United States). RNA integrity was assessed using the RNA Nano 6000 Assay Kit of the Bioanalyzer 2100 system (Agilent Technologies, CA, United States).

Library Preparation for Transcriptome Sequencing

A total amount of 1 μg RNA per mouse was used as input material for the RNA preparations. Sequencing libraries were generated using NEB Next® UltraTMRNA Library Prep Kit for Illumina® (NEB, United States) following manufacturer's recommendations and index codes were added to attribute sequences to each sample. Briefly, mRNA was purified from total RNA using poly-T oligo-attached magnetic beads. Fragmentation was carried out using divalent cations under elevated temperature in NEB Next First Strand Synthesis Reaction Buffer (5X). First-strand cDNA was synthesized using random hexamer primer and M-MuLV Reverse transcriptase (RNase H-). Second strand cDNA synthesis was subsequently performed using DNA Polymerase I and RNase H. Remaining overhangs were converted into blunt ends via exonuclease/polymerase activities. After adenylation of 3′ ends of DNA fragments, NEB Next Adaptors with hairpin loop structure were ligated to prepare for hybridization. In order to select cDNA fragments of preferentially 250~300 bp in length, the library fragments were purified with the AMPureXP system (Beckman Coulter, Beverly, United States). Then 3 μl USER Enzyme (NEB, United States) was used with size-selected, adaptor-ligated cDNA at 37°C for 15 min followed by 5 min at 95°C before PCR. Then PCR was performed with Phusion High-Fidelity DNA polymerase, Universal PCR primers and Index (X) Primer. At last, PCR products were

purified (AMPure XP system) and library quality was assessed on the Agilent Bioanalyzer 2100 system.

Clustering and Sequencing

The clustering of the index-coded samples was performed on a cBot Cluster Generation System using TruSeq PE Cluster Kit v3-cBot-HS (Illumina) according to the manufacturer's instructions. After cluster generation, the library preparations were sequenced on an Illumina Novaseq platform and 150 bp paired-end reads were generated.

Data Analysis

Quality Control

Raw data (raw reads) of FastQ format were firstly processed through in-house Perl scripts. In this step, clean data (clean reads) were obtained by removing reads containing adapter, reads containing ploy-N and low quality reads from raw data. At the same time, Q20, Q30 and GC content the clean data were calculated. All the downstream analyses were based on the clean data with high quality.

Reads Mapping to the Reference Genome

Reference genome and gene model annotation files were downloaded from genome website directly. Index of the reference genome was built using Hisat2 v2.0.5 and paired-end clean reads were aligned to the reference genome using Hisat2 v2.0.5. Hisat2 was selected as the mapping tool since it can generate a database of splice junctions based on the gene model annotation file and thus a better mapping result than other non-splice mapping tools.

Quantification of Gene Expression Levels

Feature Counts v1.5.0-p3 was used to count the reads numbers mapped to each gene. And then FPKM of each gene was calculated based on the length of the gene and reads count mapped to this gene. FPKM, expected number of Fragments Per Kilobase of transcript sequence per Million base pairs sequenced, was used to assess the effect of sequencing depth and gene length for the reads count. It is currently the most commonly used method for estimating gene expression levels.

Differential Expression Analysis

For DESeq2 with biological replicates, differential expression analysis of two conditions/groups (two biological replicates per condition) was performed using DESeq2 R package (1.16.1). DESeq2 provides statistical routines for determining differential expression in digital gene expression data using a model based on the negative binomial distribution. The resulting p-values were adjusted using the Benjamini and Hochberg's approach for controlling the false discovery rate. Genes with an adjusted p-value <0.05 found by DESeq2 were assigned as differentially expressed. The p values were adjusted using the Benjamini and Hochberg method. A corrected p-value of 0.05 and absolute fold change of two were set as the threshold for significantly differential expression.

GO and KEGG Enrichment Analysis of Differentially Expressed Genes

Gene Ontology (GO) enrichment analysis of differentially expressed genes were implemented using the clusterProfiler R package, in which gene length bias were corrected. GO terms with corrected p value less than 0.05 were considered significantly enriched by differential expressed genes. KEGG is a database resource for understanding high-level functions and utilities of the biological system, such as the cell, the organism and the ecosystem, from molecular-level information, especially large-scale molecular datasets generated by genome sequencing and other high-through put experimental technologies (http://www.genome.jp/kegg/). We used clusterProfiler R package to test the statistical enrichment of differential expression genes in KEGG pathways.

Elisa

Twenty-four hours after CLP, blood was collected and was left at room temperature for 30 min. The clot was removed by centrifuging at 1,500 g for 10 min at 4°C in a centrifuge. The IL-1β, IL-6, and NT-proBNP were detected using ELISA kits by an automatic biochemical analyzer (Multiskan MK3; Thermo Fisher Scientific, Waltham, MA, United States), according to the manufacturer's instructions as previously described (Lyu et al., 2018a; Chen et al., 2018).

The concentrations of IL-1β and IL-6 in the heart tissue were determined following the manufacturers' protocol. In brief, the hearts of mice were harvested and rinsed with normal saline 24 h after the CLP procedure. 10ul high-efficiency RIPA lysis buffer for every 1 mg of heart tissue and 10 ul PMSF protease inhibitor for every 1 ml lysis buffer were added to the heart tissue. Later, the tissues was homogenized with an Ultrasonic Tissue Homogenizer (Ningbo Scientz Biotechnology, Ningbo, China) on ice and the tissue supernatant was centrifuged at 13000 g for 5 min. The levels of IL-6 and IL-1β in the cardiac tissue were measured following the manufacturer's instructions.

Transthoracic Echocardiography in Mice

Cardiac left ventricular function and coronary blood flow were assessed non-invasively at 24 h after CLP using an ultrahigh resolution small animal ultrasound Vevo 2,100 Imaging System (Visual Sonics, Toronto, ON, Canada) equipped with a 30 MHz transducer (Respress and Wehrens, 2010). As described previously (Respress and Wehrens, 2010), mice were anesthetized (2% isoflurane mixed with 0.5 L/min of 100% O_2) before imaging. The animals were removed from the induction chamber and the hair on the chest was removed with a depilatory cream. The anesthetized mice were lying on a heating pad with embedded ECG leads to maintain body temperature. Nose cone connected to the anesthesia system was used to maintain a stable sedation level throughout the process (1.0–1.5% isoflurane mixed with 0.5 L/min of 100% O_2). The level of anesthesia was adjusted to achieve a target heart rate (bpm) of 450 ± 50 beats per minute. Four claws were attached to the ECG electrode with electrode gel. The probe was gently placed on the mouse's chest to locate the left ventricle during the testing. Three cardiac cycles were measured for each mouse and the average value was taken. All data were analyzed after the experiment using the software provided with the ultrasound system.

TABLE 1 | The primer sequences for real-time PCR experiments.

Gene	Forward Primer (5′-3′)	Reverse primer (5′-3′)
GAPDH	TGGTGAAGCAGGCATCTGAG	TGCTGTTGAAGTCGCAGGAG
TLR4	ATGGCATGGCTTACACCACC	GAGGCCAATTTTGTCTCCACA
HMGB1	GGCGAGCATCCTGGCTTATC	GGCTGCTTGTCATCTGCTG
POSTN	CCTGCCCTTATATGCTCTGCT	AAACATGGTCAATAGGCATCACT
GRP78	GTTTGCTGAGGAAGACAAAAAGCTC	CACTTCCATAGAGTTTGCTGATAATTG
IL-6	TAGTCCTTCCTACCCCAATTTCC	TTGGTCCTTAGCCACTCCTTC
IL-1β	GCAACTGTTCCTGAACTCAACT	ATCTTTTGGGGTCCGTCAACT
BNP	CTGAAGGTGCTGTCCCAGATG	GACGGATCCGATCCGGTC
BIRC3	ACGCAGCAATCGTGCATTTTG	CCTATAACGAGGTCACTGACGG
CEBPB	ACACGTGTAACTGTCAGCCG	GCTCGAAACGGAAAAGGTTC
PTGS2	TTCAACACACTCTATCACTGGC	AGAAGCGTTTGCGGTACTCAT
CXCL5	TCCAGCTCGCCATTCATGC	TTGCGGCTATGACTGAGGAAG
CD14	CTCTGTCCTTAAAGCGGCTTAC	GTTGCGGAGGTTCAAGATGTT
FOS	GGTGAAGACCGTGTCAGGAGGCAG	GCCATCTTATTCCGTTCCCTTCGG
CXCL2	CCAACCACCAGGCTACAGG	GCGTCACACTCAAGCTCTG
CXCL12	CGCCAAGG-TCGTCGCCG	TTGGCTCTGGCGATGTGGC
ICAM1	GTGATGCTCAGGTATCCATCCA	CACAGTTCTCAAAGCACAGCG
IL1A	CAGTTCTGCCATTGACCATC	TCTCACTGAAACTCAGCCGT

Cell Cultures

H9C2 cells were trypsinized, washed, and then seeded in a 96-well black plate at a density of 10,000 cells per well in DMEM medium containing 10% fetal bovine serum. The cells were cultured in an incubator with 37°C, 5% CO_2 for 24 h. After stimulation with LPS (1ug/ml), Xuebijing (1:20/1:100), C0127 (1:20/1:100), and C0127-2 (1:20/1:100) were added to the cell culture. DCFH-DA (Jiang et al., 2018) and RHOD2 (Joseph et al., 2017) probes were loaded 12 h later. After incubating at 37°C for 30 min and washing 3 times with PBS, images were taken and analyzed with a PerkinElmer high-content imaging system as described (Lyu et al., 2018b).

Real-Time PCR

Real-time PCR experiments were conducted as described (Xiao et al., 2019). Twenty-four hours after surgery, the mouse hearts were taken out and stored in liquid nitrogen, and then liquid nitrogen was added to pre-cool the mortar. One ml of lysate was added to each tissue sample, and the tissue was ground. The homogenate was separated and the supernatant was removed. RNA was isolated with chloroform, precipitated with isopropyl alcohol, washed with 75% ethanol and was dissolved with ultrapure water. The RNA concentration, purity and integrity were separately measured using Qubit RNA Assay Kit in Qubit 2.0 Fluorometer (Life Technologies, CA, United States), the NanoPhotometer spectrophotometer. Immediately after RNA extraction, total RNA was reverse transcribed into cDNA following the instructions of the Transcriptor First Strand cDNA Synthesis Kit (Roche, Mannheim, Germany). Later real-time PCR was performed in 25ul reaction system. Samples were denatured at 95°C for 30s, annealed at 60°C for 30s, and extended at 72°C for 40s.The relative mRNA level was determined using the comparative CT method and was normalized to the housekeeping gene glyceraldehyde-3-phosphate dehydrogenase (GAPDH). The primers were synthesized by Sangon Company (Shanghai, China).

The primer sequences for real-time PCR were presented in **Table 1**.

Hematoxylin and Eosin Staining

Hematoxylin and eosin (H & E) staining was described previously (Xiao et al., 2019). Briefly, heart tissue was collected 24 h after CLP and was fixed at room temperature in 4% formalin for at least 48 h, dehydrated, and paraffin-embedded. Then the tissue was sectioned in 5-μm thickness, then, stained with H and E at room temperature for 1-2 min. The pictures were taken with an Olympus microscope.

Western Blot

Western Blot was conducted as described with modifications (Zhai and Guo, 2016a). Firstly, the total protein of heart tissue was extracted with a commercial available Protein Extraction Kit Solarbio (Beijing, China). The protein concentration was determined using the Bio-Rad DC Protein Determination Kit, with bovine serum albumin (BSA) as the standard. The proteins were separated by SDS-PAGE on 12% separation gels, transferred to hydrophobic polyvinylidene (PVDF) membranes, and blocked with TBST (Tris-buffered saline with Tween-20) containing 5% non-fat dry milk. Primary antibodies of CXCL2 (1:1,000 dilution), GAPDH (1:4,000 dilution) were incubated at 4°C overnight. Then, membranes were washed three times with TBST and incubated with secondary antibodies for 2 h at room temperature. The immunoblots were developed using the ECL kit.

Statistical Analysis

All tests were performed using GraphPad Prism seven software (GraphPad Software, Inc., La Jolla,CA, United States). All experiments were expressed as the mean ± SEM or mean ± SD. Statistical analysis was carried out using Student's two-tailed t-test for comparison between two groups and One-way analysis of variance (ANOVA) followed by Dunnett's test the data involved three or more groups. $p < 0.05$ was considered as statistically significant.

RESULTS

XBJ Protected the Cardiac Function in a Septic Shock Model

In vivo and *in vitro* experiments were designed to determine the influence of XBJ on the cardiac function in septic shock (**Figure 1**). A septic shock model was established using the cecal ligation and puncture (CLP) procedure. All CLP mice died in 48 h after the procedure and all mice in the sham group survived, indicating the model was established successfully (**Supplementary Figure S2B**). Cardiac function was measured 24 h after CLP to evaluate the impact of XBJ. CLP significantly compromised cardiac function by reducing ejection fraction (EF%), fractional shortening (FS%), left ventricular posterior wall diastole (LVPWd), and left ventricular posterior wall systole (LVPWs) while increasing left ventricular internal diameter diastole (LVIDd) and left ventricular internal diameter systole (LVIDs), respectively, when compared with the saline-treated sham group. XBJ significantly improved EF, FS, LVPWd, LVPWs, LVIDd, and LVIDs in septic mice (**Figure 2**).

XBJ Protected Cardiac Tissue Upon Systemic Infection and Protected Cardiomyocytes From LPS-Induced Mitochondria Ca^{2+} Overload and ROS Production

H & E staining was conducted to determine the morphology of Cardiac tissue in different groups of mice. Consistent with previous observations by dos Santos et al. (dos Santos et al., 2010), no significant differences in necrosis or fibrosis between CLP and sham mice were detected. However, increased edema associated with some myofibrillary loss was observed in CLP mice (**Supplementary Figures S5A,B**). XBJ treatments reduced edema and myofibrillary loss in CLP mice (**Supplementary Figure S5C**). Elisa assay revealed that XBJ significantly reduced N-terminal (NT)-pro hormone BNP (NT-ProBNP) in the peripheral blood (**Figure 3A**). Consistently, the mRNA expression of B-type natriuretic peptide (BNP), a marker of heart failure (McLean et al., 2008) in the heart tissue was also decreased in the XBJ treated group (**Figure 3B**). To determine whether XBJ can protect cardiac tissue on the cellular level, *in vitro* assays were conducted on H9C2 cardiomyocytes upon LPS stimulation. XBJ not only reversed LPS-induced Ca^{2+} overload in the mitochondria (**Figures 4A,C**) but also reduced ROS production (**Figures 4B,D**).

XBJ Down-Regulated the Expression of Infection and Inflammation-Related Signaling in the Cardiac Tissue of Septic Mice

To identify the potential down-stream effectors of XBJ in the cardiac tissue, RNA sequencing was conducted to determine the gene expression profiles of the cardiac tissue in the control and XBJ treated groups. GO and KEGG analysis of the RNA-seq results revealed overwhelming up-regulation of infection and inflammation-related pathways in the CLP group compared to the sham group, including NF-κB, TNF-α, and cytokine-cytokine receptor signaling (data not shown). This is consistent with the results of previous studies (Chen et al., 2018; Villa et al., 1995). XBJ treatment drastically altered the gene expression profile in CLP mice (**Figure 5A**, **Supplementary Figure S3B**). It impacted the expression of 1839 genes in CLP mice for over two-fold (**Figures 5B,D**). GO analysis revealed infection and inflammation-related gene functions were among the top 10 biological processes among the 1839 genes influenced by XBJ, such as response to LPS, response to molecules of bacteria origin, and leukocyte migration (**Supplementary Figures S6A,B**). KEGG analysis of the XBJ-impacted genes revealed that multiple signaling pathways, including Cytokine-cytokine receptor binding, IL17 signaling, NF-κB, and TNF-α signaling, were related to inflammation and cytokine storm (**Supplementary Figures 6C,D**), confirming the results of previous studies that XBJ reduced pro-inflammatory cytokine production in the septic mice (Villa et al., 1995; Chen et al., 2018).

XBJ Down-Regulated the NF-κB Signaling in the Cardiac Tissue of Septic Mice

As an early signaling activated in sepsis, NF-κB activates the transcription of a series of proinflammatory cytokines to activate cytokine storm in septic shock, including TNF-α, IL-1β, and IL-12 (Hotchkiss et al., 2016). Several groups reported that XBJ regulates NF-κB signaling which activates a series of pro-inflammatory cytokines, including TNF-α, IL-6, and IL-1 (Jiang et al., 2013; Chen et al., 2018). Our RNA-seq assay revealed that XBJ regulated NF-κB signaling spanning from the receptor, intracellular effectors, transcription factor, and downstream targets (**Figure 6A**). The expression of at least six genes in NF-κB signaling was confirmed by Real-time PCR assay, including CD14, CXCL2, and Ptgs2 (**Figures 6B–G**).

XBJ Down-Regulated TNF-α Signaling and the Expression of Proinflammatory Cytokines and Cytokine Receptors in the Cardiac Tissue of Septic Mice

Expressed early in the pathogenesis of sepsis, TNF-α is a potential therapeutic target in sepsis (Hotchkiss et al., 2016; Huang et al., 2019). XBJ reduced TNF-α production in patients and pre-clinical models (Chen et al., 2018; He et al., 2018). RNA-seq analysis did not reveal a significant difference of TNF-α expression between CLP and XBJ treated group in the cardiac tissue on RNA level 24 h after CLP (data not shown). However, the expression of multiple TNF-α downstream targets was significantly reduced in XBJ treated septic mice, compared with the CLP group (**Figure 7A**). The expression of more than six genes in TNF-α signaling was confirmed with real-time PCR, including intracellular protein Birc3 (cIAP2), transcription factor C/EPBβ, TNF-α downstream targets ICAM1, CXCL2, CXCL5, FOS, and PTGS2 (COX2) (**Figures 7B–G**). Some of them were molecules in NF-κB signaling (ICAM1, PTGS2 (COX2) (Aronoff, 2012), and Birc3) (**Figure 6**). Besides, XBJ impacted the expression of more than 50 Cytokine-cytokine receptor interaction molecules in the cardiac tissue of septic mice, including key pro-inflammatory cytokines causing tissue damages, such as IL-6, IL-1α and IL-1β (**Figures 8A–D**). The down-regulation of IL-6, IL-1α, and IL-1β by XBJ was further confirmed by Real-time PCR

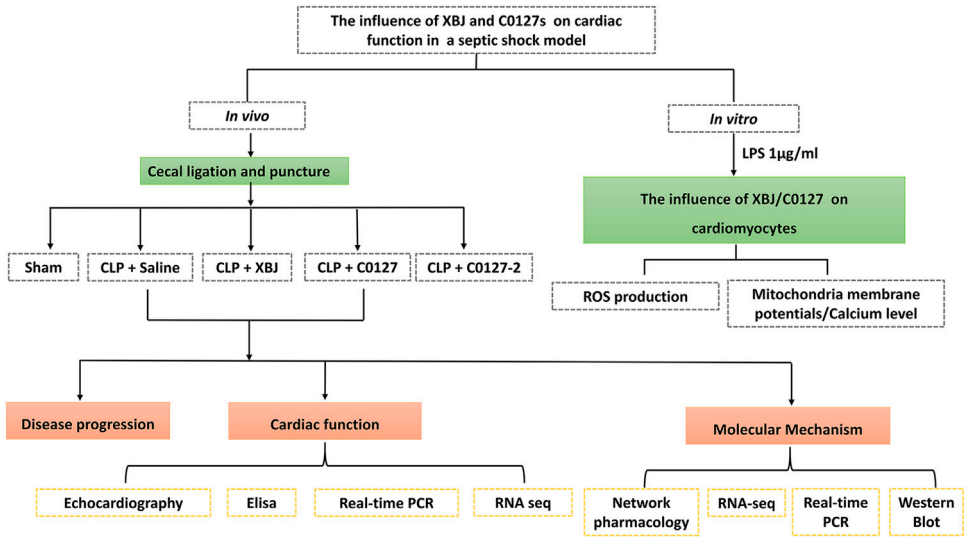

FIGURE 1 | Scheme of the experimental design. *In vivo* and *in vitro* assays were used to determine the impacts of XBJ, C0127, and C0127-2 on infection-induced cardiac dysfunction and potential mechanisms.

(**Figures 8E–G**). Elisa assay confirmed that XBJ inhibited IL-6 and IL-1β in the serum and cardiac tissue (**Figures 9A,B,D,E**). Western Blot analysis validated that XBJ inhibited the expression of CXCL2 in the cardiac tissue (**Figures 9C,F**).

C0127s Represented XBJ Function in Improving the Survival and Protecting the Cardiac Function in a Septic Shock Model

So far, the potential material base of XBJ in sepsis management and infection-related cardiac protection was not clear. Since a combination of four compounds in XBJ (C0127) prevented Candida-induced sepsis and kidney failure (Shang et al., 2019), we hypothesized that XBJ attenuates infection-induced cardiac dysfunction and C0127 plays a major role in managing septic shock and infection-induced cardiac depression. Like XBJ, C0127 and C0127-2 rescued about 35% of septic mice from acute death. There was no significant difference among the treatment groups (**Supplementary Figure S2B**).

C0127s Protected the Cardiac Tissue During Systemic Infection Partially by Preventing LPS Induced Injuries in Cardiomyocytes

Echocardiography was used to address the question of whether active ingredients in XBJ render cardiac protection in septic mice. C0127s showed similar effects as XBJ in most parameters, including LVIDd, LVIDs, LVPWs, LVEF %, and LVFS (**Figure 2**). Nonetheless, C0127s did not significantly alter the LVPWd (**Figure 2D**). C0127-2 treatment did not significantly impact the LVPWs (**Figure 2E**).

Consistently, C0127s reduced N-terminal (NT)-pro hormone BNP (NT-ProBNP) in the peripheral blood (**Figure 3A**). They also reduced the mRNA expression of B-type natriuretic peptide (BNP) (McLean et al., 2008) in the cardiac tissue of septic mice (**Figure 3B**). In addition, the expression of TLR4, its downstream effector HMGB1, periostin, and GRP78 (an effector of ER stress (Shang et al., 2019)) were moderately decreased in C0127s treated groups (**Figures 3C–F**). H&E staining showed that C0127s reduced edema and myofibrillary loss in CLP mice. There were no obvious differences between XBJ and C0127s treated groups (**Supplementary Figures S5C–E**).

On the cellular level, C0127s reversed Ca^{2+} overload in the mitochondria (**Figures 4A,C**) and reduced ROS production (**Figures 4B,D**) in LPS-stimulated H9C2 cells, suggesting the active compounds in XBJ protect cellular functions of cardiomyocytes.

Active Ingredients in XBJ Down-Regulated Gene Expression in Infection and Inflammation-Related Signaling in the Cardiac Tissue of Septic Mice

We conducted an RNA sequencing to determine the impacts of C0127s on the expression profile of the cardiac tissue in septic mice. The gene expression patterns were consistent in each group (**Supplementary Figure S3B**). Similar to XBJ intervention, C0127s shifted the gene expression profile of the CLP group (**Figure 5A**, **Supplementary Figure S3B**). C0127s treatments triggered more changes in the gene expression profile of CLP mice, comparing to the XBJ treated group (**Figure 5B**). Notably, 952 genes were differentially regulated by XBJ and C0127s for >2 fold, revealing similar expression trends as the sham group (**Supplementary Figure S3A**). We further analyzed these genes using GO and KEGG databases as references.

GO analysis revealed infection and inflammation-related gene functions were among the top 10 biological processes in the 952

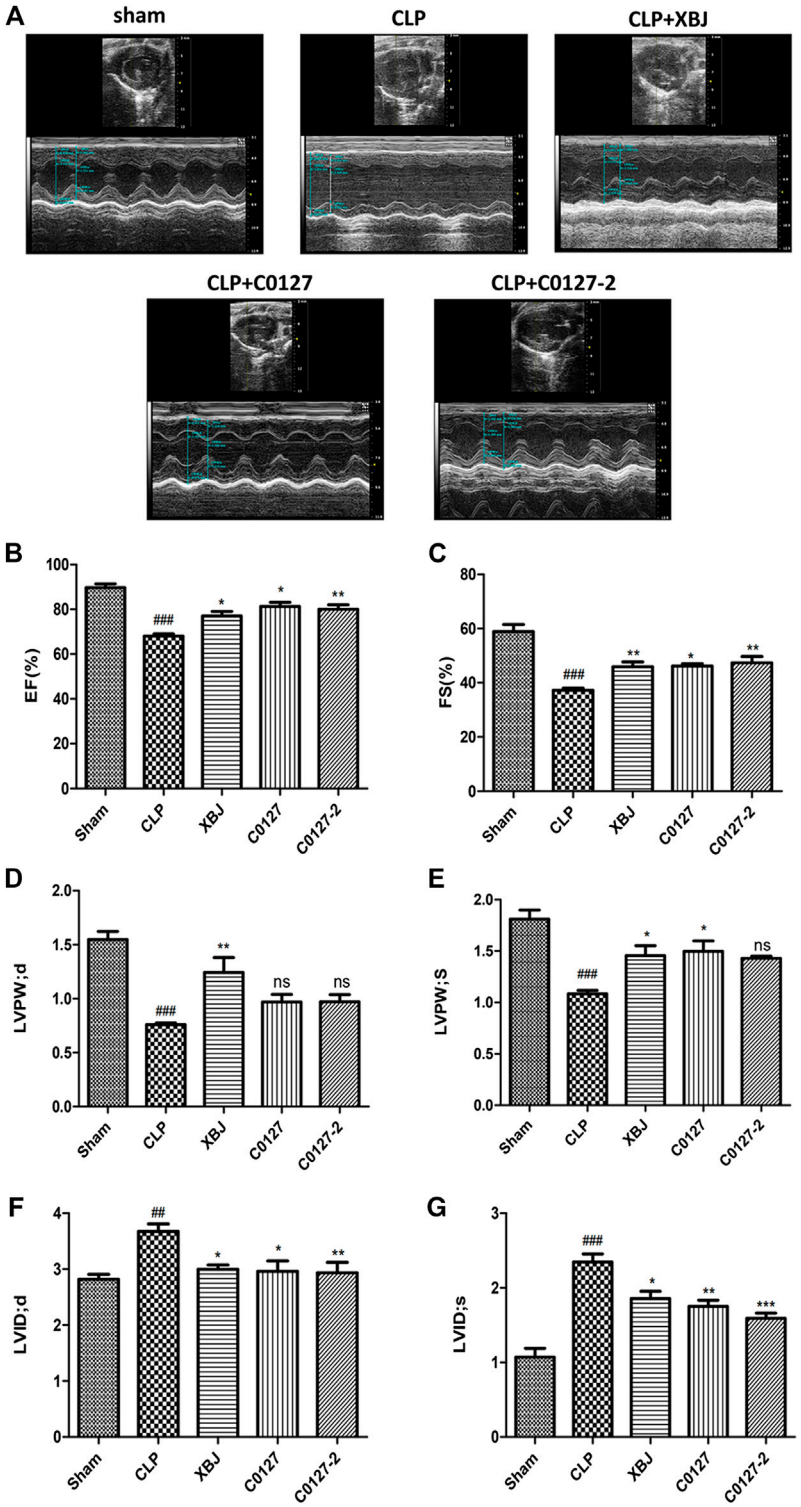

FIGURE 2 | XBJ and key compounds in XBJ protected cardiac function of septic mice. **(A)** Representative images of left ventricular echocardiography. Cardiac performance was determined by echocardiography in different groups as indicated. **(B)** Left ventricularejection fraction (LVEF) %, **(C)** Left ventricular fractional shortening (LVFS) % were measured in M-mode, **(D)** LV posterior wall diastole (LVPWd), **(E)** LV posterior wall systole (LVPWs), **(F)** Left ventricular internal dimensions at diastole (LVIDd), **(G)** Left ventricular internal diameter systole (LVIDs), Results were presented as mean ± SEM (n = 7–10/group). $^{\#}p < 0.05$, $^{\#\#}p < 0.01$, $^{\#\#\#}p < 0.001$ vs. Sham group, $^{*}p < 0.05$, $^{**}p < 0.01$ vs. CLP group.

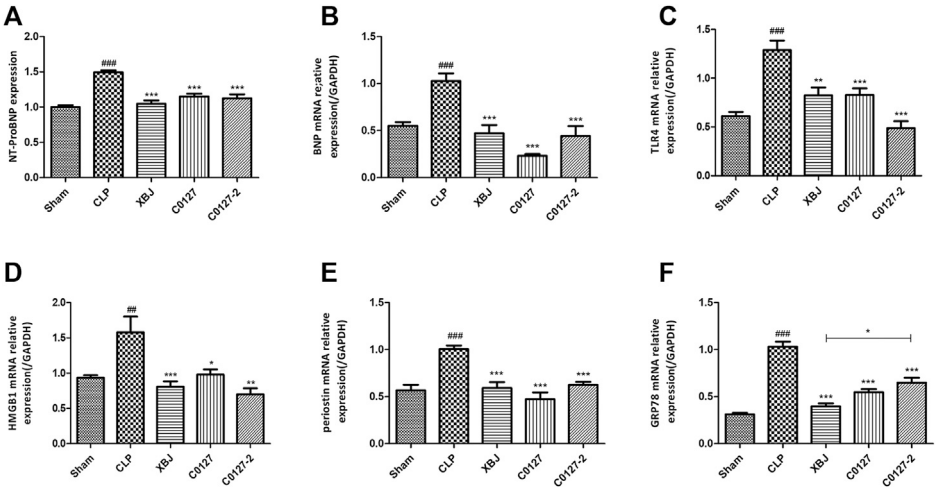

FIGURE 3 | XBJ and C0127s intervention protected hearts in septic mice. **(A)** N-terminal (NT)-pro hormone BNP (NT-ProBNP) levels in different groups were determined by Elisa assay. n = 4/group. mRNA expression of B-type natriuretic peptide (BNP) **(B)**, TLR4 **(C)**, HMGB1**(D)**, Periostin **(E)**, and GRP78 **(F)** in heart tissue of different groups were determined by real-time PCR in heart tissue of different groups. n = 4–5/group. Results were presented as mean ± SEM (n = 4-5/group). $^{\#}p < 0.05$, $^{\#\#}p < 0.01$, $^{\#\#\#}p < 0.001$ vs. Sham group, $^{*}p < 0.05$, $^{**}p < 0.01$, $^{***}p < 0.001$ vs. CLP group.

genes, such as response to LPS, response to molecules of bacteria origin, and leukocyte migration (**Figures 10A,B**). Interestingly, the top three signaling pathways impacted by C0127s among the 952 genes, such as IL17 signaling, Cytokine-cytokine receptor binding, and TNF-A signaling pathway, were also the top pathways impacted by XBJ (**Figures 10C,D**). Like XBJ, C0127s significantly down-regulated gene expression in the infection and proinflammatory signaling (**Figure 10E**). PPAR signaling was up-regulated by XBJ and C0127s (**Figure 10F**).

Active Ingredients in XBJ Down-Regulated the Expression of NF-kB Target Genes in the Cardiac Tissue of Septic Mice

Like XBJ, C0127s also regulated NF-κB signaling spanning from the receptor, intracellular effectors, transcription factors, to the downstream targets (**Figures 6A,B**, and **Supplementary Tables**). Twenty genes in NF-κB signaling which were impacted by XBJ, were also down-regulated by C0127s in the cardiac tissue of the septic mice (**Figure 6A**). The influences of C0127s on the expression of at least six genes in the NF-κB signaling were confirmed by the Real-time PCR assay, including CD14, CXCL2, and Ptgs2 (**Figures 6B–G**).

Active Ingredients in XBJ Down-Regulated TNF-α Signaling and the Expression of Pro-inflammatory Cytokine and Cytokine Receptors in the Cardiac Tissue of Septic Mice

Interestingly, C0127s not only mimicked the effect of XBJ on sepsis progression and cardiac protection, they also regulated the expression of the same genes in TNF-α signaling in the cardiac tissue (**Figure 7A**). The expression of 24 genes in TNF-α signaling and 38 Cytokine-cytokine receptor interaction molecules which were influenced by XBJ, were also similarly impacted by C0127s in the cardiac tissue in septic mice (**Figures 7A**, **8A**, and **Supplementary Tables**). The impacts of C0127s on at least six genes in TNF-α signaling were confirmed with real-time PCR, including intracellular protein Birc3 (cIAP2), transcription factor C/EPBβ, TNF-α downstream targets ICAM1, CXCL2, CXCL5, FOS, and PTGS2 (COX2) (**Figures 7B–E**, **6**). Some of them were also regulated by XBJ and C0127s in NF-κB signaling (ICAM1, PTGS2 (COX2) (Aronoff 2012), and Birc3). Similar to XBJ, C0127s significantly down-regulated the expression of IL-6, IL-1α, and IL-1β in the cardiac tissue of septic mice (**Figures 8B–D**). These results were also confirmed with real-time PCR (**Figures 8E–G**).

C0127s Inhibited the Septic Shock-Induced Myocardial Production of Inflammatory Cytokines/Chemokines

To further evaluate the impacts of C0127s on the inflammatory cytokine/chemokine production, we determine the inflammatory cytokines/chemokines in the serum and cardiac tissue of CLP mice using ELISA and Western blot. CLP induced a drastic increase of IL-6 and IL-1β in the peripheral blood and the cardiac tissue 24 h after the CLP procedure. C0127s pretreatment significantly inhibited the IL-1β and IL-6 production (**Figures 9A,B,D,E**). Western blot further confirmed that C0127s inhibited CXCL2 production in the cardiac tissue (**Figures 9C,F**). Overall, attenuating cytokine storm by XBJ and its key ingredients may play a major role in protecting cardiac function in septic shock.

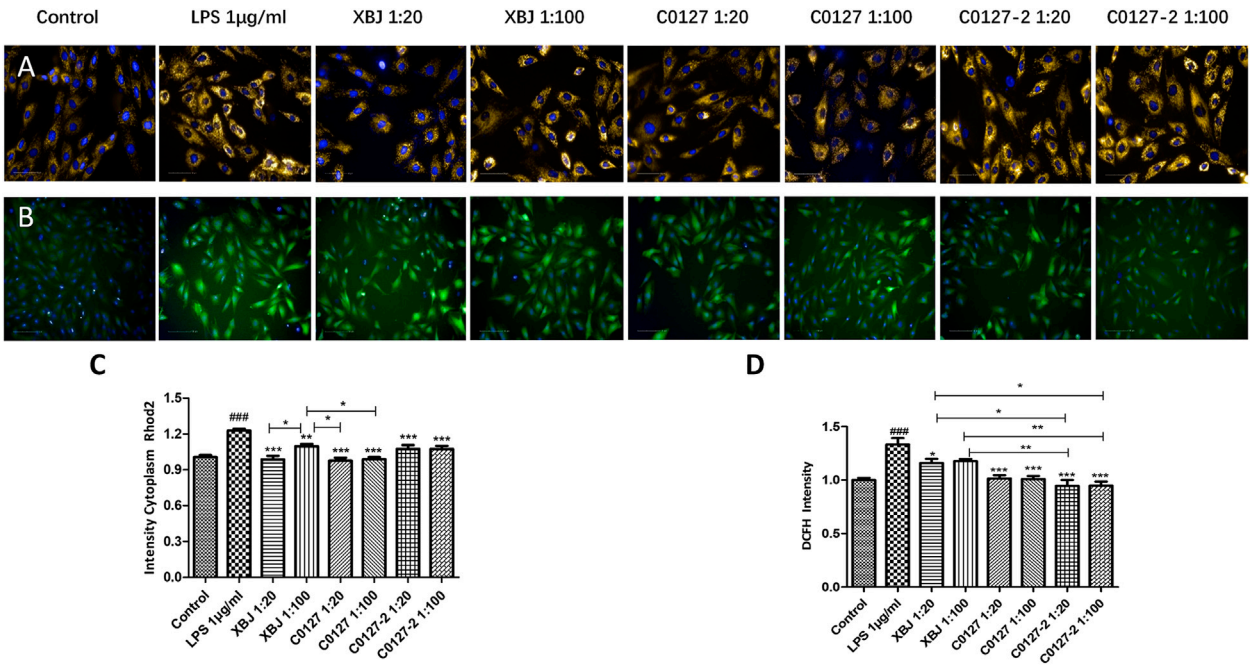

FIGURE 4 | XBJ and C0127s protected mitochondria and reduced ROS production in cardiomyocytes. H9C2 cells were treated with LPS at the presence and absence of XBJ, C0127, and C0127-2 at different concentrations. Rhode2 Florescent probe was used determine Ca^{2+} level in mitochondria and FITC probe was used to detect ROS production in a high-content imaging system. **(A)** Representative images of Ca^{2+} level in mitochondria in different treatments. **(B)** Representative images of ROS level in different treatments. **(C)** Quantification of Ca^{2+} levels in different treatments. **(D)** Quantification of ROS production in different treatments. Results were presented as mean ± SEM. $^{\#}p < 0.05$, $^{\#\#}p < 0.01$, $^{\#\#\#}p < 0.001$ vs. control, $^{*}p < 0.05$, $^{**}p < 0.01$, $^{***}p < 0.001$ vs. LPS treated cells. Experiments were repeated for 3 times.

DISCUSSION

In this study, we focused on the influence of XBJ on infection-induced cardiac dysfunction and the potential molecular mechanism of its effects. We found XBJ and C0127s improved survival and cardiac function after systemic infection. RNA-seq analysis revealed that C0127s exerted similar functions as XBJ in controlling the cytokine storm and inflammation-related signaling pathways, including NF-κB and TNF-α signaling. Real-time PCR experiments confirmed the results of RNA sequencing on the mRNA level. XBJ and C0127s protected the cardiac tissue after the septic shock by normalizing the expression of pro-inflammatory cytokines (IL-6 and IL-1β), chemokines (CXCL2, CXCL5, and CXCL12), and molecules in TNF-α and NF-κB signaling. XBJ and C0127s also protected cardiac function on the cellular level by reducing LPS-induced ROS production and calcium overload in mitochondria of cardiomyocytes. These findings partially explained the protective effects of XBJ in septic shock and severe COVID-19 patients.

C0127s Improved the Survival of Septic Mice

XBJ contains compounds derived from five different Chinese medicinal herbs (Cheng et al., 2016; Chen et al., 2018; Shang et al., 2019). It is not clear which compounds in XBJ played major roles in managing sepsis and septic shock. Our previous work showed C0127, a 4-compound formula, mimicked the effect of XBJ in preventing systemic Candida infection (Shang et al., 2019), indicating high-concentration compounds in XBJ may execute its major functions *in vivo*. Paeoniflorin (Pae) and Hydroxysafflor yellow A (HSYA) are the two compounds with the highest and 2nd highest concentrations in XBJ (Li et al., 2020a) (The chemical structures of compounds in XBJ (including Pae and HSYA) were shown in **Supplementary Figure S1**). They are key indicators for the quality control of this injection (Zhang et al., 2018; Shang et al., 2019). How these two compounds affect septic shock and infection-induced cardiac injuries/dysfunction was not well-understood. XBJ and C0127s significantly improved survival in a murine septic shock model. However, there was no significant difference between the intervention groups, indicating Pae and HSYA are major active compounds in XBJ to manage septic shock.

C0127s Improved the Cardiac Function of Septic Mice

Limited studies were conducted on cardiac dysfunction in systemic infection. Dos Santos et al. observed the down-regulation of PPAR signaling in the cardiac tissue of a murine CLP model (dos Santos et al., 2010). Consistently, our studies revealed XBJ and C0127s significantly up-regulated PPAR signaling which is critical for normal cardiac function (**Supplementary Figures 4A,B**).

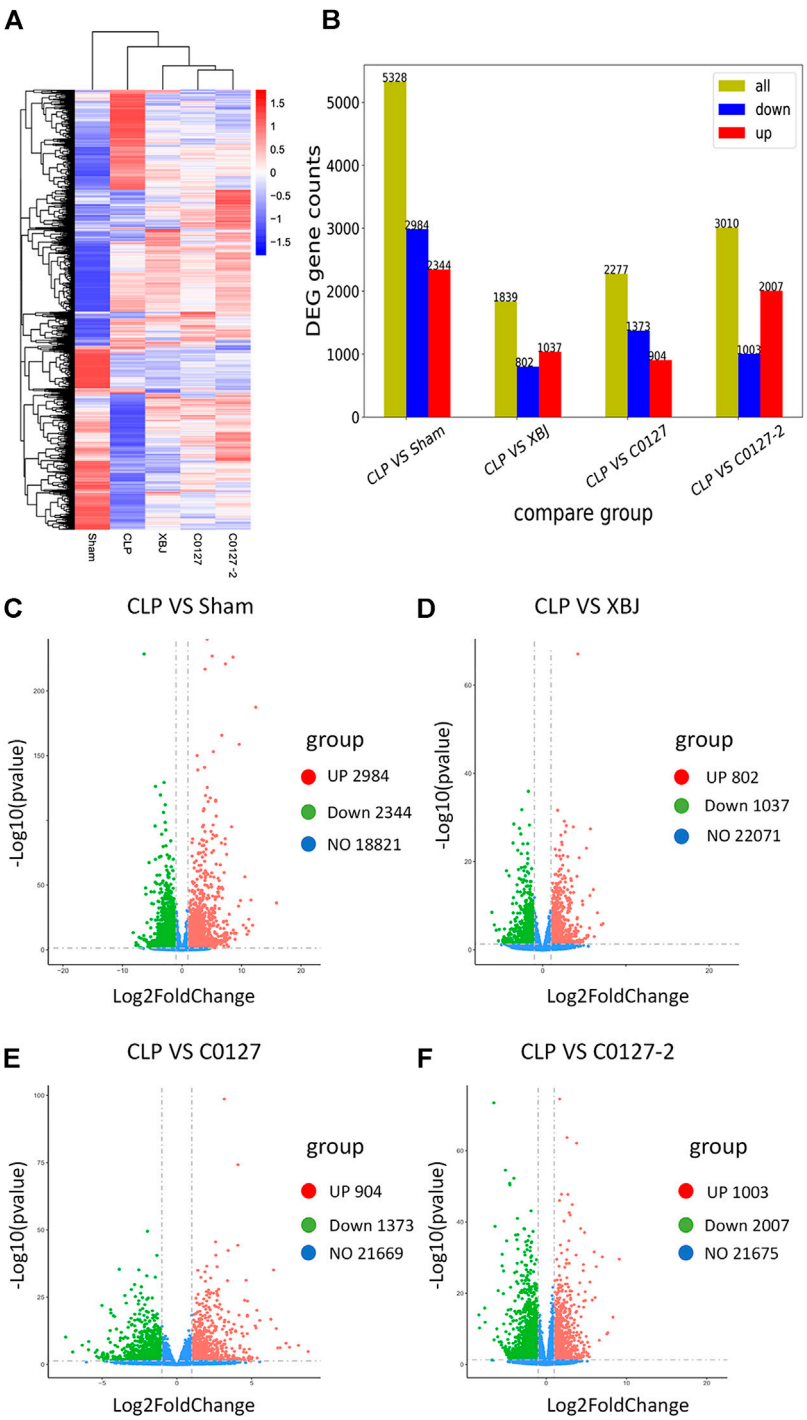

FIGURE 5 | XBJ and C0127s normalized the gene expression profile in the cardiac tissue of septic mice. 24 hs after CLP, mice were euthanized and heart tissue were harvested and subjected to RNA-seq analysis. **(A)** Heat map of the gene expression profiles in different groups. **(B)** Differential gene counts between different groups. **(C–F)** Overall distribution of differentially expressed genes (fold change >2 and *p*-Value <0.05) was reflected by the volcanic map. The X-axis represents the changes of gene expression in different samples and Y-axis represents the statistical significance of the difference in the gene expression. The up-regulated genes were in red and down-regulated genes in green. **(C)** Differentially expressed genes of CLP vs. Sham group; **(D)** Differentially expressed genes of CLP vs. XBJ group; **(E)** Differentially expressed genes of CLP vs. C0127 group; **(F)** Differentially expressed genes of CLP vs. C0127-2 group. n = 4/Group except XBJ and C0127 group (n = 3). *p* value < 0.05, |Log2FoldChange| > 1.

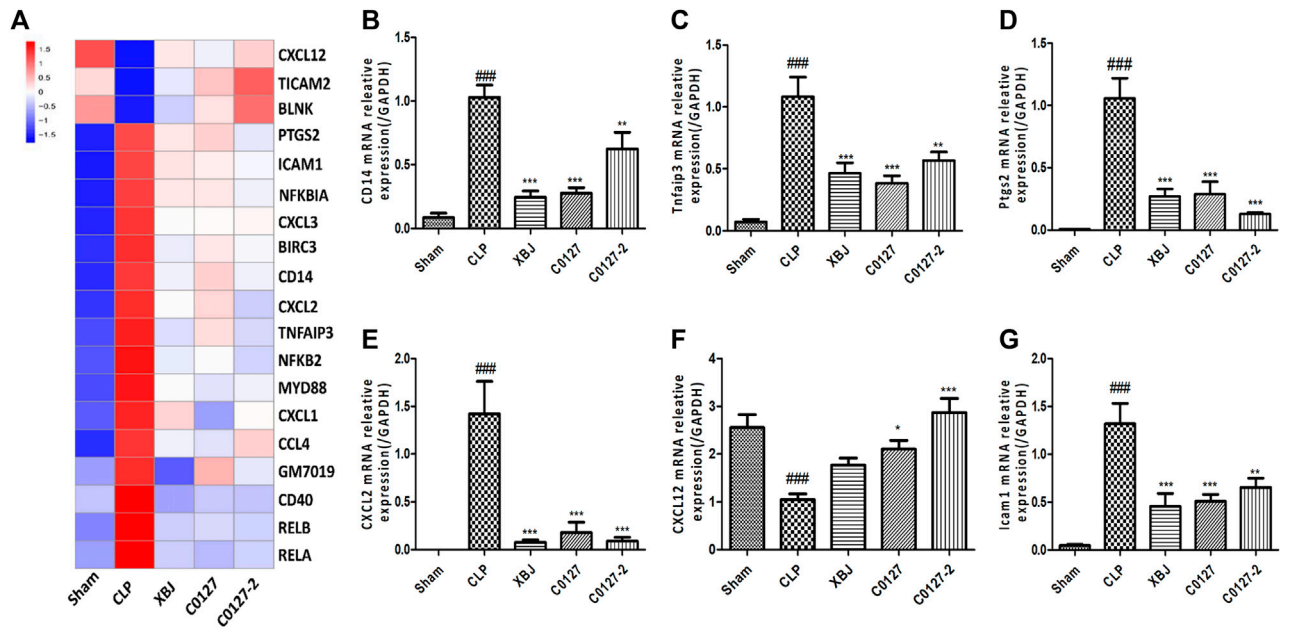

FIGURE 6 | XBJ and C0127s impacted the gene expression of NF-kB signaling pathway in the cardiac tissue of septic mice. **(A)** Heat map of the gene expression influenced by XBJ, C0127, and C0127-2 in NF-κB signaling. **(B–G)** Real-time PCR experiments were conducted to confirm the results of RNA-seq assay. **(B)** CD14; **(C)** TNFAIP3; **(D)** PTGS2; **(E)** CXCL2; **(F)** CXCL12; **(G)** ICAM1. All Real-time PCR experiments were conducted twice. n = 4/group. Results were presented as mean ± SEM (n = 4-5/group). #$p < 0.05$, ##$p < 0.01$, ###$p < 0.001$ vs. Sham group, *$p < 0.05$, **$p < 0.01$, ***$p < 0.001$ vs. CLP group.

From septic shock to COVID-19, systemic infections compromise cardiac function (dos Santos et al., 2010; Zheng et al., 2020). Patients with cardiovascular conditions are more vulnerable to the assaults of systemic bacterial infection (Zhu et al., 2020). Protecting the cardiovascular function of these high-risk patients may save tens of thousands of lives. Our IPA network pharmacology analysis predicted that XBJ, a formula of Chinese medicine activating circulation and removing stasis, may improve cardiovascular function. Some publications also provided evidence for the role of XBJ in regulating cardiovascular function (Zhai and Guo, 2016a).

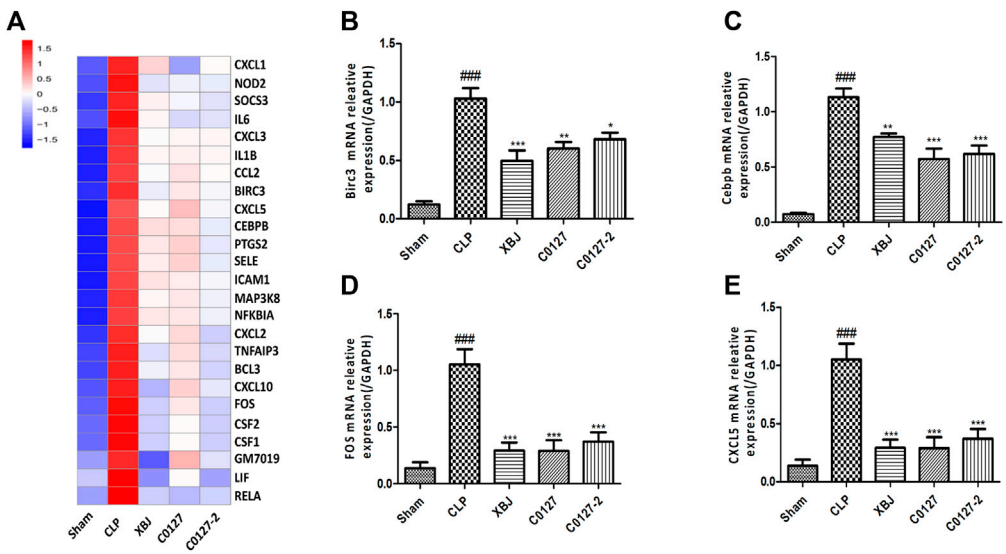

FIGURE 7 | XBJ and C0127s down-regulated TNF-α signaling in the cardiac tissue of septic mice on mRNA level. **(A)** Heat map of the gene expression influenced by XBJ and C0127s in TNF-α signaling in the RNA-seq assay. **(B–E)** Real-time PCR experiments were conducted to confirm the results of RNA-seq assay. B. Birc3; C. C/EBPβ; D. FOS; E. CXCL5. n = 4/group. All Real-time PCR experiments were conducted twice. Results were presented as mean ± SEM (n = 4/group). #$p < 0.05$, ##$p < 0.01$, ###$p < 0.001$ vs. Sham group, *$p < 0.05$, **$p < 0.01$, ***$p < 0.001$ vs. CLP group.

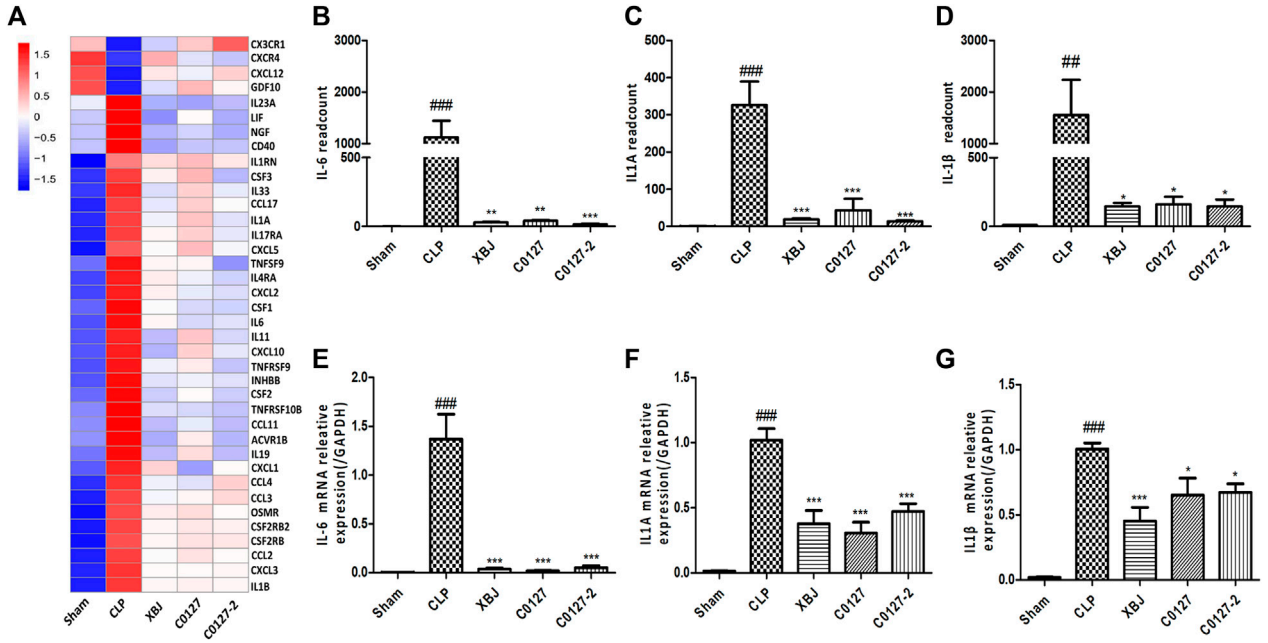

FIGURE 8 | XBJ and C0127s down-regulated the mRNA expression of pro-inflammatory cytokines and cytokine receptors in the cardiac tissue after systemic infection. **(A)** Heat map of the gene expression influenced by XBJ, C0127, and C0127-2 in Cytokine-cytokine receptor interaction in the RNA-seq assay. **(B–D)** The expression of pro-inflammatory cytokines, IL-6, IL-1α, and IL-1β were detected in the cardiac tissue of different groups of mice. B. IL-6; C. IL-1α; D. IL-1β. **(E–G)** The expression of pro-inflammatory cytokines in the cardiac tissue of different groups of mice was determined by Real-time PCR. E. IL-6; F. IL-1α; G. IL-1β. n = 4-5/group. Results were presented as mean ± SEM (n = 4-5/group). #$p < 0.05$, ##$p < 0.01$, ###$p < 0.001$ vs. Sham group, *$p < 0.05$, **$p < 0.01$, ***$p < 0.001$ vs. CLP group.

In a well-established septic shock-induced myocardial dysfunction model, we observed similar phenotypes as previously described (dos Santos et al., 2010). Overall, C0127s showed similar effects as XBJ in restoring cardiac functions in the septic mice (**Figure 2**). No significant differences were observed between C0127 and C0127-2

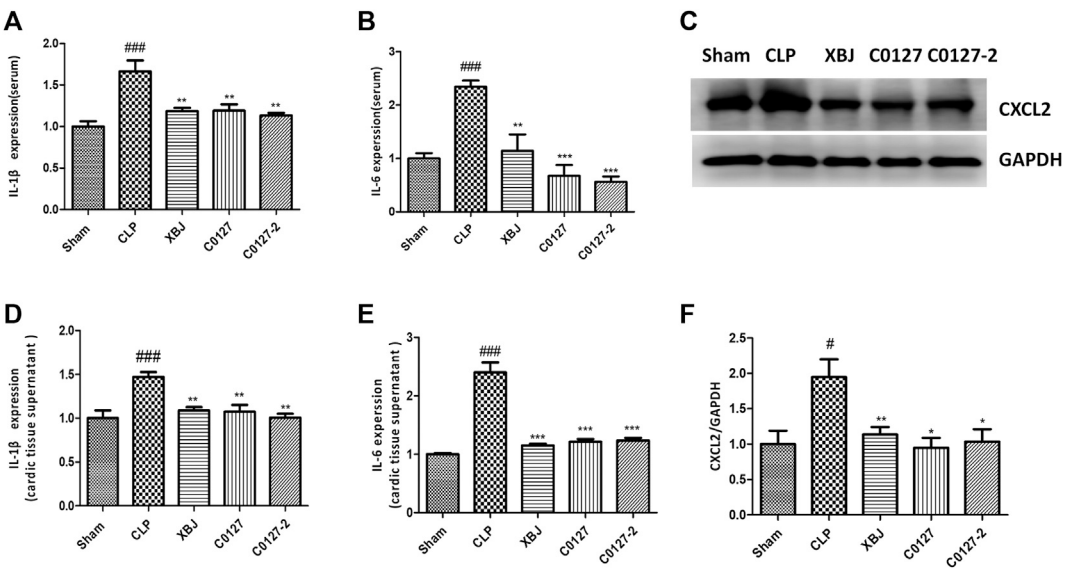

FIGURE 9 | XBJ and C0127s down-regulated the protein expression of pro-inflammatory cytokines/chemokines in the septic mice. **(A,B)** The serum levels of **(A)** IL-1β and **(B)** IL-6 were measured by ELISA. Each bar was represented as mean ± SEM (n = 5); **(D,E)** The levels of **(D)** IL-1β and **(E)** IL-6 in heart tissues were measured by ELISA. Each bar was represented as mean ± SEM (n = 5); **(C,F)** The expression of CXCL2 in the heart tissue of different groups was determined by western blot. Each bar was represented as mean ± SEM (n = 5/group). #$p < 0.05$, ##$p < 0.01$, ###$p < 0.001$ vs. Sham group, *$p < 0.05$, **$p < 0.01$, ***$p < 0.001$ vs. CLP group. Experiments were repeated for three times.

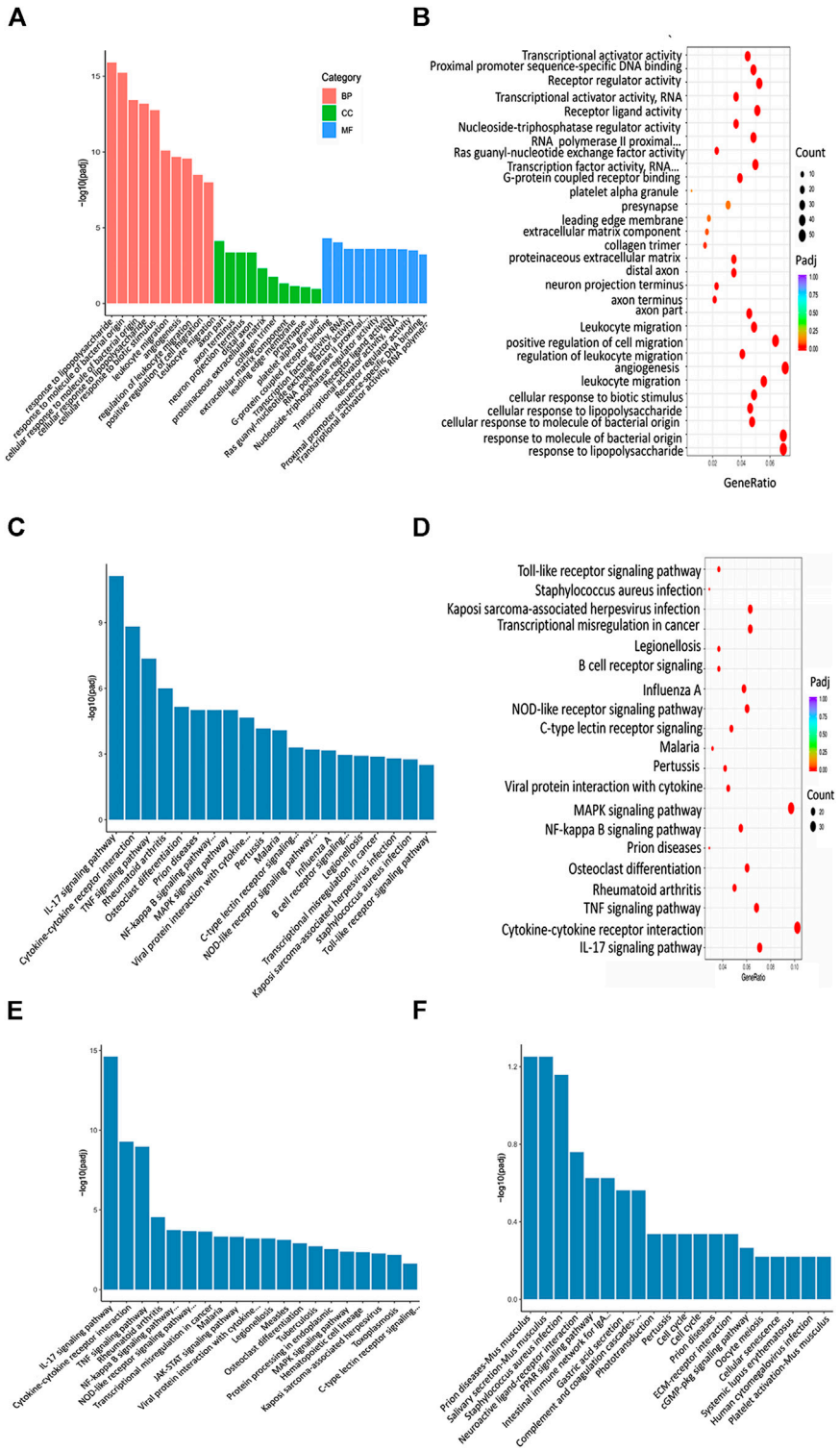

FIGURE 10 | XBJ and C0127s regulated infection and inflammation related signaling in septic shock. **(A,B)** GO analysis of the top 30 functions impacted by XBJ and C0127s. BP, biological process, CC, cellular component, MF, molecular function. Padj: P value adjusted. **(C,D)** The KEGG 676 analysis of top 20 pathways of the 952 genes impacted by XBJ and C0127s for >2 fold. The pathways/functions were ranked from left to right by –log (P value adjusted). **(E,F)** KEGG analysis of the top signaling pathways up-regulated **(E)** or down-regulated **(F)** by XBJ and C0127s were presented.

group, suggesting paeoniflorin and HSYA are the core compounds in XBJ for cardiac protection.

Two previous studies suggested paeoniflorin rendered cardiac protection in LPS-induced endotoxemia models (Zhai and Guo, 2016b; Liu et al., 2016). Liu et al. found 12 mg/kg paeoniflorin once/day reduced plasma CK-MB (a biomarker of severe heart damage) to normal level 72 h after the LPS administration (5 mg/kg) in a rat model (Liu et al., 2016). Zhai and Guo revealed that paeoniflorin reduced pro-inflammatory cytokine production in the cardiac tissue of a LPS-induced cardiac-dysfunction mouse model (Zhai and Guo, 2016b). Treating mice with paeoniflorin 15 mg/kg/day for 3 days before LPS injection (10 mg/kg) improved cardiac function in endotoxemic mice and reduced LPS-induced Leukocyte infiltration in the cardiac tissue. It reduced LPS-induced cytokine production on mRNA level (in the cardiac tissue) and protein level (in the serum), including IL-6, TNF-α, IL-12, IL-1β, and IFNγ (Zhai and Guo, 2016b). These results indicated that paeoniflorin may play an important role in XBJ and C0127s to reduce the cytokine expression in the cardiac tissue of the septic mice in our study.

HSYA, which promotes angiogenesis, was known for its anti-thrombosis effect. It is used to treat stroke and ischaemic cardiovascular diseases in China. HSYA (240 mg/kg/day) rescued CD4 T cell apoptosis in a mouse CLP model. HSYA (240 mg/kg/day) also protected mice from LPS-induced lung injury (Liu et al., 2014b; Wang et al., 2017). Another study discovered that HSYA (25 mg/kg/day) stimulated angiogenesis to improve cardiac function in a murine ischaemic model (Zou et al., 2018). This effect was mediated by nucleolin, a DNA-binding molecule that regulates angiogenesis. Huber et al. found HSYA can enter cardiac myocytes to reduce anoxia/reoxygenation-induced damage by interacting with the mitochondrial permeability transition pore *in vitro* (Huber et al., 2018).

So far, it is not clear whether HSYA can improve survival and cardiac function in CLP mice. Overall, our and other groups' results suggested paeoniflorin and HSYA may synergistically improve cardiac function during systemic infection by reducing cytokine/chemokine production.

Biochemical and molecular analysis *in vivo* and *in vitro* further confirmed the results of echocardiography. C0127s not only reduced NT-pro-BNP on the protein level but also inhibited other drivers of cardiac dysfunction, such as IL-6, IL-1β and CXCL2 expression on mRNA and protein level (**Figures 3A,B**, **8**, **9**) (McLean et al., 2008; Zhu et al., 2020). They also reduced LPS induced ROS production and Calcium overload in the mitochondria of cardiomyocytes (**Figure 4**).

The increased GRP78 expression in the cardiac tissue of CLP mice was a response to the CLP- induced acute cardiac stress (**Figure 3F**). This result echoed findings by a recent study (Bi et al., 2018). Bi et al. revealed that overexpressing GRP78 protected myocytes from I/R-induced cell death by activating AKT signaling. It is likely that the decreased expression of GRP78 after XBJ and C0127s treatment indicated the reduced ER stress an improved cardiac function in CLP mice.

XBJ and C0127s Directly or Indirectly Attenuate Cytokine Storm to Protect Cardiac Function and Improve Survival in Septic Shock

To explore the molecular mechanism of XBJ on infection-induced cardiac dysfunction, we conducted RNA–seq assay in different groups of mice to determine the impact of XBJ and C0127s on the gene expression profile of septic hearts. GO and KEGG analysis revealed that XBJ and C0127s regulate infection and inflammation related signalings in septic mice (**Figure 10**). The most pronounced change in the gene expression profile of XBJ-treated CLP mice was the pan-reduction of gene expression related to cytokine storms during infection (**Figure 10** and **Supplementary Figures S6C,D**). Not only pro-inflammatory cytokines such as IL-1α, IL-1β, and IL-6 but also the cytokine receptors, cellular mediators, downstream transcription factors, and target genes were down-regulated by the treatments (**Figures 6**, **7**, **8**). Consistently, C0127s also down-regulated the same groups of pro-inflammatory cytokines and receptors (**Figures 6**, **7**, **8**), indicating paeoniflorin and HSYA are the core compounds in XBJ to regulate the local expression of inflammation-related signaling in the cardiac tissue of septic mice. CD40-NF-κB signaling pathways is a representative signaling pathway significantly down-regulated by XBJ and C0127s. CD154, a marker of cardiac ischemia and the ligand of CD40, was often elevated in septic patients (McLean et al., 2008). Both CD154 and CD40 are potential therapeutic targets of cardiovascular disease (Bosmans et al., 2020). In our study, XBJ and C0127s significantly reduced the expression of CD40. In addition, the expression of NF-κB p65 subunit (RELA) was also reduced upon XBJ and C0127s treatments (**Figure 6A**). This result was consistent with a previous report that XBJ reduced NF-κB protein expression in the lung (He et al., 2018).

Additionally, XBJ and C0127s down-regulated the mRNA and protein expression of NF-κB targets, IL-6 and IL-1β, in the cardiac tissue. Given that IL-6 is a marker of cardiac ischemia (McLean et al., 2008), XBJ and C0127s may improve circulation in the cardiac function of septic mice. These results suggested Pae and HSYA are core compounds in XBJ to regulate pro-inflammation cytokine production in the cardiac tissue.

The Influence of XBJ and C0127s on CXCL2

CLP stimulated the expression of a series of chemokines in the cardiac tissue, including CXCL1, CXCL2, and CXCL5. XBJ and C0127s significantly down-regulated the expression of these chemokines (**Figures 7A**, **8A**, **9A**). Real-time PCR confirmed these effects on CXCL2, CXCL5, and CXCL12 in the cardiac tissue (**Figures 8E**, **9C,F**). Western blot analysis further validated that XBJ and C0127s inhibited CXCL2 protein expression (**Figures 4E,F**). Consistent with our results, Li et al., found XBJ down-regulated CXCL2 expression in a methicillin-resistant *Staphylococcus aureus* (MRSA) infection model (Li et al., 2020a).

CXCL2, which is also known as Macrophage Inflammatory Protein 2 (MIP-2) and GRO2, is a small cytokine that is expressed in a spectrum of tissues and organs including the heart (https://www.ncbi.nlm.nih.gov/gene/20310). CXCL1 (GRO1) shares 90%

of sequences with CXCL2. Both CXCL1 and CXCL2 can be secreted by monocytes and neutrophils at the site of inflammation. They function through the chemokine receptor CXCR2 to act as chemotactic agents for leukocytes and hematopoietic cells (Sawant et al., 2020).

Two studies revealed that CXCL2 polymorphism is related to the severity of sepsis in patients, suggesting CXCL2 playing an important role in the development of severe sepsis (Flores et al., 2006; Villar et al., 2007). IL-17, NF-κB, and IL-1β can stimulate CXCL2 expression in pathological conditions (Guo et al., 2020). CXCL2 is believed to be a critical therapeutic target in myocardial infarctions (MI) (Guo et al., 2020). A high level of CXCL2 worsens MI by stimulating neutrophil-mediated cardiac injuries. Interventions that down-regulate CXCL2 relieved neutrophil-mediated cardiac injuries (Montecucco et al., 2010; Montecucco et al., 2013; Mylonas et al., 2017). Our results suggested XBJ improves cardiac function partially by reducing CXCL1 and CXCL2 production to limit the neutrophil-mediated cardiac injury. Interestingly, C0127s also down-regulated the mRNA and protein expression of CXCL2 (**Figures 6A,E**, **9C,F**). How XBJ and C0127s regulate CXCL2 signaling in different cell types remains to be determined.

The balance of CXCL12 (SDF-1) and CXCL2 chemokines favors neutrophil retention in the BM in steady-state conditions (Eash et al., 2010; Day and Link, 2012). Under stress situations such as infections, G-CSF induces massive neutrophil egress into the circulation. G-CSF inhibits SDF-1 expression in the BM. It also causes cleavage of surface CXCR4 (a CXCL12 receptor) on neutrophils, disrupting SDF-1/CXCR4 signaling, which leads to their mobilization (Day and Link, 2012). Guan et al. found that combining CTCE (a peptide analogue of CXCL12) and antibiotics improves survival and neutrophil recruitment in a murine sepsis model (Guan et al., 2014). However, Liehn et al.'s results raised a concern about the expression of endogenous CXCL12 on cardiovascular function in a myocardial infarction (MI) model (Liehn et al., 2011). Increased expression of CXCL12 in the cardiac tissue after XBJ and C0127s treatments may indicate a balanced neutrophil mobilization or improved clearance of infection (**Figure 6F**). More studies need to be conducted to explain this phenomenon in the cardiac tissue.

The Implication of This Study for COVID-19 Management

COVID-19 patients having cardiac complications are suffering the second-highest mortality rate in the global pandemic. Cardiovascular complications occurred in up to 16% of critically ill COVID-19 patients (Li et al., 2020a; Zhu et al., 2020). Myocardial injury is a leading cause of severe illness and mortality in SARS-CoV-2 infection (Tersalvi et al., 2020; Zheng et al., 2020). About 5% of COVID-19 patients undergo septic shock and multiple organ failure (Russell et al., 2020; Zhu et al., 2020). Stunningly, 70% of patients who died of COVID-19 had septic shock (Hantoushzadeh and Norooznezhad, 2020). Sharing multiple traits with septic shock, severe COVID-19 was defined as viral sepsis (Shankar-Hari et al., 2016; Li et al., 2020a).

High levels of IL-6 and IL-1β drive the cytokine storm in severe COVID-19 patients, causing organ injuries and MODS. Deceased COVID-19 patients had significantly higher IL-6 expression than the survivors of COVID-19 (Ruan et al., 2020; Zhou et al., 2020). As a promising therapeutic target of severe COVID-19, IL-6 was downregulated by XBJ in clinical studies and pre-clinical studies.

Approved to treat COVID-19 in China, XBJ was effective in managing moderate and severe COVID-19. The results of this study partially revealed the working mechanism of XBJ in protecting cardiac function and controlling cytokine storm upon systemic infection. Our results suggested that XBJ might be a safe option for protecting cardiac function, controlling infection-induced cytokine storm, and preventing bacteria superinfection in severe COVID-19 patients.

Future Directions

Clearing of dying/dead cells and extracellular matrix is a key function of cardiac resident macrophages (Li et al., 2021). Enhancing macrophage efferocytosis can activate the anti-inflammatory program and reduce the damages caused by apoptotic neutrophils (Greenlee-Wacker, 2016). Limited studies have been conducted on the impact of cardiac resident macrophages on sepsis-induced cardiac dysfunction and the influence of XBJ on cardiac resident macrophages. Liu et al. found XBJ (5 mg/mL) enhanced the survival and the expression of M2 markers in LPS-stimulated mouse peritoneal macrophages (Liu et al., 2015). It is important to understand the influence of XBJ and C0127s on the bone marrow derived macrophages and cardiac resident macrophages in sepsis. Several important questions remain to be answered. It will be important to understand the influences of bone marrow-derived macrophages and cardiac resident macrophages on the cardiac function in septic shock models. It is not clear how XBJ and C0127s influence the function of macrophages in the cardiac tissue of the CLP mice. Whether they influence the infiltration of bone marrow derived macrophages in the CLP model is not known either.

GDF3 and Sectm1a have been shown to influence cardiac function of septic mice and are potential therapeutic targets of sepsis-induced cardiac dysfunction (Li et al., 2020b; Mu et al., 2020; Wang et al., 2020). XBJ and C0127s may impact cardiac function of septic mice by influence these potential therapeutic targets. How XBJ and C0127s regulate these signaling remains to be unveiled.

SUMMARY

In summary, XBJ protects cardiac function partially by easing the cytokine storm during systemic infection. Paeoniflorin and Hydroxysafflor yellow A are key compounds in XBJ which exert major functions of XBJ in managing septic shock. Like XBJ, they protected cardiac function in septic shock. NF-κB, TNF-α, and CXCL2 signaling are potential targets of XBJ and C0127s in infection-induced cardiac dysfunction. This work indicated XBJ may attenuate cytokine storm to protect the cardiac function of septic shock and COVID-19 patients.

DATA AVAILABILITY STATEMENT

All datasets generated for this study are included in the article and the **Supplementary data**.

ETHICS STATEMENT

This study was carried out in accordance with the recommendations of the Guide for the Care and Use of Laboratory Animals (NIH Publication No. 85-23, revised 1996, USA) and the recommendations in the Guidance for the Care and Use of Laboratory Animals issued by the Ministry of Science and Technology of China. All experiments were approved by the Experimental Animal Ethics Committee of Tianjin University of Traditional Chinese Medicine (Tianjin, China) and performed in accordance with its guidelines (license number: TCM-LAE-20170017).

AUTHOR CONTRIBUTIONS

X-TW, YF, and YZ designed the study and developed the methodologies. X-TW, YF, ZP, Y-YA, TS, SH, G-XX, conducted research. X-TW, YF, TS, XC, TW, HZ, XG, YZ, YW, J-HZ analyzed the data, reviewed the manuscript, and contributed critical reagents. X-TW, YF, and YZ wrote and revised the manuscript.

FUNDING

This project was supported by the National Natural Science Foundation of China (no: 81774018, 81973581, 81873037); Tianjin Municipal Education Commission (Grant number: TD13-5046); Tianjin Municipal Science and Technology Bureau (No.20ZYJDJC00070).

ACKNOWLEDGMENTS

We thank our colleagues for their supports. We thank Zhengcan Zhou, Xiao-Li Du, Yu-Le Wang, and Zhi-Xiong Li for their technical supports and constructive discussions. We thank Feng Wang (Tianjin Medical University) and Ruiqiong Ran for their constructive comments and editing our manuscript.

SUPPLEMENTARY MATERIAL

The Supplementary Material for this article can be found online at: https://www.frontiersin.org/articles/10.3389/fphar.2020.614024/full#supplementary-material.

REFERENCES

Abraham, E., Anzueto, A., Gutierrez, G., Tessler, S., San Pedro, G., Wunderink, R., et al. (1998). Double-blind randomised controlled trial of monoclonal antibody to human tumour necrosis factor in treatment of septic shock. NORASEPT II Study Group. *Lancet*. 351, 929–933.

Aronoff, D. M. (2012). Cyclooxygenase inhibition in sepsis: is there life after death?. *Mediat. Inflamm*. 2012, 696897. doi:10.1155/2012/696897

Barth, E., Radermacher, P., Thiemermann, C., Weber, S., Georgieff, M., and Albuszies, G. (2006). Role of inducible nitric oxide synthase in the reduced responsiveness of the myocardium to catecholamines in a hyperdynamic, murine model of septic shock. *Crit. Care Med*. 34, 307–313. doi:10.1097/01.ccm.0000199070.46812.21

Beesley, S. J., Weber, G., Sarge, T., Nikravan, S., Grissom, C. K., Lanspa, M. J., et al. (2018). Septic cardiomyopathy. *Crit. Care Med*. 46, 625–634. doi:10.1097/CCM.0000000000002851

Bi, X., Zhang, G., Wang, X., Nguyen, C., May, H. I., Li, X., et al. (2018). Endoplasmic reticulum chaperone GRP78 protects heart from ischemia/reperfusion injury through akt activation. *Circ. Res*. 122, 1545–1554. doi:10.1161/CIRCRESAHA.117.312641

Bosmans, L. A., Bosch, L., Kusters, P. J. H., Lutgens, E., and Seijkens, T. T. P. (2020). The CD40-CD40L dyad as immunotherapeutic target in cardiovascular disease. *J. Cardiovasc. Transl. Res*. doi:10.1007/s12265-020-09994-3

Cao, W., Zhang, W., Liu, J., Wang, Y., Peng, X., Lu, D., et al. (2011). Paeoniflorin improves survival in LPS-challenged mice through the suppression of TNF-α and IL-1β release and augmentation of IL-10 production. *Int. Immunopharm*. 11, 172–178. doi:10.1016/j.intimp.2010.11.012

Chen, X., Feng, Y., Shen, X., Pan, G., Fan, G., Gao, X., et al. (2018). Anti-sepsis protection of Xuebijing injection is mediated by differential regulation of pro- and anti-inflammatory Th17 and T regulatory cells in a murine model of polymicrobial sepsis. *J. Ethnopharmacol*. 211, 358–365. doi:10.1016/j.jep.2017.10.001

Cheng, C., Lin, J. Z., Li, L., Yang, J. L., Jia, W. W., Huang, Y. H., et al. (2016). Pharmacokinetics and disposition of monoterpene glycosides derived from Paeonia lactiflora roots (Chishao) after intravenous dosing of antiseptic XueBiJing injection in human subjects and rats. *Acta Pharmacol. Sin*. 37, 530–544. doi:10.1038/aps.2015.103

Day, R. B., and Link, D. C. (2012). Regulation of neutrophil trafficking from the bone marrow. *Cell. Mol. Life Sci*. 69, 1415–1423. doi:10.1007/s00018-011-0870-8

dos Santos, C. C., Gattas, D. J., Tsoporis, J. N., Smeding, L., Kabir, G., Masoom, H., et al. (2010). Sepsis-induced myocardial depression is associated with transcriptional changes in energy metabolism and contractile related genes: a physiological and gene expression-based approach. *Crit. Care Med*. 38, 894–902. doi:10.1097/CCM.0b013e3181ce4e50

Eash, K. J., Greenbaum, A. M., Gopalan, P. K., and Link, D. C. (2010). CXCR2 and CXCR4 antagonistically regulate neutrophil trafficking from murine bone marrow. *J. Clin. Invest*. 120, 2423–2431. doi:10.1172/JCI41649

Ehrman, R. R., Sullivan, A. N., Favot, M. J., Sherwin, R. L., Reynolds, C. A., Abidov, A., et al. (2018). Pathophysiology, echocardiographic evaluation, biomarker findings, and prognostic implications of septic cardiomyopathy: a review of the literature. *Crit. Care*. 22, 112. doi:10.1186/s13054-018-2043-8

Fan, T., Chen, Y., Bai, Y., Ma, F., Wang, H., Yang, Y., et al. (2020). Analysis of medication characteristics of traditional Chinese medicine in treating COVID-19 based on data mining. *Zhejiang Da Xue Xue Bao Yi Xue Ban*. 49, 260–269. doi:10.3785/j.issn.1008-9292.2020.03.14

Flores, C., Maca-Meyer, N., Perez-Mendez, L., Sanguesa, R., Espinosa, E., Muriel, A., et al. (2006). A CXCL2 tandem repeat promoter polymorphism is associated with susceptibility to severe sepsis in the Spanish population. *Gene Immun*. 7, 141–149. doi:10.1038/sj.gene.6364280

Gordon, A. C., Perkins, G. D., Singer, M., McAuley, D. F., Orme, R. M., Santhakumaran, S., et al. (2016). Levosimendan for the prevention of acute organ dysfunction in sepsis. *N. Engl. J. Med*. 375, 1638–1648. doi:10.1056/NEJMoa1609409

Greenlee-Wacker, M. C. (2016). Clearance of apoptotic neutrophils and resolution of inflammation. *Immunol. Rev*. 273, 357–370. doi:10.1111/imr.12453

Guan, S., Guo, C., Zingarelli, B., Wang, L., Halushka, P. V., Cook, J. A., et al. (2014). Combined treatment with a CXCL12 analogue and antibiotics improves survival and neutrophil recruitment and function in murine sepsis, *Immunology*. 144, 405–411. doi:10.1111/imm.12382

Guo, L. Y., Yang, F., Peng, L. J., Li, Y. B., and Wang, A. P. (2020). CXCL2, a new critical factor and therapeutic target for cardiovascular diseases. *Clin. Exp. Hypertens*. 42, 428–437. doi:10.1080/10641963.2019.1693585

Hantoushzadeh, S., and Norooznezhad, A. H. (2020). Possible cause of inflammatory storm and septic shock in patients diagnosed with (COVID-19). *Arch. Med. Res.* 51 (4), 347–348. doi:10.1016/j.arcmed.2020.03.015

He, F., Wang, J., Liu, Y., Wang, X., Cai, N., Wu, C., et al. (2018). Xuebijing injection induces anti-inflammatory-like effects and downregulates the expression of TLR4 and NF-κB in lung injury caused by dichlorvos poisoning. *Biomed. Pharmacother*. 106, 1404–1411. doi:10.1016/j.biopha.2018.07.111

Hotchkiss, R. S., Moldawer, L. L., Opal, S. M., Reinhart, K., Turnbull, I. R., and Vincent, J. L. (2016). Sepsis and septic shock. *Nat. Rev. Dis. Primers* 2, 16045. doi:10.1038/nrdp.2016.45

Huang, M., Cai, S., and Su, J. (2019). The pathogenesis of sepsis and potential therapeutic targets. *Int. J. Mol. Sci*. 20(21), 5376. doi:10.3390/ijms20215376

Huber, G. A., Priest, S. M., and Geisbuhler, T. P. (2018). Cardioprotective effect of hydroxysafflor yellow A via the cardiac permeability transition pore. *Planta Med*. 84, 507–518. doi:10.1055/s-0043-122501

Jiang, J., Yin, H., Sun, Y., Huang, H., and Hu, X. (2018). Clonorchis sinensis cyclophilin A immunization protected mice from CLP-induced sepsis. *Int. Immunopharm*. 59, 347–353. doi:10.1016/j.intimp.2018.03.039

Jiang, M., Zhou, M., Han, Y., Xing, L., Zhao, H., Dong, et al. (2013). Identification of NF-κB Inhibitors in Xuebijing injection for sepsis treatment based on bioactivity-integrated UPLC-Q/TOF. *J. Ethnopharmacol.* 147, 426–433. doi:10.1016/j.jep.2013.03.032

Joseph, L. C., Kokkinaki, D., Valenti, M. C., Kim, G. J., Barca, E., Tomar, D., et al. (2017). Inhibition of NADPH oxidase 2 (NOX2) prevents sepsis-induced cardiomyopathy by improving calcium handling and mitochondrial function. *JCI insight*. 2, e94248. doi:10.1172/jci.insight.94248

Li, T., Qian, Y., Miao, Z., Zheng, P., Shi, T., Jiang, X., et al. (2020a). Xuebijing injection alleviates Pam3CSK4-induced inflammatory response and protects mice from sepsis caused by methicillin-resistant Staphylococcus aureus. *Front. Pharmacol.* 11, 104. doi:10.3389/fphar.2020.00104

Li, Y., Deng, S., Wang, X., Huang, W., Chen, J., Robbins, N., et al. (2020b). Sectm1a deficiency aggravates inflammation-triggered cardiac dysfunction through disruption of LXRalpha signaling in macrophages. *Cardiovasc. Res*. doi:10.1093/cvr/cvaa067

Li, Y., Li, Q., and Fan, G. C. (2021). Macrophage efferocytosis in cardiac pathophysiology and repair. *Shock* 55 (2), 177–188. doi:10.1097/SHK.0000000000001625

Li, W., Li, J., Ashok, M., Wu, R., Chen, D., Yang, L., et al. (2007). A cardiovascular drug rescues mice from lethal sepsis by selectively attenuating a late-acting proinflammatory mediator, high mobility group box 1, *J. Immunol*. 178, 3856–3864. doi:10.4049/jimmunol.178.6.3856

Liehn, E. A., Tuchscheerer, N., Kanzler, I., Drechsler, M., Fraemohs, L., Schuh, A., et al. (2011). Double-edged role of the CXCL12/CXCR4 axis in experimental myocardial infarction. *J. Am. Coll. Cardiol*. 58, 2415–2423. doi:10.1016/j.jacc.2011.08.033

Liu, M. W., Su, M. X., Zhang, W., Wang, Y. Q., Chen, M., Wang, L., et al. (2014a). Protective effect of Xuebijing injection on paraquat-induced pulmonary injury via down-regulating the expression of p38 MAPK in rats. *BMC Compl. Alternative Med*. 14, 498. doi:10.1186/1472-6882-14-498

Liu, Y. L., Liu, Y. J., Liu, Y., Li, X. S., Liu, S. H., Pan, Y. G., et al. (2014b). Hydroxysafflor yellow A ameliorates lipopolysaccharide-induced acute lung injury in mice via modulating toll-like receptor 4 signaling pathways. *Int. Immunopharm*. 23, 649–657. doi:10.1016/j.intimp.2014.10.018

Liu, X. R., Xu, J., Wang, Y. M., Ji, M. S., and Liu, F. S. (2016). The effects of paeoniflorin injection on soluble triggering receptor expressed on myeloid-1 (sTREM-1) levels in severe septic rats. *Korean J. Physiol. Pharmacol*. 20, 565–571. doi:10.4196/kjpp.2016.20.6.565

Liu, Y. C., Yao, F. H., Chai, Y. F., Dong, N., Sheng, Z. Y., and Yao, Y. M. (2015). Xuebijing injection promotes M2 polarization of macrophages and improves survival rate in septic mice. *Evid. Based Complement Alternat. Med*. 2015, 352642. doi:10.1155/2015/352642

Liu, Y. C., Yu, M. M., Shou, S. T., and Chai, Y. F. (2017). Sepsis-induced cardiomyopathy: mechanisms and treatments. *Front. Immunol*. 8, 1021. doi:10.3389/fimmu.2017.01021

Lyu, M., Cui, Y., Zhao, T., Ning, Z., Ren, J., Jin, X., et al. (2018a). Tnfrsf12a-Mediated atherosclerosis signaling and inflammatory response as a common protection mechanism of shuxuening injection against both myocardial and cerebral ischemia-reperfusion injuries. *Front. Pharmacol*. 9, 312. doi:10.3389/fphar.2018.00312

Lyu, M., Zhou, Z., Wang, X., Lv, H., Wang, M., Pan, G., et al. (2018b). Network pharmacology-guided development of a novel integrative regimen to prevent acute graft-vs.-host disease. *Front. Pharmacol*. 9, 1440. doi:10.3389/fphar.2018.01440

Martin, L., Derwall, M., Al Zoubi, S., Zechendorf, E., Reuter, D. A., Thiemermann, C., et al. (2019). The septic heart: current understanding of molecular mechanisms and clinical implications. *Chest*. 155, 427–437. doi:10.1016/j.chest.2018.08.1037

McLean, A. S., Huang, S. J., and Salter, M. (2008). Bench-to-bedside review: the value of cardiac biomarkers in the intensive care patient. *Crit. Care*. 12, 215. doi:10.1186/cc6880

Montecucco, F., Bauer, I., Braunersreuther, V., Bruzzone, S., Akhmedov, A., Lüscher, T. F., et al. (2013). Inhibition of nicotinamide phosphoribosyltransferase reduces neutrophil-mediated injury in myocardial infarction. *Antioxidants Redox Signal.* 18, 630–641. doi:10.1089/ars.2011.4487

Montecucco, F., Lenglet, S., Braunersreuther, V., Pelli, G., Pellieux, C., Montessuit, C., et al. (2010). Single administration of the CXC chemokine-binding protein Evasin-3 during ischemia prevents myocardial reperfusion injury in mice. *Arterioscler. Thromb. Vasc. Biol.* 30, 1371–1377. doi:10.1161/ATVBAHA.110.206011

Mu, X., Wang, P., Wang, X., Li, Y., Zhao, H., Li, Q., et al. (2020). Identification of a novel antisepsis pathway: Sectm1a enhances macrophage phagocytosis of bacteria through activating GITR. *J. Immunol*. 205, 1633–1643. doi:10.4049/jimmunol.2000440

Mylonas, K. J., Turner, N. A., Bageghni, S. A., Kenyon, C. J., White, C. I., McGregor, K., et al. (2017). 11β-HSD1 suppresses cardiac fibroblast CXCL2, CXCL5 and neutrophil recruitment to the heart post MI. *J. Endocrinol*. 233, 315–327. doi:10.1530/JOE-16-0501

Opal, S. M., Laterre, P. F., Francois, B., LaRosa, S. P., Angus, D. C., Mira, J. P., et al. (2013). Effect of eritoran, an antagonist of MD2-TLR4, on mortality in patients with severe sepsis: the ACCESS randomized trial. *J. Am. Med. Assoc*. 309, 1154–1162. doi:10.1001/jama.2013.2194

Pathan, N., Hemingway, C. A., Alizadeh, A. A., Stephens, A. C., Boldrick, J. C., Oragui, E. E., et al. (2004). Role of interleukin 6 in myocardial dysfunction of meningococcal septic shock. *Lancet*. 363, 203–209. doi:10.1016/S0140-6736(03)15326-3

Respress, J. L., and Wehrens, X. H. (2010). Transthoracic echocardiography in mice. *JoVE*. 28, 1738. doi:10.3791/1738

Rittirsch, D., Huber-Lang, M. S., Flierl, M. A., and Ward, P. A. (2009). Immunodesign of experimental sepsis by cecal ligation and puncture. *Nat. Protoc*. 4, 31–36. doi:10.1038/nprot.2008.214

Ruan, Q., Yang, K., Wang, W., Jiang, L., and Song, J. (2020). Clinical predictors of mortality due to COVID-19 based on an analysis of data of 150 patients from Wuhan, China. *Intensive Care Med.* 46, 846–848. doi:10.1007/s00134-020-05991-x

Russell, C. D., Millar, J. E., and Baillie, J. K. (2020). Clinical evidence does not support corticosteroid treatment for 2019-nCoV lung injury. *Lancet* 395(10223), 473–475. doi:10.1016/S0140-6736(20)30317-2

Sawant, K. V., Sepuru, K. M., Lowry, E., Penaranda, B., Frevert, C. W., Garofalo, R. P., et al. (2020). Neutrophil recruitment by chemokines Cxcl1/KC and Cxcl2/MIP2: role of Cxcr2 activation and glycosaminoglycan interactions. *J. Leukoc. Biol*. doi:10.1002/JLB.3A0820-207R

Shang, T., Yu, Q., Ren, T., Wang, X. T., Zhu, H., Gao, J. M., et al. (2019). Xuebijing injection maintains GRP78 expression to prevent Candida albicans-induced epithelial death in the kidney. *Front. Pharmacol.* 10, 1416. doi:10.3389/fphar.2019.01416

Shankar-Hari, M., Phillips, G. S., Levy, M. L., Seymour, C. W., Liu, V. X., Deutschman, C. S., et al. (2016). Developing a new definition and assessing new clinical criteria for septic shock: for the third international consensus definitions for sepsis and septic shock (Sepsis-3). *Jama*. 315, 775–787. doi:10.1001/jama.2016.0289

Song, Y., Yao, C., Yao, Y., Han, H., Zhao, X., Yu, K., et al. (2019). XueBiJing injection versus placebo for critically ill patients with severe

community-acquired pneumonia: a randomized controlled trial. *Crit. Care Med*. 47, e735–e743. doi:10.1097/CCM.0000000000003842

Tersalvi, G., Vicenzi, M., Calabretta, D., Biasco, L., Pedrazzini, G., and Winterton, D. (2020). Elevated troponin in patients With coronavirus disease 2019: possible mechanisms. *J. Card. Fail*. 26(6), 470–475. doi:10.1016/j.cardfail.2020.04.009

Villar, J., Perez-Mendez, L., Flores, C., Maca-Meyer, N., Espinosa, E., Muriel, A., et al. (2007). A CXCL2 polymorphism is associated with better outcomes in patients with severe sepsis. *Crit. Care Med*. 35, 2292–2297. doi:10.1097/01.ccm.0000284511.73556.59

Villa, P., Sartor, G., Angelini, M., Sironi, M., Conni, M., Gnocchi, P., et al. (1995). Pattern of cytokines and pharmacomodulation in sepsis induced by cecal ligation and puncture compared with that induced by endotoxin. *Clin. Diagn. Lab. Immunol*. 2(5), 549–553. doi:10.1378/chest.101.3.810

Vincent, J. L., Bakker, J., Marécaux, G., Schandene, L., Kahn, R. J., and Dupont, E. (1992). Administration of anti-TNF antibody improves left ventricular function in septic shock patients. Results of a pilot study. *Chest*. 101, 810–815. doi:10.1378/chest.101.3.810

Walley, K. R. (2018). Sepsis-induced myocardial dysfunction. *Curr. Opin. Crit. Care*. 24, 292–299. doi:10.1097/MCC.0000000000000507

Wang, J., Wang, P., Gui, S., Li, Y., Chen, R., Zeng, R., et al. (2017). Hydroxysafflor yellow A attenuates the apoptosis of peripheral blood CD4. *Front. Pharmacol*. 8, 613. doi:10.3389/fphar.2017.00613

Wang, L., Li, Y., Wang, X., Wang, P., Essandoh, K., Cui, S., et al. (2020). GDF3 protects mice against sepsis-induced cardiac dysfunction and mortality by suppression of macrophage pro-inflammatory phenotype. *Cells*. 9. 120. doi:10.3390/cells9010120

Xiao, G., Lyu, M., Wang, Y., He, S., Liu, X., Ni, J., et al. (2019). Ginkgo flavonol glycosides or ginkgolides tend to differentially protect myocardial or cerebral ischemia-reperfusion injury via regulation of TWEAK-fn14 signaling in heart and brain. *Front. Pharmacol*. 10, 735. doi:10.3389/fphar.2019.00735

Zhai, J., and Guo, Y. (2016a). Paeoniflorin attenuates cardiac dysfunction in endotoxemic mice via the inhibition of nuclear factor-kappaB. *Biomed. Pharmacother*. 80, 200–206. doi:10.1016/j.biopha.2016.03.032

Zhai, J., and Guo, Y. (2016b). Paeoniflorin attenuates cardiac dysfunction in endotoxemic mice via the inhibition of nuclear factor-κB. *Biomedicine and pharmacotherapy = Biomedecine and pharmacotherapie*. 80, 200–206. doi:10.1016/j.biopha.2016.03.032

Zhang, N., Cheng, C., Olaleye, O. E., Sun, Y., Li, L., Huang, Y., et al. (2018). Pharmacokinetics-based identification of potential therapeutic phthalides from XueBiJing, a Chinese herbal injection used in sepsis management. *Drug Metab. Dispos*. 46, 823–834. doi:10.1124/dmd.117.079673

Zheng, Y. Y., Ma, Y. T., Zhang, J. Y., and Xie, X. (2020). COVID-19 and the cardiovascular system. *Nat. Rev. Cardiol*. 17, 259–260. doi:10.1038/s41569-020-0360-5

Zhou, F., Yu, T., Du, R., Fan, G., Liu, Y., Liu, Z., et al. (2020). Clinical course and risk factors for mortality of adult inpatients with COVID-19 in Wuhan, China: a retrospective cohort study. *Lancet*. 395, 1054–1062. doi:10.1016/S0140-6736(20)30566-3

Zhu, H., Rhee, J. W., Cheng, P., Waliany, S., Chang, A., Witteles, R. M., et al. (2020). Cardiovascular complications in patients with COVID-19: consequences of viral toxicities and host immune response. *Curr. Cardiol. Rep*. 22, 32. doi:10.1007/s11886-020-01292-3

Zou, J., Wang, N., Liu, M., Bai, Y., Wang, H., Liu, K., et al. (2018). Nucleolin mediated pro-angiogenic role of Hydroxysafflor Yellow A in ischaemic cardiac dysfunction: post-transcriptional regulation of VEGF-A and MMP-9. *J. Cell Mol. Med*. 22, 2692–2705. doi:10.1111/jcmm.13552

Conflict of Interest: The authors declare that the research was conducted in the absence of any commercial or financial relationships that could be construed as a potential conflict of interest. The authors have no conflicts of interest to declare.

frontiers in Pharmacology

ORIGINAL RESEARCH
published: 27 April 2021
doi: 10.3389/fphar.2021.659015

Capsaicin protects cardiomyocytes against lipopolysaccharide-induced damage via 14-3-3γ-mediated autophagy augmentation

Yang Qiao[1], Liang Wang[2], Tianhong Hu[3], Dong Yin[4], Huan He[3] and Ming He[1]**

[1]Institute of Cardiovascular Diseases, Jiangxi Academy of Clinical Medical Sciences, The First Affiliated Hospital of Nanchang University, Nanchang, China, [2]Department of Rehabilitation, The First Affiliated Hospital of Nanchang University, Nanchang, China, [3]Jiangxi Provincial Key Laboratory of Basic Pharmacology, Nanchang University School of Pharmaceutical Science, Nanchang, China, [4]Jiangxi Provincial Key Laboratory of Molecular Medicine, The Second Affiliated Hospital, Nanchang University, Nanchang, China

OPEN ACCESS

Edited by:
Yan Kang,
Sichuan University, China

Reviewed by:
Yuesheng Huang,
Jinan University, China
Fausto Chiazza,
University of Eastern Piedmont, Italy

***Correspondence:**
Huan He
hehuan0118@ncu.edu.cn
Ming He
jxhm56@hotmail.com

Specialty section:
This article was submitted to Experimental Pharmacology and Drug Discovery, a section of the journal Frontiers in Pharmacology

Received: 26 January 2021
Accepted: 30 March 2021
Published: 27 April 2021

Citation:
Qiao Y, Wang L, Hu T, Yin D, He H and He M (2021) Capsaicin protects cardiomyocytes against lipopolysaccharide-induced damage via 14-3-3γ-mediated autophagy augmentation. Front. Pharmacol. 12:659015. doi: 10.3389/fphar.2021.659015

Background: The myocardium is susceptible to lipopolysaccharide (LPS)-induced damage in sepsis, and cardiac dysfunction is a leading cause of mortality in patients with sepsis. The changes in cardiomyocyte autophagy in sepsis and the effects and mechanism of action of capsaicin (Cap) remain unclear.

Methods and Results: The potential pathway of 14-3-3γ-dependent autophagy and the effects and mechanisms of Cap were studied in LPS-induced injury to primary cultured neonatal rat cardiomyocytes. The results showed that cardiomyocyte viability decreased, lactate dehydrogenase and creatine kinase activities increased, 14-3-3γ expression was downregulated, and autophagy was inhibited after LPS challenge. Cap pretreatment augmented autophagy by upregulating 14-3-3γ expression and activating AMP-activated protein kinase (AMPK) and unc-51 like autophagy-activating kinase 1 (ULK1), suppressing mammalian target of rapamycin (mTOR), alleviating cardiac dysfunction and improving the inflammation response, whereas pAD/14-3-3γ-shRNA nullified the above effects. Cap pretreatment also decreased the levels of IL-1β, TNF-α, IL-6, and IL-10; suppressed intracellular oxidative stress; reduced the intracellular/mitochondrial reactive oxygen species (ROS); balanced GSH/GSSG; increased GSH-Px, catalase, and SOD activities; and decreased MDA contents. It also increased ATP content, activated complex I and complex III, stabilized the mitochondrial membrane potential, and decreased the mitochondrial permeability transition pore opening, thereby improving mitochondrial function.

Abbreviations: AMPK, AMP-activated protein kinase; BafA, Bafilomycin A1; Cap, Capsaicin; CK, creatine phosphate kinase; DHE, dihydroethidium; LDH, lactate dehydrogenase; LPS, lipopolysaccharide; MDC, dansylcadaverine; mTOR, mammalian targets of rapamycin; MMP, mitochondrial membrane potential; mPTP, mitochondrial permeability transition pore; mtROS, mitochondrial ROS; NDUFB8, NADH dehydrogenase [ubiquinone] 1 beta subcomplex subunit 8; NRCMs, neonatal rat cardiomyocytes; NS, nonsignificant; ROS, reactive oxygen species; ULK1, Unc-51 like- autophagy-activating kinase 1; UQCRC2, cytochrome b-c1 complex subunit 2.

Conclusion: Pretreatment with Cap can regulate autophagy by upregulating 14-3-3γ expression, inhibiting oxidative stress and inflammation, maintaining mitochondrial function, and protecting cardiomyocytes against LPS-induced injury.

Keywords: 14-3-3γ, Autophagy, Cardiac dysfunction, Capsaicin, lipopolysaccharide, Mitochondria

INTRODUCTION

Sepsis is characterized by high mortality in intensive care units (Angus et al., 2006; Schorr et al., 2014). Lipopolysaccharide (LPS), an essential component of the gram-negative bacterial outer membrane, is recognized as the leading cause of multi-organ failure in sepsis (Tsiotou et al., 2005; Zanotti-Cavazzoni Hollenberg, 2009). LPS-induced sepsis occurs due to excessive release of inflammatory cytokines, overproduction of oxygen radicals, and mitochondrial dysfunction, and it is a major contributor to cardiac dysfunction (Li et al., 2016; Okuhara et al., 2017; Liu et al., 2019). Mitochondria in cardiomyocytes not only generate ATP but also modulate oxidative stress, signaling, and cell fate (Kolwicz et al., 2013). Mitochondrial impairment is correlated with overproducing intracellular/mitochondrial reactive oxygen species (ROS) and inflammatory responses during LPS-induced sepsis in cardiomyocytes (Zang et al., 2007; Zang et al., 2010; Sun et al., 2018).

Accumulating studies indicated that organelles damaged by LPS-induced sepsis (such as mitochondria) were cleared by the activation of autophagy (Hsiao et al., 2012; Lin et al., 2014). Autophagy protects cardiomyocytes during LPS-induced sepsis by activating AMP-activated protein kinase (AMPK) pathways (Nishida et al., 2009). AMPK is a central energy sensor in eukaryotes that responds to disequilibrium of AMP/ADP (Lee et al., 2010; Roach, 2011). Besides, 14-3-3 proteins are evidence that it interacts directly or indirectly with multiple molecules, including AMPK, mammalian targets of rapamycin (mTOR), and Unc-51-like autophagy activating kinase 1 (ULK1), to regulate the autophagy process (Ma et al., 2012). 14-3-3γ, an isoform of the 14-3-3 protein family, was demonstrated in our previous studies to offer a cardioprotective role in response to LPS-induced cardiotoxicity (He et al., 2006; Liu et al., 2014; Huang et al., 2018a). However, the specific mechanism of 14-3-3γ-dependent autophagy remained unclear and further exploration in in cardiomyocyte LPS-induced sepsis was needed.

Several studies have confirmed many pharmacological agents as potential preconditioning strategies to prevent myocardial injury (Hausenloy and Yellon, 2011). Our previous studies suggested that pretreatment with astragaloside Ⅳ or tanshinone ⅡA could elicit similar protective effects as ischemic preconditioning against anoxia/reoxygenation (A/R)-induced cardiomyocyte injury (Zhang et al., 2018; Luo et al., 2019). Capsaicin (Cap) targets multiple pathways and possesses many pharmacological properties, including antimicrobial, analgesic, antiinflammation and antioxidant (Sun et al., 2015; Fernandes et al., 2016; Gerber et al., 2019). In our previous study, pretreatment with Cap improved cardiac function via 14-3-3η or SIRT1/Bcl2 following A/R injury (He et al., 2017; Huang et al., 2018a; Qiao et al., 2020). However, the effect of Cap pretreatment on LPS-induced cardiotoxicity remains unclear. Here, we used the LPS-induced sepsis model in neonatal rat cardiomyocytes (NRCMs), to explore (1) the role of Cap during 14-3-3γ-related autophagy process via the AMPK-mTOR/ULK1 pathway in LPS-challenged cardiomyocytes; (2) the effects of Cap in LPS-induced cardiotoxicity via regulating inflammatory cytokine release, oxidative stress, and mitochondrial dysfunction.

MATERIALS AND METHODS

Materials

The following reagents were purchased: LPS, from Sigma-Aldrich (St. Louis, MO, USA); Cap (purity ≥ 98%), from the National Institutes for Food and Drug Control (Beijing, China); adenovirus pAD/14-3-3γ-shRNA, from Gene Chem Co., Ltd (Shanghai, China); bafilomycin A1 (BafA1) and compound C, from Sigma-Aldrich (St. Louis, MO, USA); antibodies against 14-3-3γ, P62, NADH dehydrogenase [ubiquinone] 1 beta subcomplex subunit 8 (NDUFB8) and cytochrome b-c1 complex subunit 2 (UQCRC2), from Abcam (Cambridge, UK). Anti-LC3, -AMPKα, -phospho-AMPK (phosphorylation at Ser172), -mTOR, -phospho-mTOR (phosphorylation at Ser2448), -ULK1, -phospho-ULK1 (phosphorylation at Ser757) antibodies, from Cell Signaling Technology (Beverly, MA, USA), and horseradish peroxidase-conjugated IgG secondary antibody, from Zsbio (Beijing, China).

Primary culture of neonatal rat cardiomyocytes (NRCMs) and adenoviral infection equations

All experimental procedures were performed according to the Guide for the Care and Use of Laboratory Animals published by the US National Institutes of Health (NIH Publication no. 85–23, revised 1996) and approved by the Ethics Committee of Nanchang University (No. 2019–0036). The NRCMs from 0–3 days-old Sprague-Dawley rats (the Animal Center of Nanchang University, Nanchang, China) were prepared as previously published (He et al., 2017). Cardiomyocytes were cultured in high-glucose Dulbecco's modified Eagle medium (DMEM, Gibco-BRL, Grand Island, NY, USA) supplemented with 20% fetal bovine serum (FBS, Gibco-BRL), 100 U/ml of penicillin and streptomycin, and 1% bromodeoxyuridine (Brdu, Solarbio Science & Technology, Beijing, China), and incubated in a 95% air and 5% CO_2 humidified atmosphere incubator at 37 °C.

Cardiomyocytes were infected by adenovirus pAD/14-3-3γ-shRNA and infection efficiency was approximately 85% after 48 h (Qiao et al., 2020). Before conducting subsequent experiments,

the transfected cardiomyocytes were cultured in 95% O_2 and 5% CO_2 for 12 h at 37 °C.

Experimental grouping and reagent treatment

Phase A

First, we investigated whether Cap could protect cardiomyocytes against LPS-induced injury. Cardiomyocytes were randomly distributed into four groups: LPS, Cap, pAD/14-3-3γ-shRNA, and control. Cells in the control group were cultured in a complete medium throughout the experiments. LPS grouped-cardiomyocytes were treated with 1 mg/L LPS for 24 h (Liu et al., 2014; Huang et al., 2018a). Then, the cells in the Cap group were pretreated with 5, 10, 20, 40, 80 μM Cap for 12 h, placed in the fresh culture medium, and then exposed to 1 mg/L LPS for 24 h. Cardiomyocytes in the pAD/14-3-3γ-shRNA group were treated with pAD/14-3-3γ-shRNA for 12 h before Cap pretreatment. Cell viability, LDH and CK activities, and 14-3-3γ expression were determined after processing.

Phase B

Next, we examined the changes in autophagy in LPS-induced cardiomyocyte injury and the effects of Cap on these changes. Cardiomyocytes were cotreated with or without 100 nM BafA1, an autophagy inhibitor (Mauthe et al., 2018), and LPS for 24 h. The expression of LC3 and P62 were determined after processing. After, cardiomyocytes were pretreated with 10 μM Cap for 12 h according to the method of phase A before LPS treatment. Cardiomyocytes in the control, LPS, and pAD/14-3-3γ-shRNA group were treated according to phase A. The expressions of 14-3-3γ, LC3, and P62, along with autolysosome contents were determined again after processing.

Phase C

Furthermore, we explored the role of the AMPKα/mTOR signaling pathway in LPS-induced cardiomyocyte injury. Cardiomyocytes were randomly distributed into four groups: control, LPS, compound C, and Cap. Cardiomyocytes in the control, LPS, and Cap groups were treated similarly as mentioned above. Cardiomyocytes in the compound C group were coincubated with 5 μM compound C (AMPK inhibitor, Dasgupta and Seibel, 2018) and 10 μM Cap for 12 h according to phase A before LPS treatment. The expressions of 14-3-3γ, LC3, P62, AMPKα, AMPK phospho-Ser172, mTOR, mTOR phospho-Ser2448, ULK1, and ULK1 phospho-Ser757 were then determined .

Phase D

Finally, we studied how LPS disrupts intracellular redox equilibrium and cytokines and impairs mitochondrial function. In brief, the control, LPS, Cap, and pAD/14-3-3γ-shRNA group were treated as in phase A. Intracellular/mitochondrial ROS, the activities of GSH-Px, SOD, catalase, MDA, and ATP levels, GSH/GSSG ratio, cytokine (IL-1β, TNF-α, IL-6, IL-10) contents, mitochondrial membrane potential (MMP), and mitochondrial permeability transition pore (mPTP) opening were determined at the end of experiments.

Measurement of cell viability and biochemical parameters

Cell viability was measured using a commercially available kit (CCK-8, TransGen Biotech, Beijing, China). In brief, cells were cultured in 96-well plates at a density of 3×10^3 cells/well and treated as in phase A. Then, we added the tetrazolium salt WST-8 to the medium at a certain ratio incubated for 1–2 h at 37 °C, and measured the number of viable cells using a microplate reader (Bio-Rad 680, Hercules, CA, USA).

The culture medium was collected after LPS challenge to examine lactate dehydrogenase (LDH) and creatine phosphate kinase (CK) activities using commercially available kits (Jiancheng, Nanjing, China, Qiao et al., 2020).

Measurements of inflammatory cytokines

The culture medium was collected after LPS challenge and centrifuged for 10 min at 3000 rpm, and the inflammatory cytokine (IL-1β, TNF-α, IL-6, and IL-10) levels were measured by enzyme-linked immunosorbent assay (ELISA) (BestBio, Shanghai, China).

Measurements of intracellular/mitochondrial ROS

Intracellular/mitochondrial ROS levels were detected using the oxidation-sensitive probe (DCFH-DA or Mito-SOX) as previously described (Zuo et al., 2018). After treatment as in phase A, cardiomyocytes were harvested and incubated with DCFH-DA (Beyotime, Shanghai, China) or Mito-SOX (Invitrogen™ Oregon, USA) in the dark at 37 °C. Then, fluorescence was detected by a flow cytometer (Beckman Coulter, Brea, CA, USA).

Moreover, intracellular/mitochondrial ROS intensity was observed under a fluorescence microscope (×100 magnification, Olympus, Japan). In brief, cells were seeded in 24-well plates at a density of 1×10^4 cells/coverslip, then washed with prewarmed PBS and incubated with the fluorescence dye dihydroethidium (DHE, BestBio, Shanghai, China) or Mito-SOX in the dark at 37 °C.

Measurement of endogenous antioxidant enzyme activities and glutathione (GSH) and glutathione disulfide (GSSG)

The endogenous antioxidant enzyme activities, including glutathione peroxidase (GSH-Px), superoxide dismutase (SOD), and catalase; levels of malondialdehyde (MDA) (Jiancheng, Nanjing, China); and contents of the nonenzymatic antioxidant system (GSH, GSSG, and GSH/GSSG ratio; Beyotime, Shanghai, China) were detected by spectrophotometry, respectively (Chen et al., 2020; Qiao et al.,

2020). Cells were lysed after treatment as in phase A, and the supernatant was collected and examined based on manufacturer instructions of commercial kits.

Dansylcadaverine (MDC) and LysoTracker Red Staining

Cells were seeded in 24-well plates at a density of 1×10^4 cells/coverslip and treated as described in phase A. Then, cardiomyocytes were washed with prewarmed PBS and incubated with fluorescence dye MDC (Beyotime, Shanghai, China) or LysoTracker Red DND-99 (Invitrogen™, Oregon, USA) in darkness for 30 min at 37 °C. After that, images were captured by a fluorescence microscope (Olympus, Japan).

Western blotting

Proteins were extracted by a protein extraction kit (Applygen Technologies Inc, Beijing, China), and quantified by a bicinchoninic acid (BCA) protein assay kit (Thermo Fisher, Massachusetts, USA). Equal amounts of protein (30 μg) were separated by SDS-PAGE and later transferred to a polyvinylidene fluoride (PVDF) membrane. The PVDF membrane was then blocked with 5% bull serum albumin, and subsequently incubated with primary antibodies (14-3-3γ, LC3, P62, AMPKα, p-AMPKα, mTOR, p-mTOR, ULK1, p-ULK1, NDUFB8, UQCRC2, and β-actin) overnight at 4 °C. The membranes were blotted with horseradish peroxidase conjugated secondary antibody and immersed with an enhanced-chemiluminescence substrate. Finally, protein bands were imaged and analyzed with the Quantity One software (Bio-Rad, USA, Qiao et al., 2020).

ATP production

Intercellular ATP levels were measured using an Enhanced ATP Assay Kit (Beyotime, Shanghai, China). Cells were lysed and the supernatant was collected. It was then added to a detecting solution in a lightproof 96-well plate and incubated for 5 min at 25 °C. Total cellular ATP levels were determined from real-time luminescence signals and were normalized to the protein concentrations (Li et al., 2017).

Measurement of MMP and mPTPs openness

MMP was detected by Fluorescent probe JC-1 (BestBio, Shanghai, China). Briefly, cells were harvested by trypsin without EDTA and incubated with JC-1 in the dark for 30 min at 37 °C. Then, cells were suspended in an incubation buffer and MMP measured by flow cytometer (Beckman Coulter, Brea, CA, USA) at 530/580 nm (red) and 485/530 nm (green). The ratio of Red:green fluorescence intensity represents the MMP level (Qiao et al., 2020).

The mPTP opening was examined as described previously (He et al., 2020). The carmidiocyte mitochondria were isolated using a mitochondrial isolation kit (Thermo Fisher, Massachusetts, USA). Afterward, fractions were resuspended in 160 μl swelling buffer (KCl 120 mM, Tris-HCl 10 mM, MOPS 20 mM, KH_2PO_4 5 mM), the suspensions plated onto a 96-well microtiter plate and florescence measured at 520 nm. Then, we added a 40-μl $CaCl_2$ solution (200 nM) to stimulate the mPTP openings. The absorbance values were calculated per minute at 520 nm until the trends stabilized. The degree of mPTP openness were determined by the extent of changes at 520 nm.

Statistical Analysis

All experiments values were represented as Mean ± S.E.M., and tested by one-way ANOVA, the differences of biochemical data between each group were further tested by Tukey's honestly significant difference test. $P < 0.05$ was considered to be statistically significant.

RESULTS

Cap protects cardiomyocytes by upregulating 14-3-3γ expression against LPS challenge

Cardiomyocytes were pretreated with Cap (0 μM-80 μM) for 12 h and again coincubated with 1 mg/L LPS for 24 h. Cap caused a concentration-dependent increase in cell viability and decrease in LDH activity; the optimal concentration of Cap was 10 μM (**Figures 1A,B**). Cap increased cell viability and inhibited the leakage of LDH and CK in response to LPS-induced injury significantly ($P < 0.01$); however, these positive effects were nullified by pAD/14-3-3γ-shRNA ($P < 0.01$, **Figures 1C–E**). Besides, 14-3-3γ expression was significantly decreased in the LPS group compared to that in the control group ($P < 0.01$), whereas Cap upregulated 14-3-3γ expression ($P < 0.01$, **Figure 1F**).

Together, these data indicated that LPS toxicity could downregulate 14-3-3γ expression and trigger cardiomyocyte injury, but pretreatment with Cap could upregulate the 14-3-3γ protein and alter the cell viability plus LDH and CK activities to protect cardiomyocytes.

Cap activates cardiomyocyte autophagy against LPS-induced injury

Previous studies documented the role of autophagy in LPS-induced cardiac injury (Sun et al., 2018; Huang et al., 2020). The levels of LC3II, an indicator of autophagy levels, and the expression of P62, an autophagic substrate protein (Ma et al., 2012), were increased ($P < 0.01$) and decreased ($P < 0.01$), respectively, after LPS challenge (**Figure 2A**). To identify LC3II changes, which reflected as the increase in autophagy levels rather than the impairment of autophagic flux, cardiomyocytes were treated with BafA1-an inhibitor that blocks the alternation of autophagosomes to autolysosomes (Yamamoto et al., 1998). **Figure 2A** showed that BafA1

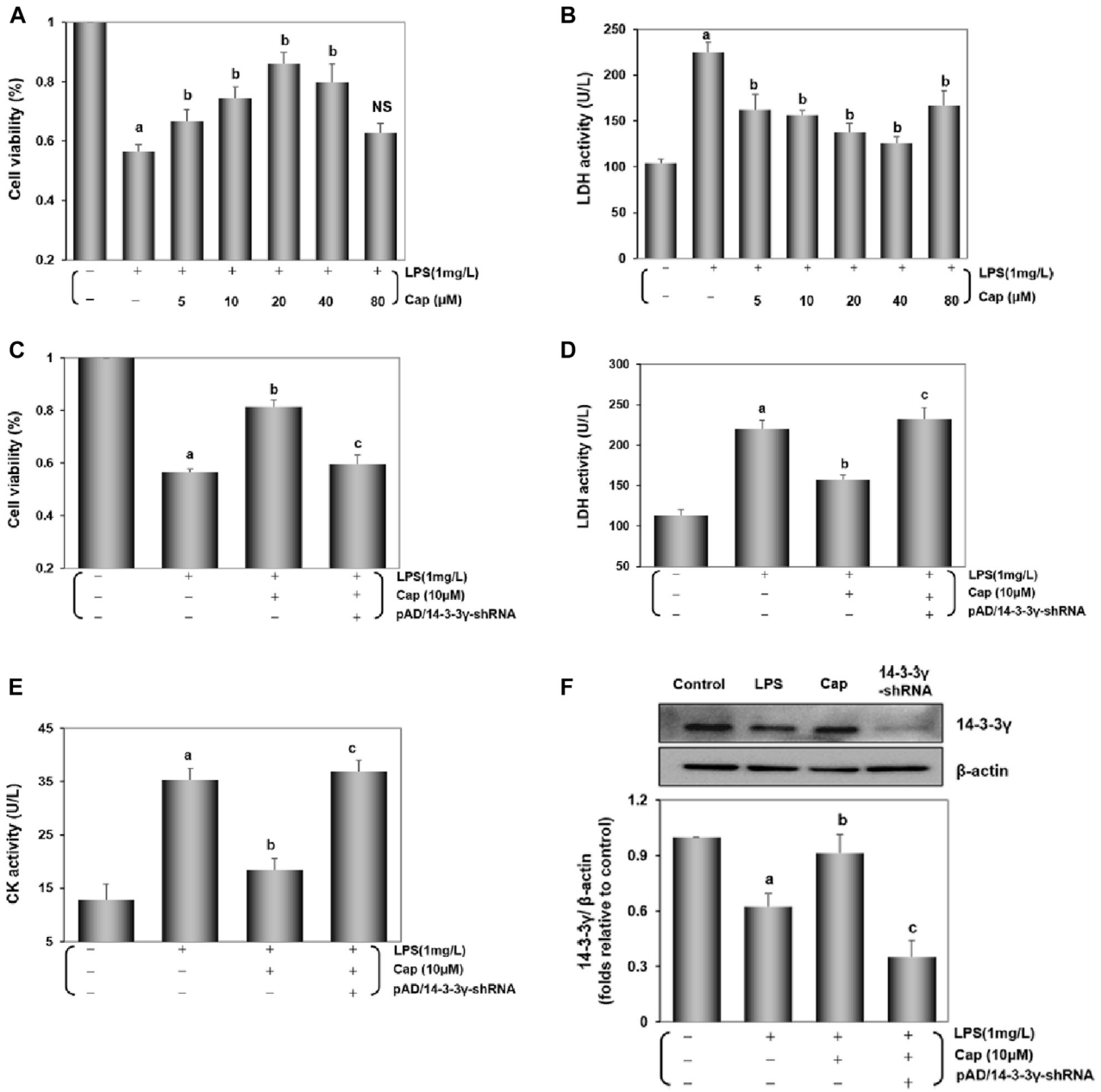

FIGURE 1 | Cap protects cardiomyocytes by upregulating 14-3-3γ levels after LPS challenge. **(A)** and **(B)** Cap presented a concentration-dependent effect on cell viability and LDH activity against LPS-induced cardiomyocyte injury. **(C)** Cap increased cell viability, and cotreatment with pAD/14-3-3γ-shRNA nullified Cap effects after LPS challenge. **(D)** and **(E)** LDH and CK activity in culture medium. **(F)** The representative western blot bands and the relative band intensity of 14-3-3γ expression in cardiomyocytes. Values are presented as mean ± SEM. For five individual experiments, a: P<0.01 vs. the control group; b: P<0.01 vs. the LPS group; c: P<0.01 vs. the Cap+LPS group.

induced an increase in LC3II and P62 levels in the control and LPS group.

Unlike in the LPS group, pretreatment with Cap led to significant LC3II accumulation ($P < 0.01$) and P62 ($P < 0.05$) led to the reverse; however, these responses were nullified by pAD/14-3-3γ-shRNA (**Figures–E**).

Furthermore, the acidotropic dyes can stain intracellular acid compartments. MDC is used in labeling early autophagosomes (Bampton et al., 2005; Wang et al., 2020) and Lyso Tracker Red is a marker for the later stages of autophagy (Scott et al., 2004). As illustrated in **Figure 2F**, MDC-specific dots (green) and autolysosome signals (red) were detected after LPS challenge, and both fluorescence intensities were significantly enhanced with Cap pretreatment. Moreover, coincubation with pAD/14-3-3γ-shRNA reduced the green and red dots. These results corroborate the above the data on LC3II and P62 expression.

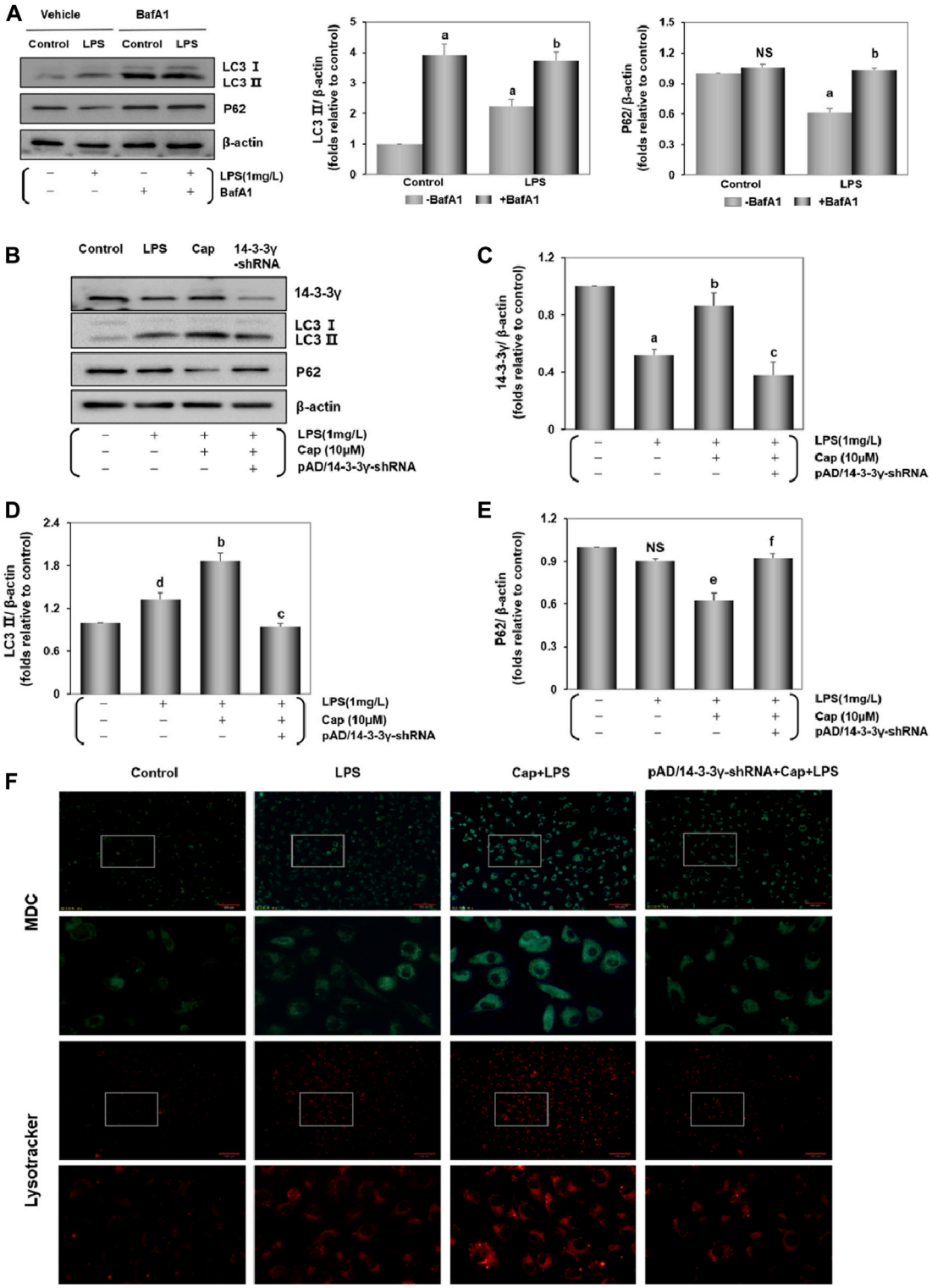

FIGURE 2 | Cap activates cardiomyocyte autophagy against LPS-induced injury. **(A)** LPS-induced autophagy flux confirmed by the contrast of P62 and LC3 II between cells with and without BafA1 addition. **(B)** The representative western blot bands of 14-3-3γ, LC3 II, and P62 expression in the cardiomyocytes. **(C-E)** The relative band intensity of 14-3-3γ, LC3 II, and P62 expression in the cardiomyocytes. **(F)** Cardiomyocytes incubated with dansylcadaverine (MDC) or LysoTracker Red DND-99. Green or red intensity showed the autophagosome and autolysosomes. Values were presented as mean ± SEM. For five individual experiments, a: $P<0.01$ vs. the control group; b: $P<0.01$ vs. the LPS group; c: $P<0.01$ vs. the Cap+LPS group. d: $P<0.05$ vs. the control group; e: $P<0.05$ vs. the LPS group; f: $P<0.05$ vs. the Cap+LPS group; NS, nonsignificant.

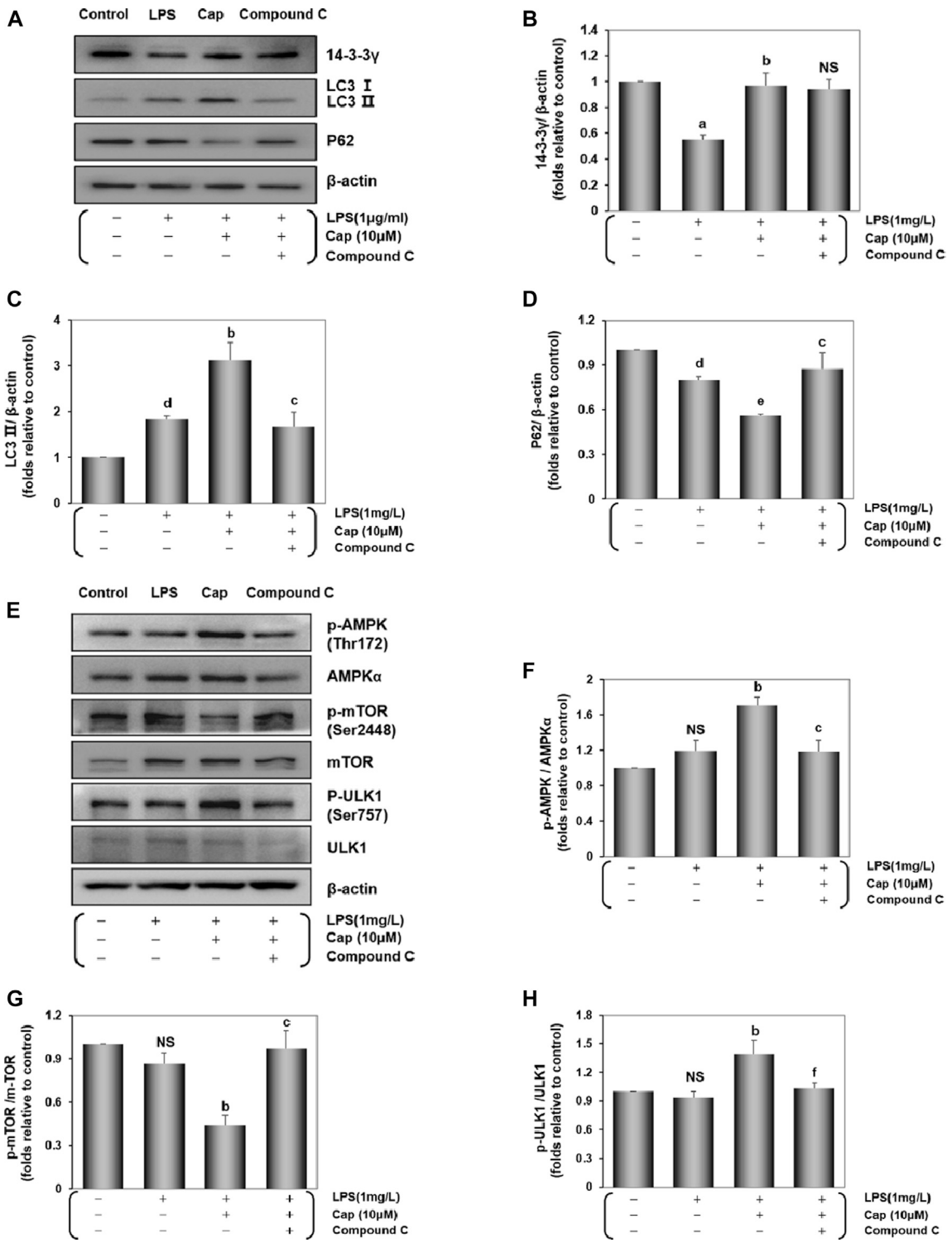

FIGURE 3 | Cap upregulates 14-3-3γ and integrates AMPKα/mTOR pathway against LPS-induced injury. **(A)** The representative western blot bands of 14-3-3γ, LC3 II, and P62 expression in the cardiomyocytes. **(B-D)** The relative band intensity of 14-3-3γ, LC3 II, and P62 expression in the cardiomyocytes. **(E)** The representative western blot bands of total and phosphorylated mTOR, AMPK and ULK1 expression in the cardiomyocytes. **(F-H)** The relative band intensity of p-mTOR/mTOR, p-AMPK/AMPK, and p-ULK1/ULK1 expression in the cardiomyocytes. Values are presented as mean ± SEM. For five individual experiments, a: $P<0.01$ vs. the control group; b: $P<0.01$ vs. the LPS group; c: $P<0.01$ vs. the Cap+LPS group. d: $P<0.05$ vs. the control group; e: $P<0.05$ vs. the LPS group; f: $P<0.05$ vs. the Cap+LPS group; NS, nonsignificant.

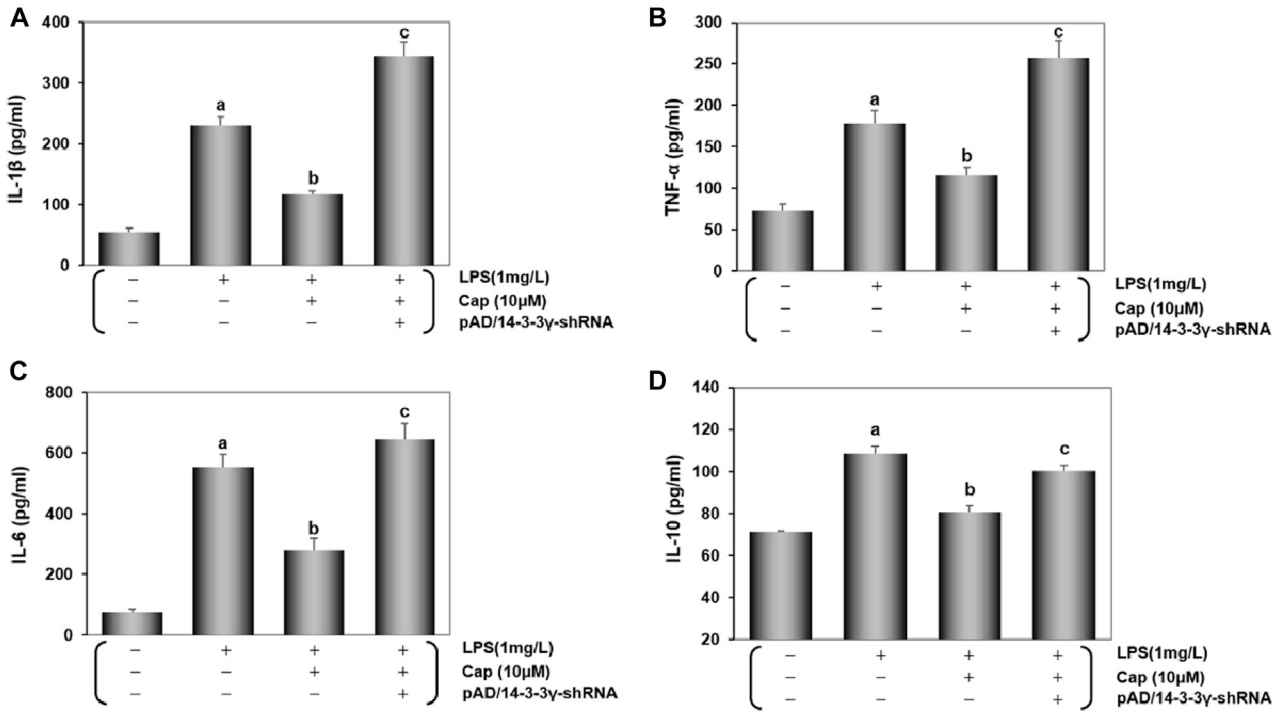

FIGURE 4 | Cap inhibits the activation of inflammatory cytokines in LPS- challenged cardiomyocytes. **(A-D)** IL-1β, TNF-α, IL-6, and IL-10 were measured in the culture supernatant of cardiomyocytes by diversiform ELISA assays. Values are presented as mean ± SEM. For five individual experiments, a: P<0.01 vs. the control group; b: P<0.01 vs. the LPS group; c: P<0.01 vs. the Cap+LPS group.

Taken together, these results indicated that LPS induced an accumulation of LC3II to active autophagy; pretreatment with Cap could further enhance the autophagic flux to scavenge the misfolded proteins and dysfunctional cellular components. Conversely, these protective effects were nullified by coincubation with pAD/14-3-3γ-shRNA.

Cap upregulates 14-3-3γ and integrates AMPKα/mTOR pathway against LPS-induced injury

The 14-3-3 protein influences the autophagy process (Lee et al., 2020). We investigated the underlying molecular pathway involved in 14-3-3γ regulation of autophagic levels. As shown in **Figures 3A–D,** compared with the LPS group, pretreatment with Cap significantly increased 14-3-3γ ($P < 0.01$) and LC3II ($P < 0.01$) expression, but decreased P62 ($P < 0.05$) expression. Interestingly, cotreatment with Cap and Compound C, an inhibitor of AMPK, upregulated 14-3-3γ (NS, nonsignificant vs. Cap+LPS), increased P62 expression ($P < 0.01$ vs. Cap+LPS), but reduced LC3II ($P < 0.01$ vs. Cap+LPS) after LPS challenge, indicating that the effects of 14-3-3γ upregulation by Cap during LPS-mediated autophagy might be related to AMPK.

Then, we examined changes in the expressions of AMPKα, mTOR, a common negative factor of autophagy (Kim and Guan, 2015), and ULK1. The p-AMPK/AMPKα and p-ULK1/ULK1 ratio in the Cap-pretreated cardiomyocytes were higher than in the LPS group ($P < 0.01$, **Figures 3E,F,H**), while p-mTOR expression was lower than that in the LPS group ($P < 0.01$, **Figures 3E,G**). Conversely, active phosphorylation sites of AMPK and ULK1, plus mTOR levels were reversed by Compound C addition.

These results demonstrated that Cap pretreatment involved a positive adjustment in autophagy level by upregulating 14-3-3γ, AMPK, and ULK1 levels, and suppressing mTOR expression. The results also demonstrated that the underlying mechanism of 14-3-3γ-dependent autophagy might be related with AMPK activity after LPS-induced cardiomyocyte injury.

Cap inhibits the activation of inflammatory cytokines in LPS-challenged cardiomyocytes

As an important index of LPS-induced damage (Schwerd et al., 2017), cytokine activities in cardiomyocytes were measured by ELISA (**Figure 4**). Contrasted with normal cardiomyocytes, IL-1β, TNF-α, IL-6, and IL-10 levels were significantly increased after LPS-induced injury ($P < 0.01$), but this index levels declined significantly with Cap pretreatment ($P < 0.01$). In contrast, the protective effects of Cap were weakened by adding pAD/14-3-3γ-shRNA ($P < 0.01$).

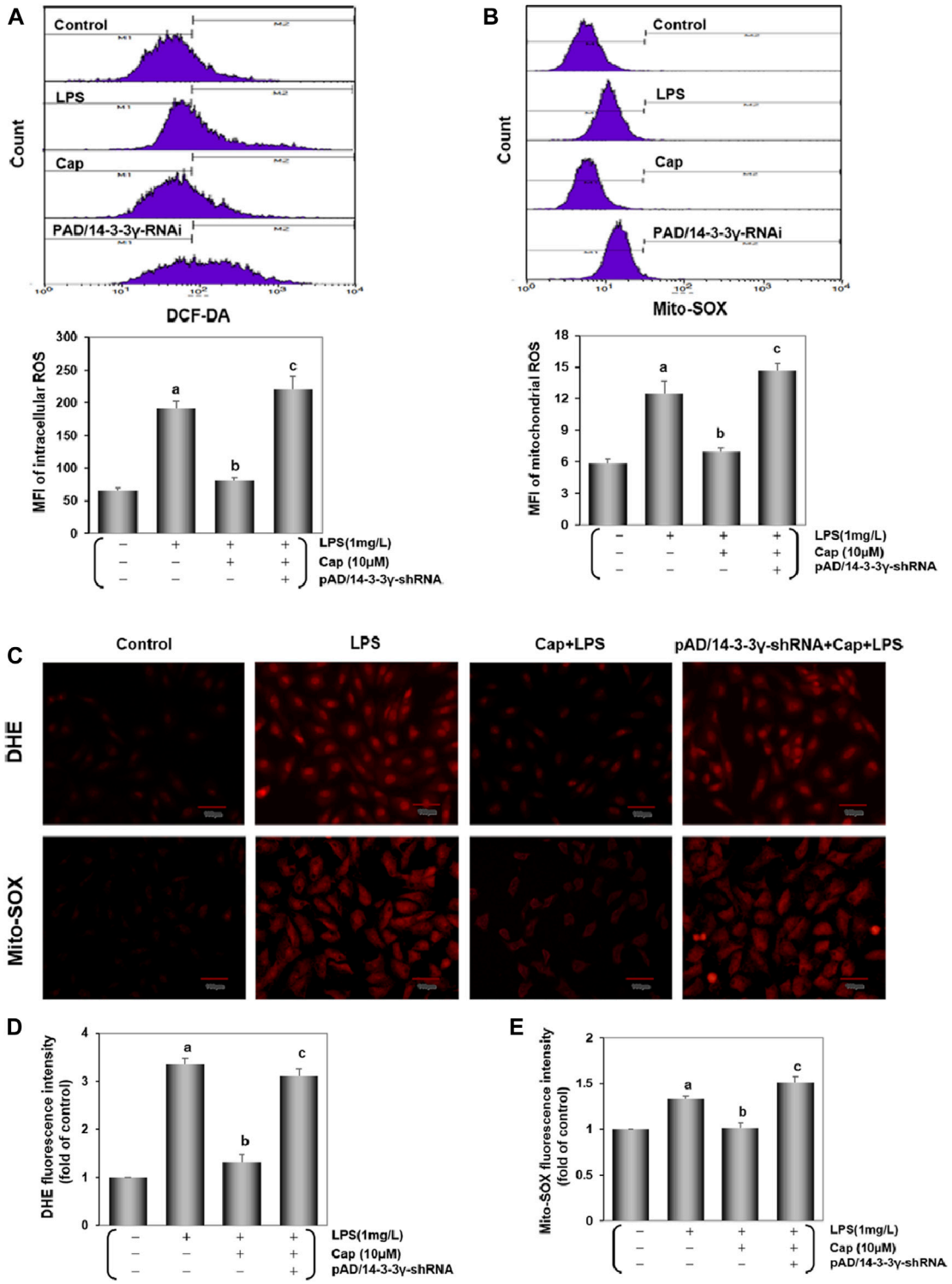

FIGURE 5 | Cap decreases Intracellular/mitochondrial ROS generation in cardiomyocytes injured after LPS challenge. **(A)** DCF-DA indicated intracellular ROS generation. **(B)** Mito-SOX measured mitochondrial ROS level. **(C)** Intracellular/ mitochondrial ROS were stained by DHE/Mito-SOX probe. **(D)** and **(E)** Fluorescence intensity of DHE and Mito-SOX were analyzed by ImageJ software. Values were presented as mean ± SEM. For five individual experiments, a: $P<0.01$ vs. the control group; b: $P<0.01$ vs. the LPS group; c: $P<0.01$ vs. the Cap+LPS group.

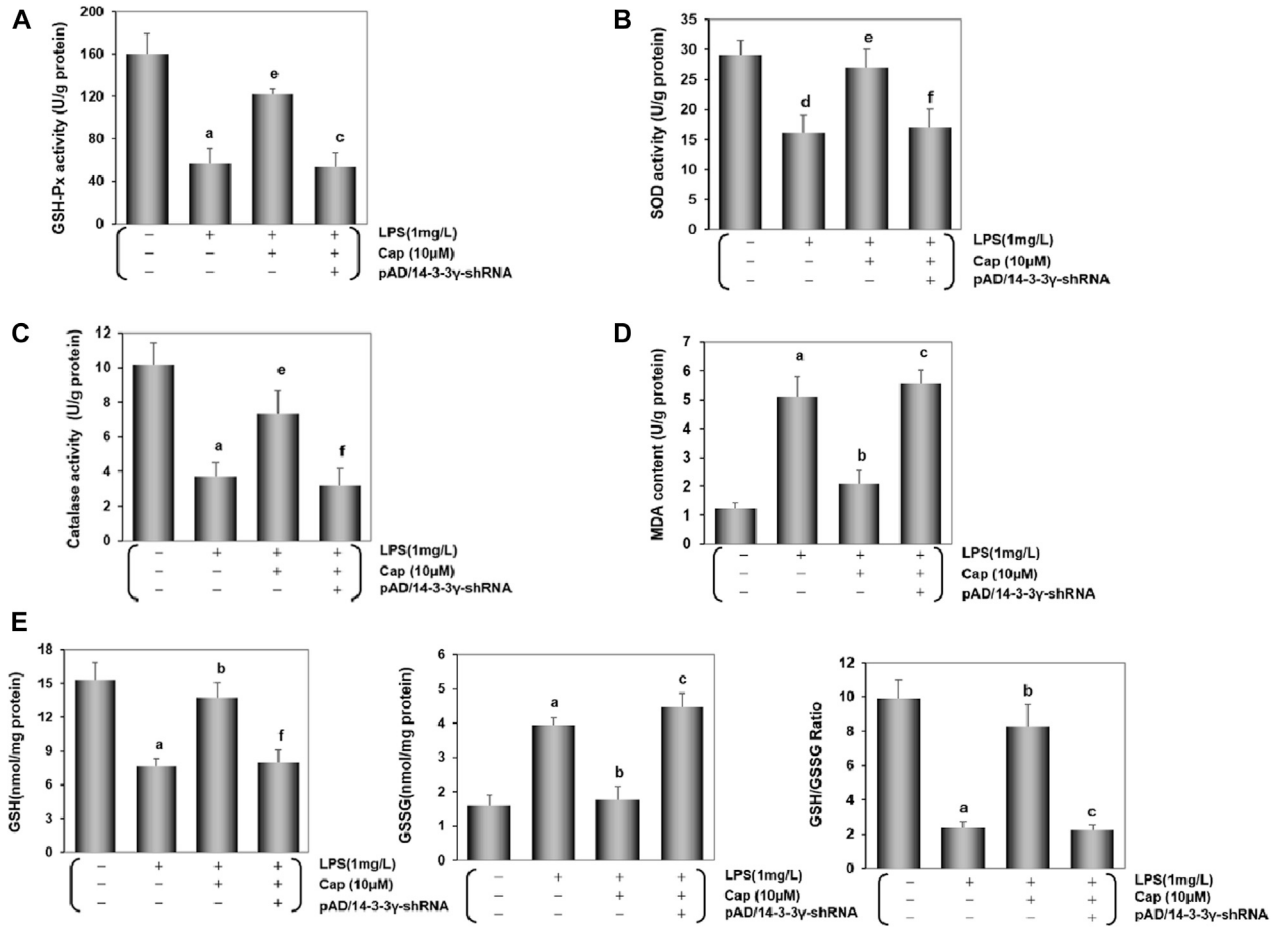

FIGURE 6 | Cap inhibits oxidative stress in injured cardiomyocytes after LPS challenge. **(A-D)** Activities of GSH-Px, SOD, and catalase, and MDA content in cardiomyocytes after different treatments. **(E)** Levels of intracellular glutathione in the cardiomyocyte. Left: intracellular GSH levels; middle: intracellular GSSG levels; right: intracellular GSH/GSSG ratio. Values are presented as mean ± SEM. For five individual experiments, a: $P<0.01$ vs. the control group; b: $P<0.01$ vs. the LPS group; c: $P<0.01$ vs. the Cap+LPS group. d: $P<0.05$ vs. the control group; e: $P<0.05$ vs. the LPS group; f: $P<0.05$ vs. the Cap+LPS group.

These results were consistent with Cap protecting cardiomyocytes from LPS-induced sepsis by upregulating 14-3-3γ expression.

Cap inhibits oxidative stress in injured cardiomyocytes after LPS challenge

Accumulating studies demonstrated that excessive ROS generation could induce cardiac inflammation following LPS challenge (Suzuki et al., 2012; Zhao et al., 2016). Intracellular/ mitochondrial ROS were detected by flow cytometry and fluorescence microscopy. As shown in **Figures 5A,B**, after adding LPS 24 h, the intracellular/ mitochondrial ROS curve moved significantly toward the right and the peak value was progressively enhanced ($P < 0.01$), while the change was inverted with Cap pretreatment ($P < 0.01$). The addition of pAD/14-3-3γ-shRNA nullified the protective effect of Cap ($P < 0.01$). Consistent with the results above, in LPS-challenged cardiomycetes, intense fluorescent dots were observed under fluorescence microscopy using DHE or Mito-SOX, but pretreatment with Cap reduced the fluorescence intensity (**Figures 5C–E**).

To confirm the change of oxidative status in cardiomyocytes, we examined the activities of endogenous antioxidant enzymes (GSH-Px, SOD, and catalase), lipid metabolite content (MDA), and non-enzymatic antioxidant system levels (GSH, GSSG and GSH/GSSG). Contrasted with the control group, the activities of GSH-Px, SOD and catalase exhibited a sharp decline while MDA contentshowed a progressive increase in the LPS-treated group ($P < 0.01$, **FiguresA–D**). Pretreatment with Cap reversed these indices to scavenge oxygen radicals in the cardiomyocytes, but the mentioned beneficial effects on the cardiomyocytes were offset after deregulating 14-3-3γ expression. Moreover, GSH and GSH/GSSG decreased, while GSSG exhibited the reverse trend after LPS-induced toxic effects ($P < 0.01$, **Figure 6E**). Pretreatment with Cap could protect the cardiomyocytes from LPS-induced damage by excessive oxygen species, but pAD/14-3-3γ-shRNA addition could aggravate the damage induced by LPS.

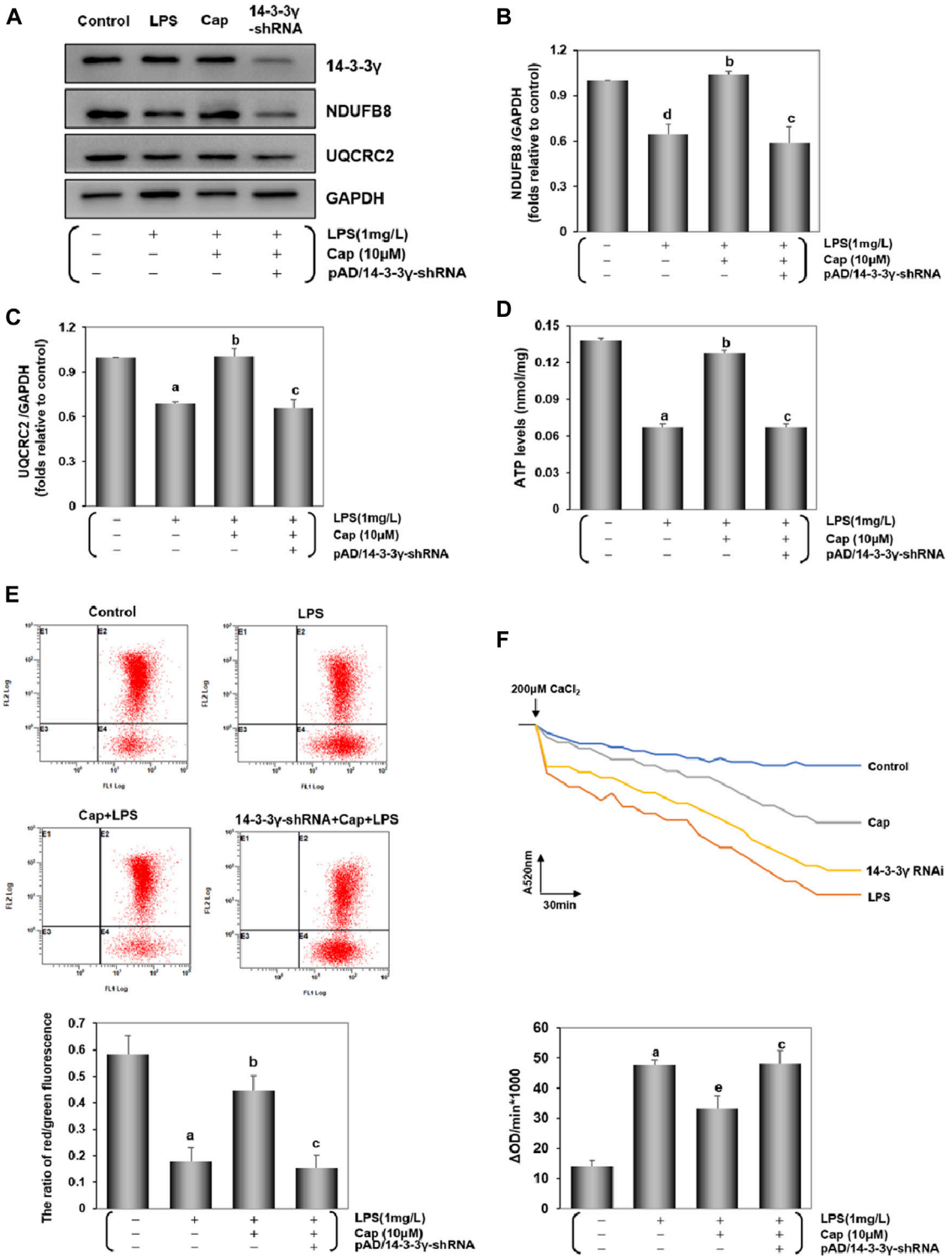

FIGURE 7 | Cap maintains mitochondrial function by regulating mitochondrial bioenergetics in cardiomyocytes after LPS challenge. **(A)** The representative western blot bands of NDUFB8 and UQCRC2 expression in the cardiomyocytes. **(B)** and **(C)** The relative band intensity of NDUFB8 and UQCRC2 expression in the cardiomyocytes. **(D)** Cardiomyocyte ATP levels were measured by firefly luciferase assay. **(E)** Levels of MMP were detected by JC-1, and red/green fluorescence ratio indicated MMP levels. **(F)** Mitochondrial swelling by Ca^{2+}-induced cells was used for measuring mPTP opening. The changes in absorbance values at 520 nm per minute were recorded and the mPTP opening levels are shown by fluctuations in absorbance ($\Delta OD = A520_{0min}\text{-}A520_{30min}$). Values are presented as mean ± SEM. For five individual experiments, a: $P<0.01$ vs. the control group; b: $P<0.01$ vs. the LPS group; c: $P<0.01$ vs. the Cap+LPS group. d: $P<0.05$ vs. the control group; e: $P<0.05$ vs. the LPS group.

These data demonstrated that LPS generated excessive ROS and decreased the scavenging of oxygen radicals. However, pretreatment with Cap could protect the cardiomyocytes from reducing oxidative stress by upregulating 14-3-3γ expression.

Cap maintains mitochondrial function by regulating mitochondrial bioenergetics in cardiomyocytes after LPS challenge

Studies have suggested that mitochondrial dysfunction via LPS toxicity triggers cardiomyocytes damage (Zhou et al., 2011; Liu et al., 2018). The expression of NDUFB8 and UQCRC2 can reflect mt complex Ⅰ/Ⅲ activities. Comparison of NDUFB8 or UQCRC2 expression between the control and LPS groups (**Figures 7A–C**) revealed that NDUFB8 ($P < 0.05$) and UQCRC2 ($P < 0.01$) expressions were decreased after LPS challenge, indicating an impairment of the mitochondrial electron transport chain (ETC) following LPS-induced injury. Meanwhile, LPS induced a significant decrease in ATP levels ($P < 0.01$, **Figure 7D**). Pretreatment with Cap upregulated NDUFB8 and UQCRC2 ($P < 0.01$, **Figures 7B,C**), and restored ATP levels ($P < 0.01$), but these positive effects were nullified by adding pAD/14-3-3γ- shRNA.

The alternation of MMP and mPTP opening served as biological markers for the mitochondrial function (Dai et al., 2020; Kinnally et al., 2011). The ratio of red/green fluorescence represents the degree of MMP oscillation in cells. Compared with the control group, the decline in the red/green ratio reflected a loss of MMP in the LPS group, whereas Cap-pretreatment restored the cardiomyocytes from MMP loss ($P < 0.01$, **Figure 7E**). Additionally, **Figure 7F** shows that the mPTP opening was activated following LPS challenge unlike in the control group ($P < 0.01$); however, pretreatment with Cap presented a steady downward trend ($P < 0.05$). The above protective effects could be blunted when 14-3-3γ expression was significantly reduced using pAD/14-3-3γ-shRNA.

From these results, we discovered that LPS-induced toxicity could trigger mitochondrial damage in the cardiomyocytes. Nevertheless, pretreatment with Cap effectively improved the mitochondrial function by upregulating the 14-3-3γ protein.

DISCUSSION

The study explored whether (i) upregulating 14-3-3γ via Cap pretreatment contributed to autophagy via the AMPK-mTOR/ULK1 pathway against LPS-induced sepsis to myocardial injury (ii) Cap protected cardiomyocytes from LPS-induced inflammation, excessive oxidative stress, and mitochondrial dysfunction. Accumulating studies indicated that LPS triggered cellular damage, especially in cardiomyocytes (Drosatos et al., 2013; Beesley et al., 2018). Here, we found that cell viability was significantly decreased and the LDH and CK activities were increased following LPS stimulation (**Figures 1C–E**). Interestingly, Cap presented a concentration-dependent increase to protect cardiomyocytes in response to LPS-induced cardiotoxicity (**Figures 1A,B**), indicating a beneficial role in cardiomyocytes following damage.

Our previous studies have demonstrated that Cap has multiple targets, including 14-3-3η and SIRT1, by which it protects cardiomyocytes against anoxia/reoxygenation-induced damage (Qiao et al., 2020; Huang et al., 2018a; He et al., 2017). In the study, Cap-mediated positive effects on cardiomyocytes were related to 14-3-3γ expression after LPS-induced injury (**Figures 1–7**). 14-3-3γ (an isoform of the 14-3-3 family proteins in mammals) was evidenced by its involvement in variable cellular processes, for example cell proliferation (Kumar et al., 2003), survival (Masters et al., 2002) and apoptosis (Zha et al., 1996). In the previously published work, we focused on 14-3-3γ/Bcl-2-mediated apoptotic pathway regulation in cardiomyocytes or human umbilical vein endothelial cells (HUVECs) against LPS or doxorubicin toxicity (He et al., 2006; Liu et al., 2014; Huang et al., 2018b; Yang et al., 2019). The specific mechanism of 14-3-3γ upregulation via Cap pretreatment remained unclear, as well as the effects by other programmed cell death pathways in cardiomyocytes after LPS-induced injury were also worth studying.

Autophagy-dependent cell death, which is driven by autophagy-related genes, significantly affects LPS-induced cardiotoxicity and ischemia/reperfusion-induced injury in cardiomyocytes (Ma et al., 2012; Tang et al., 2019; Di et al., 2020). In this study, the level of LC3Ⅱ increased and P62 presented reversed trend in cardiomyocytes following the LPS challenge. Besides, after coincubation with BafA1, LC3Ⅱ and P62 levels were significantly improved, indicating that LPS treatment could trigger a low level of autophagy instead of impairment in autophagic flux (**Figure 2A**). Previous studies have suggested that activation of autophagy could contribute to suppressing LPS-induced cell toxicity (Sun et al., 2018; Quach et al., 2019; Wu et al., 2020), autophagy influences the clearance of damaged proteins and organelles (Yang and Klionsky, 2010). After pretreatment with Cap, LC3Ⅱ was significantly increased and P62 degradation was declined (**Figures 2B–E**). Furthermore, autophagosomes, autolysosomes, and lysosomes were increased in Cap-pretreated cardiomyocytes (**Figure 2F**). These results correlated with the above data and suggested that Cap-mediated protection effects on cardiomyocytes might be related to activating autophagy.

AMPK is a well-known energy sensor in eukaryotes (de Pablos et al., 2019; Mihaylova and Shaw, 2011), and is also a key regulator in multiple cellular processes, such as ferroptosis (Lee et al., 2020), pyroptosis (He et al., 2016), and autophagy (Wang et al., 2018). Interestingly, our study showed that upregulating 14-3-3γ by Cap pretreatment could accumulate the markers of autophagy, however, the level of autophagy was significantly reduced when AMPK was inhibited by cotreatment with Compound C (**Figures 3A–D**). These results indicated that the effect of Cap in activating autophagy might be mediated via the AMPK pathway in cardiomyocytes following LPS challenge. AMPK-caused induction of autophagy may be partially related to mTOR and ULK1 (Ghavami et al., 2014). In detail, AMPK could promote 14-3-3 protein binding to Raptor (an effector of mTOR), which is needed for inhibiting mTOR activity (Meijer and Codogno, 2007). Moreover, evidence showed that the 14-3-3 protein was recruited to interfere with ULK1-mTOR binding by activating AMPK (Gwinn et al., 2008; Lee et al., 2010). Our results

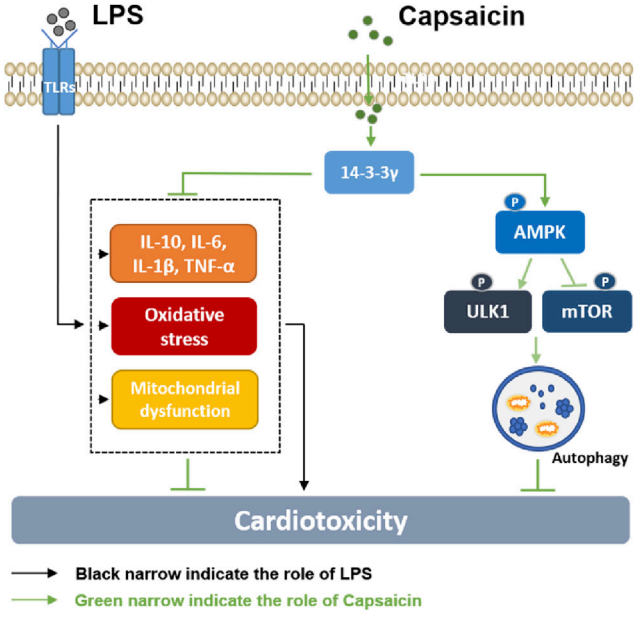

FIGURE 8 | Diagram showing the possible mechanism by which Cap alleviates LPS-induced cardiotoxicity. LPS-induced cardiotoxicity was manifested in activating inflammatory cytokines, producing excess oxygen radicals, and causing mitochondrial damage. The negative effects of LPS on cardiomyocytes are reversed by Cap, and the underlying mechanism may be involved in Cap-mediated 14-3-3γ expression and autophagy regulation via the AMPK-mTOR/ULK1 pathway.

showed that AMPK and ULK1 were activated, but mTOR activation was suppressed in the pretreatment with the Cap group after LPS-induced toxicity. Conversely, these beneficial effects of Cap-pretreatment were offset by adding Compound C (**Figures 3E–H**). These data suggested that the potential mechanism of 14-3-3γ action on AMPK involves suppression of mTOR and activation of ULK1. Thus, these consistent results indicated a positive feedback during the autophagy process in LPS-damaged cardiomyocytes by Cap pretreatment.

LPS is a known stimulator in the systemic inflammatory mechanism of sepsis (Fu et al., 2015), LPS-triggered ROS generation, and the release of inflammatory cytokines, such as IL-1β, TNF-α, IL-6, and IL-10 (Ceni et al., 2014). Some studies have confirmed that 14-3-3 proteins could regulate the inflammatory response at the genetic, molecular, and cellular levels (Munier et al., 2021; McGowan et al., 2020). Cap could also inhibit inflammatory process though TRPV1-dependent or TRPV1-independent mechanisms (Fernandes et al., 2016; Braga Ferreira, et al., 2020; Ilie et al., 2019). Here, cytokine release was significantly increased in cardiomyocytes after LPS stimulation, while the high levels of IL-1β, TNF-α, IL-6, and IL-10 in the LPS group were reversed by Cap pretreatment; however, these positive changes were nullified after adding pAD/14-3-3γ-shRNA (**Figure 4**). Hence, our results suggested that pretreatment with Cap could alleviate inflammation by upregulating 14-3-3γ in LPS-stimulated cardiomyocytes. Moreover, autophagy plays a key role in controlling inflammation and maintaining cardiomyocyte homeostasis (Turdi et al., 2012; Zhou et al., 2018). Our findings were consistent with the above alternations of autophagy, likely because temperate activation of autophagy could scavenge damaged organelles of cardiomyocytes, which might be related to the generation of inflammatory signals. Certainly, the specific mechanism needs to be explored further.

Sepsis-induced cardiac inflammation is regulated via ROS-dependent activation (Chen et al., 2015). Our previous studies have proven that excessive ROS generation was responsible for doxorubicin-induced endotheliotoxicity and cardiotoxicity (He et al., 2020; Qiao et al., 2020). In this study, we explored the role of intracellular ROS in the LPS-stimulated cardiomyocytes. We found that intracellular ROS generation was enhanced in the LPS group (**Figure 5A**). Moreover, DHE, a common fluorescent probe was used to detect oxygen radicals in cardiovascular systems (Griendling et al., 2016): strong fluorescent dots were observed in the LPS group (**Figures 5C,D**). These changes coincided with the above results. Additionally, the endogenous antioxidant enzyme system including GSH-Px, SOD, catalase, and MDA, is the mechanism of defense against internal oxidative stress (Prasai et al., 2018). Our results showed that GSH-Px, SOD, and catalase activities were inhibited, and MDA content was increased in the cardiomyocytes after LPS injury (**Figures 6A–D**). The GSH/GSSG ratio maintains the redox equilibrium in cardiomyocytes by decreasing excessive ROS production (Quintana-Cabrera et al., 2012; Giustarini et al., 2016). The GSH content and GSH/GSSG ratio were reduced, while the GSSG content was significantly increased by LPS-induced cardiomyocyte injury (**Figure 6E**). Cap-pretreatment besides reducing intracellular ROS concentrations, also improved the activities of the endogenous antioxidant system and the abilities of the nonenzymatic antioxidant system in the cardiomyocytes after LPS-induced injury, and its protective effects were inextricably linked to the expression of 14-3-3γ (**Figures 5**, **6**).

Mitochondria are the sites where molecules that impact the inflammation, especially the overwhelming mitochondrial ROS (mtROS), are generated (Zorov et al., 2014). We showed that mtROS generation was stimulated in LPS-treated cardiomyocytes. As expected, the curve of mtROS was significantly skewed to the left in the Cap pretreatment group (**Figures 5B,C,E**). Combined with prior results, we confirmed that pretreatment with Cap could protect cardiomyocytes from LPS-induced inflammation by reducing the degree of intracellular/mitochondrial ROS. Moreover, LPS triggered excessive mtROS generation, resulting in severe mitochondrial dysfunction, an overflow of the mtDNA fragment (Zhang et al., 2010) and mtROS (Brealey et al., 2002), ATP loss (Schwiebert and Zsembery, 2003) and so on. Complex I/III on mitochondria are the major sites of ROS generation. In our study, NDUFB8 (a subunit of mt complex I) and UQCRC2 (a subunit of mt complex III) expression were inhibited by LPS-induced toxicity, but Cap pretreatment could promote NDUFB8 and UQCRC2 expression by upregulating 14-3-3γ levels (**Figures 7A–C**). These findings indicated that LPS stimulated intracellular/mitochondrial ROS by inhibiting Complex I/III activities in the cardiomyocytes, but these negative effects could be weakened by Cap pretreatment. Mitochondria are also essential organelles in modulating energy generation (Wang et al., 2018). The decline in ATP production is

closely relevant to the impairment of mitochondrial respiration in cardiomyocytes (Makrecka-Kuka et al., 2019). Our results showed a decrease in ATP levels in the LPS-treated group, but counter outcomes were presented in the Cap pretreatment group (**Figure 7D**). These series of results demonstrated that pretreatment with Cap alleviated mitochondrial damage in LPS-challenged cardiomyocytes by maintaining mitochondrial metabolism, and subsequently reinforced the key role of mitochondrial function as an essential component against LPS-induced cardiotoxicity.

Mitochondrial dysfunction is sensed by a decline in MMP (De Biasi et al., 2015); simultaneously, damaged mitochondria release mitophagy-related factors such as Parkin and BNIP3 to modulate the mitophagy pathway (Sun et al., 2018) and promote the opening of mPTPs (Hamacher-Brady et al., 2007; Zhang et al., 2008). In LPS-induced cardiomyocyte injury, pretreatment with Cap could sustain MMP and inhibit mPTP opening, while the downregulation of 14-3-3γ presented an opposite trend (**Figures 7E,F**). These results suggested that mitochondria were the major organelles of LPS-induced cardiotoxicity, and might also be the targets for Cap in protecting cardiomyocytes against LPS-induced injury via 14-3-3γ expression upregulation.

LIMITATION OF THE STUDY

Mitophagy significantly influences LPS-induced cardiotoxicity (Sun et al., 2018). Further studies are needed to explore the potential mechanism of Cap-upregulated 14-3-3γ expression, and how the AMPK-mTOR/ULK1 pathway regulates IL-1β, TNF-α, IL-6, and IL-10 in LPS-stimulated cardiotoxicity during the mitophagy process.

CONCLUSIONS

In this study, we investigated the possible mechanism of Cap-upregulated 14-3-3γ expression in cardioprotection against LPS-induced injury. LPS-induced cardiotoxicity was manifested in activating inflammatory cytokines, producing excess oxygen radicals, and triggering mitochondrial damage. However, the negative effects of LPS on cardiomyocytes are reversed by Cap, and the underlying mechanism may be involved in Cap-mediated 14-3-3γ expression and autophagy regulation via the AMPK-mTOR/ULK1 pathway (**Figure 8**).

DATA AVAILABILITY STATEMENT

The raw data supporting the conclusions of this article will be made available by the authors, without undue reservation, to any qualified researcher.

ETHICS STATEMENT

The animal study was reviewed and approved by The animal study was reviewed and approved by Ethics Committee of Nanchang University(No. 2019-0036).

AUTHOR CONTRIBUTIONS

MH and HH conceived and designed the experiments. YQ, LW, TH and HH performed the experiments. DY and HH analyzed the data. HH and DY contributed reagents/materials/analysis tools. YQ, HH and MH wrote the paper.

FUNDING

This research was supported by grants from the National Natural Science Foundation of China (No: 81803534, 81660538) and the Natural Scientific Foundation of Jiangxi province (No: 20171BAB215077).

ACKNOWLEDGMENTS

We would like to thank Editage (www.editage.cn) for English language editing.

REFERENCES

Angus, D., Pires Pereira, C., and Silva, E. (2006). Epidemiology of severe sepsis around the world. *Emiddt* 6, 207–212. doi:10.2174/187153006777442332

Bampton, E. T. W., Goemans, C. G., Niranjan, D., Mizushima, N., and Tolkovsky, A. M. (2005). The dynamics of autophagy visualised in live cells: from autophagosome formation to fusion with endo/lysosomes. *Autophagy* 1, 23–36. 10.4161/auto.1.1.1495

Beesley, S. J., Weber, G., Sarge, T., Nikravan, S., Grissom, C. K., Lanspa, M. J., et al. (2018). Septic cardiomyopathy. *Crit. Care Med.* 46, 625–634. doi:10.1097/CCM.0000000000002851

Braga Ferreira, L. G., Faria, J. V., Dos Santos, J. P. S., and Faria, R. X. (2020). Capsaicin: TRPV1-independent mechanisms and novel therapeutic possibilities. *Eur. J. Pharmacol.* 887, 173356. doi:10.1016/j.ejphar.2020.173356

Brealey, D., Brand, M., Hargreaves, I., Heales, S., Land, J., Smolenski, R., et al. (2002). Association between mitochondrial dysfunction and severity and outcome of septic shock. *The Lancet* 360, 219–223. doi:10.1016/S0140-6736(02)09459-X

Ceni, E., Mello, T., and Galli, A. (2014). Pathogenesis of alcoholic liver disease: role of oxidative metabolism. *Wjg* 20, 17756–17772. doi:10.3748/wjg.v20.i47.17756

Chen, S., Yuan, J., Yao, S., Jin, Y., Chen, G., Tian, W., et al. (2015). Lipopolysaccharides may aggravate apoptosis through accumulation of autophagosomes in alveolar macrophages of human silicosis. *Autophagy* 11, 2346–2357. doi:10.1080/15548627.2015.1109765

Chen, X., Li, H., Wang, Z., Zhou, Q., Chen, S., Yang, B., et al. (2020). Quercetin protects the vascular endothelium against iron overload damages via ROS/ADMA/DDAHII/eNOS/NO pathway. *Eur. J. Pharmacol.* 868, 172885. doi:10.1016/j.ejphar.2019.172885

Dai, Q., Provost, M. P., Raburn, D. J., and Price, T. M. (2020). Progesterone increases mitochondria membrane potential in non-human primate oocytes and embryos. *Reprod. Sci.* 27, 1206–1214. doi:10.1007/s43032-019-00132-2

Dasgupta, B., and Seibel, W. (2018). Compound C/dorsomorphin: its use and misuse as an AMPK inhibitor. *Methods Mol. Biol.* 1732, 195–202. doi:10.1007/978-1-4939-7598-3_12

De Biasi, S., Gibellini, L., and Cossarizza, A. (2015). Uncompensated polychromatic analysis of mitochondrial membrane potential using JC-1 and multilaser excitation. *Curr. Protoc. Cytom* 72, 7–327. doi:10.1002/047114295610.1002/0471142956.cy0732s72132.11

de Pablos, R. M., Espinosa-Oliva, A. M., Hornedo-Ortega, R., Cano, M., and Arguelles, S. (2019). Hydroxytyrosol protects from aging process via AMPK and autophagy; a review of its effects on cancer, metabolic syndrome, osteoporosis, immune-mediated and neurodegenerative diseases. *Pharmacol. Res.* 143, 58–72. doi:10.1016/j.phrs.2019.03.005

Di, S., Wang, Z., Hu, W., Yan, X., Ma, Z., Li, X., et al. (2020). The protective effects of melatonin against LPS-induced septic myocardial injury: a potential role of AMPK-mediated autophagy. *Front. Endocrinol. (Lausanne).* 11, 162. doi:10.3389/fendo.2020.00162

Drosatos, K., Khan, R. S., Trent, C. M., Jiang, H., Son, N.-H., Blaner, W. S., et al. (2013). Peroxisome proliferator-activated receptor-γ activation prevents sepsis-related cardiac dysfunction and mortality in mice. *Circ. Heart Fail.* 6, 550–562. doi:10.1161/CIRCHEARTFAILURE.112.000177

Fernandes, E. S., Cerqueira, A. R. A., Soares, A. G., and Costa, S. K. P. (2016). Capsaicin and its role in chronic diseases. *Adv. Exp. Med. Biol.* 929, 91–125. doi:10.1007/978-3-319-41342-6_5

Fu, Y., Hu, X., Cao, Y., Zhang, Z., and Zhang, N. (2015). Saikosaponin a inhibits lipopolysaccharide-oxidative stress and inflammation in Human umbilical vein endothelial cells via preventing TLR4 translocation into lipid rafts. *Free Radic. Biol. Med.* 89, 777–785. doi:10.1016/j.freeradbiomed.2015.10.407

Gerber, W., Steyn, D., Kotzé, A., Svitina, H., Weldon, C., and Hamman, J. (2019). Capsaicin and piperine as functional excipients for improved Drug delivery across nasal epithelial models. *Planta Med.* 85, 1114–1123. doi:10.1055/a-0978-5172

Ghavami, S., Gupta, S., Ambrose, E., Hnatowich, M., Freed, D. H., and Dixon, I. M. C. (2014). Autophagy and heart disease: implications for cardiac ischemia-reperfusion damage. *Cmm* 14, 616–629. doi:10.2174/1566524014666140603101520

Giustarini, D., Tsikas, D., Colombo, G., Milzani, A., Dalle-Donne, I., Fanti, P., et al. (2016). Pitfalls in the analysis of the physiological antioxidant glutathione (GSH) and its disulfide (GSSG) in biological samples: an elephant in the room. *J. Chromatogr. B* 1019, 21–28. doi:10.1016/j.jchromb.2016.02.015

Griendling, K. K., Touyz, R. M., Zweier, J. L., Dikalov, S., Chilian, W., Chen, Y.-R., et al. (2016). Measurement of reactive oxygen species, reactive nitrogen species, and redox-dependent signaling in the cardiovascular system. *Circ. Res.* 119, e39–75. doi:10.1161/RES.0000000000000110

Gwinn, D. M., Shackelford, D. B., Egan, D. F., Mihaylova, M. M., Mery, A., Vasquez, D. S., et al. (2008). AMPK phosphorylation of raptor mediates a metabolic checkpoint. *Mol. Cel* 30, 214–226. doi:10.1016/j.molcel.2008.03.003

Hamacher-Brady, A., Brady, N. R., Logue, S. E., Sayen, M. R., Jinno, M., Kirshenbaum, L. A., et al. (2007). Response to myocardial ischemia/reperfusion injury involves Bnip3 and autophagy. *Cell Death Differ* 14, 146–157. doi:10.1038/sj.cdd.440193610

Hausenloy, D. J., and Yellon, D. M. (2011). The therapeutic potential of ischemic conditioning: an update. *Nat. Rev. Cardiol.* 8, 619–629. doi:10.1038/nrcardio.2011.85

He, H., Wang, L., Qiao, Y., Zhou, Q., Li, H., Chen, S., et al. (2020). Doxorubicin induces endotheliotoxicity and mitochondrial dysfunction via ROS/eNOS/NO pathway. *Front. Pharmacol.* 10, 1531. 10.3389/fphar.2019.01531.

He, H., Zhou, Y., Huang, J., Wu, Z., Liao, Z., Liu, D., et al. (2017). Capsaicin protects cardiomyocytes against anoxia/reoxygenation injury via preventing mitochondrial dysfunction mediated by SIRT1. *Oxidative Med. Cell Longevity* 2017, 1. doi:10.1155/2017/1035702

He, M., Zhang, J., Shao, L., Huang, Q., Chen, J., Chen, H., et al. (2006). Upregulation of 14-3-3 isoforms in acute rat myocardial injuries induced by burn and lipopolysaccharide. *Clin. Exp. Pharmacol. Physiol.* 33, 374–380. doi:10.1111/j.1440-1681.2006.04378.x

He, Y., Zeng, M. Y., Yang, D., Motro, B., and Núñez, G. (2016). NEK7 is an essential mediator of NLRP3 activation downstream of potassium efflux. *Nature* 530, 354–357. doi:10.1038/nature16959

Hsiao, H.-W., Tsai, K.-L., Wang, L.-F., Chen, Y.-H., Chiang, P.-C., Chuang, S.-M., et al. (2012). The decline of autophagy contributes to proximal tubular dysfunction during sepsis. *Shock* 37, 289–296. doi:10.1097/SHK.0b013e318240b52a

Huang, B., You, J., Qiao, Y., Wu, Z., Liu, D., Yin, D., et al. (2018a). Tetramethylpyrazine attenuates lipopolysaccharide-induced cardiomyocyte injury via improving mitochondrial function mediated by 14-3-3γ. *Eur. J. Pharmacol.* 832, 67–74. doi:10.1016/j.ejphar.2018.05.019

Huang, J., Liu, Z., Xu, P., Zhang, Z., Yin, D., Liu, J., et al. (2018b). Capsaicin prevents mitochondrial damage, protects cardiomyocytes subjected to anoxia/reoxygenation injury mediated by 14-3-3η/Bcl-2. *Eur. J. Pharmacol.* 819, 43–50. doi:10.1016/j.ejphar.2017.11.028

Huang, S., Xu, M., Liu, L., Yang, J., Wang, H., Wan, C., et al. (2020b). Autophagy is involved in the protective effect of p21 on LPS-induced cardiac dysfunction. *Cell Death Dis* 11, 554. doi:10.1038/s41419-020-02765-7

Ilie, M., Caruntu, C., Tampa, M., Georgescu, S.-R., Matei, C., Negrei, C., et al. (2019). Capsaicin: physicochemical properties, cutaneous reactions and potential applications in painful and inflammatory conditions (Review). *Exp. Ther. Med.* 18, 916–925. doi:10.3892/etm.2019.7513

Kim, Y. C., and Guan, K.-L. (2015). mTOR: a pharmacologic target for autophagy regulation. *J. Clin. Invest.* 125, 25–32. doi:10.1172/JCI73939

Kinnally, K. W., Peixoto, P. M., Ryu, S.-Y., and Dejean, L. M. (2011). Is mPTP the gatekeeper for necrosis, apoptosis, or both?. *Biochim. Biophys. Acta (Bba) - Mol. Cel Res.* 1813, 616–622. doi:10.1016/j.bbamcr.2010.09.013

Kolwicz, S. C., Jr., Purohit, S., and Tian, R. (2013). Cardiac metabolism and its interactions with contraction, growth, and survival of cardiomyocytes. *Circ. Res.* 113, 603–616. doi:10.1161/CIRCRESAHA.113.302095

Kumar, A. P., Garcia, G. E., Orsborn, J., Levin, V. A., and Slaga, T. J. (2003). 2-Methoxyestradiol interferes with NFkappaB transcriptional activity in primitive neuroectodermal brain tumors: implications for management. *Carcinogenesis* 24, 209–216. doi:10.1093/carcin/24.2.209

Lee, H., Zandkarimi, F., Zhang, Y., Meena, J. K., Kim, J., Zhuang, L., et al. (2020). Energy-stress-mediated AMPK activation inhibits ferroptosis. *Nat. Cel Biol* 22, 225–234. doi:10.1038/s41556-020-0461-8

Lee, J. W., Park, S., Takahashi, Y., and Wang, H. G. (2010). The association of AMPK with ULK1 regulates autophagy. *PLoS One* 5, e15394. doi:10.1371/journal.pone.0015394

Li, F., Lang, F., Zhang, H., Xu, L., Wang, Y., and Hao, E. (2016). Role of TFEB mediated autophagy, oxidative stress, inflammation, and cell death in endotoxin induced myocardial toxicity of young and aged mice. *Oxidative Med. Cell Longevity* 2016, 1. doi:10.1155/2016/53803192016

Li, Y., Ye, Z., Lai, W., Rao, J., Huang, W., Zhang, X., et al. (2017). Activation of sirtuin 3 by silybin attenuates mitochondrial dysfunction in cisplatin-induced acute kidney injury. *Front. Pharmacol.* 8, 178. doi:10.3389/fphar.2017.00178

Lin, Z., Liu, T., Kamp, D. W., Wang, Y., He, H., Zhou, X., et al. (2014). AKT/mTOR and c-Jun N-terminal kinase signaling pathways are required for chrysotile asbestos-induced autophagy. *Free Radic. Biol. Med.* 72, 296–307. doi:10.1016/j.freeradbiomed.2014.04.004

Liu, D., Yi, B., Liao, Z., Tang, L., Yin, D., Zeng, S., et al. (2014). 14-3-3γ protein attenuates lipopolysaccharide-induced cardiomyocytes injury through the Bcl-2 family/mitochondria pathway. *Int. Immunopharmacology* 21, 509–515. doi:10.1016/j.intimp.2014.06.014

Liu, Q., Zhang, D., Hu, D., Zhou, X., and Zhou, Y. (2018). The role of mitochondria in NLRP3 inflammasome activation. *Mol. Immunol.* 103, 115–124. doi:10.1016/j.molimm.2018.09.01010

Liu, Y., Yang, W., Sun, X., Xie, L., Yang, Y., Sang, M., et al. (2019). SS31 ameliorates sepsis-induced heart injury by inhibiting oxidative stress and inflammation. *Inflammation* 42, 2170–2180. doi:10.1007/s10753-019-01081-3

Luo, Y., Wan, Q., Xu, M., Zhou, Q., Chen, X., Yin, D., et al. (2019). Nutritional preconditioning induced by astragaloside Ⅳ on isolated hearts and cardiomyocytes against myocardial ischemia injury via improving Bcl-2-mediated mitochondrial function. *Chemico-Biological Interactions* 309, 108723. doi:10.1016/j.cbi.2019.06.036

Ma, X., Liu, H., Foyil, S. R., Godar, R. J., Weinheimer, C. J., Hill, J. A., et al. (2012). Impaired autophagosome clearance contributes to cardiomyocyte death in ischemia/reperfusion injury. *Circulation* 125, 3170–3181. doi:10.1161/CIRCULATIONAHA.111.041814

Makrecka-Kuka, M., Korzh, S., Vilks, K., Vilskersts, R., Cirule, H., Dambrova, M., et al. (2019). Mitochondrial function in the kidney and heart, but not the brain, is mainly altered in an experimental model of endotoxaemia. *Shock* 52, e153–e162. doi:10.1097/SHK.0000000000001315

Masters, S. C., Subramanian, R. R., Truong, A., Yang, H., Fujii, K., Zhang, H., et al. (2002). Survival-promoting functions of 14-3-3 proteins. *Biochem. Soc. Trans.* 30, 360–365. doi:10.1042/bst0300360

Mauthe, M., Orhon, I., Rocchi, C., Zhou, X., Luhr, M., Hijlkema, K.-J., et al. (2018). Chloroquine inhibits autophagic flux by decreasing autophagosome-lysosome fusion. *Autophagy* 14, 1435–1455. doi:10.1080/15548627.2018.1474314

McGowan, J., Peter, C., Kim, J., Popli, S., Veerman, B., Saul-McBeth, J., et al. (2020). 14-3-3ζ-TRAF5 axis governs interleukin-17A signaling. *Proc. Natl. Acad. Sci. USA* 117, 25008–25017. doi:10.1073/pnas.2008214117

Meijer, A. J., and Codogno, P. (2007). AMP-activated protein kinase and autophagy. *Autophagy* 3, 238–240. doi:10.4161/auto.3710

Mihaylova, M. M., and Shaw, R. J. (2011). The AMPK signalling pathway coordinates cell growth, autophagy and metabolism. *Nat. Cel Biol* 13, 1016–1023. doi:10.1038/ncb2329

Munier, C. C., Ottmann, C., and Perry, M. W. D. (2021). 14-3-3 modulation of the inflammatory response. *Pharmacol. Res.* 163, 105236. doi:10.1016/j.phrs.2020.105236

Murphy, M. P. (2009). How mitochondria produce reactive oxygen species. *Biochem. J.* 417, 1–13. doi:10.1042/BJ20081386

Nishida, K., Kyoi, S., Yamaguchi, O., Sadoshima, J., and Otsu, K. (2009). The role of autophagy in the heart. *Cel Death Differ* 16, 31–38. doi:10.1038/cdd.2008.163

Okuhara, Y., Yokoe, S., Iwasaku, T., Eguchi, A., Nishimura, K., Li, W., et al. (2017). Interleukin-18 gene deletion protects against sepsis-induced cardiac dysfunction by inhibiting PP2A activity. *Int. J. Cardiol.* 243, 396–403. doi:10.1016/j.ijcard.2017.04.082

Prasai, P. K., Shrestha, B., Orr, A. W., and Pattillo, C. B. (2018). Decreases in GSH: GSSG activate vascular endothelial growth factor receptor 2 (VEGFR2) in human aortic endothelial cells. *Redox Biol.* 19, 22–27. doi:10.1016/j.redox.2018.07.015

Qiao, Y., Hu, T., Yang, B., Li, H., Chen, T., Yin, D., et al. (2020). Capsaicin alleviates the deteriorative mitochondrial function by upregulating 14-3-3η in anoxic or anoxic/reoxygenated cardiomyocytes. *Oxidative Med. Cell Longevity* 2020, 1. doi:10.1155/2020/1750289

Quach, C., Song, Y., Guo, H., Li, S., Maazi, H., Fung, M., et al. (2019). A truncating mutation in the autophagy gene UVRAG drives inflammation and tumorigenesis in mice. *Nat. Commun.* 10, 5681. doi:10.1038/s41467-019-13475-w

Quintana-Cabrera, R., Fernandez-Fernandez, S., Bobo-Jimenez, V., Escobar, J., Sastre, J., Almeida, A., et al. (2012). γ-Glutamylcysteine detoxifies reactive oxygen species by acting as glutathione peroxidase-1 cofactor. *Nat. Commun.* 3, 718. doi:10.1038/ncomms1722

Roach, P. J. (2011). AMPK -> ULK1 -> autophagy. *Mol. Cell Biol.* 31, 3082–3084. doi:10.1128/MCB.05565-11

Schorr, C. A., Zanotti, S., and Dellinger, R. P. (2014). Severe sepsis and septic shock. *Virulence* 5, 190–199. doi:10.4161/viru.2740910.4161/viru.27409

Schwerd, T., Pandey, S., Yang, H.-T., Bagola, K., Jameson, E., Jung, J., et al. (2017). Impaired antibacterial autophagy links granulomatous intestinal inflammation in Niemann-Pick disease type C1 and XIAP deficiency with NOD2 variants in Crohn's disease. *Gut* 66, 1060–1073. doi:10.1136/gutjnl-2015-310382

Schwiebert, E. M., and Zsembery, A. (2003). Extracellular ATP as a signaling molecule for epithelial cells. *Biochim. Biophys. Acta (Bba) - Biomembranes* 1615, 7–32. doi:10.1016/s0005-2736(03)00210-4

Scott, R. C., Schuldiner, O., and Neufeld, T. P. (2004). Role and regulation of starvation-induced autophagy in the *Drosophila* fat body. *Developmental Cel* 7, 167–178. doi:10.1016/j.devcel.2004.07.009

Sun, K., Fan, J., and Han, J. (2015). Ameliorating effects of traditional Chinese medicine preparation, Chinese materia medica and active compounds on ischemia/reperfusion-induced cerebral microcirculatory disturbances and neuron damage. *Acta Pharmaceutica Sinica B* 5, 8–24. doi:10.1016/j.apsb.2014.11.002

Sun, Y., Yao, X., Zhang, Q.-J., Zhu, M., Liu, Z.-P., Ci, B., et al. (2018). Beclin-1-Dependent autophagy protects the heart during sepsis. *Circulation* 138, 2247–2262. doi:10.1161/CIRCULATIONAHA.117.032821

Suzuki, Y., Hattori, K., Hamanaka, J., Murase, T., Egashira, Y., Mishiro, K., et al. (2012). Pharmacological inhibition of TLR4-NOX4 signal protects against neuronal death in transient focal ischemia. *Sci. Rep.* 2, 896. doi:10.1038/srep00896

Tang, D., Kang, R., Berghe, T. V., Vandenabeele, P., and Kroemer, G. (2019). The molecular machinery of regulated cell death. *Cell Res* 29, 347–364. doi:10.1038/s41422-019-0164-510

Tsiotou, A. G., Sakorafas, G. H., Anagnostopoulos, G., and Bramis, J. (2005). Septic shock; current pathogenetic concepts from a clinical perspective. *Med. Sci. Monit.* 11, RA76–85.

Turdi, S., Han, X., Huff, A. F., Roe, N. D., Hu, N., Gao, F., et al. (2012). Cardiac-specific overexpression of catalase attenuates lipopolysaccharide-induced myocardial contractile dysfunction: role of autophagy. *Free Radic. Biol. Med.* 53, 1327–1338. doi:10.1016/j.freeradbiomed.2012.07.084

Wang, B., Nie, J., Wu, L., Hu, Y., Wen, Z., Dong, L., et al. (2018). AMPKα2 protects against the development of heart failure by enhancing mitophagy via PINK1 phosphorylation. *Circ. Res.* 122, 712–729. doi:10.1161/CIRCRESAHA.117.312317

Wang, X.-R., Kurtti, T. J., Oliver, J. D., and Munderloh, U. G. (2020). The identification of tick autophagy-related genes in Ixodes scapularis responding to amino acid starvation. *Ticks Tick-borne Dis.* 11, 101402. doi:10.1016/j.ttbdis.2020.101402

Wu, B., Song, H., Fan, M., You, F., Zhang, L., Luo, J., et al. (2020). Luteolin attenuates sepsisi–nduced myocardial injury by enhancing autophagy in mice. *Int. J. Mol. Med.* 45, 1477–1487. doi:10.3892/ijmm.2020.4536

Yamamoto, A., Tagawa, Y., Yoshimori, T., Moriyama, Y., Masaki, R., and Tashiro, Y. (1998). Bafilomycin A1 prevents maturation of autophagic vacuoles by inhibiting fusion between autophagosomes and lysosomes in rat hepatoma cell line, H-4-II-E cells. *Cell Struct. Funct.* 23, 33–42. doi:10.1247/csf.23.33

Yang, B., Li, H., Qiao, Y., Zhou, Q., Chen, S., Yin, D., et al. (2019). Tetramethylpyrazine attenuates the endotheliotoxicity and the mitochondrial dysfunction by doxorubicin via 14-3-3γ/bcl-2. *Oxidative Med. Cell Longevity* 2019, 1. doi:10.1155/2019/5820415

Yang, Z., and Klionsky, D. J. (2010). Mammalian autophagy: core molecular machinery and signaling regulation. *Curr. Opin. Cel Biol.* 22, 124–131. doi:10.1016/j.ceb.2009.11.014

Zang, Q., Maass, D. L., Tsai, S. J., and Horton, J. W. (2007). Cardiac mitochondrial damage and inflammation responses in sepsis. *Surg. Infections* 8, 41–54. doi:10.1089/sur.2006.033

Zang, Q. S., Maass, D. L., Wigginton, J. G., Barber, R. C., Martinez, B., Idris, A. H., et al. (2010). Burn serum causes a CD14-dependent mitochondrial damage in primary cardiomyocytes. *Am. J. Physiology-Heart Circulatory Physiol.* 298, H1951–H1958. doi:10.1152/ajpheart.00927.2009

Zanotti-Cavazzoni, S. L., and Hollenberg, S. M. (2009). Cardiac dysfunction in severe sepsis and septic shock. *Curr. Opin. Crit. Care* 15, 392–397. doi:10.1097/MCC.0b013e3283307a4e

Zha, J., Harada, H., Yang, E., Jockel, J., and Korsmeyer, S. J. (1996). Serine phosphorylation of death agonist BAD in response to survival factor results in binding to 14-3-3 not BCL-XL. *Cell* 87, 619–628. doi:10.1016/s0092-8674(00)81382-3

Zhang, H., Bosch-Marce, M., Shimoda, L. A., Tan, Y. S., Baek, J. H., Wesley, J. B., et al. (2008). Mitochondrial autophagy is an HIF-1-dependent adaptive metabolic response to hypoxia. *J. Biol. Chem.* 283, 10892–10903. doi:10.1074/jbc.M800102200

Zhang, Q., Raoof, M., Chen, Y., Sumi, Y., Sursal, T., Junger, W., et al. (2010). Circulating mitochondrial DAMPs cause inflammatory responses to injury. *Nature* 464, 104–107. doi:10.1038/nature08780

Zhang, Z., He, H., Qiao, Y., Huang, J., Wu, Z., Xu, P., et al. (2018). Tanshinone IIA pretreatment protects H9c2 cells against anoxia/reoxygenation injury: involvement of the translocation of bcl-2 to mitochondria mediated by 14-3-3η. *Oxidative Med. Cell Longevity* 2018, 1. doi:10.1155/2018/35839212018

Zhao, H., Zhang, M., Zhou, F., Cao, W., Bi, L., Xie, Y., et al. (2016). Cinnamaldehyde ameliorates LPS-induced cardiac dysfunction via TLR4-NOX4 pathway: the regulation of autophagy and ROS production. *J. Mol. Cell Cardiol.* 101, 11–24. doi:10.1016/j.yjmcc.2016.10.017

Zhou, M., Xu, W., Wang, J., Yan, J., Shi, Y., Zhang, C., et al. (2018). Boosting mTOR-dependent autophagy via upstream TLR4-MyD88-MAPK signalling and downstream NF-κB pathway quenches intestinal inflammation and

oxidative stress injury. *EBioMedicine* 35, 345–360. doi:10.1016/j.ebiom.2018.08.035

Zhou, R., Yazdi, A. S., Menu, P., and Tschopp, J. (2011). A role for mitochondria in NLRP3 inflammasome activation. *Nature* 469, 221–225. doi:10.1038/nature09663

Zorov, D. B., Juhaszova, M., and Sollott, S. J. (2014). Mitochondrial reactive oxygen species (ROS) and ROS-induced ROS release. *Physiol. Rev.* 94, 909–950. doi:10.1152/physrev.00026.2013

Zuo, Y.-H., Han, Q.-B., Dong, G.-T., Yue, R.-Q., Ren, X.-C., Liu, J.-X., et al. (2018). Panax ginseng polysaccharide protected H9c2 cardiomyocyte from hypoxia/reoxygenation injury through regulating mitochondrial metabolism and RISK pathway. *Front. Physiol.* 9. doi:10.3389/fphys.2018.00699

Conflicts of Interest: The authors declare that the research was conducted in the absence of any commercial or financial relationships that could be construed as a potential conflict of interest.

frontiers in Pharmacology

REVIEW
published: 28 April 2021
doi: 10.3389/fphar.2021.671164

Exosome: The Regulator of the Immune System in Sepsis

Peng Qiu[1], *Jing Zhou*[1], *Jin Zhang*[1], *Youjing Dong*[1] *and Yang Liu*[2]*

[1]*Department of Anesthesiology, Shengjing Hospital of China Medical University, Shenyang, China,* [2]*Department of Oncology, Shengjing Hospital of China Medical University, Shenyang, China*

Sepsis is a syndrome comprised of a series of life-threatening organ dysfunctions caused by a maladjusted body response to infection with no effective treatment. There is growing evidence that the immune system plays a core role in sepsis. Pathogens cause abnormal host immune response and eventually lead to immunosuppression, which is an important cause of death in patients with sepsis. Exosomes are vesicles derived from double invagination of plasma membrane, associating with immune responses closely. The cargos delivered by exosomes into recipient cells, especially immune cells, effectively alter their response and functions in sepsis. In this review, we focus on the effects and mechanisms of exosomes on multiple immune cells, as well as the role of immune cell-derived exosomes in sepsis. This is helpful for us to have an in-depth understanding of the mechanism of immune disorders in sepsis. Exosomes is also expected to become a novel target and therapeutic approach for sepsis.

Keywords: exosome, extracellular vesicle, sepsis, immune, antigen presentation, innate immune, adaptive immune

OPEN ACCESS

Edited by:
Yan Kang,
Sichuan University, China

Reviewed by:
Laurent Muller,
University Hospital Basel, Switzerland
Sandhya Bansal,
St. Joseph's Hospital and Medical Center, United States

***Correspondence:**
Yang Liu
13998843583@163.com

Specialty section:
This article was submitted to Experimental Pharmacology and Drug Discovery, a section of the journal Frontiers in Pharmacology

Received: *23 February 2021*
Accepted: *06 April 2021*
Published: *28 April 2021*

Citation:
Qiu P, Zhou J, Zhang J, Dong Y and Liu Y (2021) Exosome: The Regulator of the Immune System in Sepsis. Front. Pharmacol. 12:671164. doi: 10.3389/fphar.2021.671164

INTRODUCTION

Sepsis is a syndrome of multiple life-threatening organ dysfunction caused by the dysregulated host response to infection (Singer et al., 2016). With the progress of intensive care management and goal-directed interventions, early mortality of sepsis has diminished (Delano and Ward, 2016; Steinhagen et al., 2020). However, persistent inflammation, immunosuppression and catabolism syndrome (PICS) in later phase of sepsis remains unsolved, which is the main cause of death in septic patients (Venet and Monneret, 2018). At present, increasing evidence supports the core role of the immune system in sepsis (van der Poll et al., 2017; Rubio et al., 2019). In sepsis, the immune response initiated by invading pathogens failed to return homeostasis, which eventually leads to a pathological syndrome characterized by persistent excessive inflammation and immunosuppression (van der Poll et al., 2017). Therefore, understanding the complex mechanism of immune imbalance in sepsis and the application of targeted immunotherapy has become a research hotspot in the field of sepsis. Abnormal activation, massive apoptosis, phenotypic, and functional changes of immune cells are the pathological basis of immune disorders, especially immunosuppression in sepsis (Hotchkiss et al., 2013). The use of cytokines such as interleukin-7 (IL-7), interleukin-15 (IL-15), granulocyte-macrophage colony-stimulating factor (GM-CSF) and co-inhibitory molecules blockade involving anti-programmed cell death receptor-1 (anti-PD-1) and anti-B and T lymphocyte attenuator (anti-BTLA) have been proven to reduce the mortality of sustained sepsis (Leentjens et al., 2013; Hutchins et al., 2014; Delano and Ward, 2016; van der Poll et al., 2017; Venet and Monneret, 2018; Steinhagen et al., 2020).

Exosomes are a subset of extracellular vesicles (EVs), with a diameter of 40–160 nm, derived from endosome (Kalluri and LeBleu, 2020). The biogenesis of exosomes includes the double invagination

of plasma membrane and the formation of multivesicular body (MVB) which containing intraluminal vesicles (ILVs). ILVs are subsequently released into extracellular space according to MVB fusion with the plasma membrane and exocytosis, which are named exosomes ultimately (Robbins and Morelli, 2014; Kalluri and LeBleu, 2020). Exosomes are enriched in a variety of cell surface proteins, intracellular proteins, amino acids, nucleic acids (DNA and RNA), lipids and metabolites, which can mediate intercellular communication and affect the biological function of recipient cells (Kalluri and LeBleu, 2020) (**Figure 1C**). Exosomes have been proved to play an important role in multiple diseases (Pegtel and Gould, 2019), including tumor (Hoshino et al., 2015), infection (Rialdi et al., 2017), inflammation (Choi et al., 2020), cardiovascular diseases (Barile et al., 2017) and autoimmune diseases (Majer et al., 2019). The effects of exosomes on immune system involving antigen presentation, immune cells maturation, differentiation and activation, as well as their applications as drug carriers for immunotherapy have been widely studied (Chaput and Théry, 2010; Bobrie et al., 2011; Robbins and Morelli, 2014; Robbins et al., 2016). In addition, exosomes have also become an important target and approach for the treatment of sepsis (Terrasini and Lionetti, 2017; Wu et al., 2017; Raeven et al., 2018; Murao et al., 2020). This review focuses on the immunomodulatory effect of exosomes in sepsis. We summarized the effects (activation or inhibition) and underlying mechanisms of exosomes of different origins (non-immune and immune cells) and components on the immune system.

IMMUNOPATHOLOGY OF SEPSIS

The pathological process of sepsis is mainly manifested by excessive inflammatory response and consequent immunosuppression (van der Poll et al., 2017). When infection occurs, the pathogen-associated molecular patterns (PAMPs) of invading pathogens are recognized by innate immune cells through various pattern recognition receptors (PRRs), involving toll-like receptors (TLRs), nucleotide oligomerization domain-like receptors (NLRs), C-type lectin receptors (CLRs), and RigI-helicases (Takeuchi and Akira, 2010; Kumar et al., 2011). In general, the innate immune system eliminates pathogens and restores homeostasis through a variety of pro-inflammatory reactions. Once the pathogen prevails and is not effectively cleared, the host immune response becomes unbalanced, and eventually leading to sepsis (van der Poll et al., 2017). Excessive inflammatory responses are mobilized against the threat of pathogens, which can induce abnormal activation of the complement system and coagulation system and vascular endothelial dysfunction (van der Poll et al., 2017). Complements C3a and C5a have powerful pro-inflammatory effects, including recruitment and activation of leukocytes and platelets (Merle et al., 2015), which adhere to the surface of endothelial cells and lead to barrier dysfunction through excessive inflammatory response. Intense activation of the coagulation system can lead to disseminated intravascular coagulation (DIC). In addition, excessive inflammation trigger cell injury and the release of damage-associated molecular patterns (DAMPs), which result in further activation of the innate immune system and inflammation outbreak, eventually leading to organ damage and dysfunction (van der Poll et al., 2017).

Persistent excessive inflammation triggers extensive apoptosis in immune cells (especially lymphocytes and dendritic cells) (Boomer et al., 2011; Hotchkiss et al., 2013), while delays apoptosis of neutrophils (Tamayo et al., 2012). However, these neutrophils have lower bactericidal functions and decreased cytokine production (Tamayo et al., 2012). The expression of programmed cell death 1 (PD1) of CD4+ T cells and the proportion of regulatory T (Treg) cells increase, resulting in the inhibition of effector T cell function (Leentjens et al., 2013). Monocytes and macrophages have a reduced ability to release pro-inflammatory cytokines under stimulation such as LPS, which also known as "immuno-paralysis" (Hotchkiss et al., 2013). These factors contribute to severe immunosuppression in sepsis, especially in the later stages, leading to an increased chance of secondary infection (van der Poll et al., 2017). In summary, the immune mechanism is the core throughout the occurrence and progression of sepsis. Immunotherapy will become the key to the treatment of sepsis.

BIOGENESIS AND UPTAKE OF EXOSOMES

The biogenesis of exosomes mainly depends on the endosomal sorting complexes required for transport (ESCRT) mechanism (Robbins and Morelli, 2014; Kalluri and LeBleu, 2020) (**Figure 1A**). Extracellular components, including proteins, lipids, metabolites can enter cells together with cell surface proteins through endocytosis or plasma membrane invagination (Kalluri and LeBleu, 2020). With the participation of endoplasmic reticulum (ER), trans-Golgi network (TGN) and mitochondrial constituents, this membrane budding process drives the formation of early-sorting endosome (ESE) and gradually matures into late-sorting endosome (LSE)(Kalluri, 2016; Hessvik and Llorente, 2018; Mathieu et al., 2019). LSE eventually transforms into multivesicular body (MVB) which containing Intraluminal vesicles (ILVs) through ESCRT-mediated secondary invagination of the plasma membrane (Raiborg and Stenmark, 2009; Hurley and Hanson, 2010). After the fusion of MVB with plasma membrane, these ILVs are released out of the cell *via* exocytosis and become exosomes (Robbins and Morelli, 2014; Kalluri and LeBleu, 2020). Some of MVBs can also be degraded through autophagy or lysosomal pathway (Robbins and Morelli, 2014; Kalluri and LeBleu, 2020). In addition, certain proteins, such as PLP, are also sorted into ILVs through a machinery independently of ESCRT (Stuffers et al., 2009). The uptake of exosomes by target cells may involve plasma membrane fusion, receptor-mediated endocytosis (i.e. ICAM1 binding with LFA1), clathrin-coated pits, lipid raft, caveolae and phagocytosis (such as PS binding with its ligands MFGE8 and Tim1/4). In addition, exosomes can bind to cells directly *via* surface receptor or ligand proteins (**Figure 1B**) (Chaput and Théry, 2010; Kalluri and

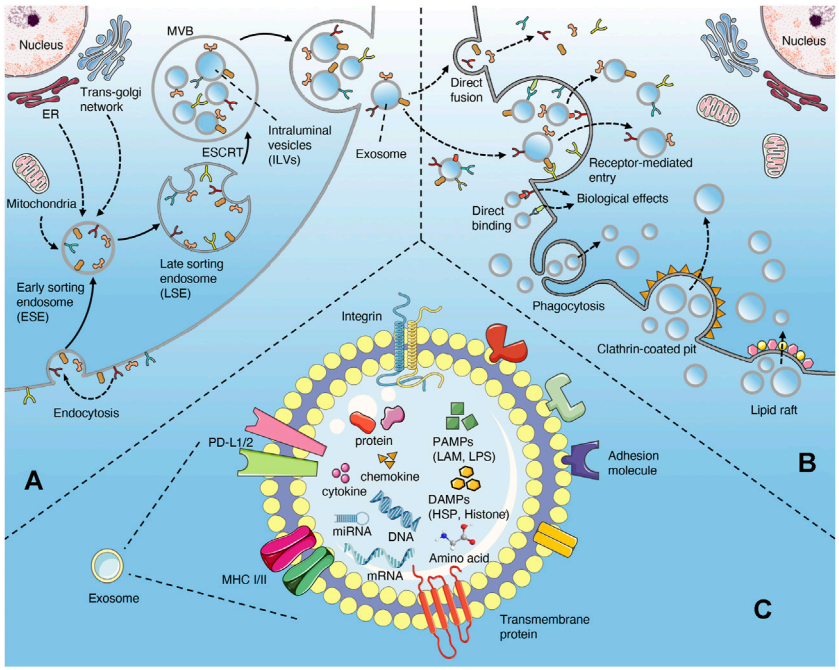

FIGURE 1 | Biogenesis and uptake of exosomes **(A)** the exosomes originate from the invagination of the plasma membrane, followed by the formation of ESE, LSE, MVB (contain ILVs), and ultimately be released through the fusion of MVB with the plasma membrane **(B)** the uptake of exosomes may involve directly fusion, receptor-mediated endocytosis, phagocytosis, clathrin-coated pits and lipid raft. In addition, exosomes can interact with cells *via* directly binding way **(C)** the contents of exosomes in sepsis include proteins, nucleic acids, cytokines, chemokines, PAMPs, and DAMPs.

LeBleu, 2020). Exosomes release bioactive contents to recipient cells after internalization, or directly induce the activation of intracellular signaling pathways through ligand-receptor binding (Kalluri and LeBleu, 2020).

EXOSOMES AND IMMUNE SYSTEM

Exosomes derived from both immune and non-immune cells play an important role in immune regulation, which may promote the pathology of multiple diseases through mediating immune stimulation or suppression (Robbins and Morelli, 2014). The immune regulation of exosomes may be due to the antigenic peptides transfer and presentation, the transmission of cGAS-STING signals induced by DNA in recipient cells, the regulation of gene expression by exosome miRNA, and the induction of different signaling by exosome surface ligands (such as PD-L1 and FasL) (Kalluri and LeBleu, 2020). Interestingly, recent study has revealed that exosomes also provide protection similar to innate immunity by neutralizing bacterial toxins actively (Keller et al., 2020).

Exosomes Participate in Antigen Presentation

Traditional antigen presentation requires antigen presenting cells (APCs) to process antigenic peptides and form MHC-peptide complexes, which subsequently promote T cell activation and proliferation *via* binding to the T cell receptor (TCR) with the synergism of co-stimulatory molecules. However, exosomes can complete antigen presentation without the interaction between APCs and T cells, or even without the reprocessing of MHC-peptide complex by the recipient APCs, which promote the efficiency of presentation and favor the host to initiate immuno-defense against invading pathogens more quickly. Exosomes participate in antigen presentation mainly through the following three mechanisms (Segura et al., 2005; Chaput and Théry, 2010; Robbins and Morelli, 2014; Tung et al., 2018) (**Figure 2**). 1) direct presentation: exosomes derived from the professional APCs (that is, dendritic cells (DCs), which carry the MHC-peptide complexes, co-stimulatory and adhesion molecules, bind with T cells directly. 2) indirect presentation: exosomes transfer their antigenic peptide to the MHC molecules of the recipient APCs. After loading with the exosome-derived peptide, the recipient APCs then present the MHC-peptide complexes to T cells. 3) cross-dressing: the captured exosomes that are retained on the APCs surface present their MHC- peptide complexes directly to T cells, although the co-stimulatory molecules are provided by the APCs.

In addition, dendritic cells may transfer the ability of activating T cells to non-professional antigen presenting cells (B cell and macrophage) through exosome-mediated antigen presentation (Segura et al., 2005; Robbins and Morelli, 2014).

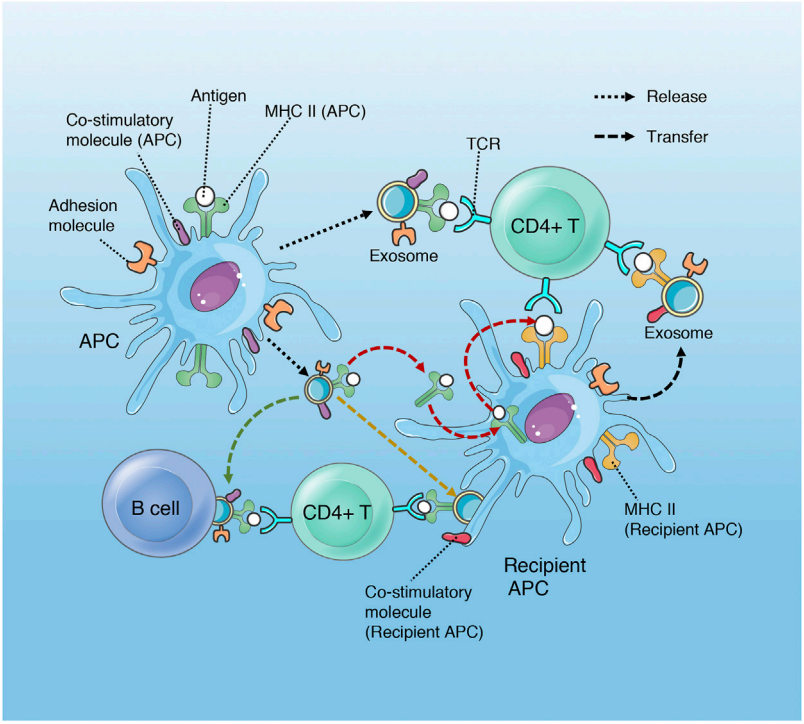

FIGURE 2 | Role of exosomes in antigen presentation. Exosomes released by APCs (DCs) contain MHC II- antigen peptide complexes (MHC II-p) and can present antigen to CD4+T cell directly, deliver antigen to MHC II of recipient APC (red arrow), present antigen *via* cross-dressing (orange arrow) and transport MHC II-p to B cell (green arrow). Although only MHC II and CD4+ T cell are shown, exosomal MHC I has a similar process in the regulation of CD8+ T cells.

Active Immuno-Defense of Exosomes

Bacteria disrupt the plasma membrane of host cells by releasing pore-forming toxins and cause cell death during infection (Dal Peraro and van der Goot, 2016; Seilie and Bubeck Wardenburg, 2017; Spaan et al., 2017). Matthew et al. found that cells exposed to bacteria release exosomes that containing ADAM10 in an ATG-dependent manner, which can neutralize α-toxin (a pore-forming toxin) produced by methicillin-resistant Staphylococcus aureus (MRSA) and protect host cells from death (Keller et al., 2020). These exosomes serve as decoy to bind bacterial toxins and play the role of scavenger similar to innate immune cells (Keller et al., 2020). This finding indicates the active immuno-defensive role of exosomes during infection, except for mediating intercellular communication.

EFFECTS OF EXOSOMES ON IMMUNE CELLS IN SEPSIS

The immuno-modulatory effect of exosomes depends on multiple factors involving type of disease, cellular sources and the cargos transmitted to the recipient cells (Robbins and Morelli, 2014; Kalluri and LeBleu, 2020). The immune regulation of exosomes in sepsis also exhibit pleiotropy and complexity. Exosomes from distinct cellular sources or the same source with different cargos can activate or suppress immune cells. The role of endogenous exosomes is both beneficial and harmful, while exogenous exosomes are often used as drug carriers for sepsis immunotherapy (Terrasini and Lionetti, 2017; Wu et al., 2017; Raeven et al., 2018; Murao et al., 2020).

Immunomodulatory Effect of Exosomes Derived From Non-immune Cells in Sepsis

Serum and Platelets

At present, a number of studies have proved that abundant exosomes exist in the plasma of septic patients and animal models (**Table 1**), which affect the function of a variety of immune cells (**Figure 3**), including T lymphocytes (Alexander et al., 2015; Deng et al., 2019; Gao et al., 2019), macrophages (Xu et al., 2018; Jiang et al., 2019), neuroglia cells (Li et al., 2018a) and neutrophils (Jiao et al., 2020).

Gao et al. (Gao et al., 2019)found that plasma exosomes enriched with IL-12 and IL-4 effectively promote the differentiation of Th1/Th2 cells in the middle and late phase of sepsis, while the growth factor GM-CSF in the exosomes augments the proliferation of T cells through TLR4-dependent pathway. Although failed to recruit lymphocytes directly, the exosomes with chemokine enhance the migration of lymphocytes (Gao et al., 2019). All these are beneficial to the resuscitation of immunosuppressive state in the late phase of sepsis and reduce the mortality. Similarly, Deng et al. (Deng et al., 2019) demonstrated that exosomes derived from plasma of septic patients downregulate the mRNA and protein levels of

TABLE 1 | Immunomodulatory effect of exosomes derived from non-immune cells in sepsis.

Donor cell/ tissue	Contents	Transfer pathway	Target cell	Signaling pathway/Protein	Immuno-effect	Immune outcome	References
Serum	Cytokines(IL, TNF-α, IFN-γ), chemokine, GM-CSF	TCR	T cell	TLR4 (+)	T cell differentiation, proliferation and chemotaxis ↑	Activation	Gao et al. (2019)
Serum	Has-miR-7-5p	N/A	T cell	cGMP-PKG (+)	T cell apoptosis ↓ (BAD ↓, caspase3 ↓, bax ↓, Bcl2 ↑)	Activation	Deng et al. (2019)
Serum	miR-155	N/A	Macrophage	SHIP1-CDKN1B (–) SOCS1 (–) NF-κb (+)	Macrophage proliferation ↑, M1 ↑, TNF-α ↑, IL-6 ↑	Activation	Jiang et al. (2019)
Serum	EVs[a]: miR-16a, miR-122, miR-34a	N/A	Macrophage neutrophil	TLR7-MyD88 (+)	Macrophage and neutrophil migration ↑, MIP-2 ↑, IL-6 ↑, IL-1β↑, TNF-α ↑, FB ↑, C3 ↑	Activation	Xu et al. (2018)
Serum	miR-21, miR-125a, miR-146a, miR-155	N/A	Microglia Astrocyte	N/A	Inflammation ↑	Activation	Li et al. (2018a)
Serum	miR-125b, miR-27a, mRNA	N/A	N/A	N/A	MPO ↑, FOXM1 ↑, inflammation ↑	N/A	Real et al. (2018)
Serum	EVs[a]: Integrin β2, PDL-1/2	Integrin β2	Lymphocyte	PD-1/PDL-1/2 (+)	Lymphocyte numbers ↓	Suppression	Kawamoto et al. (2019)
Serum	MHC-II, CD11b	N/A	N/A	Fas/FasL (+)	Inflammation ↓	Suppression	Kim et al. (2007)
Platelet	HMGB1, miR-15b-5p, miR-378a-3p	IKK	Neutrophil	Akt-mTOR (+)	dsDNA + MPO-DNA complex ↑, NETs ↑	Activation	Jiao et al. (2020)
BMSC	N/A	N/A	Macrophage	HIF-1α-glycolysis (–)	M2 ↑, M1 ↓	Suppression	Deng et al. (2020)
BMSC	miR-21	IL-1β	Macrophage	PDCD4 (–)	M2 ↑, M1 ↓	Suppression	Yao et al. (2021)
AMSC	miR-34a-5p, miR-146a-5p, miR-21	TNF-α, IFN-γ	Macrophage	Notch1 (–), IRAK1-TRAF6 (–), Sirp-β1 (late) (–), STAT3 (early) (+), MEK/ERK1/2 (+)	M2 ↑, M1 ↓, M1 ↑ (early)	Suppression	Domenis et al. (2018)
BMSC	miR-223	N/A	Cardiac myocyte	Sema3A (–), STAT3 (–)	Myocardial protection	Suppression	Wang et al. (2015c)
MSC	N/A	N/A	THP1 (direct), CD4+T cell (indirect)	TLR-MyD88-NF-κB (+)	M2 Phenotype↑, Treg ↑, IL-10 ↑	Suppression	Zhang et al. (2014)
AMSC	N/A	N/A	T cell	NF-κB (?)	$CD4^+$T and $CD8^+$T cell proliferation ↓, T cell differentiation ↓, IFN-γ ↓	Suppression	Blazquez et al. (2014)
MSC	N/A	N/A	PBMC (PMN, lymphocyte)	N/A	TGF-β↑, IL-4↑, TNF-α ↓, IL-1β ↓, IFN-γ ↓, IL-17 ↓Th1 ↓, Th2 ↑, Th17 ↓, Treg ↑, CTP4 ↑, PBMC and $CD3^+$T cell apoptosis↑	Suppression	Chen et al. (2016)
BMSC	miR-146a	N/A	Macrophage	IRAK1 (-), TRAF6 (-), IRF5 (-)	M2 ↑, TNF-α ↓, IL-10 ↑	Suppression	Song et al. (2017)
MSC	MV[a]: KGF mRNA	KGF	Alveolar epithelial cell (direct) Macrophage (indirect) Neutrophil (indirect)	N/A	TNF-α↓, IL-10↑, MIP2↓, neutrophil influx ↓	Suppression	Zhu et al. (2014)
MSC	MV[a]: CD44, mRNA (KGF, COX2, IL-10, mitochondria)	CD44-L-selectin/ osteopontin, TLR-2/3/4	Alveolar epithelial type II cell, monocyte/ Macrophage	COX2-PGE2 (+)	ATP (Alveolar epithelial cell) ↑, phagocytosis (monocyte) ↑, M2 ↑, M1 ↓, PGE2 ↑, IL-10 ↑, TNF-α ↓	Suppression	Monsel et al. (2015)
BMSC	EVs[a]: CD44, mRNA (mitochondria)	CD44-L-selectin/ osteopontin	Macrophage	OXPHOS (+)	Phagocytosis ↑, M2 ↑, M1 ↓, TNF-α ↓, IL-8 ↓	Suppression	Morrison et al. (2017)
MSC	N/A	N/A	Microglia Astrocyte	N/A	Microglia proliferation ↓ (Ibα-1 ↓, CD68 ↓) Astrocyte proliferation ↓ (GFAP ↓)	Suppression	Drommelschmidt et al. (2017)
MSC	EVs[a]: TGF-β, IL-10	N/A	Motor neuron	N/A	Inflammation ↓	Suppression	Rajan et al. (2016)
MSC	miR-181c	N/A	Macrophage Neutrophil	TLR4- NF-κB (-)	Macrophage and neutrophil infiltration ↓, IL-1β ↓, TNF-α↓	Suppression	Li et al. (2016)

(Continued on following page)

TABLE 1 | (*Continued*) Immunomodulatory effect of exosomes derived from non-immune cells in sepsis.

Donor cell/ tissue	Contents	Transfer pathway	Target cell	Signaling pathway/Protein	Immuno-effect	Immune outcome	References
MSC	N/A	TLR	DC (direct) T cell (indirect)	N/A	IL-6 ↓, IL-10 ↑, TGF-β ↑, TolDC ↑, treg ↑	Suppression	Shahir et al. (2020)
EC	HSPA12B	N/A	Macrophage	PI3K/AKT (+) NF-κB (-)	Macrophage infiltration ↓, monocyte/Macrophage activation ↓, IL-1β ↓, TNF-α ↓, IL-10 ↑	Suppression	Tu et al. (2020)
HMEC-1	MV[a]: EMP	Sodium-proton exchanges, Intact cytoskeleton	PDC (plasmacytoid dendritic cell)	N/A	IL-6 ↑, IL-8 ↑, co-stimulatory molecules (CD80/86/40) ↑, HLA-DR ↑, CD83 ↑, CCR7 ↑, TNF-α ↑, IFN-γ ↑, Th1 ↑	Activation	Angelot et al. (2009)
HUVEC	EVs[a]: miR-10a, miR-12b, miR-181b	N/A	Monocyte (THP-1)	Nucleus: NF-κB (–), IRF5 (–) Cytoplasm: IRAK4 (–), TAK1/ MAP3K7 (–), βTRC-NF-κB (–)	Pro-inflammatory response ↓, immunomodulatory phenotype ↑, M2 ↑, M1 ↓	Suppression	Njock et al. (2015)
EC	EVs[a]: miR-155	N/A	Monocyte (THP-1)	N/A	OX-LDL: M1 ↑, M2 ↓, KLF2: M2 ↑, M1 ↓	Activation/ Suppression	He et al. (2018)
Alveolar epithelial type II cell	miR-146a	N/A	Alveolar macrophage	TLR4-IRAK1-TRAF6-NF-κB (–)	IL-6 ↓, IL-8 ↓, IL-1β ↓, TNF-α ↓	Suppression	Zheng et al. (2020)
TEC	miR-19b-3p	N/A	Macrophage	SOCS1 (–)	M1 ↑	Activation	Lv et al. (2019)
Lung epithelial cell	EVs[a]: Caspase-3	N/A	Alveolar macrophage Neutrophil	ROCK1 (+)	MIP-2 ↑, pro-inflammatory cytokines ↑, macrophage and neutrophil infiltration ↑	Activation	Moon et al. (2015)
Lung epithelial cell	EVs[a]: miR-17, miR-221	N/A	Macrophage	PTEN (-), c-fos-rab11 (+)	Integrin β1 expression and circulation ↑, Macrophage recruitment and migration ↑	Activation	Lee et al. (2017)
Lung epithelial cell	EVs[a]: miR-320a, miR-221	N/A	Macrophage	MMP9 (+), NF-κb (+)	Macrophage migration and activation ↑, IL-1β ↑, TNF-α ↑	Activation	Lee et al. (2016)
CPE	EVs[a]: miR-146a, miR-155	Cross the ependymal cell layer	Microglia Astrocyte	Target mRNA (–)	Inflammatory gene ↑	Activation	Balusu et al. (2016)
IEC	EVs[a]: miRNA	N/A	IEC	N/A	TNF-α ↓, IL-17a ↓	Suppression	Appiah et al. (2020)
IEC	PGE2	N/A	Hepatocyte (direct) NKT cell (indirect) CD4+T cell (indirect)	EP2/4-CAMP-PKA (+)	Hepatocyte apoptosis ↓, NKT cell activation ↓, $CD4^+$T cell activation ↓, IFN-γ ↓, TNF-α ↓, IL-4 ↓, IL-2 ↓	Suppression	Deng et al. (2013)
IEC Neutrophils	EVs[a]: miRNA, IL-6/8, TNF-α	N/A	IEC, Macrophage	N/A	Macrophage migration ↑, pro-inflammation ↑	Activation	Mitsuhashi et al. (2016)
Synovial fibroblasts	TNF-α (membrane form)	TNF-α ubiquitin	T cell	AKT-NF-κb (+)	T Cell apoptosis ↓ (caspase-3 ↓)	Activation	Zhang et al. (2006)

[a]*Exosomes are subsets of EVs or MVs, however, their immunomodulatory effects may exist unpredictable differences.*

pro-apoptotic gene Bad, active Caspase-3 and Bax, while upregulate that of anti-apoptotic gene Bcl-2 *via* hsa-miR-7-5p, thus inhibit apoptosis of T lymphocytes induced by lipopolysaccharide (LPS). The inhibition of Bad by hsa-miR-7-5p may be related to the activation of CGMP-PKG pathway (Deng et al., 2019). Exosomes derived from the serum of septic mice deliver miR-155 to macrophages and promote M1 polarization *via* activating NF-kB, while enhance macrophages proliferation by targeting inhibition of SHIP1 and SOCS1(Jiang et al., 2019). Similarly, miR-155 in the serum exosomes also leads to the proliferation and activation of microglia and astrocytes in LPS-treated mice, which aggravate the inflammatory response of the nervous system (Li et al., 2018a). In addition, miR-34a, miR-122 and miR-146a in plasma EVs of septic mice increase the release of pro-inflammatory cytokines (IL-6, IL-1 β, TNF- α and MIP-2) by macrophages in a TLR7-MyD88-dependent manner and promote the migration of macrophages and neutrophils, all of which activate immune system and aggravate the inflammatory response of sepsis (Xu et al., 2018).

On the contrary, plasma-derived exosomes can also lead to immunosuppression. Integrins have been shown to be involved in regulating the biological distribution of exosomes and the binding and internalization of target cells (Hoshino et al., 2013; Wang et al., 2015b). Kawamoto et al. (Kawamoto et al., 2019) found that integrins and PD-1 ligands (PDL-1 and PDL-2) enriched in plasma EVs of septic patients synergistically promote the binding of EVs and lymphocytes, and inhibit the activation of T cells through the negative signal transmitted by PD-1. Similarly, Kim et al. (Kim et al., 2007) found that plasma exosomes carrying MHC II and CD11b suppress antigen-specific immune responses partially through Fas/FasL-dependent pathways.

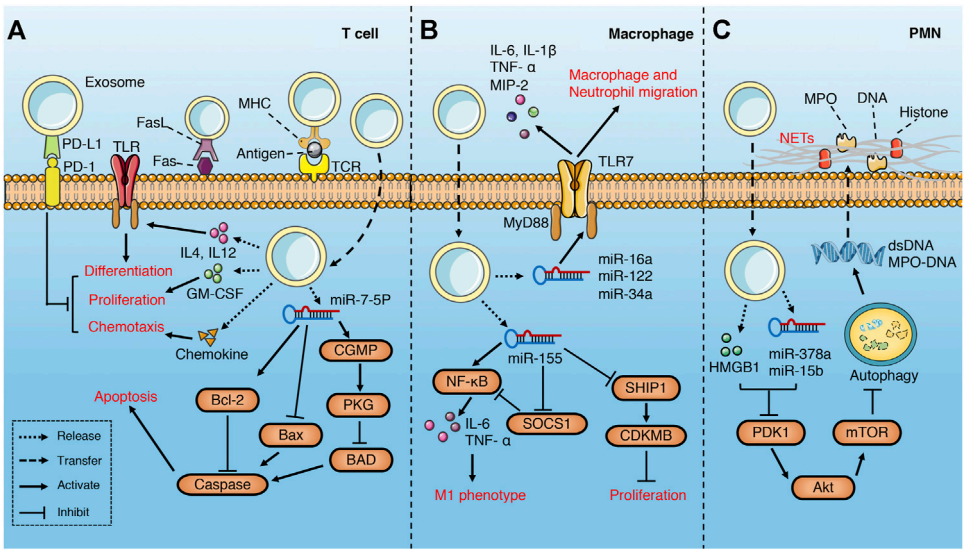

FIGURE 3 | Role of exosomes derived from serum in sepsis. **(A)** serum exosomes can promote differentiation, proliferation and chemotaxis of T cell *via* pro-inflammatory cytokines, GM-CSF and chemokines separately, while play the opposite role through PD1/PDL1 pathway. In addition, exosomes may attenuate T cell apoptosis through miR-7-5p-mediated inhibition of caspase. However, exosomes may also induce T cell apoptosis *via* FasL/Fas signaling pathway. **(B)** serum exosomes promote macrophage migration, proliferation and M1 polarization through multiple miRNAs-mediated signaling pathways. **(C)** Platelet exosomes induce excessive NETs formation through Akt/mTOR autophagy pathway.

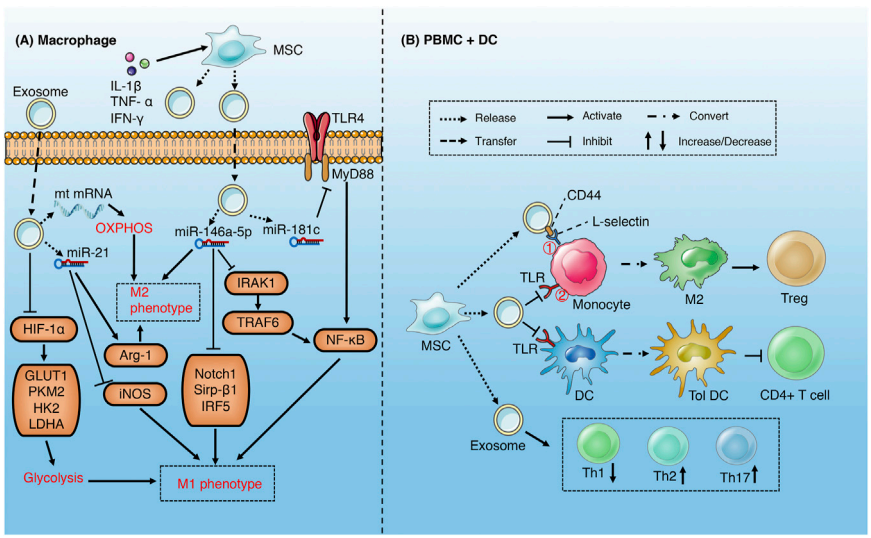

FIGURE 4 | Role of exosomes derived from MSC in sepsis **(A)** MSC-derived exosomes increase M2 and decrease M1 phenotype of macrophages through metabolism reprogramming and multiple miRNAs-mediated signaling pathways **(B)** MSC-derived exosomes induce M2-like phenotype in monocytes *via* activating COX2-PGE2① and inhibiting TLR/NF-KB② signaling pathways, which in turn induce the expansion of Treg. MSCs-derived exosomes induce DCs into a tolerogenic population and modulate the differentiation spectrum of T cell subsets.

Platelets are the main source of circulating exosomes (Ogura et al., 2001). Platelet-derived exosomes containing HMGB1, miR-15b-5p and miR-378a-3p induce excessive neutrophil extracellular trap (NET) formation through Akt/mTOR autophagy pathway (Jiao et al., 2020), which aggravates vascular endothelial injury and coagulation dysfunction (Caudrillier et al., 2012; Leppkes et al., 2019).

Mesenchymal Stem Cell

Mesenchymal stem cell (MSCs) can be easily isolated from tissue and expanded *in vitro*. For the pluripotency and immune activity, MSCs has become an effective treatment for many diseases including sepsis. MSCs can inhibit T cell proliferation and cytotoxicity, regulate the function of regulatory T cells, inhibit B cell proliferation, regulate the maturation, activation and

antigen presentation of dendritic cells, regulate natural killer cell activation (Gao et al., 2016). MSC-derived exosomes play an anti-inflammatory role in sepsis by suppressing the immune function of monocytes/macrophages, dendritic cells, neutrophils and T cells (**Table 1**) (**Figure 4**).

Studies have demonstrated that MSCs-derived exosomes may alleviate the inflammatory injury induced by sepsis *via* reprogramming the metabolism of macrophages (Morrison et al., 2017; Deng et al., 2020). M1 macrophages acquire energy from aerobic glycolysis, while M2 macrophages obtain energy through mitochondrial oxidative phosphorylation (Zhu et al., 2015). In addition, aerobic glycolysis is an important pathway of macrophage activation and M1 polarization (Pan et al., 2020; Zhao et al., 2020). MSCs-derived exosomes suppress LPS-induced glycolysis of macrophage *via* inhibition of HIF-α and its downstream pathway and reduce M1 polarization. Correspondingly, exosomes promote oxidative phosphorylation through delivering mitochondrial mRNA to macrophages, which increases M2 polarization (Morrison et al., 2017). The effect of MSCs-derived exosomes on macrophage polarization can be enhanced by the stimulation of pro-inflammatory factors (Domenis et al., 2018; Yao et al., 2021). Under stimulation of pro-inflammatory cytokines (IL-1β, TNF-α and IFN-γ), MSCs released exosomes rich in miR-34a-5p (Domenis et al., 2018), miR-146a-5p (Song et al., 2017; Domenis et al., 2018) and miR-21 (Domenis et al., 2018; Yao et al., 2021), which promote the phenotypic transition from M1 to M2 by inhibiting Notch1, IRAK1/TRAF6, IRF5, and Sirp-β1 signaling pathways and related proteins. In addition, CD44 in exosomes can enhance the phagocytosis of macrophages and inhibit the release of TNF-α (Morrison et al., 2017). The exosomes derived from human umbilical cord mesenchymal stem cells carrying miR-181c reduce macrophage infiltration and excessive release of inflammatory factors, which is partly attributed to the inhibition of TLR4/NF-κB signaling pathway (Li et al., 2016).

MSCs-derived exosomes can induce an anti-inflammatory M2-like phenotype in monocytes *via* inhibiting TLR/NF-KB signaling pathway in sepsis, which subsequently induce the expansion of regulatory T (Treg) cells (Zhang et al., 2014; Chen et al., 2016). Similarly, EVs (exosomes) up-regulated the expression of PGE2 *via* transferring COX2 mRNA to monocytes, which may increase M2-like phenotype (Monsel et al., 2015). MSCs-derived exosomes can also regulate the proliferation and activation of T cells in different subsets, including inducing the conversion of Th1 to Th2, reducing the potential of T cells to differentiate into Th17 (Blazquez et al., 2014; Chen et al., 2016), and reducing the release of pro-inflammatory factors such as IFN- γ (Blazquez et al., 2014). MSCs-derived exosomes induce DCs into a tolerogenic DC (TolDC) population, which are capable of suppressing lymphocyte activities, increasing secretion of IL-10 and TGF-β and decreasing secretion of IL-6 (Shahir et al., 2020). In addition, MSCs-derived exosomes may also reduce septic nervous system inflammation by suppressing the proliferation of microglia and astrocytes (Rajan et al., 2016; Drommelschmidt et al., 2017).

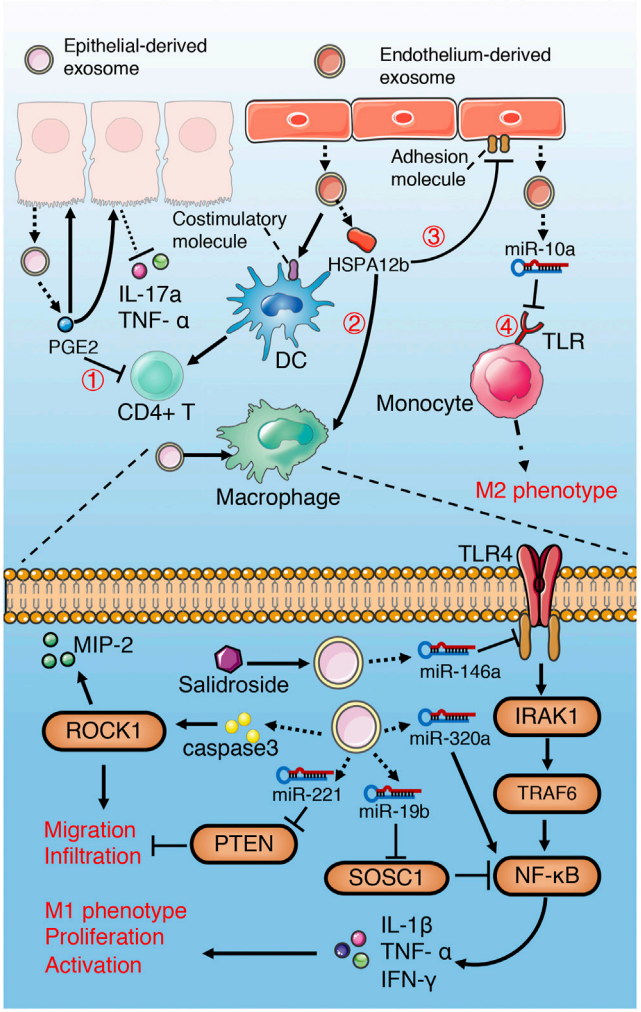

FIGURE 5 | Role of exosomes derived from epithelial and endothelial cells in sepsis. Epithelium-derived exosomes promote activation, proliferation, migration, infiltration and M1 polarization of macrophages through multiple miRNAs-mediated NF-κB activation, PTEN inhibition and caspase3-mediated ROCK1 activation. However, salidroside can induce epithelial exosomes releasing miR-146a, which inhibit TLR4/IRAK1/TRAF6/NF-κB signaling pathway. Exosomal PGE2 of IEC inhibit T cells through cAMP/PKA-dependent pathway①, and decrease pro-inflammatory cytokines release *via* autocrine and paracrine. Exosomal HSPA12b of endothelium reduce pro-inflammatory cytokines release and adhesion of macrophages by Inhibiting NF-κB② and activating PI3K/Akt③ signaling separately. Endothelial exosomes can induce a M2-like phenotype in monocyte through Inhibiting TLR/IRAK4/TAK1/NF-κB④ signaling pathway and promote DC maturation and T cell activation.

Endothelial Cell

Heat shock protein A12B (HSPA12B) is mainly expressed in endothelial cells and transferred from released exosomes to macrophages (**Figure 5**). By inhibiting the activation and nuclear translocation of NF-kB, it significantly increases the IL-10 level of LPS-stimulated macrophages and reduces the production of TNF-α and IL-1β (Tu et al., 2020). In addition,

HSPA12B reduces the expression of LPS-induced adhesion molecules and the production of pro-inflammatory cytokines *via* activating the PI3K/Akt signaling pathway of target cells (Li et al., 2013), which contribute to reduce the migration and adhesion of macrophages to target cells in sepsis (Tu et al., 2020). Endothelial microparticles (EMP) has been shown to promote the maturation of plasma cell-derived dendritic cell (PDC) by up-regulating the expression of costimulatory molecules and promoting the release of IL-6 and IL-8 (Angelot et al., 2009). PDC is considered to be the main cell secreting IFN- α under bacterial stimulation (Gilliet et al., 2008), and can induce the activation of prime T cells (Angelot et al., 2009). EVs (including exosomes) released by unstimulated endothelial cells are rich in a variety of miRNA (Njock et al., 2015). miR-10a in exosomes inhibits NF-κB by targeting suppression of IRAK4, TAK1/MAP3K7, and β-TRC, while miR-12b and miR-181b reduce the expression of pro-inflammatory genes and increase the expression of immuno-modulatory genes of monocytes *via* inhibiting the nuclear translocation of NF-κB and IRF5, and promote the differentiation of monocytes to anti-inflammatory M2-like phenotype (Njock et al., 2015). The regulation of endothelial EVs (including exosomes) on monocyte differentiation is stimulus dependent. EVs secreted by human umbilical vein endothelial cells stimulated by OX-LDL induce M1-like phenotype *via* miR-155, while EVs stimulated by KLF2 lead to M2-like phenotype in monocytes (He et al., 2018). These findings indicate that exosomes derived from endothelial cells have multiple effects and may play a role in balancing immunity in sepsis.

Epithelial Cell

The effect of lung epithelium-derived exosomes on macrophages in sepsis is mainly characterized by immune activation and pro-inflammation (**Figure 5**). Hyperoxia-induced, lung epithelial cell-derived and caspase-3 enriched EVs (including exosomes) activate macrophage *via* the ROCK1 pathway, and increase secretion of pro-inflammatory cytokines and macrophage inflammatory protein 2 (MIP-2) (Moon et al., 2015). Similarly, hyperoxia increase the levels of miR-320a and miR-221 in EVs derived from epithelial cells, and promote the activation and recruitment of macrophages and the release of pro-inflammatory cytokines by activating MMP9 and NF-κB (Lee et al., 2016). EVs derived from acid-induced lung epithelial cell are rich in miR-17 and miR-221, which increase macrophage infiltration through promoting integrin β1 circulation, inhibiting PTEN and activating c-fos-Rab11 signaling pathways (Lee et al., 2017). However, salidroside can upregulated the expression of miR-146a in LPS-induced pulmonary epithelial cell-derived exosomes, which reduce the pro-inflammatory cytokines release of macrophages *via* inhibiting TLR4/IRAK1/TRAF6/NF-κB signaling pathway (Zheng et al., 2020).

The intestinal epithelial cell (IEC)-derived luminal EVs during sepsis inhibit the release of pro-inflammatory cytokines TNF- α and IL-17a through autocrine and paracrine (Appiah et al., 2020). Exosomal PGE2 of IEC inhibit the activation of NKT and CD4+ T cells through cAMP/PKA-dependent pathway (Deng et al., 2013). In addition, IEC-derived pro-inflammatory cytokine enriched exosomes promote the migration of macrophages and aggravate the inflammatory response (Mitsuhashi et al., 2016). Exosomal miRNA-19b-3p of tubular epithelial cells (TEC) promotes M1 macrophage activation *via* SOCS-1 inhibition and NF- κB activation (Lv et al., 2019). Choroid plexus epithelial cells (CPE) release EVs containing miR-146a and miR-155 into cerebrospinal fluid (CSF) during sepsis, which trigger target mRNA repression in glial cells and induce an inflammatory response (Balusu et al., 2016).

Fibroblasts

The exosomes produced by synovial fibroblasts from patients with rheumatoid arthritis (RASF) contain membrane bound forms of TNF- α, which contributes to T cells apoptosis resistance *via* AKT and NF-kB activation (Zhang et al., 2006). According to the result, we may infer that exosomes derived from fibroblasts may play a similar role and alleviate immunosuppression in the later phase of sepsis, which need further study.

Immunomodulatory Effect of Exosomes Derived From Immune Cells in Sepsis

Macrophage

As an important part of the innate immune system, macrophages are the first line of defense against pathogen invasion. A number of studies have shown that exosomes derived from activated macrophages can affect the immune function of inactivated macrophages through autocrine and paracrine (Bhatnagar et al., 2007; Neyrolles et al., 2010; Ojcius et al., 2011; Sakaki et al., 2013; McDonald et al., 2014; Li et al., 2018b; Nair et al., 2018) (**Table 2**) (**Figure 6**). In addition, exosomes derived from macrophages also affect neutrophils (Esser et al., 2010; Jiao et al., 2017; Zhang et al., 2019b), alveolar epithelial cells (Soni et al., 2016), endothelial cells (Lee et al., 2014) and hepatocytes (Wang et al., 2018a) in sepsis (**Table 2**) (**Figure 6**).

Pathogen-associated molecular patterns (PAMPs) can stimulate macrophages to release ATP, while extracellular ATP, as a damage-associated molecular patterns (DAMPs), can activate the innate immune system and promote the production of inflammasome (Sutterwala et al., 2006; Piccini et al., 2008). Hayato et al. found that ATP enriched exosomes derived from LPS-challenged macrophages can promote recipient macrophage activation *via* activating P2Y11 receptors (Sakaki et al., 2013). Similarly, several studies have illustrated that PAMPs (such as HSP70, LAM, LPS)-containing exosomes released by pathogen-infected macrophages promote the activation, maturation and phagocytosis of uninfected macrophages *via* activation of TLR/MyD88/NF-KB signaling pathway (Bhatnagar et al., 2007; Neyrolles et al., 2010; Nair et al., 2018). Therefore, the extracellular release of exosomes containing PAMPs may be one of the important mechanisms of immune surveillance. This exosome-mediated autocrine or paracrine pathway accelerates immune activation triggered by PAMPs. However, exosomes derived from macrophages infected with Mycobacterium tuberculosis inhibit the expression of MHC

TABLE 2 | Immunomodulatory effect of exosomes derived from immune cells in sepsis.

Donor cell	Contents	Transfer pathway	Target cell	Signaling pathway/ Protein	Immuno-effect	Immune outcome	References
Macrophage	19KD lipoprotein	N/A	Macrophage	TLR2-MyD88 (+), CIITA (–)	MHC-II ↓, CD64 ↓	Suppression	Ojcius et al. (2011)
Macrophage	HSP70	N/A	Macrophage	NF-κB (+)	Macrophage mutation and phagocytosis ↑, TNF-α ↑	Activation	Neyrolles et al. (2010)
Macrophage, THP1	PAMPs (19KD lipoprotein, LAM, LPS)	N/A	Macrophage	TLR2/4-MyD88 (+)	Macrophage and neutrophil recruitment ↑, macrophage activation ↑, TNF-1/α ↑, IL-12 ↑	Activation	Bhatnagar et al. (2007)
Macrophage	miR-146a	N/A	Neutrophil	SOD (–)	ROS ↑, NETs ↑	Activation	Zhang et al. (2019b)
Alveolar macrophage	MV[a]: TNF	N/A	Alveolar epithelial cell	N/A	ICAM-1 ↑	Activation	Soni et al. (2016)
Macrophage	N/A	N/A	Macrophage	NF-κB (+)	TNF-α ↑	Activation	Li et al. (2018b)
Macrophage	N/A	N/A	PMN	NADPH oxidase (+)	ROS ↑, pyroptosis ↑	Activation	Jiao et al. (2017)
Macrophage	N/A	N/A	HUVEC	Integrin β1 ubiquitin, internalization and degradation (+), integrin β1 recycle to endosome (–), MEK-ERK (–)	MMP9 ↓, ECs migration ↓	N/A	Lee et al. (2014)
Macrophage	N/A	N/A	Hepatocyte	NOD (+)	NLRP3 ↑	Activation	Wang et al. (2018a)
Macrophage	MV[a]: Histone	N/A	Naive macrophage	TLR4 (+)	TNF-α ↑, IL-6 ↑, IL-1β ↑	Activation	Nair et al. (2018)
Macrophage	miR-126-5p, miR-146a/b, miR-21-3p, let7b, mRNA (encoding GADPH, CXCL2, CCL2/4, TNF-α), leb2, creb, G-CSF, IL-1Ra, TNF-α, chemokines	N/A	Macrophage	TLR-NF-κB	Anti-inflammation, pro-inflammation	Suppression/ Activation	McDonald et al. (2014)
MDM, MDDC, PMNL	LTC4S, LTA4H, 5-LO	TGF-β1	PMNL	5-KETE (+), LTA4-LTB4-LTC4 (+)	PMNL chemotaxis ↑, inflammatory cytokines ↑	Activation	Esser et al. (2010)
Macrophage	IL-1β, NLRP3	ATP/P2X7R	N/A	NF-κB (+)	Inflammatory cytokines ↑	Activation	Qu et al. (2007)
Monocyte	MP[a]: mt DNA	N/A	PMNs	TLR9 (+)	PMNs chemotaxis ↓	Suppression	Konecna et al. (2021)
Monocyte	N/A	N/A	Monocyte	TLR4 (–)	TNF-α ↓	Suppression	Wisler et al. (2020)
Monocyte	miR-155, miR-223	N/A	ECs (direct) PMNs (indirect)	TLR4-NF-κB (+)	ICAM-1 ↑, CCL-2 ↑, IL-6 ↑, monocyte chemotaxis and adhesion ↑	Activation	Tang et al. (2016)
Monocyte (THP1)	ATP	SLC179A	THP1	P2Y11 (+)	M1 phenotype ↑, IL-6 ↑	Activation	Sakaki et al. (2013)
PMN	MP[a]: AnxA1	N/A	PMNs	ALX (bind to AnxA1)	PMNs chemotaxis and adhesion ↓	Suppression	Dalli et al. (2008)
PMN	MP[a]: Anti-inflammatory cytokines (late stage in sepsis), PS	N/A	THP1 Macrophage	N/A	THP1 (MP): TGF-α ↑, PGE2 ↑, IL-10 ↑, THP1 (bystander): activity ↓, M2 ↑, M1 ↓	Suppression	Prakash et al. (2012)
PMN	PS	N/A	IMoDC	TLR4 (+)	iMoDC maturation, phagocytosis and chemotaxis ↓, induce T cell proliferation ↓, TGF-β1 ↑, CCR7 ↓	Suppression	Eken et al. (2008)
IDC (immature dendritic cell)	MFGE8	N/A	Macrophage	N/A	Phagocytosis ↑ (direct), TNF-α ↓, HMGB1 ↓ (indirect)	Activation (direct) Suppression (indirect)	Miksa et al. (2009)
BMDC	EVs[a]: TLR4	N/A	BMDC	NF-κB (+)	IL-6 ↑, TNF-α ↑	Activation	Zhang et al. (2019a)

(Continued on following page)

TABLE 2 | (*Continued*) Immunomodulatory effect of exosomes derived from immune cells in sepsis.

Donor cell	Contents	Transfer pathway	Target cell	Signaling pathway/ Protein	Immuno-effect	Immune outcome	References
DC	ICAM-1, MHC-II-peptide, CD86, MFG-E8	ICAM-1/ LFA-1, ICAM-1/ Mac-1	Naive T cell B cell Macrophage	ICAM-1/LFA-1 (+), ICAM-1/Mac-1 (+), MHC-II-peptide/TCR (+)	Naive T cell activation ↑, T Cell proliferation ↑, Transfer the ability of priming naive T cells to B cell and macrophage	Activation	Segura et al. (2005)
IDC	MFGE8	N/A	Macrophage	αVβ3- MFGE8-PS (+)	Phagocytosis ↑, IL-6 ↓, TNF-α ↓	Suppression	Miksa et al. (2006)
DC	miR-155, miR-146a	N/A	DC	miR-155: AGO-BACH1 (–), AGO-SHIP1 (–), miR-146a: IRAK1 (–), TRAF6 (–)	miR-155: IL-6 ↑, miR-146a: IL-10 ↑, IL-6↓, IL-12p40 ↓	Activation/ Suppression	Alexander et al. (2015)
DC (LMoDC)	EVs: HLA-1, ICAM-1, miR-155, CD63	N/A	CD8+ T cell	MHC-peptide complex	$CD8^+$ T cell activation ↑, TNF ↑, IFN ↑	Activation	Lindenbergh et al. (2019)
Treg	EVs[a]: miR-142-3p, miR-150-5p	N/A	DC	ICAM-1/LFA-1 (+)	IL-6 ↓, IL-10 ↑, MHC-II ↓, CD80 ↓	Suppression	Tung et al. (2018)
Treg	miR-155, let-7b, let-7d	Rab27, ceramide	Th1 cell	COX2 (+)	IFN-γ ↓, T cell proliferation ↓	Suppression	Okoye et al. (2014)
B cell	miR-155 inhibitor	N/A	Macrophage	N/A	TNF-α↓, SOCS1 mRNA↑	Suppression	Momen-Heravi et al. (2014)
B cell	MHC-peptide complex	Igα/β, TCR	CD4+ T cell	MHC-peptide-TCR (+)	$CD4^+$ T cell activation ↑, antigen specific memory T cells ↑	Activation	Muntasell et al. (2007)
CD8+T cell	TCR, FasL	TCR-MHC-I CD54-LFA-1	DC (direct) CD8+T cell (indirect)	TCR-MHC-I (–) FasL-FasL (+)	DC antigen presentation ↓, apoptosis ↑, $CD8^+$ CTL ↓	Suppression	Xie et al. (2010)
T cell	MP[a]: Monocyte activating factors	N/A	Monocyte/ macrophage	N/A	TNF-α ↑, IL-1 ↑, SIL-Ira ↑	Activation	Scanu et al. (2008)
MDSC (inhibitory phenotype)	lncRNA (Hotairm1)	N/A	MDSC (activation phenotype)	S100A9 nuclear translocation + +)	S100A9 release ↓, pro-inflammatory cytokines ↓, MDSCs transfer to inhibitory phenotype	Suppression	Alkhateeb et al. (2020)
G-MDSC	N/A	N/A	Neutrophil Monocyte/ macrophage	L-arginine metabolism (–), ROS (–)	Neutrophil and monocyte/macrophage infiltration ↓, Th1 proliferation ↓, Treg ↑, IFN-γ ↓, TNF-α ↓	Suppression	Wang et al. (2016)

[a]*Exosomes are subsets of EVs or MVs, however, their immunomodulatory effects may exist unpredictable differences.*

II and CD64 molecules on the surface of naïve macrophages in a TLR2-MyD88-dependent manner, and reduce their ability of antigen presentation (Ojcius et al., 2011). The effect of exosomes on the immune response is dynamic and multifactorial. Exosomes released from LPS-challenged macrophages can both promote and inhibit aspects of immunity and inflammation. For instance, macrophages stimulated with LPS secrete exosomes containing elevated levels of cytokines and miRNAs, some of which display the opposite effects (McDonald et al., 2014). MiR-21-3p, miR-146a and miR-146b in exosomes prevent over-activation of innate immune system by inhibiting TLR/NF-κB signaling pathway (Taganov et al., 2006; Hsu et al., 2011; McDonald et al., 2014), while pro-inflammatory cytokines and chemokines in exosomes lead to activation of NF- κB and promote inflammatory response and innate immune cell chemotaxis (McDonald et al., 2014; Kovach et al., 2016).

Exosomes secreted by human macrophages contain enzymes for leukotriene biosynthesis (LTC4S, LTA4H, 5-LO) and promote granulocyte migration (Esser et al., 2010). miR-146a enriched exosomes derived from oxLDL-stimulated macrophages induce ROS production and NETs formation *via* targeted inhibition of SOD2 (Zhang et al., 2019b). Exosomes released from macrophages induced by hemorrhagic shock increase the ROS production and pyroptosis of neutrophils by activating NADPH oxidase (Jiao et al., 2017), which may be involved in the immunosuppression during sepsis.

Macrophage-derived exosomes promote the adhesion of inflammatory cells in sepsis by up-regulating the expression of ICAM-1 in alveolar epithelial cells (Soni et al., 2016). In addition, exosomes secreted by macrophages suppress endothelial cell migration through regulating integrin trafficking (Lee et al., 2014). Therefore, the exosomes released by macrophages may aggravate physiological barrier dysfunction and organ damage induced by sepsis.

In conclusion, the macrophage-derived exosomes in sepsis mainly promote immune activation and mediate pro-inflammatory response and tissue damage.

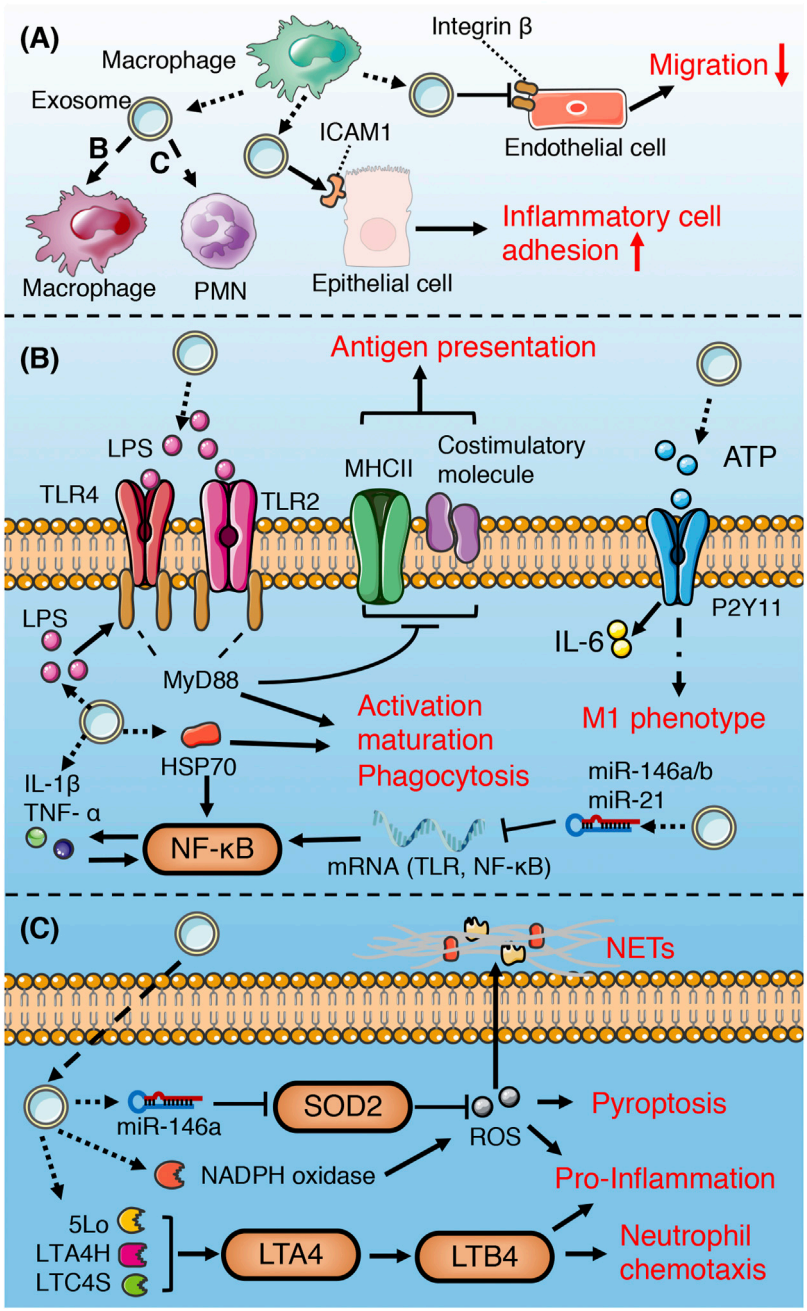

FIGURE 6 | Role of macrophage-derived exosomes in sepsis **(A)** macrophage-derived exosomes can induce pro-inflammatory response in recipient macrophage and PMN, promote inflammatory cell adhesion to endothelium, and suppress migration of epithelial cells **(B)** macrophage-derived exosomes containing DAMPs and PAMPs promote recipient macrophage activation, maturation, phagocytosis, and M1 polarization, while suppress the ability of antigen presentation. **(C)** Exosomal enzymes and miRNA increase NETs formation, chemotaxis, pro-inflammatory response, and pyroptosis of PMN.

Monocyte

Monocytes stimulated by Inflammation and infection release exosomes containing mitochondrial damage-associated molecular patterns (mt-DAMPs), which reduce the chemotaxis and sterilization of neutrophils through TLR9 inhibition mediated by endosomal acidification (Itagaki et al., 2011; Konecna et al., 2021). LPS can stimulate endothelial cells to express adhesion molecule ICAM-1, which can bind to monocytes and trigger inflammatory response (Wang et al., 2015a). In addition, miR-155 and miR-223, in monocyte-derived exosomes stimulated by LPS upregulate the expression of ICAM-1, chemokine ligand (CCL)-2 and cytokine IL-6 by activating TLR4/NF-KB signaling pathway in endothelial cells (Tang et al., 2016), which further aggravates inflammatory

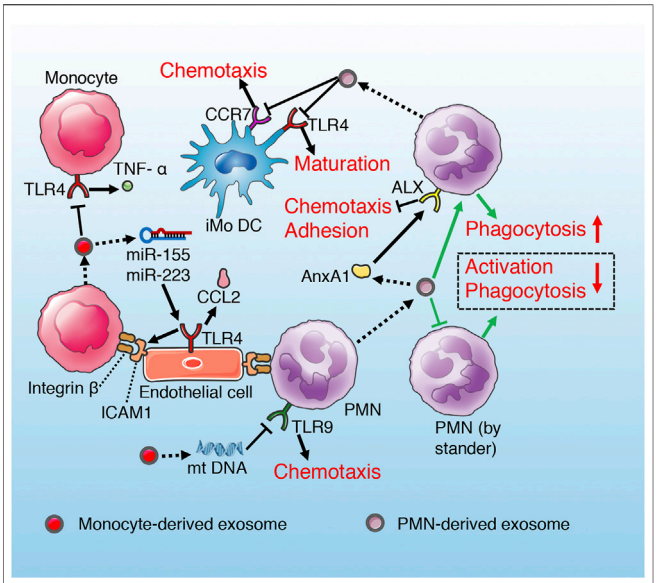

FIGURE 7 | Role of exosomes derived from monocyte and PMN in sepsis. Monocyte exosomes reduce TNF-α release of recipient monocyte and PMN chemotaxis *via* TLR inhibition. However, exosomal miRNAs of monocyte promote endothelium adhesion by activating TLR. PMN-derived exosomes suppress maturation and chemotaxis of iMoDC through inhibiting CCR7 and TLR4 separately. PMN-derived exosomes suppress recipient PMN chemotaxis and adhesion to endothelium *via* AnxA1/ALX pathway. In addition, exosomes secrete by PMN promote anti-inflammatory cytokines release of recipient PMN, while induce immune anergy of bystander PMN (green routes).

response and endothelial injury through positive feedback loop (**Figure 7**). Thus, we can infer that monocyte-derived exosomes not only promote the aggregation of monocytes to endothelial cells to cope with PAMPs, but also control excessive inflammatory response by inhibiting the chemotaxis of neutrophils. In addition, proteomic analysis demonstrated that exosomes derived from LPS-stimulated monocytes contain protein networks with potential immunosuppressive patterns (Wisler et al., 2020). These exosomes reduce LPS-induced TNF-α release from recipient monocytes (Wisler et al., 2020), which suggests a exosomal negative feedback mode of monocyte limiting self-overactivation (**Figure 7**).

Neutrophils/Polymorphonuclear Leukocytes

The exosomes derived from polymorphonuclear leukocytes (PMNs) contain functional annexin 1 (AnxA1), which is an endogenous anti-inflammatory protein by controlling activation and trafficking of the inflammatory cells (Dalli et al., 2008; Senchenkova et al., 2019). AnxA1 can activate and bind ALX receptors in PMNs, and inhibit the chemotaxis, adhesion and migration of PMNs to endothelial cells (Chiang et al., 2006; Hayhoe et al., 2006; Senchenkova et al., 2019). It has been demonstrated that AnAX1-rich exosomes derived from PMNs suppress recipient PMN migration and adhesion to human umbilical vein endothelial cell (HUVEC), which is a manner of self-regulation alleviating inflammatory response and endothelial injury induced by excessive PMNs aggregation (Dalli et al., 2008). Similar study also supports the anti-inflammatory effects of exosomes derived from neutrophils (Prakash et al., 2012). However, this anti-inflammatory effect may aggravate immunosuppression in the late stage of sepsis. PMN-derived exosomes lead to increased activation and enhanced phagocytosis and increased secretion of antimicrobial factors (TGF-α, PGE2, IL-10) of the recipient PMN, while result in immune anergy of the by stander PMN characterized by deactivation and decreased phagocytosis (Prakash et al., 2012) (**Figure 7**). The immunosuppressive effect of PMN-derived exosomes is also reflected in the hindrance of DCs maturation (**Figure 7**). Ceylan et al. (Eken et al., 2008) found that extracellular vesicles (including exosomes) derived from PMN interfere with the maturation of immature monocyte-derived dendritic cell (iMoDC) induced by LPS, decrease its phagocytosis and chemotaxis, and weaken its capacity to promote T cell activation and proliferation (**Figure 7**). Phosphatidylserine (PS) in PMN-derived exosomes has been identified as a major factor influencing iMoDC maturation and function (Eken et al., 2008; Ohyagi et al., 2013). In addition, iMoDC exposed to PMN-derived exosomes release TGF-β1, which is responsible for the downregulation of TLR4-mediated maturation of iMoDC and CCR7-mediated chemotaxis of DCs (Eken et al., 2008; Pang et al., 2016; Wang et al., 2018b).

Dendritic Cell

Dendritic cells (DCs) are the professional antigen presenting cell (APCs), which can efficiently uptake, process and present antigens. Immature DC (IDC) has stronger phagocytosis and migration ability, while mature DC expresses higher levels of adhesion and co-stimulatory molecules, which can effectively activate prime T cells and play a central role in initiating, regulating and maintaining immune response (Miksa et al., 2006; Yang et al., 2014). It has been demonstrated that DC-derived exosomes contain MFGE8, CD63, Toll-like receptors, adhesion molecules, co-stimulatory molecules, MHC-peptide complexes, and miRNA, which regulate the immune function of DCs, macrophages and lymphocytes during sepsis (Segura et al., 2005; Miksa et al., 2006; Miksa et al., 2009; Alexander et al., 2015; Zhang et al., 2019a; Lindenbergh et al., 2019).

The exosomes released by IDCs contain MFGE8 (Miksa et al., 2006; Miksa et al., 2009), which is a required protein for the opsonization of apoptotic cells for phagocytosis (Hanayama et al., 2004). The integrin α V β 3 expressed on the surface of macrophages binds to the exposed PS on the surface of apoptotic cells through the mediation of MFGE8 to complete the phagocytosis process (Miksa et al., 2006). The decrease of MFGE8 contributes to the accumulation of apoptotic cells, leading to a surge in pro-inflammatory cytokines, which is responsible for the progression and deterioration of sepsis (Shah et al., 2012). The IDC-derived exosomes promote the clearance of apoptotic cells *via* transferring MFGE8 to macrophages, which in turn reduce the release of TNF-α and HMGB1 (Miksa et al., 2006; Miksa et al., 2009) (**Figure 8A**). Compared with exosomes from IDC, LPS-stimulated mature

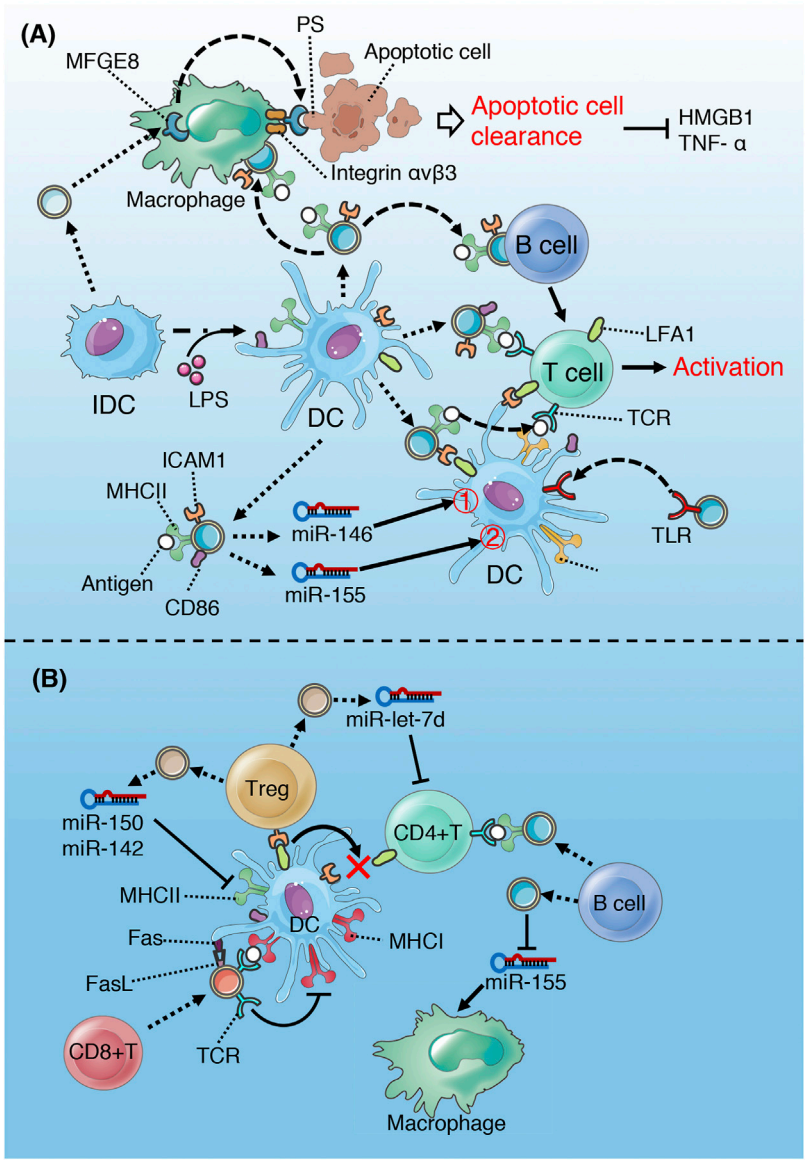

FIGURE 8 | Role of exosomes derived from DC and lymphocyte in sepsis. **(A)** IDC-derived exosomes promote MFGE8-mediated phagocytosis of apoptotic cells by macrophage. DC-derived exosomes can activate antigen-specific T cells according to antigen presentation described above. In addition, miR-146 in DC-derived exosomes alleviate inflammatory response of recipient DC *via* inhibiting IRAK1/TRAF6/NF-κB①, while exosomal miR-155 aggravate inflammatory response by suppressing BACH1 and SHIP1② signaling pathways. **(B)** exosomes derived from Treg induce an immune tolerance phenotype of DC and inhibit T cell proliferation. Exosomes released by CD8+ T cell inhibit the ability of DC to activate T cells and induce DC apoptosis. However, exosomes derived B cell can activate T cell, and also be used as drug carrier of immunotherapy.

DC-derived exosomes contain more MHC-II-peptide complexes, ICAM-1 and CD86, which can activate antigen-specific T cells more effectively (Segura et al., 2005). DC-derived exosomes perform antigen presentation and activate T cells through the pathways described above (**Figure 2**). It is noteworthy that the ability of DC-released exosomes to activate naive T cells may also be magnified by activated bystander T cells (Lindenbergh et al., 2019). After migration to the lymph node, the gradually matured DC stimulated by LPS interact with activated bystander T cells, which promote the further maturation of DC and subsequent release of exosomes containing more HLA-1, ICAM-1, miR-155, and CD63 (Lindenbergh et al., 2019).

It has been found that EVs (exosomes) can mediate the transmission of TLRs between DCs, which may improve the reactivity of DC to LPS and accelerate the activation of immune defense and inflammatory response (Zhang et al., 2019a). In addition, LPS-stimulated DC-derived exosomes are enrich in miR-155 and miR-146a, which can modulate the inflammatory response of recipient DC through paracrine (Alexander et al., 2015) (**Figure 8A**). Exosomal miR-155 reduces the expression of

anti-inflammatory target genes BACH1 and SHIP1, while exosomal miR-146a reduces the expression of pro-inflammatory target genes IRAK1 and TRAF6 (Alexander et al., 2015). The inflammatory response of recipient cells is buffered by the two exosomal microRNAs with opposite functions, so as to achieve the best response amplitude. One hypothesis may be that miR-155 and miR-146a exist in different exosomes or be released at different phase during the dynamic process of the disease to balance immune status and inflammatory response, which needs to be confirmed by further studies.

Lymphocyte

T Lymphocyte

It has been demonstrated that molecular transfer between DCs and T cells is bidirectional. Similar to DCs, active T cells can also release bioactive exosomes, which can be recruited by APCs or B cells (Xie et al., 2010). Xie et al. found that TCR-carrying exosomes released by activated CD8 + T cells could weak the ability of DCs to activate other antigen-specific T cells (Xie et al., 2010). On the one hand, the exosomes down-regulate the expression of MHC-I in DC *via* TCR-mediated internalization, on the other hand, the TCR released by the exosomes compete with antigen-specific T cells to bind to the MHC-I-peptide complex on the surface of DC, thus interfere with T cell activation (Xie et al., 2010). In addition, exosomal FasL induces DC apoptosis through Fas/FasL signaling pathway (Xie et al., 2010). Therefore, activated T cell-derived exosomes inhibit immune over-activation through negative feedback mechanism (**Figure 8B**).

Regulatory T cells (Tregs) are a subset of T cells, which can maintain self-tolerance and limit other immune responses. The over-activation of Tregs is considered to be an important cause of immunosuppression in late sepsis. It has been found that DCs and Th1 cells are the main targets for the immuno-modulatory function of Treg and its derived exosomes (Okoye et al., 2014; Tung et al., 2018) (**Figure 8B**). MiR-150-5p and miR-142-3p in Treg-derived exosomes induce the immune tolerance phenotype of DC by down-regulating the expression of surface molecules MHC-II and CD80 (Tung et al., 2018). Similarly, let-7d in Treg-derived exosomes inhibits IFN-γ release and Th1 cell proliferation through COX2-dependent pathway (Okoye et al., 2014). It is worth noting that the immune synapse (IS) formed between Treg and DC can enhance the functional transmission of exosomes to recipient DC (Gutierrez-Vazquez et al., 2013; Tung et al., 2018). However, the consumption of adhesion molecules (such as Fascin-1) to build IS between Treg and DC can reduce the efficiency of IS formation between DC and effector T cells, thus affecting the antigen presentation and activation of effector T cells by DC and its exosomes, which may aggravate immunosuppression to some extent (Tung et al., 2018) (**Figure 8B**).

B Lymphocyte

It has been found that engagement of antigen-loaded B cells with specific CD4 T cells can trigger exosomes release form B cells (Muntasell et al., 2007). The MHC-II-peptide complexes carried by the exosomes can effectively activate CD4+T cells (Muntasell et al., 2007) (**Figure 8B**). Although B cells can not play a major role in the early initiation of naive T cells compared with DCs, the exosomes secreted by B cells can act as a modulator of continuous immune response or play a role in maintaining antigen-specific memory T cells (Muntasell et al., 2007). In addition, exosomes derived from B cells can also be used as carriers to transport miR-155 inhibitor to macrophages, reducing the TNF- α release through SOCS1/NF-KB-dependent pathway (Momen-Heravi et al., 2014).

Natural Killer Cell

As an important cell of the immune system, Natural killer (NK) cells play the role of non-specific target cell killing and immune regulation. The research on NK cells and their exosomes mainly focuses on the field of anti-tumor and anti-virus, but little is known about the role of NK cells in sepsis. It has been found that the exosomes derived from NK cells is structural and independent on the activation of donor cells, which only has an effect on activated recipient immune cells, suggesting a role in immune surveillance and homeostasis in sepsis (Lugini et al., 2012).

Myeloid-Derived Suppressor Cell

Myeloid-derived suppressor cells (MDSCs) is a group of heterogeneous cells derived from bone marrow, which are the precursor of DCs, macrophages and granulocytes and have significant inhibitory effect on immune cell response. It has been demonstrated that, MDSCs play different roles in the modulation of inflammation and immune response with the development of sepsis (Brudecki et al., 2012; Dai et al., 2017). MDSCs produced in acute/early sepsis is pro-inflammatory phenotype (Brudecki et al., 2012), while in chronic/late sepsis is immunosuppressive phenotype (Dai et al., 2017). In late sepsis, MDSCs-derived exosomes contain high levels of LncRNA Hotairm1, which can transform MDSCs from pro-inflammatory phenotype to immunosuppressive phenotype by promoting nuclear translocation of pro-inflammatory protein S100A9 (Alkhateeb et al., 2020). Exosomes released by granulocytic MDSCs (G-MDSCs) can attenuate the inflammatory response of mice with colitis induced by DSS, reduce the infiltration of innate immune cells, suppress the proliferation of Th1 cells and promote the activation of Treg cells (Wang et al., 2016). This inhibitory effect on innate and adaptive immunity may be achieved through the inhibition of L-arginine metabolism and ROS (Zea et al., 2005; Tian et al., 2015).

THE THERAPEUTIC USE OF EXOSOMES IN SEPSIS

Exosomes are considered to be natural nanoliposomes, which are relatively stable in the circulation, and have the ability to resist complement lysis and ribonuclease attack (Chaput and Théry, 2010). In addition, exosomes are low in immunogenicity and well tolerated (Wu et al., 2017). These characteristics ensure exosomes to be excellent therapeutic vehicles.

MSCs-derived exosomes are most used in the treatment of sepsis. Exosomes isolated from MSCs treated by LPS *in vitro* can stimulate the regenerative and reparative properties of the target cells (Wu et al., 2017). Intravenous injection of miR-223 enriched exosomes derived from MSCs can reduce myocardial injury in sepsis through inhibiting the release of pro-inflammatory cytokines from macrophages (Wang et al., 2015c). EVs released from MSCs can reduce pulmonary edema induced by LPS and alleviated inflammation (Zhu et al., 2014). In addition, MSC-derived EVs have been shown to reduce LPS-induced motor neuron inflammation and brain injury of septic rats (Rajan et al., 2016; Drommelschmidt et al., 2017).

Exosomes isolated from the peritoneum and bronchoalveolar lavage fluid of patients with surgical sepsis can significantly enhance the activity and phagocytic capacity of THP-1 monocytes *in vitro* (Prakash et al., 2012). Exogenous administration of exosomes containing MFG-E8 from DC or IDC can accelerate the clearance of apoptotic cells accumulated in sepsis (Miksa et al., 2009). Studies have shown that exosomes isolated from B cells can be used as ideal carriers of synthetic miRNA inhibitors to reduce the release of macrophage pro-inflammatory factors in sepsis (Momen-Heravi et al., 2014). Injection of curcumin-containing exosomes can reduce the inflammatory response in septic rats and increase the survival rate (Sun et al., 2010). Similarly, curcumin-containing exosomes can pass through the blood-brain barrier when administered intranasally, and effectively reduce brain inflammation caused by LPS (Zhuang et al., 2011). In addition, tumor-derived exosomes are used to reduce excessive inflammation in sepsis by virtue of their immunosuppressive properties. It has been demonstrated that exosomes produced by H22 hepatic tumor cells can protect mice from severe tissue injury induced by LPS (Teng et al., 2012). However, the potential tumorigenicity of these exosomes should be taken into consideration more carefully.

CONCLUSION AND PERSPECTIVES

The role of exosomes in sepsis is multiple and complex. The exosomes derived from antigen-presenting cells (DCs, macrophages and B cells) mainly contribute to immune activation, including promoting the activation, differentiation, maturation and proliferation of immune cells, which assist the innate and adaptive immune system to respond to the invasion of pathogens more efficiency. On the contrary, MSC and Treg derived exosomes mainly exert immunosuppressive and anti-inflammatory effects. However, exosomes from other cell sources show two sides. Especially exosomes derived from activated inflammatory cells (monocytes and neutrophils) may inhibit their over-activation through autocrine or paracrine-mediated negative feedback mechanism, while may also accelerate the recruitment to the inflammatory site through the positive feedback pathway. This bi-directional and self-limited regulation of exosomes play an important role in maintaining the homeostasis of sepsis, which may act as the regulator or balance switch of the immune system.

It is worth noting that exosomes from the same source have different regulatory effects on the immune system in sepsis, which may be due to the following reasons: 1) the same origin exosomes contain a variety of contents with different bioactivities. 2) the effects of exosomes *in vivo* and *in vitro* may be different. 3) sepsis is a dynamic and complex pathological process, and the same origin exosomes in the early stage (excessive inflammatory response) and the late stage of sepsis (immunosuppression) may have opposite effects.

In conclusion, the complex role of exosomes in sepsis is related to multiple factors involving cell sources, contents and phase of disease. Endogenous exosomes can not only aggravate the inflammatory response and organ injury of sepsis, but also play a protective role by balancing immunity. While the engineered exogenous exosomes are used for immunotherapy in different stages of sepsis according to their immune characteristics or as a drug carrier. Understanding the specific immunomodulatory characteristics and mechanism of exosomes from various cell sources in sepsis is helpful for us to choose the right time and target, seeking benefits and avoiding disadvantages in the treatment of sepsis. As an immunomodulatory switch, exosomes may bring a new dawn for the treatment of sepsis in the future.

AUTHOR CONTRIBUTIONS

PQ collected the documentations and wrote the original manuscript; JZ and YD classified literatures; PQ and YL drew the figures; JZ and YL proposed amendments and modified the paper. All authors contributed to the article and approved the submitted version.

FUNDING

This work was funded by the National Natural Science Foundation of China (Grant Number 81701951), the Liaoning Education Department (Grant Number LK201634), 345 Talent Project and the Shenyang Municipal Science and Technology Commission (Grant Number 17-230-9-45).

REFERENCES

Alexander, M., Hu, R., Runtsch, M. C., Kagele, D. A., Mosbruger, T. L., Tolmachova, T., et al. (2015). Exosome-delivered microRNAs Modulate the Inflammatory Response to Endotoxin. *Nat. Commun.* 6, 7321. doi:10.1038/ncomms8321

Alkhateeb, T., Bah, I., Kumbhare, A., Youssef, D., Yao, Z. Q., McCall, C. E., et al. (2020). Long Non-coding RNA Hotairm1 Promotes S100A9 Support of MDSC Expansion during Sepsis. *J. Clin. Cel Immunol.* 11, 600.

Angelot, F., Seilles, E., Biichle, S., Berda, Y., Gaugler, B., Plumas, J., et al. (2009). Endothelial Cell-Derived Microparticles Induce Plasmacytoid Dendritic Cell Maturation: Potential Implications in Inflammatory Diseases. *Haematologica.* 94 (11), 1502–1512. doi:10.3324/haematol.2009.010934

Appiah, M. G., Park, E. J., Darkwah, S., Kawamoto, E., Akama, Y., Gaowa, A., et al. (2020). Intestinal Epithelium-Derived Luminally Released Extracellular Vesicles in Sepsis Exhibit the Ability to Suppress TNF-A and IL-17A Expression in Mucosal Inflammation. *Int. J. Mol. Sci.* 21, 8445. doi:10.3390/ijms21228445

Balusu, S., Van Wonterghem, E., De Rycke, R., Raemdonck, K., Stremersch, S., Gevaert, K., et al. (2016). Identification of a Novel Mechanism of Blood-Brain Communication during Peripheral Inflammation *via* Choroid Plexus-derived Extracellular Vesicles. *EMBO Mol. Med.* 8 (10), 1162–1183. doi:10.15252/emmm.201606271

Barile, L., Moccetti, T., Marbán, E., and Vassalli, G. (2017). Roles of Exosomes in Cardioprotection. *Eur. Heart J.* 38 (18), 1372–1379. doi:10.1093/eurheartj/ehw304

Bhatnagar, S., Shinagawa, K., Castellino, F. J., and Schorey, J. S. (2007). Exosomes Released from Macrophages Infected with Intracellular Pathogens Stimulate a Proinflammatory Response *In Vitro* and *In Vivo*. *Blood*. 110 (9), 3234–3244. doi:10.1182/blood-2007-03-079152

Blazquez, R., Sanchez-Margallo, F. M., de la Rosa, O., Dalemans, W., Alvarez, V., Tarazona, R., et al. (2014). Immunomodulatory Potential of Human Adipose Mesenchymal Stem Cells Derived Exosomes on *In Vitro* Stimulated T Cells. *Front. Immunol.* 5, 556. doi:10.3389/fimmu.2014.00556

Bobrie, A., Colombo, M., Raposo, G., and Théry, C. (2011). Exosome Secretion: Molecular Mechanisms and Roles in Immune Responses. *Traffic*. 12 (12), 1659–1668. doi:10.1111/j.1600-0854.2011.01225.x

Boomer, J. S., To, K., Chang, K. C., Takasu, O., Osborne, D. F., Walton, A. H., et al. (2011). Immunosuppression in Patients Who Die of Sepsis and Multiple Organ Failure. *JAMA*. 306 (23), 2594–2605. doi:10.1001/jama.2011.1829

Brudecki, L., Ferguson, D. A., McCall, C. E., and El Gazzar, M. (2012). Myeloid-derived Suppressor Cells Evolve during Sepsis and Can Enhance or Attenuate the Systemic Inflammatory Response. *Infect. Immun.* 80 (6), 2026–2034. doi:10.1128/IAI.00239-12

Caudrillier, A., Kessenbrock, K., Gilliss, B. M., Nguyen, J. X., Marques, M. B., Monestier, M., et al. (2012). Platelets Induce Neutrophil Extracellular Traps in Transfusion-Related Acute Lung Injury. *J. Clin. Invest.* 122 (7), 2661–2671. doi:10.1172/JCI61303

Chaput, N., and Théry, C. (2010). Exosomes: Immune Properties and Potential Clinical Implementations. *Semin. Immunopathol.* 33 (5), 419–440. doi:10.1007/s00281-010-0233-9

Chen, W., Huang, Y., Han, J., Yu, L., Li, Y., Lu, Z., et al. (2016). Immunomodulatory Effects of Mesenchymal Stromal Cells-Derived Exosome. *Immunol. Res.* 64 (4), 831–840. doi:10.1007/s12026-016-8798-6

Chiang, N., Serhan, C. N., Dahlén, S. E., Drazen, J. M., Hay, D. W. P., Rovati, G. E., et al. (2006). The Lipoxin Receptor ALX: Potent Ligand-specific and Stereoselective Actions *In Vivo*. *Pharmacol. Rev.* 58 (3), 463–487. doi:10.1124/pr.58.3.4

Choi, H., Kim, Y., Mirzaaghasi, A., Heo, J., Kim, Y. N., Shin, J. H., et al. (2020). Exosome-based Delivery of Super-repressor IκBα Relieves Sepsis-Associated Organ Damage and Mortality. *Sci. Adv.* 6, eaaz6980. doi:10.1126/sciadv.aaz6980

Dai, J., Kumbhare, A., Youssef, D., McCall, C. E., and El Gazzar, M. (2017). Intracellular S100A9 Promotes Myeloid-Derived Suppressor Cells during Late Sepsis. *Front. Immunol.* 8, 1565. doi:10.3389/fimmu.2017.01565

Peraro, M. D., and van der Goot, F. G. (2016). Pore-forming Toxins: Ancient, but Never Really Out of Fashion. *Nat. Rev. Microbiol.* 14 (2), 77–92. doi:10.1038/nrmicro.2015.3

Dalli, J., Norling, L. V., Renshaw, D., Cooper, D., Leung, K.-Y., and Perretti, M. (2008). Annexin 1 Mediates the Rapid Anti-inflammatory Effects of Neutrophil-Derived Microparticles. *Blood*. 112 (6), 2512–2519. doi:10.1182/blood-2008-02-140533

Delano, M. J., and Ward, P. A. (2016). Sepsis-induced Immune Dysfunction: Can Immune Therapies Reduce Mortality? *J. Clin. Invest.* 126 (1), 23–31. doi:10.1172/jci82224

Deng, Z. B., Zhuang, X., Ju, S., Xiang, X., Mu, J., Liu, Y., et al. (2013). Exosome-like Nanoparticles from Intestinal Mucosal Cells Carry Prostaglandin E2 and Suppress Activation of Liver NKT Cells. *J. Immunol.* 190 (7), 3579–3589. doi:10.4049/jimmunol.1203170

Deng, J. N., Li, Y. Q., Liu, Y., Li, Q., Hu, Y., Xu, J. Q., et al. (2019). Exosomes Derived from Plasma of Septic Patients Inhibit Apoptosis of T Lymphocytes by Down-Regulating Bad *via* Hsa-miR-7-5p. *Biochem. Biophysical Res. Commun.* 513 (4), 958–966. doi:10.1016/j.bbrc.2019.04.051

Deng, H., Wu, L., Liu, M., Zhu, L., Chen, Y., Zhou, H., et al. (2020). Bone Marrow Mesenchymal Stem Cell-Derived Exosomes Attenuate LPS-Induced ARDS by Modulating Macrophage Polarization through Inhibiting Glycolysis in Macrophages. *Shock*. 54, 828. doi:10.1097/shk.0000000000001549

Domenis, R., Cifu, A., Quaglia, S., Pistis, C., Moretti, M., Vicario, A., et al. (2018). Pro Inflammatory Stimuli Enhance the Immunosuppressive Functions of Adipose Mesenchymal Stem Cells-Derived Exosomes. *Sci. Rep.* 8 (1), 13325. doi:10.1038/s41598-018-31707-9

Drommelschmidt, K., Serdar, M., Bendix, I., Herz, J., Bertling, F., Prager, S., et al. (2017). Mesenchymal Stem Cell-Derived Extracellular Vesicles Ameliorate Inflammation-Induced Preterm Brain Injury. *Brain Behav. Immun.* 60, 220–232. doi:10.1016/j.bbi.2016.11.011

Eken, C., Gasser, O., Zenhaeusern, G., Oehri, I., Hess, C., and Schifferli, J. A. (2008). Polymorphonuclear Neutrophil-Derived Ectosomes Interfere With the Maturation of Monocyte-Derived Dendritic Cells. *J. Immunol.* 180 (2), 817–824. doi:10.4049/jimmunol.180.2.817

Esser, J., Gehrmann, U., D'Alexandri, F. L., Hidalgo-Estévez, A. M., Wheelock, C. E., Scheynius, A., et al. (2010). Exosomes from Human Macrophages and Dendritic Cells Contain Enzymes for Leukotriene Biosynthesis and Promote Granulocyte Migration. *J. Allergy Clin. Immunol.* 126 (5), 1032–1040.e1034. doi:10.1016/j.jaci.2010.06.039

Gao, F., Chiu, S. M., Motan, D. A. L., Zhang, Z., Chen, L., Ji, H.-L., et al. (2016). Mesenchymal Stem Cells and Immunomodulation: Current Status and Future Prospects. *Cell Death Dis.* 7, e2062. doi:10.1038/cddis.2015.327

Gao, K., Jin, J., Huang, C., Li, J., Luo, H., Li, L., et al. (2019). Exosomes Derived from Septic Mouse Serum Modulate Immune Responses *via* Exosome-Associated Cytokines. *Front. Immunol.* 10, 1560. doi:10.3389/fimmu.2019.01560

Gilliet, M., Cao, W., and Liu, Y. J. (2008). Plasmacytoid Dendritic Cells: Sensing Nucleic Acids in Viral Infection and Autoimmune Diseases. *Nat. Rev. Immunol.* 8 (8), 594–606. doi:10.1038/nri2358

Gutiérrez-Vázquez, C., Villarroya-Beltri, C., Mittelbrunn, M., and Sánchez-Madrid, F. (2013). Transfer of Extracellular Vesicles during Immune Cell-Cell Interactions. *Immunol. Rev.* 251 (1), 125–142. doi:10.1111/imr.12013

Hanayama, R., Tanaka, M., Miyasaka, K., Aozasa, K., Koike, M., Uchiyama, Y., et al. (2004). Autoimmune Disease and Impaired Uptake of Apoptotic Cells in MFG-E8-Deficient Mice. *Science*. 304 (5674), 1147–1150. doi:10.1126/science.1094359

Hayhoe, R. P. G., Kamal, A. M., Solito, E., Flower, R. J., Cooper, D., and Perretti, M. (2006). Annexin 1 and its Bioactive Peptide Inhibit Neutrophil-Endothelium Interactions Under Flow: Indication of Distinct Receptor Involvement. *Blood*. 107 (5), 2123–2130. doi:10.1182/blood-2005-08-3099

He, S., Wu, C., Xiao, J., Li, D., Sun, Z., and Li, M. (2018). Endothelial Extracellular Vesicles Modulate the Macrophage Phenotype: Potential Implications in Atherosclerosis. *Scand. J. Immunol.* 87, e12648. doi:10.1111/sji.12648

Hessvik, N. P., and Llorente, A. (2018). Current Knowledge on Exosome Biogenesis and Release. *Cell. Mol. Life Sci.* 75 (2), 193–208. doi:10.1007/s00018-017-2595-9

Hoshino, D., Kirkbride, K. C., Costello, K., Clark, E. S., Sinha, S., Grega-Larson, N., et al. (2013). Exosome Secretion Is Enhanced by Invadopodia and Drives Invasive Behavior. *Cel Rep.* 5 (5), 1159–1168. doi:10.1016/j.celrep.2013.10.050

Hoshino, A., Costa-Silva, B., Shen, T.-L., Rodrigues, G., Hashimoto, A., Tesic Mark, M., et al. (2015). Tumour Exosome Integrins Determine Organotropic Metastasis. *Nature*. 527 (7578), 329–335. doi:10.1038/nature15756

Hotchkiss, R. S., Monneret, G., and Payen, D. (2013). Sepsis-induced Immunosuppression: from Cellular Dysfunctions to Immunotherapy. *Nat. Rev. Immunol.* 13 (12), 862–874. doi:10.1038/nri3552

Hsu, S. D., Lin, F. M., Wu, W. Y., Liang, C., Huang, W. C., Chan, W. L., et al. (2011). miRTarBase: a Database Curates Experimentally Validated microRNA-Target Interactions. *Nucleic Acids Res.* 39 (Database issue), D163–D169. doi:10.1093/nar/gkq1107

Hurley, J. H., and Hanson, P. I. (2010). Membrane Budding and Scission by the ESCRT Machinery: It's All in the Neck. *Nat. Rev. Mol. Cel Biol.* 11 (8), 556–566. doi:10.1038/nrm2937

Hutchins, N. A., Unsinger, J., Hotchkiss, R. S., and Ayala, A. (2014). The New Normal: Immunomodulatory Agents Against Sepsis Immune Suppression. *Trends Mol. Med.* 20 (4), 224–233. doi:10.1016/j.molmed.2014.01.002

Itagaki, K., Adibnia, Y., Sun, S., Zhao, C., Sursal, T., Chen, Y., et al. (2011). Bacterial DNA Induces Pulmonary Damage *via* TLR-9 through Cross-Talk with Neutrophils. *Shock* 36 (6), 548–552. doi:10.1097/SHK.0b013e3182369fb2

Jiang, K., Yang, J., Guo, S., Zhao, G., Wu, H., and Deng, G. (2019). Peripheral Circulating Exosome-Mediated Delivery of miR-155 as a Novel Mechanism for Acute Lung Inflammation. *Mol. Ther.* 27 (10), 1758–1771. doi:10.1016/j.ymthe.2019.07.003

Jiao, Y., Li, Z., Loughran, P. A., Fan, E. K., Scott, M. J., Li, Y., et al. (2017). Frontline Science: Macrophage-Derived Exosomes Promote Neutrophil Necroptosis Following Hemorrhagic Shock. *J. Leukoc. Biol.* 103 (2), 175–183. doi:10.1189/jlb.3HI0517-173R

Jiao, Y., Li, W., Wang, W., Tong, X., Xia, R., Fan, J., et al. (2020). Platelet-derived Exosomes Promote Neutrophil Extracellular Trap Formation during Septic Shock. *Crit. Care* 24, 380. doi:10.1186/s13054-020-03082-3

Kalluri, R., and LeBleu, V. S. (2020). The Biology, Function, and Biomedical Applications of Exosomes. *Science* 367. doi:10.1126/science.aau6977

Kalluri, R. (2016). The Biology and Function of Exosomes in Cancer. *J. Clin. Invest.* 126 (4), 1208–1215. doi:10.1172/JCI81135

Kawamoto, E., Masui-Ito, A., Eguchi, A., Soe, Z. Y., Prajuabjinda, O., Darkwah, S., et al. (2019). Integrin and PD-1 Ligand Expression on Circulating Extracellular Vesicles in Systemic Inflammatory Response Syndrome and Sepsis. *Shock* 52 (1), 13–22. doi:10.1097/SHK.0000000000001228

Keller, M. D., Ching, K. L., Liang, F.-X., Dhabaria, A., Tam, K., Ueberheide, B. M., et al. (2020). Decoy Exosomes Provide Protection against Bacterial Toxins. *Nature* 579 (7798), 260–264. doi:10.1038/s41586-020-2066-6

Kim, S. H., Bianco, N. R., Shufesky, W. J., Morelli, A. E., and Robbins, P. D. (2007). MHC Class II+ Exosomes in Plasma Suppress Inflammation in an Antigen-specific and Fas ligand/Fas-dependent Manner. *J. Immunol.* 179 (4), 2235–2241. doi:10.4049/jimmunol.179.4.2235

Konecna, B., Park, J., Kwon, W.-Y., Vlkova, B., Zhang, Q., Huang, W., et al. (2021). Monocyte Exocytosis of Mitochondrial Danger-Associated Molecular Patterns in Sepsis Suppresses Neutrophil Chemotaxis. *J. Trauma Acute Care Surg.* 90 (1), 46–53. doi:10.1097/TA.0000000000002973

Kovach, M. A., Singer, B. H., Newstead, M. W., Zeng, X., Moore, T. A., White, E. S., et al. (2016). IL-36γ Is Secreted in Microparticles and Exosomes by Lung Macrophages in Response to Bacteria and Bacterial Components. *J. Leukoc. Biol.* 100 (2), 413–421. doi:10.1189/jlb.4A0315-087R

Kumar, H., Kawai, T., and Akira, S. (2011). Pathogen Recognition by the Innate Immune System. *Int. Rev. Immunol.* 30 (1), 16–34. doi:10.3109/08830185.2010.529976

Lee, H. D., Kim, Y. H., and Kim, D. S. (2014). Exosomes Derived from Human Macrophages Suppress Endothelial Cell Migration by Controlling Integrin Trafficking. *Eur. J. Immunol.* 44 (4), 1156–1169. doi:10.1002/eji.201343660

Lee, H., Zhang, D., Zhu, Z., Dela Cruz, C. S., and Jin, Y. (2016). Epithelial Cell-Derived Microvesicles Activate Macrophages and Promote Inflammation *via* Microvesicle-Containing microRNAs. *Sci. Rep.* 6, 35250. doi:10.1038/srep35250

Lee, H., Zhang, D., Wu, J., Otterbein, L. E., and Jin, Y. (2017). Lung Epithelial Cell-Derived Microvesicles Regulate Macrophage Migration *via* MicroRNA-17/221-Induced Integrin β1 Recycling. *J. Immunol.* 199 (4), 1453–1464. doi:10.4049/jimmunol.1700165

Leentjens, J., Kox, M., van der Hoeven, J. G., Netea, M. G., and Pickkers, P. (2013). Immunotherapy for the Adjunctive Treatment of Sepsis: From Immunosuppression to Immunostimulation. Time for a Paradigm Change? *Am. J. Respir. Crit. Care Med.* 187 (12), 1287–1293. doi:10.1164/rccm.201301-0036CP

Leppkes, M., Schick, M., Hohberger, B., Mahajan, A., Knopf, J., Schett, G., et al. (2019). Updates on NET Formation in Health and Disease. *Semin. Arthritis Rheum.* 49 (3S), S43–S48. doi:10.1016/j.semarthrit.2019.09.011

Li, J., Zhang, Y., Li, C., Xie, J., Liu, Y., Zhu, W., et al. (2013). HSPA12B Attenuates Cardiac Dysfunction and Remodelling after Myocardial Infarction through an eNOS-dependent Mechanism. *Cardiovasc. Res.* 99 (4), 674–684. doi:10.1093/cvr/cvt139

Li, X., Liu, L., Yang, J., Yu, Y., Chai, J., Wang, L., et al. (2016). Exosome Derived from Human Umbilical Cord Mesenchymal Stem Cell Mediates MiR-181c Attenuating Burn-Induced Excessive Inflammation. *EBioMedicine*. 8, 72–82. doi:10.1016/j.ebiom.2016.04.030

Li, J. J., Wang, B., Kodali, M. C., Chen, C., Kim, E., Patters, B. J., et al. (2018a). *In vivo* evidence for the Contribution of Peripheral Circulating Inflammatory Exosomes to Neuroinflammation. *J. Neuroinflam.* 15, 8. doi:10.1186/s12974-017-1038-8

Li, Z. G., Scott, M. J., Brzóska, T., Sundd, P., Li, Y. H., Billiar, T. R., et al. (2018b). Lung Epithelial Cell-Derived IL-25 Negatively Regulates LPS-Induced Exosome Release from Macrophages. *Mil. Med. Res.* 5, 24. doi:10.1186/s40779-018-0173-6

Lindenbergh, M. F. S., Koerhuis, D. G. J., Borg, E. G. F., van 't Veld, E. M., Driedonks, T. A. P., Wubbolts, R., et al. (2019). Bystander T-Cells Support Clonal T-Cell Activation by Controlling the Release of Dendritic Cell-Derived Immune-Stimulatory Extracellular Vesicles. *Front. Immunol.* 10, 448. doi:10.3389/fimmu.2019.00448

Lugini, L., Cecchetti, S., Huber, V., Luciani, F., Macchia, G., Spadaro, F., et al. (2012). Immune Surveillance Properties of Human NK Cell-Derived Exosomes. *J.Immunol.* 189 (6), 2833–2842. doi:10.4049/jimmunol.1101988

Lv, L.-L., Feng, Y., Wu, M., Wang, B., Li, Z.-L., Zhong, X., et al. (2019). Exosomal miRNA-19b-3p of Tubular Epithelial Cells Promotes M1 Macrophage Activation in Kidney Injury. *Cell Death Differ* 27 (1), 210–226. doi:10.1038/s41418-019-0349-y

Majer, O., Liu, B., Kreuk, L. S. M., Krogan, N., and Barton, G. M. (2019). UNC93B1 Recruits Syntenin-1 to Dampen TLR7 Signalling and Prevent Autoimmunity. *Nature* 575 (7782), 366–370. doi:10.1038/s41586-019-1612-6

Mathieu, M., Martin-Jaular, L., Lavieu, G., and Théry, C. (2019). Specificities of Secretion and Uptake of Exosomes and Other Extracellular Vesicles for Cell-To-Cell Communication. *Nat. Cel Biol.* 21 (1), 9–17. doi:10.1038/s41556-018-0250-9

McDonald, M. K., Tian, Y., Qureshi, R. A., Gormley, M., Ertel, A., Gao, R., et al. (2014). Functional Significance of Macrophage-Derived Exosomes in Inflammation and Pain. *Pain* 155 (8), 1527–1539. doi:10.1016/j.pain.2014.04.029

Merle, N. S., Noe, R., Halbwachs-Mecarelli, L., Fremeaux-Bacchi, V., and Roumenina, L. T. (2015). Complement System Part II: Role in Immunity. *Front. Immunol.* 6, 257. doi:10.3389/fimmu.2015.00257

Miksa, M., Wu, R., Dong, W., Das, P., Yang, D., and Wang, P. (2006). Dendritic Cell-Derived Exosomes Containing Milk Fat Globule Epidermal Growth Factor-Factor VIII Attenuate Proinflammatory Responses in Sepsis. *Shock* 25 (6), 586–593. doi:10.1097/01.shk.0000209533.22941.d0

Miksa, M., Wu, R., Dong, W., Komura, H., Amin, D., Ji, Y., et al. (2009). Immature Dendritic Cell-Derived Exosomes Rescue Septic Animals *via* Milk Fat Globule Epidermal Growth Factor VIII. *J. Immunol.* 183 (9), 5983–5990. doi:10.4049/jimmunol.0802994

Mitsuhashi, S., Feldbrügge, L., Csizmadia, E., Mitsuhashi, M., Robson, S. C., and Moss, A. C. (2016). Luminal Extracellular Vesicles (EVs) in Inflammatory Bowel Disease (IBD) Exhibit Proinflammatory Effects on Epithelial Cells and Macrophages. *Inflamm. Bowel Dis.* 22 (7), 1587–1595. doi:10.1097/MIB.0000000000000840

Momen-Heravi, F., Bala, S., Bukong, T., and Szabo, G. (2014). Exosome-mediated Delivery of Functionally Active miRNA-155 Inhibitor to Macrophages. *Nanomedicine* 10 (7), 1517–1527. doi:10.1016/j.nano.2014.03.014

Monsel, A., Zhu, Y.-g., Gennai, S., Hao, Q., Hu, S., Rouby, J.-J., et al. (2015). Therapeutic Effects of Human Mesenchymal Stem Cell-Derived Microvesicles in Severe Pneumonia in Mice. *Am. J. Respir. Crit. Care Med.* 192 (3), 324–336. doi:10.1164/rccm.201410-1765OC

Moon, H.-G., Cao, Y., Yang, J., Lee, J. H., Choi, H. S., and Jin, Y. (2015). Lung Epithelial Cell-Derived Extracellular Vesicles Activate Macrophage-Mediated Inflammatory Responses *via* ROCK1 Pathway. *Cel Death Dis.* 6 (12), e2016. doi:10.1038/cddis.2015.282

Morrison, T. J., Jackson, M. V., Cunningham, E. K., Kissenpfennig, A., McAuley, D. F., O'Kane, C. M., et al. (2017). Mesenchymal Stromal Cells Modulate Macrophages in Clinically Relevant Lung Injury Models by Extracellular Vesicle Mitochondrial Transfer. *Am. J. Respir. Crit. Care Med.* 196 (10), 1275–1286. doi:10.1164/rccm.201701-0170OC

Muntasell, A., Berger, A. C., and Roche, P. A. (2007). T Cell-Induced Secretion of MHC Class II-Peptide Complexes on B Cell Exosomes. *EMBO J.* 26 (19), 4263–4272. doi:10.1038/sj.emboj.7601842

Murao, A., Brenner, M., Aziz, M., and Wang, P. (2020). Exosomes in Sepsis. *Frontiers In Immunol.* 11. 2140. doi:10.3389/fimmu.2020.02140

Nair, R. R., Mazza, D., Brambilla, F., Gorzanelli, A., Agresti, A., and Bianchi, M. E. (2018). LPS-challenged Macrophages Release Microvesicles Coated with Histones. *Front. Immunol.* 9, 1463. doi:10.3389/fimmu.2018.01463

Anand, P. K., Anand, E., Bleck, C. K., Anes, E., Griffiths, G., and Griffiths, G. (2010). Exosomal Hsp70 Induces a Pro-Inflammatory Response to Foreign Particles Including Mycobacteria. *PLoS One* 5, e10136. doi:10.1371/journal.pone.0010136

Njock, M.-S., Cheng, H. S., Dang, L. T., Nazari-Jahantigh, M., Lau, A. C., Boudreau, E., et al. (2015). Endothelial Cells Suppress Monocyte Activation through Secretion of Extracellular Vesicles Containing Antiinflammatory MicroRNAs. *Blood*. 125 (20), 3202–3212. doi:10.1182/blood-2014-11-611046

Ogura, H., Kawasaki, T., Tanaka, H., Koh, T., Tanaka, R., Ozeki, Y., et al. (2001). Activated Platelets Enhance Microparticle Formation and Platelet-Leukocyte Interaction in Severe Trauma and Sepsis. *J. Trauma Inj. Infect. Crit. Care* 50 (5), 801–809. doi:10.1097/00005373-200105000-00005

Ohyagi, H., Onai, N., Sato, T., Yotsumoto, S., Liu, J., Akiba, H., et al. (2013). Monocyte-derived Dendritic Cells Perform Hemophagocytosis to Fine-Tune Excessive Immune Responses. *Immunity* 39 (3), 584–598. doi:10.1016/j.immuni.2013.06.019

Singh, P. P., LeMaire, C., Tan, J. C., Zeng, E., Schorey, J. S., and Schorey, J. S. (2011). Exosomes Released from M. tuberculosis Infected Cells Can Suppress IFN-γ Mediated Activation of Naïve Macrophages. *PLoS One* 6, e18564. doi:10.1371/journal.pone.0018564

Okoye, I. S., Coomes, S. M., Pelly, V. S., Czieso, S., Papayannopoulos, V., Tolmachova, T., et al. (2014). MicroRNA-containing T-Regulatory-Cell-Derived Exosomes Suppress Pathogenic T Helper 1 Cells. *Immunity* 41 (1), 89–103. doi:10.1016/j.immuni.2014.05.019

Pan, L., Hu, L., Zhang, L., Xu, H., Chen, Y., Bian, Q., et al. (2020). Deoxyelephantopin Decreases the Release of Inflammatory Cytokines in Macrophage Associated with Attenuation of Aerobic Glycolysis *via* Modulation of PKM2. *Int. Immunopharmacol.* 79, 106048. doi:10.1016/j.intimp.2019.106048

Pang, M. F., Georgoudaki, A. M., Lambut, L., Johansson, J., Tabor, V., Hagikura, K., et al. (2016). TGF-β1-induced EMT Promotes Targeted Migration of Breast Cancer Cells through the Lymphatic System by the Activation of CCR7/CCL21-Mediated Chemotaxis. *Oncogene* 35 (6), 748–760. doi:10.1038/onc.2015.133

Pegtel, D. M., and Gould, S. J. (2019). Exosomes. *Annu. Rev. Biochem.* 88, 487–514. doi:10.1146/annurev-biochem-013118-111902

Piccini, A., Carta, S., Tassi, S., Lasiglie, D., Fossati, G., and Rubartelli, A. (2008). ATP Is Released by Monocytes Stimulated with Pathogen-Sensing Receptor Ligands and Induces IL-1 and IL-18 Secretion in an Autocrine Way. *Proc. Natl. Acad. Sci.* 105 (23), 8067–8072. doi:10.1073/pnas.0709684105

Prakash, P. S., Caldwell, C. C., Lentsch, A. B., Pritts, T. A., and Robinson, B. R. H. (2012). Human Microparticles Generated during Sepsis in Patients with Critical Illness Are Neutrophil-Derived and Modulate the Immune Response. *J. Trauma Acute Care Surg.* 73 (2), 401–407. doi:10.1097/TA.0b013e31825a776d

Qu, Y., Franchi, L., Nunez, G., and Dubyak, G. R. (2007). Nonclassical IL-1β Secretion Stimulated by P2X7 Receptors Is Dependent on Inflammasome Activation and Correlated with Exosome Release in Murine Macrophages. *J. Immunol.* 179 (3), 1913–1925. doi:10.4049/jimmunol.179.3.1913

Raeven, P., Zipperle, J., and Drechsler, S. (2018). Extracellular Vesicles as Markers and Mediators in Sepsis. *Theranostics* 8 (12), 3348–3365. doi:10.7150/thno.23453

Raiborg, C., and Stenmark, H. (2009). The ESCRT Machinery in Endosomal Sorting of Ubiquitylated Membrane Proteins. *Nature* 458 (7237), 445–452. doi:10.1038/nature07961

Rajan, T. S., Giacoppo, S., Trubiani, O., Diomede, F., Piattelli, A., Bramanti, P., et al. (2016). Conditioned Medium of Periodontal Ligament Mesenchymal Stem Cells Exert Anti-inflammatory Effects in Lipopolysaccharide-Activated Mouse Motoneurons. *Exp. Cel Res.* 349 (1), 152–161. doi:10.1016/j.yexcr.2016.10.008

Real, J. M., Ferreira, L. R. P., Esteves, G. H., Koyama, F. C., Dias, M. V. S., Bezerra-Neto, J. E., et al. (2018). Exosomes from Patients with Septic Shock Convey miRNAs Related to Inflammation and Cell Cycle Regulation: New Signaling Pathways in Sepsis? *Crit. Care* 22, 68. doi:10.1186/s13054-018-2003-3

Rialdi, A., Hultquist, J., Jimenez-Morales, D., Peralta, Z., Campisi, L., Fenouil, R., et al. (2017). The RNA Exosome Syncs IAV-RNAPII Transcription to Promote Viral Ribogenesis and Infectivity. *Cell* 169 (4), 679–692 e14. doi:10.1016/j.cell.2017.04.021

Robbins, P. D., and Morelli, A. E. (2014). Regulation of Immune Responses by Extracellular Vesicles. *Nat. Rev. Immunol.* 14 (3), 195–208. doi:10.1038/nri3622

Robbins, P. D., Dorronsoro, A., and Booker, C. N. (2016). Regulation of Chronic Inflammatory and Immune Processes by Extracellular Vesicles. *J. Clin. Invest.* 126 (4), 1173–1180. doi:10.1172/jci81131

Rubio, I., Osuchowski, M. F., Shankar-Hari, M., Skirecki, T., Winkler, M. S., Lachmann, G., et al. (2019). Current Gaps in Sepsis Immunology: New Opportunities for Translational Research. *Lancet Infect. Dis.* 19 (12), e422–e436. doi:10.1016/s1473-3099(19)30567-5

Sakaki, H., Tsukimoto, M., Harada, H., Moriyama, Y., and Kojima, S. (2013). Autocrine Regulation of Macrophage Activation *via* Exocytosis of ATP and Activation of P2Y11 Receptor. *PLoS One* 8 (4), e59778. doi:10.1371/journal.pone.0059778

Scanu, A., Molnarfi, N., Brandt, K. J., Gruaz, L., Dayer, J.-M., and Burger, D. (2008). Stimulated T Cells Generate Microparticles, Which Mimic Cellular Contact Activation of Human Monocytes: Differential Regulation of Pro- and Anti-inflammatory Cytokine Production by High-Density Lipoproteins. *J. Leukoc. Biol.* 83 (4), 921–927. doi:10.1189/jlb.0807551

Segura, E., Nicco, C., Lombard, B., Véron, P., Raposo, G., Batteux, F., et al. (2005). ICAM-1 on Exosomes from Mature Dendritic Cells Is Critical for Efficient Naive T-Cell Priming. *Blood* 106 (1), 216–223. doi:10.1182/blood-2005-01-0220

Seilie, E. S., and Bubeck Wardenburg, J. (2017). Staphylococcus aureus Pore-Forming Toxins: The Interface of Pathogen and Host Complexity. *Semin. Cel Developmental Biol.* 72, 101–116. doi:10.1016/j.semcdb.2017.04.003

Senchenkova, E. Y., Ansari, J., Becker, F., Vital, S. A., Al-Yafeai, Z., Sparkenbaugh, E. M., et al. (2019). Novel Role for the AnxA1-Fpr2/ALX Signaling Axis as a Key Regulator of Platelet Function to Promote Resolution of Inflammation. *Circulation* 140 (4), 319–335. doi:10.1161/CIRCULATIONAHA.118.039345

Shah, K. G., Wu, R., Jacob, A., Molmenti, E. P., Nicastro, J., Coppa, G. F., et al. (2012). Recombinant Human Milk Fat Globule-EGF Factor 8 Produces Dose-dependent Benefits in Sepsis. *Intensive Care Med.* 38 (1), 128–136. doi:10.1007/s00134-011-2353-7

Shahir, M., Mahmoud Hashemi, S., Asadirad, A., Varahram, M., Kazempour-Dizaji, M., Folkerts, G., et al. (2020). Effect of Mesenchymal Stem Cell-derived Exosomes on the Induction of Mouse Tolerogenic Dendritic Cells. *J. Cel Physiol* 235 (10), 7043–7055. doi:10.1002/jcp.29601

Singer, M., Deutschman, C. S., Seymour, C. W., Shankar-Hari, M., Annane, D., Bauer, M., et al. (2016). The Third International Consensus Definitions for Sepsis and Septic Shock (Sepsis-3). *JAMA* 315 (8), 801–810. doi:10.1001/jama.2016.0287

Song, Y., Dou, H., Li, X., Zhao, X., Li, Y., Liu, D., et al. (2017). Exosomal miR-146a Contributes to the Enhanced Therapeutic Efficacy of Interleukin-1β-Primed Mesenchymal Stem Cells against Sepsis. *Stem Cells* 35 (5), 1208–1221. doi:10.1002/stem.2564

Soni, S., Wilson, M. R., O'Dea, K. P., Yoshida, M., Katbeh, U., Woods, S. J., et al. (2016). Alveolar Macrophage-Derived Microvesicles Mediate Acute Lung Injury. *Thorax* 71 (11), 1020–1029. doi:10.1136/thoraxjnl-2015-208032

Spaan, A. N., van Strijp, J. A. G., and Torres, V. J. (2017). Leukocidins: Staphylococcal Bi-component Pore-Forming Toxins Find Their Receptors. *Nat. Rev. Microbiol.* 15 (7), 435–447. doi:10.1038/nrmicro.2017.27

Steinhagen, F., Schmidt, S. V., Schewe, J. C., Peukert, K., Klinman, D. M., and Bode, C. (2020). Immunotherapy in Sepsis - Brake or Accelerate? *Pharmacol. Ther.* 208, 107476. doi:10.1016/j.pharmthera.2020.107476

Stuffers, S., Sem Wegner, C., Stenmark, H., and Brech, A. (2009). Multivesicular Endosome Biogenesis in the Absence of ESCRTs. *Traffic* 10 (7), 925–937. doi:10.1111/j.1600-0854.2009.00920.x

Sun, D., Zhuang, X., Xiang, X., Liu, Y., Zhang, S., Liu, C., et al. (2010). A Novel Nanoparticle Drug Delivery System: the Anti-inflammatory Activity of Curcumin Is Enhanced when Encapsulated in Exosomes. *Mol. Ther.* 18 (9), 1606–1614. doi:10.1038/mt.2010.105

Sutterwala, F. S., Ogura, Y., Szczepanik, M., Lara-Tejero, M., Lichtenberger, G. S., Grant, E. P., et al. (2006). Critical Role for NALP3/CIAS1/Cryopyrin in Innate and Adaptive Immunity through its Regulation of Caspase-1. *Immunity* 24 (3), 317–327. doi:10.1016/j.immuni.2006.02.004

Taganov, K. D., Boldin, M. P., Chang, K.-J., and Baltimore, D. (2006). NF- B-dependent Induction of microRNA miR-146, an Inhibitor Targeted to Signaling Proteins of Innate Immune Responses. *Proc. Natl. Acad. Sci.* 103 (33), 12481–12486. doi:10.1073/pnas.0605298103

Takeuchi, O., and Akira, S. (2010). Pattern Recognition Receptors and Inflammation. *Cell* 140 (6), 805–820. doi:10.1016/j.cell.2010.01.022

Tamayo, E., Gomez, E., Bustamante, J., Gomez-Herreras, J. I., Fonteriz, R., Bobillo, F., et al. (2012). Evolution of Neutrophil Apoptosis in Septic Shock Survivors and Nonsurvivors. *J. Crit. Care* 27 (4), 415. doi:10.1016/j.jcrc.2011.09.001

Tang, N., Sun, B., Gupta, A., Rempel, H., and Pulliam, L. (2016). Monocyte Exosomes Induce Adhesion Molecules and Cytokines *via* Activation of NF-κB in Endothelial Cells. *FASEB j.* 30 (9), 3097–3106. doi:10.1096/fj.201600368RR

Teng, H., Hu, M., Yuan, L.-X., Liu, Y., Guo, X., Zhang, W.-J., et al. (2012). Suppression of Inflammation by Tumor-Derived Exosomes: a Kind of Natural Liposome Packaged with Multifunctional Proteins. *J. Liposome Res.* 22 (4), 346–352. doi:10.3109/08982104.2012.710911

Terrasini, N., and Lionetti, V. (2017). Exosomes in Critical Illness. *Crit. Care Med.* 45 (6), 1054–1060. doi:10.1097/CCM.0000000000002328

Tian, X., Tian, J., Tang, X., Rui, K., Zhang, Y., Ma, J., et al. (2015). Particulate β-glucan Regulates the Immunosuppression of Granulocytic Myeloid-Derived Suppressor Cells by Inhibiting NFIA Expression. *Oncoimmunology* 4 (9), e1038687. doi:10.1080/2162402X.2015.1038687

Tu, F., Wang, X., Zhang, X., Ha, T., Wang, Y., Fan, M., et al. (2020). Novel Role of Endothelial Derived Exosomal HSPA12B in Regulating Macrophage Inflammatory Responses in Polymicrobial Sepsis. *Front. Immunol.* 11, 825. doi:10.3389/fimmu.2020.00825

Tung, S. L., Boardman, D. A., Sen, M., Letizia, M., Peng, Q., Cianci, N., et al. (2018). Regulatory T Cell-Derived Extracellular Vesicles Modify Dendritic Cell Function. *Sci. Rep.* 8 (1), 6065. doi:10.1038/s41598-018-24531-8

van der Poll, T., van de Veerdonk, F. L., Scicluna, B. P., and Netea, M. G. (2017). The Immunopathology of Sepsis and Potential Therapeutic Targets. *Nat. Rev. Immunol.* 17 (7), 407–420. doi:10.1038/nri.2017.36

Venet, F., and Monneret, G. (2018). Advances in the Understanding and Treatment of Sepsis-Induced Immunosuppression. *Nat. Rev. Nephrol.* 14 (2), 121–137. doi:10.1038/nrneph.2017.165

Wang, H., Hong, L.-J., Huang, J.-Y., Jiang, Q., Tao, R.-R., Tan, C., et al. (2015a). P2RX7 Sensitizes Mac-1/icam-1-dependent Leukocyte-Endothelial Adhesion and Promotes Neurovascular Injury during Septic Encephalopathy. *Cell Res.* 25 (6), 674–690. doi:10.1038/cr.2015.61

Wang, R., Ding, Q., Yaqoob, U., de Assuncao, T. M., Verma, V. K., Hirsova, P., et al. (2015b). Exosome Adherence and Internalization by Hepatic Stellate Cells Triggers Sphingosine 1-phosphate-dependent Migration. *J. Biol. Chem.* 290 (52), 30684–30696. doi:10.1074/jbc.M115.671735

Wang, X., Gu, H., Qin, D., Yang, L., Huang, W., Essandoh, K., et al. (2015c). Exosomal miR-223 Contributes to Mesenchymal Stem Cell-Elicited Cardioprotection in Polymicrobial Sepsis. *Sci. Rep.* 5, 13721. doi:10.1038/srep13721

Wang, Y., Tian, J., Tang, X., Rui, K., Tian, X., Ma, J., et al. (2016). Exosomes Released by Granulocytic Myeloid-Derived Suppressor Cells Attenuate DSS-Induced Colitis in Mice. *Oncotarget* 7 (13), 15356–15368. doi:10.18632/oncotarget.7324

Wang, G., Jin, S., Ling, X., Li, Y., Hu, Y., Zhang, Y., et al. (2018a). Proteomic Profiling of LPS-Induced Macrophage-Derived Exosomes Indicates Their Involvement in Acute Liver Injury. *Proteomics* 19 (3), e1800274. doi:10.1002/pmic.201800274

Wang, Y. C., Chen, R. F., Brandacher, G., Lee, W. P. A., and Kuo, Y. R. (2018b). The Suppression Effect of Dendritic Cells Maturation by Adipose-Derived Stem Cells through TGF-B1 Related Pathway. *Exp. Cel Res.* 370 (2), 708–717. doi:10.1016/j.yexcr.2018.07.037

Wisler, J. R., Singh, K., McCarty, A. R., Abouhashem, A. S. E., Christman, J. W., and Sen, C. K. (2020). Proteomic Pathway Analysis of Monocyte-Derived Exosomes during Surgical Sepsis Identifies Immunoregulatory Functions. *Surg. Infections* 21 (2), 101–111. doi:10.1089/sur.2019.051

Wu, J., Wang, Y., and Li, L. (2017). Functional Significance of Exosomes Applied in Sepsis: A Novel Approach to Therapy. *Biochim. Biophys. Acta. Mol. Basis Dis.* 1863 (1), 292–297. doi:10.1016/j.bbadis.2016.10.024

Xie, Y., Zhang, H., Li, W., Deng, Y., Munegowda, M. A., Chibbar, R., et al. (2010). Dendritic Cells Recruit T Cell Exosomes *via* Exosomal LFA-1 Leading to Inhibition of CD8+ CTL Responses through Downregulation of Peptide/MHC Class I and Fas Ligand-Mediated Cytotoxicity. *J.Immunol.* 185 (9), 5268–5278. doi:10.4049/jimmunol.1000386

Xu, J., Feng, Y., Jeyaram, A., Jay, S. M., Zou, L., and Chao, W. (2018). Circulating Plasma Extracellular Vesicles from Septic Mice Induce Inflammation *via* MicroRNA- and TLR7-dependent Mechanisms. *J.Immunol.* 201 (11), 3392–3400. doi:10.4049/jimmunol.1801008

Yang, A. X., Chong, N., Jiang, Y., Catalano, J., Puri, R. K., and Khleif, S. N. (2014). Molecular Characterization of Antigen-Peptide Pulsed Dendritic Cells: Immature Dendritic Cells Develop a Distinct Molecular Profile when Pulsed with Antigen Peptide. *PLoS One* 9 (1), e86306. doi:10.1371/journal.pone.0086306

Yao, M., Cui, B., Zhang, W., Ma, W., Zhao, G., and Xing, L. (2021) Exosomal miR-21 Secreted by IL-1β-primed-mesenchymal Stem Cells Induces Macrophage M2 Polarization and Ameliorates Sepsis. *Life Sci.* 264, 118658. doi:10.1016/j.lfs.2020.118658

Zea, A. H., Rodriguez, P. C., Atkins, M. B., Hernandez, C., Signoretti, S., Zabaleta, J., et al. (2005). Arginase-producing Myeloid Suppressor Cells in Renal Cell Carcinoma Patients: A Mechanism of Tumor Evasion. *Cancer Res.* 65 (8), 3044–3048. doi:10.1158/0008-5472.CAN-04-4505

Zhang, H.-G., Liu, C., Su, K., Yu, S., Zhang, L., Zhang, S., et al. (2006). A Membrane Form of TNF-α Presented by Exosomes Delays T Cell Activation-Induced Cell Death. *J. Immunol.* 176 (12), 7385–7393. doi:10.4049/jimmunol.176.12.7385

Zhang, B., Yin, Y., Lai, R. C., Tan, S. S., Choo, A. B. H., and Lim, S. K. (2014). Mesenchymal Stem Cells Secrete Immunologically Active Exosomes. *Stem Cell Develop.* 23 (11), 1233–1244. doi:10.1089/scd.2013.0479

Zhang, Y., Meng, J., Zhang, L., Ramkrishnan, S., and Roy, S. (2019a). Extracellular Vesicles with Exosome-like Features Transfer TLRs between Dendritic Cells. *Immunohorizos* 3 (6), 186–193. doi:10.4049/immunohorizons.1900016

Zhang, Y. G., Song, Y., Guo, X. L., Miao, R. Y., Fu, Y. Q., Miao, C. F., et al. (2019b). Exosomes Derived from oxLDL-Stimulated Macrophages Induce Neutrophil Extracellular Traps to Drive Atherosclerosis. *Cell Cycle* 18 (20), 2672–2682. doi:10.1080/15384101.2019.1654797

Zhao, M., Li, F., Jian, Y., Wang, X., Yang, H., Wang, J., et al. (2020). Salvianolic Acid B Regulates Macrophage Polarization in Ischemic/reperfused Hearts by Inhibiting mTORC1-Induced Glycolysis. *Eur. J. Pharmacol.* 871, 172916. doi:10.1016/j.ejphar.2020.172916

Zheng, L., Su, J., Zhang, Z., Jiang, L., Wei, J., Xu, X., et al. (2020). Salidroside Regulates Inflammatory Pathway of Alveolar Macrophages by Influencing the Secretion of miRNA-146a Exosomes by Lung Epithelial Cells. *Sci. Rep.* 10, 20750. doi:10.1038/s41598-020-77448-6

Zhu, Y. G., Feng, X. M., Abbott, J., Fang, X. H., Hao, Q., Monsel, A., et al. (2014). Human Mesenchymal Stem Cell Microvesicles for Treatment ofEscherichia coliEndotoxin-Induced Acute Lung Injury in Mice. *Stem Cells* 32 (1), 116–125. doi:10.1002/stem.1504

Zhu, L., Zhao, Q., Yang, T., Ding, W., and Zhao, Y. (2015). Cellular Metabolism and Macrophage Functional Polarization. *Int. Rev. Immunol.* 34 (1), 82–100. doi:10.3109/08830185.2014.969421

Zhuang, X., Xiang, X., Grizzle, W., Sun, D., Zhang, S., Axtell, R. C., et al. (2011). Treatment of Brain Inflammatory Diseases by Delivering Exosome Encapsulated Anti-inflammatory Drugs from the Nasal Region to the Brain. *Mol. Ther.* 19 (10), 1769–1779. doi:10.1038/mt.2011.164

Conflict of Interest: The authors declare that the research was conducted in the absence of any commercial or financial relationships that could be construed as a potential conflict of interest.

frontiers in Pharmacology

MINI REVIEW
published: 14 July 2021
doi: 10.3389/fphar.2021.706908

GLP-1 Receptor: A New Target for Sepsis

Fuxun Yang†, Fan Zeng†, Xiaoxiu Luo, Yu Lei, Jiajia Li, Sen Lu, Xiaobo Huang, Yunping Lan and Rongan Liu**

Department of ICU, Sichuan Provincial People's Hospital, University of Electronic Science and Technology of China, Chengdu, China

Patients with sepsis often exhibit hyperglycemia, which increases mortality. glucagon-like peptide-1 receptor agonists (GLP-1RAs) not only regulate blood glucose homeostasis but also improve organ dysfunction, regulate immunity, and control inflammation and other functions in patients with sepsis. Here, we review the possible application of GLP-1RAs in sepsis, to provide a new perspective for the clinical diagnosis and treatment of patients with sepsis complicated with stress hyperglycemia.

Keywords: GLP-1 receptor, sepsis, hyperglycemia, GLP-1 receptor agonist, insulin

OPEN ACCESS

Edited by:
Hong Zhou,
Zunyi Medical University, China

Reviewed by:
Weiying Zhou,
Chongqing Medical University, China
Xin Liu,
Third Military Medical University, China

****Correspondence:***
Yunping Lan
lanyunping929@163.com
Rongan Liu
frog007_119@qq.com

†These authors have contributed equally to this work

Specialty section:
This article was submitted to Translational Pharmacology, a section of the journal Frontiers in Pharmacology

Received: *08 May 2021*
Accepted: *29 June 2021*
Published: *14 July 2021*

Citation:
Yang F, Zeng F, Luo X, Lei Y, Li J, Lu S, Huang X, Lan Y and Liu R (2021) GLP-1 Receptor: A New Target for Sepsis. Front. Pharmacol. 12:706908. doi: 10.3389/fphar.2021.706908

INTRODUCTION

Sepsis is a dysfunctional response to infection that leads to life-threatening organ dysfunction (Seymour et al., 2016; Singer et al., 2016) with a mortality rate of more than 10%, of which 40% is due to septic shock (Seymour et al., 2016; Singer et al., 2016). Sepsis is often accompanied by stress hyperglycemia, which damages the immune response of the host, increases the risk of organ damage, and affects the prognosis of patients (Leonidou et al., 2007). A large number of studies on stress hyperglycemia (Sapolsky et al., 2000; Hunt and Ivy 2002; Jennifer et al., 2007; Saberi et al., 2008; Borst 2015; Rague. 2017) showed that stress hyperglycemia caused due to various reasons occurs through the whole pathophysiological process of sepsis, especially at the septic shock stage. Insulin is a commonly used drug to treat hyperglycemia, but excessive use of insulin could lead to frequent hypoglycemia and greatly increase the mortality of patients with sepsis (Ali et al., 2008). Therefore, the accurate regulation of the blood glucose level of the patients with sepsis is an urgent problem for clinicians.

Glucagon-like peptide-1 (GLP-1) receptor agonists (GLP-1RAs) are one of the new drugs used in the treatment of diabetes. The GLP-1 receptor is a member of the glucagon receptor family of G protein-coupled receptors (Mayo et al., 2003). The receptor protein consists of 463 amino acids. The receptor protein is glycosylated. Glycosylation can regulate the function of the receptor. GLP1R consists of two domains as follows: an extracellular domain, which binds to the C-terminal helix of GLP-1, and a transmembrane domain, which binds to the N-terminal region of GLP-1 (Mayo et al., 2003). Different domains in the third intracellular loop of the GLP-1 receptor are responsible for specific G protein coupling (Gαs, Gαi, and Gαo) (Hällbrink et al., 2001). In addition to the pancreatic tissue, the central nervous system, cardiovascular system, gastrointestinal tract, lung, kidney, thyroid, skin, and mesenchymal stem cells also express GLP-1 receptors (Wei and Mojsov 1995). GLP-1 receptors are activated by mimicking the endogenous GLP-1 to enhance insulin secretion and inhibit glucagon secretion in a glucose-dependent manner, as well as delay gastric emptying and reduce food intake through the suppression of appetite, thereby reducing blood sugar.

With recent studies, researchers have found that GLP-1RA has many functions in addition to regulating blood glucose homeostasis, such as improving organ dysfunction, regulating immunity, and controlling inflammatory response in patients with sepsis. However, the research and

application of GLP-1RA in sepsis is limited, and the mechanism of action is still unclear. This paper intends to review its application in sepsis, to provide a new idea for the clinical diagnosis and treatment of patients with sepsis complicated with stress hyperglycemia.

MECHANISM OF ACTION OF GLP-1RAS

Enteroglycin is released primarily in response to enteral nutrition and promotes insulin secretion from pancreatic β cells in a glucose-dependent manner; for instance, through glucose-dependent insulin-stimulating peptide (GIP) and GLP-1. GIP is secreted by enteral endocrine cells (K cells), which are mainly located in the proximal small intestine and release GIP after enteral nutrition (including carbohydrates and fatty acids) (Campbell and Drucker 2013). GLP-1 is a member of a family of naturally occurring hormones, released after meals by the L cells in the small intestine (mainly composed of jejunum, ileum, and colon at the end of the lang Abraham's cells secrete) and by the pancreas, which possesses a particular GLP-1 receptor, GLP-1R. GLP-1R stimulates adenylate cyclase and increases the level of cyclic AMP (cAMP) through Gαs (Drucker et al., 1987). It then stimulates protein kinase A (PKA)-dependent intracellular signaling, and cAMP-regulated guanine nucleotide exchange factor II (cAMP-GEFII, Epac2) directly activates the exchange protein. With the activation of the above signaling cascade, GLP-1 activates T cell nuclear factor. Insulin release and genetic changes are ultimately triggered through PKA- and calcineurin (CaN)-dependent pathways in pancreatic β cells (Lawrence et al., 2002; Holst 2007; Smith et al., 2019). GLP-1 inhibits ATP-regulated potassium channels through PKA and EPAC (cAMP-dependent mechanisms) (Holz 2004), leading to increased calcium influx, thereby increasing calcium-induced insulin secretion by stimulating glucose-dependent insulin release (Lee. 2014). In humans, GLP-1 has two bioactive forms, the 31-amino acid GLP-1 (7–37) and the 30-amino acid GLP-1 (7–36), with a difference of only one amino acid residue. Approximately 80% of the cyclic activity of GLP-1 comes from the GLP-1 (7–36) peptide (Talchai et al., 2012). The hypoglycemic effect of GLP-1 is glucose dependent. As an enterogenous hormone, GLP-1 can only exert its hypoglycemic effect when nutrients, especially carbohydrates, cause the blood glucose level to rise; however, it does not further reduce blood glucose when the blood glucose level is normal.

The new class of GLP-1RAs includes short-acting GLP-1 analogs, such as exenatid, and long-acting GLP-1 analogs, such as abirutide and liraglutide. There are several main mechanisms of glucose control. For instance, one mechanism involves promoting the production and secretion of GLP-1RAs, which significantly enhances glucose-induced insulin secretion by their interaction with specific receptors on pancreatic beta cells, which then simultaneously activates sensitive nerves and glucose receptors on beta cells to exert hypoglycemic effects (Ahrén 2004). The effects of GLP-1RAs are concentration-dependent. GLP-1RAs do not induce insulin secretion when the blood glucose concentration is less than 3.6 mmol/L. Therefore, they do not cause severe hypoglycemia. Another mechanism is the inhibition of glucagon secretion, where GLP-1RAs act on islet α cells and inhibit the release of glucagon (Ahrén 2004). They also act on pancreatic islet δ cells to promote the secretion of somatostatin, which can act as parastrin to inhibit glucagon. The third mechanism entails the protection of islet β cells through the stimulation of their proliferation and differentiation as well as the promotion of their regeneration and repair (Flamez et al., 1998). β cells are protected by maintaining β cell morphology and inhibiting the expression of pre-apoptotic genes. The fourth mechanism is activated when GLP-1RAs reduce the concentration of free fatty acids and liver glucose production, thereby reducing insulin resistance (Mette et al., 2002). The final mechanism is slowing gastric emptying, inhibiting the inappropriate release of postprandial glucagon, and possibly inhibiting the appetite control center of the brain (Schirra et al., 2006) CLP-1 analogs are currently used for patients with type 2 diabetes (T2DM), as well as for patients with obesity. In 2018, the American Diabetes Association/European Association for the Study of Diabetes new consensus recommended GLP-1RAs as the first choice for glucose-lowering therapy in T2DM patients with ASCVD (Davies et al., 2018).

In the event of acute infection, the pro-inflammatory factor IL-6 can induce the secretion of GLP-1 to optimize the level of blood sugar (Kahles et al., 2014). In a mouse model of acute kidney injury caused by sepsis, the expression of GLP-1R in the renal tubules increases in the early stage of sepsis, and the endogenous GLP-1 regulation reduces kidney injury (Choi et al., 2019). In addition, dipeptidyl peptidase 4 (DPP-4), a drug that inhibits the degradation of GLP-1, reduces kidney damage through antiapoptotic, immunological, and antioxidative changes (Glorie et al., 2012). After LPS-induced sepsis in rats with *DPP-4* knockout, the administration of GLP-1 RAs can increase cardiac cAMP levels, improve cardiovascular function in animals with endotoxemia, and improve the prognosis of endotoxemia (Ku et al., 2010).

EFFECT OF GLP-1RAS ON BLOOD GLUCOSE IN PATIENTS WITH SEPSIS

L-cells that secrete GLP-1 are a type of multifunctional endocrine cells that only exist in the intestinal mucosal epithelium. GLP-1 is mainly secreted upon stimulation by intestinal nutrients, but recent studies have found that inflammation can also stimulate the secretion of incretin (Kahles et al., 2014) (**Figure 1**). As the only carrier of L-cells, the intestine is one of the most important targets of organ function in sepsis. The gastrointestinal tract of patients with sepsis is often the first organ affected, which often manifests as gastrointestinal intolerance. Patients in the acute stage of the disease are often in a state of fasting due to unstable hemodynamics, and the decreased secretion of endogenous intestinal glucagon hormone is an important factor leading to the fluctuation of blood glucose levels in patients with sepsis. GLP-1 expression in patients in the early stage of sepsis can quickly increase to more than twice that in healthy people, reaching as high as 9.5 times higher in patients with severe

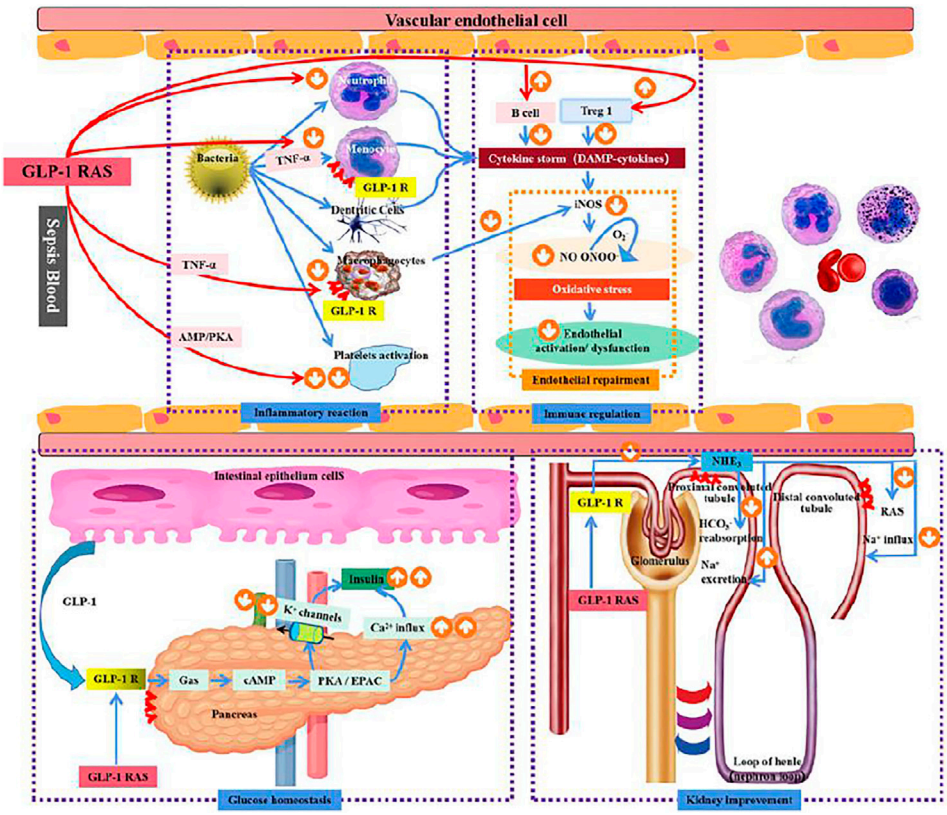

FIGURE 1 | Mechanism of GLP-1R in sepsis.

sepsis. This may be a feedback protection mechanism when the body suffers severe damage (Perl et al., 2018). To resist the inflammatory reaction, as the disease progresses, the GLP-1 system is inhibited, causing hyperglycemia. Most patients with sepsis have stress hyperglycemia, which reduces the ability to resist pathogen invasion (Jafar et al., 2016). Acute hypoglycemia increases oxidative stress, platelet aggregation, production of pro-inflammatory cytokines, and the expression of vascular adhesion molecules (Gogitidze Joy et al., 2010; Wright et al., 2010). If blood glucose is unstable in patients with sepsis, nosocomial mortality is remarkably increased (Leonidou et al., 2007). Furthermore, in patients with sepsis, increased glucagon levels caused by a decreased endogenous secretion of intestinal glucagon have been associated with disease severity and poor prognosis (Jung and Park. 2015; Perl et al., 2018). In animal models of sepsis, intestinal glucose can induce the decrease of intestinal glucose levels and blood sugar, and GIP promotes insulin secretion, reduces glucagon secretion, increases insulin secretion, weakens the systemic inflammatory response, and improves hemodynamics (Shah et al., 2017). Results of previous studies suggest that sepsis at a steady state depends on endogenous glucose and blood sugar levels, as well as hormonal regulation. Patients with stress hyperglycemia caused by sepsis may benefit from the exogenous supplementation of GLP-1RAs to optimize blood glucose control while reducing blood glucose variation rate, and the protective effect of GLP-1RAs on multiple organ functions may improve the prognosis of sepsis.

The effect of GLP-1Ras on sepsis: 1) The effect of blood glucose homeostasis: The endogenous GLP-1 and exogenous GLP-1Ras secreted in the small intestine bind to GLP-1R on the surface of the pancreas, stimulate Ca2+ influx and reduce K+ outflow through cAMP activation of PKA/EPAC signaling pathway, promote insulin secretion, and regulate blood glucose homeostasis 2) Inflammation response: GLP-1R is expressed in macrophages and monocytes, and can inhibit the release of inflammatory factors through TNF-α, AMP/PKA and other pathways to reduce systemic inflammatory response. Meanwhile, macrophages can inhibit the release of iNOS to improve vascular endothelial cell dysfunction. GLP-1 RAS can also reduce platelet activation through the AMP/PKA pathway and reduce microthrombosis in sepsis patients. 3) Immune function: GLP-1R is expressed in B lymphocytes and T lymphocytes. The activation of GLP-1R can promote the proliferation of B lymphocytes and T lymphocytes, especially the expression of Treg1, to inhibit systemic inflammatory response in sepsis patients. 4) Effects of GLP-IR activation on endothelial cells: GLP-IR activation can reduce oxidative stress of endothelial cells by reducing iNOS secretion, thereby improving endothelial cell dysfunction; 5) Renal effects: the expression of GLP-1 receptor in renal tubules, GLP-1 RAS can prevent inflammation and septicaemic induced AKI by blocking the

sodium-hydrogen exchanger (NHE3), enhance the excretion of sodium in renal tubules, and reduce RAS activation; Thus play the role of kidney protection.

EFFECT OF GLP-1RAS ON ORGAN FUNCTION

GLP-1RAs are relatively safe for controlling blood glucose. Current studies suggest that the GLP-1R is distributed in all organs, mainly located on the β cells in the pancreas. In kidneys and lungs, GLP-1R is expressed in the smooth muscle cells of the arteries and arterioles. In the heart, GLP-1R is located on the muscle cells of the sinoatrial node. In the gastrointestinal tract, the expression of GLP-1R in Bruner's gland of the duodenum has been detected (pyke et al., 2014). A large number of studies have shown that GLP-1RAs have protective effects on multiple organs. In one study of patients with cardiovascular disease, treatment with a GLP-1 analog (liraglutid) resulted in significantly lower rates of non-fatal myocardial infarction, non-fatal stroke, and hospitalization for heart failure, compared with the placebo groups (Marso et al., 2016). Many GLP-1 analogs have been shown to reduce the incidence and progression of diabetic nephropathy compared with the results obtained with the conventional therapy for patients with T2DM(Orsted et al., 2017). In a mouse model of ischemic stroke, GLP-1RA treatment was shown to exert neuroprotective effects and prevent memory impairment (Teramoto et al., 2011). Since GLP-1 receptors are distributed in the pancreas, kidneys, lungs, heart, gastrointestinal tract, and other organs (Pyke et al., 2014), an increasing number of studies have focused on the effect of GLP-1RAs on organ function, and the results have confirmed the protective effect of GLP-1RAs on the heart (Marso et al., 2016), kidneys (Orsted et al., 2017) and the nervous system (Teramoto et al., 2011). In comatose out-of-hospital cardiac arrest patients with elevated blood glucose levels, GLP-1 analogs can reduce blood glucose and improve lactic acid clearance, possibly improving neurological prognosis through its effect on glycolysis and hemodynamics (Wiberg et al., 2017). In animal experiments, GLP-1 has been shown to improve the metabolic efficiency of myocardial glucose, reduce systemic and pulmonary vascular resistance, and activate the ischemic preconditioning pathway (Aravindhan et al., 2015) GLP-1-mediated positive effects on cardiac function have been observed in clinical studies, and the application of a GLP-1 analog in patients with ischemic injury resulted in improved left ventricular function and reduced infarct size (Lazaros. 2004). In the LEADER trial, patients with diabetes treated with liraglutide had a lower incidence of major adverse cardiovascular events, including cardiovascular death, compared to the placebo group (Marso et al., 2016). With the increasing understanding of the roles and functions of GLP-1RAs, some scientists have begun to pay attention to the effect of GLP-1RAs on the organs in the pathological process of sepsis. GLP-1, a marker of early intestinal mucosal injury, was significantly increased after LPS injection in a mouse model of intestinal injury induced by lipopolysaccharide (IPOLPS) (Lebrun et al., 2017). There are a large number of bacteria in the intestinal tract, and when the intestinal mucosal barrier is damaged, LPS produced by bacteria can enter the blood circulation, leading to an increase in GLP-1 levels, which can improve mucosal integrity and reduce local and systemic inflammation (Lebrun et al., 2017). Exogenous GLP-1 can protect the intestinal tract from oxidative damage, regulate intestinal homeostasis through local effects, and restore intestinal integrity (Deniz et al., 2015). In a rat model of acute kidney injury in early sepsis, Glp-1 receptor expression in renal tubules increased, and the induction of Glp-1 receptor expression prevented inflammation and sepsis-induced AKI (Choi et al., 2019), a Glp-1 analog, by blocking sodium hydrogen exchanger, enhancing renal tubular sodium (Girardi et al., 2008), and reducing the activity of angiotensin (Jeppe et al., 2013); thus, playing a role in kidney protection. Also, the systemic inflammatory reaction caused by sepsis may lead to multiple organ function impairment in patients. Whether GLP-1RAs can benefit such patients warrants further clinical confirmation.

EFFECT OF GLP-1RAS ON INFLAMMATORY RESPONSE INDUCED BY SEPSIS

In an observational study of patients with sepsis, it was found that endogenous GLP-1 was activated during sepsis, and GLP-1 levels were significantly elevated in patients with sepsis who died early (2–4 days post-admission) (Perl et al., 2018). Scott Brakenridge et al. found that increased GLP-1 levels within 24 h of sepsis are closely associated with early death, and in survivors, a sustained increase in GLP-1 levels after 14 days was also associated with severe dysfunction after 6 months, and the changes were associated with IL-6 secretion (Brakenridge et al., 2019). GLP-1RAs inhibit TNFα-induced activation of NF-κB and decrease the expression of adhesion molecules, including VCAM-1, ICAM-1, and E-selectin (Hattori et al., 2010). In animal models and *in vitro* experiments of sepsis, GLP-1 analogs inhibited TNFα and LPS-induced monocyte adhesion, thereby reducing vascular endothelial injury (Krasner et al., 2014). Inhibition of the NF-κB pathway and the secretion of inflammatory cytokines in macrophages improve inflammatory macrophage-derived insulin resistance (Guo et al., 2016), while the inhibition of LPS-induced inflammatory pathways and iNOS expression, and the decrease in AMPK activation improve vascular dysfunction and alleviate oxidative stress in endotoxemia rats (Steven et al., 2015). The GLP-1 receptor is expressed on eosinophils and neutrophils, and GLP-1RAs can reduce the expression of eosinophil surface activation markers after LPS stimulation, and reduce the production of IL-4, IL-8, and IL-13, thereby reducing the inflammatory response (Mitchell et al., 2017). Activation of the GLP-1 receptor reduces the expression of LPS-induced pro-inflammatory cytokines, including IL-1β, IL-6, TNF-α, and IFN-γ, *in vivo* and *in vitro* (Ofer et al., 2015; Young-Sun and Hee-Sook 2016). GLP-1RA activates the GLP-1 receptor in platelets, through an cyclic adenosine monophosphate/protein kinase (AMP/PKA)-dependent mechanism to prevent systemic inflammation, vascular dysfunction, and end-organ damage,

thereby significantly reducing the microvascular thrombosis induced by endotoxin blood disease and mortality (Steven et al., 2016) (Tests on human vascular endothelial cells exposed to LPS have demonstrated that GLP-1 analogs reduce vascular permeability and lower the levels of pro-inflammatory cytokines (Wonhwa et al., 2016).

EFFECT OF GLP-1RAS ON IMMUNE RESPONSE INDUCED BY SEPSIS

GLP-1R is expressed in macrophages, monocytes, B cells, and T cell lymphocytes. The lack of GLP-1R signal will impair the ability of mouse lymphocytes to divide and proliferate. GLP-1R activation causes increased cAMP levels, which activates and regulates Treg function and promotes peripheral T cell proliferation (Hadjiyanni et al., 2010). Treg cells have obvious anti-inflammatory effects, and can secrete anti-inflammatory cytokines, such as IL-4, IL-10, and TGF-β, to inhibit auto-inflammatory response and prevent pathological immune responses that cause tissue destruction. (Sakaguchi 2004). After activation, GLP-1R can inhibit the release of pro-inflammatory cytokines IL-2, IL-17A, interferon gamma, and tumor necrosis factor alpha triggered by anti-CD3 and -CD28 antibodies produced by intestinal intraepithelial lymphocytes (Yusta et al., 2015). The results of studies on sepsis-related cells and animal models suggested that GLP-1RAs activate the cAMP/PKA pathway to reduce the expression of iNOS in Raw264.7 macrophages induced by LPS (Chang et al., 2013). GLP-1RAs inhibit the activation of leukocytes and the differentiation of antigen-presenting cells, thereby reducing the adhesion and infiltration of activated leukocytes on the vascular endothelium, and reducing endothelial cell damage (Steven et al., 2015). GLP-1 RAs inhibit platelet activation through the cAMP/PKA pathway, reduce endotoxemia-induced microvascular thrombosis, and reduce the occurrence of diffuse intravascular coagulation, thereby preventing systemic inflammation, improving vascular dysfunction, reducing organ injure, and improving the outcome of patients with sepsis (Steven et al., 2017). GLP-1 receptor is also expressed in CD14-positive monocytes of healthy people (Arakawa et al., 2010). In endotoxemia, after LPS binds to CD14 on the surface of monocytes and phagocytoses, the TLR-4/CD14 complex is cleaved into sCD14 (the water-soluble form of CD14). The increase in the level of circulating sCD14 is associated with the high fatality rate of septic shock caused by Gram-negative bacteria (Landmann et al., 1995). In sepsis caused by Gram-negative bacteria, it was found that the GLP-1 system is over-activated. On the one hand, its over-activity is related to increased sCD14 levels, which activates the innate immune response to resist the invasion of pathogenic microorganisms. On the other hand, it may reduce excessive inflammation to prevent immune system disorders and the adverse consequences of sepsis (Bloch et al., 2021).

Due to the complex etiology of sepsis, the need to balance infection and inflammation in the treatment process, and the abnormal fluctuation of blood glucose due to endocrine abnormalities during the course of the disease, maintaining "reasonable" blood glucose in sepsis patients is still a challenge. Current studies suggest that hyperglycemia is associated with a variety of poor clinical outcomes, and critically ill patients with hyperglycemia have a higher mortality rate than patients with normal blood glucose (Krinsley. 2003). However, the incidence of hypoglycemia is also significantly increased in patients using insulin, and previous studies have shown that hypoglycemia is an independent predictor of hospitalization and one-year mortality in critically ill patients (Krinsley et al., 2007; Waeschle et al., 2008; Park et al., 2012). Selection in critically ill patients can effectively control blood glucose without increasing the risk of hypoglycemia, which is of great significance for improving the prognosis of patients with sepsis. GLP-1 analogs can regulate immune response and the release of inflammatory factors in severely ill patients, especially in patients with sepsis, and exert organ protection effects, which may benefit patients. However, there is still a lack of large-scale high-quality clinical studies, and ascertaining the clinical safety and effectiveness of GLP-1RA treatment warrants further study.

AUTHOR CONTRIBUTIONS

FY and FZ: Writing–original draft, XL, XH, JL, YL, and SL: Validation, XH: RL and YL review and editing.

FUNDING

This study was supported by the Sichuan Province Science and Technology Support Program (grant number 2017SZ0138).

REFERENCES

Ahrén, B. (2004). Sensory Nerves Contribute to Insulin Secretion by Glucagon-like Peptide-1 in Mice. *Am. J. Physiology-Regulatory, Integr. Comp. Physiol.* 286, R269–R272. doi:10.1152/ajpregu.00423.2003

Ali, N. A., O'Brien, J. M., Dungan, K., Phillips, G., Marsh, C. B., Lemeshow, S., et al. (2008). Glucose Variability and Mortality in Patients with Sepsis*. 'Glucose Variability and Mortality in Patients with Sepsis'. *Crit. Care Med.* 36, 2316–2321. doi:10.1097/ccm.0b013e3181810378

Arakawa, M., Mita, T., Azuma, K., Ebato, C., Goto, H., Nomiyama, T., et al. (2010). Inhibition of Monocyte Adhesion to Endothelial Cells and Attenuation of Atherosclerotic Lesion by a Glucagon-like Peptide-1 Receptor Agonist, Exendin-4. *Diabetes* 59, 1030–1037. doi:10.2337/db09-1694

Aravindhan, K., Bao, W., Harpel, M. R., Willette, R. N., and Beat, M. J. (2015). 'Cardioprotection Resulting from Glucagon-like Peptide-1 Administration Involves Shifting Metabolic Substrate Utilization to Increase Energy Efficiency in the Rat Heart. *Plos One* 10, e0130894. doi:10.1371/journal.pone.0130894

Bloch, O., Perl, S. H., Lazarovitch, T., Zelnik-Yovel, D., Love, I., Mendel-Cohen, L., et al. (2021). Hyper-Activation of Endogenous GLP-1 System to Gram-Negative Sepsis Is Associated with Early Innate Immune Response and Modulated by Diabetes. *Shock* 55, 796–805. doi:10.1097/SHK.0000000000001683

Borst, S. E. (2015). The Role of TNF-Alpha in Insulin Resistance. *Endocrine* 23, 177. doi:10.1385/ENDO:23:2-3:177

Brakenridge, S. C., Moore, F. A., Mercier, N. R., Cox, M., Wu, Q., Moldawer, L. L., et al. (2019). Persistently Elevated Glucagon-like Peptide-1 Levels Among Critically Ill Surgical Patients after Sepsis and Development of Chronic Critical Illness and Dismal Long-Term Outcomes. *J. Am. Coll. Surgeons* 229, 58–67. doi:10.1016/j.jamcollsurg.2019.04.014

Campbell, J. E., and Drucker, D. J. (2013). Pharmacology, Physiology, and Mechanisms of Incretin Hormone Action. *Cel Metab.* 17, 819–837. doi:10.1016/j.cmet.2013.04.008

Chang, S. Y., Kim, D.-B., Ryu, G. R., Ko, S. H., Jeong, I. K., Ahn, Y. B., et al. (2013). Exendin-4 Inhibits iNOS Expression at the Protein Level in LPS-Stimulated Raw264.7 Macrophage by the Activation of cAMP/PKA Pathway. *J. Cel. Biochem.* 114, 844–853. doi:10.1002/jcb.24425

Choi, J. H., Kim, S. J., Kwon, S. K., Kim, H. Y., and Jeon, H. (2019). Renal Tubular Glucagon-like Peptide-1 Receptor Expression Is Increased in Early Sepsis but Reduced in Chronic Kidney Disease and Sepsis-Induced Kidney Injury. *Int. J. Mol. Sci.* 20, 6024. doi:10.3390/ijms20236024

Davies, M. J., D'Alessio, D. A., Fradkin, J., Kernan, W. N., Mathieu, C., Mingrone, G., et al. (2018). Management of Hyperglycemia in Type 2 Diabetes, 2018. A Consensus Report by the American Diabetes Association (ADA) and the European Association for the Study of Diabetes (EASD). *Dia Care* 41, 2669–2701. doi:10.2337/dci18-0033

Deniz, M., Atasoy, B. M., Dane, F., Can, G., Erzik, C., Çetinel, Ş., et al. (2015). Radiation-induced Oxidative Injury of the Ileum and colon Is Alleviated by Glucagon-like Peptide-1 and -2. *J. Radiat. Res. Appl. Sci.* 8, 234–242. doi:10.1016/j.jrras.2015.01.010

Drucker, D. J., Philippe, J., Mojsov, S., Chick, W. L., and Habener, J. F. (1987). Glucagon-like Peptide I Stimulates Insulin Gene Expression and Increases Cyclic AMP Levels in a Rat Islet Cell Line. *Proc. Natl. Acad. Sci.* 84, 3434–3438. doi:10.1073/pnas.84.10.3434

Flamez, D., Van Breusegem, A., Scrocchi, L. A., Quartier, E., Pipeleers, D., Drucker, D. J., et al. (1998). Mouse Pancreatic Beta-Cells Exhibit Preserved Glucose Competence after Disruption of the Glucagon-like Peptide-1 Receptor Gene. *Diabetes* 47, 646–652. doi:10.2337/diabetes.47.4.646

Girardi, A. C. C., Fukuda, L. E., Rossoni, L. V., Malnic, G., and Rebouças, N. A. (2008). Dipeptidyl Peptidase IV Inhibition Downregulates Na+-H+exchanger NHE3 in Rat Renal Proximal Tubule. *Am. J. Physiology-Renal Physiol.* 294, F414–F422. doi:10.1152/ajprenal.00174.2007

Glorie, L. L. F., Verhulst, A., Matheeussen, V., Baerts, L., Magielse, J., Hermans, N., et al. (2012). DPP4 Inhibition Improves Functional Outcome after Renal Ischemia-Reperfusion Injury. *Am. J. Physiology-Renal Physiol.* 303, F681–F688. doi:10.1152/ajprenal.00075.2012

Gogitidze Joy, N., Hedrington, M. S., Briscoe, V. J., Tate, D. B., Ertl, A. C., and Davis, S. N. (2010). Effects of Acute Hypoglycemia on Inflammatory and Pro-atherothrombotic Biomarkers in Individuals with Type 1 Diabetes and Healthy Individuals. *Diabetes Care* 33, 1529–1535. doi:10.2337/dc09-0354

Guo, C., Huang, T., Chen, A., Chen, X., Wang, L., Shen, F., et al. (2016). 'Glucagon-like Peptide 1 Improves Insulin Resistance *In Vitro* through Anti-inflammation of Macrophages. *Braz. J. Med. Biol. Res.* 49, e5826. doi:10.1590/1414-431x20165826

Hällbrink, M., Holmqvist, T., Olsson, M., Östenson, C.-G., Efendic, S., and Langel, Ü. (2001). Different Domains in the Third Intracellular Loop of the GLP-1 Receptor Are Responsible for Gαs and Gαi/Gαo Activation. *Biochim. Biophys. Acta (Bba) - Protein Struct. Mol. Enzymol.* 1546, 79–86. doi:10.1016/s0167-4838(00)00270-3

Hadjiyanni, I., Siminovitch, K. A., Danska, J. S., and Drucker, D. J. (2010). Glucagon-like Peptide-1 Receptor Signalling Selectively Regulates Murine Lymphocyte Proliferation and Maintenance of Peripheral Regulatory T Cells. *Diabetologia* 53, 730–740. doi:10.1007/s00125-009-1643-x

Hattori, Y., Jojima, T., Tomizawa, A., Satoh, H., Hattori, S., Kasai, K., et al. (2010). RETRACTED ARTICLE: A Glucagon-like Peptide-1 (GLP-1) Analogue, Liraglutide, Upregulates Nitric Oxide Production and Exerts Anti-inflammatory Action in Endothelial Cells. *Diabetologia* 53, 2256–2263. doi:10.1007/s00125-010-1831-8

Holst, J. J. (2007). The Physiology of Glucagon-like Peptide 1. *Physiol. Rev.* 87, 1409–1439. doi:10.1152/physrev.00034.2006

Holz, G. G. (2004). Epac: A New cAMP-Binding Protein in Support of Glucagon-like Peptide-1 Receptor-Mediated Signal Transduction in the Pancreatic -Cell. *Diabetes* 53, 5–13. doi:10.2337/diabetes.53.1.5

Hunt, D. G., and Ivy., J. L. (2002). Epinephrine Inhibits Insulin-Stimulated Muscle Glucose Transport. *J. Appl. Physiol.* 93, 1638–1643. doi:10.1152/japplphysiol.00445.2002

Jafar, N., Edriss, H., and Nugent, K. (2016). The Effect of Short-Term Hyperglycemia on the Innate Immune System. *Am. J. Med. Sci.* 351, 201–211. doi:10.1016/j.amjms.2015.11.011

Jennifer, J., Thierry, G., Mireille, C., Yannick, L. M. B., and Jean-François, T. (2007). 'Interleukin-1β-Induced Insulin Resistance in Adipocytes through Down-Regulation of Insulin Receptor Substrate-1 Expression'. *Endocrinology* 148 (1), 241–251. doi:10.1210/en.2006-0692

Jeppe, S., Anders, D., Jørgen, F., Juul, H. J., Thomas, J., Søren, R., et al. (2013). 'Glucagon-Like Peptide-1 (GLP-1): Effect on Kidney Hemodynamics and Renin-Angiotensin-Aldosterone System in Healthy Men'. *J. Clin. Endocrinol. Metab.* 98, E664–E71. doi:10.1210/jc.2012-3855

Jung, W. J., Park, B. H., Chung, K. S., Song, Y. K., Park, B. H., Chung, K. S., et al. (2015). Glucagon Levels, Disease Severity, and Outcome in Severe Sepsis. *Shock* 43, 563–568. doi:10.1097/shk.0000000000000344

Kahles, F., Meyer, C., Möllmann, J., Diebold, S., Findeisen, H. M., Lebherz, C., et al. (2014). GLP-1 Secretion Is Increased by Inflammatory Stimuli in an IL-6-Dependent Manner, Leading to Hyperinsulinemia and Blood Glucose Lowering. *Diabetes* 63, 3221–3229. doi:10.2337/db14-0100

Krasner, N. M., Yasuo, I., Ruderman, N. B., Cacicedo, J. M., and Bauer, P. M. (2014). 'Glucagon-Like Peptide-1 (GLP-1) Analog Liraglutide Inhibits Endothelial Cell Inflammation through a Calcium and AMPK Dependent Mechanism'. *Plos One* 9, e97554. doi:10.1371/journal.pone.0097554

Krinsley, J. S., and Grover, A. (2007). Severe Hypoglycemia in Critically Ill Patients: Risk Factors and Outcomes*. *Crit. Care Med.* 35, 2262–2267. doi:10.1097/01.ccm.0000282073.98414.4b

Krinsley, J. S. (2003). Association between Hyperglycemia and Increased Hospital Mortality in a Heterogeneous Population of Critically Ill Patients. *Mayo Clin. Proc.* 78, 1471–1478. doi:10.4065/78.12.1471

Ku, H. C., Chen, W. P., and Su, M. J. (2010). GLP-1 Signaling Preserves Cardiac Function in Endotoxemic Fischer 344 and DPP4-Deficient Rats. *Naunyn-schmied Arch. Pharmacol.* 382, 463–474. doi:10.1007/s00210-010-0559-9

Landmann, R., Zimmerli, W., Sansano, S., Link, S., Hahn, A., Glauser, M. P., et al. (1995). Increased Circulating Soluble Cd14 Is Associated with High Mortality in Gram-Negative Septic Shock. *J. Infect. Dis.* 171, 639–644. doi:10.1093/infdis/171.3.639

Lawrence, M. C., Bhatt, H. S., and Easom, R. A. (2002). NFAT Regulates Insulin Gene Promoter Activity in Response to Synergistic Pathways Induced by Glucose and Glucagon-like Peptide-1. *Diabetes* 51, 691–698. doi:10.2337/diabetes.51.3.691

Lazaros, A. N. (2004). 'Effects of Glucagon-like Peptide-1 in Patients with Acute Myocardial Infarction and Left Ventricular Dysfunction after Successful Reperfusion'. *Circulation* 109 (8), 962–965. doi:10.1161/01.CIR.0000120505.91348.58

Lebrun, L. J., Lenaerts, K., Kiers, D., Pais de BarrosDe Barros, J.-P., Le Guern, N., Plesnik, J., et al. (2017). Enteroendocrine L Cells Sense LPS after Gut Barrier Injury to Enhance GLP-1 Secretion. *Cel Rep.* 21, 1160–1168. doi:10.1016/j.celrep.2017.10.008

Lee, Y. S., and Jun, H. S. (2014). Anti-diabetic Actions of Glucagon-like Peptide-1 on Pancreatic Beta-Cells. *Metabolism* 63, 9–19. doi:10.1016/j.metabol.2013.09.010

Leonidou, L., Mouzaki, A., Michalaki, M., DeLastic, A. L., Kyriazopoulou, V., Bassaris, H. P., et al. (2007). Cytokine Production and Hospital Mortality in Patients with Sepsis-Induced Stress Hyperglycemia. *J. Infect.* 55, 340–346. doi:10.1016/j.jinf.2007.05.177

Marso, S. P., Daniels, G. H., Brown-Frandsen, K., Kristensen, P., Mann, J. F. E., Nauck, M. A., et al. (2016). 'Liraglutide and Cardiovascular Outcomes in Type 2 Diabetes'. *New Engl. J. Med.* 375 (4), 311–322. doi:10.1056/NEJMoa1603827

Mayo, K. E., Miller, L. J., Bataille, D., Dalle, S., Göke, B., Thorens, B., et al. (2003). International Union of Pharmacology. XXXV. The Glucagon Receptor Family. *Pharmacol. Rev.* 55, 167–194. doi:10.1124/pr.55.1.6

Mette, Z., Madsbad, S., and Madsen, J. L. (2002). 'Effect of 6-week Course of Glucagon-like Peptide 1 on Glycaemic Control, Insulin Sensitivity, and β-cell Function in Type 2 Diabetes: a Parallel-Group Study. *Lancet* 359 (9309), 824–830. doi:10.1016/S0140-6736(02)07952-7

Mitchell, P. D., Salter, B. M., Oliveria, J. P., El-Gammal, A., Tworek, D., Smith, S. G., et al. (2017). Glucagon-like Peptide-1 Receptor Expression on Human Eosinophils and its Regulation of Eosinophil Activation. *Clin. Exp. Allergy* 47, 331–338. doi:10.1111/cea.12860

Yanay, O., Bailey, A. L., Kernan, K., Zimmerman, J. J., and Osborne, W. R. (2015). Effects of Exendin-4, a Glucagon like Peptide-1 Receptor Agonist, on Neutrophil Count and Inflammatory Cytokines in a Rat Model of Endotoxemia. *J. Inflamm. Res.* 8, 129–135. doi:10.2147/JIR.S84993

Orsted, D. D., Brown-Frandsen, K., Marso, P. S., Rasmussen, S., and Mann, F. E. J. (2017). 'Liraglutide and Renal Outcomes in Type 2 Diabetes'. *New Engl. J. Med.* 377 (9), 839–848. doi:10.1056/NEJMoa1616011

Park, S., Kim, D. G., Suh, G., Kang, J., Ju, Y. S., Lee, Y. J., et al. (2012). Mild Hypoglycemia Is Independently Associated with Increased Risk of Mortality in Patients with Sepsis: a 3-year Retrospective Observational Study. *Crit. Care* 16, R189. doi:10.1186/cc11674

Perl, S. H., Bloch, O., Zelnic-Yuval, D., Love, I., Mendel-Cohen, L., Flor, H., et al. (2018). 'Sepsis-induced Activation of Endogenous GLP-1 System Is Enhanced in Type 2 Diabetes'. *Diabetes/Metabolism Res. Rev.* 34, e2982. doi:10.1002/dmrr.2982

Pyke, C., Heller, R. S. H., Kirk, R. K., Ørskov, C., Reedtz-Runge, S., Kaastrup, P., et al. (2014). 'GLP-1 Receptor Localization in Monkey and Human Tissue: Novel Distribution Revealed with Extensively Validated Monoclonal Antibody'. *Endocrinology* 155, 1280–1290. doi:10.1210/en.2013-1934

Rague, J. M. (2017). Effect of Hydrocortisone on Development of Shock Among Patients with Severe Sepsis: The HYPRESS Randomized Clinical Trial. *J. Emerg. Med.* 52, 387–388. doi:10.1016/j.jemermed.2017.01.029

Saberi, F., Heyland, D., Lam, M., Rapson, D., and Jeejeebhoy, K. (2008). Prevalence, Incidence, and Clinical Resolution of Insulin Resistance in Critically Ill Patients: An Observational Study. *Jpen J. Parenter. Enteral Nutr.* 32, 227–235. doi:10.1177/0148607108316195

Sakaguchi, S. (2004). 'Naturally Arising CD4+ Regulatory T Cells for Immunologic Self-Tolerance and Negative Control of Immune Responses'. *Annu. Rev. Immunol.* 22, 531–562. doi:10.1146/annurev.immunol.21.120601.141122

Sapolsky, R. M., Romero, L. M., and Munck, A. U. (2000). 'How Do Glucocorticoids Influence Stress Responses? Integrating Permissive, Suppressive, Stimulatory, and Preparative Actions'. *Endocr. Rev.* 21, 55–89. doi:10.1210/edrv.21.1.0389

Schirra, J., Nicolaus, M., Roggel, R., Martin, K., Storr, M., Woerle, H. J., et al. (2006). Endogenous Glucagon-like Peptide 1 Controls Endocrine Pancreatic Secretion and Antro-Pyloro-Duodenal Motility in Humans. *Gut* 55, 243–251. doi:10.1136/gut.2004.059741

Seymour, C. W., Liu, V. X., Iwashyna, T. J., Brunkhorst, F. M., Rea, T. D., Scherag, A., et al. (2016). Assessment of Clinical Criteria for Sepsis. *Jama* 315, 762–774. doi:10.1001/jama.2016.0288

Shah, F. A., Singamsetty, S., Guo, L., Chuan, B. W., Mcdonald, S., Bryce, A., et al. (2017). 'Stimulation of the Endogenous Incretin Glucose-dependent Insulinotropic Peptide by Enteral Dextrose Improves Glucose Homeostasis and Inflammation in Murine Endotoxemia'. *Translational Res.* 193, 1–12. doi:10.1016/j.trsl.2017.11.001

Singer, M., Deutschman, C. S., Seymour, C. W., Shankar-Hari, M., Annane, D., Bauer, M., et al. (2016). The Third International Consensus Definitions for Sepsis and Septic Shock (Sepsis-3). *JAMA* 315, 801–810. doi:10.1001/jama.2016.0287

Smith, N. K., Hackett, T. A., Galli, A., and Flynn, C. R. (2019). GLP-1: Molecular Mechanisms and Outcomes of a Complex Signaling System. *Neurochem. Int.* 128, 94–105. doi:10.1016/j.neuint.2019.04.010

Steven, S., Hausding, M., Kroller-Schon, S., Mader, M., Mikhed, Y., Stamm, P., et al. (2015). 'Gliptin and GLP-1 Analog Treatment Improves Survival and Vascular Inflammation/dysfunction in Animals with Lipopolysaccharide-Induced Endotoxemia'. *Basic Res. Cardiol.* 110, 6. doi:10.1007/s00395-015-0465-x

Steven, S., Jurk, K., Kopp, M., Kr, S., Ller-Sch?, N., Mikhed, Y., et al. (2016). 'Glucagon-like Peptide-1 Receptor Signalling Reduces Microvascular Thrombosis, Nitrosative and Oxidative Stress, Systemic Inflammation and Platelet Activation in Endotoxaemic Mice'. *Br. J. Pharmacol.* 174 (12), 1620–1632. doi:10.1111/bph.13549

Steven, S., Jurk, K., Kopp, M., Kröller-Schön, S., Mikhed, Y., Schwierczek, K., et al. (2017). Glucagon-like Peptide-1 Receptor Signalling Reduces Microvascular Thrombosis, nitro-oxidative Stress and Platelet Activation in Endotoxaemic Mice. *Br. J. Pharmacol.* 174, 1620–1632. doi:10.1111/bph.13549

Talchai, C., Xuan, S., Lin, H. V., Sussel, L., and Accili, D. (2012). Pancreatic β Cell Dedifferentiation as a Mechanism of Diabetic β Cell Failure. *Cell* 150, 1223–1234. doi:10.1016/j.cell.2012.07.029

Teramoto, S., Miyamoto, N., Yatomi, K., Tanaka, Y., Oishi, H., Arai, H., et al. (2011). Exendin-4, a Glucagon-like Peptide-1 Receptor Agonist, Provides Neuroprotection in Mice Transient Focal Cerebral Ischemia. *J. Cereb. Blood Flow Metab.* 31, 1696–1705. doi:10.1038/jcbfm.2011.51

Waeschle, R. M., Moerer, O., Hilgers, R., Herrmann, P., et al. (2008). The Impact of the Severity of Sepsis on the Risk of Hypoglycaemia and Glycaemic Variability. *Crit. Care* 12, R129–R29. doi:10.1186/cc7097

Wei, Y., and Mojsov, S. (1995). Tissue-specific Expression of the Human Receptor for Glucagon-like Peptide-I: Brain, Heart and Pancreatic Forms Have the Same Deduced Amino Acid Sequences. *FEBS Lett.* 358, 219–224. doi:10.1016/0014-5793(94)01430-9

Wiberg, S., Kjaergaard, J., Schmidt, H., Thomsen, J. H., Frydland, M., Winther-Jensen, M., et al. (2017). The Glucagon-like Peptide-1 Analog Exenatide Increases Blood Glucose Clearance, Lactate Clearance, and Heart Rate in Comatose Patients after Out-Of-Hospital Cardiac Arrest. *Crit. Care Med.* 46 (2), e118–e125. doi:10.1097/CCM.0000000000002814

Lee, W., Park, E. J., Kwak, S., Lee, K. C., Na, D. H., Bae, J. S., et al. (2016). Trimeric PEG-Conjugated Exendin-4 for the Treatment of Sepsis. *Biomacromolecules* 17, 1160–1169. doi:10.1021/acs.biomac.5b01756

Wright, R. J., Newby, D. E., Stirling, D., Ludlam, C. A., Macdonald, I. A., and Frier, B. M. (2010). Effects of Acute Insulin-Induced Hypoglycemia on Indices of Inflammation. *Diabetes Care* 33 (7), 1591–1597. doi:10.2337/dc10-0013

Young-Sun, L., and Hee-Sook, J. (2016). Anti-Inflammatory Effects of GLP-1-Based Therapies beyond Glucose Control. *Mediators Inflamm.* 2016, 1–11. doi:10.1155/2016/3094642

Yusta, B., Baggio, L. L., Koehler, J., Holland, D., Cao, X., Pinnell, L. J., et al. (2015). GLP-1R Agonists Modulate Enteric Immune Responses through the Intestinal Intraepithelial Lymphocyte GLP-1R. *Diabetes* 64, 2537–2549. doi:10.2337/db14-1577

Conflict of Interest: The authors declare that the research was conducted in the absence of any commercial or financial relationships that could be construed as a potential conflict of interest.

frontiers in Pharmacology

MINI REVIEW
published: 26 November 2021
doi: 10.3389/fphar.2021.794298

TFEB Dependent Autophagy-Lysosomal Pathway: An Emerging Pharmacological Target in Sepsis

Xin Liu[1†], Xinchuan Zheng[2†], Yongling Lu[1†], Qian Chen[1], Jiang Zheng[1] and Hong Zhou[3]**

[1]Medical Research Center, Southwest Hospital, Army Military Medical University, Chongqing, China, [2]Chongqing Institute of Green and Intelligent Technology, Chinese Academy of Sciences, Chongqing, China, [3]Key Laboratory of Basic Pharmacology of Ministry of Education and Joint International Research Laboratory of Ethnomedicine of Ministry of Education, Zunyi Medical University, Zunyi, China

Sepsis is a life-threatening syndrome induced by aberrant host response towards infection. The autophagy-lysosomal pathway (ALP) plays a fundamental role in maintaining cellular homeostasis and conferring organ protection. However, this pathway is often impaired in sepsis, resulting in dysregulated host response and organ dysfunction. Transcription factor EB (TFEB) is a master modulator of the ALP. TFEB promotes both autophagy and lysosomal biogenesis via transcriptional regulation of target genes bearing the coordinated lysosomal expression and regulation (CLEAR) motif. Recently, increasing evidences have linked TFEB and the TFEB dependent ALP with pathogenetic mechanisms and therapeutic implications in sepsis. Therefore, this review describes the existed knowledge about the mechanisms of TFEB activation in regulating the ALP and the evidences of their protection against sepsis, such as immune modulation and organ protection. In addition, TFEB activators with diversified pharmacological targets are summarized, along with recent advances of their potential therapeutic applications in treating sepsis.

Keywords: sepsis, TFEB, TFEB activators, autophagy-lysosomal pathway, inflammation, immunity

OPEN ACCESS

Edited by:
Salvatore Salomone, University of Catania, Italy

Reviewed by:
Yang Chen, Guangzhou University of Chinese Medicine, China
Bo Pan, Wayne State University, United States

****Correspondence:***
Hong Zhou
zhouh64@163.com
Jiang Zheng
zhengj99219@163.com

[†]These authors have contributed equally to this work

Specialty section:
This article was submitted to Experimental Pharmacology and Drug Discovery, a section of the journal Frontiers in Pharmacology

Received: *13 October 2021*
Accepted: *05 November 2021*
Published: *26 November 2021*

Citation:
Liu X, Zheng X, Lu Y, Chen Q, Zheng J and Zhou H (2021) TFEB Dependent Autophagy-Lysosomal Pathway: An Emerging Pharmacological Target in Sepsis. Front. Pharmacol. 12:794298. doi: 10.3389/fphar.2021.794298

INTRODUCTION

Sepsis is the most common and severe syndrome that can affect a population of critically ill patients (Cecconi et al., 2018). Each year, there are an estimated 48.9 million causes of sepsis globally and 11.0 million sepsis-related deaths (Rudd et al., 2020). The latest definition ("Sepsis-3") defines sepsis as life-threatening organ dysfunction induced by a dysregulated host response to infection (Cecconi et al., 2018). In this regard, the current pathogenic model refers to sepsis arising from infection. This is followed by the release of pathogen-associated molecular patterns (PAMPs) which induce excessive inflammation, aberrant immunity, and abnormalities in the complement and coagulatory systems; ultimately, these processes can lead to organ dysfunction and life-threatening shock (van der Poll et al., 2017; Cecconi et al., 2018). Although the main route of sepsis has been extensively characterized, there are several new paradigms being investigated with regards to the mechanisms that drive the progression of sepsis, including the disruption of cellular homeostasis and the induction of cell injury and organ damage (Cecconi et al., 2018). For example, there is an accumulating body of evidence indicating that the autophagy-lysosomal pathway (ALP),

which plays a fundamental role in cellular homeostasis, antimicrobial immunity and organ protection, is commonly impaired in sepsis, thus resulting in a dysregulated host response and organ dysfunction (Venet and Monneret, 2018; Yin et al., 2019). Previous research has also demonstrated that the restoration or enhancement of autophagy and lysosomal function are highly beneficial and can improve the outcomes of patients with sepsis (Sun et al., 2018; Venet and Monneret, 2018; Ballabio and Bonifacino, 2020). Therefore, the regulation of the ALP may provide us with additional options for the therapeutic intervention of sepsis.

Transcriptional factor EB (TFEB) is a member of the microphthalmia (MiTF/TFE) transcriptional factor family (Irazoqui, 2020). TFEB binds directly to a conserved "GTCACGTGAC" motif, termed as the coordinated lysosomal expression and regulation (CLEAR) element in the promoter regions of targeted genes to upregulate their expression (Pan et al., 2019). Previous work has shown that the CLEAR element is highly enriched in a group of autophagy and lysosomal genes, thereby indicating that TFEB may play a key role in the ALP (Sardiello et al., 2009; Irazoqui, 2020). In addition, emerging evidence has associated TFEB and the TFEB-dependent ALP with pathogenic mechanisms in inflammatory diseases, including sepsis, thus creating the potential for the discovery of new therapeutic options (Jin et al., 2017; Li et al., 2017; Irazoqui, 2020; Ouyang et al., 2021). In this mini-review, we aim to summarize recent advances in the regulatory mechanisms associated with the TFEB- dependent ALP and discuss how the targeting of TFEB may provide us with pharmacological options for the intervention of sepsis.

THE ALP AND SEPSIS

The ALP mainly consists of the autophagy machinery and its associated lysosomal degradation processes (Martini-Stoica et al., 2016). This pathway is evolutionarily conserved in eukaryotic cells and fundamental for the maintenance of cellular homeostasis under stressful conditions (Levine and Kroemer, 2019). Autophagy is characterized by the formation of intracellular double membrane autophagosomes, which deliver cytoplasmic cargo to the lysosomes for degradation (Yu et al., 2018; Levine and Kroemer, 2019). The formation of autophagosome is mediated by a group of core proteins encoded by the autophagy associated genes (ATG). ATG proteins are assembled as kinase complexes at specific stages to control the initiation, formation and elongation of autophagosomes. Then autophagosomes are fused with lysosomes, in which hydrolases and lysosome-associated proteins mediate the degradation of cargo substances (Ballabio and Bonifacino, 2020). Due to its key role in the sequential mechanisms that allow the clearance of cellular debris, the ALP is indispensable for overcoming metabolic insufficiency, organelle damage, and pathogen invasion. Moreover, defects in the ALP pathway are strongly implicated in numerous disease conditions associated with sepsis, including inflammation, organ injury, and aberrant immunity (Deretic, 2021).

It has been extensively demonstrated that the ALP is beneficial for balancing the immune response and protecting organ function during sepsis. A recent review article described autophagy features extensive crosstalk with innate immune cells, thereby exerting influence on phagocytosis in neutrophils, degranulation in mast cells, along with differentiation and migration in NK cells (Germic et al., 2019). Research has also demonstrated that the activation of autophagy in macrophages can confer protection against sepsis by restoring antimicrobial responses against bacterial infection (Lee et al., 2014; Fang F. et al., 2020) or by restricting the production of inflammatory mediators (Xu et al., 2018; Xia et al., 2019). It has been also widely demonstrated that the induction of autophagy alleviates liver damage (Lin et al., 2014), attenuates pulmonary inflammatory impairment (Nikouee et al., 2021), reduces acute kidney injury (Sunahara et al., 2018), protects against neuromuscular dysfunction (Chen G. et al., 2019) and improves cardiac function (Sun et al., 2018) in preclinical models of sepsis. In contrast, the suppression of autophagy during sepsis has been shown to result in accelerated apoptosis in T cells (Oami et al., 2017), the impairment of phagocytic capacity in microglia (Lee et al., 2019), and the aggravation of acute lung or liver injury (Oami et al., 2018; Liu et al., 2021). Similarly, defects in the degradative function of lysosomes is known to amplify sepsis-induced acute lung injury (Mo et al., 2018) and drive septic cardiac dysfunction (Jia et al., 2018). Moreover, disruption of the fusion between lysosomes and autophagosomes can be induced by excessively low doses of LPS, thus leading to persistent low-grade inflammation in macrophages (Baker et al., 2015). It is notable that the ALP is often disrupted during sepsis; this has been shown to worsen outcomes in preclinical models (Chien et al., 2011) and in clinical populations (Huang et al., 2021). Therefore, targeting the ALP may represent a promising strategy for the intervention of sepsis.

TFEB IS A CENTRAL REGULATORY HUB OF THE ALP

It is possible that the induction of initial acute cellular responses by ALP may not involve transcriptional machinery. However, the sustained upregulation of autophagy and lysosomal activity requires modulation by several key transcriptional factors (Levine and Kroemer, 2019). TFEB is a master transcriptional factor of the ALP (Martini-Stoica et al., 2016) and was initially identified as a master regulator of lysosomal biogenesis and degradation (Sardiello et al., 2009). Further studies confirmed that TFEB enhances lysosomal proteostasis of mutated or misfolded proteins (Song et al., 2013), induces a Ca^{2+}-dependent exocytosis in the lysosomes (Medina et al., 2011), mediates the clearance of damaged lysosomes, and controls lysosomal membrane repair (Palmieri et al., 2011). Research has also shown that TFEB is an essential regulator at multiple stages of autophagy. For example, TFEB upregulates the expression of several autophagic genes (e.g., *Becn1*, *Gabarap*, and *Maplc3b*) bearing the CLEAR element (Palmieri et al., 2011)

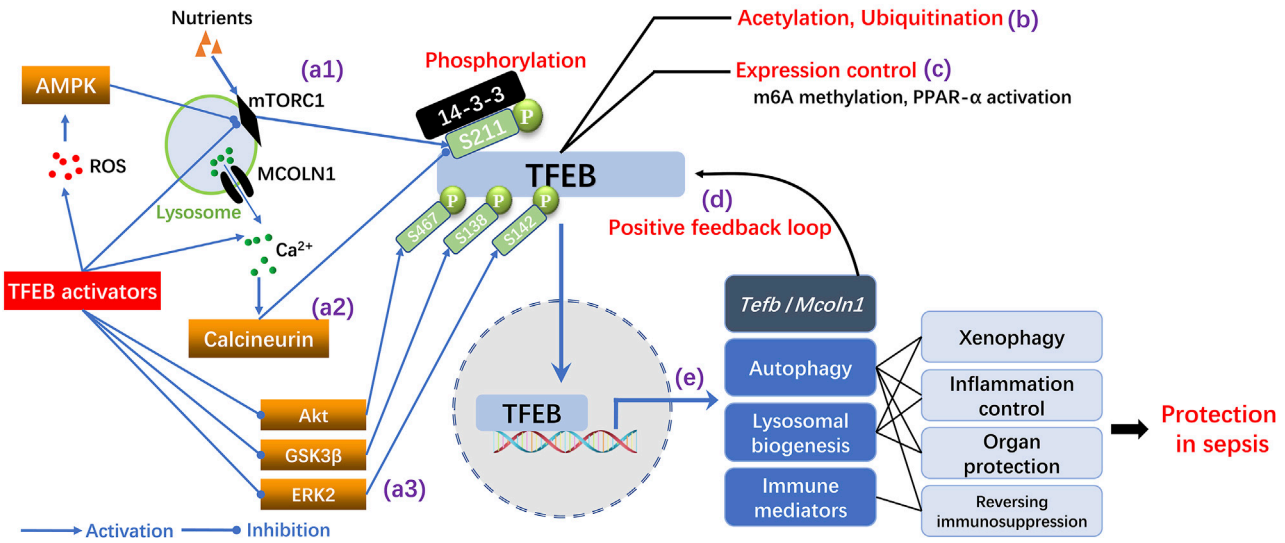

FIGURE 1 | Mechanisms of TFEB activation and the protective roles of TFEB dependent ALP in sepsis. **(A)** Regulation of TFEB activation by phosphorylation. TFEB is inactivated by mTORC1 dependent phosphorylation at S211 while ROS generation and nutrition deprivation inhibit mTORC1 and suppress TFEB phosphorylation (a1). Lysosomal Ca2+ release through the Mcoln-1 channel activate calcineurin and inhibit TFEB phosphorylation (a2). Inhibition of Akt, GSK3β or ERK2 dependent phosphorylation of TFEB promotes TFEB activation (a3) **(B–C)** Modulation of TFEB activation by epigenetic regulation (e.g., acetylation, ubiquitination) or expression control (e.g., m6A methylation, PPAR-α activation). **(D)** Positive feedback regulation of TFEB by transcriptional upregulation of tfeb and mcoln1 by TFEB. **(E)** TFEB upregulates autophagy, promotes lysosomal biogenesis and enhance immunity, thereby conferring protection in sepsis.

while the overexpression of TFEB is known to enhance the biogenesis of autophagosomes in multiple cell lines (Settembre et al., 2011). In addition, TFEB coordinates the fusion of autophagosomes with lysosomes, thereby providing balance in the ALP (Settembre et al., 2011). Collectively, these results suggest that TFEB is a central modulator in the ALP.

The activation of TFEB is mainly regulated by post-translational mechanisms (Zhu et al., 2021) (**Figure 1**). The mechanistic target of rapamycin complex 1 (mTORC1) and calcineurin are two central modulators that function in an opposing manner to connect upstream pathways with the phosphorylation of TFEB and its cytoplasmic/nuclear distribution (Zhu et al., 2021). Activated mTORC1 phosphorylates the Ser/Thr residue (S211) of TFEB; this allows binding to the YWHA/14-three to three protein that restricts TFEB from nuclear translocation (Irazoqui, 2020). In contrast, the activation of calcineurin by mechanisms that increase the cytosolic concentration of Ca^{2+} induces dephosphorylation of the S211 residue in TFEB, thereby releasing TFEB and enabling its nuclear translocation. Subsequently, TFEB upregulates the CLEAR gene network and enhances autophagy and the biogenesis of lysosomes (Irazoqui, 2020). TFEB can also be directly dephosphorylated by protein kinase B (Akt) (S467), glycogen synthase kinase 3β (GSK3β) (S138), and extracellular regulated protein kinase 2 (ERK2) (S142), thus suggesting a complicated regulatory pattern of phosphorylation/dephosphorylation that balances the activation of TFEB (Zhu et al., 2021). In addition to phosphorylation, epigenetic mechanisms may also modulate the activity of TFEB (Zhu et al., 2021). For example, the deacetylation of TFEB enhances its activation in microglia cells (Bao et al., 2016) while ubiquitination degrades phosphorylated TFEB and subsequently enhances activity of the ALP (Sha et al., 2017). In contrast, the modification of TFEB by N6-methyladenosine (m^6A) mRNA has been shown to reduce the expression of TFEB and impair the TFEB-dependent autophagic process (Song HL. et al., 2019). Other research has shown that TFEB is regulated by multiple positive feedback loops. TFEB possesses the CLEAR sequences within its promoter, thus implicating an autoregulatory mechanism (Martini-Stoica et al., 2016). Moreover, TFEB has been shown to upregulate the expression of mucolipin 1 (Mcoln-1), a calcium channel in the lysosomal membrane, to increase calcium efflux from the lysosomes and activate calcineurin; this also suggests the existence of a positive feedback loop (Martini-Stoica et al., 2016).

TFEB AND TFEB DEPENDENT ALP IN SEPSIS

TFEB is an important pharmacological target in neurodegenerative, metabolic and malignant diseases, which was comprehensively summarized by previous literatures (Martini-Stoica et al., 2016; Raben and Puertollano, 2016). Meanwhile, recent studies have increasingly focused on its putative roles in immune modulation and organ protection,

thereby implicating a close relationship with the development and outcomes of sepsis (Irazoqui, 2020; Zhu et al., 2021) (**Figure 1**).

Modulation of the Immune Response

The cellular machinery of autophagy is featured by its ability to eliminate intracellular microbes in a process known as xenophagy (Deretic, 2021). In innate immune cells, TFEB is activated downstream of a phagocytosis event or can be stimulated by lipopolysaccharide (LPS) or interferon (IFN)-γ, thereby enhancing autophagy and lysosomal degradation and promoting the antimicrobial responses against intracellular pathogens (Kumar et al., 2020). It has also been demonstrated the antimicrobial activity is recovered through autophagy activation by overexpression of TFEB in sirtuin-3 KO macrophages (Kim et al., 2019). Of note, the membrane penetrating *Mycobacterium tuberculosis* was shown to repress the expression of *Tfeb* and inhibit autophagy in macrophages to support intracellular replication, implicating an underlying mechanism that disrupts xenophagy in sepsis (Ouimet et al., 2016). This may offer an alternative strategy for eliminating pathogens during sepsis by modulating the activity of TFEB.

The control of inflammation is another prominent effect of TFEB in sepsis. Several recent reviews have highlighted the functions of TFEB in modulating innate immunity and inflammation with wide diversity (Brady et al., 2018; Irazoqui, 2020). TFEB was shown to be rapidly activated in a *Caenorhabditis elegans* model following *Staphylococcus aureus* infection; this process drove the expression of proinflammatory cytokines and chemokines (Visvikis et al., 2014). The activation of TFEB has also been shown to induce M1 macrophage polarization, thus causing transition into a proinflammatory state (Pastore et al., 2016). In contrast, TFEB may exert anti-inflammatory effects indirectly by activating autophagy and lysosomes to suppress the activation of inflammasomes and the excessive production of proinflammatory cytokines (Irazoqui, 2020). TFEB also regulates lipid metabolism and restores homeostasis in the endoplasmic reticulum, thereby controlling the resolution of inflammation (Irazoqui, 2020). Therefore, TFEB may inhibit inflammation in sepsis *via* several different mechanisms.

Immunosuppression is also a well-recognized feature of sepsis and is characterized by monocytes/macrophage tolerance, T cell exhaustion, impaired antigen presentation and increased susceptibility to opportunistic nosocomial infection (Cecconi et al., 2018). Induction of the ALP may reverse these phenotypes (Venet and Monneret, 2018). Although there has been no direct report relating to TFEB and immunosuppression during sepsis, existing studies have demonstrated that TFEB intensifies immune responses by promoting antigen presentation in dendritic cells (Samie and Cresswell, 2015), resetting suppressive tumor-associated macrophages towards the M1 phenotype (Chen et al., 2018), reversing B cell senescence (Zhang et al., 2019), and by enhancing T cell immunity (Jin et al., 2021). Furthermore, the activation of TFEB mediates high levels of glucose-induced interleukin-1β secretion in human monocytic cells (Tseng et al., 2017) and rescues the dysfunctional lysosomal phenotype to improve viability in macrophages upon co-treatment with palmitate and LPS (Schilling et al., 2013). These findings also suggest that TFEB may reverse immunosuppression by restoring cellular response and preventing cell death.

Organ Protection

The TFEB dependent ALP is fundamental for organ protection in sepsis by reducing tissue inflammation, alleviating oxidative stress and controlling metabolic process (Irazoqui, 2020). The overexpression of TFEB increases the autophagy levels in major organs and protects against LPS induce acute lung injury (Liu et al., 2019) or inflammatory liver injury and pancreatitis (Chao et al., 2018; Wang et al., 2019). Moreover, the pharmacological activation of TFEB by extrinsic stimuli or intrinsic signaling molecules is known to protect against septic liver injury, acute kidney injury (Li D. et al., 2021), and cardiac dysfunction (Unuma et al., 2013).

THE PHARMACOLOGICAL APPLICATION OF TFEB ACTIVATORS AS A THERAPEUTIC OPTION FOR SEPSIS

Although the overexpression of TFEB has been investigated in cells and experimental rodents to evaluate its ability to activate the ALP, the pharmacological modulation of TFEB by means of activators is more desirable for therapeutic applications in the short term. For example, recent research has reported that small molecules and biomacromolecules (e.g., microRNAs (miRNA), polysaccharides and peptides) can modulate the ALP by activating TFEB (Xu H. et al., 2020; Chen et al., 2021). These activators have been categorized according to the pharmacological mechanisms by which they regulate TFEB. Here, we summarize recent findings related to the therapeutic implications of some of these molecules and biomacromolecules for sepsis.

TFEB Activators and Their Pharmacological Targets

A variety of small compounds have been demonstrated to either increase the levels of TFEB or promote its activation at the post-translational level. The first target is the expression or synthesis of TFEB, thus leading to increased intracellular levels of TFEB. For example, peroxisome proliferator-activated receptor α (PPAR-α) agonists (e.g., GW7647 and cinnamic acid) and other natural compounds (e.g., genistein, ATRA, GDC-0941, and luteolin) have been shown to upregulate the mRNA expression of TFEB, thereby activating the ALP and enhancing the cellular clearance machinery (Enzenmuller et al., 2013; Moskot et al., 2014; Kim et al., 2017; Chandra et al., 2019; Xu H. et al., 2020; Orfali et al., 2020). Moreover, polyamines (e.g., spermidine) have been shown to activate translation factor eIF5A by inducing its hypusination, thereby promoting the synthesis of TFEB and the upregulation of autophagy in immune cells (Puleston et al., 2019; Zhang et al., 2019). The second target is the regulation of phosphorylation/dephosphorylation and translocation

TABLE 1 | Small-molecular TFEB activators and their pharmacological targets.

Pharmacological targets	Name of compounds	References
TFEB expression	PPARα agonists (e.g., GW7647, cinnamic acid)	Kim et al. (2017), Chandra et al. (2019)
	Other compounds (genistein, ATRA, GDC-0941, luteolin)	Moskot et al. (2014), Orfali et al. (2020), Enzenmuller et al. (2013), Xu et al. (2020a)
TFEB synthesis	Polyamines (e.g., spermidine)	Zhang et al. (2019), Puleston et al. (2019)
TFEB binding	Curcumin and analogues (e.g., curcumin-c1)	Zhang et al. (2016), Song et al. (2016)
mTOR inhibition	Tool mTOR inhibitors (e.g. torin-1, rapamycin)	Xu et al. (2020b), Chen et al. (2021)
	Flavonoids (e.g., quercetin)	Huang et al. (2018)
	Polyphenols (e.g., 3,4-dimethoxychalcone, chlorogenic acid)	Chen et al. (2019b), Gao et al. (2020)
Ca^{2+}/calcineurin modulation	Na^{+}/K^{+}-ATPase inhibitors (e.g., digoxin, Ouabain)	Wang et al. (2017), Song et al. (2019b)
	Other compounds (bedaquiline, liraglutide, carbon monoxide	Kim et al. (2018), Giraud-Gatineau et al. (2020), Fang et al. (2020b)
AMPK/SIRT1 activation	Resveratrol, licochalcone A	Huang et al. (2019), Lv et al. (2019)
Akt activation	Trehalose	Sharma et al. (2021)
ROS generation	Docetaxel, sulforaphane	Zhang et al. (2018), Li et al. (2021b)
TFEB dephosphorylation	Acacetin	Ammanathan et al. (2020)
TFEB nuclear translocation	Naringenin, Apigenin	Jin et al. (2017), Li et al. (2017)

of TFEB in either a direct or indirect manner. For example, curcumin and analogues (e.g., curcumin-C1) are direct modulators that bind to the N terminus of TFEB, weaken TFEB-YWHA interaction, and promote the nuclear translocation of TFEB (Song et al., 2016; Zhang et al., 2016). The translocation of TFEB can be enhanced by the induction of dephosphorylation or the translation of TFEB in a manner that is mediated indirectly by mTOR inhibitors, AMPK/SIRT1 activators, ROS inducers, Akt inhibitors and Ca^{2+}-calcineurin modulators (described in detail in **Table 1**).

In addition to small molecular activators, other larger biomolecules, such as polysaccharides, peptides and miRNAs, can also regulate the activity of TFEB. A few recent studies have reported that polysaccharides (e.g., tea polysaccharide and cyclodextrin) and peptides (e.g., apelin and cell-penetrating peptides) can activate TFEB and enhance the ALP process by inhibiting mTOR activity (Zhou et al., 2021) or promoting TFEB translocation (Song et al., 2014; Jiang et al., 2020; Kondow-Mcconaghy et al., 2020). In contrast, miRNAs are predominantly negative regulators of TFEB expression or its activity to promote autophagy and lysosome biogenesis. For example, a recent review article reported that specific miRNAs, such as the miR-128 and miR-29 families, are predicted to bind to the 3' UTRs of TFEB mRNA, thereby downregulating its expression at the post-transcriptional levels (Cora et al., 2021). Other miRNAs such as miR-30b-5p (Guo et al., 2021) and miR-33 (Ouimet et al., 2016) have also been demonstrated to disrupt TFEB activation and inhibit autophagy by either inhibiting its transcriptional activity or interfering with its nuclear translocation. Therefore, downregulating these inhibitory non-coding RNAs may provide alternative approaches to activating the TFEB dependent ALP.

Therapeutic Implications of TFEB Activators in Sepsis

Given that the impairment of ALP in sepsis results in unresolved infection, inflammation, organ injury, and immunodysfunction, researchers have begun to investigate TFEB modulators in preclinical models to examine their therapeutic efficacy in ameliorating sepsis-induced dysfunction by promoting autophagy and lysosomal functions.

TFEB-dependent xenophagy is critical for antimicrobial defense and is fundamental for the prevention and control of sepsis. TFEB-activating agents, such as trehalose (Sharma et al., 2021), bedaquiline (Giraud-Gatineau et al., 2020), and acacetin (Ammanathan et al., 2020), can upregulate autophagy- and lysosome-associated genes, thus resulting in enhanced bactericidal activity in macrophages or mice infected by intracellular pathogens (e.g., *Mycobacterium tuberculosis* and *Salmonella typhimurium*). It is notable that opportunistic pathogens, such as mycobacterial species, can commonly induce secondary infection in post-sepsis patients or trigger sepsis in patients who are immunocompromised. Moreover, pathogens like *Mycobacterium tuberculosis* inhibit autophagy and lysosomal function by inducing miR-33 dependent inactivation of TFEB (Ouimet et al., 2016). Therefore, TFEB activators may provide additional benefit in these circumstances.

The TFEB-dependent ALP is widely regarded as a critical pathway that can control excessive inflammation and restore immune homeostasis during sepsis. Several recent studies have described pivotal immunomodulatory roles for TFEB activators in sepsis. The activation of TFEB by flavonoid compounds, such as naringenin and apigenin, has been shown to reduce inflammatory cytokines following an LPS challenge by either enhancing the degradation of intracellular cytokines *via* lysosome-dependent mechanisms (Jin et al., 2017) or by enhancing the control of autophagy (Li et al., 2017). Two recent studies reported that polyamines can promote the synthesis of TFEB and induce autophagy; this ability was successfully used to reverse immune senescence in B lymphocytes (Zhang et al., 2019) or to promote macrophage M2 polarization (Puleston et al., 2019). These findings further indicate that TFEB activators may also modulate the status of immune cells in addition to their anti-inflammatory activity *via* a common mechanism to activate the ALP.

TFEB activators have also been demonstrated to confer organ protection in sepsis. For example, licochalcone A, curcumin, and cobalt protoporphyrin, have been shown to alleviate liver injury (Lv et al., 2019), intestinal barrier injury (Cao et al., 2020), and septic insults in the heart (Unuma et al., 2013), induced by LPS challenge; these effects were all related to the ability of these TFEB activators to activate the ALP. Other non-conventional TFEB inducers, such as hydrogen rich saline (Fu et al., 2020) and carbon monoxide (Kim et al., 2018), have been found to confer protection against lipopolysaccharide-induced acute injury or inflammatory liver injury, respectively. Furthermore, the activation of TFEB by mTORC1 inhibitors has been shown to rescue a mouse model from lethal pancreatitis (Wang et al., 2019) and chronic ethanol-induced liver injury (Chao et al., 2018); these effects were closely associated with the onset of sepsis or during sepsis and worsened clinical outcomes.

CONCLUSION AND PERSPECTIVES

A multitude of studies have aimed to explore the therapeutic efficacy of TFEB and the TFEB-dependent ALP pathway in sepsis *via* the pharmacological modulation of TFEB activation. This research has led to encouraging outcomes in preclinical models of sepsis or diseases associated with sepsis, including antimicrobial, anti-inflammatory, and organ protective activities. In addition, lower nuclear levels of TFEB have been detected in patients with alcohol-induced hepatitis or acute pancreatitis. These results further implicate the significance of activating TFEB and the TFEB-dependent ALP in clinical conditions associated with sepsis (Chao et al., 2018; Wang et al., 2019). However, despite these encouraging findings, there are still several concerns that need to be addressed in future research activities.

First, the kinetics and specificity of TFEB in sepsis should be investigated. Both the activity of TFEB and the status of autophagy are altered during the progression of sepsis. Therefore, further investigations are needed to evaluate time-dependent changes in the expression and activity of TFEB in sepsis; these studies are vital if we are to use TFEB activators appropriately for therapeutic intervention. In addition, it is known that the dephosphorylation/phosphorylation balance of TFEB is central for its regulation. Multiple pathways, such as mTORC1 and Ca^{2+}/calcineurin, target the phosphorylating sites on TFEB. However, these mechanisms are identified in different cells. Further research is needed to find the specific upstream regulatory pathways in each cell type and determining their function of modulating TFEB in sepsis (Pan et al., 2017; Pan et al., 2020). Moreover, most existing studies investigated the activation of TFEB by assessing the efficacy of TFEB activators in cell lines or homogenates from a single organ. The entire tissue- and organ-specific profiles of TFEB and the TFEB-dependent ALP in sepsis have yet to be elucidated in detail. In this regard, it is important that we investigate the overall activity of TFEB and the TFEB-dependent ALP in major organs (e.g., liver, lung, spleen, kidney and intestine) or specific cells (e.g., immune cells, hepatocytes and endothelial cells). It is also important to compare the involvement of TFEB and the TFEB-dependent ALP in organ-specific functions (e.g., hepatic metabolic regulation, cardiac and renal protection, and immunomodulation) to determine their influences on the outcomes of sepsis.

Second, the activation of the TFEB-dependent ALP can be triggered by nutritional deficiency, infection, and other stressful conditions, that are commonly observed in sepsis. Thus, future studies need to investigate whether TFEB activators can synergize or counteract with these environmental factors in the regulation of TFEB and the ALP. Prolonged deficiency or dysregulation in sepsis is increasingly regarded as an epigenetic consequence (van der Poll et al., 2017) while post-translational mechanisms may also be key to the activation of TFEB and how the ALP is affected over the long term. Therefore, further studies should focus on the epigenetic regulation of TFEB and identify post-translational mechanisms (e.g., miRNAs, long non-coding RNA (lncRNAs) and new protein modifications) that may exert functional roles during sepsis.

Third, the current safety and efficacy data for TFEB activators are not convincing and require further validation. For example, the efficacy of TFEB activators should be verified in more standardized models of sepsis (e.g., the cecal ligation and puncture model) instead of endotoxemia models or otherwise tested in clinical settings. Moreover, most TFEB activators target the upstream regulators of TFEB, such as mTORC1 and Ca^{2+}/calcineurin; these are also involved in other intracellular events (Song et al., 2021). Therefore, more direct TFEB activators (e.g., curcumin-c1) need to be developed in future studies as these may increase functional specificity and reduce side effects. In addition, we must consider that the activation of the TFEB-dependent ALP may induce tumorigenesis, a disease condition that is frequently concurrent with sepsis (Levine and Kroemer, 2019). Therefore, it is important that we evaluate the relative risks and benefits before the widespread therapeutic application of TFEB activators by investigating their consequences in septic conditions concomitant with tumor.

AUTHOR CONTRIBUTIONS

XL, XZ and YL reviewed literatures, wrote the manuscript and prepared figures and tables. QC reviewed literature and help to prepare figures. JZ and HZ conceived the review article and made substantial revision before submission. All authors contributed to the article and approved the submission.

FUNDING

This work was supported by grants from the National Natural Science Foundation (81873955, 81772137, 81803394).

REFERENCES

Ammanathan, V., Mishra, P., Chavalmane, A. K., Muthusamy, S., Jadhav, V., Siddamadappa, C., et al. (2020). Restriction of Intracellular Salmonella Replication by Restoring TFEB-Mediated Xenophagy. *Autophagy* 16 (9), 1584–1597. doi:10.1080/15548627.2019.1689770

Baker, B., Geng, S., Chen, K., Diao, N., Yuan, R., Xu, X., et al. (2015). Alteration of Lysosome Fusion and Low-Grade Inflammation Mediated by Super-low-dose Endotoxin. *J. Biol. Chem.* 290 (10), 6670–6678. doi:10.1074/jbc.M114.611442

Ballabio, A., and Bonifacino, J. S. (2020). Lysosomes as Dynamic Regulators of Cell and Organismal Homeostasis. *Nat. Rev. Mol. Cel Biol* 21 (2), 101–118. doi:10.1038/s41580-019-0185-4

Bao, J., Zheng, L., Zhang, Q., Li, X., Zhang, X., Li, Z., et al. (2016). Deacetylation of TFEB Promotes Fibrillar Aβ Degradation by Upregulating Lysosomal Biogenesis in Microglia. *Protein Cell* 7 (6), 417–433. doi:10.1007/s13238-016-0269-2

Brady, O. A., Martina, J. A., and Puertollano, R. (2018). Emerging Roles for TFEB in the Immune Response and Inflammation. *Autophagy* 14 (2), 181–189. doi:10.1080/15548627.2017.1313943

Cao, S., Wang, C., Yan, J., Li, X., Wen, J., and Hu, C. (2020). Curcumin Ameliorates Oxidative Stress-Induced Intestinal Barrier Injury and Mitochondrial Damage by Promoting Parkin Dependent Mitophagy through AMPK-TFEB Signal Pathway. *Free Radic. Biol. Med.* 147, 8–22. doi:10.1016/j.freeradbiomed.2019.12.004

Cecconi, M., Evans, L., Levy, M., and Rhodes, A. (2018). Sepsis and Septic Shock. *Lancet* 392 (10141), 75–87. doi:10.1016/S0140-6736(18)30696-2

Chandra, S., Roy, A., Jana, M., and Pahan, K. (2019). Cinnamic Acid Activates PPARα to Stimulate Lysosomal Biogenesis and Lower Amyloid Plaque Pathology in an Alzheimer's Disease Mouse Model. *Neurobiol. Dis.* 124, 379–395. doi:10.1016/j.nbd.2018.12.007

Chao, X., Wang, S., Zhao, K., Li, Y., Williams, J. A., Li, T., et al. (2018). Impaired TFEB-Mediated Lysosome Biogenesis and Autophagy Promote Chronic Ethanol-Induced Liver Injury and Steatosis in Mice. *Gastroenterology* 155 (3), 865–e12. e12. doi:10.1053/j.gastro.2018.05.027

Chen, D., Xie, J., Fiskesund, R., Dong, W., Liang, X., Lv, J., et al. (2018). Chloroquine Modulates Antitumor Immune Response by Resetting Tumor-Associated Macrophages toward M1 Phenotype. *Nat. Commun.* 9 (1), 873. doi:10.1038/s41467-018-03225-9

Chen, G., Xie, W., Nah, J., Sauvat, A., Liu, P., Pietrocola, F., et al. (2019a). 3,4-Dimethoxychalcone Induces Autophagy through Activation of the Transcription Factors TFE3 and TFEB. *EMBO Mol. Med.* 11 (11), e10469. doi:10.15252/emmm.201910469

Chen, J., Min, S., Xie, F., Yang, J., and Wang, X. (2019b). Enhancing Autophagy Protects against Sepsis-Induced Neuromuscular Dysfunction Associated with Qualitative Changes to Acetylcholine Receptors. *Shock* 52 (1), 111–121. doi:10.1097/SHK.0000000000001189

Chen, M., Dai, Y., Liu, S., Fan, Y., Ding, Z., and Li, D. (2021). TFEB Biology and Agonists at a Glance. *Cells* 10 (2), 333. doi:10.3390/cells10020333

Chien, W. S., Chen, Y. H., Chiang, P. C., Hsiao, H. W., Chuang, S. M., Lue, S. I., et al. (2011). Suppression of Autophagy in Rat Liver at Late Stage of Polymicrobial Sepsis. *Shock* 35 (5), 506–511. doi:10.1097/SHK.0b013e31820b2f05

Corà, D., Bussolino, F., and Doronzo, G. (2021). TFEB Signalling-Related MicroRNAs and Autophagy. *Biomolecules* 11 (7), 985. doi:10.3390/biom11070985

Deretic, V. (2021). Autophagy in Inflammation, Infection, and Immunometabolism. *Immunity* 54 (3), 437–453. doi:10.1016/j.immuni.2021.01.018

Enzenmüller, S., Gonzalez, P., Karpel-Massler, G., Debatin, K. M., and Fulda, S. (2013). GDC-0941 Enhances the Lysosomal Compartment via TFEB and Primes Glioblastoma Cells to Lysosomal Membrane Permeabilization and Cell Death. *Cancer Lett.* 329 (1), 27–36. doi:10.1016/j.canlet.2012.09.007

Fang, F., Ge, Q., Li, R., Lv, J., Zhang, Y., Feng, A., et al. (2020a). LPS Restores Protective Immunity in Macrophages against *Mycobacterium tuberculosis* via Autophagy. *Mol. Immunol.* 124, 18–24. doi:10.1016/j.molimm.2020.05.001

Fang, Y., Ji, L., Zhu, C., Xiao, Y., Zhang, J., Lu, J., et al. (2020b). Liraglutide Alleviates Hepatic Steatosis by Activating the TFEB-Regulated Autophagy-Lysosomal Pathway. *Front Cel Dev Biol* 8, 602574. doi:10.3389/fcell.2020.602574

Fu, Z., Zhang, Z., Wu, X., and Zhang, J. (2020). Hydrogen-Rich Saline Inhibits Lipopolysaccharide-Induced Acute Lung Injury and Endothelial Dysfunction by Regulating Autophagy through mTOR/TFEB Signaling Pathway. *Biomed. Res. Int.* 2020, 9121894. doi:10.1155/2020/9121894

Gao, L., Li, X., Meng, S., Ma, T., Wan, L., and Xu, S. (2020). Chlorogenic Acid Alleviates Aβ25-35-Induced Autophagy and Cognitive Impairment via the mTOR/TFEB Signaling Pathway. *Drug Des. Devel Ther.* 14, 1705–1716. doi:10.2147/DDDT.S235969

Germic, N., Frangez, Z., Yousefi, S., and Simon, H. U. (2019). Regulation of the Innate Immune System by Autophagy: Neutrophils, Eosinophils, Mast Cells, NK Cells. *Cell Death Differ* 26 (4), 703–714. doi:10.1038/s41418-019-0295-8

Giraud-Gatineau, A., Coya, J. M., Maure, A., Biton, A., Thomson, M., Bernard, E. M., et al. (2020). The Antibiotic Bedaquiline Activates Host Macrophage Innate Immune Resistance to Bacterial Infection. *eLife* 9, e55692. doi:10.7554/eLife.55692

Guo, H., Pu, M., Tai, Y., Chen, Y., Lu, H., Qiao, J., et al. (2021). Nuclear miR-30b-5p Suppresses TFEB-Mediated Lysosomal Biogenesis and Autophagy. *Cel Death Differ* 28 (1), 320–336. doi:10.1038/s41418-020-0602-4

Huang, J., Wang, X., Zhu, Y., Li, Z., Zhu, Y. T., Wu, J. C., et al. (2019). Exercise Activates Lysosomal Function in the Brain through AMPK-SIRT1-TFEB Pathway. *CNS Neurosci. Ther.* 25 (6), 796–807. doi:10.1111/cns.13114

Huang, W., Liu, D. W., Wang, G. J., Zhang, H. M., Zhou, G. S., Liu, J. J., et al. (2021). Serum Microtubule-Associated Protein Light Chain 3 Type II Levels Correlate with Aggravation and Multi-Organ Dysfunction in Septic Patients. *Chin. Med. J. (Engl)* 134 (14), 1732–1734. doi:10.1097/CM9.0000000000001640

Huang, Y., Chen, Y., Shaw, A. M., Goldfine, H., Tian, J., and Cai, J. (2018). Enhancing TFEB-Mediated Cellular Degradation Pathways by the mTORC1 Inhibitor Quercetin. *Oxid. Med. Cel. Longev.* 2018, 5073420. doi:10.1155/2018/5073420

Irazoqui, J. E. (2020). Key Roles of MiT Transcription Factors in Innate Immunity and Inflammation. *Trends Immunol.* 41 (2), 157–171. doi:10.1016/j.it.2019.12.003

Jia, L., Wang, Y., Wang, Y., Ma, Y., Shen, J., Fu, Z., et al. (2018). Heme Oxygenase-1 in Macrophages Drives Septic Cardiac Dysfunction via Suppressing Lysosomal Degradation of Inducible Nitric Oxide Synthase. *Circ. Res.* 122 (11), 1532–1544. doi:10.1161/CIRCRESAHA.118.312910

Jiang, W., Zhao, P., and Zhang, X. (2020). Apelin Promotes ECM Synthesis by Enhancing Autophagy Flux via TFEB in Human Degenerative NP Cells under Oxidative Stress. *Biomed. Res. Int.* 2020, 4897170. doi:10.1155/2020/4897170

Jin, J., Kim, C., Xia, Q., Gould, T. M., Cao, W., Zhang, H., et al. (2021). Activation of mTORC1 at Late Endosomes Misdirects T Cell Fate Decision in Older Individuals. *Sci. Immunol.* 6 (60), eabg0791. doi:10.1126/sciimmunol.abg0791

Jin, L., Zeng, W., Zhang, F., Zhang, C., and Liang, W. (2017). Naringenin Ameliorates Acute Inflammation by Regulating Intracellular Cytokine Degradation. *J. Immunol.* 199 (10), 3466–3477. doi:10.4049/jimmunol.1602016

Kim, H. J., Joe, Y., Rah, S. Y., Kim, S. K., Park, S. U., Park, J., et al. (2018). Carbon Monoxide-Induced TFEB Nuclear Translocation Enhances Mitophagy/mitochondrial Biogenesis in Hepatocytes and Ameliorates Inflammatory Liver Injury. *Cell Death Dis* 9 (11), 1060. doi:10.1038/s41419-018-1112-x

Kim, T. S., Jin, Y. B., Kim, Y. S., Kim, S., Kim, J. K., Lee, H. M., et al. (2019). SIRT3 Promotes Antimycobacterial Defenses by Coordinating Mitochondrial and Autophagic Functions. *Autophagy* 15 (8), 1356–1375. doi:10.1080/15548627.2019.1582743

Kim, Y. S., Lee, H. M., Kim, J. K., Yang, C. S., Kim, T. S., Jung, M., et al. (2017). PPAR-α Activation Mediates Innate Host Defense through Induction of TFEB and Lipid Catabolism. *J. Immunol.* 198 (8), 3283–3295. doi:10.4049/jimmunol.1601920

Kondow-Mcconaghy, H. M., Muthukrishnan, N., Erazo-Oliveras, A., Najjar, K., Juliano, R. L., and Pellois, J. P. (2020). Impact of the Endosomal Escape Activity of Cell-Penetrating Peptides on the Endocytic Pathway. *ACS Chem. Biol.* 15 (9), 2355–2363. doi:10.1021/acschembio.0c00319

Kumar, S., Jain, A., Choi, S. W., da Silva, G. P. D., Allers, L., Mudd, M. H., et al. (2020). Mammalian Atg8 Proteins and the Autophagy Factor IRGM Control mTOR and TFEB at a Regulatory Node Critical for Responses to Pathogens. *Nat. Cel Biol.* 22 (8), 973–985. doi:10.1038/s41556-020-0549-1

Lee, J. W., Nam, H., Kim, L. E., Jeon, Y., Min, H., Ha, S., et al. (2019). TLR4 (Toll-like Receptor 4) Activation Suppresses Autophagy through Inhibition of FOXO3 and Impairs Phagocytic Capacity of Microglia. *Autophagy* 15 (5), 753–770. doi:10.1080/15548627.2018.1556946

Lee, S., Lee, S. J., Coronata, A. A., Fredenburgh, L. E., Chung, S. W., Perrella, M. A., et al. (2014). Carbon Monoxide Confers protection in Sepsis by Enhancing Beclin 1-dependent Autophagy and Phagocytosis. *Antioxid. Redox Signal.* 20 (3), 432–442. doi:10.1089/ars.2013.5368

Levine, B., and Kroemer, G. (2019). Biological Functions of Autophagy Genes: A Disease Perspective. *Cell* 176 (1-2), 11–42. doi:10.1016/j.cell.2018.09.048

Li, D., Shao, R., Wang, N., Zhou, N., Du, K., Shi, J., et al. (2021a). Sulforaphane Activates a Lysosome-dependent Transcriptional Program to Mitigate Oxidative Stress. *Autophagy* 17 (4), 872–887. doi:10.1080/15548627.2020.1739442

Li, F., Lang, F., Zhang, H., Xu, L., Wang, Y., Zhai, C., et al. (2017). Apigenin Alleviates Endotoxin-Induced Myocardial Toxicity by Modulating Inflammation, Oxidative Stress, and Autophagy. *Oxid. Med. Cel. Longev.* 2017, 2302896. doi:10.1155/2017/2302896

Li, R., Zhao, X., Zhang, S., Dong, W., Zhang, L., Chen, Y., et al. (2021b). RIP3 Impedes Transcription Factor EB to Suppress Autophagic Degradation in Septic Acute Kidney Injury. *Cel Death Dis* 12 (6), 593. doi:10.1038/s41419-021-03865-8

Lin, C. W., Lo, S., Perng, D. S., Wu, D. B., Lee, P. H., Chang, Y. F., et al. (2014). Complete Activation of Autophagic Process Attenuates Liver Injury and Improves Survival in Septic Mice. *Shock* 41 (3), 241–249. doi:10.1097/SHK.0000000000000111

Liu, Q., Wu, J., Zhang, X., Li, X., Wu, X., Zhao, Y., et al. (2021). Circulating Mitochondrial DNA-Triggered Autophagy Dysfunction via STING Underlies Sepsis-Related Acute Lung Injury. *Cel Death Dis* 12 (7), 673. doi:10.1038/s41419-021-03961-9

Liu, W., Li, C. C., Lu, X., Bo, L. Y., and Jin, F. G. (2019). Overexpression of Transcription Factor EB Regulates Mitochondrial Autophagy to Protect Lipopolysaccharide-Induced Acute Lung Injury. *Chin. Med. J. (Engl)* 132 (11), 1298–1304. doi:10.1097/CM9.0000000000000243

Lv, H., Yang, H., Wang, Z., Feng, H., Deng, X., Cheng, G., et al. (2019). Nrf2 Signaling and Autophagy Are Complementary in Protecting Lipopolysaccharide/d-Galactosamine-Induced Acute Liver Injury by Licochalcone A. *Cel Death Dis* 10 (4), 313. doi:10.1038/s41419-019-1543-z

Martini-Stoica, H., Xu, Y., Ballabio, A., and Zheng, H. (2016). The Autophagy-Lysosomal Pathway in Neurodegeneration: A TFEB Perspective. *Trends Neurosci.* 39 (4), 221–234. doi:10.1016/j.tins.2016.02.002

Medina, D. L., Fraldi, A., Bouche, V., Annunziata, F., Mansueto, G., Spampanato, C., et al. (2011). Transcriptional Activation of Lysosomal Exocytosis Promotes Cellular Clearance. *Dev. Cel.* 21 (3), 421–430. doi:10.1016/j.devcel.2011.07.016

Mo, Y., Lou, Y., Zhang, A., Zhang, J., Zhu, C., Zheng, B., et al. (20182018). PICK1 Deficiency Induces Autophagy Dysfunction via Lysosomal Impairment and Amplifies Sepsis-Induced Acute Lung Injury. *Mediators Inflamm.* 2018, 6757368. doi:10.1155/2018/6757368

Moskot, M., Montefusco, S., Jakóbkiewicz-Banecka, J., Mozolewski, P., Węgrzyn, A., Di Bernardo, D., et al. (2014). The Phytoestrogen Genistein Modulates Lysosomal Metabolism and Transcription Factor EB (TFEB) Activation. *J. Biol. Chem.* 289 (24), 17054–17069. doi:10.1074/jbc.M114.555300

Nikouee, A., Kim, M., Ding, X., Sun, Y., and Zang, Q. S. (2021). Beclin-1-Dependent Autophagy Improves Outcomes of Pneumonia-Induced Sepsis. *Front Cel Infect Microbiol* 11, 706637. doi:10.3389/fcimb.2021.706637

Oami, T., Watanabe, E., Hatano, M., Sunahara, S., Fujimura, L., Sakamoto, A., et al. (2017). Suppression of T Cell Autophagy Results in Decreased Viability and Function of T Cells through Accelerated Apoptosis in a Murine Sepsis Model. *Crit. Care Med.* 45 (1), e77–e85. doi:10.1097/CCM.0000000000002016

Oami, T., Watanabe, E., Hatano, M., Teratake, Y., Fujimura, L., Sakamoto, A., et al. (2018). Blocking Liver Autophagy Accelerates Apoptosis and Mitochondrial Injury in Hepatocytes and Reduces Time to Mortality in a Murine Sepsis Model. *Shock* 50 (4), 427–434. doi:10.1097/SHK.0000000000001040

Orfali, N., O'Donovan, T. R., Cahill, M. R., Benjamin, D., Nanus, D. M., Mckenna, S. L., et al. (2020). All-trans Retinoic Acid (ATRA)-induced TFEB Expression Is Required for Myeloid Differentiation in Acute Promyelocytic Leukemia (APL). *Eur. J. Haematol.* 104 (3), 236–250. doi:10.1111/ejh.13367

Ouimet, M., Koster, S., Sakowski, E., Ramkhelawon, B., van Solingen, C., Oldebeken, S., et al. (2016). *Mycobacterium tuberculosis* Induces the miR-33 Locus to Reprogram Autophagy and Host Lipid Metabolism. *Nat. Immunol.* 17 (6), 677–686. doi:10.1038/ni.3434

Ouyang, X., Becker, E., Bone, N. B., Johnson, M. S., Craver, J., Zong, W.-X., et al. (2021). ZKSCAN3 in Severe Bacterial Lung Infection and Sepsis-Induced Immunosuppression. *Lab. Invest.* 101, 1467–1474. doi:10.1038/s41374-021-00660-z

Palmieri, M., Impey, S., Kang, H., di Ronza, A., Pelz, C., Sardiello, M., et al. (2011). Characterization of the CLEAR Network Reveals an Integrated Control of Cellular Clearance Pathways. *Hum. Mol. Genet.* 20 (19), 3852–3866. doi:10.1093/hmg/ddr306

Pan, B., Lewno, M. T., Wu, P., and Wang, X. (2019). Highly Dynamic Changes in the Activity and Regulation of Macroautophagy in Hearts Subjected to Increased Proteotoxic Stress. *Front. Physiol.* 10, 758. doi:10.3389/fphys.2019.00758

Pan, B., Li, J., Parajuli, N., Tian, Z., Wu, P., Lewno, M. T., et al. (2020). The Calcineurin-TFEB-P62 Pathway Mediates the Activation of Cardiac Macroautophagy by Proteasomal Malfunction. *Circ. Res.* 127 (4), 502–518. doi:10.1161/CIRCRESAHA.119.316007

Pan, B., Zhang, H., Cui, T., and Wang, X. (2017). TFEB Activation Protects against Cardiac Proteotoxicity via Increasing Autophagic Flux. *J. Mol. Cel. Cardiol.* 113, 51–62. doi:10.1016/j.yjmcc.2017.10.003

Pastore, N., Brady, O. A., Diab, H. I., Martina, J. A., Sun, L., Huynh, T., et al. (2016). TFEB and TFE3 Cooperate in the Regulation of the Innate Immune Response in Activated Macrophages. *Autophagy* 12 (8), 1240–1258. doi:10.1080/15548627.2016.1179405

Puleston, D. J., Buck, M. D., Klein Geltink, R. I., Kyle, R. L., Caputa, G., O'Sullivan, D., et al. (2019). Polyamines and eIF5A Hypusination Modulate Mitochondrial Respiration and Macrophage Activation. *Cell Metab* 30 (2), 352–e8. e8. doi:10.1016/j.cmet.2019.05.003

Raben, N., and Puertollano, R. (2016). TFEB and TFE3: Linking Lysosomes to Cellular Adaptation to Stress. *Annu. Rev. Cel Dev Biol* 32, 255–278. doi:10.1146/annurev-cellbio-111315-125407

Rudd, K. E., Johnson, S. C., Agesa, K. M., Shackelford, K. A., Tsoi, D., Kievlan, D. R., et al. (2020). Global, Regional, and National Sepsis Incidence and Mortality, 1990-2017: Analysis for the Global Burden of Disease Study. *Lancet* 395 (10219), 200–211. doi:10.1016/S0140-6736(19)32989-7

Samie, M., and Cresswell, P. (2015). The Transcription Factor TFEB Acts as a Molecular Switch that Regulates Exogenous Antigen-Presentation Pathways. *Nat. Immunol.* 16 (7), 729–736. doi:10.1038/ni.3196

Sardiello, M., Palmieri, M., di Ronza, A., Medina, D. L., Valenza, M., Gennarino, V. A., et al. (2009). A Gene Network Regulating Lysosomal Biogenesis and Function. *Science* 325 (5939), 473–477. doi:10.1126/science.1174447

Schilling, J. D., Machkovech, H. M., He, L., Diwan, A., and Schaffer, J. E. (2013). TLR4 Activation under Lipotoxic Conditions Leads to Synergistic Macrophage Cell Death through a TRIF-dependent Pathway. *J. Immunol.* 190 (3), 1285–1296. doi:10.4049/jimmunol.1202208

Settembre, C., Di Malta, C., Polito, V. A., Garcia Arencibia, M., Vetrini, F., Erdin, S., et al. (2011). TFEB Links Autophagy to Lysosomal Biogenesis. *Science* 332 (6036), 1429–1433. doi:10.1126/science.1204592

Sha, Y., Rao, L., Settembre, C., Ballabio, A., and Eissa, N. T. (2017). STUB1 Regulates TFEB-Induced Autophagy-Lysosome Pathway. *EMBO J.* 36 (17), 2544–2552. doi:10.15252/embj.201796699

Sharma, V., Makhdoomi, M., Singh, L., Kumar, P., Khan, N., Singh, S., et al. (2021). Trehalose Limits Opportunistic Mycobacterial Survival during HIV Co-infection by Reversing HIV-Mediated Autophagy Block. *Autophagy* 17 (2), 476–495. doi:10.1080/15548627.2020.1725374

Song, H., Feng, X., Zhang, H., Luo, Y., Huang, J., Lin, M., et al. (2019b). METTL3 and ALKBH5 Oppositely Regulate m6A Modification of TFEB mRNA, Which Dictates the Fate of Hypoxia/reoxygenation-Treated Cardiomyocytes. *Autophagy* 15 (8), 1419–1437. doi:10.1080/15548627.2019.1586246

Song, H. L., Demirev, A. V., Kim, N. Y., Kim, D. H., and Yoon, S. Y. (2019a). Ouabain Activates Transcription Factor EB and Exerts Neuroprotection in Models of Alzheimer's Disease. *Mol. Cel. Neurosci.* 95, 13–24. doi:10.1016/j.mcn.2018.12.007

Song, J. X., Liu, J., Jiang, Y., Wang, Z. Y., and Li, M. (2021). Transcription Factor EB: An Emerging Drug Target for Neurodegenerative Disorders. *Drug Discov. Today* 26 (1), 164–172. doi:10.1016/j.drudis.2020.10.013

Song, J. X., Sun, Y. R., Peluso, I., Zeng, Y., Yu, X., Lu, J. H., et al. (2016). A Novel Curcumin Analog Binds to and Activates TFEB *In Vitro* and *In Vivo* Independent of MTOR Inhibition. *Autophagy* 12 (8), 1372–1389. doi:10.1080/15548627.2016.1179404

Song, W., Wang, F., Lotfi, P., Sardiello, M., and Segatori, L. (2014). 2-Hydroxypropyl-β-cyclodextrin Promotes Transcription Factor EB-Mediated Activation of Autophagy: Implications for Therapy. *J. Biol. Chem.* 289 (14), 10211–10222. doi:10.1074/jbc.M113.506246

Song, W., Wang, F., Savini, M., Ake, A., di Ronza, A., Sardiello, M., et al. (2013). TFEB Regulates Lysosomal Proteostasis. *Hum. Mol. Genet.* 22 (10), 1994–2009. doi:10.1093/hmg/ddt052

Sun, Y., Yao, X., Zhang, Q. J., Zhu, M., Liu, Z. P., Ci, B., et al. (2018). Beclin-1-Dependent Autophagy Protects the Heart during Sepsis. *Circulation* 138 (20), 2247–2262. doi:10.1161/CIRCULATIONAHA.117.032821

Sunahara, S., Watanabe, E., Hatano, M., Swanson, P. E., Oami, T., Fujimura, L., et al. (2018). Influence of Autophagy on Acute Kidney Injury in a Murine Cecal Ligation and Puncture Sepsis Model. *Sci. Rep.* 8 (1), 1050. doi:10.1038/s41598-018-19350-w

Tseng, H. H. L., Vong, C. T., Kwan, Y. W., Lee, S. M., and Hoi, M. P. M. (2017). Lysosomal Ca2+ Signaling Regulates High Glucose-Mediated Interleukin-1β Secretion via Transcription Factor EB in Human Monocytic Cells. *Front. Immunol.* 8, 1161. doi:10.3389/fimmu.2017.01161

Unuma, K., Aki, T., Funakoshi, T., Yoshida, K., and Uemura, K. (2013). Cobalt Protoporphyrin Accelerates TFEB Activation and Lysosome Reformation during LPS-Induced Septic Insults in the Rat Heart. *PLoS One* 8 (2), e56526. doi:10.1371/journal.pone.0056526

van der Poll, T., van de Veerdonk, F. L., Scicluna, B. P., and Netea, M. G. (2017). The Immunopathology of Sepsis and Potential Therapeutic Targets. *Nat. Rev. Immunol.* 17 (7), 407–420. doi:10.1038/nri.2017.36

Venet, F., and Monneret, G. (2018). Advances in the Understanding and Treatment of Sepsis-Induced Immunosuppression. *Nat. Rev. Nephrol.* 14 (2), 121–137. doi:10.1038/nrneph.2017.165

Visvikis, O., Ihuegbu, N., Labed, S. A., Luhachack, L. G., Alves, A. F., Wollenberg, A. C., et al. (2014). Innate Host Defense Requires TFEB-Mediated Transcription of Cytoprotective and Antimicrobial Genes. *Immunity* 40 (6), 896–909. doi:10.1016/j.immuni.2014.05.002

Wang, C., Niederstrasser, H., Douglas, P. M., Lin, R., Jaramillo, J., Li, Y., et al. (2017). Small-molecule TFEB Pathway Agonists that Ameliorate Metabolic Syndrome in Mice and Extend *C. elegans* Lifespan. *Nat. Commun.* 8 (1), 2270. doi:10.1038/s41467-017-02332-3

Wang, S., Ni, H. M., Chao, X., Wang, H., Bridges, B., Kumer, S., et al. (2019). Impaired TFEB-Mediated Lysosomal Biogenesis Promotes the Development of Pancreatitis in Mice and Is Associated with Human Pancreatitis. *Autophagy* 15 (11), 1954–1969. doi:10.1080/15548627.2019.1596486

Xia, Y., Liu, N., Xie, X., Bi, G., Ba, H., Li, L., et al. (2019). The Macrophage-specific V-ATPase Subunit ATP6V0D2 Restricts Inflammasome Activation and Bacterial Infection by Facilitating Autophagosome-Lysosome Fusion. *Autophagy* 15 (6), 960–975. doi:10.1080/15548627.2019.1569916

Xu, C., Wang, W., Zhong, J., Lei, F., Xu, N., Zhang, Y., et al. (2018). Canagliflozin Exerts Anti-inflammatory Effects by Inhibiting Intracellular Glucose Metabolism and Promoting Autophagy in Immune Cells. *Biochem. Pharmacol.* 152, 45–59. doi:10.1016/j.bcp.2018.03.013

Xu, H., Yu, W., Sun, S., Li, C., Zhang, Y., and Ren, J. (2020a). Luteolin Attenuates Doxorubicin-Induced Cardiotoxicity through Promoting Mitochondrial Autophagy. *Front. Physiol.* 11, 113. doi:10.3389/fphys.2020.00113

Xu, J., Zhang, X. Q., and Zhang, Z. (2020b). Transcription Factor EB Agonists from Natural Products for Treating Human Diseases with Impaired Autophagy-Lysosome Pathway. *Chin. Med.* 15 (1), 123. doi:10.1186/s13020-020-00402-1

Yin, X., Xin, H., Mao, S., Wu, G., and Guo, L. (2019). The Role of Autophagy in Sepsis: Protection and Injury to Organs. *Front. Physiol.* 10, 1071. doi:10.3389/fphys.2019.01071

Yu, L., Chen, Y., and Tooze, S. A. (2018). Autophagy Pathway: Cellular and Molecular Mechanisms. *Autophagy* 14 (2), 207–215. doi:10.1080/15548627.2017.1378838

Zhang, H., Alsaleh, G., Feltham, J., Sun, Y., Napolitano, G., Riffelmacher, T., et al. (2019). Polyamines Control eIF5A Hypusination, TFEB Translation, and Autophagy to Reverse B Cell Senescence. *Mol. Cel.* 76 (1), 110–e9. e9. doi:10.1016/j.molcel.2019.08.005

Zhang, J., Wang, J., Wong, Y. K., Sun, X., Chen, Y., Wang, L., et al. (2018). Docetaxel Enhances Lysosomal Function through TFEB Activation. *Cel Death Dis* 9 (6), 614. doi:10.1038/s41419-018-0571-4

Zhang, J., Wang, J., Xu, J., Lu, Y., Jiang, J., Wang, L., et al. (2016). Curcumin Targets the TFEB-Lysosome Pathway for Induction of Autophagy. *Oncotarget* 7 (46), 75659–75671. doi:10.18632/oncotarget.12318

Zhou, Y., Zhou, X., Huang, X., Hong, T., Zhang, K., Qi, W., et al. (2021). Lysosome-Mediated Cytotoxic Autophagy Contributes to Tea Polysaccharide-Induced Colon Cancer Cell Death via mTOR-TFEB Signaling. *J. Agric. Food Chem.* 69 (2), 686–697. doi:10.1021/acs.jafc.0c07166

Zhu, S. Y., Yao, R. Q., Li, Y. X., Zhao, P. Y., Ren, C., Du, X. H., et al. (2021). The Role and Regulatory Mechanism of Transcription Factor EB in Health and Diseases. *Front. Cel Dev Biol* 9, 667750. doi:10.3389/fcell.2021.667750

Conflict of Interest: The authors declare that the research was conducted in the absence of any commercial or financial relationships that could be construed as a potential conflict of interest.

Publisher's Note: All claims expressed in this article are solely those of the authors and do not necessarily represent those of their affiliated organizations, or those of the publisher, the editors and the reviewers. Any product that may be evaluated in this article, or claim that may be made by its manufacturer, is not guaranteed or endorsed by the publisher.

frontiers in Pharmacology

ORIGINAL RESEARCH
published: 29 November 2021
doi: 10.3389/fphar.2021.792741

Effect of Anti-Inflammatory and Antimicrobial Cosupplementations on Sepsis Prevention in Critically Ill Trauma Patients at High Risk for Sepsis

Noha A. Kamel[1†], *Moetaza M. Soliman*[1*†], *Maha A. Abo-Zeid*[2†] *and Mona I. Shaaban*[3†]

[1]Department of Clinical Pharmacy and Pharmacy Practice, Faculty of Pharmacy, Mansoura University, Mansoura, Egypt, [2]Department of Anesthesia, Surgical Intensive Care Unit and Pain Management, Faculty of Medicine, Mansoura University, Mansoura, Egypt, [3]Department of Microbiology and Immunology, Faculty of Pharmacy, Mansoura University, Mansoura, Egypt

OPEN ACCESS

Edited by:
Yan Kang,
Sichuan University, China

Reviewed by:
Lana Nezic,
University of Banja Luka, Bosnia and Herzegovina
Michael Super,
Harvard University, United States

***Correspondence:**
Moetaza M. Soliman
moetaza@mans.edu.eg

†ORCID:
Noha A. Kamel,
orcid.org/0000-0002-3299-9555;
Moetaza M. Soliman,
orcid.org/0000-0002-8651-9385;
Maha A. Abo-Zeid,
orcid.org/0000-0002-6389-406X;
Mona I. Shaaban,
orcid.org/0000-0003-3044-6102

Specialty section:
This article was submitted to Translational Pharmacology, a section of the journal Frontiers in Pharmacology

Received: 11 October 2021
Accepted: 01 November 2021
Published: 29 November 2021

Citation:
Kamel NA, Soliman MM, Abo-Zeid MA and Shaaban MI (2021) Effect of Anti-Inflammatory and Antimicrobial Cosupplementations on Sepsis Prevention in Critically Ill Trauma Patients at High Risk for Sepsis. Front. Pharmacol. 12:792741. doi: 10.3389/fphar.2021.792741

Background: Sepsis development in patients with trauma is associated with bad prognosis. This study investigated the effect of immunomodulatory interventions in major trauma patients at high risk for sepsis.

Methods: In a randomized, double-blinded, controlled design, severe trauma patients were stratified by leukocyte anti-sedimentation rate (LAR) test into high risk (HR) and low risk (LR) for sepsis. The HR patients were randomly allocated into intravenous vitamin C plus vitamin B1 (HR-CB), intramuscular vitamin D plus oral *Lactobacillus* probiotics (HR-DP), or control (HR-C) groups. The clinical trial was registered at clinicaltrials.gov (https://clinicaltrials.gov/show/NCT04216459).

Outcomes: The primary outcome was Acute Physiologic Assessment and Chronic Health Evaluation score II (APACHE II) score. Secondary outcomes included sepsis incidence, changes in Sequential Organ Failure Assessment (SOFA) score, and serum monocyte chemoattractant protein-1 (MCP-1) on day 6 from baseline, 28-day mortality, intensive care unit (ICU), and hospital discharge.

Results: The HR-DP, HR-CB, and LR groups showed a significantly lower incidence of sepsis development (20%, 20%, and 16%, respectively, versus 60% in the HR-C group, p-value = 0.004). The three groups also showed a significant improvement in APACHE II and SOFA scores. Besides, MCP-1 levels were significantly decreased in HR-DP and HR-CB groups compared to the HR-C group (p-value ≤ 0.05). Significantly decreased mortality (10% and 16% versus 60% in the HR-C group) and increased ICU discharge

Abbreviations: APACHE II, acute Physiologic Assessment and Chronic Health Evaluation score II; CB, vitamin C plus vitamin B1; CRP, C-reactive protein; DP, vitamin D plus probiotics; ELISA, enzyme-linked immunosorbent assay; ESR, erythrocyte sedimentation rate; HR, high-risk; HR-DP, high-risk vitamin D plus probiotics; HR-CB, high-risk vitamin C plus vitamin B1; IL-6, interleukin-6; IDT, intradermal skin test; ISS, injury severity score; LAR, leukocyte anti-sedimentation rate; LR, low-risk; MCP-1, monocyte chemoattractant protein-1; ROC curve, receiver operating characteristics curve; SOFA, sequential Organ Failure Assessment.

(95% and 84% versus 45% in the HR-C group) were observed in HR-CB and LR groups (p-value = 0.001).

Conclusion: Both combinations of interventions improved APACHE II scores and reduced sepsis incidence in trauma patients. The LAR combined with injury severity score were good sepsis predictors.

Keywords: vitamin C, vitamin B1, vitamin D, probiotics, leukocyte antisedimentation rate, monocyte chemoattractant protein 1, controlled trial, sepsis

1 INTRODUCTION

Sepsis is a life-threatening illness associated with poor prognosis (Rudd et al., 2020). Patients with major trauma are prone to septic complications due to the immune dysregulation that occurs after trauma (Hesselink et al., 2019). The incidence of mortality due to post-traumatic sepsis development in the intensive care unit (ICU) is still high (Wafaisade et al., 2011). Both trauma and sepsis cause tissue and cell damages, systemic inflammatory response syndrome, and multiple organ failure in severe cases. The reason for the similarity in body response to trauma and sepsis might be that the antigen structures of mitochondria released during trauma are very similar to the genetic structure of pathogens in sepsis. Nevertheless, the exact underlying mechanisms are not the same (Rozanovic et al., 2016).

The prevention of sepsis in patients with trauma could greatly help avoid the poor prognosis of sepsis and improve patient survival (Ma et al., 2016). The ideal prevention strategy should involve first identifying patients with major trauma at high risk for sepsis who would benefit most from the used immunomodulatory interventions. Early prediction of sepsis development is a key factor that would allow the use of preventive interventions to improve patient prognosis (Jin et al., 2014).

First, the early prediction of sepsis in trauma patients is likely to face many challenges. The surviving sepsis campaign in 2016 defined sepsis as a life-threatening organ dysfunction caused by a dysregulated host response to infection. Organ dysfunction is identified as acute change in the total Sequential Organ Failure Assessment Score (SOFA) score ≥2 points (Singer et al., 2016). On applying sepsis-3 definition in clinical practice, by the time the patient is diagnosed as septic, organ dysfunction has already occurred. Patients with sepsis often have a bad prognosis. Even the survivors suffer from long term physical, psychological, and cognitive disabilities (Sartelli et al., 2018).

Identifying patients at high risk for sepsis before reaching multi-organ failure was never mentioned in the surviving sepsis campaign's latest guidelines (Singer et al., 2016). On the other hand, relying on the blood culture results to identify patients at high risk for sepsis is not possible either. Infection is rarely confirmed microbiologically. Culture-positive sepsis is observed only in 30%–40% of cases (Singer et al., 2016). The time delay in obtaining culture results and the possibility of false-negative findings limit the usefulness of culture in the early recognition of sepsis (Sweeney et al., 2019).

The limitation of the 2016 sepsis guidelines was addressed in the following 2021 surviving sepsis campaign's guidelines that recommended implementing sepsis performance improvement programs in healthcare settings. These programs consist mainly of two arms: sepsis screening tools and standard operating procedures. Sepsis screening tools were defined as means of identifying high-risk critically ill patients to allow timely interventions that help improve their prognosis. Standard operating procedures involved usual care by obtaining cultures and administering fluids and antibiotics (Evans et al., 2021). Two methods, leukocyte antisedimentation rate (LAR) and monocyte chemoattractant protein-1 (MCP-1), were used in previous studies for the early prediction of sepsis in trauma and showed positive results (Rozanovic et al., 2016; Wang et al., 2018). The LAR failing to exceed 15% on day 1 (second day from the ICU admission) was used to predict the high risk for sepsis in trauma patients (Rozanovic et al., 2016), whereas the serum MCP-1 levels >240.7 pg/ml on day 0 (within 24 h of admission) was used for the same purpose of identifying patients with trauma at high risk for sepsis development (Wang et al., 2018).

The LAR test offered some advantages that made its use more feasible and affordable in this trial for prediction of sepsis than the MCP-1. These advantages include the performance of LAR using whole blood samples; no storage, preparation, or isolation procedures could cause false activation of leukocytes. Moreover, the LAR test is cheap, reproducible, easy to perform, and time-saving (Bogár et al., 1997). Conversely, the levels of MCP-1 were measured by enzyme-linked immunosorbent assay (ELISA) (Wang et al., 2018). Some disadvantages hinder the clinical use of ELISA in Egyptian ICUs including the tedious and time-consuming procedure besides the necessity for centralized laboratory equipment (Hosseini et al., 2018).

Second, for sepsis prevention in patients with trauma at high risk for sepsis development, using a combination of interventions was recommended. The rationale behind this recommendation was the complex pathophysiology of sepsis involving hundreds of mediators and the failure of previous studies using single intervention targeting a single biomarker (Aird, 2003). Several immunomodulatory interventions have been used in previous studies including intravenous (IV) high-dose vitamin C and vitamin B1, IV stress dose steroids, IV N-acetyl cysteine, intramuscular (IM) or oral high-dose vitamin D, and oral probiotics (Kotzampassi et al., 2006; Bedreag et al., 2015; Sandesc et al., 2018; Tessa et al., 2018; Hasanloei et al., 2020).

Positive results were reported including lower incidence of sepsis development and multi-organ dysfunction syndrome with vitamin C and N-acetyl cysteine (Sandesc et al., 2018) and lower peak SOFA scores with vitamin C and vitamin B1 (Tessa et al., 2018). In other contexts, involving the management of sepsis and septic shock in the medical ICU, hydrocortisone, ascorbic acid, and thiamine combination has shown promise (Marik et al., 2017). Vitamin C has antibacterial effects, whereas both vitamin C and vitamin B1 have anti-inflammatory, antioxidant, and mitochondrial protective effects (Marik, 2018). None of the previous studies specifically targeted patients with major trauma at high risk for sepsis.

Vitamin D and probiotics have been used separately in the previous trials focusing on patients with trauma. The reported positive outcomes included reduced incidence of sepsis with synbiotics (Kotzampassi et al., 2006), significantly lower SOFA score, duration of mechanical ventilation, and ICU stay with high-dose oral and IM vitamin D3 (Hasanloei et al., 2020). Vitamin D and probiotics have been used together in contexts other than trauma and have shown a synergistic effect as anti-inflammatory and antimicrobial combination (Abboud et al., 2021).

Previous studies on immunomodulatory interventions in trauma usually monitored the change in interleukin 6 (IL-6) as a proinflammatory cytokine (Kotzampassi et al., 2006; Sandesc et al., 2018; Hasanloei et al., 2020). However, none of the previous studies investigated the effect of immunomodulatory interventions on MCP-1 levels among patients with major trauma. Wang et al. suggested that future studies should investigate their hypothesis that decreasing MCP-1 could confer an associated therapeutic benefit among ICU patients with major trauma (Wang et al., 2018).

Therefore, the aims of the current study were, first, to re-validate LAR as a cheap and available test combined with Injury Severity Score (ISS) to predict the risk for sepsis development in major trauma ICU patients and, second, to investigate the effect of IM vitamin D3 supplementation plus oral probiotics cosupplementation versus IV vitamin C plus vitamin B1 on prevention of sepsis compared to no additional supplementation. This was based on the combined predictable anti-inflammatory and antimicrobial effects of each set of study regimens on sepsis prevention in ICU patients with major trauma at high risk for sepsis development.

2 MATERIALS AND METHODS

2.1 Study Design and Location

This was a prospective, randomized, controlled, double-blind study conducted among trauma patients at high risk for sepsis in the ICU. Data were collected from February to November 2020 in the ICUs of Mansoura University Emergency Hospital, Egypt.

2.2 Ethics Approval

Study procedures complied with the 1964 Declaration of Helsinki and its later amendments (Rickham, 1964; Baker, 2020). Confidentiality of patient data was preserved. No patient identifiers were used in the datasheet. The study was approved by the Institutional Review Board (IRB), Faculty of Medicine (IRB # R.19.12.707) and Research Ethics Committee, Faculty of Pharmacy, Mansoura University. Informed consent was obtained from all patients or their relatives in case the patient was unable to provide consent. The clinical trial had been registered at clinicaltrials.gov (https://clinicaltrials.gov/show/NCT04216459).

2.3 Inclusion and Exclusion Criteria

Inclusion criteria consisted of admission to ICU within 24 h from trauma onset with ISS ≥ 16 and age ≥ 18 years. The exclusion criteria included pregnant or breastfeeding women and immune deficient patients or patients receiving immunosuppressant drugs. Patients at high risk for sepsis (LAR < 15%) who had serum vitamin D level <10 ng/ml or >30 ng/ml or serum calcium level >10 mg/dl were excluded. Besides, patients with a history of primary parathyroid disease and those with contraindications to enteral administration were also excluded. Patients with end-stage renal disease on renal replacement therapy were not eligible for the study. Moreover, patients with oxalate nephropathy or glucose-6 phosphate dehydrogenase deficiency were also not eligible for the study.

2.4 Outcomes

The primary outcome of the study was the change in Acute Physiologic Assessment and Chronic Health Evaluation score II (APACHE II) score defined as day 6 minus day 0 score, while the secondary outcomes included the change in SOFA score and MCP-1 in addition to number of patients who developed sepsis within the first week. Blood cultures were used as a possible documentation for infection. Moreover, C-reactive protein (CRP) level and erythrocyte sedimentation rate (ESR) were also measured on days 0 and 6 for all included patients. Additional secondary outcomes included ICU discharge, hospital discharge, and mortality within 28 days for all patients.

In a secondary analysis, the predictive value of LAR combined with ISS to predict the risk for sepsis development in severe trauma ICU patients was evaluated.

2.5 Sample Size

Sample size calculation was based on APACHE II scores achieved after receiving vitamin C, vitamin D, and probiotics in previous studies (Sanaie et al., 2014; Atalan and Güçyetmez, 2017; Sandesc et al., 2018; Hasanloei et al., 2020). For vitamin C, the mean ± standard deviation (SD) APACHE II score was 8.00 ± 0.99 in the treated group versus 10.50 ± 2.10 in the control group (Sandesc et al., 2018). The estimated mean ± SD APACHE II score after receiving IM vitamin D injection was 9.30 ± 0.95 compared to 10.20 ± 0.50 in the placebo arm (Atalan and Güçyetmez, 2017; Hasanloei et al., 2020). For probiotics, the mean APACHE II score was 13.85 ± 4.82 in patients treated with probiotics versus 20.85 ± 7.55 in the control arm (Sanaie et al., 2014).

G*Power version 3.0.10 was used for sample size calculation. The *t*-test was used to detect difference between two independent means (two groups), two-tailed, with α error = 0.05 and power

= 89%. The effect sizes were 1.5228481, 1.1855969, and 1.1051758, whereas the total calculated sample sizes were 10, 16, and 18 patients in each arm for vitamin C, vitamin D, and probiotics, respectively. To overlap the probable dropout of patients, 10% of the calculated sizes were added, making the total calculated sample sizes of 11, 18, and 20 for vitamin C, vitamin D, and probiotics, respectively. Thus, we decided to include 20 patients in each group.

2.6 Patient Allocation

After ICU admission of patients with ISS ≥ 16, all patients were evaluated. The included patients with high risk for sepsis (LAR < 15%) were randomly allocated, at 1:1:1 ratio, into one of three groups each consisting of 20 patients, using sealed opaque envelopes. Patients in the first group did not receive any additional supplement and represented the control group (HR-C group). Patients in the second group received vitamin D plus probiotics (HR-DP group), while patients in the third group received vitamin C plus vitamin B1 (HR-CB group). The low-risk (LR) group (LAR ≥ 15%) did not receive any special therapy.

2.7 Clinical Data Collection

2.7.1 Baseline Characteristics

Demographic characteristics (age, sex, weight, and height), comorbidities, initial ventilatory status, Glasgow coma score (GCS), and laboratory values were collected on admission. The ISS determination was performed according to Baker et al. (1974). Abbreviated injury scale for each type of injury in different body regions was determined according to chart for clinical use (Civil and Schwab, 1988).

On day 0, recordings of APACHE II (Knaus et al., 1985) and SOFA (Vincent et al., 1996) scores were conducted for all included patients. Then, 3 cm of blood sample was drawn within 24 h of ICU admission for measurement of MCP-1. Besides, ESR and CRP levels were measured initially on day 0. After that, on day 1, peripheral venous blood samples were collected for determination of LAR and serum 25-hydroxyvitamin D levels.

2.7.2 Medications Used in the Intervention Groups

In the HR-DP group, patients received vitamin D as one IM injection (400,000 IU of vitamin D3; two ampoules of Devarol-S®, Memphis Co. for Pharmaceutical and Chemical Industries, Egypt) on day 1 in addition to *Lactobacillus* probiotics (Lacteol Fort ® 10 billion colony-forming unit sachets, manufactured by Rameda Pharmaceutical Company under license of Axcan Pharma S.A, France) in a dose of six sachets (one pack) twice a day (at 9 a.m. and 9 p.m.) orally (either directly or through Ryle's tube feeding) starting from day 1 for 48 h.

Patients of the HR-CB group received from day 1 a dose of 1 g of vitamin C (one ampoule of Wörwag Pharma GmbH and Co. KG® Vitamin C 1000 mg) plus 200 mg of vitamin B1 (two ampoules of Pascoe pharmaceutical preparations GmbH® vitamin B1 100 mg). Vitamin C plus vitamin B1 were infused intravenously in 500 ml of saline over 30 min four times at 12-h intervals for 48 h.

Intradermal skin testing (IDT) for vitamin B1 hypersensitivity was conducted in patients of the HR-CB group with unspecified history of allergy to vitamin B1. Patients showing allergy to vitamin B1 were excluded from the study. Blood gases were investigated for metabolic acidosis. Patients in the HR-CB group showing metabolic acidosis on day 1 were also excluded from the study.

The investigator who knew the allocation of groups and was responsible for the drug administration was excluded in all data collection.

2.7.3 Patient Follow up

On day 6, SOFA and APACHE II scores were recorded for all groups. Moreover, a blood sample was obtained from all patients for determination of MCP-1 (in HR groups), ESR, and CRP level (in all groups) measurements. Changes in SOFA and MCP-1 were defined as day 6 minus initial (day 0) values. For LR group, outcomes were the same as the other three groups except for change in MCP-1 as MCP-1 for this group was only measured on day 0. Eight centimeters of blood were collected for aerobic blood culture (30-ml bottle manufactured by Zhuhai DL Biotech Co., Ltd., China).

During the whole ICU admission, all patients in the four groups were carefully monitored and managed according to the ICU protocol. The number of patients who developed sepsis in each group within 7 days was recorded. Sepsis development within 7 days was confirmed according to the sepsis-3 criteria (Singer et al., 2016). Sepsis was assigned if there was an increase in patient's SOFA score by two or more points in addition to suspected or documented source of infection (Singer et al., 2016). Furthermore, the duration of mechanical ventilation for patients who needed mechanical ventilation from day 0 in each group was observed by the end of the first week. All included patients were followed for ICU discharge and hospital discharge within 28 days. Also, ICU mortality and hospital mortality (including patients who died in the ICU or after discharge from it in the ward) within 28 days were recorded.

For fear that the patient cannot complete the study (due to transfer outside hospital or death), after completion of study treatment regimen, and before the patient completes day 6, a reserved blood sample and blood culture were collected on day 3. This reserved blood sample was used for MCP-1 (in HR groups), ESR, and CRP level measurements. These reserved samples and blood culture taken on day 3 were collected to be analyzed immediately (except for MCP-1), recorded if the patient did not complete the study, and discarded if day 6 blood sample and blood culture were collected. Also, for those patients, the last recorded APACHE II and SOFA scores (after day 2) were forwarded for assessment, whereas if a patient was discharged to the ward before day 6 but after completing the study regimen in the ICU, the last recorded APACHE II score in the ICU just before discharge was used. Then, the patient was followed in the ward, and the final SOFA score, ESR, CRP level, MCP-1 level (if HR group), and blood culture were collected in the ward on day 6. Patients who were unable to complete their study treatment regimens in the ICU due to very early discharge or death were excluded from the study.

2.7.4 Monitoring of Adverse Events

Serum creatinine level in the ICU was routinely monitored for any significant elevations. Moreover, the serum creatinine level on day 6 was compared to day 0 to record the occurrence of acute kidney injury (AKI). Patients with AKI were managed according to the Kidney disease Improving Global Outcomes (KDIGO) guidelines (Khwaja, 2012).

2.7.5 Details of the Performed Measurements

2.7.5.1 Serum 25-Hydroxyvitamin D Measurement

Serum vitamin D level was assessed using the LIAISON® analyzer, DiaSorin S.p.A. The LIAISON® 25-hydroxyvitamin D assay is a direct, competitive chemiluminescent immunoassay for quantitative determination of total 25-hydroxyvitamin D in serum or plasma. This method of immunoassay is FDA approved (FDA, 2007).

2.7.5.2 MCP-1 Measurement

Blood samples (3 cm) were obtained in vacuum red cap disposable plain blood tubes (GD050A, Gong Dong, China) and centrifuged at 370 × g for 5 min (Centrifuge, Sigma, Germany, model 2-16P). Serum samples were collected and stored at −80°C, analyzed together after all patient enrollments. The MCP-1 was assessed using the commercially available Invitrogen Human C-C motif chemokine ligand 2 [CCL2 (MCP-1)] ELISA kit (Thermo Fisher Scientific, Catalog Number BMS281).

Two sets of the ELISA kits were used according to the manufacturer's instructions. Each kit contained one plate [Microwell Plate (12 strips of eight wells each) coated with monoclonal antibody to human MCP-1]. Samples were diluted at 1:5 [20 µl sample +80 µl assay buffer (1×)]. The standard curve was constructed, and the MCP-1 level in each sample was retrieved from the standard curve and multiplied by the dilution factor (×5). Samples exceeding standard concentration were further externally prediluted.

2.7.5.3 ESR and CRP Measurement

The ESR was measured by modified Westergren method using Streck® ESR-10 Manual Rack for the Modified Westergren Sed Rate, Streck® 240321. However, the CRP level was measured by nephelometry using the BN™ II System nephelometric analyzer.

2.7.5.4 LAR Measurement

Peripheral venous blood (1.28 ml) was collected in sodium citrate anticoagulated tube (vacuum blood tube containing buffered sodium citrate solution with a concentration of 3.8%, 8 × 120 mm, 1.28 ml, GD0128ESR, Gong Dong, China). After 1 h of blood sedimentation, using an automatic cell counter (Mindray BC-2800 Auto Hematology Analyzer), leukocyte count in the upper (U) and lower (L) half of blood column was determined. LAR was calculated according to the equation described by Rozanovic et al. (2016): $LAR = \frac{U-L}{U+L} \times 100$.

2.8 Statistical Analysis

The IBM® SPSS® 26.0.0 statistical software was used to perform statistical analyses. Shapiro–Wilk test for normality was performed. Quantitative data were summarized as mean ± SD or median, interquartile range according to normality. Qualitative data were summarized as frequency (percentage). To detect differences between groups, analysis of variance (ANOVA), Kruskal–Wallis, and chi-square tests were used for parametric, nonparametric, and categorical variables, respectively. If significant differences between groups were found, appropriate post-hoc tests were performed. Post-hoc tests after ANOVA were determined according to homogeneity of variances. Dunn's and Monte Carlo post-hoc tests were conducted after Kruskal–Wallis and chi-square tests, respectively.

To determine if there were significant differences between day 0 and 6 scores (SOFA or APACHE II) within the same group, paired *t*-test and Wilcoxon signed-rank test were used for parametric and nonparametric data, respectively.

Kaplan–Meier and log rank test were used to compare ICU mortality between HR groups. Cox's proportional hazards model was used to identify significant independent predictors associated with ICU mortality with calculation of the hazard ratios and 95% confidence intervals. Univariate models were used for determining which variables could be associated with ICU mortality in HR groups (60 patients). The tested variables in the univariate model included the effect of study treatment (CB and DP interventions compared to no intervention in the HR-C group), the initial GCS (three to eight versus higher GCS), the need for vasopressors, ISS (≥25 versus lower ISS), sepsis development (by the end of the first week), and needing mechanical ventilation at admission. Only variables that showed statistical significance in univariate models were included in the multivariate model.

Receiver operating characteristics (ROC) curve was used to evaluate the predictive ability of different sepsis predictors (MCP-1, ISS, 100-LAR, and combinations of 100-LAR + ISS or MCP-1+ISS) among the HR-C and LR groups. Test performance for predictors was evaluated as failed (AUC, 0.5–0.6), poor (AUC, 0.6–0.7), fair (AUC, 0.7–0.8), good (AUC, 0.8–0.9), and excellent (0.9–1) (Hosmer et al., 2013). Probability value (*p*-value) ≤ 0.05 was considered statistically significant.

3 RESULTS

Between February and November 2020, 156 patients were evaluated. After ruling out patients who did not fulfill the study criteria, 112 patients were enrolled after obtaining informed consent. Then, 27 patients were excluded as they did not complete the steps of the study. Afterward, 85 patients had successfully completed the study (**Figure 1**).

3.1 Patients' Demographics, Initial Ventilatory Status, and Basal Lab Values

Patients' demographic data and initial ventilatory status (**Table 1**) showed no statistically significant difference between groups. **Table 2** demonstrates the basal laboratory values. The highest value of LAR was found in the LR group, showing significant increase when compared to the other three groups (*p*-value < 0.0001). Similarly, arterial oxygen saturation and serum 25-hydroxyvitamin D level were significantly high in the LR group compared to high-risk groups with *p*-values of 0.002 and <0.0001, respectively.

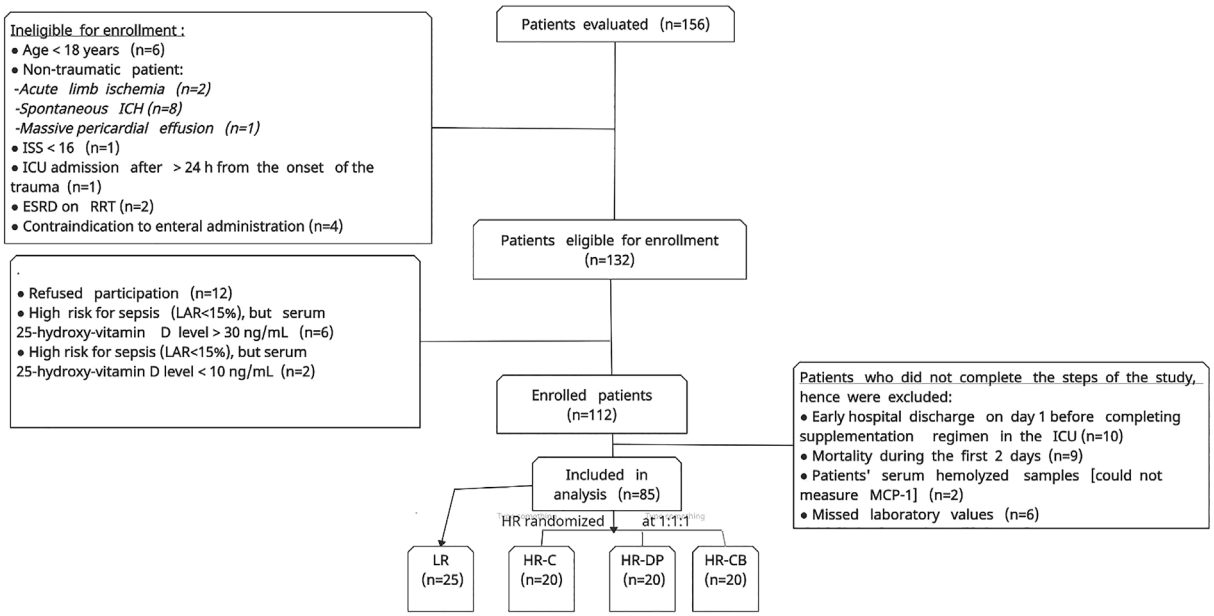

FIGURE 1 | Flow chart of patient enrollment process. ICH: intracerebral hemorrhage, ISS: injury severity score, ESRD: end-stage renal disease, RRT: renal replacement therapy, LR: low risk for sepsis group, HR-C: high risk for sepsis control group, HR-DP: high risk for sepsis vitamin D and probiotics group, HR-CB: high risk for sepsis vitamin C and vitamin B1 group, MCP-1: monocyte chemoattractant protein-1. LAR: leukocyte anti-sedimentation rate.

TABLE 1 | Patients' demographics and initial ventilatory status on admission in each group.

Characteristic	LR (*n* = 25)	HR-C (*n* = 20)	HR-DP (*n* = 20)	HR-CB (*n* = 20)	*p*-value
Age (years)	42.52 ± 18.84	48.75 ± 19.65	44.95 ± 17.54	42.15 ± 15.90	0.63[a]
Male/female number (%)	23 (92%)/2 (8%)	19 (95%)/1 (5%)	17 (85%)/3 (15%)	16 (80%)/4 (20%)	0.47[b]
Height (cm)	165.00 (160.00,170.00)	167.50 (161.25,173.00)	167.50 (160.00,173.00)	165.00 (160.00,171.50)	0.65[c]
Weight (kg)	74.72 ± 7.00	74.50 ± 7.24	74.50 ± 6.67	72.00 ± 7.33	0.56[a]
Comorbidities					
No comorbidities	19 (70.4%)	13 (52%)	13 (54.2%)	17 (77.3%)	0.83[b]
Hypertension	2 (7.4%)	4 (16%)	4 (16.7%)	2 (9.1%)	
Diabetes mellitus	2 (7.4%)	4 (16%)	4 (16.7%)	2 (9.1%)	
Chronic liver disease	2 (7.4%)	2 (8%)	1 (4.2%)	1 (4.5%)	
History of cerebral stroke	2 (7.4%)	0 (0%)	1 (4.2%)	0 (0%)	
Other comorbidities	0 (0%)	2 (8%)	1 (4.2%)	0 (0%)	
Ventilatory status on day 0					0.49[b]
On room air	13 (52%)	5 (25%)	6 (30%)	12 (60%)	
On nasal cannula	2 (8%)	1 (5%)	1 (5%)	1 (5%)	
On Oxygen mask	5 (20%)	5 (25%)	5 (25%)	3 (15%)	
On Mechanical ventilation	5 (20%)	9 (45%)	8 (40%)	4 (20%)	

Data are mean ± standard deviation, median (interquartile range) or number (incidence). LR: low risk for sepsis group, HR-C: high risk for sepsis control group, HR-DP: high risk for sepsis vitamin D and probiotics group, HR-CB: high risk for sepsis vitamin C and vitamin B1 group.

[a]: Analysis of variance (ANOVA) used to detect differences among groups.

[b]: Monte Carlo test with 95% confidence interval used to detect differences among groups.

[c]: Kruskal–Wallis test used to detect differences among groups.

3.2 Injury Characteristics of Each Group

There were no significant differences between the groups with respect to ISS, cause of trauma, and primary diagnosis (type of trauma), even in the segmental injury description. Intracranial hematoma (≤100 ml or unspecified) represented the most prevalent injury in all patient groups either isolated or combined with other traumas (**Tables 3**, **4**).

3.3 Change in Inflammatory Indices on Day 6 Compared to Day 0

Table 5 shows the serum levels of the investigated inflammatory indices on day 0 and 6 in each group. The MCP-1 level was significantly high on day 0 in HR groups compared to the LR group (p-value < 0.0001). On day 6, a significant decrease was

TABLE 2 | Basal laboratory values.

Laboratory test	LR (*n* = 25)	HR-C (*n* = 20)	HR-DP (*n* = 20)	HR-CB (*n* = 20)	*p*-value
Day 0					
Virology					
HBV positive	0 (0%)	2 (10%)	0 (0%)	2 (10%)	0.24[e]
HCV positive	7 (28%)	6 (30%)	3 (15%)	3 (15%)	0.58[e]
Hemoglobin (g/dl)	12.1 (10.40, 12.75)	12.15 (10.20, 13.8)	11.25 (9.60, 13.05)	11.55 (10.03, 13.43)	0.73[c]
MCHC (g/dl)	33 (32.10, 33.85)	32.30 (31.20, 33.25)	33.05 (32.03, 33.30)	33.25 (32.30, 33.78)	0.064[c]
Prothrombin time (seconds)	15 (14.35, 15.80)	15.55 (14.63, 16.50)	14.85 (13.90, 16.08)	15.35 (14.80, 16.20)	0.47[c]
INR	1.15 (1.08, 1.28)	1.20 (1.10, 1.32)	1.13 (1.03, 1.25)	1.2 (1.13, 1.30)	0.41[c]
Lymphocyte %	8.1 (6.95, 11.95)	8.45 (6.30, 12.00)	8.25 (6.70, 11.73)	9.35 (6.63, 13.05)	0.96[c]
ALT (U/L)	28 (25.00, 44.1)	44 (29.75, 68.75)	32 (27.00, 66.25)	26 (21.50, 75.50)	0.31[c]
Albumin (g/dl)	3.67 ± 0.67	3.52 ± 0.68	3.55 ± 0.72	3.83 ± 0.66	0.47[a]
Serum calcium (mg/dl)	7.55 ± 0.94	7.88 ± 0.76	7.74 ± 0.95	7.86 ± 0.92	0.59[a]
RBG (mg/dl)	163.00 (140.00,187.00)	180.00 (152.50,252.00)	187.50 (143.50,239.00)	168.50 (154.00,211.00)	0.29[c]
Blood gases					
PH	7.39 (7.37, 7.43)	7.37 (7.31, 7.40)	7.37 (7.33, 7.42)	7.37 (7.31, 7.40)	0.059[c]
$PaCO_2$ (mmHg)	35.26 ± 6.08	34.73 ± 8.42	33.29 ± 7.58	34.47 ± 5.63	0.82[a]
SaO_2 (%)	97.60 (93.00,100.00)	87.35 (64.28, 95.93)[f]	80.40 (62.43, 93.10)[f]	93.35 (65.78, 97.50)[f]	<0.0001[d]
Serum 25-hydroxy vitamin D level (ng/ml)	32.30 (25.05, 36.91)	16.00 (12.22, 21.63)[f]	16.22 (12.12, 23.32)[f]	20.50 (17.50, 23.00)[f]	<0.0001[d]
Day 1					
LAR (%)	34.15 ± 9.18	5.60 ± 3.17[f]	6.00 ± 2.71[f]	6.68 ± 4.28[f]	<0.0001[b]

Data are mean ± standard deviation, median (interquartile range) or number (incidence). LR: low risk for sepsis group, HR-C: high risk for sepsis control group, HR-DP: high risk for sepsis vitamin D and probiotics group, HR-CB: high risk for sepsis vitamin C and vitamin B1 group. MCHC: mean corpuscular hemoglobin concentration, INR: international normalized ratio, ALT: alanine aminotransferase, HBV: hepatitis B virus, HCV: hepatitis C virus, $PaCO_2$: arterial partial pressure of carbon dioxide, SaO_2: arterial oxygen saturation, LAR: leukocyte anti-sedimentation rate, RBG: random blood glucose.

[a]: Analysis of variance (ANOVA) used to detect differences among groups.

[b]: Analysis of variance (ANOVA) followed by post-hoc test according to homogeneity of variances (Levine's test), where we used Bonferroni post-hoc test if equal variances were assumed and Games-Howell post-hoc test if no homogeneity of variances was found. For both Bonferroni and Games-Howell post-hoc tests, the mean difference was significant at the 0.05 level.

[c]: Kruskal–Wallis test used to detect differences among groups.

[d]: Kruskal–Wallis test followed by post-hoc test (Dunn's test).

[e]: Monte Carlo test with 95% confidence interval used to detect differences among groups.

[f]= significant with LR group. Significance level at p-value ≤ 0.05.

TABLE 3 | Injury characteristics of patients in each group.

	LR (*n* = 25)	HR-C (*n* = 20)	HR-DP (*n* = 20)	HR-CB (*n* = 20)	*p*-value
ISS	16 (16, 21)	20 (16, 25)	19 (16, 24.25)	21 (17, 28.5)	0.07[a]
Cause of trauma					
Road traffic accident	15 (60%)	11 (55%)	15 (75%)	14 (70%)	0.32[b]
Stab (abdomen or chest)	2 (8%)	1 (5%)	0 (0%)	1 (5%)	
Fall injury (from height, to the ground or downstairs)	8 (32%)	8 (40%)	5 (25%)	5 (25%)	
Primary diagnosis					
Multiple trauma	11 (44%)	14 (70%)	12 (60%)	16 (80%)	0.24[b]
Head trauma	8 (32%)	3 (15%)	6 (30%)	3 (15%)	
Spine trauma	0 (0%)	1 (5%)	0 (0%)	0 (0%)	
Extremity trauma	2 (8%)	0 (0%)	0 (0%)	1 (5%)	
Thoracic trauma	1 (4%)	2 (10%)	1 (5%)	0 (0%)	
Abdominal trauma	3 (12%)	0 (0%)	1 (5%)	0 (0%)	

Data are median (interquartile range) or number (incidence). LR: low risk for sepsis group, HR-C: high risk for sepsis control group, HR-DP: high risk for sepsis vitamin D and probiotics group, HR-CB: high risk for sepsis vitamin C and vitamin B1 group. ISS: injury severity score.

[a]: Kruskal–Wallis test used to detect differences among groups.

[b]: Monte Carlo test with 95% confidence interval used to detect differences among groups.

detected in both HR-CB and HR-DP groups compared to the HR-C group (p-value = 0.006).

Comparing the serum MCP-1 levels within the same group, the HR-C group showed a significant increase in MCP-1 level on day 6 compared to day 0 (p-value = 0.014). Interestingly, both HR-DP and HR-CB groups showed a significant decrease in MCP-1 level on day 6 compared to that on day 0 (p-value < 0.0001).

The ESR, at the first and second hours, revealed no significant differences between groups. Within the same group, the ESR showed a significant increase in the HR-DP and HR-C groups on

TABLE 4 | Segmental injury descriptions in study groups.

	LR (*n* = 25)	HR-C (*n* = 20)	HR-DP (*n* = 20)	HR-CB (*n* = 20)	*p*-value
Hematoma epidural, subdural or intracranial ≤ 100 ml or unspecified	10 (20.8%)	7 (16.7%)	10 (25.6%)	11 (20.4%)	0.95[a]
Traumatic subarachnoid hemorrhage	2 (4.2%)	1 (2.4%)	1 (2.6%)	2 (3.7%)	
Traumatic cerebral edema	2 (4.2%)	2 (4.8%)	2 (5.1%)	3 (5.6%)	
Fracture base without CSF leak	3 (6.3%)	2 (4.8%)	2 (5.1%)	3 (5.6%)	
Fracture orbit, maxilla or zygoma (unspecified)	1 (2.1%)	0 (0%)	3 (7.7%)	1 (1.9%)	
Fracture orbit open or displaced	1 (2.1%)	1 (2.4%)	1 (2.6%)	0 (0%)	
Cervical cord lesion (incomplete) with preservation of significant sensation	0 (0%)	1 (2.4%)	1 (2.6%)	1 (1.9%)	
Dislocation or fracture of thoracic or lumbar spine (unspecified)	0 (0%)	1 (2.4%)	0 (0%)	0 (0%)	
Dislocation of lamina, body, facet, or pedicle of thoracic spine	1 (2.1%)	0 (0%)	0 (0%)	0 (0%)	
Fracture radius, ulna, clavicle, scapula, tibia, fibula, or tarsals	4 (8.3%)	5 (11.9%)	4 (10.3%)	9 (16.7%)	
Fracture tibia, radius, or ulna open or displaced	4 (8.3%)	2 (4.8%)	1 (2.6%)	3 (5.6%)	
Sprain or contusion wrist	3 (6.3%)	4 (9.5%)	0 (0%)	3 (5.6%)	
Fracture femur (open)	1 (2.1%)	1 (2.4%)	0 (0%)	0 (0%)	
Traumatic above knee amputation	1 (2.1%)	0 (0%)	0 (0%)	1 (1.9%)	
Multi-lobar lung contusion	3 (6.3%)	5 (11.9%)	5 (12.8%)	2 (3.7%)	
Lung contusion< 1 lobe	5 (10.4%)	2 (4.8%)	2 (5.1%)	3 (5.6%)	
Bilateral hemothorax	1 (2.1%)	3 (7.1%)	0 (0%)	1 (1.9%)	
Bilateral pneumothorax	1 (2.1%)	3 (7.1%)	1 (2.6%)	3 (5.6%)	
Unilateral pneumothorax	0 (0%)	0 (0%)	1 (2.6%)	2 (3.7%)	
Unilateral hemothorax	0 (0%)	0 (0%)	1 (2.6%)	3 (5.6%)	
Rib fracture with pneumothorax	0 (0%)	1 (2.4%)	1 (2.6%)	2 (3.7%)	
Superficial or unspecified laceration of duodenum, ileum, or liver	2 (4.2%)	0 (0%)	0 (0%)	1 (1.9%)	
Grade III splenic hematoma	2 (4.2%)	0 (0%)	1 (2.6%)	0 (0%)	
Retroperitoneal hematoma, symphysis pubis separation	1 (2.1%)	0 (0%)	1 (2.6%)	0 (0%)	
Minor contusion kidney	0 (0%)	1 (2.4%)	1 (2.6%)	0 (0%)	

Data are number (incidence). LR: low risk for sepsis group, HR-C: high risk for sepsis control group, HR-DP: high risk for sepsis vitamin D and probiotics group, HR-CB: high risk for sepsis vitamin C and vitamin B1 group. CSF: cerebrospinal fluid.

[a]: Monte Carlo test with 95% confidence interval used to detect differences among groups.

day 6 compared to that on day 0 at both the first and second hours (p-value ≤ 0.05).

The serum CRP level on day 6 revealed a significant decrease in both the LR and HR-CB groups compared to that in the HR-C group (p-value = 0.03). Within the same group, the HR-CB group showed a significant decrease in serum CRP level on day 6 compared to that on day 0 (p-value = 0.02).

3.4 APACHE II and SOFA Scores

Monitoring the improvement (decrease) or deterioration (increase) in clinical and laboratory items of APACHE II score on day 6 compared to those on day 0 within the same group, the HR-C group showed a significant deterioration in APACHE II score (p-value = 0.014). Noteworthily, the LR, HR-DP, and HR-CB groups showed a significant improvement in APACHE II score on day 6 compared to their initial score on day 0 (p-value = 0.003, 0.003 and <0.0001 for LR, HR-DP and HR-CB groups, respectively) and a significant improvement compared to the HR-C group on day 6 (**Tables 6**, **7**, **Supplementary Figure S1A**).

Comparing the increase or decrease in parameters of SOFA score from day 0 to day 6 within the same group, the HR-C group showed a significant deterioration in SOFA score on day 6 compared to its initial score on day 0 (p-value = 0.002), while the LR, HR-DP, and HR-CB groups showed a significant improvement in SOFA score (p-value = 0.04, 0.026, and 0.02 for LR, HR-DP, and HR-CB groups, respectively). Furthermore, a significant improvement was observed in SOFA score of the HR-DP, HR-CB, and LR groups compared to the HR-C group on day 6 (**Tables 8**, **9**, **Supplementary Figure S1B**).

3.5 Patients Who Completed Treatment Regimen in the ICU, but Transferred Outside, Died, or Discharged to Ward Before Day 6

Three, three, two, and one patient in the LR, HR-C, HR-DP, and HR-CB groups, respectively, died or were discharged home before day 6 but after completing the study treatment regimen in the ICU. However, two, one, two, and four patients in the LR, HR-C, HR-DP, and HR-CB groups, respectively, were discharged to the ward before day 6 and after completion of the study regimen in the ICU.

3.6 Sepsis Development

The incidence of sepsis by the end of the first week in each group according to the sepsis-3 criteria (Singer et al., 2016) is presented in **Figure 2A**. The highest incidence of sepsis development was revealed in the HR-C group compared to the other three groups (p-value = 0.004). The coagulase negative *Staphylococcus aureus* (CONS) represented the most abundant species isolated from positive aerobic blood cultures in all groups (**Supplementary Figure S2**).

3.7 Duration of Mechanical Ventilation

Patients in the LR, HR-DP, and HR-CB groups who needed mechanical ventilation upon admission had a significantly shorter duration of mechanical ventilation compared to the HR-C group by the end of the first week (p-value = 0.014) (**Figure 2B**).

TABLE 5 | Serum levels of inflammatory indices among groups on day 0 and day 6.

Serum level	Day	LR (n = 25)	HR-C (n = 20)	HR-DP (n = 20)	HR-CB (n = 20)	p-value
MCP-1 (pg/ml)	Day 0	89.26 (57.29,133.97)	193.07 (118.67,427.23)[a]	320.15 (172.86,493.62)[a]	351.82 (179.37,759.99)[a]	<0.0001[h]
	Day 6	—	247.56 (191.15, 503.30)[d]	151.83 (81.50, 274.13)[b,d]	144.79 (82.94, 187.12)[b,d]	0.006[h]
—	Delta MCP-1	—	44.82 (17.49, 119.67)	−113.61 (−283.54, −76.62)[b]	−219.30 (−494.19, −109.43)[b]	<0.0001[h]
ESR 1st hour	Day 0	32.00 (16.00, 50.00)	24.00 (10.00, 50.00)	26.00 (9.00, 39.00)	29.00 (19.25, 62.25)	0.47[g]
(mm/h)	Day 6	31.00 (15.00, 57.50)	53.50 (27.50, 87.50)[d]	37.50 (20, 63.75)[d]	46.50 (26.25, 58.75)	0.15[g]
—	Delta ESR 1st hour	1.56 ± 19.87[b]	24.25 ± 24.28	14.65 ± 29.70	4.75 ± 26.65	0.02[f]
ESR 2nd hour	Day 0	64.16 ± 38.04	55.15 ± 39.55	51.20 ± 30.56	68.65 ± 38.54	0.41[e]
(mm/h)	Day 6	60.00 (30.00,100.00)	85.00 (57.50,120.00)[d]	82.50 (41.25,107.50)[d]	79.50 (52.50, 99.50)	0.13[g]
—	Delta ESR 2nd hour	−1.16 ± 38.80[b]	31.10 ± 30.19	23.90 ± 37.52	10.90 ± 35.60	0.02[f]
CRP (mg/L)	Day 0	24.00 (12.00, 48.00)	36.00 (15.00, 84.00)	48.00 (15.00, 48.00)	48.00 (24.00, 88.09)	0.31[g]
	Day 6	12.00 (6.00, 48.00)[b]	36.00 (24.00, 96.00)	48.00 (15.00, 96.00)	24.00 (12.00, 48.00)[b,d]	0.03[h]
—	Delta CRP	0.00 (−15.00, 0.00)	2.20 (0.00, 40.50)	0.00 (−24.00, 42.00)	−30.00 (−48.00, 0.00)[b,c]	0.008[h]

Data are mean ± standard deviation or median (interquartile range). LR: low risk for sepsis group, HR-C: high risk for sepsis control group, HR-DP: high risk for sepsis vitamin D and probiotics group, HR-CB: high risk for sepsis vitamin C and vitamin B1 group. MCP-1: monocyte chemoattractant protein-1, ESR: erythrocyte sedimentation rate, CRP: C-reactive protein. Delta MCP-1: change in monocyte chemoattractant protein-1 on day 6 compared to day 0, Delta ESR 1st hour: change in erythrocyte sedimentation rate value of first hour on day 6 compared to day 0, Delta ESR 2nd hour: change in erythrocyte sedimentation rate value of second hour on day 6 compared to day 0, Delta CRP: change in C-reactive protein on day 6 compared to day 0.

[a]= Significant with LR group.

[b]= Significant with HR-C group.

[c]= Significant with HR-DP group.

[d]= Significant difference between day 0 and day 6 serum level of inflammatory index within the same group. Significance level at p-value ≤ 0.05.

[e]: Analysis of variance (ANOVA) used to detect differences between groups.

[f]: Analysis of variance (ANOVA) followed by post-hoc test according to homogeneity of variances (Levine's test), where we used Bonferroni post-hoc test if equal variances were assumed and Games-Howell post-hoc test if no homogeneity of variances was found. For both Bonferroni and Games-Howell post-hoc tests, the mean difference was significant at 0.05 level.

[g]: Kruskal–Wallis test used to detect differences between groups.

[h]: Kruskal–Wallis test followed by post-hoc test (Dunn's test).

TABLE 6 | Clinical and laboratory items of the Acute Physiologic Assessment and Chronic Health Evaluation score II (APACHE II) on day 0.

Variable	LR (n = 25)	HR-C (n = 20)	HR-DP (n = 20)	HR-CB (n = 20)	p-value
Day 0 APACHE II score	12.64 ± 4.55[a]	15.45 ± 6.57	16.30 ± 4.29	13.10 ± 3.84	0.044[c]
Variables of day 0 APACHE II score					
Temperature (°C)	36.30 (36.10, 37.00)	36.40 (36.10, 37.88)	36.55 (36.23, 37.10)	36.45 (36.20, 37.58)	0.52[d]
MAP (mmHg)	88.44 ± 10.46[a]	85.93 ± 11.48	79.59 ± 6.56	87.70 ± 11.40	0.03[c]
HR (beats/min)	101.00 (71.00,117.00)	110.00 (97.00,119.75)	108.50 (93.75,122.00)	105.00 (94.50,110.00)	0.51[d]
RR (breaths/min)	25.00 (21.50, 27.00)	22.00 (20.00, 27.50)	25.00 (21.25, 27.75)	25.00 (20.50, 27.00)	0.77[d]
GCS	13.00 (9.50, 15.00)	13.50 (10.25, 15.00)	10.00 (8.00, 14.00)	13.50 (10.00, 15.00)	0.47[d]
A-aO_2 (mmHg)	326.90 (318.65,328.10)	322.40 (300.70,454.03)	309.60 (270.28,333.03)	325.70 (253.40,382.00)	0.86[d]
PaO_2 (mmHg)	91.85 (69.65,124.58)	73.30 (38.88,127.5)	60.45 (40.68, 86.15)	63.90 (41.80, 82.95)	0.08[d]
Serum sodium (mmol/L)	141.00 (136.50,142.95)	142.75 (136.25,143.75)	138.00 (136.40,142.75)	140.40 (137.25,141.23)	0.28[d]
Serum potassium (mmol/L)	3.10 (2.60, 3.42)	3.33 (2.53, 3.60)	3.22 (2.70, 3.50)	3.17 (2.66, 3.40)	0.84[d]
Serum bicarbonate (mmol/L)	20.81 ± 4.16	18.95 ± 3.51	19.96 ± 3.48	19.72 ± 3.34	0.41[b]
Cr (mg/dl)	1.00 (0.82, 1.13)	1.16 (0.98, 1.50)	1.07 (1.01, 1.33)	1.05 (0.88, 1.34)	0.14[d]
HCT (%)	35.16 ± 6.32	35.45 ± 7.05	33.16 ± 6.14	34.61 ± 6.84	0.69[b]
WBCs (cells/mm^3)	16.00 (10.25, 20.45)	17.85 (15.18, 21.40)	18.30 (14.65, 23.38)	17.40 (12.20, 21.68)	0.34[d]

Data are mean ± standard deviation, median (interquartile range). LR: low risk for sepsis group, HR-C: high risk for sepsis control group, HR-DP: high risk for sepsis vitamin D and probiotics group, HR-CB: high risk for sepsis vitamin C and vitamin B1 group, MAP: mean arterial blood pressure, HR: heart rate, RR: respiratory rate, GCS: Glasgow coma score, A-a O_2: alveolo-arterial oxygen gradient, PaO_2: arterial partial pressure of oxygen, HCT: hematocrit, WBC: white blood cells count.

[a]= Significant with HR-DP group. Significance level at p-value ≤ 0.05.

[b]: Analysis of variance (ANOVA) used to detect differences between groups.

[c]: Analysis of variance (ANOVA) followed by post-hoc test according to homogeneity of variances (Levine's test), where we used Bonferroni post-hoc test if equal variances were assumed and Games-Howell post-hoc test if no homogeneity of variances was found. For both Bonferroni and Games-Howell post-hoc tests, the mean difference was significant at 0.05 level.

[d]: Kruskal–Wallis test used to detect differences between groups.

TABLE 7 | Clinical and laboratory items of the Acute Physiologic Assessment and Chronic Health Evaluation score II (APACHE II) on day 6.

Variable	LR (*n* = 25)	HR-C (*n* = 20)	HR-DP (*n* = 20)	HR-CB (*n* = 20)	*p*-value
Day 6 APACHE II score	7.00 (5.50, 13.00)[a,c]	17.50 (11.75, 25.75)[c]	10.00 (6.25, 14.50)[a,c]	8.00 (5.00, 11.75) [a,c]	<0.0001[g]
Variables of day 6 APACHE II score					
Temperature (°C)	36.40 (36.00, 37.00)[a]	35.85 (34.85, 36.33)	36.45 (36.10, 37.00)[a]	36.45 (36.00, 37.00)[a]	0.011[g]
MAP (mmHg)	89.38 ± 9.54	80.38 ± 15.93	85.65 ± 5.67	91.75 ± 7.44[a,b]	0.005[e]
HR (beats/min)	94.35 ± 21.84[a]	118.35 ± 30.77	93.90 ± 18.73[a]	89.80 ± 20.91[a]	0.001[e]
RR (breaths/min)	22.00 (20.00, 24.50)[a]	25.00 (23.50, 27.75)	22.00 (20.00, 24.00)[a]	22.00 (20.50, 25.75)[a]	0.012[g]
GCS	15.00 (13.00, 15.00)[a,b]	12.00 (5.25, 13.00)	13.00 (9.25, 15.00)	14.00 (12.00, 15.00)[a]	0.001[g]
A-aO_2 (mmHg)	—	290.20 (265.90,324.55)	250.65 (223.20,278.1)	291.70 (231.05,332.40)	0.52[f]
PaO_2 (mmHg)	80.80 (62.23,104.50)	72.70 (44.50, 91.10)	79.35 (65.68, 88.68)	96.70 (47.33,108.78)	0.44[f]
Serum sodium (mmol/L)	139.70 (137.00,144.05)[a]	146.00 (139.70,160.75)	140.00 (137.00,143.95)[a]	137.65 (135.00,143.00)[a]	0.006[g]
Serum potassium (mmol/L)	3.23 (2.94, 3.54)	3.20 (2.85, 3.40)	3.05 (2.83, 3.50)	3.20 (2.79, 3.58)	0.96[f]
Serum bicarbonate (mmol/L)	24.65 ± 3.86	24.12 ± 5.00	24.54 ± 4.67	24.54 ± 2.76	0.98[d]
Serum creatinine (mg/dl)	0.86 (0.70, 1.1)[a]	1.04 (0.93, 1.75)	0.83 (0.76, 1.20)	0.80 (0.67, 0.89)[a]	0.01[g]
HCT (%)	32.33 ± 6.93	32.54 ± 7.43	31.26 ± 6.40	31.58 ± 5.21	0.91[d]
WBCs (cells/mm^3)	10.50 (7.44, 12.25)	11.65 (9.05, 13.23)	12.65 (7.90, 15.00)	10.25 (8.45, 13.18)	0.35[f]
Delta APACHE II (day 6 compared to day 0)	−3.00 (−7.00, −1.00)[a,c]	3(−0.75, 5.00)[c]	−7.00 (−8.00, −2.00)[a,c]	−4.00 (−7.50, −2.00)[a,c]	<0.0001[g]

Data are mean ± standard deviation, median (interquartile range). LR: low risk for sepsis group, HR-C: high risk for sepsis control group, HR-DP: high risk for sepsis vitamin D and probiotics group, HR-CB: high risk for sepsis vitamin C and vitamin B1 group, MAP: mean arterial blood pressure, HR: heart rate, RR: respiratory rate, GCS: Glasgow coma score, A-a O_2: alveolo-arterial oxygen gradient, PaO_2: arterial partial pressure of oxygen, HCT: hematocrit, WBC: white blood cells count.

[a]= Significant with HR-C group.

[b]= Significant with HR-DP group.

[c]= Significant difference between day 0 and day 6 score within the same group. Significance level at p*-value ≤ 0.05. For A-aO_2 on day 6 APACHE II, only one value existed for LR group (A-aO_2 = 309.7 mmHg) and thus could not obtain median (IQR).*

[d]: Analysis of variance (ANOVA) used to detect differences between groups.

[e]: Analysis of variance (ANOVA) followed by post-hoc test according to homogeneity of variances (Levine's test), where we used Bonferroni post-hoc test if equal variances were assumed and Games-Howell post-hoc test if no homogeneity of variances was found. For both Bonferroni and Games-Howell post-hoc tests, the mean difference was significant at 0.05 level.

[f]: Kruskal–Wallis test used to detect differences between groups.

[g]: Kruskal–Wallis test followed by post-hoc test (Dunn's test).

TABLE 8 | Clinical and laboratory items of Sequential Organ Failure Assessment (SOFA) score on day 0.

Variable	LR (*n* = 25)	HR-C (*n* = 20)	HR-DP (*n* = 20)	HR-CB (*n* = 20)	*p*-value
Day 0 SOFA score	3.00 (2.00, 4.50)[b]	4.50 (3.00, 7.00)	6.00 (4.25, 6.75)	3.50 (3.00, 5.00)[b]	0.001[f]
Variables of SOFA score on day 0					
PaO_2 (mmHg)	89.50 (63.75,125.15)	75.15 (56.75, 98.15)	65.30 (46.70,101.18)	66.00 (43.38, 79.1)	0.15[e]
FiO_2	0.21 (0.21, 0.40)	0.40 (0.23, 0.60)	0.40 (0.21, 0.60)	0.21 (0.21, 0.58)	0.10[e]
PaO_2/FiO_2	340.00 (217.99,450.00)[a, b]	139.17 (102.53,340.50)	175.00 (133.13,242.92)	231.19 (104.00,344.29)	0.76[f]
PLT (K/uL)	166.00 (132.00,226.50)	197.00 (143.00,226.75)	146.00 (138.25,194.75)	177.00 (128.75,220.00)	0.49[e]
Bilirubin (mg/dl)	0.58 (0.49, 0.78)	0.51 (0.39, 0.77)	0.65 (0.43, 0.99)	0.67 (0.46, 1.27)	0.27[e]
MAP (mmHg)	88.44 ± 10.46[b]	85.93 ± 11.48	79.59 ± 6.56	87.7 ± 11.40	0.03[c]
On vasopressors (Dopamine, Epinephrine or Norepinephrine)	1 (4%)	2 (10%)	1 (5%)	0 (0%)	0.73[d]
GCS	13.00 (9.50, 15.00)	13.50 (10.25, 15.00)	10.00 (8.00, 14.00)	13.50 (10.00, 15.00)	0.47[e]
Serum Creatinine (mg/dl)	1.00 (0.82, 1.13)	1.16 (0.98, 1.50)	1.07 (1.01, 1.33)	1.05 (0.88, 1.34)	0.14[e]

Data are mean ± standard deviation, median (interquartile range) or number (incidence). LR: low risk for sepsis group, HR-C: high risk for sepsis control group, HR-DP: high risk for sepsis vitamin D and probiotics group, HR-CB: high risk for sepsis vitamin C and vitamin B1 group. PaO_2: arterial partial pressure of oxygen, FiO_2: fraction of inspired oxygen, PLT: platelets, MAP: mean arterial blood pressure, GCS: Glasgow coma score.

[a]= Significant with HR-C group.

[b]= Significant with HR-DP group. Significance level at p*-value ≤ 0.05.*

[c]: Analysis of variance (ANOVA) followed by post-hoc test according to homogeneity of variances (Levine's test), where we used Bonferroni post-hoc test if equal variances were assumed and Games-Howell post-hoc test if no homogeneity of variances was found. For both Bonferroni and Games-Howell post-hoc tests, the mean difference was significant at 0.05 level.

[d]: Monte Carlo test with 95% confidence interval used to detect differences among groups.

[e]: Kruskal–Wallis test used to detect differences among groups.

[f]: Kruskal–Wallis test followed by post-hoc test (Dunn's test).

TABLE 9 | Clinical and laboratory items of Sequential Organ Failure Assessment (SOFA) score on day 6.

Variable	LR (*n* = 25)	HR-C (*n* = 20)	HR-DP (*n* = 20)	HR-CB (*n* = 20)	*p*-value
Day 6 SOFA score	2.00 (1.00, 3.50)[a, b, c]	7.00 (3.00, 9.75)[c]	4.00 (2.25, 6.00) [c]	2.00 (1.00, 4.00)[a, b, c]	<0.0001[g]
Variables of SOFA score on day 6					
PaO_2 (mmHg)	79.80 (60.85,100.45)	78.05 (42.78, 94.20)	80.85 (67.10, 99.40)	95.95 (51.60, 109.45)	0.48[f]
FiO_2	0.21 (0.21, 0.22)[a]	0.51 (0.40, 0.60)	0.21 (0.21, 0.40)[a]	0.21 (0.21, 0.40)[a]	<0.0001[g]
PaO_2/FiO_2	353.81 (221.67,460.71)[a]	157.08 (88.46, 227.60)	254.29 (181.55, 391.18)[a]	284.25 (184.12, 464.64)[a]	0.001[g]
PLT (K/uL)	174.00 (147.50, 228.50)[b]	166.00 (105.75, 249.00)	127.50 (108.75, 181.00)	180.00 (165.50, 232.25) [b]	0.04[g]
Bilirubin (mg/dl)	0.69 (0.52, 0.96)	0.81 (0.56, 1.10)	0.80 (0.63, 1.15)	0.60 (0.45, 0.93)	0.38[f]
MAP (mmHg)	89.38 ± 9.54	80.38 ± 15.93	85.65 ± 5.67	91.75 ± 7.44[a, b]	0.005[d]
On Vasopressors (Dopamine, Epinephrine or Norepinephrine)	0 (0%)[a]	7 (35%)	0 (0%)[a]	0 (0%)[a]	<0.0001[e]
GCS	15.00 (13.00, 15.00)[a, b]	12.00 (5.25, 13.00)	13.00 (9.25, 15.00)	14.00 (12.00, 15.00)[a]	0.001[g]
Serum Creatinine (mg/dl)	0.86 (0.70, 1.10)[a]	1.04 (0.93, 1.75)	0.83 (0.76, 1.20)	0.80 (0.67, 0.89)[a]	0.01[g]
Delta SOFA (on day 6 compared to day 0)	−1.00 (−2.00, 0.50)[a, c]	2.00 (0.00, 4.50)[c]	−2.00 (−3.00, 0.75)[a, c]	−1.50 (−3.00, 0.00)[a, c]	<0.0001[g]

Data are mean ± standard deviation, median (interquartile range) or number (incidence). LR: low risk for sepsis group, HR-C: high risk for sepsis control group, HR-DP: high risk for sepsis vitamin D and probiotics group, HR-CB: high risk for sepsis vitamin C and vitamin B1 group. PaO_2: arterial partial pressure of oxygen, FiO_2: fraction of inspired oxygen, PLT: platelets, MAP: mean arterial blood pressure, GCS: Glasgow coma score.

[a]= Significant with HR-C group

[b]= significant with HR-DP group.

[c]= Significant difference between day 0 and day 6 score within the same group. Significance level at p-value ≤ 0.05.

[d]: Analysis of variance (ANOVA) followed by post-hoc test according to homogeneity of variances (Levine's test), where we used Bonferroni post-hoc test if equal variances were assumed and Games-Howell post-hoc test if no homogeneity of variances was found. For both Bonferroni and Games-Howell post-hoc tests, the mean difference was significant at 0.05 level.

[e]: Monte Carlo test with 95% confidence interval followed by post-hoc test where significant p-value is determined against adjusted α = 0.00625 (when using Bonferroni correction).

[f]: Kruskal Wallis test used to detect differences among groups.

[g]: Kruskal Wallis test followed by post-hoc test (Dunn's test).

3.8 Mortality, ICU Discharge, and Hospital Discharge

During the first 28 days, both LR and HR-CB groups showed a significant increase in ICU (p-value = 0.001) and hospital discharge (p-value = 0.001) (**Figures 3A,B**) in addition to a significant decrease in mortality incidence (p-value = 0.001) (**Figure 3C**) compared to the HR-C group.

3.9 Incidence of AKI

To evaluate the occurrence of AKI among the study population, serum creatinine levels on day 6 were compared to the initial values on day 0. It was observed that 10 patients developed AKI. These patients were distributed as follows: two, five, one, and two patients in the LR, HR-C, HR-CB, and HR-DP groups, respectively, with no statistically significant differences (p-value = 0.22).

3.10 Survival Analysis and Multivariate Cox Proportional Hazard Model

Survival analysis showed that the HR-CB group had a significantly lower ICU mortality compared to the HR-C group (**Figure 4**). The univariate Cox proportional hazard models showed significance for both the effect of study treatment (p-value = 0.022 and 0.309 for HR-CB and HR-DP, respectively, compared to HR-C group) and sepsis development (p-value = 0.009), whereas all the other tested variables in HR groups were non-significant (p-value > 0.05). Hence, the multivariate Cox proportional hazard model was performed using effect of study treatment and sepsis development as covariates (**Table 10**). Patients who developed sepsis by the end of the first week had a significantly higher hazard of ICU mortality than those who did not develop sepsis (hazard ratio = 3.291; p = 0.034; 95% CI, 1.097–9.869). Regarding the effect of study treatment versus control in HR groups, the HR-CB group showed the lowest hazard ratio for ICU mortality compared to the HR-C group. However, the difference between hazard ratios did not reach the threshold of statistical significance (hazard ratio = 0.137; p = 0.06; 95% CI, 0.017–1.091).

3.11 Evaluating Predictive Value of Different Sepsis Predictors in the No-Intervention Groups

The predictive value for different sepsis predictors was evaluated in the no-intervention groups (HR-C and LR). Areas under the ROC curve (AUCs) of MCP-1 (day 0), ISS (day 0), and 100-LAR (day 1) were 0.793 (95% CI, 0.66–0.93; p-value = 0.001), 0.734 (95% CI, 0.58–0.89; p-value = 0.01), and 0.758 (95% CI, 0.62–0.9; p-value = 0.005), respectively (**Figure 5**). Hence, the test performance of each predictor alone was fair (Hosmer et al., 2013). Combining the predictors, MCP-1 + ISS and 100-LAR + ISS, yielded higher AUCs of 0.797 and 0.825, respectively. Therefore, the combined use of either MCP-1 or LAR with ISS was better than each indicator alone. The test performance for combined predictors was good (Hosmer et al., 2013) with higher sensitivity for MCP-1 + ISS compared to higher specificity for 100-LAR + ISS. Sensitivity and specificity for MCP-1 + ISS were 94% and 59%, respectively. Conversely, sensitivity and specificity for 100-LAR + ISS were 63% and 93%, respectively. Optimal cutoff values to predict sepsis were determined on the ROC curve with maximum Youden-index [sensitivity − (1 − specificity)]. The best thresholds of MCP-1, 100-LAR, and ISS for sepsis prediction were 138.98 pg/ml, 70.85%, and 16.5, respectively.

3.12 Safety and Adverse Effects

Throughout the patients' follow-up, few complications were recorded. Two patients in the HR-CB group showed

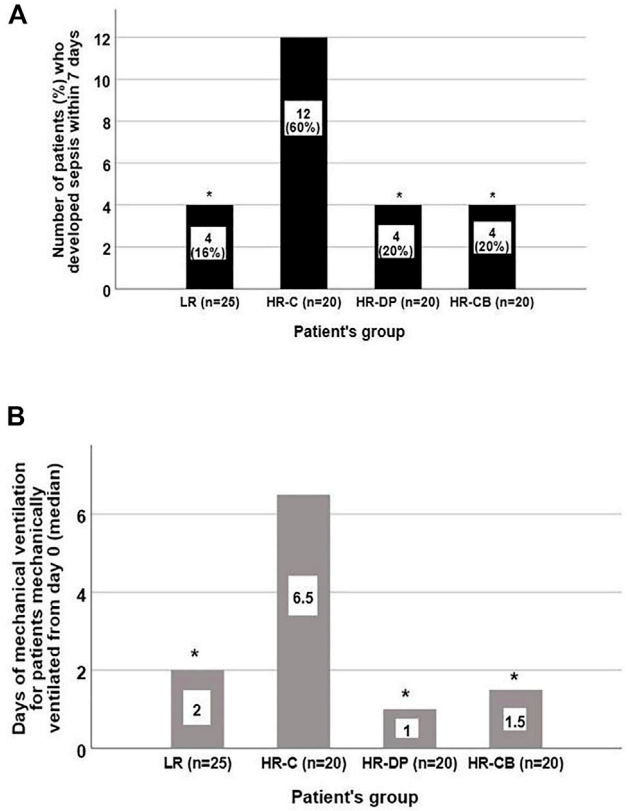

FIGURE 2 | Number of patients who developed sepsis besides the duration of mechanical ventilation for patients mechanically ventilated from day 0 in each group by the end of the first week. **(A)** Number of patients developing sepsis (by the end of the first week) in each group. **(B)** Days of mechanical ventilation for patients ventilated from day 0 in each group. (* = significant compared to HR-C group, p-value ≤ 0.05). LR: low risk for sepsis group, HR-C: high risk for sepsis control group, HR-DP: high risk for sepsis vitamin D and probiotics group, HR-CB: high risk for sepsis vitamin C and vitamin B1 group. Data are number (incidence), median (IQR).

hypersensitivity (positive IDT for vitamin B1) with no other complications. Consequently, these patients were excluded from the study. No other adverse events were deemed related to the study drugs in the HR-CB and HR-DP groups in the entire study period.

4 DISCUSSION

4.1 The Effect of Study Drugs on Patient Clinical Outcomes

In the current study, LAR was used for determination of patients who have high risk for sepsis development. The effects of immunomodulatory interventions (IV vitamin C plus vitamin B1 versus IM vitamin D plus oral probiotics) on prevention of sepsis development were investigated among patients with major trauma at high risk for sepsis. Both interventions decreased the incidence of sepsis development to the same extent (20%). However, vitamin C plus vitamin B1 were associated with lower 28-day mortality rate and higher ICU and hospital discharge rates than vitamin D plus probiotics.

4.2 The Proposed Mechanisms for Vitamin D Plus Probiotics' Effects on Sepsis and Inflammation

This current study showed that vitamin D plus probiotics significantly decreased scores for illness severity (APACHE II and SOFA), proinflammatory biomarker MCP-1, and sepsis development. The overall good clinical outcomes observed in the HR-DP group may be attributed to the synergistic effects of vitamin D plus probiotic combination. The benefits of vitamin D

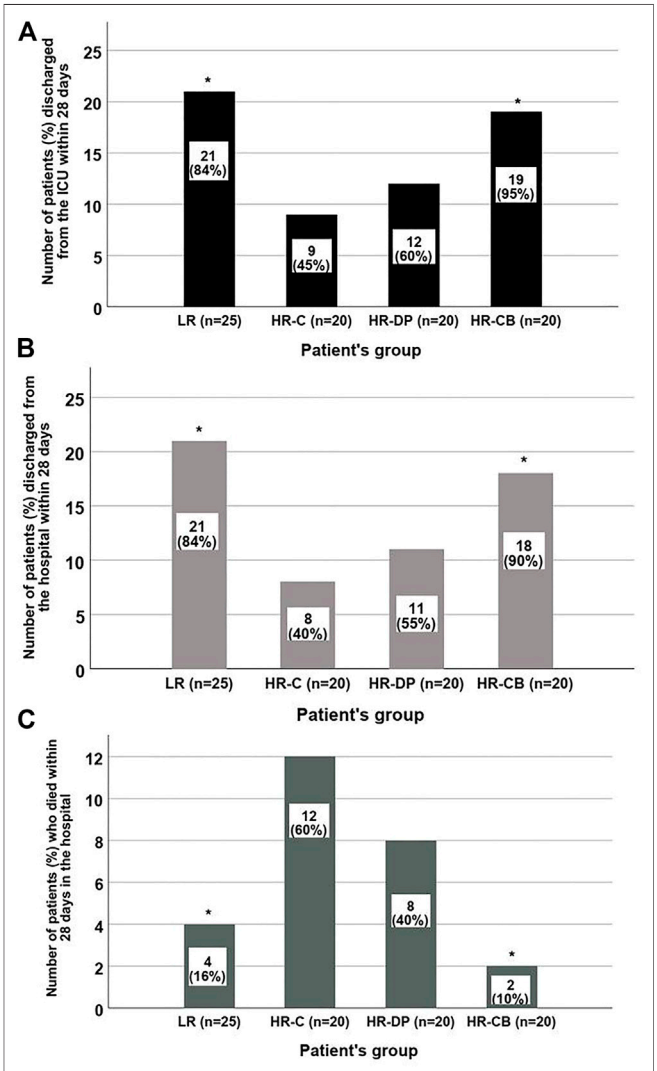

FIGURE 3 | Number of patients discharged from the ICU, from the hospital or died during the first 28 days in each group. **(A)** ICU discharge within 28 days. **(B)** Hospital discharge within 28 days. **(C)** The 28-day hospital mortality in each group (* = significant compared to HR-C group, p-value ≤ 0.05). LR: low risk for sepsis group, HR-C: high risk for sepsis control group, HR-DP: high risk for sepsis vitamin D and probiotics group, HR-CB: high risk for sepsis vitamin C and vitamin B1 group. Data are number (incidence).

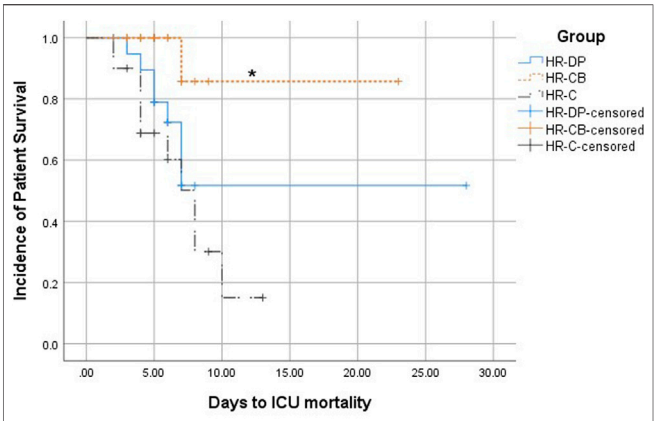

Group	Overall survival duration in days		Log rank test
	Mean (SE)	95% CI	
HR-C (20)	7.33 (0.89)	5.58-9.09	X^2= 8.55, overall p-value=0.01, p-value for HR-DP compared to HR-C= 0.29, p-value for HR-CB compared to HR-C=0.004
HR-DP (20)	17.21 (3.18)	10.98-23.44	
HR-CB (20)	20.71 (2.12)	16.57-24.86	

FIGURE 4 | Kaplan–Meier survival estimates of ICU Mortality HR-C: High risk for sepsis control group, HR-DP: High risk for sepsis vitamin D and probiotics group, HR-CB: High risk for sepsis vitamin C and vitamin B1 group, SE: standard error, 95% CI: 95% confidence interval, $\square^2$: chi-square, * = Significant compared to HR-C group, *p*-value ≤ 0.05.

TABLE 10 | Multivariate Cox regression model of risk factors for ICU mortality during the first 28 days from the onset of trauma.

	p-value	Hazard ratio	95% Confidence interval	
			Lower	Upper
HR-C (reference group)	0.137	—	—	—
HR-DP group	0.833	1.130	0.363	3.516
HR-CB group	0.060	0.137	0.017	1.091
Sepsis development	0.034[a]	3.291	1.097	9.869

HR-C: high risk for sepsis control group, HR-DP: high risk for sepsis vitamin D and probiotics group, HR-CB: high risk for sepsis vitamin C and vitamin B1 group.
[a]= Significant compared to no sepsis development by the end of the first week.
Significance level at p-value ≤ 0.05.

and probiotic cosupplementation on inflammation and antioxidant capacity have been studied in other contexts than ICU severe trauma (Abboud et al., 2021). *Lactobacillus fermentum*, one of the components of probiotic product used in this study, is among the most studied *Lactobacilli* strains with antimicrobial activity (de Melo Pereira et al., 2018; Silva et al., 2020). The antimicrobial effect of probiotics may be attributed to their gut barrier protective effects (Crooks et al., 2012; Assimakopoulos et al., 2018). Probiotics block adhesion sites of pathogenic microorganisms in the intestinal mucosa, compete with them for nutrients, and produce antibacterial substances during their elimination process. These substances include lactic acid, bacteriocin, exopolysaccharides, and hydrogen peroxide (Bermudez-Brito et al., 2012). Bacteriocin has been used by researchers to synthesize probiotic-derived bacteriocin-modified antimicrobial peptides. These peptides demonstrated strong antibacterial activity against multidrug-resistant bacteria in preclinical studies and are expected to replace antibiotics in the future (Mazumdar et al., 2020). Besides, vitamin D supplementation has been suggested for sepsis prevention in the critically ill due to its immunomodulatory effects (Takeuti et al., 2018). The anti-inflammatory characteristics of probiotics are dependent on vitamin D receptor (VDR) expression, and alternatively, probiotics in preclinical studies enhanced VDR and m-RNA antimicrobial cathelicidin expression (Yoon and Sun, 2011). Both high-dose vitamin D and probiotics have been studied separately among the ICU trauma population and showed potential benefits (Kotzampassi et al., 2006; Hasanloei et al., 2020).

4.3 The Possible Mechanisms of Vitamin C Plus Vitamin B1's Influence on Sepsis Prevention

The overall improved patient outcomes in the HR-CB group compared to the HR-C group could be attributed to the synergistic effect of vitamin C plus vitamin B1, which could be explained by a twofold mechanism. First, both vitamin C and vitamin B1 have an anti-inflammatory effect *via* inhibition of nuclear factor kappa B signaling, antioxidant potential, and mitochondrial protective mechanisms (Marik, 2018). The effects of vitamin C and vitamin B1 on mitochondrial biogenesis are critical elements in their sepsis-preventing effects compared to N-acetyl cysteine, whose unproven effects were attributed to its low ability to enter the mitochondria (Molnár, 2008). Second, vitamin B1 mitigates vitamin C-induced renal toxicity by acting as a cofactor for glyoxylate aminotransferase, the enzyme that converts glyoxylate (metabolic product of vitamin C) to carbon dioxide instead of oxalate, which causes nephropathy (Oudemans-van Straaten et al., 2017). Besides that, vitamin C supplementation enhances both innate and adaptive immunity (Carr and Maggini, 2017). The antibacterial effect of vitamin C is both concentration and bacterial strain dependent (Kallio et al., 2012; Mehmeti et al., 2013). Vitamin C has been shown to act synergistically with some antibiotics against different types of bacteria in previous studies such as synergism with rifampicin and isoniazid against multidrug-resistant *Staphylococcus aureus* and *Mycobacterium tuberculosis* isolates (Khameneh et al., 2016; Pandit et al., 2017). Vitamin C has also been suggested as an antibiotic modifier acting synergistically with chloramphenicol, kanamycin, streptomycin, and tetracycline against multi-resistant *Pseudomonas aeruginosa* isolates obtained from burn patients (Cursino et al., 2005). Additionally, both trauma and sepsis fall under the umbrella of endothelial dysfunction-dependent pathophysiology (Lehr et al., 2006). Vitamin C reduces endothelial dysfunction and capillary leakage syndrome by reducing detachment in tight gap junctions, detoxification of histamine, and synthesis of endogenous vasopressors (Carr et al., 2015).

4.4 The Predictive Value of the LAR Test

In this study, the fair test performance of LAR (AUC, 0.758) as a predictor of sepsis is concordant with a previous study reporting good test performance of LAR (AUC, 0.8) as a predictor of bacteremia in a

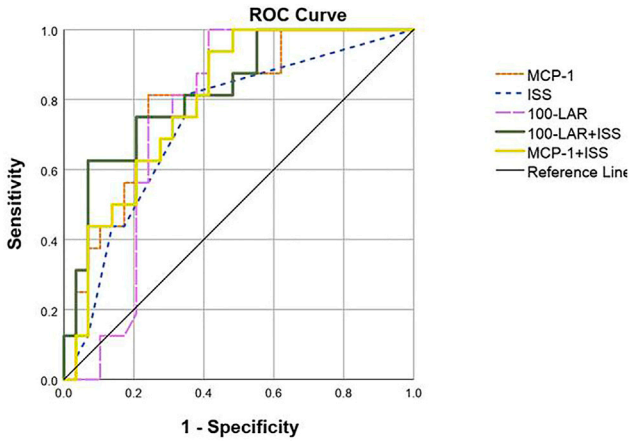

Parameter(s)	Area under the ROC curve (AUC)	SE	*p*-value	95% Confidence Interval	
				Lower Bound	Upper Bound
MCP-1	0.793	0.069	0.001 #	0.659	0.928
ISS	0.734	0.078	0.010 #	0.580	0.887
100-LAR	0.758	0.073	0.005 #	0.615	0.900
100-LAR+ISS	0.825	0.063	< 0.0001 #	0.701	0.950
MCP-1+ISS	0.797	0.065	0.001 #	0.670	0.925

FIGURE 5 | Receiver operating characteristics (ROC) curve for predictive value of different sepsis predictors among non-intervention groups (HR-C and LR groups). MCP-1: Monocyte chemoattractant protein-1, ISS: Injury severity score. LAR: Leukocyte anti sedimentation rate. SE: standard error. # = Significant *p*-value. Significance level at $p \leq 0.05$.

general surgical ICU population (Bogar et al., 2006). Furthermore, combining LAR with ISS further increased AUC to 0.825, resulting in a good test performance comparable to that of MCP-1 and ISS (AUC of 0.87) reported in a previous study (Wang et al., 2018).

4.5 Similar Previous Studies in Trauma Patients

The significant decrease in SOFA score and consequently the significantly lower incidence of sepsis among the intervention groups compared to control were concordant with previous studies conducted on the use of synbiotics (Kotzampassi et al., 2006), vitamin D (Hasanloei et al., 2020), vitamin C, and N-acetyl cysteine (Sandesc et al., 2018) among the ICU trauma population. However, in a previous trial using 300,000 IU vitamin D in trauma, patients did not develop sepsis (Hasanloei et al., 2020). Compared to this study; the difference in sepsis development may be attributed to the many variable comorbidities in this study that were not mentioned in the study by Hasanloei et al. (2020). Patient comorbidities have been shown to be risk factors for sepsis development in other previous literature (Kisat et al., 2013).

Bedreag et al. found no reduced incidence of sepsis development with the use of vitamin C, vitamin B1, and N-acetyl cysteine together among ICU trauma patients (Bedreag et al., 2015). However, no exclusion criteria were stated in their retrospective study. As known, patients with immune suppression (iatrogenic or caused by a disease) are much more vulnerable to sepsis development (Kumar et al., 2015). Thus, they were excluded from our study. Moreover, Wiley et al., after administration of vitamin C and vitamin B1 in trauma, found a significantly lower peak SOFA score in the intervention group compared to that in the control group on day 3 (a concordant finding with this study's results). However, they recorded no significant effect on shock resolution (Tessa et al., 2018).

4.6 The Rationale for Timing of Collection of Reserve Samples

If any patient was discharged to the ward before day 6 after completing the study treatment regimen in the ICU, final SOFA score and blood culture were collected in the ward on day 6. However, the last APACHE II score in the ICU just before discharge was recorded and forwarded for assessment. This is based on evidence from literature that full SOFA score is the best tool for identifying patients with sepsis in the ward setting (better than quick SOFA) (Szakmany et al., 2018). However, the APACHE II score represents a physiologically based ICU scoring system for measuring illness severity. The APACHE II was used to predict in-hospital mortality (incorporated both death in the ICU and the ward) for critical care patients (Knaus et al., 1981; Cardoso and Chiavone, 2013). The evidence from literature showed that discharge APACHE II score (calculated 24 h prior to ICU discharge) was related to mortality after ICU discharge. The discharge APACHE II scores of ≥17 were associated with poor post-ICU prognosis (Cardoso and Chiavone, 2013).

4.7 Sepsis and Mortality

All three groups (LR, HR-CB, and HR-DP) revealed a significantly lower incidence of sepsis than the HR-C group by the end of the first week. Consequently, these three groups showed lower 28-day mortality than the HR-C group. Multivariate Cox regression showed that sepsis development was a significant risk factor for ICU mortality in HR groups. These results comply with a previous study reporting sepsis as a leading cause of mortality contributing to 11 million deaths annually worldwide (Rudd et al., 2020). Another study conducted in all trauma centers of Pennsylvania also showed that sepsis was associated with significantly higher mortality in patients with trauma (Osborn et al., 2004).

4.8 The MCP-1 in the Current and Previous Studies

Differently from this study, previous studies investigating the effects of interventions (CB and DP) on MCP-1 levels were either preclinical or clinical on patients without trauma (Dong et al., 2011; Alvarez et al., 2013; Lauer et al., 2021). The significantly reduced incidence of sepsis development by the end of the first week in both the HR-DP and HR-CB groups compared to the HR-C group was accompanied by a significant reduction in the proinflammatory chemokine MCP-1 level within these intervention groups compared to a significant increase within

the control group. These results comply with a previous study revealing the key role of MCP-1 in sepsis pathogenesis (Zhu et al., 2017). Moreover, these results confirm Wang et al.'s hypothesis (Wang et al., 2018) that lowering MCP-1 level might confer an associated clinical progress in ICU patients with major trauma as decreasing MCP-1 level was accompanied by a significant reduction in incidence of sepsis development. The significant reduction in proinflammatory chemokine MCP-1 level on day 6 was concordant with previous studies on patients with trauma, but these studies investigated IL-6 as a proinflammatory cytokine (Kotzampassi et al., 2006; Sandesc et al., 2018; Hasanloei et al., 2020). Furthermore, preclinical studies suggest that the nephroprotective effects of vitamin D involve MCP-1 lowering mechanisms (Arfian et al., 2020). This was manifested by the significantly decreased MCP-1 level within the HR-DP group accompanying the reduced incidence of AKI in the HR-DP group compared to that in the HR-C group.

Alvarez et al. have shown that vitamin D inhibited MCP-1 production in patients with early CKD and *in vitro* study. The 1,25 dihydroxyvitamin D concentration used in Alvarez et al. 's *in vitro* study (16 ng/ml) was in the range of 25-hyroxivitamin D levels of patients in the HR-DP group (10–30 ng/ml) (Alvarez et al., 2013). The effect of probiotics as MCP-1 inhibitors has been shown previously in preclinical studies concordant with this study's findings (Dong et al., 2011; Wachi et al., 2014). In the Dong et al.'s study conducted on many Lactobacilli strains, MCP-1 levels were lower than those in positive controls (Dong et al., 2011). Another study declared that exopolysaccharides of *Lactobacillus delbrueckii* TUA4408L act on intestinal epithelial cells via toll-like receptors 2 and 4, leading to decreased production of MCP-1 (Wachi et al., 2014). *Lactobacillus delbrueckii* is one of the two probiotic strain constituents of the probiotic product used in this study (Lacteol Forte [package insert], 2018). The results of the *ex vivo* study of Lauer et al. (2021) support the findings of the significantly reduced MCP-1 level on day 6 within the HR-CB group. The average steady-state serum vitamin C concentration in the HR-CB group [0.4 mM, estimated based on dosing rate (1 g every 12 h), salt value (0.889), and clearance (0.92 L/h)] is within the range of vitamin C concentration as investigated in the Lauer et al. study (0.2–2 mM) (Lauer et al., 2021).

4.9 The ESR and CRP Changes in This Study Compared to Similar Previous Studies

A significant increase in ESR and a nonsignificant increase in CRP level were found within both HR-DP and HR-C groups on day 6 compared to those on day 0. However, in the HR-CB group, a nonsignificant increase in ESR besides a significant reduction in CRP level were observed on day 6 compared to those on day 0. These ESR and CRP changes in HR groups agreed with previous studies reporting the higher sensitivity of CRP to changes in acute phase response than ESR (Markanday, 2015). Kotzampassi et al. (2006) reported a significantly lower CRP level in the synbiotics group with respect to placebo on day 7. However, within the synbiotics group, no significant decrease in CRP level on day 7 compared to that on day 0 was reported. Perhaps, probiotics could not significantly lower CRP level within the HR-DP group similar to Kotzampassi et al. who used a larger dose of synbiotics (Kotzampassi et al., 2006).

4.9.1 The Proposed Explanation for CRP Changes in HR-DP and HR-CB Groups

Controversially, Hasanloei et al. (2020) found a significant reduction in ESR and CRP levels in the IM vitamin D group on day 7 compared to those at baseline. One explanation for the nonsignificantly different CRP level on day 6 compared to that on day 0 in the HR-DP group could be the inverse relationship between CRP and vitamin D levels reported in literature that occurs only at serum vitamin D levels <53 nmol/L (21.2 ng/ml, conversion factor 2.496) (Cannell et al., 2014). As patients in the HR-DP group received vitamin D plus probiotics on day 1, the IM 400,000 IU vitamin D dose was expected to increase serum vitamin D level by 25 ng/ml according to Amrein et al. (2011) to reach the level of approximately 41 ng/ml on day 3 and remain on that level for 1 month (Amrein et al., 2014). Therefore, the vitamin D level on day 6 was probably ≥21.2 ng/ml in most patients in the HR-DP group; thus, the inverse relationship between vitamin D and CRP levels was no longer obvious. The IM vitamin D dose in this study exceeded that of Hasanloei et al. by 100,000 IU (Hasanloei et al., 2020). Hence, there were probably more patients with vitamin D levels ≥21.2 ng/ml in the HR-DP group than in the IM vitamin D group of Hasanloei et al. (2020).

The CRP level of the HR-CB group on day 6 was significantly lower compared to that in the control group. This result was concordant with the previous study of Sandesc et al. who found a significant decrease in CRP level and ESR in the intervention group compared to those in the control group upon ICU discharge (Sandesc et al., 2018).

4.9.2 The Suggested Explanation for the ESR Changes in HR-DP and HR-CB Groups

The ESR showed an increase that was significant within the HR-DP group and insignificant within the HR-CB group on day 6 compared to that on day 0. One explanation is that fibrinogen and immunoglobulin G are the main proteins influencing ESR. Both fibrinogen and immunoglobulin G have long half-lives (Litao and Kamat, 2014). Thus, elevated ESR can take weeks to return to normal and can stay elevated after inflammation has resolved (Litao and Kamat, 2014). Perhaps in this study, if ESR had been measured after 2 weeks, it might have decreased in the HR-DP and HR-CB groups as mentioned in the study by Sandesc et al. in which ESR significantly decreased after approximately 14 days in the vitamin C and N-acetyl cysteine group compared to the control group (Sandesc et al., 2018).

4.10 The Rationale for Using Aerobic Bacterial Blood Cultures

Aerobic bacterial blood cultures were used as a possible documentation for infection due to their prevalence in sepsis diagnosis among the critically ill rather than anaerobic bacteria, fungi, or viruses (Dolin et al., 2019;

Gajdács and Urbán, 2020). The most prevalent bacterial strain detected in aerobic bacterial positive blood cultures was CONS concordant with previous studies in Egypt (Ahmed et al., 2009) and the United States (Edmond et al., 1999).

4.11 The Duration of Mechanical Ventilation in this Trial Compared to a Previous Similar Trial

Patients in the HR-CB group mechanically ventilated from day 0 showed a significantly shorter duration of mechanical ventilation compared to those in the HR-C group by the end of the first week. These findings were discordant with the results of Sandesc et al., who attributed the nonsignificant difference in duration of mechanical ventilation between their groups to the high prevalence of thoracic trauma and pulmonary infections (Sandesc et al., 2018). However, in the current study, multiple trauma was the most common, followed by head trauma. The highest percentage of thoracic trauma in this study was 10% in the HR-C group, which showed the longest duration of mechanical ventilation supporting the hypothesis of Sandesc et al. (2018). The reduced duration of mechanical ventilation in the HR-CB group may be attributed to the antioxidant effects of vitamin C plus vitamin B1, which agrees with a previous meta-analysis conducted on this subject (Hemilä and Chalker, 2019).

4.12 The Protective Effects of Vitamin B1 and Vitamin D Against AKI

At the end of the first week, the occurrence of AKI detected by comparing day 6 and day 0 serum creatinine values followed the KDIGO guidelines. The KDIGO guidelines define the AKI as an increase in serum creatinine level to 1.5 times the baseline creatinine or more within the last 7 days (Khwaja, 2012). AKI is reported in literature as a complication of oxalate nephropathy (secondary to high dose IV vitamin C) and hypercalcemia (secondary to hypervitaminosis D) (Lamarche et al., 2011; Graidis et al., 2020). However, by monitoring the reported adverse effects, AKI was the least common in the HR-CB group [1 (5%)] and the most common in the HR-C group [5 (25%)], which could be explained by the addition of IV vitamin B1 in the HR-CB group with its renoprotective effects (Moskowitz et al., 2017). Vitamin B1 mitigates oxalate nephropathy, a side effect reported with high-dose vitamin C (Hoppe et al., 2009). Additionally, the HR-DP group also showed a lower incidence of AKI [2 (10%)] compared to the HR-C group [5 (25%)]. Vitamin D deficiency (<15 ng/ml) or insufficiency (15–30 ng/ml) predicts increased risk of AKI development (Braun et al., 2012). All patients in the HR-DP and HR-C groups had basal vitamin D levels of 10–30 ng/ml and consequently had an increased risk for AKI development. After supplementation with 400,000 IU vitamin D in the HR-DP group, serum 25-hydroxyvitamin D level was expected to reach the level of 41 ng/ml (bypassed the range associated with increased risk of AKI) (Amrein et al., 2011). The incidence of AKI in the HR-DP group was lower than that in the HR-C group, confirming the nephroprotective effects of vitamin D supplementation.

4.13 Strengths of the Study

One strength for this study is that, to the best of our knowledge, it is the first study to demonstrate the lowering effects of vitamin C plus vitamin B1 (CB) and vitamin D plus probiotic (DP) combinations on MCP-1 in ICU trauma patients. The average estimated serum vitamin C level in this trial (0.4 mM) was far from the level reported in a previous preclinical study to be associated with prooxidant effects (2 mM) (Park and Lee, 2008). Besides, the parenteral route of vitamin C administration bypassed the vitamin C intestinal uptake ceiling effect that occurs with oral route and is responsible for its inefficacy in critically ill patients (van Zanten et al., 2014). The use of continuous infusion rather than bolus injection fostered lower excretion of vitamin C and oxalate (de Grooth et al., 2018). The use of single IM vitamin D dose avoided the problems of slow absorption and low bioavailability encountered with oral doses (Hasanloei et al., 2020). Moreover, the use of LAR enabled sepsis-risk prediction that was not possible with leukocyte count due to its limited prognostic value (Hesselink et al., 2020). The LAR can be used as an affordable and easy method for sepsis prediction until newer methods for assessment of neutrophil dysfunction become available (Hesselink et al., 2019). The LAR combined with ISS were good sepsis predictors comparable to MCP-1 combined with ISS suggested by Wang et al. (2018), with a much lower cost.

4.14 Limitations of the Study

This study may be limited by the inability to measure vitamin C and vitamin B1 levels at baseline due to the requirement of high-performance liquid chromatography (HPLC), which was expensive and unavailable. Moreover, HPLC may be unable to detect the very low levels of vitamin C in critical illness (Long et al., 2003; Collie et al., 2017). Vitamin D level after supplementation could not be measured due to financial limitations. However, it was expected to be normalized and exceed the level found in a similar study of Hasanloei et al. on 300,000 IU of IM vitamin D [where mean ± SD serum 25-hyroxyvitamin D level in the IM vitamin D group on day 7 was 29.43 ± 5.18 ng/ml (Hasanloei et al., 2020)] due to the higher IM vitamin D dose in this study (400,000 IU). The probability of patient transfer outside hospital or death after completing the supplementation regimen in the ICU and before day 6 prompted the investigators of this study to collect a reserve sample and blood culture on day 3, which was used in case day 6 sample and blood culture could not be collected.

5 CONCLUSION

Early prediction of sepsis in severe trauma represents an unmet clinical need. The use of LAR as a point-of-care test combined with ISS as a cheap and available alternative to MCP-1 plus ISS enabled determination of patients at high risk for sepsis development who would benefit most from the prophylactic immunomodulatory interventions. Vitamin D plus probiotics synergistic combination reduced the incidence of sepsis development similar to IV vitamin C plus vitamin B1

in the ICU patients with trauma. Both combinations reduced MCP-1 level, proving the therapeutic progress accompanying MCP-1 level decrease in severe trauma. Hence, the administration of immunomodulatory interventions for prevention of sepsis in clinical practice could help improve major trauma patient prognosis and decrease the incidence of sepsis.

DATA AVAILABILITY STATEMENT

The raw data supporting the conclusion of this article will be made available by the authors, upon request.

ETHICS STATEMENT

The studies involving human participants were reviewed and approved by the Institutional Review Board (IRB), Faculty of Medicine (IRB # R.19.12.707), and Research Ethics Committee, Faculty of Pharmacy, Mansoura University. The patients/participants provided their written informed consent to participate in this study.

AUTHOR CONTRIBUTIONS

NK, MMS, MA-Z, and MIS contributed to the conceptualization and design of the study. NK and MA-Z carried out the investigation part. NK, MMS, and MA-Z performed the formal statistical analysis. NK and MMS wrote the first draft. MIS supervised and administrated the project. All authors reviewed, edited, and approved the manuscript.

SUPPLEMENTARY MATERIAL

The Supplementary Material for this article can be found online at: https://www.frontiersin.org/articles/10.3389/fphar.2021.792741/full#supplementary-material

Supplementary Figure S1 | APACHE II and SOFA scores on day 0 and day 6 in the tested groups, **(A)**: APACHE II score on day 0 and day 6, **(B)**: SOFA score on day 0 and day 6.

Supplementary Figure S2 | The number of patients (incidence) with positive aerobic bacterial blood culture (obtained on day 6) in each group and the incidence of bacterial strains in each group.

REFERENCES

Abboud, M., Rizk, R., AlAnouti, F., Papandreou, D., Haidar, S., and Mahboub, N. (2021). The Health Effects of Vitamin D and Probiotic Co-Supplementation: A Systematic Review of Randomized Controlled Trials. *Nutrients.* 13 (1), 111. doi:10.3390/nu13010111

Ahmed, S. H., Daef, E. A., Badary, M. S., Mahmoud, M. A., and Abd-Elsayed, A. A. (2009). Nosocomial Blood Stream Infection in Intensive Care Units at Assiut University Hospitals (Upper Egypt) with Special Reference to Extended Spectrum Beta-Lactamase Producing Organisms. *BMC Res. Notes.* 2, 76. doi:10.1186/1756-0500-2-76

Aird, W. C. (2003). The Role of the Endothelium in Severe Sepsis and Multiple Organ Dysfunction Syndrome. *Blood.* 101 (10), 3765–3777. doi:10.1182/blood-2002-06-1887

Alvarez, J. A., Zughaier, S. M., Law, J., Hao, L., Wasse, H., Ziegler, T. R., et al. (2013). Effects of High-Dose Cholecalciferol on Serum Markers of Inflammation and Immunity in Patients With Early Chronic Kidney Disease. *Eur. J. Clin. Nutr.* 67 (3), 264–269. doi:10.1038/ejcn.2012.217

Amrein, K., Schnedl, C., Holl, A., Riedl, R., Christopher, K. B., Pachler, C., et al. (2014). Effect of High-Dose Vitamin D3 on Hospital Length of Stay in Critically Ill Patients With Vitamin D Deficiency: the VITdAL-ICU Randomized Clinical Trial. *Jama.* 312 (15), 1520–1530. doi:10.1001/jama.2014.13204

Amrein, K., Sourij, H., Wagner, G., Holl, A., Pieber, T. R., Smolle, K. H., et al. (2011). Short-Term Effects of High-Dose Oral Vitamin D3 in Critically Ill Vitamin D Deficient Patients: a Randomized, Double-Blind, Placebo-Controlled Pilot Study. *Crit. Care.* 15 (2), R104. doi:10.1186/cc10120

Arfian, N., Budiharjo, S., Wibisono, D. P., Setyaningsih, W. A. W., Romi, M. M., Saputri, R. L. A. A. W., et al. (2020). Vitamin D Ameliorates Kidney Ischemia Reperfusion Injury via Reduction of Inflammation and Myofibroblast Expansion. *Kobe J. Med. Sci.* 65 (4), E138–e43.

Assimakopoulos, S. F., Triantos, C., Thomopoulos, K., Fligou, F., Maroulis, I., Marangos, M., et al. (2018). Gut-origin Sepsis in the Critically Ill Patient: Pathophysiology and Treatment. *Infection.* 46 (6), 751–760. doi:10.1007/s15010-018-1178-5

Atalan, H. K., and Güçyetmez, B. (2017). Serum Vitamin D Level at ICU Admission and Mortality. *Turk J. Anaesthesiol Reanim.* 45 (4), 193–196. doi:10.5152/tjar.2017.60234

Baker, R. (2020). *The Declaration of Helsinki and the Foundations of Global Bioethics. Ethical Research: The Declaration of Helsinki, and the Past, Present, and Future of Human Experimentation*. New York: Oxford University Press, 47.

Baker, S. P., O'Neill, B., Haddon, W., Jr., and Long, W. B. (1974). The Injury Severity Score: a Method for Describing Patients With Multiple Injuries and Evaluating Emergency Care. *J. Trauma.* 14 (3), 187–196. doi:10.1097/00005373-197403000-00001

Bedreag, O. H., Rogobete, A. F., Sărăndan, M., Cradigati, A. C., Păpurică, M., Roşu, O. M., et al. (2015). Influence of Antioxidant Therapy on the Clinical Status of Multiple Trauma Patients. A Retrospective Single Center Study. *Rom. J. Anaesth. Intensive Care.* 22 (2), 89–96.

Bermudez-Brito, M., Plaza-Díaz, J., Muñoz-Quezada, S., Gómez-Llorente, C., and Gil, A. (2012). Probiotic Mechanisms of Action. *Ann. Nutr. Metab.* 61 (2), 160–174. doi:10.1159/000342079

Bogar, L., Molnar, Z., Kenyeres, P., and Tarsoly, P. (2006). Sedimentation Characteristics of Leucocytes Can Predict Bacteraemia in Critical Care Patients. *J. Clin. Pathol.* 59 (5), 523–525. doi:10.1136/jcp.2005.033035

Bogar, L., Horvath, J. A., and Tekeres, M. (1997). "Leucocyte Motion During Gravity Sedimentation of Whole Blood," in *Advances in Critical Care Testing*. Editors List, W. F., Müller, M. M., and McQueen, M. J. (Berlin: Springer), 13–19.

Braun, A. B., Litonjua, A. A., Moromizato, T., Gibbons, F. K., Giovannucci, E., and Christopher, K. B. (2012). Association of Low Serum 25-Hydroxyvitamin D Levels and Acute Kidney Injury in the Critically Ill. *Crit. Care Med.* 40 (12), 3170–3179. doi:10.1097/CCM.0b013e318260c928

Cannell, J. J., Grant, W. B., and Holick, M. F. (2014). Vitamin D and Inflammation. *Dermatoendocrinol.* 6 (1), e983401. doi:10.4161/19381980.2014.983401

Cardoso, L. G., and Chiavone, P. A. (2013). The Apache II Measured on Patients' Discharge From the Intensive Care Unit in the Prediction of Mortality. *Rev. Lat Am. Enfermagem.* 21, 811–819. doi:10.1590/S0104-11692013000300022

Carr, A. C., and Maggini, S. (2017). Vitamin C and Immune Function. *Nutrients.* 9 (11). doi:10.3390/nu9111211

Carr, A. C., Shaw, G. M., Fowler, A. A., and Natarajan, R. (2015). Ascorbate-Dependent Vasopressor Synthesis: a Rationale for Vitamin C Administration in Severe Sepsis and Septic Shock? *Crit. Care.* 19, 418. doi:10.1186/s13054-015-1131-2

Civil, I. D., and Schwab, C. W. (1988). The Abbreviated Injury Scale, 1985 Revision: a Condensed Chart for Clinical Use. *J. Trauma.* 28 (1), 87–90. doi:10.1097/00005373-198801000-00012

Collie, J. T. B., Greaves, R. F., Jones, O. A. H., Lam, Q., Eastwood, G. M., and Bellomo, R. (2017). Vitamin B1 in Critically Ill Patients: Needs and Challenges. *Clin. Chem. Lab. Med.* 55 (11), 1652–1668. doi:10.1515/cclm-2017-0054

Crooks, N. H., Snaith, C., Webster, D., Gao, F., and Hawkey, P. (2012). Clinical Review: Probiotics in Critical Care. *Crit. Care.* 16 (6), 237. doi:10.1186/cc11382

Cursino, L., Chartone-Souza, E., and Nascimento, A. M. A. (2005). Synergic Interaction Between Ascorbic Acid and Antibiotics Against *Pseudomonas aeruginosa*. *Braz. Arch. Biol. Technol.* 48, 379–384. doi:10.1590/S1516-89132005000300007

de Grooth, H. J., Manubulu-Choo, W. P., Zandvliet, A. S., Spoelstra-de Man, A. M. E., Girbes, A. R., Swart, E. L., et al. (2018). Vitamin C Pharmacokinetics in Critically Ill Patients: A Randomized Trial of Four IV Regimens. *Chest.* 153 (6), 1368–1377. doi:10.1016/j.chest.2018.02.025

de Melo Pereira, G. V., de Oliveira Coelho, B., Magalhães Júnior, A. I., Thomaz-Soccol, V., and Soccol, C. R. (2018). How to Select a Probiotic? A Review and Update of Methods and Criteria. *Biotechnol. Adv.* 36 (8), 2060–2076. doi:10.1016/j.biotechadv.2018.09.003

Dolin, H. H., Papadimos, T. J., Chen, X., and Pan, Z. K. (2019). Characterization of Pathogenic Sepsis Etiologies and Patient Profiles: A Novel Approach to Triage and Treatment. *Microbiol. Insights.* 12, 1178636118825081. doi:10.1177/1178636118825081

Dong, H., Rowland, I., and Yaqoob, P. (2011). Comparative Effects of Six Probiotic Strains on Immune Function *In Vitro*. *Br. J. Nutr.* 108 (3), 459–470. doi:10.1017/S0007114511005824

Edmond, M. B., Wallace, S. E., McClish, D. K., Pfaller, M. A., Jones, R. N., and Wenzel, R. P. (1999). Nosocomial Bloodstream Infections in United States Hospitals: a Three-Year Analysis. *Clin. Infect. Disan Official Publication Infect. Dis. Soc. America.* 29 (2), 239–244. doi:10.1086/520192

Evans, L., Rhodes, A., Alhazzani, W., Antonelli, M., Coopersmith, C. M., French, C., et al. (2021). Surviving Sepsis Campaign: International Guidelines for Management of Sepsis and Septic Shock 2021. *Intensive Care Med.* 47 (11), 1181–1247. doi:10.1007/s00134-021-06506-y

FDA (2007). DiaSorin Inc. LIASON 510(K) FDA submission. Available at: http://www.accessdata.fda.gov/cdrh_docs/reviews/K071480.pdf (Accessed April 14, 2021).

Gajdács, M., and Urbán, E. (2020). Relevance of Anaerobic Bacteremia in Adult Patients: A Never-Ending story? *Eur. J. Microbiol. Immunol. (Bp).* 10 (2), 64–75. doi:10.1556/1886.2020.00009

Graidis, S., Papavramidis, T. S., and Papaioannou, M. (2020). Vitamin D and Acute Kidney Injury: A Two-Way Causality Relation and a Predictive, Prognostic, and Therapeutic Role of Vitamin D. *Front. Nutr.* 7, 630951. doi:10.3389/fnut.2020.630951

Hasanloei, M. A. V., Rahimlou, M., Eivazloo, A., Sane, S., Ayremlou, P., and Hashemi, R. (2020). Effect of Oral Versus Intramuscular Vitamin D Replacement on Oxidative Stress and Outcomes in Traumatic Mechanical Ventilated Patients Admitted to Intensive Care Unit. *Nutr. Clin. Pract.* 35 (3), 548–558.

Hemilä, H., and Chalker, E. (2019). Vitamin C Can Shorten the Length of Stay in the ICU: A Meta-Analysis. *Nutrients.* 11 (4), 708. doi:10.3390/nu11040708

Hesselink, L., Spijkerman, R., de Fraiture, E., Bongers, S., Van Wessem, K. J. P., Vrisekoop, N., et al. (2020). New Automated Analysis to Monitor Neutrophil Function Point-of-Care in the Intensive Care Unit after Trauma. *Intensive Care Med. Exp.* 8 (1), 12. doi:10.1186/s40635-020-0299-1

Hesselink, L., Spijkerman, R., van Wessem, K. J. P., Koenderman, L., Leenen, L. P. H., Huber-Lang, M., et al. (2019). Neutrophil Heterogeneity and its Role in Infectious Complications After Severe Trauma. *World J. Emerg. Surg.* 14 (1), 24. doi:10.1186/s13017-019-0244-3

Hoppe, B., Beck, B. B., and Milliner, D. S. (2009). The Primary Hyperoxalurias. *Kidney Int.* 75 (12), 1264–1271. doi:10.1038/ki.2009.32

Hosmer, D. W., Jr, Lemeshow, S., and Sturdivant, R. X. (2013). *Applied Logistic Regression*. Hoboken, NJ: John Wiley & Sons.

Hosseini, S., Vázquez-Villegas, P., Rito-Palomares, M., and Martinez-Chapa, S. O. (2018). *Advantages, Disadvantages and Modifications of Conventional ELISA. Enzyme-Linked Immunosorbent Assay (ELISA): From A to Z*. Singapore: Springer Singapore, 67–115. doi:10.1007/978-981-10-6766-2_5

Jin, H., Liu, Z., Xiao, Y., Fan, X., Yan, J., and Liang, H. (2014). Prediction of Sepsis in Trauma Patients. *Burns Trauma.* 2 (3), 106–113. doi:10.4103/2321-3868.135479

Kallio, J., Jaakkola, M., Mäki, M., Kilpeläinen, P., and Virtanen, V. (2012). Vitamin C Inhibits staphylococcus Aureus Growth and Enhances the Inhibitory Effect of Quercetin on Growth of *Escherichia coli In Vitro*. *Planta Med.* 78 (17), 1824–1830. doi:10.1055/s-0032-1315388

Khameneh, B., Fazly Bazzaz, B. S., Amani, A., Rostami, J., and Vahdati-Mashhadian, N. (2016). Combination of Anti-Tuberculosis Drugs With Vitamin C or NAC Against Different *Staphylococcus aureus* and *Mycobacterium tuberculosis* Strains. *Microb. Pathog.* 93, 83–87. doi:10.1016/j.micpath.2015.11.006

Khwaja, A. (2012). KDIGO Clinical Practice Guidelines for Acute Kidney Injury. *Nephron Clin. Pract.* 120 (4), c179–84. doi:10.1159/000339789

Kisat, M., Villegas, C. V., Onguti, S., Zafar, S. N., Latif, A., Efron, D. T., et al. (2013). Predictors of Sepsis in Moderately Severely Injured Patients: an Analysis of the National Trauma Data Bank. *Surg. Infect. (Larchmt).* 14 (1), 62–68. doi:10.1089/sur.2012.009

Knaus, W. A., Draper, E. A., Wagner, D. P., and Zimmerman, J. E. (1985). Apache II: a Severity of Disease Classification System. *Crit. Care Med.* 13 (10), 818–829. doi:10.1097/00003246-198510000-00009

Knaus, W. A., Zimmerman, J. E., Wagner, D. P., Draper, E. A., and Lawrence, D. E. (1981). Apache-Acute Physiology and Chronic Health Evaluation: a Physiologically Based Classification System. *Crit. Care Med.* 9 (8), 591–597. doi:10.1097/00003246-198108000-00008

Kotzampassi, K., Giamarellos-Bourboulis, E. J., Voudouris, A., Kazamias, P., and Eleftheriadis, E. (2006). Benefits of a Synbiotic Formula (Synbiotic 2000Forte) in Critically Ill Trauma Patients: Early Results of a Randomized Controlled Trial. *World J. Surg.* 30 (10), 1848–1855. doi:10.1007/s00268-005-0653-1

Kumar, G., Ahmad, S., Taneja, A., Patel, J., Guddati, A. K., Nanchal, R., et al. (2015). Severe Sepsis in Hematopoietic Stem Cell Transplant Recipients*. *Crit. Care Med.* 43 (2), 411–421. doi:10.1097/CCM.0000000000000714

Lacteol Forte [package insert] (2018). *Tenth of Ramadan for Pharmaceutical Industries and Diagnostic Reagents (Rameda)*. Houdan, France: AXCAN pharma SA France.

Lamarche, J., Nair, R., Peguero, A., and Courville, C. (2011). Vitamin C-Induced Oxalate Nephropathy. *Int. J. Nephrol.* 2011, 146927. doi:10.4061/2011/146927

Lauer, A., Burkard, M., Niessner, H., Leischner, C., Renner, O., Vollbracht, C., et al. (2021). *Ex Vivo* Evaluation of the Sepsis Triple Therapy High-Dose Vitamin C in Combination with Vitamin B1 and Hydrocortisone in a Human Peripheral Blood Mononuclear Cells (PBMCs) Model. *Nutrients.* 13 (7), 2366. doi:10.3390/nu13072366

Lehr, H. A., Germann, G., McGregor, G. P., Migeod, F., Roesen, P., Tanaka, H., et al. (2006). Consensus Meeting on "Relevance of Parenteral Vitamin C in Acute Endothelial Dependent Pathophysiological Conditions (EDPC)". *Eur. J. Med. Res.* 11 (12), 516–526.

Litao, M. K., and Kamat, D. (2014). Erythrocyte Sedimentation Rate and C-Reactive Protein: How Best to Use Them in Clinical Practice. *Pediatr. Ann.* 43 (10), 417–420. doi:10.3928/00904481-20140924-10

Long, C. L., Maull, K. I., Krishnan, R. S., Laws, H. L., Geiger, J. W., Borghesi, L., et al. (2003). Ascorbic Acid Dynamics in the Seriously Ill and Injured. *J. Surg. Res.* 109 (2), 144–148. doi:10.1016/s0022-4804(02)00083-5

Ma, X. Y., Tian, L. X., and Liang, H. P. (2016). Early Prevention of Trauma-Related Infection/Sepsis. *Mil. Med. Res.* 3 (1), 33. doi:10.1186/s40779-016-0104-3

Marik, P. E. (2018). Hydrocortisone, Ascorbic Acid and Thiamine (HAT Therapy) for the Treatment of Sepsis. Focus on Ascorbic Acid. *Nutrients.* 10 (11), 1762. doi:10.3390/nu10111762

Marik, P. E., Khangoora, V., Rivera, R., Hooper, M. H., and Catravas, J. (2017). Hydrocortisone, Vitamin C, and Thiamine for the Treatment of Severe Sepsis and Septic Shock: A Retrospective Before-After Study. *Chest.* 151 (6), 1229–1238. doi:10.1016/j.chest.2016.11.036

Markanday, A. (2015). Acute Phase Reactants in Infections: Evidence-Based Review and a Guide for Clinicians. *Open Forum Infect. Dis.* 2 (3), ofv098. doi:10.1093/ofid/ofv098

Mazumdar, A., Haddad, Y., Sur, V. P., Milosavljevic, V., Bhowmick, S., Michalkova, H., et al. (2020). Characterization and *In Vitro* Analysis of Probiotic-Derived Peptides Against Multi Drug Resistance Bacterial Infections. *Front. Microbiol.* 11, 1963. doi:10.3389/fmicb.2020.01963

Mehmeti, I., Solheim, M., Nes, I. F., and Holo, H. (2013). *Enterococcus faecalis* Grows on Ascorbic Acid. *Appl. Environ. Microbiol.* 79 (15), 4756–4758. doi:10.1128/AEM.00228-13

Molnár, Z. (2008). N-acetylcysteine as the Magic Bullet: Too Good to Be True. *Crit. Care Med.* 36 (2), 645–646. doi:10.1097/01.ccm.0000299841.13197.94

Moskowitz, A., Andersen, L. W., Cocchi, M. N., Karlsson, M., Patel, P. V., and Donnino, M. W. (2017). Thiamine as a Renal Protective Agent in Septic Shock.

A Secondary Analysis of a Randomized, Double-Blind, Placebo-Controlled Trial. *Ann. Am. Thorac. Soc.* 14, 737–741. doi:10.1513/AnnalsATS.201608-656BC

Osborn, T. M., Tracy, J. K., Dunne, J. R., Pasquale, M., and Napolitano, L. M. (2004). Epidemiology of Sepsis in Patients With Traumatic Injury. *Crit. Care Med.* 32 (11), 2234–2240. doi:10.1097/01.ccm.0000145586.23276.0f

Oudemans-van Straaten, H. M., Elbers, P. W. G., and Spoelstra-de Man, A. M. E. (2017). How to Give Vitamin C a Cautious but Fair Chance in Severe Sepsis. *Chest.* 151 (6), 1199–1200. doi:10.1016/j.chest.2017.01.008

Pandit, S., Ravikumar, V., Abdel-Haleem, A. M., Derouiche, A., Mokkapati, V. R. S. S., Sihlbom, C., et al. (2017). Low Concentrations of Vitamin C Reduce the Synthesis of Extracellular Polymers and Destabilize Bacterial Biofilms. *Front. Microbiol.* 8 (2599), 2599. doi:10.3389/fmicb.2017.02599

Park, S. W., and Lee, S. M. (2008). Antioxidant and Prooxidant Properties of Ascorbic Acid on Hepatic Dysfunction Induced by Cold Ischemia/reperfusion. *Eur. J. Pharmacol.* 580 (3), 401–406. doi:10.1016/j.ejphar.2007.11.023

Rickham, P. P. (1964). Human Experimentation. Code of Ethics of the World Medical Association. Declaration of Helsinki. *Br. Med. J.* 2 (5402), 177. doi:10.1136/bmj.2.5402.177

Rozanovic, M., Csontos, C., Bogár, L., Szélig, L., Bocskai, T., Kovács, P., et al. (2016). Can Leukocyte Antisedimentation Rate (LAR) Predict Septic Complications and Critical Care Survival Early in Polytrauma and Burn Victims? *Clin. Hemorheol. Microcirc.* 64 (4), 875–885. doi:10.3233/CH-168024

Rudd, K. E., Johnson, S. C., Agesa, K. M., Shackelford, K. A., Tsoi, D., Kievlan, D. R., et al. (2020). Global, Regional, and National Sepsis Incidence and Mortality, 1990-2017: Analysis for the Global Burden of Disease Study. *Lancet.* 395 (10219), 200–211. doi:10.1016/s0140-6736(19)32989-7

Sanaie, S., Ebrahimi-Mameghani, M., Hamishehkar, H., Mojtahedzadeh, M., and Mahmoodpoor, A. (2014). Effect of a Multispecies Probiotic on Inflammatory Markers in Critically Ill Patients: A Randomized, Double-Blind, Placebo-Controlled Trial. *J. Res. Med. Sci.* 19 (9), 827–833.

Sandesc, M., Rogobete, A. F., Bedreag, O. H., Dinu, A., Papurica, M., Cradigati, C. A., et al. (2018). Analysis of Oxidative Stress-Related Markers in Critically Ill Polytrauma Patients: An Observational Prospective Single-center Study. *Bosn J. Basic Med. Sci.* 18 (2), 191–197. doi:10.17305/bjbms.2018.2306

Sartelli, M., Kluger, Y., Ansaloni, L., Hardcastle, T. C., Rello, J., Watkins, R. R., et al. (2018). Raising Concerns About the Sepsis-3 Definitions. *World J. Emerg. Surg.* 13, 6. doi:10.1186/s13017-018-0165-6

Silva, D. R., Sardi, J. d. C. O., Pitangui, N. d. S., Roque, S. M., Silva, A. C. B. d., and Rosalen, P. L. (2020). Probiotics as an Alternative Antimicrobial Therapy: Current Reality and Future Directions. *J. Funct. Foods.* 73, 104080. doi:10.1016/j.jff.2020.104080

Singer, M., Deutschman, C. S., Seymour, C. W., Shankar-Hari, M., Annane, D., Bauer, M., et al. (2016). The Third International Consensus Definitions for Sepsis and Septic Shock (Sepsis-3). *JAMA.* 315 (8), 801–810. doi:10.1001/jama.2016.0287

Sweeney, T. E., Liesenfeld, O., and May, L. (2019). Diagnosis of Bacterial Sepsis: Why Are Tests for Bacteremia Not Sufficient? *Expert Rev. Mol. Diagn.* 19 (11), 959–962. doi:10.1080/14737159.2019.1660644

Szakmany, T., Pugh, R., Kopczynska, M., Lundin, R. M., Sharif, B., Morgan, P., et al. (2018). Defining Sepsis on the Wards: Results of a Multi-Centre Point-Prevalence Study Comparing Two Sepsis Definitions. *Anaesthesia.* 73 (2), 195–204. doi:10.1111/anae.14062

Takeuti, F. A. C., Guimaraes, F. S. F., and Guimaraes, P. S. F. (2018). Applications of Vitamin D in Sepsis Prevention. *Discov. Med.* 25 (140), 291–297.

Tessa, L., Wiley, P. D., JeremyRainey, T. D. O., Alan, V., Dukes, P. D., and Matthew Kutcher, M. D. (2018). *University of Mississippi Medical Center J, Mississippi, United States. An Evaluation of Vitamin C and Thiamine in Trauma and Surgical Patients with Shock. Anesthesiology Annual Meeting*. US: American Society of Anesthesiologists.

van Zanten, A. R., Sztark, F., Kaisers, U. X., Zielmann, S., Felbinger, T. W., Sablotzki, A. R., et al. (2014). High-Protein Enteral Nutrition Enriched With Immune-Modulating Nutrients vs Standard High-Protein Enteral Nutrition and Nosocomial Infections in the ICU: a Randomized Clinical Trial. *Jama.* 312 (5), 514–524. doi:10.1001/jama.2014.7698

Vincent, J. L., Moreno, R., Takala, J., Willatts, S., De Mendonça, A., Bruining, H., et al. (1996). The SOFA (Sepsis-Related Organ Failure Assessment) Score to Describe Organ Dysfunction/failure. On Behalf of the Working Group on Sepsis-Related Problems of the European Society of Intensive Care Medicine. *Intensive Care Med.* 22 (7), 707–710. doi:10.1007/bf01709751

Wachi, S., Kanmani, P., Tomosada, Y., Kobayashi, H., Yuri, T., Egusa, S., et al. (2014). Lactobacillus Delbrueckii TUA4408L and its Extracellular Polysaccharides Attenuate Enterotoxigenic Escherichia Coli-Induced Inflammatory Response in Porcine Intestinal Epitheliocytes via Toll-like Receptor-2 and 4. *Mol. Nutr. Food Res.* 58 (10), 2080–2093. doi:10.1002/mnfr.201400218

Wafaisade, A., Lefering, R., Bouillon, B., Sakka, S. G., Thamm, O. C., Paffrath, T., et al. (2011). Epidemiology and Risk Factors of Sepsis After Multiple Trauma: an Analysis of 29,829 Patients from the Trauma Registry of the German Society for Trauma Surgery. *Crit. Care Med.* 39 (4), 621–628. doi:10.1097/CCM.0b013e318206d3df

Wang, Y., Liu, Q., Liu, T., Zheng, Q., Xu, X., Liu, X., et al. (2018). Early Plasma Monocyte Chemoattractant Protein 1 Predicts the Development of Sepsis in Trauma Patients: A Prospective Observational Study. *Medicine (Baltimore).* 97 (14), e0356. doi:10.1097/MD.0000000000010356

Yoon, S. S., and Sun, J. (2011). Probiotics, Nuclear Receptor Signaling, and Anti-Inflammatory Pathways. *Gastroenterol. Res. Pract.* 2011, 971938. doi:10.1155/2011/971938

Zhu, T., Liao, X., Feng, T., Wu, Q., Zhang, J., Cao, X., et al. (2017). Plasma Monocyte Chemoattractant Protein 1 as a Predictive Marker for Sepsis Prognosis: A Prospective Cohort Study. *Tohoku J. Exp. Med.* 241 (2), 139–147. doi:10.1620/tjem.241.139

Conflict of Interest: The authors declare that the research was conducted in the absence of any commercial or financial relationships that could be construed as a potential conflict of interest.

Publisher's Note: All claims expressed in this article are solely those of the authors and do not necessarily represent those of their affiliated organizations, or those of the publisher, the editors, and the reviewers. Any product that may be evaluated in this article, or claim that may be made by its manufacturer, is not guaranteed or endorsed by the publisher.

frontiers in Pharmacology

ORIGINAL RESEARCH
published: 06 December 2021
doi: 10.3389/fphar.2021.791648

Exosome-Mediated eCIRP Release From Macrophages to Induce Inflammation in Sepsis

Atsushi Murao[1], *Chuyi Tan*[1], *Alok Jha*[1], *Ping Wang*[1,2*†] and *Monowar Aziz*[1,2*†]

[1]Center for Immunology and Inflammation, The Feinstein Institutes for Medical Research, Manhasset, NY, United States, [2]Departments of Surgery and Molecular Medicine, Zucker School of Medicine at Hofstra/Northwell, Manhasset, NY, United States

Extracellular cold-inducible RNA-binding protein (eCIRP) is an important damage-associated molecular pattern (DAMP). Despite our understanding of the potentially harmful effects of eCIRP in sepsis, how eCIRP is released from cells remains elusive. Exosomes are endosome-derived extracellular vesicles, which carry proteins, lipids, and nucleic acids to facilitate intercellular communication and several extracellular functions. We hypothesized that eCIRP is released via exosomes to induce inflammation in sepsis. Exosomes isolated from the supernatants of LPS-treated macrophage culture and serum of endotoxemia and polymicrobial sepsis mice showed high purity, as revealed by their unique median sizes ranging between 70 and 126 nm in diameter. eCIRP levels of the exosomes were significantly increased after LPS treatment in the supernatants of macrophage culture, mouse serum, and cecal ligation and puncture (CLP)-induced sepsis mouse serum. Protease protection assay demonstrated the majority of eCIRP was present on the surface of exosomes. Treatment of WT macrophages and mice with exosomes isolated from LPS-treated WT mice serum increased TNFα and IL-6 production. However, treatment with $CIRP^{-/-}$ mice serum exosomes significantly decreased these levels compared with WT exosome-treated conditions. $CIRP^{-/-}$ mice serum exosomes significantly decreased neutrophil migration *in vitro* compared with WT exosomes. Treatment of mice with serum exosomes isolated from $CIRP^{-/-}$ mice significantly reduced neutrophil infiltration into the peritoneal cavity. Our data suggest that eCIRP can be released via exosomes to induce cytokine production and neutrophil migration. Thus, exosomal eCIRP could be a potential target to inhibit inflammation.

Keywords: eCIRP, exosomes, sepsis, cytokines, macrophage, neutrophil

OPEN ACCESS

Edited by:
Daolin Tang,
University of Texas Southwestern Medical Center, United States

Reviewed by:
Liliang Jin,
Louisiana State University, United States
Dongze Qin,
Albert Einstein College of Medicine, United States

***Correspondence:**
Ping Wang
pwang@northwell.edu
Monowar Aziz
maziz1@northwell.edu

†These authors share senior authorship

Specialty section:
This article was submitted to Experimental Pharmacology and Drug Discovery, a section of the journal Frontiers in Pharmacology

Received: *08 October 2021*
Accepted: *15 November 2021*
Published: *06 December 2021*

Citation:
Murao A, Tan C, Jha A, Wang P and Aziz M (2021) Exosome-Mediated eCIRP Release From Macrophages to Induce Inflammation in Sepsis. Front. Pharmacol. 12:791648. doi: 10.3389/fphar.2021.791648

INTRODUCTION

Cold-inducible RNA-binding protein (CIRP) is an 18-kD stress-responsive glycoprotein primarily present in the nucleus under normal conditions (Nishiyama et al., 1997). Under stressed conditions such as hypothermia, hypoxia, and ultra-violate irradiation, it migrates from the nucleus to the cytoplasm to act as an intracellular RNA chaperone (Wellmann et al., 2004; Zhu et al., 2016). We have recently identified that CIRP is also present in the extracellular space while stimulating macrophages with hypoxia

Abbreviations: CLP, cecal ligation and puncture; DAMPs, damage-associated molecular patterns; eCIRP, extracellular cold-inducible RNA-binding protein; HMGB1, high mobility group box 1; LPS, lipopolysaccharides; PAMPs, pathogen-associated molecular patterns; TLR, Toll-like receptor; TREM-1, triggering receptor expressed on myeloid cells-1.

and lipopolysaccharides (LPS) (Qiang et al., 2013). We further determined the presence of extracellular CIRP (eCIRP) in the blood of humans and mice with various clinical conditions such as sepsis, ischemia/reperfusion (I/R) injuries, and hemorrhagic shock (Qiang et al., 2013; Cen et al., 2017; Gurien et al., 2020). Hypoxia induces CIRP expression and release by activating the transcription factor, hypoxia-inducible factor 1α (HIF1α), while LPS induces CIRP expression and release through toll-like receptor 4 (TLR4) and nuclear factor-κB (NF-κB) pathway (Aziz et al., 2019). Unlike the release mechanism of cytokines and chemokines mediated through their N-terminal signal peptide, CIRP does not have a leader sequence to be released from cells during inflammation (Aziz et al., 2019). We previously reported that following hypoxia exposure to the macrophages, intracellular CIRP migrates from the nucleus to the cytoplasm, fuses with stress granules, and then is released *via* lysosomal secretion (Qiang et al., 2013). This finding enlightened the possibility of CIRP's secretion through a mechanism that causes loading or connecting to the vesicles/granules to be actively released from cells.

Following its secretion from cells, eCIRP acts as an important damage-associated molecular pattern (DAMP) (Zindel and Kubes, 2020). DAMPs are endogenous molecules which activate the immune system by stimulating pattern recognition receptors (PRRs) to contribute to various diseases (Zindel and Kubes, 2020). eCIRP induces inflammation by binding to its receptors such as TLR4 and triggering receptor expressed on myeloid cells-1 (TREM-1) (Qiang et al., 2013; Denning et al., 2020). Macrophages and neutrophils treated with eCIRP release pro-inflammatory cytokines, chemokines, and extracellular traps (ETs) (Aziz et al., 2019; Ode et al., 2019; Murao et al., 2020a). Normal mice injected with eCIRP exhibit systemic inflammation and acute lung injury (ALI), while $CIRP^{-/-}$ mice are protected from sepsis, I/R injuries, and other inflammatory diseases (Qiang et al., 2013; Denning et al., 2020; Gurien et al., 2020). Recent studies identified several antagonists of CIRP to inhibit eCIRP's binding to its receptors, TLR4 and TREM-1 (Qiang et al., 2013; Denning et al., 2020). We found that these antagonists abrogated inflammation and tissue injury in various diseases. Thus, eCIRP plays a significant role in inflammation, and targeting eCIRP is a potential approach to mitigate inflammatory diseases.

DAMPs are released passively by cell death as well as actively via exocytosis of secretory lysosomes and exosomes (Murao et al., 2021). Exosomes are 30–150 nm extracellular vesicles (EV) with lipid bilayer membrane structures carrying proteins, lipids, and nucleic acids to facilitate intercellular communication (Murao et al., 2020b; Kalluri and Lebleu, 2020). Following endocytosis, inward invagination of endosome gives rise to the generation of intraluminal vesicles (ILVs), future exosomes, concomitant with the cargo sorting. The subset of endosomes containing ILVs is called multivesicular bodies (MVBs). Exosomes are released into the extracellular space when the MVBs fuse with the plasma membrane (Murao et al., 2020b; Kalluri and Lebleu, 2020). Released exosomes migrate to the site of action and are absorbed by the recipient cells to be eliminated from the body through metabolism and excretion (Kim et al., 2019). Almost all cell types secrete exosomes, and the exosomes are found in various biological fluids, such as blood, urine, saliva, and breast milk (de la Torre Gomez et al., 2018). Studies have shown that exosomes carry different DAMPs, including high mobility group box 1 (HMGB1), heat shock proteins, histones, adenosine triphosphate, extracellular RNA, and cell-free DNA. In fact, the release of DAMPs via exosomes can be upregulated by stimulation of the cells with LPS (Sakaki et al., 2013; Tulapurkar et al., 2015; Balusu et al., 2016; Nair et al., 2018; Li et al., 2020). Exosomal DAMPs are functionally active and contribute to the pathogenesis of inflammatory diseases by inducing cytokine production, immune cell polarization, and cell death (Murao et al., 2020b).

The current study tested our hypothesis that eCIRP is released through exosomal secretion to contribute to inflammation by inducing cytokine production by the macrophages and neutrophil migration. Thus, identifying a new mechanism of eCIRP's release through exosomes may reveal a novel therapeutic avenue to mitigate inflammation by controlling eCIRP's release from cells during inflammation.

MATERIALS AND METHODS

Mice

Male 8–12-week-old wild-type (WT) C57BL/6 mice were purchased from Charles River (Charles River, Wilmington, MA) and were acclimated to the environment for 5–7 days before we performed studies with them. $CIRP^{-/-}$ mice (C57BL/6 background) initially obtained from Jun Fujita (Kyoto University, Kyoto, Japan) were bred and maintained in our facility. Mice were housed in a temperature-controlled room on a 12-h (h) light-dark cycle and fed a standard mouse chow diet. All experiments were performed following the guidelines for using experimental animals by the National Institutes of Health and were approved by our Institutional Animal Care and Use Committees (IACUC).

In vivo LPS Administration

WT and $CIRP^{-/-}$ mice were intraperitoneally (*i.p*) injected with 5 mg/kg LPS (MilliporeSigma, Burlington, MA). After 4 h of the injection of LPS, mice were anesthetized, and blood was drawn to collect the serum for isolating exosomes.

Mouse Model of Sepsis

Polymicrobial sepsis was induced in mice by cecal ligation and puncture (CLP) (Gurien et al., 2020). WT mice were anesthetized with isoflurane and a midline abdominal incision was created. The cecum was ligated with a 4–0 silk suture 1 cm proximal from its distal extremity and punctured twice with a 22-gauge needle. The wound was closed in layers. Sham animals underwent a laparotomy without cecal ligation and puncture. Following the surgery, 1 ml of normal saline was subcutaneously injected to avoid surgery-induced dehydration. After 20 h of the surgery, the serum was harvested to isolate exosomes.

Cell Culture and Isolation of Primary Mouse Peritoneal Macrophages

Mouse macrophage cell line RAW 264.7 cells were obtained from ATCC. Murine peritoneal macrophages were isolated from WT

mice (Denning et al., 2020). Briefly, mice were euthanized using CO_2 asphyxiation, and peritoneal cells were collected using peritoneal lavage with PBS. Total peritoneal cells were isolated by centrifugation at 200 *g* for 10 min and subsequently cultured in DMEM (Thermo Fisher Scientific, Waltham, MA). After 4 h nonadherent cells were removed, and adherent cells, primarily macrophages, were collected, counted, and plated in the cell culture plate for subsequent studies.

Isolation of Exosomes

Exosomes were isolated from cell culture media and serum using a total exosome isolation kit (Themo Fisher Scientific) by following the manufacturer's protocol. Isolated exosomes were resuspended in PBS. The protein concentrations of the exosomes were determined by the Bio-Rad protein assay reagent (Hercules, CA). The size distribution of the exosomes was assessed by nanoparticle tracking analysis (NTA) using ZetaView TWIN (Particle Matrix, Inning am Ammersee, Germany), and the histogram was created with FlowJo software (Tree Star, Ashland, OR). NTA determines the size of nanoparticles within the range of 10–1,000 nm by using a special algorithm based on their movement recorded by a light sensitive camera under a laser illumination.

Assessment of Exosomal Levels of eCIRP *in vitro*

RAW 264.7 cells were cultured in DMEM (Thermo Fisher Scientific) and stimulated with 1 μg/ml LPS for 20 h. Exosomes were isolated from the culture supernatants, and the protein amount of the exosomes was determined by a Bio-Rad protein assay reagent. Equal protein amounts of the exosomes were supplemented with Lane Marker Non-Reducing Sample Buffer (Thermo Fisher Scientific), which contains SDS sufficient to lyse exosomes to release and denature the proteins. The crude exosomal proteins contained in the sample buffer were then subjected to Western blotting. The blots were reacted with anti-CIRP Ab (Proteintech, Rosemont, IL) followed by fluorescent-labeled secondary Abs (Li-Cor Biosciences, Lincoln, NE), and detection was done using an Odyssey FC Dual-Mode Imaging system (Li-Cor Biosciences, Lincoln, NE). The densitometry intensities of the bands were measured using ImageJ software (NIH). The blots were also reacted with anti-CD63 Ab (Abcam, Cambridge, UK) followed by the same procedures for the loading control.

Assessment of Exosomal Levels of eCIRP *in vivo*

Exosomes isolated from the serum of LPS-injected or CLP mice were lysed using extraction buffer containing 25 mM Tris, 0.15 M NaCl, 1 mM EDTA, 1% NP-40, 5% glycerol, 2 mM Na_3VO_4, and protease inhibitor cocktail (Roche Diagnostics, Basel, Switzerland), at pH 7.4. Protein concentration was determined by the Bio-Rad protein assay reagent. CIRP levels of exosomal lysates were assessed using mouse CIRP ELISA Kit (LSBio, Seattle, WA) and normalized by protein concentrations.

Assessment of the Effect of Exosome Inhibitor GW4869 on the Release of eCIRP

RAW 264.7 cells were cultured in Opti-MEM (Thermo Fisher Scientific) and pre-treated with GW4869 (MilliporeSigma) at a dose of 10 μg/ml for 2 h followed by 20 h stimulation with 1 μg/ml LPS. An equal volume of the supernatants was supplemented with Lane Marker Non-Reducing Sample Buffer (Thermo Fisher Scientific) to perform Western blotting for CIRP. LPS at a dose of 5 mg/kg was intraperitoneally injected to WT mice with or without 1 mg/kg GW4869 injection simultaneously. Serum was harvested 4 h after the injection and eCIRP levels of the serum were assessed by mouse CIRP ELISA Kit (LSBio). CLP was performed in WT mice with or without intraperitoneal instillation of GW4869 before closing the abdomen. 20 h after CLP, serum was harvested to assess eCIRP levels by mouse CIRP ELISA Kit (LSBio).

Homology Modeling of CIRP and CD63

The amino acid sequences of mouse CIRP (P60824) and CD63 (P41731) were retrieved from the Uniprot database. The models were generated using Iterative Threading ASSEmbly Refinement (I-TASSER) server based on templates identified by threading approach to maximize the percentage identity, sequence coverage, and confidence (Yang et al., 2015). The CIRP structure has RNA binding domain (aa 6–84), disordered region (aa 70–172), and polar residues (aa 143–172). The CD63 has different topological and transmembrane domains and a lysosomal targeting motif (234–238). Models were refined based on repetitive relaxations by short molecular dynamics simulations for mild (0.6 ps) and aggressive (0.8 ps) relaxations with 4 fs time step after structure perturbations. The model refinement enhanced specific parameters, including Rama favored residues and a decrease in poor rotamers.

Protein-Protein Docking

The docking of CIRP and CD63 protein structure models was performed using ATTRACT tool (Schindler et al., 2015), which uses an approach of conformational flexibility of binding partners. The docking process includes pre-calculation of potential energy on a grid and then interactions are calculated by interpolation from nearest grid points. Moreover, docking process includes several Monte Carlo simulations or energy minimization steps.

Protein-Protein Interaction

The analysis of CIRP-CD63 complex interactions were calculated using PDBePISA tool (Krissinel and Henrick, 2007). The surface area of interaction interface and thermodynamic parameters were calculated. The complex structure was visualized using PyMOL and Chimera (Sanner et al., 1996).

Assessment of Intracellular Interaction Between CIRP and CD63

RAW 264.7 cells (1×10^6 cells) were stimulated with 1 μg/ml LPS for 20 h. We also isolated cells from the peritoneal lavage of mice

4 h after LPS injection and 20 h after CLP. The cells were lysed using a buffer containing 25 mM Tris, 0.15 M NaCl, 1 mM EDTA, 1% NP-40, 5% glycerol, 2 mM Na_3VO_4, and protease inhibitor cocktail (Roche Diagnostics), pH 7.4. The extracted proteins were immunoprecipitated with anti-CD63 Ab (Abcam) and protein A/G plus agarose beads (Themo Fisher Scientific), and the eluted samples were subjected to Western blotting. Finally, the blots were detected with anti-CIRP Ab (Proteintech). Total lysates were subjected to Western blotting, and the blots were detected with anti-CD63 Ab (Abcam) for internal control.

Protease Protection Assay

Equal amounts of exosomes isolated from the supernatants of LPS-treated RAW 264.7 cells were separated into 3 groups: 1. control, 2. 100 ng/ml protease K (Thermo Fisher Scientific), 3. 1% Triton-X 100 + 100 ng/ml protease K. The samples were incubated in 37°C for 30 min and denatured with 99°C Lane Marker Non-Reducing Sample Buffer (Themo Fisher Scientific) for Western blotting. The blots were reacted with anti-CIRP Ab (Proteintech) and anti-TSG101 Ab (Cell Signaling Technology, Danvers, MA). TSG101 is an important component of the endosomal sorting complex required for transport (ESCRT) machinery and serves as an internal control of exosomes (Fan et al., 2020).

Culture of Macrophages With WT and CIRP$^{-/-}$ Exosomes

RAW 264.7 cells and peritoneal macrophages were co-cultured with 5 μg/ml of exosomes isolated from WT or CIRP$^{-/-}$ mice treated with PBS or LPS. After 20 h supernatants were analyzed by ELISA kits specific for IL-6 and TNFα (both from BD Biosciences, Franklin Lakes, NJ) according to the manufacturer's protocol.

Intraperitoneal Injection of WT vs CIRP$^{-/-}$ Exosomes in Mice

WT mice were intraperitoneally injected with 10 mg/kg of exosomes isolated from WT or CIRP$^{-/-}$ mice challenged with LPS. After 4 h of injection with exosomes, serum and peritoneal lavage were collected. Serum was analyzed by ELISA for IL-6 and TNFα (both from BD Biosciences). The number of peritoneal neutrophils labeled with anti-Ly6G Ab (BioLegend, San Diego, CA) was counted by FACSymphony Flow Cytometer (BD Biosciences) using Precision Count Beads (BioLegend).

Neutrophil Migration Assay With WT vs CIRP$^{-/-}$ Exosomes

Neutrophils were isolated from the bone marrow of WT mice using the EasySep mouse neutrophil enrichment kit (STEMCELL, Vancouver, BC). Neutrophils (0.5×10^6) were added into the 3.0 μm cell culture insert (Corning, Corning, NY) placed on the cell culture plate. Exosomes were isolated from WT and CIRP$^{-/-}$ mice challenged with LPS, and exosomal protein concentration was determined. Exosomes (5 μg/ml) were added into the bottom chamber of the 24-well plate containing insert loaded with neutrophils. After 4 h, the number of migrated neutrophils in the well was counted by flow cytometry using anti-Ly6G Ab (BioLegend) and Precision Count Beads (BioLegend) as described earlier.

Statistical Analysis

Data represented in the figures are expressed as mean ± SEM. ANOVA was used for one-way comparison among multiple groups, and the significance was determined by the Student Newman-Keuls (SNK) test. The paired Student t-test was applied for two-group comparisons. Significance was considered for $p \leq 0.05$ between study groups. Data analyses were carried out using GraphPad Prism graphing and statistical software (GraphPad Software, San Diego, CA).

RESULTS

Endotoxin and Sepsis Increase eCIRP Release *via* Exosomes

We treated macrophages and mice with LPS and then collected exosomes from culture supernatants and serum to assess eCIRP levels within the exosomes. We first examined the quality of exosomes isolation by NTA based on their unique size range demarcating from other extracellular vesicles. The median size of the isolated exosomes was 126 and 72 nm for macrophage culture supernatant- and serum-derived samples, respectively, indicating efficient isolation and purity of the exosomes (**Figures 1A,B**). The size difference of the exosomes between the sources was in line with previous studies showing exosomes isolated from cell lines, including RAW 264.7 cells, exhibited larger size than primary cell- or serum-derived exosomes (Singh et al., 2012; Cai et al., 2018; Zhao et al., 2020). We also subjected mice to CLP, a model of polymicrobial sepsis. The median size of exosomes isolated from the serum of CLP mice was 70 nm, which was identical to that of LPS-injected mice (**Figure 1C**). There were no significant differences in the size of exosomes between PBS/Sham and LPS/CLP groups (**Figures 1A–C**). Next, we compared the levels of eCIRP in the exosomes released from RAW 264.7 cells subjected to PBS or LPS stimulation. While we observed basal levels of exosomal eCIRP in the PBS group, LPS stimulation significantly increased the levels of eCIRP in the exosomes (**Figure 1D**). We also assessed the levels of CD63, one of the pan markers of exosomes, and found that it was homogeneously present among the samples (**Figure 1D**). We then checked exosomal eCIRP release in mice injected with LPS. Exosomes isolated from the serum of LPS-injected mice contained significantly higher amounts of eCIRP than that of the PBS-injected mice (**Figure 1E**). Similarly, exosomes isolated from CLP mice serum exhibited significantly elevated levels of eCIRP compared to sham mice (**Figure 1F**). These findings indicate that eCIRP is released via exosomes from macrophages, and the levels of exosomal eCIRP are increased by LPS treatment of the macrophages and mice and in septic mice.

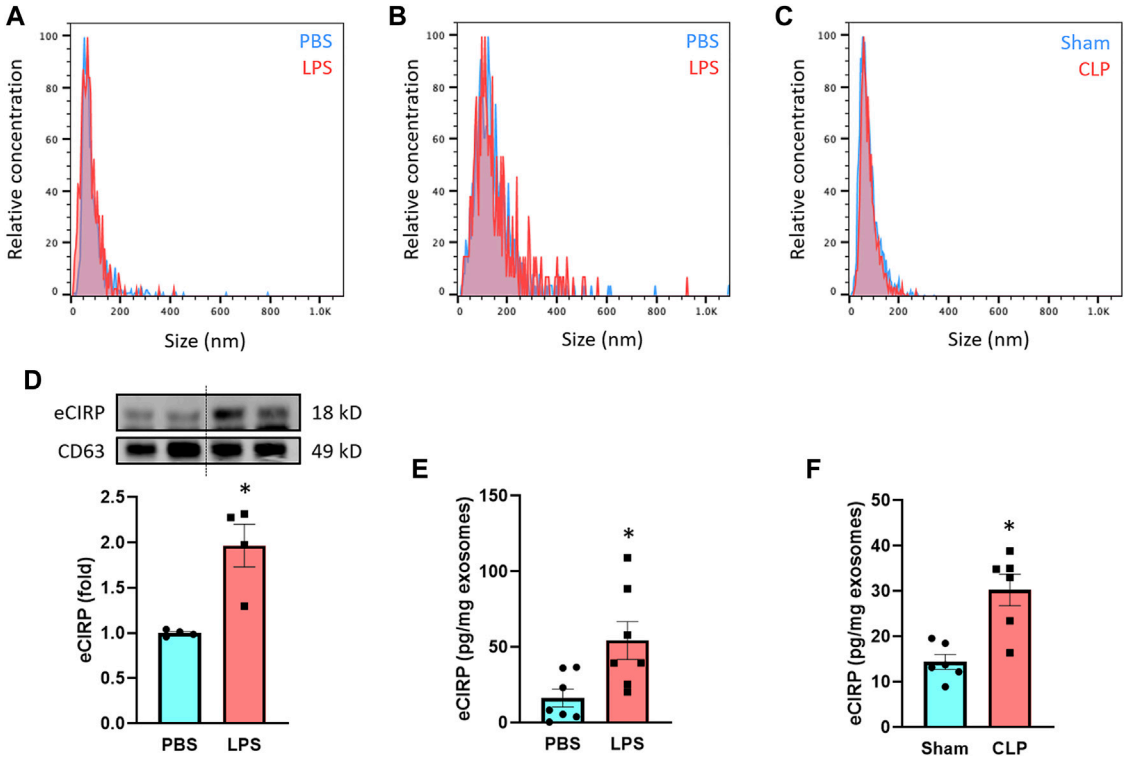

FIGURE 1 | LPS induces eCIRP release via exosomes. The size distribution of the isolated exosomes from **(A)** culture supernatants of PBS/LPS-treated RAW 264.7 cells and serum of **(B)** PBS/LPS-injected or **(C)** Sham/CLP mice was assessed by ZetaView TWIN. The experiments were repeated three times. **(D)** eCIRP levels of the exosomes isolated from the culture supernatants of PBS- or LPS-treated RAW 264.7 cells were determined by Western blotting. RAW 264.7 cells (10^6) were treated with PBS or LPS (1 μg/ml). After 20 h of LPS stimulation, exosomes were isolated from culture supernatants. Protein contents were determined in the exosomes, and an equal amount of protein (30 μg) was loaded in the gel to assess eCIRP levels by Western blot using anti-CIRP Ab. Blots were stripped off and re-probed with anti-CD63 Ab to serve as a loading control. Data are expressed as means ± SE (n = 4 samples/group). The groups were compared by paired student's t-test (*p < 0.05 vs. PBS). **(E)** eCIRP levels of the exosomes isolated from the serum of PBS- or LPS-injected mice were determined by ELISA and were normalized with the protein concentration. Data are expressed as means ± SE (n = 7 samples/group). The groups were compared by paired student's t-test (*p < 0.05 vs. PBS). **(F)** eCIRP levels of the exosomes isolated from the serum of sham or CLP mice were determined by ELISA and were normalized with the protein concentration. Data are expressed as means ± SE (n = 6 samples/group). The groups were compared by paired student's t-test (*p < 0.05 vs. Sham).

CIRP Interacts With CD63, a Member of the Tetraspanin Family Intracellularly

We next focused on the intracellular formation of exosomes containing CIRP. CD63 is one of the tetraspanin proteins and is enriched in the exosomes. CD63 is not only used as a biomarker of exosomes but is also involved in exosome cargo loading (Wei et al., 2021). First, we assessed the interaction between CIRP and CD63 by computational modeling, and it indeed predicted the direct binding (**Figure 2A**). The CIRP-CD63 structure complex showed that the disordered region and some polar residues of CIRP interacted with the 1st, 3rd, and 4th alpha-helices of the transmembrane region of CD63. The CIRP-CD63 complex structure revealed that based on the interaction interface surface area in Å2, which was 1,299 Å2 and other thermodynamic parameters such as free energy of binding upon complex formation (ΔiG) −15.6 kcal/mol indicated that the CIRP and CD63 interactions could be an intermediate type of interactions. Moreover, the free energy of dissociation (ΔGdisso) was 3.5 kcal/mol. The positive free energy of dissociation indicated that the CIRP-CD63 complex was stable. The entropy change after dissociation (TΔS) was 12.5 kcal/mol. There was one hydrogen bond formation (Gly27-Arg75), which possibly contributed to the stability of CIRP-CD63 complex structure (**Table 1**). Next, we assessed their interaction in cells by immunoprecipitation. We collected the proteins of RAW 264.7 cells challenged with LPS and peritoneal cells isolated from LPS-injected or CLP mice and subjected the total proteins to immunoprecipitation of anti-CD63 Ab. We found that cell lysates immunoprecipitated with anti-CD63 Ab revealed the presence of CIRP. In contrast, the lysates immunoprecipitated with IgG did not show the existence of CIRP, indicating the intracellular interaction between CIRP and CD63 (**Figures 2B–D**). These results suggest the formation of the CIRP-CD63 complex and the sorting of CIRP to exosomes inside the cells.

An Exosome Inhibitor GW4869 Attenuates eCIRP Release

To further confirm eCIRP's release *via* exosomes, we used GW4869, an inhibitor of exosome biogenesis and release

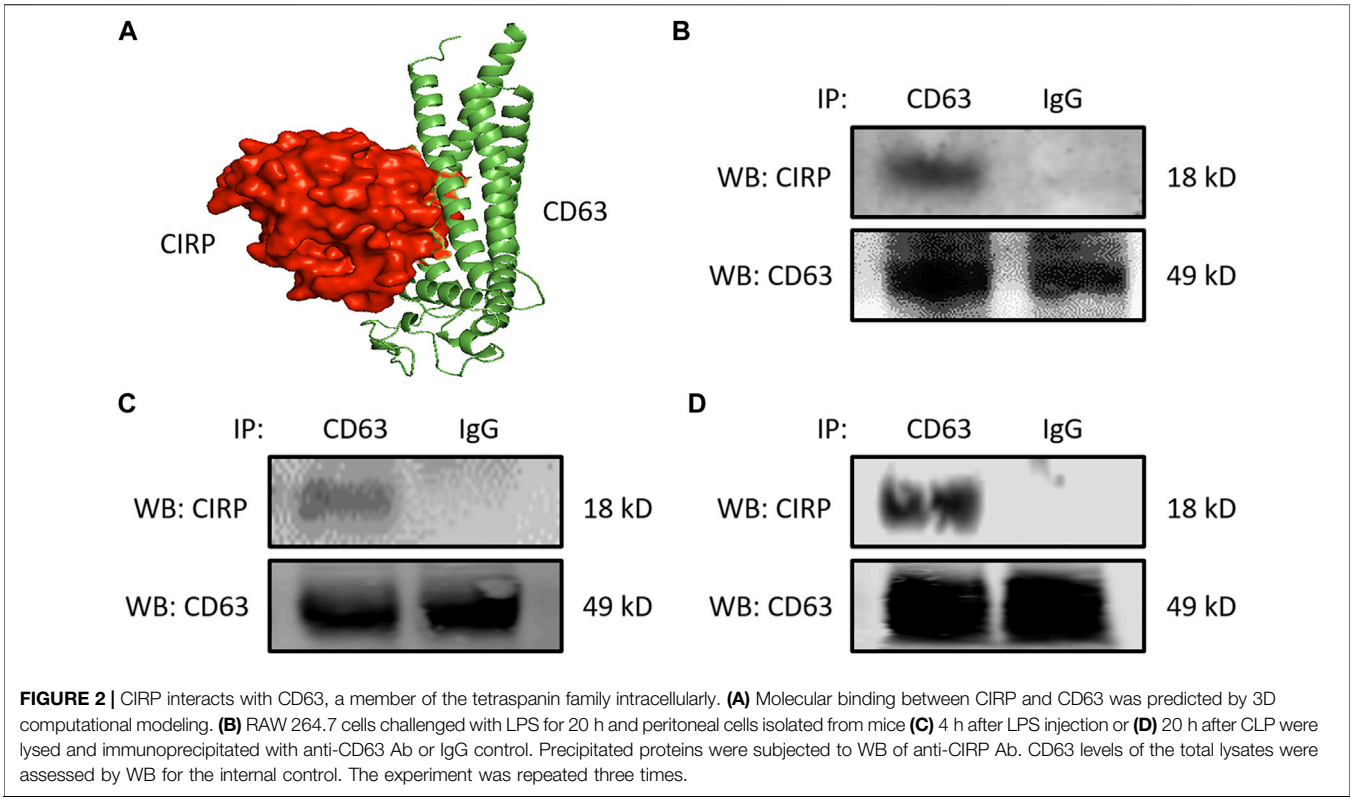

FIGURE 2 | CIRP interacts with CD63, a member of the tetraspanin family intracellularly. **(A)** Molecular binding between CIRP and CD63 was predicted by 3D computational modeling. **(B)** RAW 264.7 cells challenged with LPS for 20 h and peritoneal cells isolated from mice **(C)** 4 h after LPS injection or **(D)** 20 h after CLP were lysed and immunoprecipitated with anti-CD63 Ab or IgG control. Precipitated proteins were subjected to WB of anti-CIRP Ab. CD63 levels of the total lysates were assessed by WB for the internal control. The experiment was repeated three times.

TABLE 1 | Interaction between CIRP and CD63 as revealed by computational analysis. The analysis of CIRP-CD63 complex interactions were calculated using PDBePISA tool. The surface area of interaction interface and thermodynamic parameters were determined.

Complex	Surface area ($Å^2$)	Binding ($^{\Delta}G$) energy (Kcal/mol)	Free energy of dissociation (ΔG^{diss}) in kcal/mol	Entropy change at dissociation ($T\Delta S^{diss}$)	N_{HB}	N_{SB}
CIRP-CD63	1,299.0	−15.6	3.5	12.5	1	0

(Catalano and O'driscoll, 2020). We pre-treated the RAW 264.7 cells with GW4869 for 2 h and stimulated these cells with LPS for 20 h. Pre-treatment with GW4869 significantly decreased the levels of eCIRP in the culture supernatants of macrophages stimulated with LPS (**Figure 3A**). We also assessed the effect of GW4869 on eCIRP release in endotoxemic and septic mice. While LPS increased eCIRP levels in mice serum, GW4869 injection significantly attenuated the levels of eCIRP in the serum of LPS-injected mice (**Figure 3B**). eCIRP was significantly elevated in the serum of CLP-induced septic mice, whereas GW4869 dramatically decreased eCIRP levels in the serum of CLP mice (**Figure 3C**). Collectively, this data, along with the data of intracellular interaction between CIRP and CD63 (**Figure 2**), confirmed exosomes to be the means of eCIRP release instead of the possibility that exosomes and eCIRP make complex in the extracellular space following their release from cells separately. In addition, the significance of the decrease of eCIRP levels back to the baseline by GW4869 treatment indicated that exosomes could play a significant role in releasing the majority of eCIRP.

CIRP is Present on the Surface of Exosomes

To elucidate eCIRP's localization on exosomes, we performed a protease protection assay (**Figure 4A**). Exosomes isolated from the supernatants of LPS-challenged RAW 264.7 cells were treated with or without proteinase K and Triton-X 100. Proteinase K alone quenched CIRP even the membrane integrity of the exosomes was preserved in the absence of Triton-X 100. On the contrary, TSG101, one of the intra-exosomal proteins, required Triton-X 100 to be digested by proteinase K (**Figure 4B**). These results indicate that eCIRP is present on the surface of the exosomes, suggesting it can directly interact with cell surface receptors of eCIRP to promote eCIRP-mediated inflammation.

Exosomal eCIRP Induces Pro-inflammatory Cytokine Production

Previous studies showed that exosomes isolated from LPS-treated macrophages or mice exhibited inflammatory responses when treated to the naive immune cells (McDonald et al., 2014). To

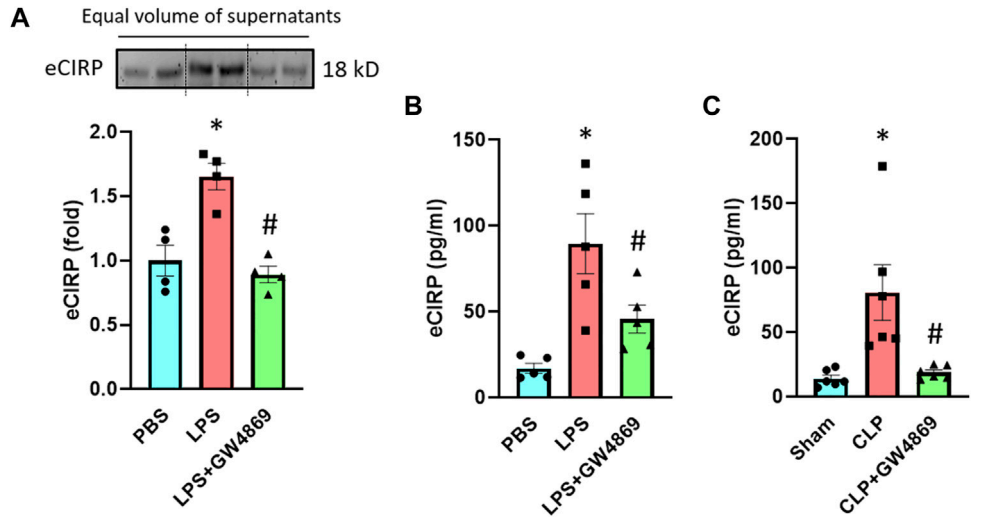

FIGURE 3 | An exosome inhibitor GW4869 attenuates eCIRP release. **(A)** RAW 264.7 cells were treated with PBS, LPS or LPS + GW4869. After 20 h eCIRP levels of the supernatants were assessed by Western blotting. Data are expressed as means ± SE (n = 4 samples/group). The groups were compared by two-way ANOVA and SNK method (*p < 0.05 vs PBS; #p < 0.05 vs LPS). **(B)** Mice were injected with PBS, LPS or LPS + GW4869. After 4 h the serum was harvested and eCIRP levels were assessed by ELISA. Data are expressed as means ± SE (n = 5 samples/group). The groups were compared by two-way ANOVA and SNK method (*p < 0.05 vs PBS; #p < 0.05 vs LPS). **(C)** Mice were subjected to sham surgery, CLP or CLP with GW4869 instillation. After 20 h the serum was harvested and eCIRP levels were assessed by ELISA. Data are expressed as means ± SE (n = 6 samples/group). The groups were compared by two-way ANOVA and SNK method (*p < 0.05 vs Sham; #p < 0.05 vs CLP).

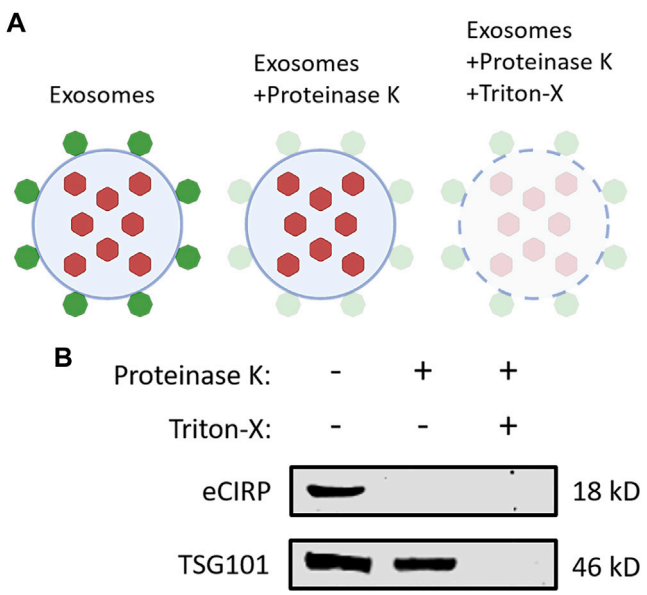

FIGURE 4 | CIRP is present on the surface of exosomes. **(A)** A schematic diagram of proteinase protection assay. Proteinase K alone only digests the proteins on the surface of exosomes. An additional treatment of Triton-X with proteinase K quenches the proteins both on the surface and inside the exosomes. **(B)** Exosomes isolated from the supernatants of LPS-treated RAW 264.7 cells were incubated with Proteinase K ± Triton-X at 37°C for 30 min and subjected to Western blotting of anti-CIRP Ab and anti-TSG101 Ab. The experiment was repeated three times.

determine the impact of exosomal eCIRP on macrophages, we first isolated exosomes from the blood of LPS-treated WT or CIRP$^{-/-}$ mice. Those exosomes contained barely detectible endotoxin contamination (data not shown), which was consistent with a previous study (Li et al., 2018). We then treated RAW 264.7 cells separately with the WT or CIRP$^{-/-}$ mice exosomes for 20 h and assessed the levels of cytokines in the culture supernatants. We found that exosomes isolated from PBS-injected WT mice did not induce cytokine production when added to the macrophages. On the other hand, exosomes isolated from LPS-injected WT mice induced IL-6 and TNFα production by the macrophages (**Figures 5A,B**). Interestingly, RAW 264.7 cells stimulated with exosomes isolated from LPS-treated CIRP$^{-/-}$ mice blood significantly decreased IL-6 and TNFα production compared to WT exosomes (**Figures 5A,B**). Similarly, primary mouse peritoneal macrophages treated with exosomes obtained from LPS-injected CIRP$^{-/-}$ mice blood showed a significant decrease in IL-6 and TNFα levels in the culture supernatants compared to exosomes isolated from LPS-injected WT mice blood (**Figures 5C,D**). These data indicate that eCIRP present in the exosomes induces inflammation in macrophages. To determine the role of eCIRP on exosome-mediated inflammation in mice, we *i. p.* administered WT mice with the exosomes isolated from LPS-treated WT or CIRP$^{-/-}$ mice blood. We found that normal mice injected (*i.p.*) with exosomes isolated from LPS-treated WT mice exhibited higher levels of IL-6 and TNFα in the serum than mice injected (*i.p.*) with exosomes isolated from LPS-treated CIRP$^{-/-}$ mice blood (**Figures 5E,F**). These data indicate that exosomal eCIRP induces cytokine production in mice.

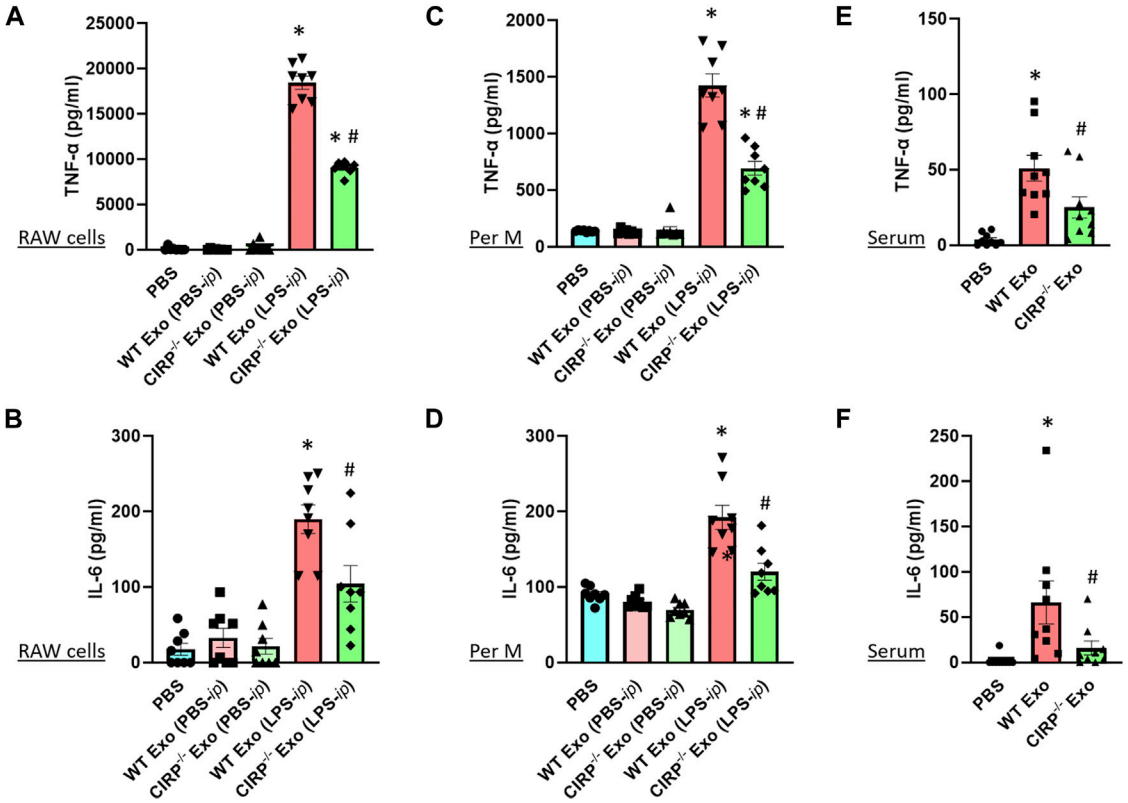

FIGURE 5 | Exosomal eCIRP induces pro-inflammatory cytokine production. **(A,B)** RAW 264.7 cells (10^5) and **(C,D)** peritoneal macrophages (10^5) were co-cultured with 5 μg/ml of exosomes isolated from WT or CIRP$^{-/-}$ mice treated with PBS or LPS. After 20 h supernatants were collected and IL-6 and TNF-α levels were assessed by ELISA. Data are expressed as means ± SE (n = 8 samples/group). The groups were compared by two-way ANOVA and SNK method (*p < 0.05 vs PBS; $^{\#}p$ < 0.05 vs exosomes from LPS- *i. p.* WT mice). **(E,F)** WT mice were intraperitoneally injected with exosomes isolated from WT or CIRP$^{-/-}$ mice challenged with LPS. After 4 h serum was harvested and IL-6 and TNF-α levels were assessed by ELISA. The groups were compared by two-way ANOVA and SNK method Data are expressed as means ± SE (n = 9 samples/group). The groups were compared by two-way ANOVA and SNK method (*p < 0.05 vs PBS; $^{\#}p$ < 0.05 vs. WT exosomes).

Exosomal eCIRP Promotes Neutrophil Migration

We assessed the chemotactic activity of eCIRP containing exosomes. *In vitro* neutrophil migration data revealed that exosomes isolated from LPS-treated WT mice induced neutrophil migration. In contrast, exosomes isolated from LPS-treated CIRP$^{-/-}$ mice significantly decreased the numbers of migrated neutrophils (**Figures 6A,B**). Furthermore, *in vivo i. p.* injection of exosomes isolated from LPS-treated WT mice blood increased neutrophil infiltration in the peritoneal cavity. By contrast, *i. p.* injection of exosomes of LPS-treated CIRP$^{-/-}$ mice blood showed a significant decrease in the infiltration of neutrophils in the peritoneal cavity compared to WT exosomes treated mice (**Figures 6C,D**). These data indicate the direct chemotaxis effects of exosomal eCIRP.

DISCUSSION

The present study reveales that eCIRP is released via exosomes and has impacts on exosome-induced inflammation. Our findings on the new mechanism of eCIRP release through exosomes are crucial in inducing innate immune response since little has been known how eCIRP is released into the extracellular space, especially in terms of active secretion. As a leaderless (devoid of signal peptide sequence) protein, eCIRP is unlikely to be released via the endoplasmic reticulum (ER)-Golgi pathway (Aziz et al., 2019). Until now, eCIRP has been regarded to be released passively by necrosis or actively by secretory lysosomes (Qiang et al., 2013; Aziz et al., 2019). We have previously shown enrichment of CIRP in lysosomes in the cells under stress conditions suggesting its release by secretory lysosomes (Qiang et al., 2013). In cells, exosomes have been known to interact with lysosomes, especially for their degradation (Kalluri and Lebleu, 2020). Together with our previous and current findings, the interaction between exosomes and lysosomes in the cells might also be a process for the release of exosomal eCIRP. We also found that eCIRP is present on the surface of exosomes, suggesting its direct interaction with cell surface receptors such as TLR4 and TREM-1 to induce inflammatory responses. It was previously reported that histones present on the surface of exosomes interact with TLR4 to induce cytokine production (Nair et al., 2018). As both being nuclear proteins, eCIRP might share similar

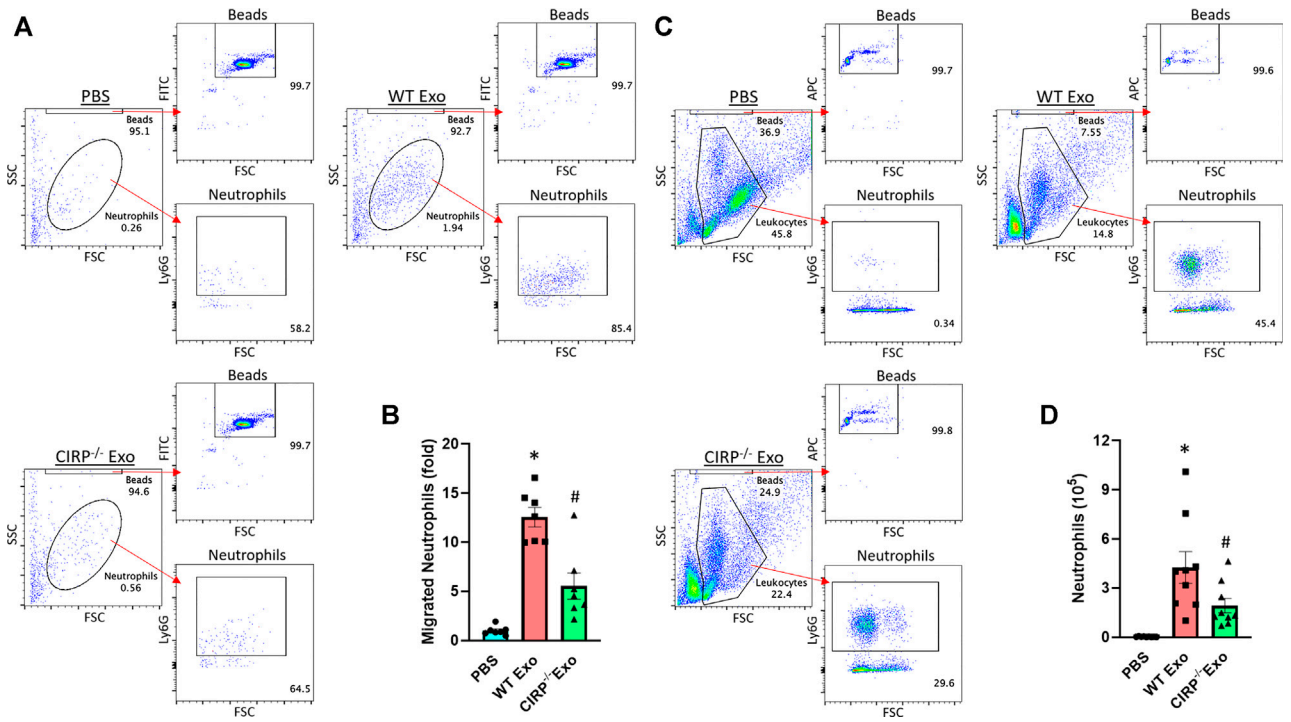

FIGURE 6 | Exosomal eCIRP promotes neutrophil migration. Migration of neutrophils (5×10^5) was assessed using 5 μg/ml of exosomes isolated from WT or CIRP$^{-/-}$ mice challenged with LPS as attractants. After 4 h the number of migrated neutrophils was counted by flow cytometry and was normalized to PBS group. **(A)** Representative dot pots and **(B)** bar diagram are shown. Data are expressed as means ± SE ($n = 7$ samples/group). The groups were compared by two-way ANOVA and SNK method (*$p < 0.05$ vs PBS; $^{\#}p < 0.05$ vs WT exosomes). WT mice were intraperitoneally injected with exosomes isolated from WT or CIRP$^{-/-}$ mice challenged with LPS. After 4 h the number of infiltrated neutrophils in the peritoneal lavage was assessed by flow cytometry. **(C)** Representative dot pots and **(D)** bar diagram are shown. Data are expressed as means ± SE ($n = 9$ samples/group). The groups were compared by two-way ANOVA and SNK method (*$p < 0.05$ vs PBS; $^{\#}p < 0.05$ vs WT exosomes).

loading mechanisms with histones to be presented on the surface of exosomes. In this study, we focused on macrophages as the source of exosomal eCIRP since macrophages significantly contribute to innate immunity and have already been shown to release eCIRP under stress such as hypoxia and LPS stimulation (Qiang et al., 2013). Although the *in vitro* studies made it feasible to know the origin/source of exosomes as we studied on macrophages, in the context of *in vivo* studies, identification of the sources of exosomes that contain eCIRP is critical as any cells can release exosomes upon different kinds of stimuli (Murao et al., 2020b; Kalluri and Lebleu, 2020). Since all cell types ubiquitously express CIRP (Zhong and Huang, 2017), it is thought that under *in vivo* conditions, exosomal eCIRP can be released by various immune and non-immune cells which respond to PAMPs, DAMPs, and other stimuli. Future studies on detecting exosomal eCIRP using different stimuli on various cell types *in vitro* or using cell type-specific knock-out animals will be of interest.

Besides confirming the exosomal release of eCIRP, we also assessed the impacts of eCIRP on exosome-induced inflammation. Exosomes have already been shown to play a crucial role in sepsis because of their inflammatory function. Exosome inhibitor GW4869 attenuated IL-6 and TNFα levels in the supernatants of LPS-challenged macrophages and the serum of CLP mice (Essandoh et al., 2015). GW4869 also ameliorated sepsis-induced cardiac dysfunction and improved the survival of septic mice, indicating its clinical potential (Essandoh et al., 2015). However, the study had not revealed which exosomal contents are responsible for sepsis pathophysiology. We have found that GW4869 significantly attenuated eCIRP release in LPS-treated macrophages as well as endotoxemic and septic mice, indicating the therapeutic effects of GW4869 on sepsis could be, at least in part, due to the reduction of exosomal eCIRP. To confirm the impacts of exosomal eCIRP more directly, we have demonstrated that exosomes isolated from LPS-challenged CIRP$^{-/-}$ mice have significantly decreased levels of inflammatory functions as compared to those of WT mice in terms of cytokine production and neutrophil migration *in vitro* and *in vivo*. It has been shown that LPS stimulation increases exosomal contents, including cytokines and DAMPs such as HMGB1, HSP, histones, ATP, and exRNAs (Sakaki et al., 2013; McDonald et al., 2014; Tulapurkar et al., 2015; Balusu et al., 2016; Nair et al., 2018; Li et al., 2020). The presence of those inflammatory molecules within the exosomes was likely to be the reason that even though the exosomes of CIRP$^{-/-}$ mice were free from CIRP, the presence of other molecules within exosomes might have induced the inflammation, which resulted in not complete inhibition of inflammatory responses in CIRP$^{-/-}$ exosome-treated group.

Neutrophils are the first line of defense against pathogen invasion, but their excessive activities including tissue migration cause organ injuries (Rittirsch et al., 2008). The present study has revealed that exosomal eCIRP plays a significant role in neutrophil migration. A previous study has shown that exosomes attracted neutrophils in an LTB4 receptor-dependent manner *in vitro* (Majumdar et al., 2021), indicating their direct effect on neutrophil migration, which is in line with our current finding. Furthermore, another study has shown that intraperitoneal injection of septic exosomes induced neutrophil migration in a MyD88-dependent manner (Xu et al., 2018), suggesting exosomal eCIRP stimulates TLR4/MyD88 pathway to cause neutrophil migration since eCIRP is one of the most potent ligands for TLR4. Besides the direct effect, the migration of neutrophils *in vivo* might have been amplified by chemokines released from the resident macrophages activated by the exosomes. Since exosomal eCIRP exhibited its effects on neutrophils, this finding further implicates its role in the production of reactive oxygen species (ROS), myeloperoxidase (MPO), and neutrophil extracellular traps (NETs) by neutrophils to exaggerate inflammation and tissue injury. We have previously shown that eCIRP induces the formation of NETs via TREM-1 (Murao et al., 2020a). Thus, it is likely that exosomal eCIRP also promotes NETosis in the same manner, but further studies are awaited to prove this theory.

eCIRP has been reported to be elevated in the circulation and correlate with the severity of patients suffering from sepsis (Zhou et al., 2015). Our study using exosome inhibitor GW4869 revealed that exosomal release is the major, if not all, source of eCIRP. Therefore, it is suggested that exosomal eCIRP plays a critical role in the development of inflammatory diseases. Exosomes, in general, have already shown their clinical potential. Exosomes are regarded as important biomarkers for cancer (Lebleu and Kalluri, 2020). Artificial liposomes, which share similar structures with exosomes, have already been used to deliver drugs and vaccines such as Amphotericin B and COVID-19 vaccine, respectively (Tenchov et al., 2021). Our study suggests targeting specific contents in biological exosomes, including exosomal eCIRP can be a novel therapeutic avenue for treating inflammatory diseases.

From this study, we identified several critical issues that need further focus. Firstly, while we showed different functions between WT and CIRP$^{-/-}$ exosomes of LPS-injected mice, it still remains inconclusive whether the differences are due to the direct effects of exosomal eCIRP or indirect exosomal changes caused by the presence or absence of CIRP. For example, the lack of CIRP might have also caused differences in other exosomal contents, which synergistically enhancing functional differences. Secondly, we have performed only two experimental models, endotoxemia and sepsis. Since eCIRP is involved in various diseases caused by different stimuli, it would be important to prove eCIRP can also be released via exosomes in other inflammatory conditions. Since increased serum levels of eCIRP are directly associated with the sepsis severity in patients (Zhou et al., 2015; Gurien et al., 2020), the clinical relevance of this study would further be supported by confirming the elevation of exosomal eCIRP in the samples of patients with inflammatory diseases.

In conclusion, eCIRP is released via exosomes and contributes to inflammation by inducing cytokine production and neutrophil migration. Therefore, targeting exosomal eCIRP has the potential to become a novel therapeutic avenue to treat inflammatory diseases.

DATA AVAILABILITY STATEMENT

The original contributions presented in the study are included in the article. Further inquiries can be directed to the corresponding authors.

ETHICS STATEMENT

All animal experiments were performed following the guidelines for using experimental animals by the National Institutes of Health and were approved by our (Feinstein Institutes) Institutional Animal Care and Use Committees (IACUC).

AUTHOR CONTRIBUTIONS

AM and MA outlined the experiments. AM performed *in vitro* and *in vivo* experiments. AM and CT perform sepsis model. AJ did computational modeling and writing the relevant methods and results. AM, MA, and PW analyzed the data. AM and MA wrote the manuscript. PW reviewed and edited the manuscript. PW conceived the idea. PW and MA supervised the project.

FUNDING

This study was supported by the National Institutes of Health (NIH) grants R35GM118337 (PW) and R01GM129633 (MA).

REFERENCES

Aziz, M., Brenner, M., and Wang, P. (2019). Extracellular CIRP (eCIRP) and Inflammation. *J. Leukoc. Biol.* 106, 133–146. doi:10.1002/jlb.3mir1118-443r

Balusu, S., Van Wonterghem, E., De Rycke, R., Raemdonck, K., Stremersch, S., Gevaert, K., et al. (2016). Identification of a Novel Mechanism of Blood-Brain Communication during Peripheral Inflammation via Choroid Plexus-Derived Extracellular Vesicles. *EMBO Mol. Med.* 8, 1162–1183. doi:10.15252/emmm.201606271

Cai, C., Koch, B., Morikawa, K., Suda, G., Sakamoto, N., Rueschenbaum, S., et al. (2018). Macrophage-Derived Extracellular Vesicles Induce Long-Lasting Immunity against Hepatitis C Virus Which Is Blunted by Polyunsaturated Fatty Acids. *Front. Immunol.* 9, 723. doi:10.3389/fimmu.2018.00723

Catalano, M., and O'driscoll, L. (2020). Inhibiting Extracellular Vesicles Formation and Release: a Review of EV Inhibitors. *J. Extracell Vesicles* 9, 1703244. doi:10.1080/20013078.2019.1703244

Cen, C., Mcginn, J., Aziz, M., Yang, W. L., Cagliani, J., Nicastro, J. M., et al. (2017). Deficiency in Cold-Inducible RNA-Binding Protein Attenuates Acute Respiratory Distress Syndrome Induced by Intestinal Ischemia-Reperfusion. *Surgery* 162, 917–927. doi:10.1016/j.surg.2017.06.004

De La Torre Gomez, C., Goreham, R. V., Bech Serra, J. J., Nann, T., and Kussmann, M. (2018). "Exosomics"-A Review of Biophysics, Biology and Biochemistry of Exosomes with a Focus on Human Breast Milk. *Front. Genet.* 9, 92. doi:10.3389/fgene.2018.00092

Denning, N. L., Aziz, M., Murao, A., Gurien, S. D., Ochani, M., Prince, J. M., et al. (2020). Extracellular CIRP as an Endogenous TREM-1 Ligand to Fuel Inflammation in Sepsis. *JCI Insight* 5, e134172. doi:10.1172/jci.insight.134172

Essandoh, K., Yang, L., Wang, X., Huang, W., Qin, D., Hao, J., et al. (2015). Blockade of Exosome Generation with GW4869 Dampens the Sepsis-Induced Inflammation and Cardiac Dysfunction. *Biochim. Biophys. Acta* 1852, 2362–2371. doi:10.1016/j.bbadis.2015.08.010

Fan, S. J., Kroeger, B., Marie, P. P., Bridges, E. M., Mason, J. D., Mccormick, K., et al. (2020). Glutamine Deprivation Alters the Origin and Function of Cancer Cell Exosomes. *Embo j* 39, e103009. doi:10.15252/embj.2019103009

Gurien, S. D., Aziz, M., Jin, H., Wang, H., He, M., Al-Abed, Y., et al. (2020). Extracellular microRNA 130b-3p Inhibits eCIRP-Induced Inflammation. *EMBO Rep.* 21, e48075. doi:10.15252/embr.201948075

Kalluri, R., and Lebleu, V. S. (2020). The Biology, Function, and Biomedical Applications of Exosomes. *Science* 367, eaau6977. doi:10.1126/science.aau6977

Kim, D. H., Kothandan, V. K., Kim, H. W., Kim, K. S., Kim, J. Y., Cho, H. J., et al. (2019). Noninvasive Assessment of Exosome Pharmacokinetics *In Vivo*: A Review. *Pharmaceutics* 11, 649. doi:10.3390/pharmaceutics11120649

Krissinel, E., and Henrick, K. (2007). Inference of Macromolecular Assemblies from Crystalline State. *J. Mol. Biol.* 372, 774–797. doi:10.1016/j.jmb.2007.05.022

Lebleu, V. S., and Kalluri, R. (2020). Exosomes as a Multicomponent Biomarker Platform in Cancer. *Trends Cancer* 6, 767–774. doi:10.1016/j.trecan.2020.03.007

Li, J. J., Wang, B., Kodali, M. C., Chen, C., Kim, E., Patters, B. J., et al. (2018). *In Vivo* evidence for the Contribution of Peripheral Circulating Inflammatory Exosomes to Neuroinflammation. *J. Neuroinflammation* 15, 8. doi:10.1186/s12974-017-1038-8

Li, W., Deng, M., Loughran, P. A., Yang, M., Lin, M., Yang, C., et al. (2020). LPS Induces Active HMGB1 Release from Hepatocytes into Exosomes through the Coordinated Activities of TLR4 and Caspase-11/GSDMD Signaling. *Front. Immunol.* 11, 229. doi:10.3389/fimmu.2020.00229

Majumdar, R., Tavakoli Tameh, A., Arya, S. B., and Parent, C. A. (2021). Exosomes Mediate LTB4 Release during Neutrophil Chemotaxis. *Plos Biol.* 19, e3001271. doi:10.1371/journal.pbio.3001271

Mcdonald, M. K., Tian, Y., Qureshi, R. A., Gormley, M., Ertel, A., Gao, R., et al. (2014). Functional Significance of Macrophage-Derived Exosomes in Inflammation and Pain. *Pain* 155, 1527–1539. doi:10.1016/j.pain.2014.04.029

Murao, A., Arif, A., Brenner, M., Denning, N. L., Jin, H., Takizawa, S., et al. (2020a). Extracellular CIRP and TREM-1 axis Promotes ICAM-1-Rho-Mediated NETosis in Sepsis. *Faseb j* 34, 9771–9786. doi:10.1096/fj.202000482R

Murao, A., Aziz, M., Wang, H., Brenner, M., and Wang, P. (2021). Release Mechanisms of Major DAMPs. *Apoptosis* 26, 152–162. doi:10.1007/s10495-021-01663-3

Murao, A., Brenner, M., Aziz, M., and Wang, P. (2020b). Exosomes in Sepsis. *Front. Immunol.* 11, 2140. doi:10.3389/fimmu.2020.02140

Nair, R. R., Mazza, D., Brambilla, F., Gorzanelli, A., Agresti, A., and Bianchi, M. E. (2018). LPS-challenged Macrophages Release Microvesicles Coated with Histones. *Front. Immunol.* 9, 1463. doi:10.3389/fimmu.2018.01463

Nishiyama, H., Itoh, K., Kaneko, Y., Kishishita, M., Yoshida, O., and Fujita, J. (1997). A Glycine-Rich RNA-Binding Protein Mediating Cold-Inducible Suppression of Mammalian Cell Growth. *J. Cel Biol* 137, 899–908. doi:10.1083/jcb.137.4.899

Ode, Y., Aziz, M., Jin, H., Arif, A., Nicastro, J. G., and Wang, P. (2019). Cold-inducible RNA-Binding Protein Induces Neutrophil Extracellular Traps in the Lungs during Sepsis. *Sci. Rep.* 9, 6252. doi:10.1038/s41598-019-42762-1

Qiang, X., Yang, W. L., Wu, R., Zhou, M., Jacob, A., Dong, W., et al. (2013). Cold-inducible RNA-Binding Protein (CIRP) Triggers Inflammatory Responses in Hemorrhagic Shock and Sepsis. *Nat. Med.* 19, 1489–1495. doi:10.1038/nm.3368

Rittirsch, D., Flierl, M. A., and Ward, P. A. (2008). Harmful Molecular Mechanisms in Sepsis. *Nat. Rev. Immunol.* 8, 776–787. doi:10.1038/nri2402

Sakaki, H., Tsukimoto, M., Harada, H., Moriyama, Y., and Kojima, S. (2013). Autocrine Regulation of Macrophage Activation via Exocytosis of ATP and Activation of P2Y11 Receptor. *PLoS One* 8, e59778. doi:10.1371/journal.pone.0059778

Sanner, M. F., Olson, A. J., and Spehner, J. C. (1996). Reduced Surface: an Efficient Way to Compute Molecular Surfaces. *Biopolymers* 38, 305–320. doi:10.1002/(sici)1097-0282(199603)38:3%3c305:aid-bip4%3e3.0.co;2-y

Schindler, C. E., De Vries, S. J., and Zacharias, M. (2015). iATTRACT: Simultaneous Global and Local Interface Optimization for Protein-Protein Docking Refinement. *Proteins* 83, 248–258. doi:10.1002/prot.24728

Singh, P. P., Smith, V. L., Karakousis, P. C., and Schorey, J. S. (2012). Exosomes Isolated from Mycobacteria-Infected Mice or Cultured Macrophages Can Recruit and Activate Immune Cells *In Vitro* and *In Vivo*. *J. Immunol.* 189, 777–785. doi:10.4049/jimmunol.1103638

Tenchov, R., Bird, R., Curtze, A. E., and Zhou, Q. (2021). Lipid Nanoparticles-From Liposomes to mRNA Vaccine Delivery, a Landscape of Research Diversity and Advancement. *ACS Nano*. doi:10.1021/acsnano.1c04996

Tulapurkar, M. E., Ramarathnam, A., Hasday, J. D., and Singh, I. S. (2015). Bacterial Lipopolysaccharide Augments Febrile-Range Hyperthermia-Induced Heat Shock Protein 70 Expression and Extracellular Release in Human THP1 Cells. *PLoS One* 10, e0118010. doi:10.1371/journal.pone.0118010

Wei, H., Chen, Q., Lin, L., Sha, C., Li, T., Liu, Y., et al. (2021). Regulation of Exosome Production and Cargo Sorting. *Int. J. Biol. Sci.* 17, 163–177. doi:10.7150/ijbs.53671

Wellmann, S., Bührer, C., Moderegger, E., Zelmer, A., Kirschner, R., Koehne, P., et al. (2004). Oxygen-regulated Expression of the RNA-Binding Proteins RBM3 and CIRP by a HIF-1-independent Mechanism. *J. Cel Sci* 117, 1785–1794. doi:10.1242/jcs.01026

Xu, J., Feng, Y., Jeyaram, A., Jay, S. M., Zou, L., and Chao, W. (2018). Circulating Plasma Extracellular Vesicles from Septic Mice Induce Inflammation via MicroRNA- and TLR7-dependent Mechanisms. *J. Immunol.* 201, 3392–3400. doi:10.4049/jimmunol.1801008

Yang, J., Yan, R., Roy, A., Xu, D., Poisson, J., and Zhang, Y. (2015). The I-TASSER Suite: Protein Structure and Function Prediction. *Nat. Methods* 12, 7–8. doi:10.1038/nmeth.3213

Zhao, F., Cheng, L., Shao, Q., Chen, Z., Lv, X., Li, J., et al. (2020). Characterization of Serum Small Extracellular Vesicles and Their Small RNA Contents across Humans, Rats, and Mice. *Sci. Rep.* 10, 4197. doi:10.1038/s41598-020-61098-9

Zhong, P., and Huang, H. (2017). Recent Progress in the Research of Cold-Inducible RNA-Binding Protein. *Future Sci. OA* 3, Fso246. doi:10.4155/fsoa-2017-0077

Zhou, Y., Dong, H., Zhong, Y., Huang, J., Lv, J., and Li, J. (2015). The Cold-Inducible RNA-Binding Protein (CIRP) Level in Peripheral Blood Predicts Sepsis Outcome. *PLoS One* 10, e0137721. doi:10.1371/journal.pone.0137721

Zhu, X., Bührer, C., and Wellmann, S. (2016). Cold-inducible Proteins CIRP and RBM3, a Unique Couple with Activities Far beyond the Cold. *Cell Mol Life Sci* 73, 3839–3859. doi:10.1007/s00018-016-2253-7

Zindel, J., and Kubes, P. (2020). DAMPs, PAMPs, and LAMPs in Immunity and Sterile Inflammation. *Annu. Rev. Pathol.* 15, 493–518. doi:10.1146/annurev-pathmechdis-012419-032847

Conflict of Interest: The authors declare that the research was conducted in the absence of any commercial or financial relationships that could be construed as a potential conflict of interest.

Publisher's Note: All claims expressed in this article are solely those of the authors and do not necessarily represent those of their affiliated organizations, or those of the publisher, the editors and the reviewers. Any product that may be evaluated in this article, or claim that may be made by its manufacturer, is not guaranteed or endorsed by the publisher.

frontiers in Pharmacology

SYSTEMATIC REVIEW
published: 21 January 2022
doi: 10.3389/fphar.2021.804250

Specific Interleukin-1 Inhibitors, Specific Interleukin-6 Inhibitors, and GM-CSF Blockades for COVID-19 (at the Edge of Sepsis): A Systematic Review

Ying Wang[1†], *Kun Zhu*[1†], *Rulin Dai*[2], *Rui Li*[1], *Miao Li*[3], *Xin Lv*[2] *and Qian Yu*[1*]

[1]*Department of Pharmacy, China-Japan Union Hospital of Jilin University, Jilin University, Changchun, China,* [2]*Center of Reproductive Medicine and Center of Prenatal Diagnosis, The First Hospital, Jilin University, Changchun, China,* [3]*Department of Neurosurgery, China-Japan Union Hospital of Jilin University, Jilin University, Changchun, China*

OPEN ACCESS

Edited by:
Yan Kang,
Sichuan University, China

Reviewed by:
Wared Nour-Eldine,
Qatar Biomedical Research Institute, Qatar
Pasquale Pagliano,
University of Salerno, Italy

***Correspondence:**
Qian Yu
yuqian@jlu.edu.cn

[†]*These authors have contributed equally to this work.*

Specialty section:
This article was submitted to Experimental Pharmacology and Drug Discovery, a section of the journal Frontiers in Pharmacology

Received: *29 October 2021*
Accepted: *23 November 2021*
Published: *21 January 2022*

Citation:
Wang Y, Zhu K, Dai R, Li R, Li M, Lv X and Yu Q (2022) Specific Interleukin-1 Inhibitors, Specific Interleukin-6 Inhibitors, and GM-CSF Blockades for COVID-19 (at the Edge of Sepsis): A Systematic Review. Front. Pharmacol. 12:804250. doi: 10.3389/fphar.2021.804250

Sepsis is a syndrome with high mortality, which seriously threatens human health. During the pandemic of coronavirus disease 2019 (COVID-19), some severe and critically ill COVID-19 patients with multiple organ dysfunction developed characteristics typical of sepsis and met the diagnostic criteria for sepsis. Timely detection of cytokine storm and appropriate regulation of inflammatory response may be significant in the prevention and treatment of sepsis. This study evaluated the efficacy and safety of specific interleukin (IL)-1 inhibitors, specific IL-6 inhibitors, and GM-CSF blockades in the treatment of COVID-19 (at the edge of sepsis) patients through systematic review and meta-analysis. Methodology: A literature search was conducted on PubMed, EMBASE, Clinical Key, Cochrane Library, CNKI, and Wanfang Database using proper keywords such as "SARS-CoV-2," "Corona Virus Disease 2019," "COVID-19," "anakinra," "tocilizumab," "siltuximab," "sarilumab," "mavrilimumab," "lenzilumab," and related words for publications released until August 22, 2021. Other available resources were also used to identify relevant articles. The present systematic review was performed based on PRISMA protocol. Results: Based on the inclusion and exclusion criteria, 43 articles were included in the final review. The meta-analysis results showed that tocilizumab could reduce the mortality of patients with COVID-19 (at the edge of sepsis) [randomized controlled trials, RCTs: odds ratio (OR) 0.71, 95%CI: 0.52–0.97, low-certainty evidence; non-RCTs: risk ratio (RR) 0.68, 95%CI: 0.55–0.84, very low-certainty evidence) as was anakinra (non-RCTs: RR 0.47, 95%CI: 0.34–0.66, very low-certainty evidence). Sarilumab might reduce the mortality of patients with COVID-19 (at the edge of sepsis), but there was no statistical significance (OR 0.65, 95%CI: 0.36–1.2, low-certainty evidence). For safety outcomes, whether tocilizumab had an impact on serious adverse events (SAEs) was very uncertain (RCTs: OR 0.87, 95%CI: 0.38–2.0, low-certainty evidence; non-RCTs 1.18, 95%CI: 0.83–1.68, very low-certainty evidence) as was on secondary infections (RCTs: OR 0.71, 95%CI: 0.06–8.75, low-certainty evidence; non-RCTs: RR 1.15, 95%CI: 0.89–1.49, very low-certainty evidence). Conclusions: This systematic review showed that tocilizumab, sarilumab, and anakinra could reduce the mortality of people with COVID-19 (at the edge of sepsis), and tocilizumab did not significantly affect SAEs and secondary infections. The current evidence of the studies on

patients treated with siltuximab, mavrilimumab, and lenzilumab is insufficient. In order to establish evidence with stronger quality, high-quality studies are needed.

Systematic Review Registration: PROSPERO (https://www.crd.york.ac.uk/prospero/), identifier CRD42020226545

Keywords: specific interleukin-1 inhibitors, specific interleukin-6 inhibitors, GM-CSF blockades, coronavirus disease 2019 (COVID-19), SARS-CoV-2, sepsis

1 INTRODUCTION

Sepsis is a life-threatening organ dysfunction syndrome caused by host response imbalance due to an infection or infectious factors. The mortality and treatment expenditure of sepsis are relatively high, and there is no specific drug so far. An article published in *The Lancet* in 2020 pointed out that the number of sepsis patients worldwide reached 48.9 million in 2017, among which 11 million patients died, accounting for one-fifth of the global death toll (Rudd et al., 2020).

During the pandemic of coronavirus disease 2019 (COVID-19), patients with severe and critically ill COVID-19 may develop circulation disorders and severe lung damage. Some patients with multiple organ dysfunction, such as that of the liver and kidney, showed typical characteristics of sepsis and meet the diagnostic criteria for sepsis (Li et al., 2020). According to Sepsis-3, sepsis is defined as a life-threatening organ dysfunction caused by a dysregulated host response to infection. The organ dysfunction can be represented by an increase in the Sequential (Sepsis-Related) Organ Failure Assessment (SOFA) score of 2 points or more, which is associated with an in-hospital mortality greater than 10% (Singer et al., 2016). Recent studies have shown that patients with severe and critical diseases may experience immune hyperactivity with increased levels of interleukin (IL)-1, IL-6, granulocyte–monocyte colony-stimulating factor (GM-CSF), interferon-γ-inducible protein 10 (IP-10), tumor necrosis factor-α (TNF-α), and other several inflammatory cytokines and were associated with adverse clinical outcomes (Huang et al., 2020; Qin et al., 2020; Coomes and Haghbayan, 2020; Lucas et al., 2020). Therefore, inhibition of proinflammatory cytokines may be a potential therapeutic strategy in COVID-19 (at the edge of sepsis) patients. This study was the first to screen COVID-19 patients with sepsis or at the edge of sepsis through the SOFA score and systematically reviewed the efficacy and safety of anti-cytokine therapy, such as specific IL-1, IL-6 inhibitors, and anti-GM-CSF in COVID-19 patients with organ dysfunction (SOFA ≥2). This paper could help sepsis treatment strategy researchers to grasp the current status of anti-cytokine therapy for COVID-19 patients (at the edge of sepsis) and provide a new perspective for clinical treatment.

2 METHODOLOGY

This study was conducted in accordance with the Preferred Reporting Items for Systematic Reviews and Meta-analyses (PRISMA) guideline (**Supplementary Material S1**) (Moher et al., 2009) and registered with the National Institute for Health Research international prospective register of systematic reviews (PROSPERO registration number: CRD42020226545) (Wang et al., 2020).

2.1 Search Strategy and Selection Criteria

Electronic searches were carried out in PubMed, EMBASE, Clinical Key, Cochrane Library, China National Knowledge Infrastructure (CNKI), and Wanfang Database. The search terms that we used were "SARS-CoV-2," "corona virus disease 2019," "COVID-19," "anakinra," "tocilizumab," "siltuximab," "sarilumab," "mavrilimumab," and "lenzilumab" and relevant keywords for publications released until August 22, 2021. The search strategies are available as supplementary data (**Supplementary Material S1**). Other available resources were also used to identify relevant articles. The language will be limited to Chinese and English. Eligible articles were identified for inclusion by screening the titles, abstracts, and full text. Other relevant studies were manually screened by investigators from the reference list of included studies for further analysis. There was no date limit. Two independent reviewers (YW and KZ) carried out the search in a standardized process, followed with identifying eligible records through the examination of each title, abstract, and full text. Disagreements were resolved by consensus, and unresolved conflicts were decided by a third reviewer (QY).

The studies were selected based on the following inclusion criteria: (1) The patients were diagnosed with SARS-CoV-2 infection and their SOFA score (include mean value, median, and absolute value) ≥2 or, according to the SOFA scoring tool, a certain system index (including mean, median, and absolute value) should be within the range corresponding to the system score ≥2—for example, PaO_2/FiO_2 ratio (P/F) (including absolute value, mean value, or median value) was less than 300 mmHg (Singer et al., 2016). A SpO_2/FiO_2 ratio (S/F) of 315 corresponded with a P/F ratio of 300 mmHg [S/F = 64 + 0.84*(P/F)] (Rice et al., 2007). In this review, we defined such COVID-19 patients to be at the edge of sepsis. (2) The intervention of interest was a specific IL-1 inhibitor (anakinra), specific IL-6 inhibitors (tocilizumab, siltuximab, and sarilumab), GM-CSF blockades (mavrilimumab and lenzilumab) with or without standard of care (or treatment), and glucocorticoids. Comparator treatments included placebo, standard of care (or treatment), glucocorticoids, or no intervention; studies with no comparator group were also included. (3) Randomized clinical trials (RCTs), cohort studies, case–control studies, case series, case reports, clinical guidelines, protocols for clinical trials, and any other gray literatures will be included. The studies will not be limited in terms of country. The exclusion criteria were as follows: (1) The patients were not diagnosed as COVID-19; (2) The SOFA score (absolute value,

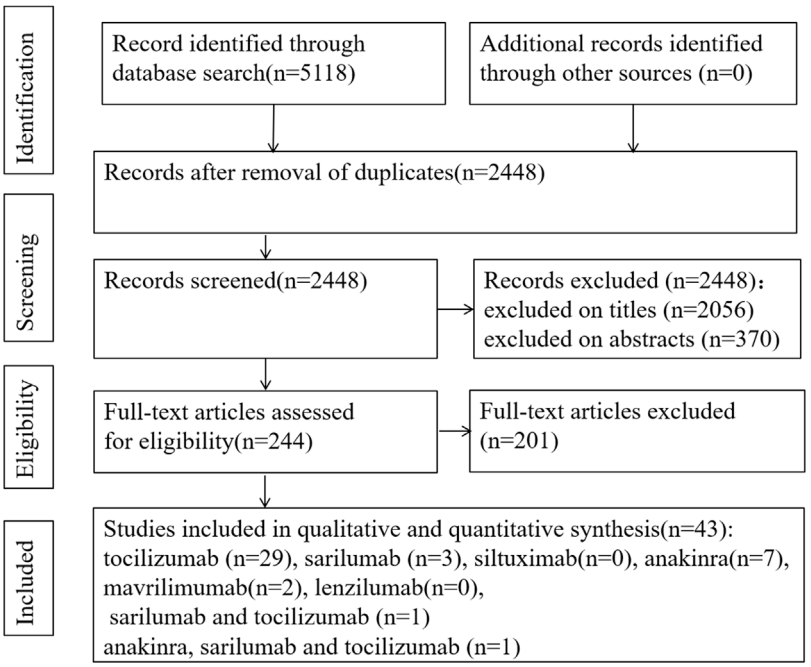

FIGURE 1 | PRISMA flow chart of study selection.

mean value, or median value) of the patients was less than 2 or did not reach 2 on any of the system indicators; (3) Data on SOFA score or certain indicators in the SOFA scoring tool for the patients studied were not available in the study text, additional materials, or any other relevant resources; and (4) Studies without an available full text or whose data were incomplete or unavailable, posters, commentaries, letters, opinion articles, and *in vitro* studies were excluded. The defined primary outcome was all-cause mortality at 28–30 days. The safety outcomes included serious adverse events (SAEs) and (serious) secondary infection. Adverse events were graded according to the Common Terminology Criteria for Adverse Events, version 4.0 (National Institutes of Health, 2017).

2.2 Data Extraction and Quality (Risk of Bias) Assessment

Two independent reviewers (YW and KZ) extracted data from the eligible studies, and a third one (QY) validated it. The following information will be extracted: year of publication, authors, country, study type, sample size, participant demographics, time of administration, intervention characteristics (name of agent, dose, and route), concomitant medications, survival outcome, treatment-related adverse events, and conclusions of the authors.

The included studies were assessed in terms of potential bias by two reviewers (RD and RL) independently. The third researcher (XL) was consulted for resolving any difference of opinion. The Quality Assessment for Case Series of the National Institute for Health and Care Excellence will be used to evaluate the quality of the case reports (series). The total score is 8 points, in which a score of 4–8 is high quality, and a score less than 4 is low quality. The methodological quality for cohort and case–control studies was assessed based on the Newcastle–Ottawa Scale (NOS) (NOS, 2020). The total score is 9 points, in which scores of 0–3, 4–6, and 7–9 are respectively considered as low, moderate, and high quality. The methodological quality of RCTs was assessed based on the "Risk of Bias" 2.0 tool (Sterne et al., 2019). Each checklist item was judged as "low," "moderate," "serious," and "critical," The quality of evidence was assessed by using the "Grading of Recommendations Assessment Development and Evaluation (GRADE)" tool (Granholm et al., 2019). The quality of evidence of each outcome is classified as "high," "moderate," "low," or "very low".

2.3 Data Synthesis and Analysis

The Review Manager version 5.4.1 software was used for analyses. One reviewer (YW) would have to enter the data into the software, and another reviewer (M.L) would have to check the data for accuracy. For dichotomous outcomes, the number of events and total number of participants in the two groups were recorded. The different types of studies were analyzed separately, such as non-RCTs (cohorts and case–control studies) and RCTs. The risk ratio (RR) and odds ratio (OR) with 95% confidence intervals (CIs) were respectively assessed for non-RCTs and RCTs. Fixed-effects model was used if the result of the Q test was not significant ($p > 0.1$) and I^2 <50%. Chi-square test, with a significance level at $p \leq 0.1$, was used to assess the heterogeneity of treatment effects between trials. The I^2 statistic was used to

TABLE 1 | Characteristics of the included studies.

Study	Country	Study type	P	SOFA score or indicators, median (IQR)	Laboratory values, median (IQR)	Intervention group	Control group	Time of administration, median (IQR)-days	Dosage	Usage	Comorbidities(n)	Concomitant medications(n)	Effective outcomes	Safety outcomes	Authors' conclusion
Salvarani et al. (2020)	Italy	RCT, MC, open-label	126; 77 M:49 F	P/F: 264.5 (243.0–290.0) mmHg	CRP- mg/dl: 8.2 (3.7–13.5).; IL-6- pg/ml: 42.1 (20.6–74.9); ferritin-ng/ml: 569.0 (317.0–1,156.0)	TCB + standard of care	Standard of care	Days from symptom onset to randomization, median (IQR): 8.0 (6.0–11.0)	A dose of 8 mg/kg up to a maximum of 800 mg, followed by a second dose after 12 h	Intravenous	DB (19), obesity: BMI ≥30 (38), HTN (56), COPD (4)	HCQ (115), antiretrovirals (52), azithromycin (26), steroids	Within 14 days, 17 of 60 in the experimental group and 17 of 63 in the control group showed clinical worsening; 1 in the control group and 2 patients in the experimental group died before 30 days from randomization	AE (*n*, %): TCB (14, 23.3%); control (7, 11.1%). SAE (*n*): TCB (1), control group (2)	No benefit on disease progression was observed compared with standard care
REMAP-CAP Investigators, et al. (2021)	United Kingdom, Australia, Canada, New Zealand, France	RCT, MC, open label	865; 629 M:236 F	P/F: 116.5 (89–165) mmHg	CRP-μg/ml: 136 (79–208)	TCB, sarilumab	Standard of care	Median days from hospital admission to enrollment (IQR): 1.2 (0.8–2.8)	TCB: 8 mg/kg (up to a maximum of 800 mg), 1 to 2 doses; sarilumab: 400 mg, 1 dose	Intravenous	DB (304), Kidney disease (81), respirator (206)	COVID-19 antivirals, corticosteroid	The analysis of 90-day survival showed that the survival rate of the IL-6 inhibitor groups was improved. Compared with the control group, the HR was 1.61 (95%CI 1.25–2.08) and the posterior probability of superiority was more than 99.9%	SAEs: 9 in the TCB group, 11 in the control group, and 0 in the sarilumab group	In critical patients with organ support, treatment with TCB and sarilumab improved the outcomes
Canziani et al. (2020)	Italy	MC, retrospective cohort	128; 94 M:34 F	P/F, mean (SD): 94 (67) mmHg	Ferritin, mean (SD)-ng/ml:1,604 (1,201); CRP, mean (SD)-g/dl: 19.1 (8.6)	TCB + standard of care	Standard of care	Time since symptom onset (SD): 11 (6)	8 mg/kg per dose, followed by a second dose 24 h later if no clinical worsening occurred	Intravenous	CCI, mean (SD): 2.4 (1.6); HTN (66)	HCQ, azithromycin, glucocorticoids	TCB did not significantly affect the risk of death, but TCB was associated with the use at baseline of NIV or invasive MV and the presence of comorbidities	TCB was not associated with the risk of infections, bleeding, or thrombosis	TCB did not affect the 30-day mortality in severe respiratory impairment patients
Menzella et al. (2020)	Italy	SC, retrospective, case–control study	79; 56 M:23 F	SOFA score: mean (SD): 4.3 (1.3)	CRP, mean (SD)-mg/dl: 11.9 (7.2); IL-6, mean (SD)-pg/m: 147.2 (180.4)	TCBb + standard therapy	Standard therapy	–	Intravenous: 8 mg/kg—max 800 mg, Q12 h; subcutaneous: 2 to 4 doses of 162 mg	Intravenous	Number of comorbidities, mean (SD): 2.9 (2.1)	HCQ (20), azithromycin (60), methylprednisolone	The probability of death and intubation in patients treated with TCB was significantly lower than that in patients not treated with TCB	2 patients treated with TCB developed cavitating lung lesions	TCB may be helpful in COVID-19 patients with severe respiratory impairment receiving NIV
Fisher et al. (2021)	United States	SC, retrospective cohort study	115; 80 M:35 F	SOFA score within 24-h intubation: 6.0 (3.0)	CRP-mg/dl: TCB 19.5 (15.7); control 17.6 (18.0); ferritin-ng/ml: TCB 1,507 (1,518), control 1,462 (1,435)	TCB + standard of care	Standard of care	Mean time from intubation to treatment was 2.5 days	400 mg/dose	Intravenous	CCI: TCB 2.0 (3.0), control 3.0 (3.0)	HCQ (108), corticosteroids	No reduction in mortality associated with receipt of TCB	The increased risk of secondary infection in patients given TCB was not observed	TCB was not associated with a reduction in mortality in MV patients with COVID-19 after controlling for severity of illness, age, and co-morbidities
Campochiaro et al. (2020)	Italy	SC, retrospective, cohort	65; 56 M:9 F	P/F-mmHg: TCB 107 (82–181), control 124 (91–172)	CRP-mg/L: TCB 156 (100–208); control: 169 (98–226); ferritin-ng/ml: TCB 1,400 (1,027–2,777); 1,448 (793—4,131)	TCB + standard treatment	Standard treatment	Duration of symptoms (days): TCB11 (8–14); control: 9 (8–10)	400 mg/dose; in case of respiratory worsening, a second dose was given after 24 h	Intravenous	HTN (28), CKD (8), DB (10), CAD (10)	HCQ, azithromycin	During the 28-day follow-up, mortality was 33% in the standard treatment group and 33% in the TCB group	The rate of pulmonary thrombosis and infection was similar between the two groups	At day 28, compared to standard treatment, the clinical improvement and mortality were not statistically different
Vazquez Guillamet et al. (2021)	United States	SC, retrospective cohort study	43; 16 M:27 F	P/F-mmHg: 171.5 (122–221)	CRP- mg/dl:142.7 (97.7–213.7); IL-6-pg/ml: 61 (28.6–439)	TCB + standard care	Standard care	–	8 mg/kg, a second dose at 12–24 h later	Intravenous	DB (12), CKD (17), CAD (11); Charlson score, median (IQR): TCB 0 (0–3), control 2 (0–4)	——	Treatment with TCB was a significant predictor of survival	Treatment with TCB might increase the risk of infection	After adjusting for severity of critical illness, administration of IL-6 inhibitor was associated with improved survival

(Continued on following page)

TABLE 1 | (*Continued*) Characteristics of the included studies.

Study	Country	Study type	P	SOFA score or indicators, median (IQR)	Laboratory values, median (IQR)	Intervention group	Control group	Time of administration, median (IQR)-days	Dosage	Usage	Comorbidities(n)	Concomitant medications(n)	Effective outcomes	Safety outcomes	Authors' conclusion
Rajendram et al. (2021)	United States	MC, retrospective observational cohort	164; 103 M:61 F	SOFA score, mean (SD): TCB 6.0 (3.3), control 6.4 (3.6); P/F, mean (SD)-mmHg: TCB 134.8 (68.4), control 149.8 (82.2)	CRP, mean (SD)-mg/dl: TCB 20.4 (10.1), control 17.2 (12.3); ferritin- ng/ml: TCB 1,398.2 (1,143.3), control 4,159.9 (13,454.1)	TCB	Did not receive TCB	–	4–8 mg/kg (maximum dose 400 mg), one dose only	Intravenous	DB (67), COPD (48)	HCQ (88), azithromycin (78), systemic corticosteroids	ICU mortality was lower in the TCB group, with more hospital-, ICU-, and vasoactive-free days at day 28 compared with those who did not receive TCB. There was no difference in MV-free days at day 28 or development of secondary infections	There was no difference in the rates of secondary infection	Administration of TCB might decrease in ICU mortality of critical COVID-19 patients with severe hypoxemic respiratory failure TCB use was associated with a significant decrease in ICU death rate in critically ill COVID-19 patients with severe hypoxemic respiratory failure
Huang et al. (2021)	United States	SC, retrospective cohort study	96; 64 M:32 F	SOFA score median (range): TCB 4 (0–13), non-TCB 5 (0–13)	CRP, median (range)-mg/L: TCB 122.3 (2.4–327.2); non-TCB 122.5 (11.10–343.1)	TCB	Non-TCB	Median (range): TCB:2 (0–16)	A single 400 mg dose	Intravenous	HTN (62), cardiac arrhythmias (33), DB (47), other comorbidities (84)	HCQ (63), azithromycin (69), and remdesivir (9), DXMS	Fewer deaths were observed among TCB-treated patients, both in the overall population and among the subgroup of patients requiring MV	Secondary infections were not different between the two groups and were predominantly related to invasive devices, such as urinary and central venous catheters	Administration of TCB was associated with fewer deaths compared to non-treatment despite predominantly being used in patients with more advanced respiratory disease
Galván-Román et al. (2021)	Spain	SC, retrospective observational study	146; 97 M:49 F	Baseline P/F, median (p25–p75): 215 (112–310)	CRP, median (p25–p75)-mg/dl: 11.55 (5.16–22.53)	TCB	Not treated with TCB	Duration of symptoms at admission, median (p25–p75)-d: 6 (4–7)	8 mg/kg (maximum 800 mg) followed by a second one after 12 h	Intravenous	Comorbidities, median (p25–p75): 100 (69)	HCQ (136), azithromycin (82), Lpv/Rtv(119), and glucocorticoids	Early TCB treatment might improve in oxygenation (P/F) in patients with high IL-6. Patients with high IL-6 not treated with TCB showed a high mortality as well as those with low IL-6 treated with TCB	Relevant SAEs were not observed in TCB-treated patients	Baseline IL-6 more than 30 pg/ml predicts IMV requirement in patients with COVID-19 and contributes to the establishment of an adequate indication for the treatment of TCB
Saffo et al. (2021)	United States	Retrospective cohort	130; 93 M:37 F	SOFA score mean (SD): TCB 5.7 (2.2); control 6.0 (3.2)	Mean (SD) IL-6-pg/ml: TCB 108.8 (179), control 62.3 (105.3); mean (SD) CRP-mg/dl: TCB 13.2 (7.4); control: 12.6 (6.4)	TCB	Did not receive TCB	Mean (SD) symptom onset to admission: TCB 6.9 (3.4); control 7.1 (4.4)	A dose of 8 mg/kg; 400 mg single dose	Intravenous	HTN (98), DB (53), COPD (27), CA (24)	HCQ, azithromycin, methylprednisolone	A Kaplan–Meier survival curve demonstrated no difference in survival between TCB and comparator patients. In the multivariable Cox regression model for mortality at 30 days, administration of TCB was not associated with decreased mortality	Positive blood culture was not statistically significant between the groups	No difference in survival was observed in critical patients treated with TCB
Somers et al. (2021)	United States	SC, observational controlled cohort	154; 102 M:52 F	P/F ($n = 80$): 165 (136.5–231.5) mmHg	CRP-mg/L: 220 (125–293); ferritin-ng/ml:1,418 (692–2,139)	TCB	Did not receive TCB	–	8 mg/kg (maximum 800 mg) × 1 dose	Intravenous	HTN (102), DB (25), CKD (64), asthma (31)	HCQ, remdesivir, corticosteroid	In IPTW-adjusted models, TCB was associated with a 45% reduction in hazard of death	TCB was associated with an increased proportion of patients with superinfections, but there was no difference in the 28-day case fatality rate between the two groups	In the cohort, administration of TCB was associated with a lower mortality in spite of higher superinfection occurrence

(Continued on following page)

TABLE 1 | (*Continued*) Characteristics of the included studies.

Study	Country	Study type	P	SOFA score or indicators, median (IQR)	Laboratory values, median (IQR)	Intervention group	Control group	Time of administration, median (IQR)-days	Dosage	Usage	Comorbidities(n)	Concomitant medications(n)	Effective outcomes	Safety outcomes	Authors' conclusion
Brosnahan et al. (2021)	United States	MC, retrospective cohort	537; 366 M:171 F	SOFA score: TCB:7 (7–9); control: 8 (3–10)	−−	Steroid + TCB	Steroid	–	A total of 90% of patients received 400 mg as a single dose	Intravenous	HTN without complication (394); DB without complication (229)	Antivirals, immune globulins, HCQ, methylprednisolone, DXMS, hydrocortisone, prednisone	The combination group (TCB 400 mg and daily equivalent DXMS 10 mg) had an improved 28-day mortality compared with the steroid-only group (daily equivalent DXMS 10 mg) without increasing the risk of infection	There was no statistical significance difference in the rate of infections between the propensity-matched groups	The combination group had an improved 28-day mortality compared with the steroid-only group without increasing the risk of infection
Corominas et al. (2021)	Spain	Single-center, observational study	104; 72 M:32 F	P/F, mean (SD): 201.3 (78.1) mmHg	IL-6-pg/ml, mean (SD): 171.6 (40–210.7); CRP-mg/L, mean (SD): 198.4 (161.5)	TCB		–	If ≥75 kg: a single dose of 600 mg, less than <75 kg: a single dose of 400 mg	–	HTN, dyslipidemia, obesity, CLD, DB	HCQ	The overall mortality rate was 5.8% patients. Mortality in hospitalized non-TCB treated patients was 10%. The regional death rate was 11%	–	Early treatment of IL-6 inhibition in COVID-19 patients with imminent hyper-inflammatory response may be safe and effective
Cavalli et al. (2021)	Italy	Cohort study	392; 301 M:91 F	P/F ≤ 300 mmHg	CRP-mg/L: 129 (100–171)	Anakinra, tocilizumab, sarilumab	No interleukin inhibitors	None	Anakinra: 5 mg/kg/dose twice daily (total daily dose of 10 mg/kg) until clinical benefit. TCB: 400 mg/dose, which was repeated after 24 h if the respiratory function further worsened; sarilumab: 400 mg/dose	Intravenous	CAD (119); history of neoplasia (66); DB (72)	HCQ, glucocorticoid	There was no difference in adverse clinical outcome risk in patients treated with IL-6 or IL-1 inhibition relative to patients who did not receive interleukin inhibitors	–	IL-1 inhibition was associated with a significant reduction of mortality in COVID-19 patients. IL-6 and IL-1 inhibition were effective in patients with low lactate dehydrogenase concentrations
Abe et al. (2020)	Japan	Case reports	2; 1 M:1 F	PLT <20*10^9/L	P1: IL-6-pg/ml: 47.8; P2: IL-6-pg/ml: 93.6	TCB		Days from symptom onset to TCB application: P1: 8 days later; P2: 4 days later	8 mg/kg of TCB twice	Intravenous	DB; KD	P1: peramivir and favipiravir; P2: peramivir and favipiravir, immunoglobulin	P1: He was released from the isolation unit on day 29. P2: She was released from the isolation unit on day 36 based on negative results of PCR assays	–	Anti-cytokine therapy might be effective for severe COVID-19 in end-stage renal disease patients
Patel et al. (2020)	United States	Case reports	1; F (12 years old)	PLT <10*10^9/L	IL-6-pg/ml: 34; CRP-mg/dl: 8.3	TCB		Days from symptoms onset to TCB application: 12	2 doses of TCB (8 mg/kg 12 h apart)	Intravenous	Severe thrombocytopenia	HCQ, remdesivir, immunoglobulin; methylprednisolone	Discharged	–	Treatment with cytokine-directed agents such as TCB could be considered in critical patients
Mady et al. (2020)	Saudi Arabia	A case series	61; 54 M:7 F	SpO_2/FiO_2, median (IQR): 162 (145–209.2) mmHg	CRP, median (IQR)-mg/L: 31.7 (30.5–49.9)	TCB		–	8 mg/kg (two consecutive intravenous infusions 12 h apart)	Intravenous	More than one comorbidity (%): 38 (62.3%)	Lpv/Rtv or ribavirin	Administration of TCB did not affect the mortality of critical COVID-19 patients	No SAEs due to TCB were recorded; 12 patients developed nosocomial acquired infections	TCB could be an adjunct safe therapy in rapidly evolving COVID-19 and associated critical illness
Bernardo et al. (2020)	Italy	Case reports	1; M	P/F: 295 mmHg	CRP-mg/L: 89.8 (9 × the upper limit of normal)	TCB		8th day of admission	Two doses of TCB 8 mg/kg administered 12 h apart	Intravenous	Hypertensive cardiomyopathy, paroxystic AF, CRD	HCQ, Lpv/Rtv	On day 30 after the TCB injections, the ANC of the patient began to improve in spite of far-from-normal values	Severe prolonged neutropenia	Considering the increasing use of TCB in COVID-19 patients, this case warrants further studies regarding the possible adverse hematological effects that need to be monitored in order to prevent superimposed infections

(Continued on following page)

TABLE 1 | (*Continued*) Characteristics of the included studies.

Study	Country	Study type	P	SOFA score or indicators, median (IQR)	Laboratory values, median (IQR)	Intervention group	Control group	Time of administration, median (IQR)-days	Dosage	Usage	Comorbidities(n)	Concomitant medications(n)	Effective outcomes	Safety outcomes	Authors' conclusion
Morillas et al. (2020)	United States	Case reports	5; 2M:3F	P1: P/F: 196 mmHg; P2: P/F: 200 mmHg; P3: P/F: 113 mmHg; P4: P/F: 283 mmHg; P5: P/F: 156 mmHg	P1: CRP-mg/dl: 9.7, IL-6-pg/ml: 7; P2: CRP-mg/dl: 18.8, IL-6-pg/ml: 13; P3: CRP-mg/dl 36.5, IL-6-pg/ml: 438; P4: CRP-mg/dl: 5.2; P5: CRP-mg/dl: 32.7	TCB		TCB administration after symptoms onset (day): P1: 7; P2: 5; P3: 10; P4: 13; P5: 12	P1: 400 mg/dose; P2: 400 mg/dose; P3: 400 mg/dose; P4: 310 mg/dose (adjusted based on weight); P5: 400 mg/dose	Intravenous	P1: HTN, kidney transplants; P2: lung transplant, DB, HF, HTN, hemodialysis, CA; P3: a motor vehicle accident on tacrolimus; P4: liver transplant, rheumatic heart disease, CKD stage 3; P5: HTN, DB, pulmonary embolism, coronary artery by-pass graft surgery, and kidney transplantation	P1: Lpv/Rtv; P2/3: HCQ, steroids	P1/2/3/5: discharged; P4: Dclied	There were no immediate drug-related side effects, although 2 patients developed 3 proven bacterial infections within 14 days after dosing	TCB can be used without major direct toxicity in SOT/CTTRs early after initiation of MV due to COVID-19, regardless of type of organ transplanted
Cascella et al. (2020)	Italy	Case reports	1; M	P/F: 150 mmHg	CRP-mg/L: 193; IL-6-pg/ml: 93	TCB		2nd day of admission	8 mg/kg, 800 mg	Intravenous	–	Lpv/Rtv, HCQ	Discharged	–	The combination of IL-6 inhibitor with calibrated ventilatory strategies may improve outcomes
AL-Kaf et al. (2021)	Kingdom of Saudi Arabia	Case reports	1; M	P/F: 133 mmHg	IL-6-pg/ml: 130	TCB		5th day of admission	–	–	Down syndrome	Hydrocortisone	After a total of 31 days of MV support, the patient was successfully weaned off and planned for tracheostomy closure	–	This is a rare critical presentation of COVID-19 in a Down syndrome patient with cardiac tamponade, ARDS, and severe hypothyroidism who responds well to pericardiocentesis, levothyroxine, hydrocortisone and TCB
Eroglu et al. (2021)	Turkey	Case reports	1; M	P/F: 204 mmHg	IL-6-pg/ml: 14 (0–6.4); CRP-mg/L: 78 (0–5)	TCB		8th day of admission	TCB 400 mg was infused 2×/day for 2 days	Infused intravenously	HTN	Favipiravir, oseltamivir, HCQ	On day 14, the patient was transferred to a negative COVID-19 service with negative PCR test and better clinical condition	–	Patients with severe COVID-19 should be monitored for hemophagocytic lympho-histiocytosis syndrome, and TCB can be used early under NIV delivered by helmet mask
Kataoka et al. (2021)	Japan	Case reports	1; M (age 85)	P/F: 100 mmHg	CRP-mg/dl: 13.02; IL-6-pg/ml: 154	TCB		–	A single dose of 480 mg/body	Intravenous	Sjögren's syndrome	Favipiravir, ciclesonide	Discharged	–	IL-6 inhibition may be an optional treatment in patients with a severe respiratory condition
Kishaba et al. (2021)	Japan	Case reports	1; M (age 74)	P/F: 115 mmHg	CRP-mg/dl: 32	TCB		On the day of admission	480 mg (8 mg/kg/day)	Intravenous	HTN	Favipiravir, methylprednisolone	Discharged	–	In order to secure good outcomes in critical COVID-19 patients, early administration of intensive combination therapy requires suppression of both viral replication and inflammation
Leelayuwatanakul et al. (2021)	Thailand	Case reports	2; 1 M:1 F	P1: P/F: 260 mmHg; P2: P/F: 130 mmHg	P1: CRP-mg/L 228; IL-6-pg/ml: 1,091; P2: hs-CRP-mg/L:225; IL-6-pg/ml: 426.2	TCB		P1: 8th day of admission; P2: 4th day of admission	400 mg/dose	Intravenous	P1: HIV infection, DB, dyslipidaemia; P2: relapse multiple myeloma, triple vessel disease, DB, HTN	Favipiravir, HCQ, darunavir/ritonavir, immunoglobulin	Discharged	–	Combined therapeutic modalities are promising treatment for severe COVID-19 infection in the immunocompromised host. Timely adjunctive therapies that alleviate overwhelming inflammation may improve the outcome
McKenzie et al. (2021)	United States	Case series	16; 9M:7 F	P/F: 84 (IQR: 69–108.6) mmHg	CRP-mmol/L: 219.6 ± 72.1; IL-6-pg/ml: 248.7 (IQR: 69.5–719.2)	TCB		Time from admission to administration: 7.08 ± 3.5 (days)	400 mg (400–600)	Intravenous	HTN (31%); DB (25%)	HCQ, convalescent plasma, steroids	8 (50%) patients were discharged home, 7 (44%) patients died, and 1 (6%) patient was still hospitalized at the end of data collection	–	The study did not support the effectiveness of TCB in the treatment of critical COVID-19 patients

(Continued on following page)

TABLE 1 | (*Continued*) Characteristics of the included studies.

Study	Country	Study type	P	SOFA score or indicators, median (IQR)	Laboratory values, median (IQR)	Intervention group	Control group	Time of administration, median (IQR)-days	Dosage	Usage	Comorbidities(n)	Concomitant medications(n)	Effective outcomes	Safety outcomes	Authors' conclusion
Nourié et al. (2021)	France	Case reports	1; M	SOFA score: 13	CRP-mg/L: 62.2	TCB		On day 7 of the illness	400 mg/dose	–	Von Hippel–Lindau; HTN; DB; CAD	HCQ, hydrocortisone	Discharged	–	A single dose of 400 mg of TCB was effective and well tolerated
Ladna et al. (2021)	United States	Case series	2; 2 M	P1: P/F: 117 mmHg; P2: P/F: 116 mmHg	P1: IL-6-pg/ml 45; hs-CRP-mg/L: 74.9; P2: IL-6 pg/ml:31; hs-CRP-mg/L: 244	TCB		First hospital day	400 mg/dose	–	P1: CAD, DB, HTN, and prior stroke; kidney and heart transplant; P2: chronic hepatitis B complicated by hepatocellular carcinoma status post orthotopic liver transplant, HTN, DB	HCQ, P1: tacrolimus, hydrocortisone, mycophenolate; P2: hydrocortisone	Discharged	–	TCB appears to hold promise for critical COVID-19 patients who require MV when given shortly after intubation
Senegaglia et al. (2021)	Brazil	Case report	1; M	P/F: 87 mmHg	CRP-mg/ml: 25.3 (<5.0)	TCB		2nd, 3rd hospital day	400 mg/dose for 2 days	Infusion	HTN, urethral stenosis	DXMS	Discharged	No adverse events	Administration of TCB and mesenchymal stromal cells proved to be safe, and the results of the report prove to be a promising alternative in patients with severe acute respiratory syndrome
Thammathiwat et al. (2021)	Thailand	Case report	1; M	P/F: 226 mmHg	IL-6-pg/ml: 17.1 (reference level <7)	TCB		6th hospital day	8 mg/kg/dose	–	Kidney transplantation, HTN, dyslipidemia, and post-transplant DB	Darunavir, ritonavir, favipiravir, tacrolimus, prednisolone, and immunoglobulin	COVID-19 was undetected	–	For this COVID-19 patient with kidney transplant, favipiravir together with decreased immunosuppression and IL-6 inhibitor antibody provides favorable outcomes. Decision on timing for IL-6 inhibitor initiation can be guided by IL-6 level monitoring
Lescure et al. (2021)	Argentina, Brazil, Canada, Chile, France, Germany, Israel, Italy, Japan, Russia, and Spain	MC, RCT	416, 261 M:155 F	SpO_2/FiO_2, median (IQR)-mmHg: 237.5 (173.6–300.0)	CRP-mg/L: 94.6 (48.1–167.9); IL-6-pg/ml: 12.3 (4.8–25.5)	Sarilumab	Placebo	Time from dyspnea onset to baseline, days: 5.0 (2.0–9.0)	200 mg, 400 mg	Intravenous	HTN (177), DB (110), CA (42), obesity (86), HL (41), CAD (22), COPD (18)	HCQ/CQ, azithromycin, remdesivir, convalescent plasma, and corticosteroids	At day 29, there were numerical, non-significant survival differences between sarilumab 400 mg and placebo for critical COVID-19 patients	No unexpected safety signals were seen	The result of this study did not show the efficacy of sarilumab in patients admitted to the hospital with COVID-19 and receiving supplemental oxygen
Della- Torre et al. (2020)	Italy	SC, open-label cohort study	56; 44 M:12 F	P/F <300 mmHg	CRP-mg/L: 152 (116–210); ferritin-ng/ml: 1,376 (1,023–6,927)	Sarilumab + standard care	Standard of care	Duration of symptoms before enrollment (days): 7 (7–10)	400 mg	Intravenous	HTN (17), DB (9), HLD (8), COPD (2), and CAD (6)	HCQ, Lpv/Rtv, azithromycin, corticosteroids	A total of 61% of patients treated with sarilumab experienced clinical improvement and 7% of patients died. These findings were not significantly different from the comparison group (clinical improvement 64%, mortality 18%)	The rate of pulmonary thrombosis and infection was similar between the 2 groups	Overall mortality and clinical improvement were not significantly different between standard of care and sarilumab. Sarilumab was associated with faster recovery in a subset of patients showing minor lung consolidation at baseline
Gremese et al. (2020)	Italy	SC, observational cohort	53; 47 M:6 F	P/F-mmHg: medical wards 146 (120–212), ICU 112 (100–141.5)	–	Sarilumab + standard care	No control group	–	400 mg, 1 to 2 doses	Intravenous	34 (64.2%) had at least one comorbidity	Darunavir/ritonavir; Lpv/Rtv	Within the medical wards, 89.7% of inpatients significantly improved, 70.6% were discharged. Within the ICU, 64.2% were discharged from ICU to the ward and 35.8% were still alive at the last follow-up	Sarilumab appears to be safe	IL-6 receptor inhibition leads to good clinical outcome in severe COVID-19 patients, and sarilumab is a safe and effective alternative in the therapeutic armamentarium of this disease without a defined standardized treatment

(Continued on following page)

TABLE 1 | (*Continued*) Characteristics of the included studies.

Study	Country	Study type	P	SOFA score or indicators, median (IQR)	Laboratory values, median (IQR)	Intervention group	Control group	Time of administration, median (IQR)-days	Dosage	Usage	Comorbidities(n)	Concomitant medications(n)	Effective outcomes	Safety outcomes	Authors' conclusion
Kyriazopoulou et al. (2021a)	Greece, Italy	MC, RCT	594; 344 M:250 F	SOFA score, mean (SD): 2.4 (1.1); P/F-mmHg: 237 (181–301)	CRP, mean (SD)-mg/L: 50.6 (25.3–99.7); IL-6, mean (SD)-pg/ml: 16.8 (7.0–39.8); ferritin, mean (SD)-ng/ml: 585.2 (294.5–1,047.0)	Anakinra + standard of care	Placebo + standard of care	From symptom onset to start of study drug (days), median (Q1–Q3) 9 (7–11)	100 mg/daily,7–10 days	Subcutaneous	CCI, mean (SD): 2.2 (1.6); DB (94), chronic heart failure (18), CRD (10), COPD (24), CAD (41), Atrial fibrillation (28), depression (34)	Remdesivir, DXMS	Anakinra protected from severe disease or death; the 28-day mortality decreased	The incidence of treatment-emergent SAEs through day 28 was lower in patients in the anakinra combined with standard of care group compared to the placebo combined with standard of care group	Early administration of anakinra guided by suPAR shows 2.78 times better improvement of overall clinical status in moderate and severe COVID-19
Bozzi et al. (2020)	Italy	SC, prospective observational cohort	120; 96 M:24 F	P/F-mHg: 151 (105–204.5), 32.5% patients on MV	Ferritin-mcg/L: 1,555 (1,239–2,679); CRP-mg/dl: 15.2 (10.8–23.1)	Anakinra + methylprednisolone + standard treatment	Methylprednisolone + standard treatment	Days between hospitalization and inclusion: intervention: 3 (1–6); control: 1 (0–2)	200 mg q8 h for 3 days and then 100 mg q8h up to day 14	Intravenous	Median CCI was 0 (IQR 0–1)	HCQ, Lpv/Rtv, remdesivir, methylprednisolone	At 28 days, mortality was 35.6% in controls and 13.9% in treated patients. Unadjusted and adjusted risk of death was significantly lower for treated patients compared to controls	No significant differences in laboratory alterations or bloodstream infections were observed	Administration of anakinra combined with methylprednisolone may be an effective therapy in COVID-19 patients with respiratory failure and hyper-inflammation, also on MV
Franzetti et al. (2021)	Italy	MC, retrospective cohort study	112; 87 M:25 F	P/F: 133 (110–196) mmHg	CRP-mg/dl: 17.5 (11.0–24.9); ferritin-ng/ml: 1,620 (918–2,988)	Anakinra + standard of care	Standard of care	Symptom duration before hospitalization: 7 (5–10)	Regular ward: 7 days at a dosage of 100 mg four times a day, subcutaneous; ICU: 200 mg three times daily, intravenous	Intravenous or subcutaneous	CCI median (IQR): 3 (2–4); HTN (59), ischemic heart disease (20), COPD (8), DB (19)	HCQ, Lpv/Rtv	Survival at day 28 was significantly higher in anakinra-treated patients than in the controls. When stratified by continuous positive airway pressure support at baseline, the survival of anakinra-treated patients was also significant compared with the controls	No significant difference was observed in the rate of infectious-related adverse events between groups	Anakinra improved the invasive ventilation-free survival and overall survival and was well tolerated in patients with ARDS associated with COVID-19
Kyriazopoulou et al. (2021b)	Greece	MC, cohort	260; 165 M:95 F	SOFA score: 2 (1); P/F mmHg: anakinra 293.3 (195.7–371.2), parallel SOC after propensity matching 285.7 (208.5–371.7)	CRP-mg/L: anakinra 47.4 (14.3–105.5), parallel SOC after propensity matching 68.8 (19.7–141.8)	Anakinra + SOC	SOC	Days from onset of symptoms to start of treatment, median (range): anakinra 8 (1–23), parallel SOC after propensity matching 7 (1–12)	100 mg once daily for 10 days	Subcutaneous	CCI, mean (SD): 3 (2); DB (73), CAD (21), CRD (5), HTN (125), COPD (18)	HCQ, remdesivir, azithromycin, DXMS	22.3% with anakinra treatment and 59.2% comparators progressed into severe respiratory failure; the 30-day mortality was 11.5 and 22.3%, respectively	The rate of SAEs was lower among anakinra-treated patients	Early soluble urokinase plasminogen activator receptor guided anakinra decreased severe respiratory failure and restored the pro-/anti-inflammatory balance
Erden et al. (2021)	Turkey	SC, retrospective case review	17; 12 M:5 F	SOFA score, median IQR: 3 (3)	CRP-mg/L: 45.6 (101.8); ferritin concentration-µg/L: 397 (307)	Anakinra	No control group	Duration of COVID-19 symptoms before anakinra, days: 7 (4.5)	100 mg/12 h from day (D) 1 to D3, then at 100 mg/24 h from D3 to D5	Subcutaneously	HTN (9), DB (4), asthma (1), CAD (3), CA (1)	HCQ, azithromycin, favipiravir	The mortality rate was 17.6%; 1 patient was receiving low-flow oxygen supply, 3 patients no longer needed oxygen supply, and 10 patients were discharged	Treatment was well tolerated	The other factors that enhance the administration of anakinra in the situation of viremia could also be sorted as no response to full-dose antiviral drugs, antiviral side effects, or no success to antiviral treatment
Filocamo et al. (2020)	Italy	Case report	1; M	P/F:160 mmHg	–	Anakinra		Day 10 after admission	200 mg intravenously followed by 100 mg/6 h subcutaneously	Intravenous and subcutaneous	–	Lpv/Rtv, HCQ	Discharged	–	This critical COVID-19 patient was successfully treated with IL-1 receptor antagonist

(Continued on following page)

TABLE 1 | (*Continued*) Characteristics of the included studies.

Study	Country	Study type	P	SOFA score or indicators, median (IQR)	Laboratory values, median (IQR)	Intervention group	Control group	Time of administration, median (IQR)-days	Dosage	Usage	Comorbidities(n)	Concomitant medications(n)	Effective outcomes	Safety outcomes	Authors' conclusion
Franzetti et al. (2020)	Italy	Case report	1; M	P/F: 50 mmHg	–	Anakinra		Day 7 after admission	100 mg/6 h	Subcutaneous	–	Lpv/Rtv, remdesivir	By day 16, a substantial improvement in the respiratory function of the patient was also noticed, with $SaPO_2$ levels of 92% while on Venturi mask	–	This report highlights the high tolerability and the interesting immunomodulatory profile of anakinra in the setting of severe patients associated with remdesivir therapy
Cremer et al. (2021)	United States	MC, RCT, double-blind	40; 26 M:14 F	Baseline SOFA score, median (IQR): 2 (2–3); baseline P/F-mmHg: 137 (88–193)	CRP-mg/dl: 13.1 (9.8–18.8); ferritin-ng/ml: 1,040 (486–1860)	Mavrilimumab	Placebo	Time from symptom onset to hospitalization: 7 (4–8)	A single dose of 6 mg/kg	Intravenous	HTN (22), DB (17), HL (18), CAD (4)	Antiviral drugs, convalescent plasma, corticosteroids, other immunosuppressive agents	At 14 days, 12 patients in the mavrilimumab group were alive and off supplemental oxygen therapy compared with 9 patients in the placebo group	Adverse events were similar between groups. Treatment-related deaths were not observed	There was no significant difference in the proportion of patients alive and off oxygen therapy at day 14; despite the harm or benefit of mavrilimumab therapy in this patient population, it remains possible given the wide confidence intervals
De Luca et al. (2021)	Italy	SC, prospective cohort	39; 29 M:10 F	P/F-mmHg (KPa): mavrilimumab 196 (167–215), control 217 (138–258)	CRP-mg/L: mavrilimumab 152 (100–177), control 123 (77–190); ferritin, μg/L: mavrilimumab 2,302 (1,040–3,217), control 1,269 (854–3,369)	Mavrilimumab + standard of care	Standard of care	Fever duration (days): mavrilimumab 11 (10–12), control 7 (4–10)	A single dose of 6 mg/kg	Intravenous	–	HCQ, Lpv/Rtv, azithromycin	During the 28-day follow-up, 7 patients in the control group died, and no patient in the mavrilimumab group died. At day 28, 17 patients in the control group showed clinical improvement and all patients in the mavrilimumab group. Fever resolution was faster in mavrilimumab recipients *versus* controls	Mavrilimumab group with no infusion reactions; 3 patients in the control group developed infectious complications	Treatment of mavrilimumab was associated with improved clinical outcomes compared with standard care in non-MV patients with severe COVID-19 and systemic hyper-inflammation

MC, multi-center; SC, single-center; F, female; M, male; IL-6, interleukin-6; CRP, C-reactive protein; ALT, alanine aminotransferase; INR, international normalized ratio; PLT, platelet; AF, atrial fibrillation; CAD, coronary artery disease; COPD, chronic obstructive pulmonary disease; DB, diabetes; CKD, chronic kidney disease; HL, hyperlipidemia; CVI, cardiovascular impairment; CVD, cardiovascular disease; HTN, hypertension; HI, hepatic impairment; HF, heart failure; CA, cancer; CLD, chronic lung disease; CCD, chronic cardiac disease; CPD, chronic pulmonary disease; AMN, active malignant neoplasm; NIV, noninvasive ventilation; MV, mechanical ventilation; CI, confidence interval; TCB, tocilizumab; CP, cumulative percentage; SAE, serious adverse events; AE, adverse events; HCQ, hydroxychloroquine; Lpv/Rtv, lopinavir/ritonavir; IFN, interferon; HR, hazard ratio; OR, odds ratios; P/F, PaO_2:FiO_2; SOC, standard of care; KD, kidney disease; IPTW, inverse probability treatment weighting; DXMS, dexamethasone; P, patient; SOT/CTTR, solid organ and composite tissue transplant recipients; CCI, Charlson Comorbidity Index; suPAR, soluble urokinase plasminogen activator receptor.

quantify possible heterogeneity (75–100% considerable heterogeneity). We would explore potential causes through sensitivity and subgroup analyses if heterogeneity had been above 80%. We would not have conducted a meta-analysis if we had not found a reason for heterogeneity. If we could not perform a meta-analysis, we had planned to comment on the results from all studies.

3 RESULTS

3.1 Search Results

Because of insufficient evidence available from RCTs, we also included cohort studies, case–control studies, and case reports (series). The search of the electronic databases on Aug 22, 2021 yielded a total of 5,118 studies. Following the elimination of duplicates and screening of titles and abstracts, we evaluated 244 articles in full text. Among these, we found 43 eligible articles (5 RCTs, 16 cohort studies, 2 case–control studies, and 20 case reports) (**Figure 1**) (Salvarani et al., 2021; REMAP-CAP Investigators et al., 2021; Canziani et al., 2020; Menzella et al., 2020; Fisher et al., 2021; Campochiaro et al., 2020; Vazquez Guillamet et al., 2021; Rajendram et al., 2021;Huang et al., 2021; Galván-Román et al., 2021; Saffo et al., 2021; Somers et al., 2021; Brosnahan et al., 2021; Corominas et al., 2021; Cavalli et al., 2021; Abe et al., 2021; Patel et al., 2020; Mady et al., 2020; Bernardo et al., 2020; Morillas et al., 2020; Cascella et al., 2020; Al-Kaf et al., 2021; Eroglu et al., 2021; Kataoka et al., 2021; Kishaba et al., 2021; Leelayuwatanakul et al., 2021; McKenzie et al., 2021; Nourié et al., 2021; Ladna et al., 2021; Senegaglia et al., 2021; Thammathiwat et al., 2021; Lescure et al., 2021; Della-Torre et al., 2020; Gremese et al., 2020; Kyriazopoulou et al., 2021a; Bozzi et al., 2021; Franzetti et al., 2021; Kyriazopoulou et al., 2021b; Erden et al., 2021; Filocamo et al., 2020; Franzetti et al., 2020; Cremer et al., 2021; De Luca et al., 2020). All studies were published in peer-reviewed journals.

In the process of full-text review, there were four articles for which we failed to obtain the full texts. The four studies were related to tocilizumab. Two studies did not report the efficacy and safety of tocilizumab (Garg et al., 2020; Kashin et al., 2020). The other two studies were case reports, in which one patient developed tuberculosis reactivation during treatment and the other patient had a secondary infection. The authors of the two case reports suggested that patients might be at a high risk for secondary infection after receiving tocilizumab or tocilizumab combined with glucocorticoid. They suggested that clinicians should use tocilizumab with caution and screen for latent tuberculosis before medication (Mazankova et al., 2020; Moideen et al., 2020).

3.2 Risk of Bias Assessment

The risk of bias of the RCTs was low to moderate, respectively. The results are shown in **Supplementary Figure S1** (**Supplementary Material S2**, Appendix p1). Some studies reported only one outcome, and we assessed the risk of bias for the results—for instance, bias in the measurement of outcomes was not available for safety for the study of Brosnahan *et al.* (2021) because they did not report it. For mortality outcomes, the methodological quality of 16 cohorts was moderate to high, and those of 2 case–control studies were moderate. For safety outcomes, the methodological quality of 14 cohorts was low to high, and those of 2 case–control studies were low to moderate (NOS assessment results are shown in **Supplementary Material S2**, Appendix p2–40). The methodological quality evaluation results of the included case reports (series) showed that the quality was low to moderate (the results of quality are shown in **Supplementary Material S2**, Appendix, p41–42).

3.3 Characteristics of Patients

The 43 studies included were identified and critically evaluated, which included a total of 4,951 patients with confirmed SARS-CoV-2 infection, of whom 2,243 received mechanical ventilation. Only 11 studies reported the SOFA score of enrolled patients, of which 4 studies reported SOFA scores greater than or equal to 6 (tocilizumab), 3 studies reported scores between 4 and 5 (tocilizumab), and 4 studies reported scores between 2 and 3 (3 for anakinra, 1 for mavrilimumab). The remaining 32 articles reported the respiratory status (including P/F or S/F) and platelet of patients, of which 5 studies included patients with P/F less than or equal to 100 mmHg and of which 13 studies reported patients with P/F between 100 and 200 mmHg.

Most patients received standard of care (or standard of treatment) based on local treatment guidelines. However, the medication regimens of the standard of care were different, mainly including antiviral drugs, antibiotics, glucocorticoids, and other symptomatic drugs. Anti-cytokine agents were mainly used by intravenous injection and, in a few studies, by subcutaneous administration. In addition, there is still no consensus on the dosage of anti-cytokine agents for such patients until now. In the included articles, the dosage of most patients was as follows: tocilizumab, 8 mg/kg/dose and up to a maximum of 800 mg; sarilumab, 400 mg/dose with 1 to 2 doses; anakinra 100 mg/dose 1–4 times a day; and mavrilimumab 6 mg/kg/dose. The characteristics of the included studies are presented in **Table 1**.

3.4 Results of the Meta-analysis

We cannot conduct a quantitative analysis of anakinra, sarilumab, and mavrilimumab for some outcomes, owing to differences in outcomes reported, study design, and limited study numbers. Especially for mavrilimumab, only one RCT and one cohort met the inclusion criteria. If we could not perform a meta-analysis, we commented on the results from all included studies.

3.4.1 Mortality Outcome (All-Cause Mortality at Days 28–30)

Tocilizumab

Among the 14 controlled studies, one RCT and 6 cohorts neither reported a difference for mortality at days 28–30 between the tocilizumab and control groups. Compared to the control group, the results of RCTs showed that the use of tocilizumab for

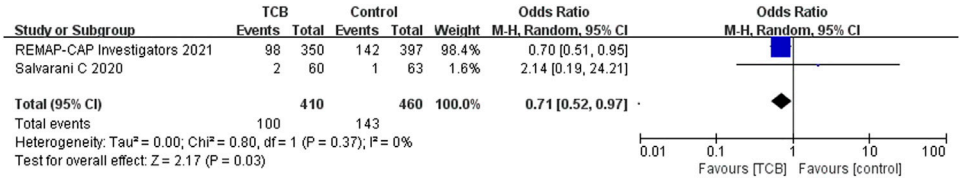

FIGURE 2 | (**A**) Results from randomized controlled trials (RCTs): the mortality outcome of tocilizumab for COVID-19 (at the edge of sepsis).

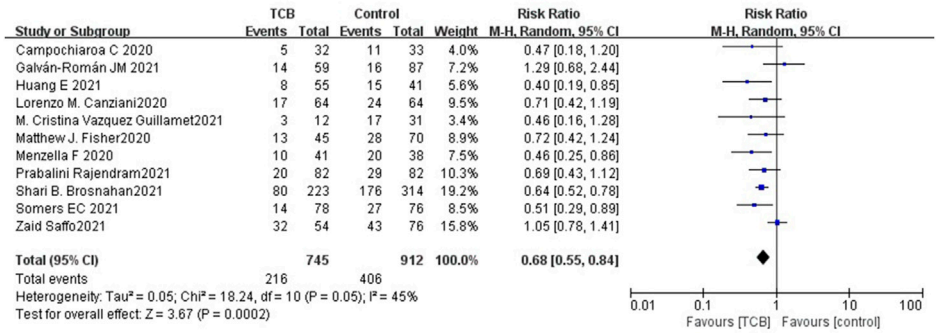

FIGURE 2 | (**B**) Results from non-RCTs: the mortality outcome of tocilizumab for COVID-19 (at the edge of sepsis).

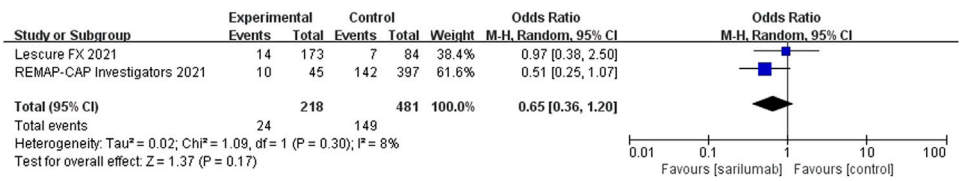

FIGURE 3 | Results from randomized controlled trials: the mortality outcome of sarilumab for COVID-19 (at the edge of sepsis).

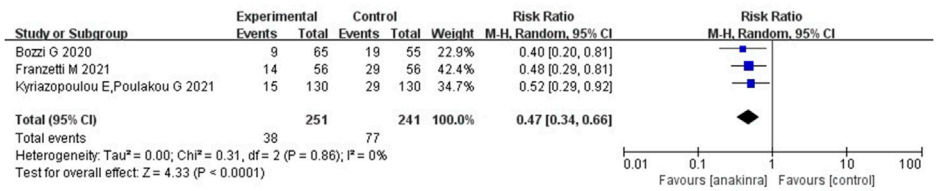

FIGURE 4 | Results from non- randomized controlled trials: the mortality outcome of anakinra for COVID-19 (at the edge of sepsis).

patients with COVID-19 (at the edge of sepsis) might decrease the mortality rate (OR 0.71, 95%CI: 0.52–0.97, I^2 = 0%), and there was a significant difference between the two groups (**Figure 2A**). The non-RCTs showed a similar result (RR 0.68, 95%CI: 0.55–0.84, I^2 = 45%), and there was statistical significance (**Figure 2B**).

Sarilumab

For sarilumab, of the studies that met the inclusion criteria, only two RCTs (one of the RCTs studied tocilizumab and sarilumab) and two non-RCTs provided data on mortality outcome. Among the two non-RCTs, one cohort did not set up a control group. Compared to the control group, the results of RCTs showed that

TABLE 2 | Adverse events (AEs) summarized from controlled studies.

Author	Immunomodulator	AEs (percentages)
Salvarani et al. (2021)	Tocilizumab	Control group: 2 severe infections; treatment group: 1 upper gastrointestinal tract bleeding. The most common adverse events were increased alanine aminotransferase level and decreased neutrophil count
REMAP-CAP Investigators et al. (2021)	Tocilizumab, sarilumab	Treatment group: 1 secondary bacterial infection, 5 bleeding events, 2 cardiac events, 1 deterioration in vision. Control group: 4 bleeding events, 7 thromboses
Canziani et al. (2020)	Tocilizumab	Thrombosis: treatment group (19%), control group (17%). Bleeding: treatment group (17%), control group (13%). Infection: treatment group (31%), control group (39)
Fisher et al. (2021)	Tocilizumab	No observed increased risk of secondary infection within 14 days of treatment with tocilizumab
Campochiaroa *et al*. (2020)	Tocilizumab	Pulmonary thrombosis: treatment group (6%), control group (9%). Raised ALT, AST level: treatment group (15%), control group (18%). Neutropenia: treatment group (16%), control group (0)
Vazquez Guillamet et al. (2021)	Tocilizumab	Culture-negative sepsis: treatment group (41.7%), control group (19.4)
Rajendram et al. (2021)	Tocilizumab	Secondary infection: treatment group (25.6%), control group (25.6%)
Huang et al. (2021)	Tocilizumab	Secondary infection: treatment group (31%), control group (17%)
Saffo et al. (2021)	Tocilizumab	Bleeding: treatment group (24.1%), control group (14.5%). Blood stream infection: treatment group (7.4%), control group (9.2%). Pulmonary infection (endotracheal aspirates/sputum): treatment group (25.9%), control group (30.3%)
Somers et al. (2021)	Tocilizumab	Superinfection: treatment group (54%), control group (26%). Bloodstream infection: treatment group (14%), control group (9%). Pneumonia: treatment group (45%), control group (20%)
Brosnahan et al. (2021)	Tocilizumab	Positive blood culture: combination group (steroid + tocilizumab) (11.6%), steroid group (12.7%). Positive Fungitell test: combination group (6.9%), steroid group (10.4%). Positive T2Candida panels: combination group (6.4%), steroids group (6.9%). Cytomegalovirus viral loads elevated: combination group (3.5%), steroids group 4.6%
Lescure et al. (2021)	Sarilumab	Serious infection: treatment group (12%), control group (12%). ALT increase: treatment group (31.02%), control group (19%). Invasive bacterial or fungal infection: treatment group (6.9%), control group (4%). Grade ≥2 hypersensitivity reaction: treatment group (2.4%), control group (0%). Grade 4 neutropenia: treatment group (2.7%), control group (0)
Della-Torre et al. (2020)	Sarilumab	Infections: treatment group (21%), control group (18%). Neutropenia: treatment group (14%), control group (0). Increase in liver enzymes: treatment group (14%), control group (0). Thromboembolism: treatment group (7%), control group (7%)
Kyriazopoulou et al. (2021a)	Anakinra	Infections and infestations: treatment group (8.4%), control group (15.9%). Anemia: treatment group (14.3%), control group (19.6%). Increase of liver function tests: treatment group (35.8%), control group (33.3%). Hyperglycemia: treatment group (36.5%), control group (40.2%). Hyponatremia: treatment group (7.9%), control group (12.2%). Hypernatremia: treatment group (11.4%), control group (9%)
Bozzi et al. (2021)	Anakinra	Treatment group: grade ≥3 GGT increase (27.7%), anemia (24.6%), ALT increase (6.2%), granulocytopenia (1.5%). Control group: a comparable proportion of these AEs
Franzetti et al. (2021)	Anakinra	Bloodstream infections: treatment group (16%), control group (7.1%). Urinary tract infections: treatment group (3.5%), control group (1.8%). Pneumonia infections: treatment group (7.1%), control group (7.1%)
Kyriazopoulou et al. (2021b)	Anakinra	Electrolyte abnormalities: treatment group (26.9%), control group (31.5%). Elevated liver function tests: treatment group (30.8%), control group (39.2%). Gastrointestinal disturbances: treatment group (11.5%), control group (6.9%). Anemia: treatment group (16.9%), control group (20%)
Cremer et al. (2021)	Mavrilimumab	Bacterial pneumonia: treatment group (10%), control group (5%). SAEs: treatment group (24%), control group (21%). Circulatory shock: treatment group (10%); control group (5%); Acute kidney injury: treatment group (19%), control group (16%). ALT ≥3ULN: treatment group (24%), control group (16%). AST ≥3ULN: treatment group (29%), control group (21%)
De Luca et al. (2020)	Mavrilimumab	Infectious complications: treatment group (0), control group (12%)

ALT, alanine aminotransferase; AST, aspartate aminotransferase; GGT, gamma-glutamyl transferase; ULN, upper limit of normal.

the use of sarilumab for patients with COVID-19 (at the edge of sepsis) might reduce the mortality rate (OR 0.65, 95%CI: 0.36–1.2, I^2 = 8%), but there was no significant difference between the two groups (**Figure 3**). However, due to the lack of research, data synthesis for outcomes of non-RCTs was not conducted.

Anakinra

For anakinra, of the studies that met the inclusion criteria, 1 RCT and 4 non-RCTs provided data on mortality outcome. Due to the insufficiency of RCTs, we only quantitatively synthesized the results of non-RCTs. Compared to the control group, the results of non-RCTs showed that the use of anakinra for patients with COVID-19 (at the edge of sepsis) might reduce the mortality rate (RR 0.47, 95%CI: 0.34–0.66, I^2 = 0%), and there was statistical significance (**Figure 4**).

Mavrilimumab

The only RCT, published in 2021, explored outcomes in 21 patients who received mavrilimumab and 19 patients who received placebo. The median (IQR) baseline SOFA score of enrolled patients was 2 (2 to 3). The study reported no significant association with the proportion of patients alive and off oxygen therapy at day 14. The other cohort, published in 2020, explored outcomes in 12 patients who received mavrilimumab and 26 patients who received standard of care. The median (IQR) P/F ratio of the mavrilimumab and control group was 196 (167–215) and 217 (138–258) mmHg, respectively. The study reported that

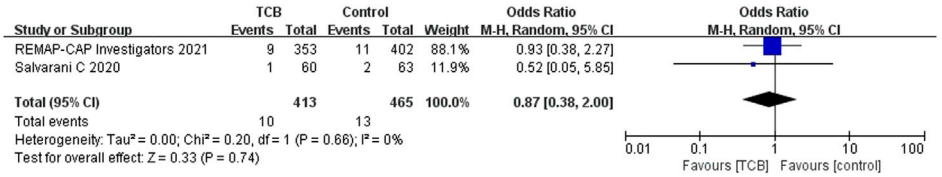

FIGURE 5 | (**A**) Results from randomized controlled trials (RCTs): the serious adverse events (SAEs) of tocilizumab for COVID-19 (at the edge of sepsis).

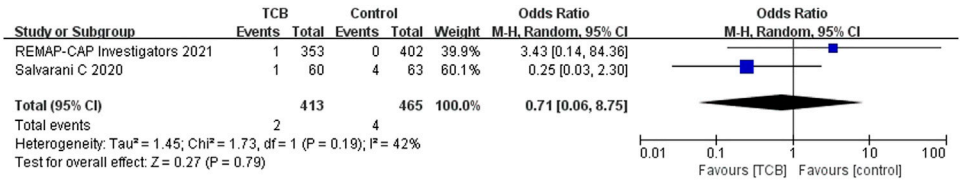

FIGURE 5 | (**B**) Results from RCTs: the secondary infections of tocilizumab for COVID-19 (at the edge of sepsis).

mavrilimumab was associated with a reduced mortality rate and improved clinical outcomes. The benefits of mavrilimumab therapy for those patients remained uncertain, given the insufficient controlled studies and the small sample size.

3.4.2 Safety Outcomes

Treatment-related adverse events (TRAEs) were reported in the majority of research and typically included neutropenia, secondary infections, increase in liver enzymes, and thromboembolism (**Table 2**). Due to the insufficient studies of safety outcome, we only conducted a quantitative synthesis for tocilizumab.

Tocilizumab

Both 2 RCTs reported SAEs and secondary infections; 4 of 11 non-RCTs reported SAEs and 10 reported secondary infections. Tocilizumab was associated with less SAEs (OR 0.87, 95%CI: 0.38–2.00, I^2 = 0%) and lower rates of secondary infections (OR 0.71, 95%CI: 0.06–8.75, I^2 = 42%) compared with the control groups, which both did not reach significance in RCTs (**Figures 5A,B**). For non-RCTs, tocilizumab was associated with slightly more SAEs (RR 1.18, 95%CI: 0.83–1.68, I^2 = 0) and secondary infections (RR 1.15, 95%CI: 0.89–1.49, I^2 = 49%) compared with the control arm, but there was no statistical significance (**Figures 6A,B**).

Other Anti-cytokine Agents

The included RCTs reported that the incidence of treatment-emergent SAEs through day 28 was higher in the placebo and standard-of-care group (21.2%) compared to the anakinra and standard-of-care group (16.5%). The non-serious TRAEs were similar in both treatment groups (Kyriazopoulou et al., 2021a). Only two cohorts reported secondary infection outcomes, and none reported SAEs. Both Franzetti M *et al.* and Bozzi G *et al.* reported that the rate of adverse events related to infection (or bloodstream infections) was similar between groups—for example, 26.8% occurred in the anakinra group and 16.1% in the control group (Bozzi et al., 2021; Franzetti et al., 2021). Among these infectious events, 9/56 developed bloodstream infections in the anakinra group and 4/56 in the control group (Franzetti et al., 2021). Meanwhile, they all suggested that special attention should be paid to possible infective reactivations or bacterial sepsis due to anakinra. In studies with a comparator arm exploring outcomes from patients who received mavrilimumab or sarilumab, the frequency of TRAEs was similar in both treatment and comparator groups.

3.5 Quality of Evidence

For mortality outcomes, the quality of evidence of tocilizumab for COVID-19 (at the edge of sepsis) was of low and very low quality for RCTs and non-RCTs, respectively. Meanwhile, the quality of evidence of sarilumab and anakinra for COVID-19 (at the edge of sepsis) was of low and very low quality, respectively. As for the SAEs and secondary infections of tocilizumab for COVID-19 (at the edge of sepsis), the quality of evidence was all low for RCTs and very low for non-RCTs, respectively. The results are shown in **Supplementary Table S8** (**Supplementary Material S2**, Appendix p43–45).

4 DISCUSSION

In terms of etiology, sepsis can be classified as bacterial sepsis, fungal sepsis, and viral sepsis based on different pathogens. Sepsis patients with a SOFA score of 2 or more in a general hospital population with presumed infection had an increased risk of death by 2–25 times compared to patients with a SOFA score of less than 2 (Singer et al., 2016; Seymour et al., 2016). The population included in this study was COVID-19 patients with SOFA score ≥2, who were already in the state of sepsis or were

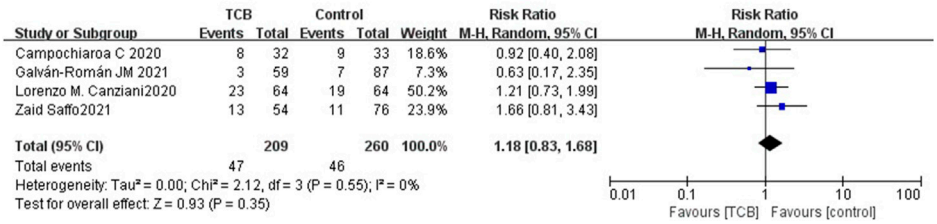

FIGURE 6 | (**A**) Results from non-randomized controlled trials (non-RCTs): the serious adverse events of tocilizumab for COVID-19 (at the edge of sepsis).

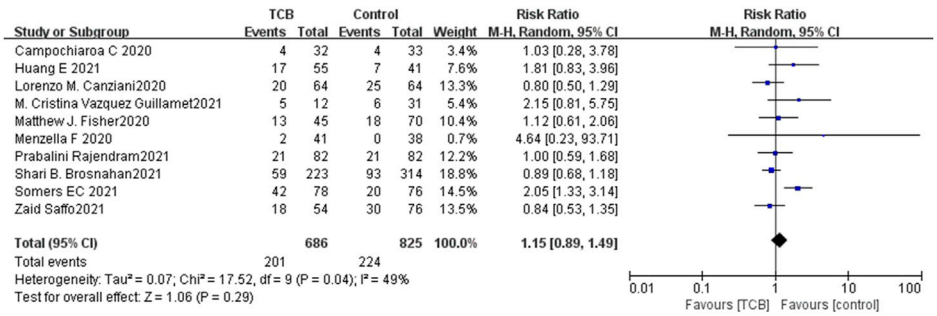

FIGURE 6 | (**B**) Results from non-RCTs: the secondary infections of tocilizumab for COVID-19 (at the edge of sepsis).

about to deteriorate into sepsis, and these patients urgently needed appropriate, safe, and effective treatment. In this study, we evaluated the efficacy and safety of tocilizumab, sarilumab, siltuximab, anakinra, mavrilimumab, and lenzilumab to provide relevant clinical evidence and research ideas for treatment.

4.1 Anti-cytokine Therapy

The local inflammatory response caused by an infection can promote the replacement of damaged tissues by new tissues and play a role in weakening the damage that has occurred, but when excessive inflammation occurs, it may cause systemic inflammatory response syndrome (SIRS) and lead to sepsis. Therefore, timely detection of cytokine storms and proper regulation of inflammatory response may be of great significance to the prevention of sepsis. The "Expert Consensus on Early Prevention and Blocking of Sepsis in China" recommended that when infected patients experience significant increases in cytokines or inflammatory imbalances, the inflammation should be adjusted as soon as possible using glucocorticoids, nonsteroidal anti-inflammatory drugs, traditional Chinese medicine preparations, antibodies targeting inflammatory mediators, *etc.* (Emergency medicine branch of CPAM et al., 2020). Many studies showed that the factors mainly involved in SIRS and compensatory anti-inflammatory response syndrome include TNF-α, IL-1, IL-6, *etc.* The Expert Consensus suggested that, for patients with high-risk sepsis infection, cytokine monitoring should be carried out regularly (2–4-h repetition) to find suspected sepsis patients in time. At present, the cytokine commonly detected in hospitals is IL-6. As a cytokine, IL-6 mainly stimulates the proliferation and differentiation of cells involved in immune response and plays an important role in the anti-infection immune response (Emergency Medicine Branch of CPAM et al., 2020).

IL-6 inhibitors include tocilizumab, sarilumab and siltuximab. Tocilizumab and sarilumab were approved for rheumatoid arthritis, and siltuximab was approved for Castleman's disease. The IL-1 receptor antagonist (anakinra) is a cornerstone treatment for hyperinflammatory conditions such as Still's disease. Some studies showed that cytokine-directed agents such as IL-6 and IL-1 inhibitors might be effective in the treatment of cytokine storm syndromes, including macrophage activation syndrome and cytokine release syndrome (La Rosée et al., 2019). The GM-CSF blockade included mavrilimumab and lenzilumab, which is designed to prevent and treat cytokine storm (De Luca et al., 2020; Aroldi et al., 2019). This systematic review identified and summarized RCTs, non-RCTs, and case reports (series) to evaluate the effect and safety of tocilizumab, sarilumab, siltuximab, anakinra, mavrilimumab, and lenzilumab. The meta-analysis results showed that tocilizumab might reduce the mortality of patients with COVID-19 (at the edge of sepsis) (RCTs: OR: 0.71, 95%CI: 0.52–0.97, low-certainty evidence; non-RCTs: RR: 0.68, 95%CI: 0.55–0.84, very low-certainty evidence) as was anakinra (non-RCTs: RR: 0.47, 95%CI: 0.34–0.66, very low-certainty evidence). Sarilumab might reduce the mortality of patients with COVID-19 (at the edge of sepsis), but there was no statistical significance (OR: 0.65, 95%CI: 0.36–1.2, low-certainty evidence). For safety outcomes, whether tocilizumab had an impact on SAEs was very uncertain (RCTs: OR: 0.87,

95%CI: 0.38–2.0, low-certainty evidence; non-RCTs: OR: 1.18, 95%CI: 0.83–1.68, very low-certainty evidence) as was on secondary infections (RCTs: OR: 0.71, 95%CI: 0.06–8.75, low-certainty evidence; non-RCTs: RR: 1.15, 95%CI: 0.89–1.49, very low-certainty evidence).

4.2 Special Population

At present, there are still few large-scale randomized controlled prospective studies on COVID-19 (at the edge of sepsis). The experiences of case or case series still have a certain reference significance for clinical treatment, especially for the individualized treatment of special populations, such as critically ill children, immunocompromised individuals, and elderly patients with a variety of chronic diseases. Patel PA *et al.* reported a case of severe pediatric COVID-19 presenting with respiratory failure and severe thrombocytopenia. On day 7, because of continued fever and elevated inflammatory markers, remdesivir and tocilizumab were given. On the next day, she had significant clinical improvement, so the treatment with cytokine-directed agents may be considered in critically ill patients (Patel et al., 2020).

Patients with impaired immune function are more at risk in case of adverse outcomes. Leelayuwatanaku N *et al.* reported two patients (P/F < 300 mmHg) with human immunodeficiency virus (HIV) infection and multiple myeloma relapse, respectively. After tocilizumab, hemoperfusion, and immunoglobulin comprehensive treatment, their P/F levels increased significantly, and they survived to discharge (Leelayuwatanaku et al., 2021). In addition, Kataoka H *et al.* reported an 85-year-old patient with Sjögren's syndrome, whose P/F decreased to 100 mmHg. After receiving a single dose of tocilizumab, the symptoms improved. This patient represents a supplementary case confirming the safety and efficacy of tocilizumab for elderly COVID-19 patients with autoimmune diseases. It is also suggested that combination therapy may be a promising treatment for severe COVID-19 in immunocompromised hosts (Kataoka et al., 2021).

The experience of COVID-19 patients with solid organ and composite tissue transplantation has not been reported in detail before. Morillas JA *et al.* reported 5 patients with COVID-19 (P/F < 300 mmHg) who received kidney transplantation, lung transplantation, face transplantation, and liver transplantation, respectively. These patients also had chronic diseases, such as heart diseases, bladder cancer, rheumatic heart disease, *etc*. Their C-reactive protein (CRP) levels decreased significantly within a few days after the application of tocilizumab. The findings showed that tocilizumab could be used without major direct toxicity in solid organ and composite tissue transfer recipients early after initiation of mechanical exploitation due to COVID-19, regardless of the type of organ transferred. However, the authors suggested that the diagnosis and side effects need to be further studied (Morillas et al., 2020). Ladna M *et al.* and Thammathiwa T *et al.* shared the treatment experiences of transplant patients, respectively. One patient who received a kidney and heart transplant in February 2020 had a relatively poor clinical condition with a P/F level of 117 mmHg. On day1, he was given a dose of 400 mg of tocilizumab, broad-spectrum antibiotics, and hydroxychloroquine, and transplant immunosuppression with tacrolimus was continued. After 11 days of treatment, he was discharged without supplemental oxygen requirement (Ladna et al., 2021; Thammathiwat et al., 2021).

In addition to tocilizumab treatment cases, there are few case reports on IL-1 receptor antagonist. Filocamo G *et al.* and Franzetti M *et al.* in Italy treated two severe patients (P/F <200 mmHg) with IL-1 receptor antagonist anakinra. These studies suggested that, in the cytokine storm occurring during severe COVID-19 pneumonia, the high tolerability, short half-life, and immunomodulatory profile of anakinra may be useful. IL-1 inhibition may represent a safe and promising strategy to reduce inflammation, thus preventing multi-organ dysfunction (Filocamo et al., 2020; Franzetti et al., 2020).

4.3 Limitation

First, the lack of RCTs limited our analyses. Some included studies were case reports or series and had no proper control groups. Meanwhile, some articles of which the full texts or data were not accessible and those in languages other than Chinese and English were excluded from the analysis. This might have led to overlooking some critical findings or observations. In addition, in this study, the SOFA score or related indicators of some patients included in the study were median or mean, so not all patients were septic patients, but the results of this population also reflected a trend problem because some patients might be or would be in a state of sepsis. Thirdly, we found that most patients use antiviral drugs, glucocorticoids, immunoglobulins, plasma, broad-spectrum antibiotics, and other drugs at the same time. We cannot rule out the impact of these drugs on the disease.

5 CONCLUSION

The results of this systematic review showed that tocilizumab, sarilumab, and anakinra might reduce the mortality of people with COVID-19 (at the edge of sepsis), and tocilizumab did not significantly affect SAEs and secondary infections. However, given the limited clinical researches and low-quality evidence, this conclusion needs more clinical evidence to be verified. In addition, so far, there is still no unified opinion on the timing, dosage, usage, and applicable population of these drugs all over the world, which also adds to the uncertainty of the conclusion of this study.

DATA AVAILABILITY STATEMENT

The original contributions presented in the study are included in the article/**Supplementary Material**. Further inquiries can be directed to the corresponding author.

AUTHOR CONTRIBUTIONS

YW and KZ contributed equally to this work. YW, KZ, and QY conceived and designed the study protocol. YW and KZ executed

the search strategy and screening and performed data extraction. RL, RD, and XL performed risk of bias assessments, and YW and RL assessed the quality of evidence. YW, ML, and RD analyzed or interpreted the data. YW and KZ drafted the manuscript. QY contributed to writing—review and editing.

SUPPLEMENTARY MATERIAL

The supplementary material for this article can be found online at: https://www.frontiersin.org/articles/10.3389/fphar.2021.804250/full#supplementary-material

REFERENCES

Abe, T., Izumo, T., Ueda, A., Hayashi, M., and Ishibashi, Y. (2021). Successful Treatment of Two Japanese ESRD Cases With Severe COVID-19 Pneumonia. *CEN Case Rep.* 10 (1), 42–45. doi:10.1007/s13730-020-00512-7

Al-Kaf, F. A., Al Garni, T. A., Al-Harbi, N., Sandokji, H., and Samargandy, S. (2021). Cardiac Tamponade, Sever Hypothyroidism and Acute Respiratory Distress Syndrome (ARDS) With COVID-19 Infection. *J. Saudi Heart Assoc.* 33 (1), 71–76. doi:10.37616/2212-5043.1235

Aroldi, A., Chiarle, R., and Gambacorti-Passerini, C. (2021). Clinical Benefit of Lenzilumab in Cases of Coronavirus Disease 2019. *Mayo Clin. Proc.* 96 (3), 817. doi:10.1016/j.mayocp.2020.12.030

Bernardo, L., Del Sesto, S., Giordano, L., Benincaso, A. R., Biondi, P., Goj, V., et al. (2020). Severe Prolonged Neutropenia Following Administration of Tocilizumab in a Patient Affected by COVID-19: a Case Report and Brief Review of the Literature. *Drugs Ther. Perspect.* 14, 1–5. doi:10.1007/s40267-020-00777-z

Bozzi, G., Mangioni, D., Minoia, F., Aliberti, S., Grasselli, G., Barbetta, L., et al. (2021). Anakinra Combined With Methylprednisolone in Patients With Severe COVID-19 Pneumonia and Hyperinflammation: An Observational Cohort Study. *J. Allergy Clin. Immunol.* 147 (2), 561–e4. e4. doi:10.1016/j.jaci.2020.11.006

Brosnahan, S. B., Chen, X. J. C., Chung, J., Altshuler, D., Islam, S., Thomas, S. V., et al. (2021). Low-Dose Tocilizumab With High-Dose Corticosteroids in Patients Hospitalized for COVID-19 Hypoxic Respiratory Failure Improves Mortality Without Increased Infection Risk. *Ann. Pharmacother.* 28, 10600280211028882. doi:10.1177/10600280211028882

Campochiaro, C., Della-Torre, E., Cavalli, G., De Luca, G., Ripa, M., Boffini, N., et al. (2020). Efficacy and Safety of Tocilizumab in Severe COVID-19 Patients: a Single-centre Retrospective Cohort Study. *Eur. J. Intern. Med.* 76, 43–49. doi:10.1016/j.ejim.2020.05.021

Canziani, L. M., Trovati, S., Brunetta, E., Testa, A., De Santis, M., Bombardieri, E., et al. (2020). Interleukin-6 Receptor Blocking with Intravenous Tocilizumab in COVID-19 Severe Acute Respiratory Distress Syndrome: A Retrospective Case-Control Survival Analysis of 128 Patients. *J. Autoimmun.* 114, 102511. doi:10.1016/j.jaut.2020.102511

Cascella, M., Mauro, I., De Blasio, E., Crispo, A., Del Gaudio, A., Bimonte, S., et al. (2020). Rapid and Impressive Response to a Combined Treatment With Single-Dose Tocilizumab and NIV in a Patient With COVID-19 Pneumonia/ARDS. *Medicina (Kaunas).* 56 (8), 377. doi:10.3390/medicina56080377

Cavalli, G., Larcher, A., Tomelleri, A., Campochiaro, C., Della-Torre, E., De Luca, G., et al. (2021). Interleukin-1 and Interleukin-6 Inhibition Compared With Standard Management in Patients With COVID-19 and Hyperinflammation: a Cohort Study. *Lancet Rheumatol.* 3 (4), e253–e261. doi:10.1016/S2665-9913(21)00012-6

Coomes, E. A., and Haghbayan, H. (2020). Interleukin-6 in Covid-19: A Systematic Review and Meta-Analysis. *Rev. Med. Virol.* 30 (6), 1–9. doi:10.1002/rmv.2141

Corominas, H., Castellví, I., Pomar, V., Antonijoan, R., Mur, I., Matas, L., et al. (2021). Effectiveness and Safety of Intravenous Tocilizumab to Treat COVID-19-Associated Hyperinflammatory Syndrome: Covizumab-6 Observational Cohort. *Clin. Immunol.* 223, 108631. doi:10.1016/j.clim.2020.108631

Cremer, P. C., Abbate, A., Hudock, K., McWilliams, C., Mehta, J., Chang, S. Y., et al. (2021). Mavrilimumab in Patients With Severe COVID-19 Pneumonia and Systemic Hyperinflammation (MASH-COVID): an Investigator Initiated, Multicentre, Double-Blind, Randomised, Placebo-Controlled Trial. *Lancet Rheumatol.* 3 (6), e410–e418. doi:10.1016/S2665-9913(21)00070-9

De Luca, G., Cavalli, G., Campochiaro, C., Della-Torre, E., Angelillo, P., Tomelleri, A., et al. (2020). GM-CSF Blockade With Mavrilimumab in Severe COVID-19 Pneumonia and Systemic Hyperinflammation: a Single-Centre, Prospective Cohort Study. *Lancet Rheumatol.* 2 (8), e465–e473. doi:10.1016/S2665-9913(20)30170-3

Della-Torre, E., Campochiaro, C., Cavalli, G., De Luca, G., Napolitano, A., La Marca, S., et al. (2020). Interleukin-6 Blockade With Sarilumab in Severe COVID-19 Pneumonia With Systemic Hyperinflammation: an Open-Label Cohort Study. *Ann. Rheum. Dis.* 79 (10), 1277–1285. doi:10.1136/annrheumdis-2020-218122

Emergency medicine branch of CPAM (2020). Emergency Medicine Branch of Chinese Medical Association, Emergency Physicians branch of Chinese Medical Doctor Association, Professional Committee of Emergency Medicine of Chinese People's Liberation Army. Expert Consensus on Early Prevention and Blocking of Sepsis in China. *Cli Emer J. (China).* 21 (7), 517–529.

Erden, A., Ozdemir, B., Karakas, O., Mutlu, N. M., Izdes, S., Kalem, A. K., et al. (2021). Evaluation of 17 Patients With COVID-19 Pneumonia Treated With Anakinra According to HScore, SOFA, MuLBSTA, and Brescia-COVID Respiratory Severity Scale (BCRSS) Scoring Systems. *J. Med. Virol.* 93 (3), 1532–1537. doi:10.1002/jmv.26473

Eroglu, A., Kartal, S., and Saral, O. B. (2021). Helmet Mask and Tocilizumab for a Patient With Hemophagocytic Lymphohistiocytosis Syndrome and COVID-19: a Case Report. *Braz. J. Anesthesiol.* 71 (1), 79–83. doi:10.1016/j.bjane.2020.10.009

Filocamo, G., Mangioni, D., Tagliabue, P., Aliberti, S., Costantino, G., Minoia, F., et al. (2020). Use of Anakinra in Severe COVID-19: A Case Report. *Int. J. Infect. Dis.* 96, 607–609. doi:10.1016/j.ijid.2020.05.026

Fisher, M. J., Marcos Raymundo, L. A., Monteforte, M., Taub, E. M., and Go, R. (2021). Tocilizumab in the Treatment of Critical COVID-19 Pneumonia: A Retrospective Cohort Study of Mechanically Ventilated Patients. *Int. J. Infect. Dis.* 103, 536–539. doi:10.1016/j.ijid.2020.12.021

Franzetti, M., Forastieri, A., Borsa, N., Pandolfo, A., Molteni, C., Borghesi, L., et al. (2021). IL-1 Receptor Antagonist Anakinra in the Treatment of COVID-19 Acute Respiratory Distress Syndrome: A Retrospective, Observational Study. *J. Immunol.* 206 (7), 1569–1575. doi:10.4049/jimmunol.2001126

Franzetti, M., Pozzetti, U., Carugati, M., Pandolfo, A., Molteni, C., Faccioli, P., et al. (2020). Interleukin-1 Receptor Antagonist Anakinra in Association With Remdesivir in Severe COVID-19: A Case Report. *Int. J. Infect. Dis.* 97, 215–218. doi:10.1016/j.ijid.2020.05.050

Galván-Román, J. M., Rodríguez-García, S. C., Roy-Vallejo, E., Marcos-Jiménez, A., Sánchez-Alonso, S., Fernández-Díaz, C., et al. (2021). IL-6 Serum Levels Predict Severity and Response to Tocilizumab in COVID-19: An Observational Study. *J. Allergy Clin. Immunol.* 147 (1), 72–80. e8. doi:10.1016/j.jaci.2020.09.018

Garg, N., and Lee, Y. I. (2020). Reactivation TB With Severe COVID-19. *Chest.* 158, A777. doi:10.1016/j.chest.2020.08.724

Granholm, A., Alhazzani, W., and Møller, M. H. (2019). Use of the GRADE Approach in Systematic Reviews and Guidelines. *Br. J. Anaesth.* 123 (5), 554–559. doi:10.1016/j.bja.2019.08.015

Gremese, E., Cingolani, A., Bosello, S. L., Alivernini, S., Tolusso, B., Perniola, S., et al. (2020). Sarilumab Use in Severe SARS-CoV-2 Pneumonia. *EClinicalMedicine.* 27, 100553. doi:10.1016/j.eclinm.2020.100553

Huang, C., Wang, Y., Li, X., Ren, L., Zhao, J., Hu, Y., et al. (2020). Clinical Features of Patients Infected With 2019 Novel Coronavirus in Wuhan, China. *Lancet.* 395 (10223), 497–506. doi:10.1016/S0140-6736(20)30183-5

Huang, E., Isonaka, S., Yang, H., Salce, E., Rosales, E., and Jordan, S. C. (2021). Tocilizumab Treatment in Critically Ill Patients With COVID-19: A Retrospective Observational Study. *Int. J. Infect. Dis.* 105, 245–251. doi:10.1016/j.ijid.2021.02.057

Kashin, M., Gorski, J., and Minkin, R. (2020). Lung Abscesses in A Patient Treated With Tocilizumab for Covid-19 Pneumonia Complicated by Severe Hypoxemic Respiratory Failure. *Chest.* 158 (4), A2568. doi:10.1016/j.chest.2020.09.165

Kataoka, H., Kodama, F., Tomita, T., Kondo, M., Nagasaka, A., Nishikawa, S., et al. (2021). Immediate Amelioration of Severe Respiratory Distress in Sjögren's Syndrome With COVID-19 Treated With a Single Dose of Off-Label Tocilizumab. *Intern. Med.* 60 (4), 639–643. doi:10.2169/internalmedicine.6010-20

Kishaba, T., Maeda, A., Fukuoka, S., Imai, T., Takakura, S., Yokoyama, S., et al. (2021). A Case Report of Super Responder of Critical COVID-19 Pneumonia. *J. Med. Invest.* 68 (1.2), 192–195. doi:10.2152/jmi.68.192

Kyriazopoulou, E., Panagopoulos, P., Metallidis, S., Dalekos, G. N., Poulakou, G., Gatselis, N., et al. (2021a). An Open Label Trial of Anakinra to Prevent Respiratory Failure in COVID-19. *Elife.* 10, e66125. doi:10.7554/eLife.66125

Kyriazopoulou, E., Poulakou, G., Milionis, H., Metallidis, S., Adamis, G., Tsiakos, K., et al. (2021b). Early Treatment of COVID-19 with Anakinra Guided by Soluble Urokinase Plasminogen Receptor Plasma Levels: a Double-Blind, Randomized Controlled Phase 3 Trial. *Nat. Med.* 27 (10), 1752–1760. doi:10.1038/s41591-021-01499-z

La Rosée, P., Horne, A., Hines, M., von Bahr Greenwood, T., Machowicz, R., Berliner, N., et al. (2019). Recommendations for the Management of Hemophagocytic Lymphohistiocytosis in Adults. *Blood.* 133 (23), 2465–2477. doi:10.1182/blood.2018894618

Ladna, M., Villanueva, F. L., Maharrey, P. B., and Lascano, J. (2021). Post-Transplant Patients With COVID-19 Associated Acute Respiratory Distress Syndrome, a Role for Tociluzumab: A Case Series. *Respir. Med. Case Rep.* 32, 101319. doi:10.1016/j.rmcr.2020.101319

Leelayuwatanakul, N., Kongpolprom, N., Sriprasart, T., Phoophiboon, V., Thanthitaweewat, V., Thawanaphong, S., et al. (2021). Multimodality Treatment in Immunocompromised Patients With Severe COVID-19: the Role of IL-6 Inhibitor, Intravenous Immunoglobulin, and Haemoperfusion. *Respirol Case Rep.* 9 (4), e0733. doi:10.1002/rcr2.733

Lescure, F. X., Honda, H., Fowler, R. A., Lazar, J. S., Shi, G., Wung, P., et al. (2021). Sarilumab COVID-19 Global Study Group. Sarilumab in Patients Admitted to Hospital With Severe or Critical COVID-19: a Randomised, Double-Blind, Placebo-Controlled, Phase 3 Trial. *Lancet Respir. Med.* 9 (5), 522–532. doi:10.1016/S2213-2600(21)00099-0

Li, H., Liu, L., Zhang, D., Xu, J., Dai, H., Tang, N., et al. (2020). SARS-CoV-2 and Viral Sepsis: Observations and Hypotheses. *Lancet.* 395 (10235), 1517–1520. doi:10.1016/S0140-6736(20)30920-X

Lucas, C., Wong, P., Klein, J., Castro, T. B. R., Silva, J., Sundaram, M., et al. (2020). Longitudinal Analyses Reveal Immunological Misfiring in Severe COVID-19. *Nature.* 584 (7821), 463–469. doi:10.1038/s41586-020-2588-y

Mady, A., Aletreby, W., Abdulrahman, B., Lhmdi, M., Noor, A. M., Alqahtani, S. A., et al. (2020). Tocilizumab in the Treatment of Rapidly Evolving COVID-19 Pneumonia and Multifaceted Critical Illness: A Retrospective Case Series. *Ann. Med. Surg. (Lond).* 60, 417–424. doi:10.1016/j.amsu.2020.10.061

Mazankova, L. N., Osmanov, I. M., Samitova, E. R., Malakhov, A. B., Koroid, V. V., Nedostoev, A. A., et al. (2020). A Teenager With a Severe Form of COVID-19. *Rossiyskiy Vestnik Perinatologii i Pediatrii.* 65 (5), 58–65. doi:10.21508/1027-4065-2020-65-5-58-65

McKenzie, M. G., Lee, Y. M., Mathew, J., Anderson, M., Vo, A. T., Akinyele, S., et al. (2021). Tocilizumab for the Critically Ill With Severe COVID-19: A Community Hospital Case Series. *J. Pharm. Pract.* 19, 8971900211002353. doi:10.1177/08971900211002353

Menzella, F., Fontana, M., Salvarani, C., Massari, M., Ruggiero, P., Scelfo, C., et al. (2020). Efficacy of Tocilizumab in Patients With COVID-19 ARDS Undergoing Noninvasive Ventilation. *Crit. Care.* 24 (1), 589. doi:10.1186/s13054-020-03306-6

Moher, D., Liberati, A., Tetzlaff, J., and Altman, D. G.PRISMA Group (2009). Preferred Reporting Items for Systematic Reviews and Meta-Analyses: the PRISMA Statement. *Plos Med.* 6 (7), e1000097. doi:10.1371/journal.pmed.1000097

Moideen, S., Maheshwari, V., Syam Prakash, K. R., Rajagopal, S., and Sherief, S. H. (2020). Different Treatment Approaches, Clinical Outcome, Effectiveness of the Drug towards Covid 19 With 5 Different Cases: A Case Series. *Int. J. Pharm. Sci. Rev. Res.* 65 (1), 98–103. doi:10.47583/ijpsrr.2020.v65i01.014

Morillas, J. A., Marco Canosa, F., Srinivas, P., Asadi, T., Calabrese, C., Rajendram, P., et al. (2020). Tocilizumab Therapy in 5 Solid and Composite Tissue Transplant Recipients With Early ARDS Due to SARS-CoV-2. *Am. J. Transpl.* 20 (11), 3191–3197. doi:10.1111/ajt.16080

National Institutes of Health(NIH) (2017). Common Terminology Criteria for Adverse Events (CTCAE) Version 5.0. Available at: https://ctep.cancer.gov/protocolDevelopment/electronic_applications/ctc.htm#ctc_40 (Accessed October 17, 2021).

NOS (2020). Abbreviations.com. STANDS4 LLC. Available at: https://www.abbreviations.com/term/1418908 (Accessed October 17, 2021).

Nourié, N., Chamaa, M. A., Mouawad, S., Kotait, M. M., Finianos, S., Azar, H., et al. (2021). Effective Treatment With Tocilizumab in a COVID-19 Patient on Maintenance Hemodialysis: A Case Report. *CEN Case Rep.* 10 (3), 364–369. doi:10.1007/s13730-021-00577-y

Patel, P. A., Chandrakasan, S., Mickells, G. E., Yildirim, I., Kao, C. M., and Bennett, C. M. (2020). Severe Pediatric COVID-19 Presenting With Respiratory Failure and Severe Thrombocytopenia. *Pediatrics.* 146 (1), e20201437. doi:10.1542/peds.2020-1437

Qin, C., Zhou, L., Hu, Z., Zhang, S., Yang, S., Tao, Y., et al. (2020). Dysregulation of Immune Response in Patients With Coronavirus 2019 (COVID-19) in Wuhan, China. *Clin. Infect. Dis.* 71 (15), 762–768. doi:10.1093/cid/ciaa248

Rajendram, P., Sacha, G. L., Mehkri, O., Wang, X., Han, X., Vachharajani, V., et al. (2021). Tocilizumab in Coronavirus Disease 2019-Related Critical Illness: A Propensity Matched Analysis. *Crit. Care Explor.* 3 (1), e0327. doi:10.1097/CCE.0000000000000327

REMAP-CAP InvestigatorsGordon, A. C., Mouncey, P. R., Al-Beidh, F., Rowan, K. M., and Nichol, A. D. (2021). Interleukin-6 Receptor Antagonists in Critically Ill Patients With Covid-19. *N. Engl. J. Med.* 384 (16), 1491–1502. doi:10.1056/NEJMoa2100433

Rice, T. W., Wheeler, A. P., Bernard, G. R., Hayden, D. L., Schoenfeld, D. A., Ware, L. B., et al. (2007). Comparison of the SpO2/FIO2 Ratio and the PaO2/FIO2 Ratio in Patients With Acute Lung Injury or ARDS. *Chest.* 132 (2), 410–417. doi:10.1378/chest.07-0617

Rudd, K. E., Johnson, S. C., Agesa, K. M., Shackelford, K. A., Tsoi, D., Kievlan, D. R., et al. (2020). Global, Regional, and National Sepsis Incidence and Mortality, 1990-2017: Analysis for the Global Burden of Disease Study. *Lancet.* 395 (10219), 200–211. doi:10.1016/S0140-6736(19)32989-7

Saffo, Z., Guo, W., Springer, K., Maksimowicz-McKinnon, K., Kak, V., McKinnon, J. E., et al. (2021). The Role of Tocilizumab Therapy in Critically Ill Patients With Severe Acute Respiratory Syndrome Coronavirus 2. *J. Osteopath Med.* 121 (8), 705–714. doi:10.1515/jom-2020-0292

Salvarani, C., Dolci, G., Massari, M., Merlo, D. F., Cavuto, S., Savoldi, L., et al. (2021). Effect of Tocilizumab vs Standard Care on Clinical Worsening in Patients Hospitalized With COVID-19 Pneumonia: A Randomized Clinical Trial. *JAMA Intern. Med.* 181 (1), 24–31. doi:10.1001/jamainternmed.2020.6615

Senegaglia, A. C., Rebelatto, C. L. K., Franck, C. L., Lima, J. S., Boldrini-Leite, L. M., Daga, D. R., et al. (2021). Combined Use of Tocilizumab and Mesenchymal Stromal Cells in the Treatment of Severe Covid-19: Case Report. *Cell Transpl.* 30, 9636897211021008. doi:10.1177/09636897211021008

Seymour, C. W., Liu, V. X., Iwashyna, T. J., Brunkhorst, F. M., Rea, T. D., Scherag, A., et al. (2016). Assessment of Clinical Criteria for Sepsis: For the Third International Consensus Definitions for Sepsis and Septic Shock (Sepsis-3). *JAMA.* 315 (8), 762–774. doi:10.1001/jama.2016.0288

Singer, M., Deutschman, C. S., Seymour, C. W., Shankar-Hari, M., Annane, D., Bauer, M., et al. (2016). The Third International Consensus Definitions for Sepsis and Septic Shock (Sepsis-3). *JAMA.* 315 (8), 801–810. doi:10.1001/jama.2016.0287

Somers, E. C., Eschenauer, G. A., Troost, J. P., Golob, J. L., Gandhi, T. N., Wang, L., et al. (2021). Tocilizumab for Treatment of Mechanically Ventilated Patients With COVID-19. *Clin. Infect. Dis.* 73 (2), e445–e454. doi:10.1093/cid/ciaa954

Sterne, J. A. C., Savović, J., Page, M. J., Elbers, R. G., Blencowe, N. S., Boutron, I., et al. (2019). RoB 2: a Revised Tool for Assessing Risk of Bias in Randomised Trials. *BMJ.* 366, l4898. doi:10.1136/bmj.l4898

Thammathiwat, T., Tungsanga, S., Tiankanon, K., Torvorapanit, P., Chumpangern, W., Udomkarnjananun, S., et al. (2021). A Case of Successful Treatment of Severe COVID-19 Pneumonia With Favipiravir and Tocilizumab in post-kidney Transplant Recipient. *Transpl. Infect. Dis.* 23 (1), e13388. doi:10.1111/tid.13388

Vazquez Guillamet, M. C., Kulkarni, H. S., Montes, K., Samant, M., Shaikh, P. A., Betthauser, K., et al. (2021). Interleukin-6 Trajectory and Secondary Infections

in Mechanically Ventilated Patients With Coronavirus Disease 2019 Acute Respiratory Distress Syndrome Treated With Interleukin-6 Receptor Blocker. *Crit. Care Explor.* 3 (2), e0343. doi:10.1097/CCE.0000000000000343

Wang, Y., Dai, R., Lv, X., Qian, Y., and Zhu, K. (2020). Specific Interleukin-1 Inhibitors, Specific Interleukin-6 Inhibitors and Anti-GM-CSF for COVID-19 (At the Edge of Sepsis): a Living System Review. PROSPERO 2020 CRD42020226545 Available at: https://www.crd.york.ac.uk/prospero/display_record.php?ID=CRD42020226545 (Accessed October 17, 2021).

Conflict of Interest: The authors declare that the research was conducted in the absence of any commercial or financial relationships that could be construed as a potential conflict of interest.

Publisher's Note: All claims expressed in this article are solely those of the authors and do not necessarily represent those of their affiliated organizations or those of the publisher, the editors, and the reviewers. Any product that may be evaluated in this article or claim that may be made by its manufacturer is not guaranteed or endorsed by the publisher.

Advantages of publishing in Frontiers

OPEN ACCESS
Articles are free to read for greatest visibility and readership

FAST PUBLICATION
Around 90 days from submission to decision

HIGH QUALITY PEER-REVIEW
Rigorous, collaborative, and constructive peer-review

TRANSPARENT PEER-REVIEW
Editors and reviewers acknowledged by name on published articles

Frontiers
Avenue du Tribunal-Fédéral 34
1005 Lausanne | Switzerland

Visit us: www.frontiersin.org
Contact us: frontiersin.org/about/contact

REPRODUCIBILITY OF RESEARCH
Support open data and methods to enhance research reproducibility

DIGITAL PUBLISHING
Articles designed for optimal readership across devices

FOLLOW US
@frontiersin

IMPACT METRICS
Advanced article metrics track visibility across digital media

EXTENSIVE PROMOTION
Marketing and promotion of impactful research

LOOP RESEARCH NETWORK
Our network increases your article's readership